

NASA Tech Briefs

National
Aeronautics and
Space
Administration

Winter 1985
Volume 9 Number 4

**Satellite Servicing
Comes of Age**



Good news

For humans, a better life on Earth.

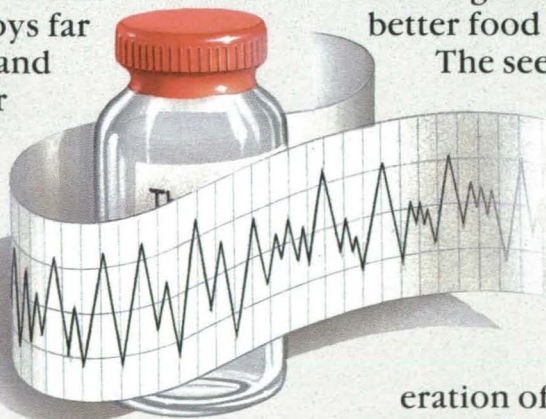
Soon, 26 years of space exploration will begin to pay off in ways few Americans can imagine. When America's first permanent space station goes into orbit, here is what NASA expects to learn:

How to manufacture purer vaccines and new drugs impossible to make on Earth.

How to manufacture computer chips with capacities that are one hundred times greater than the best we have now.

How to create metal alloys far stronger and far lighter than any made on Earth.

How to create metals that can transmit electrical energy with no



appreciable loss of power. (The savings to consumers could be billions of dollars every year!)

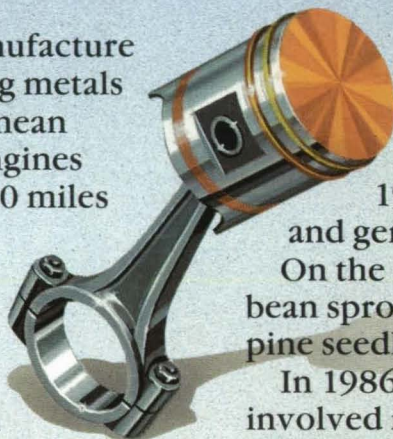
How to manufacture self-lubricating metals which could mean automobile engines lasting 500,000 miles and more.

These are only a few of over 150 experiments being planned right now that will be made possible by NASA and companies such as General Electric.

Planting the seeds of knowledge 25 years ago.

Work NASA began long ago will soon teach us not only how to grow food in space, but perhaps even how to grow more and better food on Earth.

The seeds General Electric helped send into space on Discoverer 32 in 1960 propagated a new generation of increasingly sophisticated — and fruitful — experiments.



On Bio-satellite II, wheat and peppers were successfully germinated.

On Apollo 16 in 1972, beans and watercress were studied.

On Skylab 3 in 1973, the growth and germination of rice.

On the 1982 shuttle, bean sprouts, oats, and pine seedlings.

In 1986, GE will be involved in further work on the Space Shuttle with wheat and oats.

One thing NASA hopes to learn is whether it's possible to grow more from every seed.

Good news for heart patients on Earth.

For fourteen years, GE has worked with NASA on the effects of weightlessness on the cardiovascular system. A new device GE has helped develop for use on America's permanent space station may soon make it possible for doctors on Earth to use a noninvasive

from space:

technique instead of catheterization in the treatment of heart patients.

The GE device uses a trace gas inhaled and then measured during exhalation and monitored during exercise.

This permits heart

A major achievement for the 20th century.

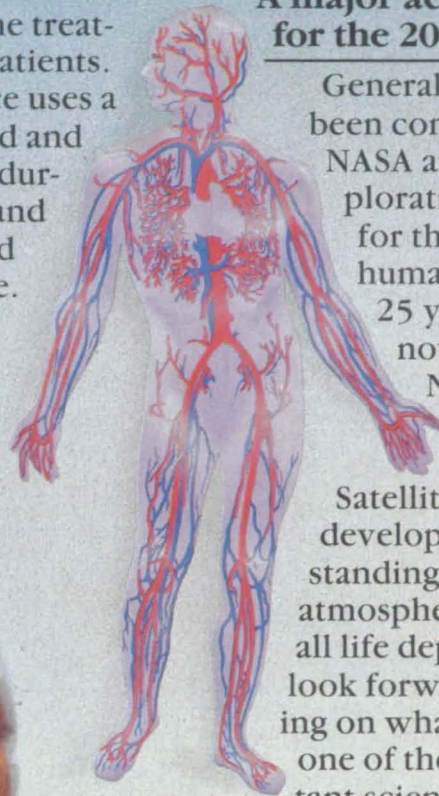
General Electric has been committed to NASA and to the exploration of space for the benefit of humanity for over 25 years. We are now building NASA's Upper Atmosphere Research

Satellite (UARS) to develop our understanding of the Earth's atmosphere on which all life depends. We look forward to working on what will be one of the most important scientific endeavors of the 20th Century — America's first permanent space station.

Space Systems Division,
Valley Forge, PA.

Leading from the start ...
and working on the future.

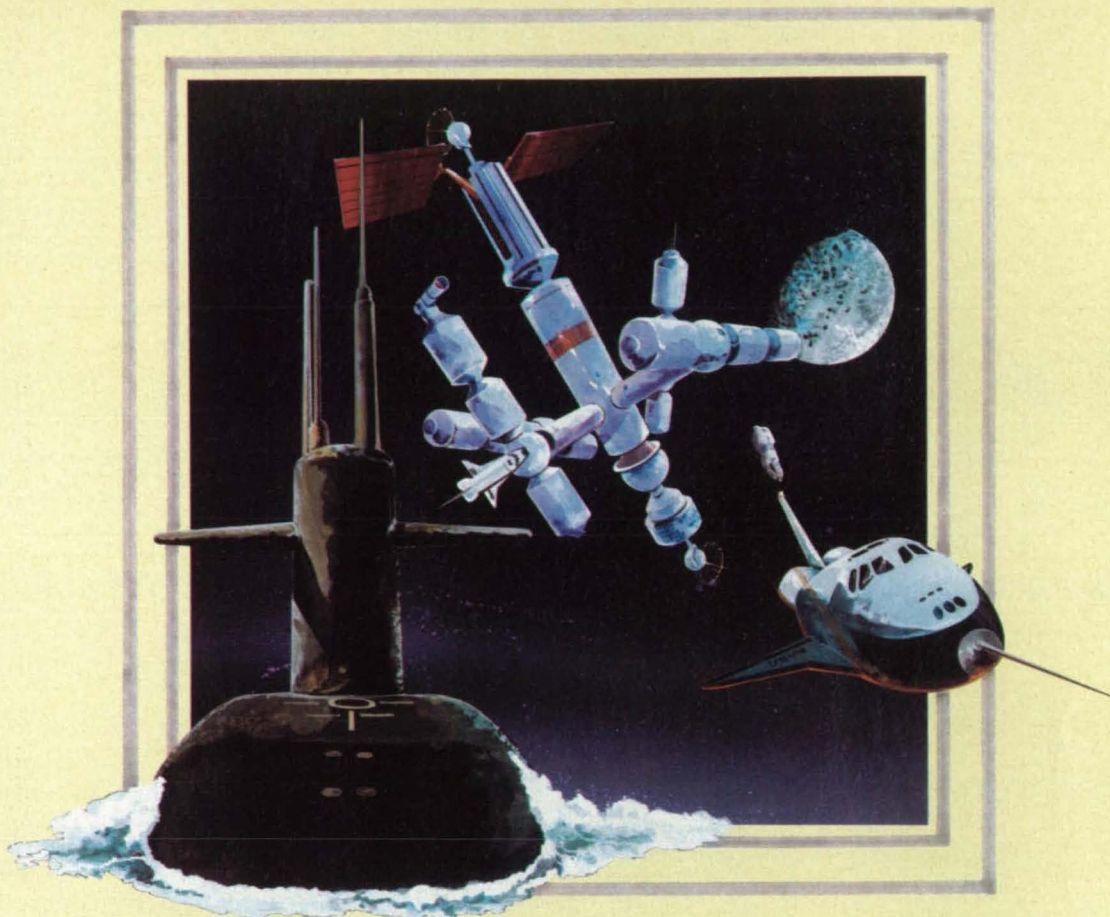
Join the GE Team: Find out about opportunities at GE Space Systems Division. Write: Professional Staffing, General Electric Company, 234 Goddard Blvd., King of Prussia, PA 19406.



behavior experimentation in space without catheterization. And for heart patients on Earth this technique would be a welcome benefit.

NASA

Excellence



What do Space Stations and Submarines Have in Common?

Space stations will be required to be self-sufficient for long periods . . . just like submarines. Vitro Corporation has long ensured the sustained on-station operation of the submarine fleet.

How does Vitro make this happen?

Full Support - Vitro provides the logistics support, maintainability support, and systems engineering necessary to keep a submarine on patrol for extended periods.

Long Experience - Vitro support capability is founded upon over 35 years of systems engineering experience. Our engineers are well-versed in the techniques that ensure optimum systems operation in a demanding environment. With

over 6,200 employees, Vitro provides mission support analysis, quality assurance, software, and modern management information systems to ensure system operability.

Extensive Resources - Yes, a space station orbiting our planet and a submarine patrolling our oceans have many needs in common. Vitro has and will continue to meet those needs. Our combination of experience, technical capability, and resources is unmatched.

This capability is available to you. Vitro Corporation stands ready now to work with you to ensure a long and successful Space Station Program . . . to continue a tradition of excellence.

Vitro
CORPORATION

14000 Georgia Avenue, Silver Spring, Maryland 20910
For information call our Marketing Manager, (301) 231-1300

Circle Reader Action No. 394

National Aeronautics and
Space Administration

NASA Tech Briefs:

Published by:

Associated Business Publications
Editor-in-Chief/Publisher: **Bill Schnirring**
Managing Editor: **Rita Nothaft**
Associate Editor: **Judith Mann**
Assistant Editor: **Elena Nacanthaer**
Creative Director: **Michael Renchiwich**
Art Director: **Melanie Gottlieb**
Production Manager: **Rita Nothaft**
Traffic Manager: **Karen Galindo**
Circulation Manager: **Anita Weissman**
Fulfillment Manager: **Elizabeth Kuzio**
Controller: **Neil B. Rose**

Technical Staff:

Briefs prepared for National Aeronautics and
Space Administration by **Logical Technical
Services Corp.:**

Technical Editor: **Jay Kirschenbaum**
Art Director: **Ernest Gillespie**
Managing Editor: **Ted Selinsky**
Administrator: **Elizabeth Texeira**
Chief Copy Editor: **Pamela Toubul**
Staff Editors: **James Boyd, Theron Cole, Jr.,
Larry Grunberger, Jordan Randjelovich,
George Watson**
Graphics: **Kenneth Blasko, Luis Martinez,
Huburn Proffitt**
Editorial & Production: **Walter J. Pawlowski,
Trudy Cavallo, Lorne Bullen, Frank Ponce,
Joe Renzler, Ivonne Valdes**

NASA:

NASA Tech Briefs are provided by the
National Aeronautics and Space Administration,
Technology Transfer Division, Washington, DC:
Administrator: **James M. Beggs**
Assistant Administrator for Commercial
Programs: **Isaac T. Gillam IV**
Deputy Administrator for Commercial
Programs: **L.J. Evans, Jr.**
Acting Director Technology Utilization
Division: **Henry J. Clarks**
Publications Manager: **Leonard A. Ault**

Associated Business Publications
41 East 42nd Street, Suite 921
New York, NY 10017-5391
(212) 490-3999

President: **Bill Schnirring**
Executive Vice President: **Frank Nothaft**
Vice President—Sales: **Wayne Pierce**
Vice President: **Patricia Neri**

Special Features and Departments

Editorial Notebook	6
Focus on Applications	12
Technology Transfer and R & D	14
by Len Ault, Deputy Director Technology Utilization Division	
Goddard – The Legacy of a Pioneer	18
Framework for Action (II)	182
Letters	186
Classified Advertising	187
Advertising Index	187
About This Publication	188
Mission Accomplished	189

ON THE FRONT COVER:

The theory of satellite servicing became practice during the April 1984 flight of the space shuttle Challenger. Astronauts James van Hoften (pictured) and George Nelson replaced a defective module and installed new components on the Solar Maximum Mission satellite. (Solar Max is shown berthed in the rear of the shuttle's cargo bay, with the blue and white earth in the background.) After servicing, the satellite was redeployed to continue its mission. The Solar Max satellite and its shuttle repair mission were both managed by Goddard Space Flight Center, Greenbelt, Maryland. For more on Goddard, see page 18 this issue.

Advertising:

New York Office: (212) 490-3999
Vice President—Sales: **Wayne Pierce**
Sales Manager: **Robin DuCharme**
Account Executive: **Dick Soule**
Chicago Office: (312) 848-8120
Account Executive: **Irene Froehlich**
Los Angeles Office: (213) 477-5866
Account Executive: **Robert Bruder**

Technical Section Thumb Index

NASA TU Services	28	
New Product Ideas	34	
Electronic Components and Circuits	40	
Electronic Systems	62	
Physical Sciences	80	
Materials	100	
Life Sciences	122	
Mechanics	126	
Machinery	152	
Fabrication Technology	162	
Mathematics and Information Sciences	166	
Subject Index	178	

This document was prepared under the sponsorship of the National Aeronautics and Space Administration. Neither Associated Business Publications, Inc., nor anyone acting on behalf of Associated Business Publications, Inc., nor the United States Government nor any person acting on behalf of the United States Government assumes any liability resulting from the use of the information contained in this document, or warrants that such use will be free from privately owned rights. The U. S. Government does not endorse any commercial product, process, or activity identified in this publication.

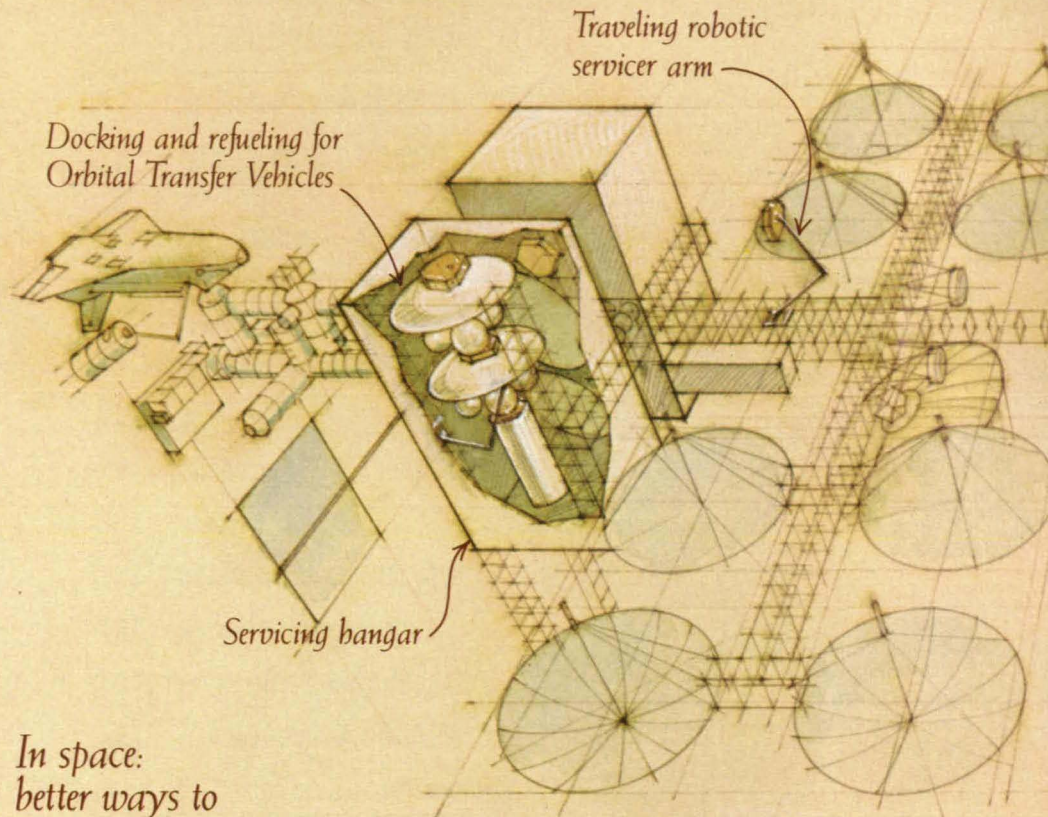
NASA Tech Briefs, ISSN 0145-319X, copyright © 1985 in U.S., is published quarterly by Associated Business Publications, Inc., 41 E. 42nd St., New York, NY 10017-5391. The copyrighted information does not include the individual Tech Briefs which are supplied by NASA. Editorial, sales, production and circulation offices at 41 E. 42nd Street, New York, NY 10017-5391. Subscriptions for non-qualified subscribers in the U.S., Panama Canal Zone, and Puerto Rico, \$50.00 for 1 year; \$100.00 for 2 years; \$150 for 3 years. Single copies \$15.00. Remit by check, draft, postal or express orders. Other remittances at sender's risk. Address all communications for subscriptions or circulation to NASA Tech Briefs, 41 E. 42nd Street, New York, NY 10017-5391. Application to mail at second-class postage rates is pending at New York, NY 10017 and additional mailing offices.

POSTMASTER: please send address changes to NASA Tech Briefs, 41 E. 42nd Street, Suite 921, New York, NY 10017-5391.

NASA Tech Briefs, Winter 1985

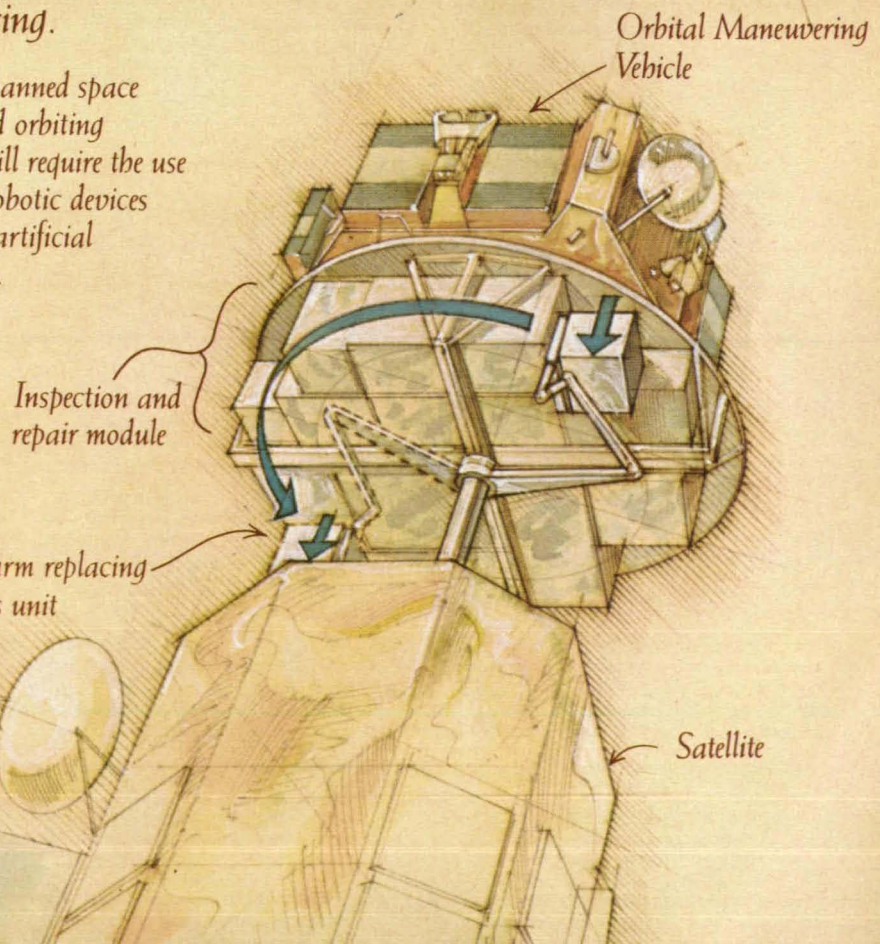
Artificial intelligence and robotics: giving machines the ability to sense, reason and act.

Much as it may hurt to think so, many things might be done better by independently functioning machines than by humans. Certain tasks may require superhuman precision or speed, or need to be done where humans can't go. Martin Marietta is creating systems that combine the ability to sense, reason and take action—to function autonomously and intelligently. And we are exploring ways to put them to work on a variety of tasks.

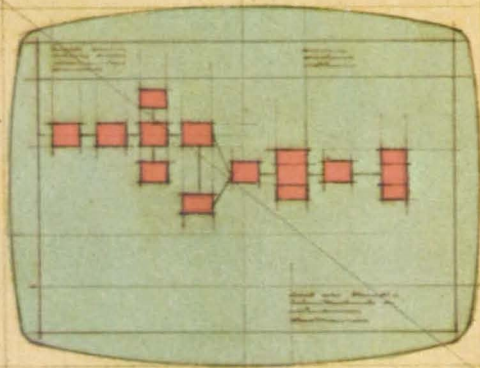


*In space:
better ways to
do servicing.*

NASA's manned space station and orbiting satellites will require the use of many robotic devices driven by artificial intelligence.



Analytical intelligence programming



On earth:
faster manufacturing
and inspections.

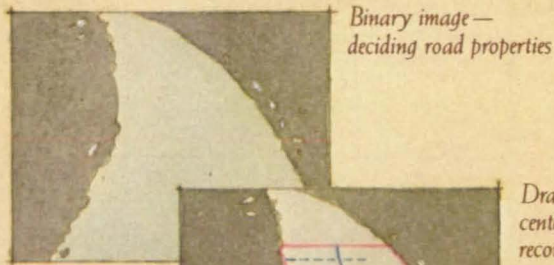
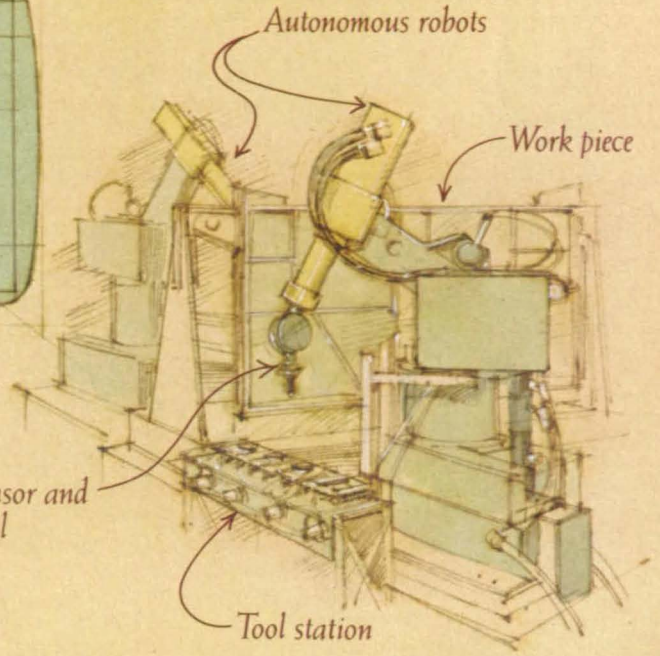
With creative intelligence stemming from software that we are developing, autonomous robots can quickly and efficiently perform batch manufacturing and precision inspections, even choose their own tools.

Autonomous robots

Work piece

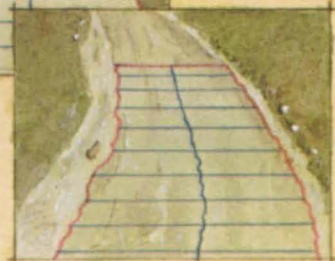
Sensor and tool

Tool station



On the road:
autonomous
navigation.

Artificial intelligence systems that use advanced sensory perception technologies are being developed and demonstrated in the Autonomous Land Vehicle. Already able to follow roads, this mobile test bed will eventually be able to plan its route, avoid obstacles and even thread its way across country.

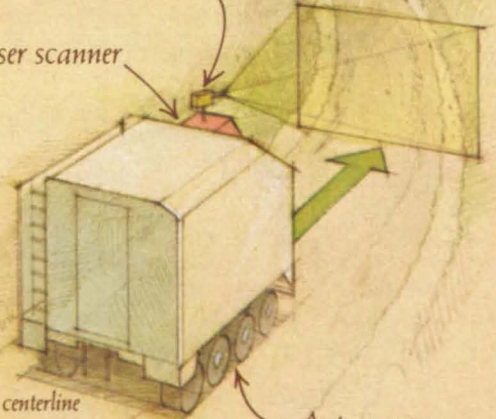


TV camera

Laser scanner

Boundaries,
direction and centerline
on TV image

Autonomous
Land Vehicle



MARTIN MARIETTA

Martin Marietta Corporation
6801 Rockledge Drive, Bethesda, Maryland 20817, USA

Circle Reader Action No. 408

Editorial Notebook

Feedback . . . Please

It's no secret that we're interested in reader response . . . that's why we include postage-paid feedback cards in every issue of *Tech Briefs*. Certainly a kind word always makes our day, and we're as delighted as anyone else by "orchid letters," but that's not our real purpose in furnishing these reply cards. We want to answer any questions you may have, handle your complaints (which we hope are few), and receive your suggestions (which we hope are many).

However, there's another use to which we'd like the feedback cards to be put. *NASA Tech Briefs* is published with the express intent of sharing with American industry the new technologies, processes, information—in short, original ideas—that have evolved through the space exploration process. From the mail we've received to date, it seems that we've been doing that successfully insofar as you, our readers, are concerned.

What we'd like to know more about is: After you get the information, what do you do with it? "Mission Accomplished," the



feature found in the back of every issue of *NASA Tech Briefs*, highlights a product or service or company that has come about as a direct result of technology transfer. Every year NASA publishes *Spinoff*, which is not only a summary of NASA's current mainline programs, but also is a compilation of products and processes that have been spunoff as a result of NASA's ongoing efforts. If you haven't seen *Spinoff*, ask for one on the feedback

card you'll find in the back of this issue. As long as supplies last, you'll get one.

With all the spinoffs that have been identified, we know that there are manifold more that have gone unheralded because we don't know about them. Please, use the feedback cards to share with us what you do, have done, or plan to do with the information you've received from *NTB*. Your answers will help us become more effective com-

Will your next proposal win...

Some of the world's most successful technology companies depend on us for their proposal needs. We supply top-caliber proposal consultants, engineers and writers in confidence. In a hurry. Anywhere in the free world. We cover every requirement put forth by government or utility RFP,

RFQ, IFB or Tender . . . in any advanced technology. Aerospace/Defense, Energy, Transportation. You name it, we've covered it. Successfully.

We increase your probability of winning—assisting or totally managing your proposal so that it's more responsive and better priced.

We develop strategy, organize and present in the latest proven formats a professional proposal.

We speak well for your corporate interests through objectivity and planning. Our risk assessments, trade-off analyses, "devil's advocate" reviews and proper man-loading estimates fine-tune the technical/cost interaction so important to the competitive edge. We know proposals. And our experience gets results.

Pride, performance and hands-on professional presentation. **A-E Systems Management, Inc.**—the winning edge.



Proposal Management/Consulting
1089 West Granada Blvd., Suite III
Ormond Beach, FL 32074

Take a closer look. Call or write for a professional, non-obligatory critique of your existing proposal style or evaluation of your next RFP.

T.F. Visconti, President
Telephone (904) 673-4725
Telex 568899 (AESMI ORBH)



It's no secret that MBC has pioneered many significant advancements in high performance hydraulic systems. What may surprise you, is that we possess equally formidable skills in the area of special metal forming techniques.

And it's no secret why. Whether its helping you optimize an existing configuration or designing an entire system utilizing pressure vessels and other MBC components, we can assist you. Our full range of engineering and manufacturing expertise also applies to specially wrapped pressure vessels, tanks and custom metal fabrications.

From CAD/CAM analytic capabilities to fracture and stress analysis, to our new 125,000 sq. ft. complex and capable staff, MBC has everything necessary to make

SUPERPLASTIC AND COLD FORMING FABRICATION FROM MBC.



© 1985 Metal Bellows Corp

superplastic and hydroformed products a more economical proposition.

In fact, compared to traditional forging and machining methods, a 5 to 1 savings in cost is readily achievable. Not to mention our proven versatility in low or high production runs.

So, before you incur the expense of tooling up in-house, look into the extensive resources at MBC. For your local sales engineer call 805/529-5800. But don't be surprised if we can't keep a secret.

MBC

Metal Bellows Corporation

P.O. Box 8010, 200 Science Drive
Moorpark, CA 93021-8010
805/529-5800 Telex: 65-1483
Datafax: 805/529-5850

THE BEST KEPT SECRET IN PRESSURE VESSELS IS NOW OUT OF THE BOTTLE.

MBC

Editorial Notebook

municators, and improve our communication with you.

■ ■ ■

There are a variety of NASA programs which solicit private-sector involvement in developing technology for commercial applications. As we continue to publish *NTB*, we will try to bring them to your attention.

Our series on NASA's field research centers continues in this issue with Goddard Space Flight Center, Greenbelt, Maryland. Goddard has a very active program in secondary technology applications. Its Office of Commercial Programs, under the direction of Don Friedman, coordinates technology transfer and utilization for a number of applications projects, a few of which are mentioned on page 12.

Goddard is also participating in the federal government's Small Business Innovation Research (SBIR) program. The SBIR program's operative assumption is that the small business/entrepreneurial company has the best chance of taking a fresh technical idea and rapidly bringing it to the marketplace. Dr. Noel Hinners, center director, sums up Goddard's involvement with the SBIR program this way: "One of the things we want to be sure we do at Goddard is to make the



Don Friedman, left, chief of Goddard's Office of Commercial Programs, Henry Clarks, acting director, NASA's Technology Utilization Division, and Bill Schnirring, NTB publisher, look on as Dr. Noel Hinners, director of Goddard Space Flight Center, examines a model of the tracking and data relay satellite.

developed technology known and available to private industry so that they can benefit from it. In terms of its ability to involve small business, the SBIR program is quite impressive. Based on announced 'Areas of Research Interest,' Goddard may sponsor about a dozen or so phase I proposals, with funding in the range of \$25,000 to \$50,000. Phase II funding may be available for up to around \$500,000 if a project is particularly promising. Goddard has been involved in SBIR for two years, and has about 25 pro-

jects in progress."

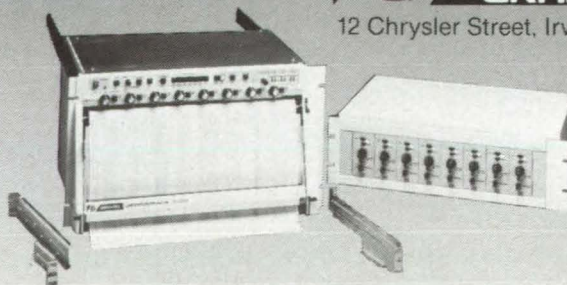
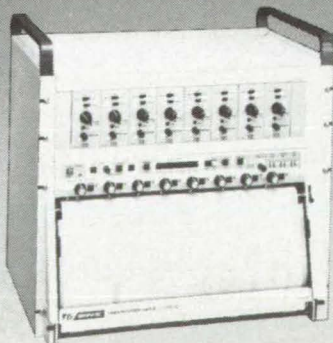
Overall, NASA's 1985 SBIR program includes 150 research projects, which were selected from a field of 1164 proposals. NASA's fiscal '85 budget includes approximately \$7.5 million for phase I of the SBIR projects. The program is administered by NASA's Office of Commercial Programs. You can get more information by writing directly to this office at NASA Headquarters, Code IC, Washington, D.C. 20546. . . or you can use the feedback card. □

***New!* Mark VIII Thermal Oscillograph offers Modular styling, computer control capability, one standard print head and capability for up to 8 additional print heads.**

Features:

- Only 10½" rack space required for WR 3502 model
- Extended viewing model, WR 3532, gives full 16" chart view
- Hot stylus pens guaranteed for 310 miles (500 km) of trace length
- Amplifier cage - optional
- 17 different amplifiers to choose from
- Frequency characteristics: DC-60 Hz at 50 divisions; DC-140 Hz at 10 divisions. Rise time - 4 milliseconds.
- Choice of roll or Z-fold, blue or black trace, chart paper
- One print head standard - 8 additional print heads optional
- Choice of RS232C or GPIB/IEEE interface for computer control

For more information on this new recorder, or for information on our complete line of oscillographs, strip chart or X-Y recorders, and digital plotters, call our Customer Service department today. In California call (714) 770-6010 - Outside California, (800) 854-8385, or write:



WESTERN GRAPHTEC
12 Chrysler Street, Irvine, CA 92718



Wyle at work.

Helping explore the new commercial frontier.

Our nation's growth was possible because of the individual's opportunity to excel. The first frontier was broken when our country's founders moved westward. Frontiers have fallen rapidly ever since.

Today we are seeing the development of one of the most exciting commercial frontiers yet. Space itself. Wyle is playing a vital part in that development. We've had an active role in all of our nation's space programs, including the Space Shuttle. We're already at work on the Space Station. We're identifying commercial opportunities in space, including materials processing in microgravity environments. And we're starting in on projects that as yet are still unnamed.

Wyle Laboratories has excelled in aerospace testing since 1949. We're the nation's leading independent testing laboratory. We have the testing facilities, experience, and scientific specialists to conduct any kind of developmental or test program. Our standards of performance are unsurpassed.

For more information on Wyle's testing programs, call collect: Drexel Smith in Norco, California, (714) 737-0871, Don McAvin in Huntsville, Alabama, (205) 837-4411, John Wood in Hampton, Virginia, (804) 865-0000, or Paul Turkheimer in El Segundo, California, (213) 322-1763.

WYLE SCIENTIFIC SERVICES
LABORATORIES & SYSTEMS
GROUP

Huntsville, AL Arlington, VA Norco, CA
Lanham, MD El Segundo, CA Hampton, VA

Circle Reader Action No. 396

Here's one supermini that's



gonna knock your socks off.

It's the IBM 4361.

And it's setting new standards for cost-performance. IBM? Supermini? For computational processing? You bet. It'll knock the socks off a centipede.

Speed. The 4361 features a high-speed cache buffer. It has a separate floating-point processor to handle multiplication. And it executes the 70 most-used instructions in the hardware. No wonder the 4361 will turn in a Whetstone that will knock your.... You get the idea.

Precision and accuracy. The 4361 has advanced 32/64-bit architecture. It can handle 31-decimal-digit precision. And as for accuracy, IBM's high-accuracy arithmetic facility (ACRITH) includes 22 special floating-point instructions that can be used to process iterative calculations accurately. The ACRITH program notifies you if the accuracy you need can't be maintained.

Ease of use. The 4361 needs no pampering. Install it almost anywhere—in a corner of your office, for example. And the 4361 can run unattended, with no onsite DP specialist.

To make life easier yet, there's the IBM Engineering/Scientific Support System (E/S³)—a consistent, menu-driven interface for interactive users. E/S³ is rich in function and offers an open architecture so you can add applications easily. It handles graphics, text and data manipulation. And it supports a wide range of administrative applications.

Attachability. What would you like to attach to your IBM 4361? Lab instruments? Personal computers? ASCII-oriented devices? Are they Multibus* or Unibus** -oriented? Or do they use a serial digital interface? The 4361 welcomes them all. It attaches to IBM and non-IBM devices of all kinds.

Growth path. The 4361 protects your investment. It can be upgraded on your premises over a processing power range of three to one. At low cost and in small steps. If you out-grow even the biggest 4361, you can move up to the IBM 4381 or one of the large 308X or 3090 processors.

There's much, much more. In technology, architecture, service and support. The 4361 is an engineering/scientific computer from head to toe. But hold our feet to the fire. Demand answers to all your questions.

To receive brochures on the 4361 and E/S³, or to have an IBM marketing representative call, return the coupon.



IBM DRM Dept. LQ/710 101 Paragon Drive Montvale, NJ 07645	11-85
<input type="checkbox"/> Please send me information on the IBM 4361 supermini and E/S ³ .	
<input type="checkbox"/> Please have an IBM marketing representative call.	
Name _____	
Title _____	
Company _____	
Address _____	
City _____ State _____ Zip _____	
Phone _____	

*Multibus is a trademark of Intel Corporation./**Unibus is a trademark of Digital Equipment Corporation.

Focus on Applications

Applying aeronautic and space technology to improve the quality of life on earth is a NASA priority. The Terrestrial Applications Program of NASA's Technology Utilization Division is directly concerned with this task, as are the technology utilization officers at each NASA center. Here, we focus on applications involving implantable biomedical systems, highlighting those managed by Goddard Space Flight Center, Greenbelt, Maryland.

PIMS...

The Programmable Implantable Medication System consists of an implantable pump, which administers required medication to patients internally, and an external programmable unit that controls the action of the pump. For diabetics, PIMS will deliver insulin as required, freeing patients from routine injections.

The microminiaturized hybrid circuitry for both the pump system and the programming unit is based on NASA technology. The system has passed all animal tests and, following FDA approval, will be available by the end of the current year. Additional applications for controlling pain and treating Parkinson's, Lou Gehrig's and

Alzheimer's diseases are under consideration. In addition to Goddard, the PIMS program drew on the resources of the Applied Physics Laboratory at Johns Hopkins University, Pacesetter Systems, Inc., and Parker-Hannifin.

AID...

The Automatic Implantable Defibrillator restores normal heart rate by delivering an electrical shock to people who experience irregular heart rhythms—a potentially fatal condition known as arrhythmia. Essentially, AID is a sensing system coupled with a shock delivery system. Intec Systems of Pittsburgh, Pa., manufactures the AID system, which has been implanted

in some 700 patients to date.

SAMS...

The Sensor Actuated Medication System is similar in concept to both PIMS and AID. It is designed to control hypertension by sensing the need for medication and administering it through an implantable pump device. SAMS is currently under development at the Applied Physics Laboratory at Johns Hopkins University in conjunction with Goddard Space Flight Center.

For the complete story on Goddard, see page 18.

**ELECTROMAGNETIC INTERFERENCE
ELECTRONIC CORES**



carbonyl iron powders

"The Right Stuff"

**POWDER METALLURGY
INJECTION MOLDING**

GAF is the sole domestic manufacturer of Carbonyl Iron Powders. For more detailed information, contact GAF Corporation, Chemical Division, 1361 Alps Road, Wayne, NJ 07470, (201) 628-3000.

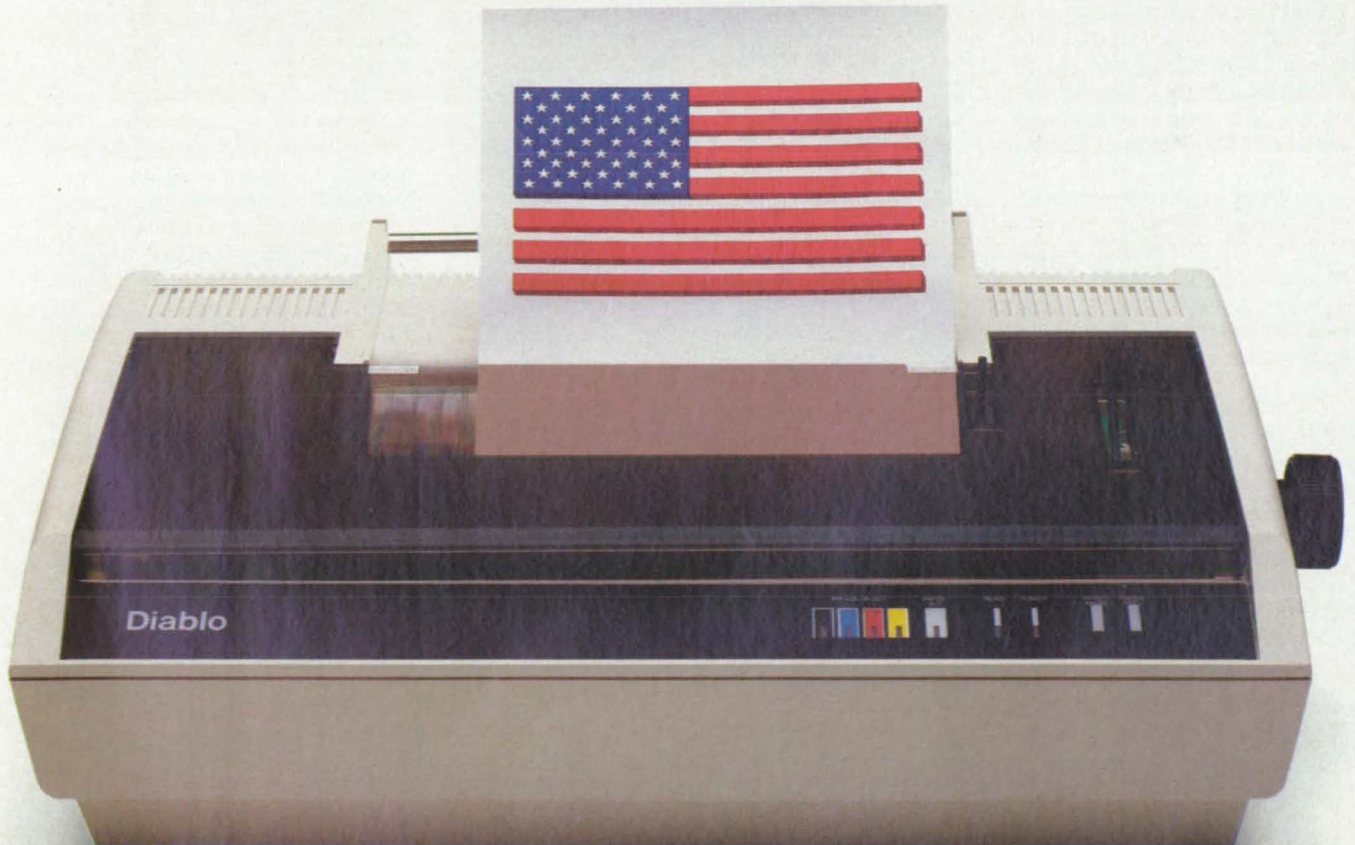
WE FEATURE 4,093 BRILLIANT COLORS BESIDES RED, WHITE, AND BLUE.

Fact is, the Xerox®/Diablo® C150 ink jet printer advantages are right before your very eyes. Like brilliant colors and shadings. The capacity to rotate text, create 3-D images, or zoom in or out for magnified, detailed graphics. There's even the versatility to work with more software than you'd ever imagined possible.

Of course this high performance business machine has the remarkable high resolution you've come to expect from Diablo. An operation that's as quiet as it is fast.

But don't just take our word on the Xerox/Diablo C150 ink jet printer. Because seeing is truly believing.

The Xerox/Diablo C150 ink jet printer is available through Zenith Data Systems under government contract. For more information call Zenith Data Systems at 1-800-582-0030 (in Virginia, call 703-821-0140) or Xerox at 415-498-7805.





Technology Transfer and R & D

By Leonard A. Ault,
Deputy Director,
Technology Utilization Division

During periods of economic uncertainty, corporations tend to focus on the here and now rather than on long-range activities such as research and development. R & D is a future-oriented activity where new technologies are created or emerging technologies are applied. Typically, these activities are the first to suffer from budget reductions during economic hard times. A well-developed technology transfer program can substantially augment a corporation's R & D effort, thus stretching its R & D investment dollar by a considerable margin.

Simply stated, technology transfer is the process of utilizing a technology for a purpose other than that for which it was developed. While technology transfer focuses on the application of previous research, there is no clear distinction between it and R & D—just as there is no clear separation between basic and applied research. Industrial technical development actually involves aspects of each.

What is the value of a technology transfer program? There are several benefits:

- It can reduce the cost of a company's R & D effort.
- It can help increase company productivity.
- It provides a broader set of technological alternatives, and increases the probability of selecting the best technology for a given task.
- It can effectively accelerate the application of a technology in new fields of use.
- It can provide a broader technological base for company diversification.

These benefits are usually sufficient reasons for companies to establish an internal technology transfer program. To be effective,

however, such a program needs to involve a good deal more than a few days' research in the company library to learn about a particular technology or process. A well-developed transfer program, while not inexpensive, can substantially increase the payback potential of the R & D effort in large and small companies alike.

How can my firm organize for technology transfer? One approach

“A well-developed technology transfer program can substantially increase the payback potential of the R & D effort.”

is the establishment of a company technology transfer team which would serve as a focal point for new technologies and new business opportunities. The team should be highly sensitive to the company's technological problems and needs, and acquainted with outside technical information resources. Systematically searching or using such resources in a highly focused manner should pay off. In making matches, the team should be concerned with these questions:

- What is the technology?
- Has the technology been demonstrated or reduced to practice?
- What are its unique characteristics?
- Can it be protected by a patent, or can my company be licensed to use the technology?
- What would be the cost of further development or commercialization?

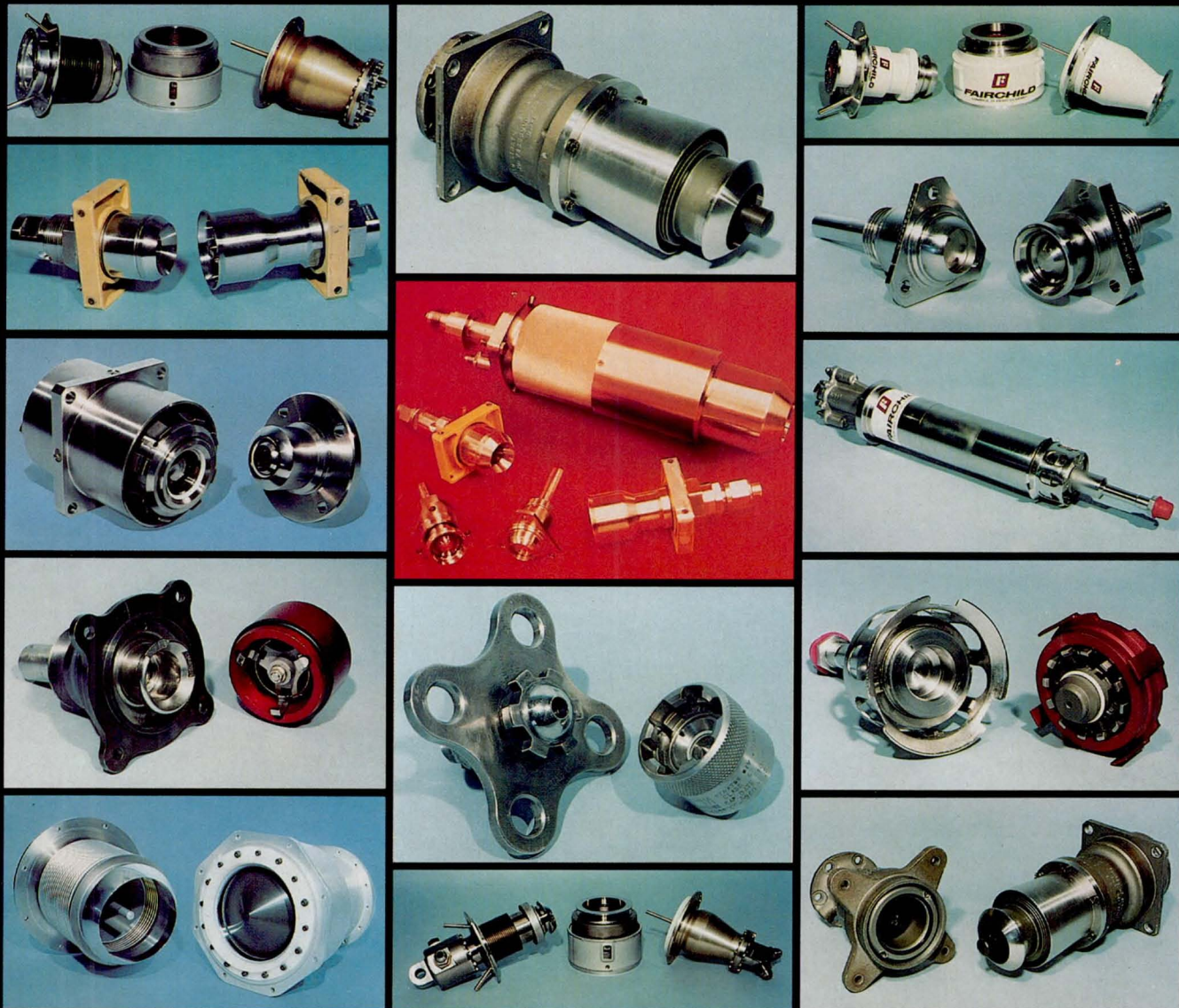
- What are the cost/performance and performance/benefit trade-offs?

In addition, the team should seek out members of the company who can be characterized as “technological gatekeepers.” Such individuals tend to keep up with developments in their chosen field and are usually very effective points of reference for others in the organization. They can be called upon to assist in evaluating the potential applicability of externally generated technologies to the company's needs.

Whatever approach is taken in technology transfer, large organizations will find it a valuable adjunct to their R & D efforts, while smaller companies can use it as an alternative to R & D since access is easy once channels of communication have been established and large laboratory facilities are not usually needed. The rewards from technology transfer can be great and should be considered by all companies, both large and small, that are seeking methods of making their R & D more productive. □

For more on enhancing productivity through effective management techniques, see “A Framework for Action,” page 182 this issue.

When the challenge is handling propellants in space...



Fairchild Control Systems Company has the answers.

Fairchild Control Systems Company has provided disconnects for every major space program requiring storable propellants, cryogenics, and gases. Our reliability and safety record is second to none.

If your system requires light weight, long life, low leakage, self-alignment, minimal pressure drop, manual or remote actuation, give the challenge to Fairchild Control Systems Company. Go with the leader in fluid transfer technology . . . with more QD's in

space than all other competitors combined.

Fairchild's fluid transfer couplings used aboard:

- VOYAGER (Hypergolic)
- SATURN/APOLLO (Cryogenic)
- LUNAR MODULE (Oxygen and EGW)
- TITAN (Hypergolic)
- SPACE SHUTTLE (Hypergolic, Cryogenic, Pneumatic)
- SHUTTLE/CENTAUR (Cryogenic)

Fairchild Control Systems Company . . . meeting the aerospace challenges of today and tomorrow.



FAIRCHILD
CONTROL SYSTEMS COMPANY

Fairchild Control Systems Company
1800 Rosecrans Avenue
Manhattan Beach, California 90266
Tel.: (213) 643-9222
Telex: 910-325-6216

THE HEREAFTER NAMED SUBSIDIARIES OF
UNITED STATES INTERNATIONAL TRADING CO., INC.

760 N. US HIGHWAY 1, SUITE 101, N. PALM BEACH, FL 33408
(305) 627-4510

Propose to register with the
Securities and Exchange Commission

A Public Offering of \$3,960,000
on Form S-1
of 6000 Jumbo Units @ \$660 per unit
Each Jumbo Unit consisting of 26
\$25 Subordinated Convertible
Debentures and 1000 Shares of
Common Stock @ \$.001 par value.

THE OFFERING WILL BE MADE ONLY BY MEANS OF PROSPECTUS

ANTICIPATED TIME OF OFFERING

NOVEMBER 15, 1985

Circle Reader Action No. 397

ZERO GRAVITY ENTERPRISES, INC.

The purpose of the Offering is to capitalize the Company to conduct the business of developing commercial products based on existing and future technology derived from space programs and to develop new technology under weightless environments.

Circle Reader Action No. 387

SPACE METALLURGY, INC.

The purpose of the Offering is to capitalize the Company to conduct the business of commercializing existing metallurgical technology and developing new metals technology related to international aerospace activities.

Circle Reader Action No. 376

**OUTER SPACE
LABORATORIES, INC.**

The purpose of the Offering is to capitalize the Company to conduct the business of developing products and services which can be used in governmental and private space environments and to contract for private, commercial experimentation related to space programs.

Circle Reader Action No. 386

**SPACE GENETICS
RESEARCH CORPORATION**

The purpose of the Offering is to capitalize the Company to conduct the business of experimentation and productivity in the fields of human, animal and plant life relating to bacteriological, geobiology, aging, gene splicing, disease control, chemo-remedial chemistry and waste control.

Circle Reader Action No. 388

**SPACE SHUTTLE
CARGO CORPORATION**

The purpose of the Offering is to capitalize the Company to conduct the business of providing international transportation systems and services related to aerospace research and development activities with governmental and private entities.

Circle Reader Action No. 366

**INTERSTELLAR COMMUNICATIONS
CORPORATION**

The purpose of the Offering is to capitalize the Company to conduct the business of commercializing existing technology from past governmental space programs and to develop new technologies of international earth and space communications.

\$300,000,000,000.00

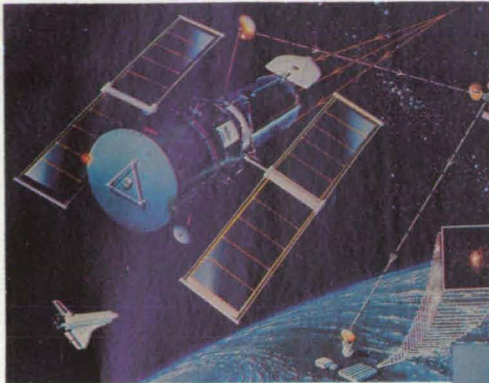
\$300 BILLION.

That's the projected Gross National Product of U.S. business in space in just fifteen years, according to the Congressional Space Caucus.

\$300 billion . . . and ten million new jobs for space construction, manufacturing, materials, medical products, metallurgy, and communications.

And that's where we come in. We're United States International Trading Co., Inc. and we're developing investment programs today, to fund research and development for the industries of tomorrow.

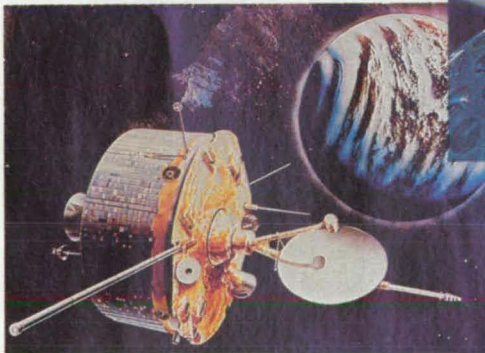
We're taking stock in America.
On its final frontier.



Zero Gravity Enterprises



Space Metallurgy, Inc.



Outer Space Laboratories, Inc.



Space Genetics Research Corporation



Space Shuttle Cargo Corporation



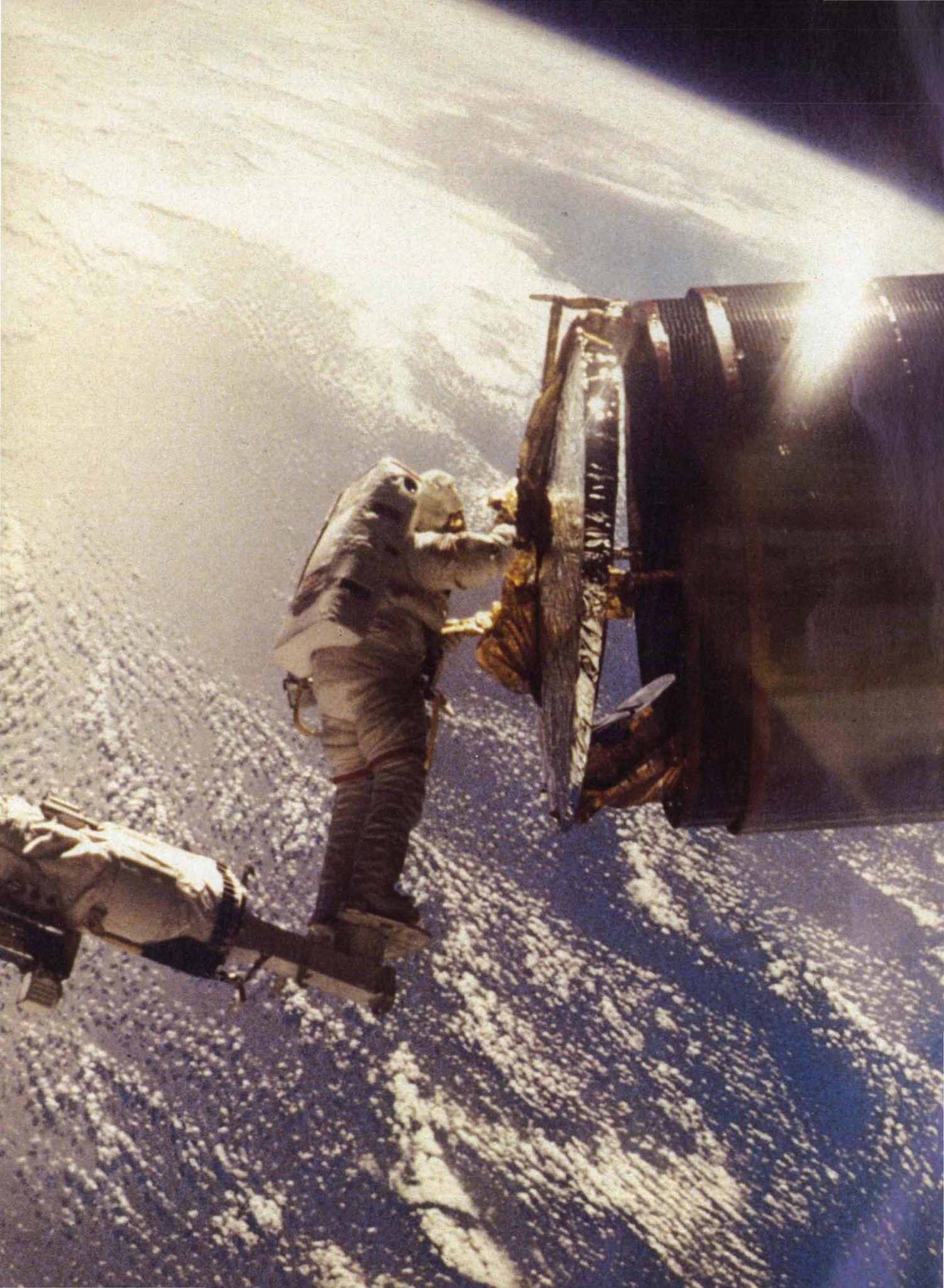
Interstellar Communications Corporation

We're the Business End of Space.

We're United States International Trading Co., Inc.

For more information, please call or write to James Miller, Chief Operations Officer, United States International Trading Co., Inc. 760 N. US Highway 1, Suite 101, N. Palm Beach, FL 33408 (305) 627-4510

Circle Reader Action No. 409



Goddard— the legacy of a pioneer

On March 17, 1926, Robert H. Goddard, professor of physics at Clark University in Worcester, Mass., wrote the following comment in his experimental notebook:

"The first flight with a rocket using liquid propellants was made yesterday at Aunt Effie's farm in Auburn." Although Goddard wrote in a style which approaches that of the press release, he had no desire to publicize his historic accomplishment. With what has come to be regarded as classic New England reticence, Goddard carried out his pioneering rocket experiments in a manner verging on secrecy. Exactly 35 years later, however, the "moon rocket man" and his legacy of original research were accorded a highly public, if posthumous, tribute.

Goddard Space Flight Center was officially dedicated on March 16, 1961, "in commemoration of Dr. Robert H. Goddard, American pioneer in rocket research." The center, located on 550 acres in Greenbelt, Maryland, was the first to be established under the aegis of NASA, which had been created by the National Aeronautics and Space Act of 1958.

The launch of the Soviet satellite SPUTNIK I a year earlier had ushered in a new era in human history—the space age. At the same time, it sparked what's commonly referred to as the "space race." For the U.S., this meant a stepped-up commitment to space exploration, which was manifested by the creation of NASA.

Prior to this, the development of launch vehicles and satellites for space exploration had been the province of the military services. Following WWII, American rocket research was given a boost by the example of the German V-2, and by one of its developers, Dr. Wernher von Braun, who joined researchers at the Army Ballistic Missile Agency (ABMA) in Huntsville, Ala. This group would later develop and launch the first U.S. satellite, EXPLORER I.

The Vanguard project, which called for the design, development and launch of a U.S. scientific satellite during the International Geophysical Year (July 1, 1957—December 31, 1958) was assigned to the Naval Research Laboratory. The Space Act, however, declared that "It is the policy of the United States that activities in space should be devoted to peaceful purposes for the benefit of all mankind," and created a civilian agency to pursue these aims.

They Make Space Calls: Astronauts Dale A. Gardner (left) and Joseph P. Allen IV work together to retrieve the Westar VI communications satellite. The satellite had been launched into an improper orbit, and was returned to earth by the shuttle Discovery for refurbishment and eventual reuse.

With the advent of NASA, all military rocket and space-related programs not primarily associated with defense were transferred to the civilian agency. These included two Air Force lunar probe programs, three satellite and two more lunar probe programs at ABMA, a variety of rocket engine projects, and the Naval Research Laboratory's Project Vanguard. Key personnel from this last program would later form the nucleus of Goddard Space Flight Center.

Other programs inherited by Goddard included the Army Signal Corps' meteorological program and the military's space communications program. In addition, Goddard was charged with conducting an active space science program, which included the launching of satellites. A global tracking, data acquisition and data reduction operation for all of NASA's space missions was established at Goddard as well.

The development of these original Goddard programs—scientific, meteorological and communications satellites, and tracking, data acquisition and reduction—set the pace for the rapid growth and expansion which occurred at Goddard throughout the 1960s.

Along with this expansion came a myriad of scientific and technological successes, many of them involving

satellites. Goddard engineers and technicians applied their expertise in all phases of satellite design and development, fabrication, integration, testing, and launch services. Once a satellite had been launched, Goddard personnel would track the satellite, monitor communications, and reduce the data it transmitted to Goddard's Space Operations Control Center. Satellites from the Explorer, Relay, Pioneer, Nimbus, Tiros, Telstar and Syncom families were among those managed by Goddard, and all of these contributed to laying a solid foundation upon which the network of scientific, meteorological and communication satellites most of us take for granted today could be built.

The wealth of data collected and transmitted by Goddard-managed satellites helped the American scientific community take great strides toward a fuller comprehension of the earth, its atmosphere, magnetic fields, radiation and other solar and cosmic phenomena. Yet, since scientific experiments have a way of posing as many questions as they answer, the data from early scientific missions—the orbiting solar, astronomical and geophysical observatories, for example—pointed up the need for further exploration. NASA's commitment to the scientific exploration of space is well in evidence today at

Goddard, where a number of scientific satellites are being developed for launch during the current decade.

Coming (and Going) Up

The Cosmic Background Explorer (COBE) satellite will test the veracity of the "big bang" theory of the origin of the universe. Scheduled for launch into a polar orbit in 1987, the 5-ton COBE will measure and map the diffuse microwave and infrared radiation that is thought to be leftover from the primeval explosion—the big bang—and other formative events in the early universe. Data from COBE will provide astronomers with maps of the entire sky at a variety of microwave and infrared wavelengths. The maps are expected to furnish answers to such questions as how old is the universe? when did the first stars appear? is the universe expanding uniformly?

Goddard is functioning as the prime contractor for the COBE spacecraft. As such, Goddard scientists, engineers and technicians are designing, fabricating, integrating and testing the COBE spacecraft and its three instruments. Goddard personnel will continue to manage COBE after its launch from Vandenberg Air Force Base in California. Goddard's all-around satellite capabilities are illustrated by the fact that, once in orbit, COBE's data will be transmitted to Goddard's data system facility through the Goddard-managed Tracking and Data Relay Satellite System (TDRSS). Finally, the processed data will be stored at the National Space Science Data Center at Goddard, where it will be available both as printouts and maps to cosmologists and to the public.

On the House

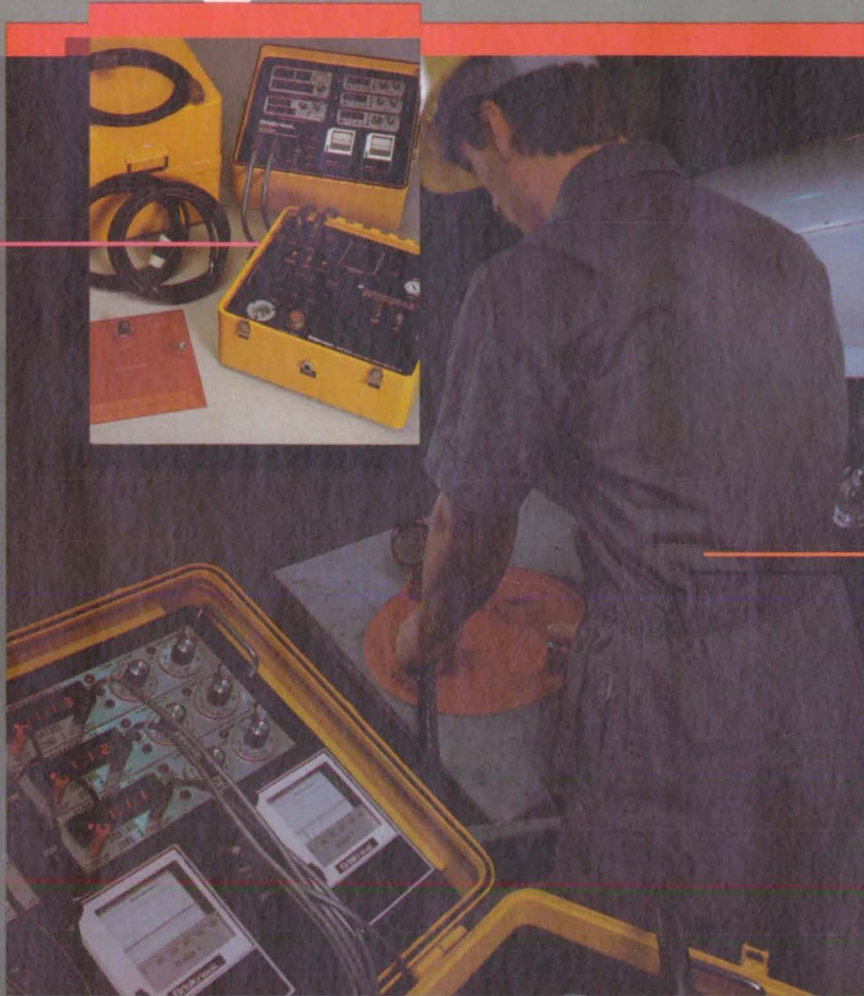
It is Goddard policy to have at least one in-house design and engineering project at all times. This way, the center assures that its technicians and engineers are conversant with the latest developments in technology. This policy also provides valuable learning experiences for recent college graduates and those earning higher degrees. They're able to gain familiarity with center opera-



Prelude to Orbit: Physicists at Goddard Space Flight Center conduct prelaunch evaluations of the laser geodynamic satellite. The satellite was designed and developed during the '70s to reflect laser pulses from their exact point of origin on earth. By timing the return of the laser, scientists can gather data about the motion of the earth's crust, which can be used to develop models. Such models are used in predicting earthquakes.

From assembly line to flight line...

BriskHeat integral vacuum curing blankets and portable ramp programmable control systems provide flight-line composite repair capability.



BriskHeat heating blankets provide evenly distributed heat across the surface for even curing of thermoset composites.

BriskHeat composite curing systems provide uniform, low watt density heat, custom designed to your application.

Tool and fixture heating elements provide evenly distributed heat up to 1600°F for composite curing. Heating elements can be designed for any tool surface regardless of complexity.

With BriskHeat composite curing systems, composite repairs can be made on the flight line without removing the part, increasing the operational readiness of equipment.

BriskHeat also provides standard heating blankets and controllers for traditional

repair systems and heated vacuum tables and fiberglass insulating blankets for depot repair of large parts.

BriskHeat is your single source for composite curing systems. For more information and our FREE booklet on composite repair, contact BriskHeat Corporation, A Yarway Company, P.O. Box 628, Columbus, Ohio 43216. For even faster action call toll-free 1-800-848-7673.

BriskHeat.
Specialty Products Group

A Yarway Company
P.O. Box 628, Columbus, Ohio 43216



In 1992, we set sail for a New World.

In 1492, a Genoese navigator and an intrepid crew crossed uncharted waters in search of a west passage to India. In the process, they uncovered the vast resources of two continents. And they opened up a new base for exploration, progress, and the hopes of mankind.

In 1992, coincident with the 500th anniversary of Columbus's voyage, we plan to



set sail for another New World. That year, or shortly thereafter, the United States and the world will begin benefiting from the first manned Space Station. The Station will be more than another giant step for mankind. It will be our stepping stone to living in new realms, and it will result in thousands of discoveries that will benefit earth.

This New World, free from gravity and atmospheric impurity, will provide that ideal environment for experimentation and production that is impossible on earth. Simultaneously we will have a permanent station for scanning the earth and the heavens — an unparalleled vantage point for predicting weather, aiding agriculture, and understanding the universe.

Of course, like Columbus, we cannot foresee all the benefits ahead. But we do know that we will have a new arena in which to conquer disease, transform the materials of earth, and generate precious energy. The resulting knowledge from countless discoveries will come down to earth for our well-being.

But, unlike Columbus, our craft will be in constant contact with the Old World. Harris Aerospace, as a member of the Rockwell, Grumman and Sperry team, is responsible for the Space Station's communications and tracking system. We are totally committed to this great endeavor, and we bring to the challenge the capabilities and experience necessary for success.

Harris has had 27 years of successful involvement with the kind of space communications and tracking required for the manned Space Station. Our space experience includes programs from Telstar to the Tracking and Data Relay Satellite as well as the manned programs of Apollo, Lunar Module, and Space Shuttle. We are also a leader in the architecture and design of large communication networks.

Now Harris is ready for the Space Station. Over the next years and centuries, the scope of scientific, commercial and technological opportunities and breadth of results are sure to exceed our wildest expectations.

For in 1992, we, too, will be very much like Columbus: carrying the sum of our knowledge into the unknown. And, like him, we, too, shall return with the bountiful gifts of a New World.



HARRIS

Circle Reader Action No. 410

For your information,



our name is Harris.

tions from a variety of perspectives, including design and development. Goddard management believes it's essential for people who will eventually become project managers to be knowledgeable in all aspects of satellite production in order to make the most efficient use of the center's resources and available technology. At the same time, this policy ensures that center personnel will keep up with steadily changing technology.

Goddard is one of the four NASA centers responsible for developing the first permanently orbiting Space Station in the early 1990s. Goddard's role focuses on the development of automated free-flying platforms, instruments and payloads which would be attached externally to the pressurized section of the Space Station, and the development of pressurized modules to be used for laboratory facilities.

The TDRSS will increase communications and data link coverage of orbiting satellites through the use of satellites. One satellite already is in operation, and two others are scheduled to be launched in 1986. The three-satellite system will provide communications coverage for approximately 85 percent of each satellite's orbit. Prior to the development of the satellite relay system, which collects communications and data from an orbiting satellite and relays them to Earth, a worldwide network of ground stations was used. With the ground stations, however, communications with a

satellite could be maintained over only about 15 percent of each orbit.

The Hubble Space Telescope, also due to be launched in 1986, is a ground-sized observatory that will be placed in orbit in order to view the universe unobscured by the Earth's atmosphere. Once in orbit, it will become the principal tool for exploring the universe through this decade and the next, and possibly beyond. It will be operated from the Goddard Space Flight Center in support of astronomers working at the Goddard-managed Space Telescope Science Institute at Johns Hopkins University in nearby Baltimore.

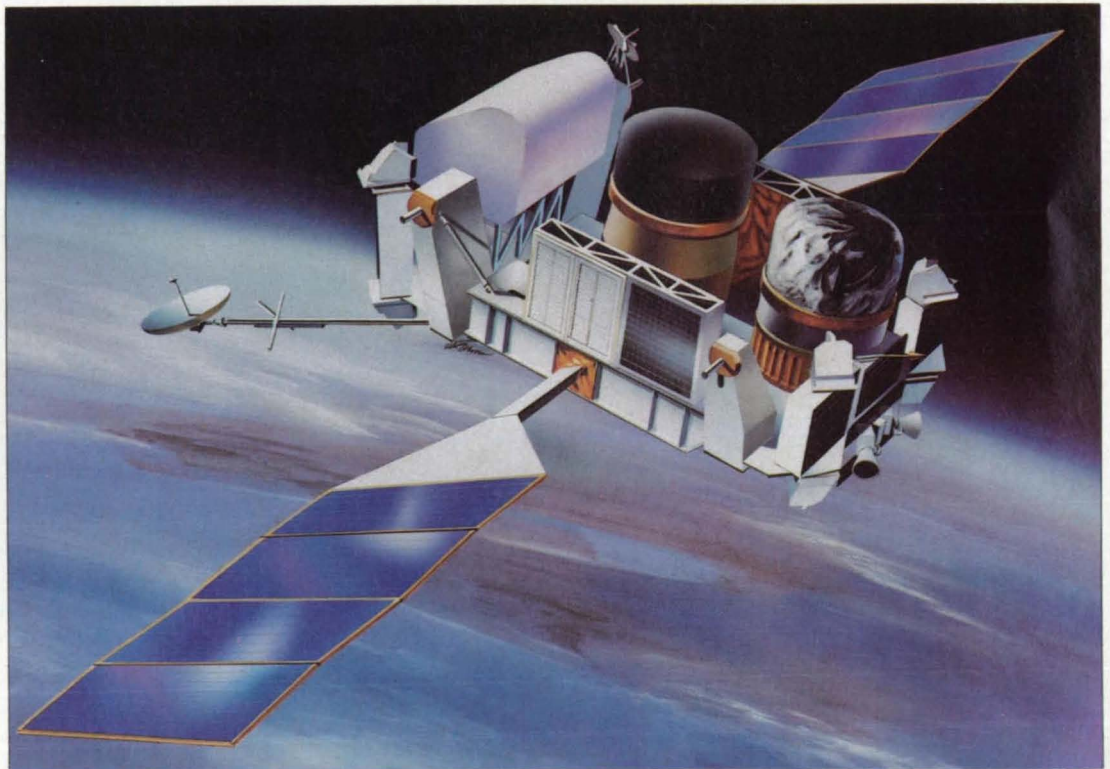
Goddard's Gamma Ray Observatory (GRO), a scientific satellite scheduled for launch aboard the shuttle in 1988, is drawing on in-house engineering and technical expertise for the design and fabrication of one of its four instruments. The Naval Research Laboratory, West Germany's Max Planck Institute and NASA's Marshall Space Flight Center are providing the other three instruments, and mission contractor TRW is responsible for spacecraft design, development and fabrication, and instrument integration.

GRO will weigh approximately 17 tons and measure 70 feet between the tips of its two solar arrays. It will be the largest scientific satellite ever launched by Goddard. Its design is based on the multimission modular spacecraft (MMS) system, which was developed at God-

dard by Frank Cepollina. The MMS system, which includes logistics support modules for communications, power, data, and attitude control, along with a flight support system located in the rear of the shuttle's cargo bay, was designed to facilitate the on-orbit repair and/or replacement of defective satellite modules. MMS development represents a move toward spacecraft design standardization, which results in cost-savings and life extension for satellite missions. Should one of a satellite's modules fail during its mission, the defective module can be replaced by crew servicing in the shuttle's cargo bay.

The efficacy of the MMS system was demonstrated in April 1984, when astronauts George Nelson and James van Hoften retrieved, repaired and re-deployed the Goddard-managed Solar Maximum Mission spacecraft. After completing nine months of its mission—observing and documenting the sun's energy build-up and release—the Solar Max spacecraft lost its ability for precision pointing at the sun, due to a failure in its attitude control system module. Following the successful repair mission, which involved replacing the faulty module, Solar Max is back in business.

Solar Max's faulty attitude control system module itself will be back in business as of October 1989, when the Upper Atmosphere Research Satellite (UARS) is launched from the space shuttle. After extensive study and analysis,



Big Bird: Goddard's Gamma Ray Observatory (GRO) will gather data on high-energy electromagnetic radiation. Gamma ray bursts, quasars, pulsars and the sun are slated for study, as is the Crab Nebula, the supernova remnant found in our galaxy.

Celerity: Speed in Accomplishing Work



The C1200 redefines the way compute-intensive tasks are accomplished in the engineering and scientific environment. By providing mainframe power under local control, the C1200 delivers the performance needed for applications that previously required offloading to a remote system: interactive solids modeling; design optimization without prototyping; simulation of mechanical behavior; analysis modeling; structural, thermal, magnetic, and fluid flow analysis; results evaluation; animation; two and three dimensional image rendering.

- Optimized native UNIX 4.2 BSD
- Up to 24 MBytes physical memory
- 4 Gigabytes virtual memory
- Industry-standard compilers, networking, and communications
- High resolution color graphics
- Up to 32 users

Processing speed, advanced 32-bit architecture, and high speed graphics interfaces enable the C1200 to be configured as a cost-effective multi-user or dedicated system. Complemented by such applications programs as PATRAN, ANSYS, MARC, MENTAT, DYNA, ADAMS, and UAI/NASTRAN, the C1200 defines a new standard of value and delivers the best price/performance available.

Redefine Your Accomplishments.
Call Celerity Computing Today.

CELERITY COMPUTING



Corporate Headquarters: 9692 Via Excelencia, San Diego, CA 92126 (619) 271-9940

PATRAN, ANSYS, MARC AND MENTAT, ADAMS, and UNIX are registered trademarks of PDA ENGINEERING, SWANSON ANALYSIS SYSTEMS, INC., MARC ANALYSIS RESEARCH CORPORATION, MECHANICAL DYNAMICS, INC., AND AT&T BELL LABORATORIES, respectively.

Circle Reader Action No. 352

Solar Max's attitude control system module was refurbished for use on UARS. This is yet another advantage of the MMS system: It introduces the concept of "off the shelf" satellite systems, consisting of parts which can be deployed, retrieved, repaired and reused with new, mission-unique instruments.

The UARS spacecraft design makes additional use of the MMS concept. A spare power module from the currently orbiting Landsat satellite series will be used on UARS. Following the completion of its mission—determining the effects of natural and man-made causes on the upper atmosphere—UARS will be retrieved. Its MMS components then may be reused on another satellite, representing considerable cost savings for NASA and the American taxpayers.

Space Science at a Bargain

The concept of reusing satellites even without retrieving them is the idea behind another unique Goddard mission, which resulted in the world's first spacecraft encounter with a comet last September. A group of engineers under

the direction of Goddard's Dr. Robert W. Farquhar devised a series of complex maneuvers whereby a satellite which had been in orbit for seven years would be re-routed to pass through the tail of the Comet Giacobini-Zinner, 44 million miles from Earth. Data from the historic encounter gave scientists new insights into the enigmatic nature of comets and indicated that comets are not at all the benign objects they were thought to be.

Another innovative Goddard program gives curious earthlings the opportunity to test their theories about the space environment aboard the space shuttle. The Get Away Special (GAS) program makes use of leftover space in the shuttle's cargo bay to allow for low-cost experimenting by individuals, small companies, educational institutions or research organizations which would otherwise be unable to afford the price of flying an experiment on the shuttle. For a \$10,000 fee, experimenters can fly their 200-lb. payloads in the Goddard-developed five cubic-foot cylindrical canisters, which are then mounted in the shuttle's cargo bay (smaller canisters are available for

smaller payloads and a lower fee). Originally, the payloads merely were exposed to the space environment in the shuttle's open cargo bay, but this year a new ejection device makes it possible for experimenters to have their payloads ejected into independent orbits.

The program is very successful and, apparently, very popular. It's received some 400 reservations, while more than 20 experiments have already flown. Another 20 are ready to go, space permitting.

The principles of economy, efficiency and simplicity underly Goddard's Spartan program as well. The Spartan is a space research subsatellite, which is deployed and retrieved on-orbit by the shuttle's remote manipulator system. Once in space, however, Spartan operates autonomously, via an onboard processor which activates stores pointing, maneuvering and stabilizing commands. The Spartan collects data in support of high-energy astrophysics, ultraviolet astronomy and solar physics research. Three Spartan carriers have already been built and two more are in the offing. The Spartan carriers, which are built in-house at Goddard, all incorporate the same basic design, which, like the MMS system, allows for the interchangeability of standard modules, while accommodating mission-unique systems as necessary.

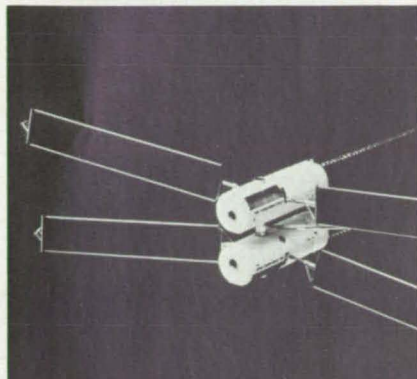
• • •

Goddard is probably the most diversified of the NASA research centers. This is not surprising, considering the sweeping breadth of the center's fundamental mission—to make possible the expansion of human knowledge of the earth, its environment, the solar system and the universe through the development and use of near-earth orbit spacecraft. Volumes can, and indeed have, been written on the variety of scientific and technical approaches Goddard employs in pursuing its mission. Yet, if the man for whom the center is named left a legacy of some 214 patents, then it is to be expected that the work of those who pursue his vision would be prodigious. Lt. Homer Boushey of the Army Air Corps knew Robert Goddard. In making the following comment, he probably had little idea how true his words would ring in describing the man and his public monument: "He reminded me of the man who plants the seed of a tree, so that others might one day sit in its shade." At Goddard Space Flight Center, that tree is still growing. □



GAS Cans: Get Away Special (GAS) canisters are seen mounted at upper right and lower left of the space shuttle's cargo bay.

NASA News in Brief



A model of the Industrial Space Facility, a privately financed commercial space platform. It will be launched from the shuttle in 1989.

New Business . . .

Space Industries, Inc. (SII) of Houston, Texas, has signed an agreement with NASA whereby the company will launch its privately-owned, commercial platform, the Industrial Space Facility (ISF), from the space shuttle in 1989. The ISF will be modular in concept and will measure 35 feet by 14.5 feet initially. While it will not be permanently manned, it is designed to be habitable and will provide a "shirt sleeve" work environment for astronauts when docked with the shuttle or space station.

Philip E. Culbertson, associate administrator for NASA's Space Station Office, says, "NASA considers the ISF to be a complementary capability to the space station. There are characteristics of the ISF and space station that are similar. For these reasons, there may be some aspects of the two programs that are of mutual interest and use to both NASA and SII."

To this end, NASA's Space Station Office and SII signed a separate agreement to provide for the beneficial exchange of information during the definition and preliminary design phase of the space station. The agreement also lays the groundwork for subsequent discussions and negotiations during the space station development period, scheduled to begin in mid-1987. SII is the first private company to sign such an agreement, and it

is hoped that the information exchange will result in a commercial facility capable of compatible operations with the space station.

NASA Administrator James M. Beggs says, "We hope the ISF will be the first of many such platforms to be funded and built by private industry that will complement the permanently-manned space station and lead eventually to an industrial park in space."

According to Max Faget, president of Space Industries, Inc., the ISF "will respond to a variety of private research and manufacturing needs. Industry could take advantage of the unique gravity-free environment of space to conduct experiments that cannot be effectively duplicated here on earth, particularly in the areas of pharmaceuticals and biological products, pure and exotic crystals, and new metals and alloys."

. . .

Another agreement between NASA and a private company provides for the supply of NASA technical expertise in the development of a commercial liquid-fuel upper stage for boosting shuttle-deployed satellites to geosynchronous orbit. Scott Science and Technology of Lancaster, California, is developing a privately-financed satellite transfer vehicle, which will have the capacity to boost satellites ranging from 2000 to 19,000 pounds.

Engineers at Johnson Space Center in Houston will monitor the stage's development and will consult with Scott Science and Technology staff regarding technical problems. Former astronaut David R. Scott is president of the company, which has agreed to reimburse NASA for the use of any test facilities, and for salaries and travel expenses of Johnson Space Center personnel.

Getting Organized . . .

To stimulate high technology research and development that takes advantage of the characteristics of space, NASA has named five teams to establish Centers for the Commercial Development of Space. The five centers are joint undertakings of

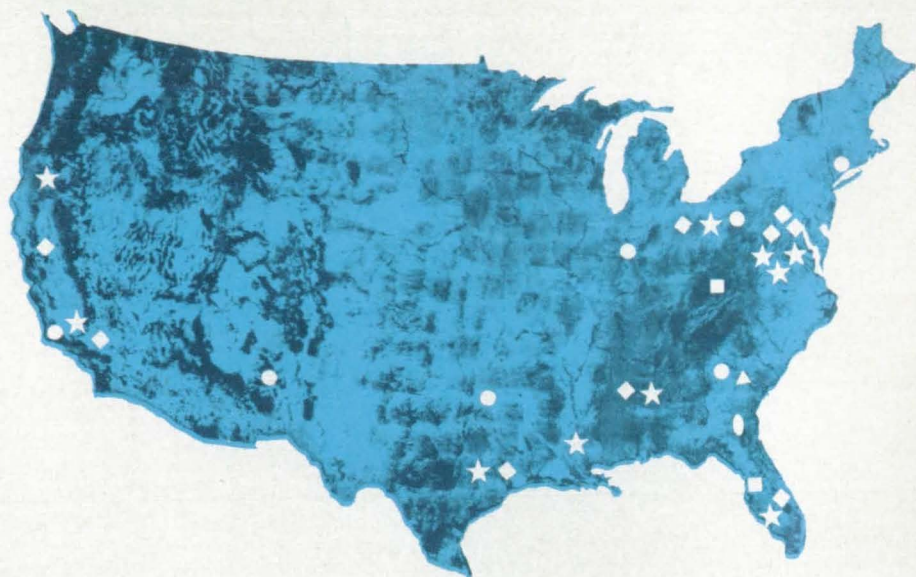
government, industry and academic teams, and all share the goal of developing new products which either have commercial potential or contribute to potential new commercial ventures. Battelle Columbus Laboratories of Columbus, Ohio, will focus its development efforts on multiphase materials processing. The University of Alabama at Birmingham will be involved in macromolecular crystallography in space. The remaining three centers—Vanderbilt University, the Institute for Technology Development, Hancock, Mississippi, and the University of Alabama at Huntsville—will focus on metallurgical processing in space, remote sensing, and materials processing, respectively. All five centers will coordinate their efforts with NASA field centers. NASA will fund the centers for a period not to exceed five years. During this period, the centers are expected to stimulate commercial ventures which will allow them to become financially self-sustaining.

Space Education . . .

NASA is making plans to broadcast live lessons from space during teacher-in-space Christa McAuliffe's shuttle flight, which is set for launch in late January. During the first lesson, "The Ultimate Field Trip," McAuliffe will take viewers on a tour of the shuttle. "Where We've Been, Where We're Going" will review technological advances resulting from the space program, and outline expectations for the future of space exploration. Other on-board activities, such as demonstrations of Newton's laws in a microgravity environment, will be filmed as well, and these will be used in developing a series of educational products.

In addition, three Student Involvement Project experiments will fly aboard the shuttle, and McAuliffe will assist mission specialists in conducting them. One experiment will use a semi-permeable membrane to direct crystal growth. Another will study chicken embryo development in the space environment, and the third will monitor the effects of weightlessness on grain formation and strength in metals.

NASA Technology Utilization Services



TECHNOLOGY UTILIZATION OFFICERS

Technology transfer experts can help you apply the innovations in NASA Tech Briefs.

The Technology Utilization Officer

at each NASA Field Center is an applications engineer who can help you make use of new technology developed at his center. He brings you NASA Tech Briefs and other special publications, sponsors conferences, and arranges for expert assistance in solving technical problems.

Technical assistance,

in the form of further information about NASA innovations and technology, is one of the services available from the TUO. Together with NASA scientists and engineers, he can often help you find and implement NASA technology to meet your specific needs.

Technical Support Packages (TSP's)

are prepared by the center TUO's. They provide further technical details for articles in NASA Tech Briefs. This additional material can help you evaluate and use NASA technology. You may receive most TSP's free of charge by using the TSP Request Card found at the back of this issue.

Technical questions about articles

in NASA Tech Briefs are answered in the TSP's. When no TSP is available, or you have further questions, contact the Technology Utilization Officer at the center that sponsored the research [see facing page for details].



COSMIC®

An economical source of computer programs developed by NASA and other government agencies.

A vast software library

is maintained by COSMIC—the Computer Software Management and Information Center. COSMIC gives you access to approximately 1,600 computer programs developed for NASA and the Department of Defense and selected programs for other government agencies. Programs and documentation are available at reasonable cost.

Available programs

range from management (PERT scheduling) to information science (retrieval systems) and computer operations (hardware and software). Hundreds of engineering programs perform such tasks as structural analysis, electronic circuit design, chemical analysis, and the design of fluid systems. Others determine building energy requirements and optimize mineral exploration.

COSMIC services

go beyond the collection and storage of software packages. Programs are checked for completeness; special announcements and an indexed software catalog are prepared; and programs are reproduced for distribution. Customers are helped to identify their software needs; and COSMIC follows up to determine the successes and problems and to provide updates and error corrections. In some cases, NASA engineers can offer guidance to users in installing or running a program.

Information about programs

described in NASA Tech Briefs articles can be obtained by circling the appropriate number on the TSP request card at the back of this issue.



★ TECHNOLOGY UTILIZATION OFFICERS

Stanley A. Miller
Ames Research Center
Mail Code 234-2
Moffett Field, CA 94035
(415) 694-6472

Donald S. Friedman
Goddard Space Flight Center
Mail Code 702.1
Greenbelt, MD 20771
(301) 344-6242

William Chmylak
Lyndon B. Johnson Space Center
Mail Code AL32
Houston, TX 77058
(713) 483-3809

U. Reed Barnett
John F. Kennedy Space Center
Mail Stop: PT-TPO-A
Kennedy Space Center, FL 32899
(305) 867-3017

John Samos
Langley Research Center
Mail Stop 139A
Hampton, VA 23665
(804) 865-3281

Daniel G. Soltis
Lewis Research Center
Mail Stop 7-3
21000 Brookpark Road
Cleveland, OH 44135
(216) 433-4000, Ext. 422

Ismail Akbay
George C. Marshall Space Flight Center
Code AT01
Marshall Space Flight Center,
AL 35812
(205) 453-2223

Leonard A. Ault
NASA Headquarters
Code IU
Washington, DC 20546
(202) 453-1920

Norman L. Chalfin
Jet Propulsion Laboratory
Mail Stop 201-110
4800 Oak Grove Drive
Pasadena, CA 91109
(818) 354-2240

Robert M. Barlow
National Space Technology Laboratories
Code GA-10
NSTL Station, MS 39529
(601) 688-1929

Gordon S. Chapman
NASA Resident Office-JPL
Mail Stop 180-801
4800 Oak Grove Drive
Pasadena, CA 91109
(818) 354-4849

● INDUSTRIAL APPLICATIONS CENTER

Aerospace Research Applications Center (ARAC)
Indianapolis Center for Advanced Research
611 N. Capitol Avenue
Indianapolis, IN 46204
John M. Ulrich, Director
(317) 262-5003

Kerr Industrial Applications Center (KIAC)
Southeastern Oklahoma State University
Station A, Box 2584
Durant, OK 74701
Tom J. McRorey, Director
(405) 924-6822

NASA Industrial Applications Center
823 William Pitt Union
University of Pittsburgh
Pittsburgh, PA 15260
Paul A. McWilliams, Executive Director
(412) 624-5211

NERAC, Inc.
Mansfield Professional Park
Storrs, CT 06268
Daniel U. Wilde, President
(203) 429-3000

North Carolina Science and Technology Research Center (NC/STRC)
Post Office Box 12235
Research Triangle Park, NC 27709
James E. Vann, Director
(919) 549-0671

Technology Application Center (TAC)
University of New Mexico
Albuquerque, NM 87131
Stanley A. Morain, Director
(505) 277-3622

NASA Industrial Applications Center (WESRAC)
University of Southern California
Research Annex
3716 South Hope Street
Room 200
Los Angeles, CA 90007
Robert Mixer, Director
(213) 743-6132

◆ PATENT COUNSELS

Robert F. Kempf, Asst. Gen.
Counsel for Patent Matters
NASA Headquarters
Code GP
Washington, DC 20546
(202) 453-2424

Darrell G. Brekke
Ames Research Center
Mail Code: 200-11A
Moffett Field, CA 94035
(415) 694-5104

John O. Tresansky
Goddard Space Flight Center
Mail Code: 204
Greenbelt, MD 20771
(301) 344-7351

Marvin F. Matthews
Lyndon B. Johnson Space Center
Mail Code: AL3
Houston, TX 77058
(713) 483-4871

James O. Harrell
John F. Kennedy Space Center
Mail Code: PT-PAT
Kennedy Space Center, FL 32899
(305) 867-2544

Howard J. Osborn
Langley Research Center
Mail Code: 279
Hampton, VA 23665
(804) 865-3725

Norman T. Musial
Lewis Research Center
Mail Code: 60-2
21000 Brookpark Road
Cleveland, OH 44135
(216) 433-4000, Ext. 346

Leon D. Wofford, Jr.
George C. Marshall Space Flight Center
Mail Code: CC01
Marshall Space Flight Center, AL
35812
(205) 453-0020

Paul F. McCaul
NASA Resident Office-JPL
Mail Code: 180-801
4800 Oak Grove Drive
Pasadena, CA 91109
(818) 354-2700

□ APPLICATION TEAM

Technology Application Team
Research Triangle Institute
Post Office Box 12194
Research Triangle Park, NC 27709
Doris Rouse, Director
(919) 541-6980

■ STATE TECHNOLOGY APPLICATIONS CENTERS

NASA/Southern Technology Applications Center
State University System of Florida
307 Weil Hall
Gainesville, FL 32611
J. Ronald Thornton, Director
(904) 392-6760

NASA/UK Technology Applications Program
University of Kentucky
109 Kinkead Hall
Lexington, KY 40506-0057
William R. Strong, Program Director
(606) 257-6322

● COMPUTER SOFTWARE MANAGEMENT & INFORMATION CENTER

COSMIC®
Computer Services Annex
University of Georgia
Athens, GA 30602
John A. Gibson, Director
(404) 542-3265

● CENTRALIZED TECHNICAL SERVICES GROUP

NASA Scientific and Technical Information Facility
Technology Utilization Office
P.O. Box 8757
BWI Airport, MD 21240
Walter M. Helland, Manager
(301) 859-5300, Ext. 242, 243

STATE TECHNOLOGY APPLICATIONS CENTERS

Technical information services for industry and state and local government agencies

Government and private industry

in Florida and Kentucky can utilize the services of NASA's State Technology Applications Centers (STAC's). The STAC's differ from the Industrial Applications Centers described on page 21, primarily in that they are integrated into existing state technical assistance programs and serve

only the host state, whereas the IAC's serve multistate regions.

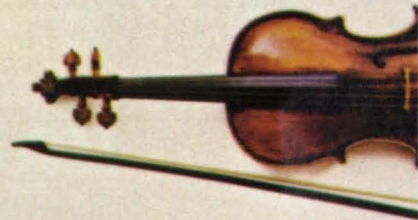
Many data bases,

including the NASA base and several commercial bases, are available for automatic data retrieval through the STAC's. Other services such as document retrieval and

special searches are also provided. (Like the IAC's, the STAC's normally charge a fee for their services.)

To obtain information

about the services offered, write or call the STAC in your state [see above].





**For years baroque music was
composed without major change,
until J.S. Bach put these
instruments together in a way
that set him apart.**

All the baroque composers were faced with the same restrictions, the same notes, the same instruments, and the same musical forms. Yet today, we remember J.S. Bach above them all. Simply because he was able to arrange scores of music in a way no one had ever seen . . . or heard before.

At IBM Federal Systems Division we know that it takes the same degree of ingenuity to design and manage within the dimensions of today's complex systems programs. It's a special ability to combine a broad range of technology — and make it work together in harmony.

And we're doing exactly that for the National Aeronautics and Space Administration's Space Shuttle program.

We've orchestrated the operations of the most sophisticated flying vehicle ever built with a team of on-board computers. And we compose software that can be tuned for each mission to make space a more available resource.

In every project we undertake, we start with a myriad of individual parts, as separate as the notes of a scale. And put them into play — together. It isn't easy.

But the more complex the task, the more we manage to make it happen.



Federal Systems Division

NASA INVENTIONS AVAILABLE FOR LICENSING

Over 3,500 NASA inventions are available for licensing in the United States—both exclusive and nonexclusive.

Nonexclusive licenses

for commercial use of NASA inventions are encouraged to promote competition and to achieve the widest use of inventions. They must be used by a negotiated target date.

Exclusive licenses

may be granted to encourage early commercial development of NASA inventions, especially when considerable private investment is required. These are generally for 5 to 10 years and usually require royalties based on sales or use.

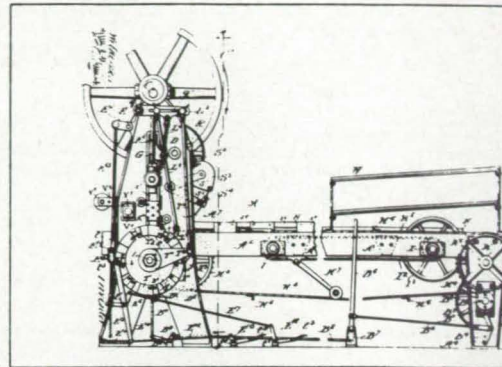
Additional licenses available

include those of NASA-owned foreign patents. In addition to inventions described in NASA Tech Briefs, "NASA Patent

Abstract Bibliography" (PAB), containing abstracts of all NASA inventions, can be purchased from National Technical Information Service, Springfield, VA 22161. The PAB is updated semiannually.

Patent licenses for Tech Briefs

are frequently available. Many of the inventions reported in NASA Tech Briefs are patented or are under consideration for a patent at the time they are published. The current patent status is described at the end of the article; otherwise, there is no statement about patents. If you want to know more about the patent program or are interested in licensing a particular invention,



contact the Patent Counsel at the NASA Field Center that sponsored the research [see page 29]. Be sure to refer to the NASA reference number at the end of the Tech Brief.

INDUSTRIAL APPLICATIONS CENTERS

Computerized access to over 10 million documents worldwide

Computerized information retrieval

from one of the world's largest banks of technical data is available from NASA's network of Industrial Applications Centers (IAC's). The IAC's give you access to 1,800,000 technical reports in the NASA data base and to more than 10 times that many reports and articles found in nearly 200 other computerized data bases.

The major sources include:

- 750,000 NASA Technical Reports
- Selected Water Resources Abstracts
- NASA Scientific and Technical Aerospace Reports
- Air Pollution Technical Information Center
- NASA International Aerospace Abstracts

- Chem Abstracts Condensates
- Engineering Index
- Energy Research Abstracts
- NASA Tech Briefs
- Government Reports
- Announcements

and many other specialized files on food technology, textile technology, metallurgy, medicine, business, economics, social sciences, and physical science.

The IAC services

range from tailored literature searches through expert technical assistance:

- **Retrospective Searches:** Published or unpublished literature is screened and documents are identified according to your interest profile. AIC engineers tailor results to your specific needs and furnish

abstracts considered the most pertinent. Complete reports are available upon request.

- **Current-Awareness Searches:** IAC engineers will help design a program to suit your needs. You will receive selected monthly or quarterly abstracts on new developments in your area of interest.
- **Technical Assistance:** IAC engineers will help you evaluate the results of your literature searches. They can help find answers to your technical problems and put you in touch with scientists and engineers at appropriate NASA Field Centers.

Prospective clients can obtain more information about these services by contacting the nearest IAC [see page 29]. User fees are charged for IAC information services.

APPLICATION TEAMS

Technology-matching and problem-solving assistance to public sector organizations

Application engineering projects

are conducted by NASA to help solve public-sector problems in such areas as safety, health, transportation, and environmental protection. Some application teams specialize in biomedical disciplines;

others, in engineering and scientific problems. Staffed by professionals from various disciplines, these teams work with other Federal agencies and health organizations to identify critical problems amenable to solution by the application of existing

NASA technology.

Public-sector organization representatives can learn more about application teams by contacting a nearby NASA Field Center Technology Utilization Office [see page 29].

TECHNOLOGY UTILIZATION OFFICE, NASA SCIENTIFIC & TECHNICAL INFORMATION FACILITY

Centralized technical office to provide service to the U.S. professional community and general public

Missing a copy of NASA Tech Briefs?

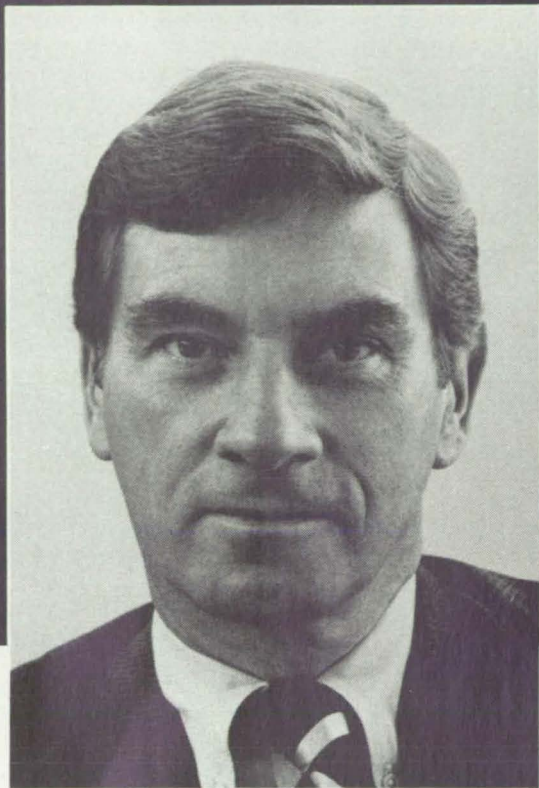
Not received Technical Support Package requested? Want to check on Tech Briefs status? Have urgent request for subscription address change? Wish to receive other

Tech Brief in area of interest? Simply confused as to whom to contact within the NASA Technology Utilization Network? Have general or specific question about the Technology Utilization Program, its

services and documents?

We are here to help you. Write or call. We have the right answer, the correct document, or the proper referral [see page 29].

"FREE ENTERPRISE ISN'T FREE.



"IT NEEDS YOUR SUPPORT!"

Andrew C. Sigler,
Chairman and CEO,
Champion International Corp.

I'm a volunteer supporter of the International Executive Service Corps, a not-for-profit organization with a vital mission:

We build free enterprise worldwide by sending retired U.S. executives to help companies in developing countries. The executives receive expenses, but no salary.

Our main purpose is to help developing countries succeed in business. But the benefit doesn't stop there. These countries consume about

40 percent of U.S. exports.

With the support of over 800 U.S. companies, we have completed 9,000 projects in 77 countries. Our Board of Directors and Advisory Council include the CEOs of many of America's largest companies.

Join me in building free enterprise throughout the free world. Write to: Andrew C. Sigler, Chairman and CEO, Champion International Corp. at P.O. Box 10005, Stamford, CT 06904-2005.



International Executive Service Corps

It's not just doing good. It's doing good business.



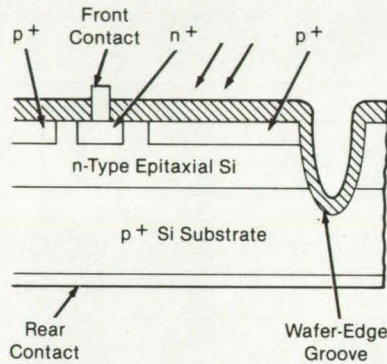
New Product Ideas



New Product Ideas are just a few of the many innovations described in this issue of *NASA Tech Briefs* and having promising commercial applications. Each is discussed further on the referenced page in the appropriate section in this issue. If you are interested in developing a product from these or other NASA innovations, you can receive further technical information by requesting the TSP referenced at the end of the full-length article or by writing to the NASA Scientific and Technical Information Facility, Technology Utilization Office, P.O. Box 8757, BWI Airport, MD 21240 (see page 29). NASA's patent-licensing program to encourage commercial development is described on page 32.

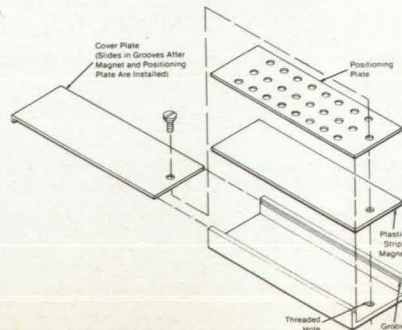
Floating-Emitter Solar-Cell Transistor

A proposed solar cell would be easy to fabricate and relatively breakage resistant, while promising efficiencies greater than 20 percent against a 15-percent efficiency for the best conventional solar cells. Gaining its increased efficiency through the incorporation of a junction transistor, the solar-cell transistor would be relatively immune to variations in the common-emitter current gain between devices. Even for a 2-to-1 spread in this gain, the open-circuit voltage will vary only about 20 mV. (See page 56.)



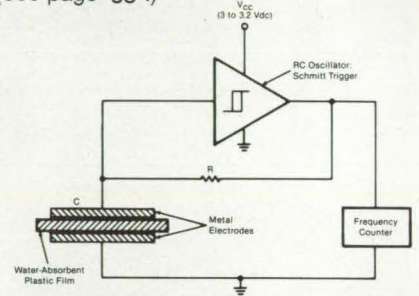
Conductive Container for Semiconductor Devices

A container for semiconductor components not only protects them from mechanical damage but also ensures that they are not harmed by electrostatic discharges. In addition, the container holds components in fixed positions so that they can be serialized and identified from their locations. The container is suitable for holding components during both storing and shipping. Because the container contains a plastic strip magnet, magnetic components will be held in place, even when the container is open. Originally developed for microwave diodes, the container concept is readily adaptable to transistors and integrated circuits. (See page 54.)



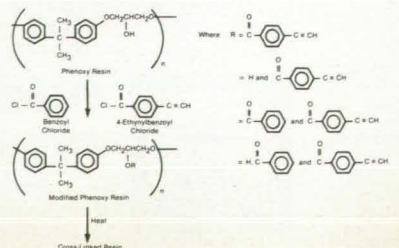
Low-Cost Humidity Sensor

A simple, inexpensive, electronic humidity sensor produces an output that is readily used by indicator or control circuits. The new sensor is a resistor/capacitor oscillator in which a water-absorbent plastic film is the insulator in the capacitive element. As the film absorbs more water with increasing atmospheric humidity, its capacitance increases, reducing the oscillation frequency. Because frequency can be measured more readily than the weak currents produced as outputs in the older sensors, the new sensor offers improved accuracy and resolution. The sensor operates at a safe, low voltage — so low that a significant electrolysis of the absorbed water does not occur. (See page 55.)



Phenoxy Resins Containing Pendant Ethynyl Groups

After curing, phenoxy resins containing pendant ethynyl groups have use temperatures and solvent resistances much greater than those of previous phenoxy and modified phenoxy resins. The ethynyl-containing phenoxy resins have an excellent shelf life in solution or in bulk. They also offer lower moisture absorption and better thermal stability over state-of-the-art cross-linked phenoxy resins. Depending upon the cross-link density, the cured ethynyl-modified phenoxy resins are solvent resistant but still thermoformable and relatively tough. These modified resins show potential for use as adhesives, composite matrices, solvent-resistant coatings, membranes, insulators, and films. (See page 109.)



**Now it's a piece of cake
to do business with Kodak.**

Systems Center and Kodak's new Government Systems Division are now open for business. The sole purpose of both: to make it easier for the government to do business with Kodak. This new division of Kodak is all divisions of Kodak. We can help you with any Kodak product from a floppy disk to a mirror for a space telescope. With special emphasis on imaging systems for information management. All it takes is one call to (703) 558-8500.



Or one visit to
1300 N. 17th Street,
Arlington, VA 22209.

**Kodak's new
Government Systems
Division.**

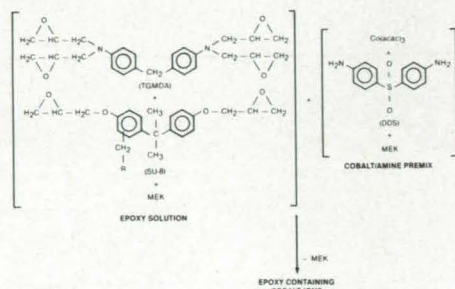


© Eastman Kodak Company, 1985

Circle Reader Action No. 339

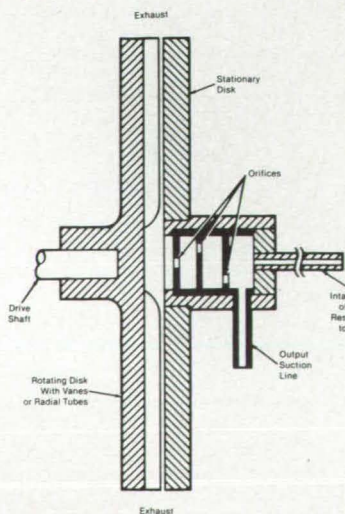
Cobalt Ions Improve the Strength of Epoxy Resins

The flexural strength of tetraglycidyl-methylenedianiline (TGMDA) epoxy resins is increased by 10 to 95 percent by the addition of cobalt ions in the form of tris(acetylacetonato)cobalt (III) complex. Any liquid or solid TGMDA resins are suitable for this technique. It is anticipated that this improved epoxy formulation will prove useful as a composite matrix resin, adhesive, or casting resin for applications on advanced aircraft. (See page 111.)



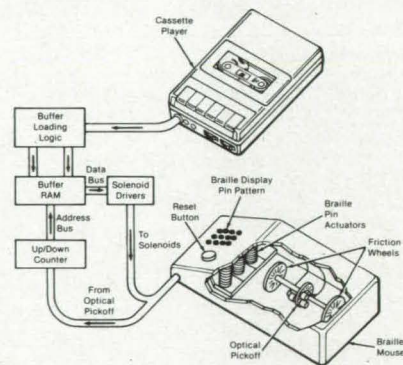
Rotary Speed Sensor for Antilocking Brakes

A rotary speed sensor, developed as part of an antilocking brake system for motorcycles, produces a negative pressure approximately proportional to rotational speed. This pressure is converted to a signal that prevents the brakes from locking. The sensor is a centrifugal air pump that is turned by a motorcycle wheel. Use of pump inlet pressure, rather than pump output pressure, as the braking-control signal eliminates the pressure pulsations caused by the pump vanes. Because the pressure signal is pulse free and directly proportional to rotational speed, a fluidic differentiation, rather than a more expensive fluidic accelerometer, is used to control the brakes. (See page 128.)



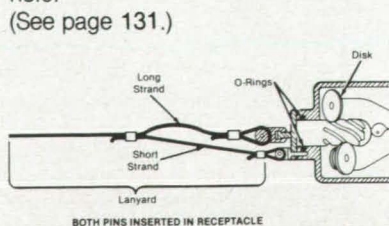
Braille Reading Systems

Two proposed electromechanical systems for making Braille characters could be produced relatively inexpensively. Similar in operating principle to dot-matrix printers, the two methods use electronically actuated pins to produce characters from information stored on magnetic tape. In the first method one or more pins would be scanned over a blank page and energized at intervals to emboss the text on paper, one or more dots at a time. In the second approach (shown in the figure) a hand-held device containing one or more character-generator cells would be used by the reader to scan the lines of text manually. In both cases the text would directly produce the Braille characters and would be fed into a RAM buffer one or more pages at a time. (See page 135.)



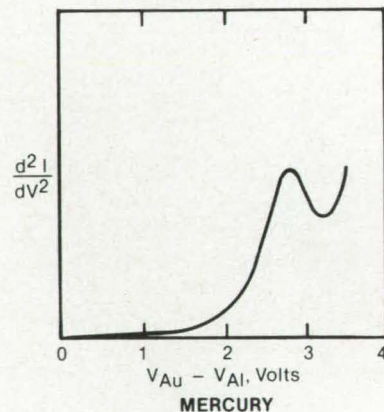
Locking Pull Pin

A proposed self-locking pull pin cannot be accidentally released by shock or vibration but can be intentionally released by a pull on a lanyard. The main pin can undergo the rotational motion necessary for its removal, only after a secondary pin in place, rotation of the main pin locks the secondary pin even more securely in its hole. A pull on the lanyard would first apply tension to a shorter end strand, pulling the secondary pin out of its hole. The tension would then shift to the longer strand attached to the main pin. Without the secondary pin to restrain it, the main pin would rotate and withdraw from the hole. (See page 131.)



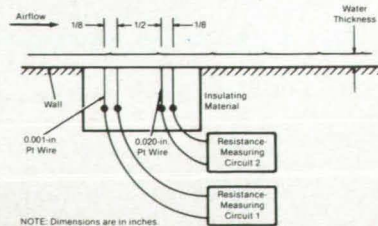
Solid-State Detector for Trace Materials

A detector that senses as few as 10^{12} molecules of a given trace chemical on its surface could find applications in industrial process control and in environmental analysis. Containing no moving parts, amenable to large-scale integration, and operating at room temperature, the detector is a thin-film, solid-state tunnel junction composed of layers of aluminum, aluminum oxide, and gold on a glazed ceramic substrate. When the trace chemical is adsorbed on the outer gold film and diffuses into it, the tunneling characteristics are altered, the nature of the alteration depending on the trace material. After adsorbing (and detecting) a trace chemical, the device can be restored to its initial state by heating or washing with an appropriate solvent. (See page 88.)



Water-Thickness Gage

A gage for determining the depth of water buildup on aircraft is relatively simple to operate and yields a result independent of the conductivity of the water. The gage can be used to evaluate the effects of water on lift and to detect water weight excess. The gage consists of two ac circuits, each of which measures the resistance between a pair of conducting platinum wires immersed in an insulating material. One pair of wires yields a resistance independent of water thickness, and hence determines the resistivity of the water. With the second pair, the resistance is proportional to the water thickness. The combination of the two outputs then gives the water thickness. (See page 127.)





Rocketdyne achieves another major milestone in Space Shuttle Main Engine durability.

The Space Shuttle Main Engine, designed and built for NASA by the Rocketdyne Division of Rockwell International, has successfully completed the NASA Phase II ten flight certification tests with improved-life high pressure fuel turbopumps.

- Turbine temperature has been reduced by 110° F.
- Turbine durability has been significantly improved to effectively reduce maintenance.
- Both sets of turbine blades have operated the equivalent of ten flights during full power level hot fire tests.

Rocketdyne



**Rockwell
International**

...where science gets down to business

Aerospace / Electronics / Automotive
General Industries / A-B Industrial Automation

Circle Reader Action No. 380

Lightweight Protective Garments

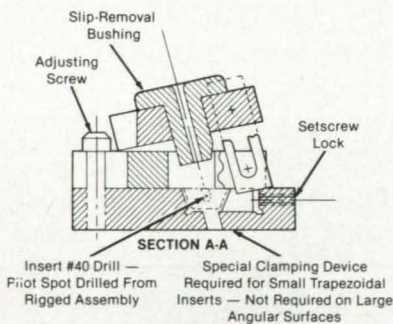
Garments made of cotton fabric coated by a thin layer of polyacrylate rubber would protect wearers from poisonous chemicals, bacteria, and radioactive particles. At the same time the garments would allow heat, moisture, and carbon dioxide to pass from the inside to the outside so that the wearers remain comfortable. While polyacrylate rubber transmits large-molecule chemical agents only at very low rates, additional protection from these agents could be achieved by various reactive additives incorporated in the rubber.

(See page 115.)

Adjustable-Angle Drill Block

The adjustable block illustrated in the figure enables holes to be drilled at precise angles to the surface of a structure. The block can be used to "transfer" (drill at the same angle) nonperpendicular holes in mating contoured assemblies; for example, in aircraft frames. In general manufacturing it can be used to transfer mating installation holes to irregular and angular surfaces.

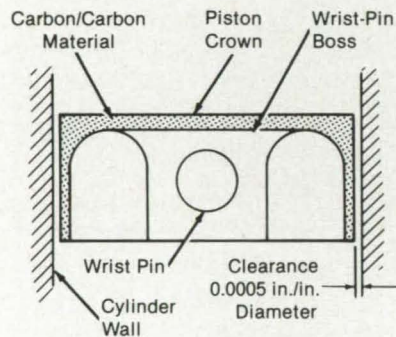
(See page 154.)



Carbon/Carbon Pistons for Internal Combustion Engines

A carbon/carbon piston for reciprocating internal combustion engines (see figure) has less weight than an aluminum piston but increases the mechanical and thermal efficiencies of the engines. Maintaining its strength at elevated temperatures, the carbon/carbon piston can operate at higher temperatures and pressures than a comparable metal piston. Moreover, the negligible thermal expansion undergone by the carbon/carbon material makes piston rings and skirts unnecessary, thus reducing friction. The high emittance and low thermal conductivity of the carbon/carbon piston will improve the thermal efficiency of the engine, because less heat energy is lost to the piston and cooling system. Heat loss could be further reduced and engine efficiency further increased through the use of a carbon/carbon cylinder wall, which can be formed by a carbon/carbon sleeve installed in a conventional cylinder block.

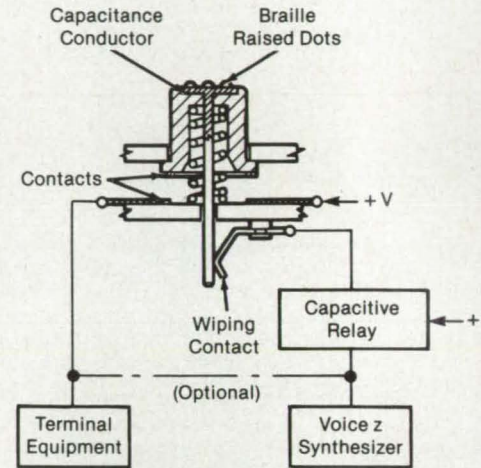
(See page 156.)



Keyboard With Voice Output

A proposed keyboard that actuates a voice synthesizer would give an operator verbal identification of a key before it is firmly pressed. The operator could then

follow through with or abandon the selection. The verbal feedback is useful for blind operators or for operators working in dim light or busy observing other things while keying data into a control system. In situations where correct data entry is critical, the feedback gives the operator added confidence. The keyboard can be used as a training aid for touch typing. The concept can be adapted to such equipment as typewriters, computers, calculators, telephones, cash registers, and on/off controls. (See page 54.)



CAPACITIVE RELAY

Titanium Heat-Pipe Wicks

Sintered titanium offers several advantages over sintered aluminum as a material for heat-pipe wicks. Titanium is both light and strong. Because its thermal conductivity is only one-seventh that of aluminum, it can be used when a high thermal resistance is needed to prevent boiling of the working fluid. Conditions yielding the best wicks have been determined. The heat flux, evaporator temperature drop, and life expectancy have been determined for all titanium heat pipe made with the best type of wick. The working fluids used were acetone, ammonia, water, and chlorofluoromethanes.

(See page 141.)

WORLD'S SMALLEST LOAD CELL

THINK OF THE POSSIBILITIES!

A.L. Design, Inc.

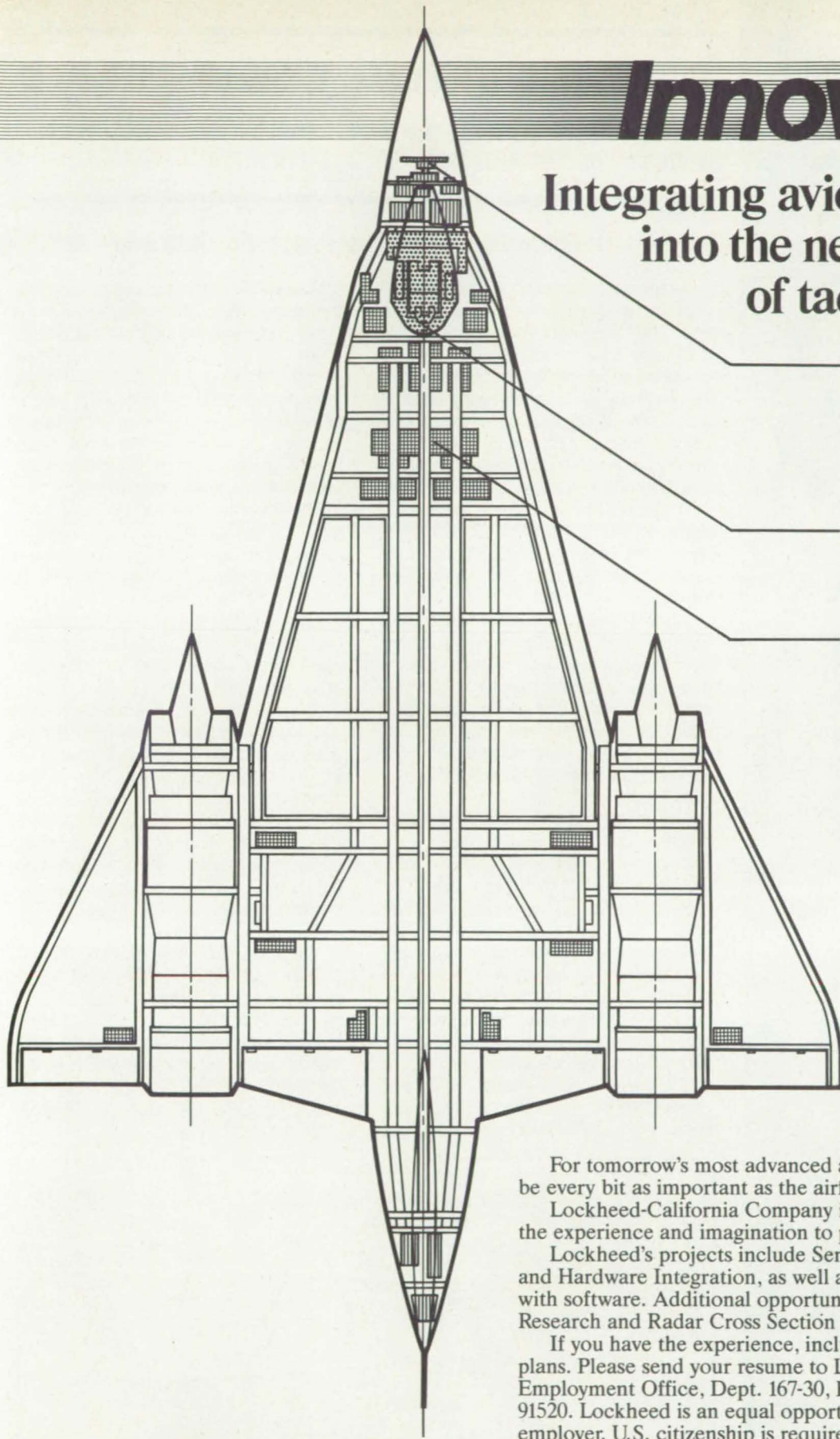
(716) 833-6272

4232 Ridge Lea Rd.

Amherst, N.Y. 14226

Innovation

Integrating avionics systems
into the next generation
of tactical aircraft.



Sensor Systems

- Antenna/Radome Design
- Radar
- IR/EO
- ESM/ECM

Cockpit Design

- Displays
- Real-Time Software

Hardware Integration

- Inertial Navigation
- Digital Computers
- Armament Support Management
- Microwave/RF

For tomorrow's most advanced aircraft, what goes inside will be every bit as important as the airframe in which it rides.

Lockheed-California Company is looking for individuals with the experience and imagination to put the pieces together.

Lockheed's projects include Sensor Systems, Cockpit Design, and Hardware Integration, as well as the integration of all systems with software. Additional opportunities exist in Operations Research and Radar Cross Section Technology.

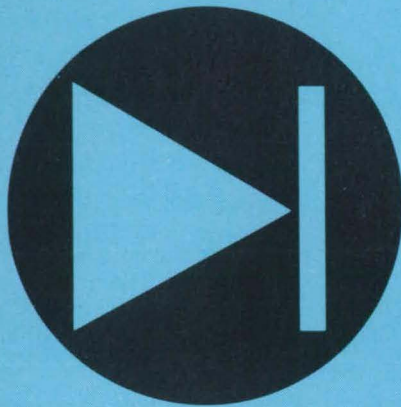
If you have the experience, include Lockheed in your career plans. Please send your resume to Lockheed-California Company, Employment Office, Dept. 167-30, P.O. Box 551, Burbank, CA 91520. Lockheed is an equal opportunity, affirmative action employer. U.S. citizenship is required.

 **Lockheed-California Company**

Giving shape to imagination.

SKUNK WORKS and the skunk design are registered service marks of the Lockheed Corporation. © 1985 Lockheed Corporation

Electronic Components and Circuits



Hardware, Techniques, and Processes

- 40 Pulse Coupling for Laser Excitation
- 42 Generating Independent Preionizing Pulses for Lasers
- 42 Magnetically-Switched, Long-Pulse XeCl Laser
- 44 Obtaining One-Degree Accuracy with Shaft Encoders
- 46 Microwave Power Combiner with Switching Diodes
- 48 Cassegrain-Antenna Gain Improvement
- 49 Multiple-Winding Output Inductors for Power Converters
- 49 Improved Waveguide Laser Array
- 50 A Quick Visual Power-Supply Monitor
- 52 Controlling Transistor Temperature During Burn-In
- 54 Keyboard with Voice Output
- 54 Conductive Container for Semiconductor Devices
- 55 Low-Cost Humidity Sensor
- 56 Floating-Emitter Solar-Cell Transistor
- 56 Tester for Distress Beacons
- 57 Control Electronics for Solar/Flywheel Power Supply
- 58 Reduced-Stress Mounting for Thermocouples
- 60 Determining Internal Connections in Capacitors
- 60 Accelerating Corrosion in Solar-Cell Tests

Pulse Coupling for Laser Excitation

A small switch is joined to a large laser with minimum energy loss.

NASA's Jet Propulsion Laboratory, Pasadena, California

A tapered transmission line couples energy from a magnetic switch to an excimer laser. The transmission line provides a constant impedance for pulses that come from the switch and distributes the pulses across the length of the laser as nearly uniform wave fronts. It also allows a smaller, more efficient magnetic core to be used in the switch. Losses and circuit capacitance are less than for a full-laser-width line and core.

The tapered line (see figure) matches the disparate geometries of the core and the laser. At the same time, it reduces unwanted reflections and reversals of current and energy flux.

The line is fed from a pulse-shaping network composed of five sections, the dimensions of which are determined by the required characteristic impedance, current density, and core size. As the core saturates, it removes its impedance from between the laser and the pulse-shaping network and thus enables the network to couple rapidly to the laser.

The characteristic impedance of the tapered line can be adjusted by including discrete capacitors spaced along the line. With an impedance mismatch thus created, the pulse waveform can be peaked by circuit ringing. The peak, superimposed on the main pulse, can be used to increase the preionization electron density and thereby reduce the magnitude of the main pulse required to excite the laser. Alternatively, the transmission line can be tapered nonuniformly to achieve the same effect.

The cross-sectional area of the core is chosen to ensure saturation at the desired pulse magnitude: Saturation should occur at

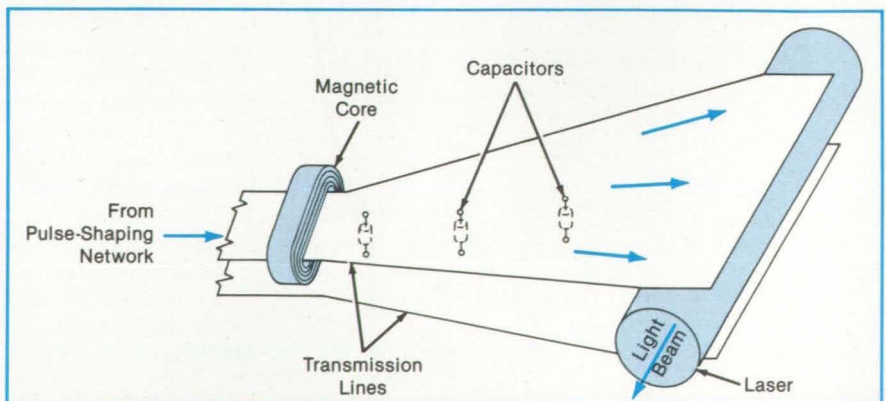
the peak of the main discharge pulse so that the entire main pulse is switched into the preionized laser. The magnetic path length of the core is chosen for efficient and fast coupling of the pulse into the laser and thus tends to determine the width of the section of the transmission line on which the core is mounted. For minimum reflection and loss, the line should generally match the impedance of the pulse-shaping network.

The size of the line should not result in too large a capacitance; this would cause an excessive amount of energy to be stored in the line and diminish overall efficiency. Increasing the taper angle reduces the capacitance, but too large a taper will produce an arced wave front in the pulse, and the pulse energy will not arrive simultaneously at all parts of the laser.

The overall capacitance can be reduced by using parallel tapered lines from multiple switches and pulse-shaping networks, joining in a single wide transmission line as they approach the laser. This alternative would require tuned pulse-shaping networks, matched magnetic switches, and precisely dimensioned, tapered sections, but would further reduce energy requirements and increase efficiency.

This work was done by Thomas J. Pacala of Caltech for NASA's Jet Propulsion Laboratory. For further information, Circle 2 on the TSP Request Card.

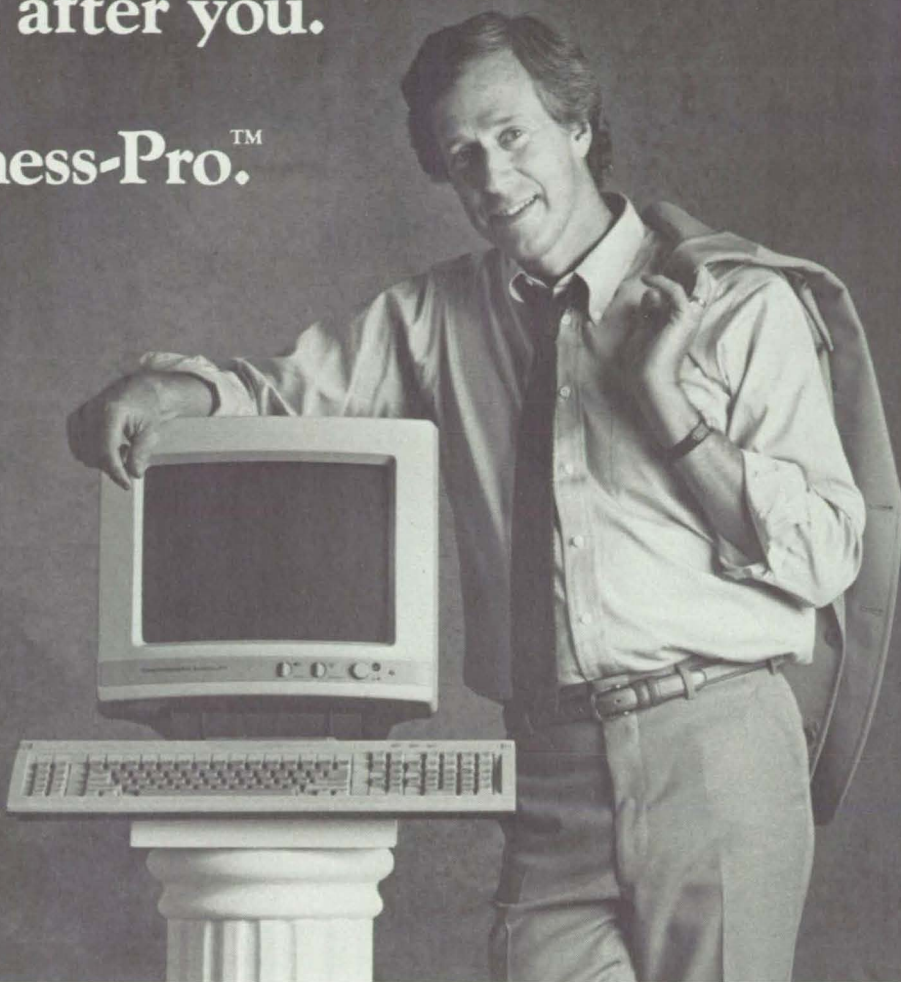
Inquiries concerning rights for the commercial use of this invention should be addressed to the Patent Counsel, NASA Resident Office-JPL [see page 29]. Refer to NPO-16403.



Conductive Tapered Strips carry pulses of energy from a switch and pulse-shaping network to a laser. The taper in the transmission line formed by the strips couples the pulse energy through the small magnetic core to the large laser. The discrete capacitors are optional components for creating peaks on the pulses.

TI presents the advanced PC so powerful, it's named after you.

The Business-Pro™



We put your name on the most powerful, expandable, versatile, compatible, personal computer ever from Texas Instruments. The Business-Pro™ computer.

Compatibility means options.

Business-Pro's ability to best the efforts of any other advanced PC begins with being able to run the most popular business software. That includes the software that runs on the IBM Personal Computer AT™. And over 1,100 TI PC business programs. Giving you the widest selection of software to best solve your specific business problems.

Tomorrow is the best reason to get Business-Pro today.

Expandability is a prime asset of Business-Pro. In fact, Michael J. Miller says in *Popular Computing*, "Its flexibility and expandability make it superior to the AT."* So, if you need the power to match the growth of your business, Business-Pro starts with 512 kilobytes of memory standard. And it expands to an extraordinary 15 megabytes of memory with 144 megabytes of data file storage!

So, for the price of a personal computer, you also get a system that performs and configures like a larger mini-computer system. Because one Business-Pro computer has the power to drive up to 50 other PCs in a local area network acting as a network server with full access and communications to mainframes, mini-computers and other PCs.

Further, no matter where your business goes, no matter how much it grows, you get TI service nationwide and the support

of industry-specific value-added resellers (VARs) with the right software solutions for your business.

If your business needs an advanced personal computer with the power and capabilities to grow into the future, get the one with your name on it. The Business-Pro from Texas Instruments. For Government sales and GSA information please call 1-800-527-3500, ext. 602.

A few of the areas served by TI industry-specific VARs: Business Accounting, Health Services, Retail Trade, Construction, Manufacturing, Auto Dealers, Educational Services, and Engineering.

© 1985 TI




**TEXAS
INSTRUMENTS**

Creating useful products
and services for you.

Business-Pro is a trademark of Texas Instruments Incorporated. IBM Personal Computer AT is a trademark of International Business Machines Corporation.

*"TI Business-Pro" by Michael J. Miller, pages 79-84, September 1985, *Popular Computing*.

Circle Reader Action No. 393

Generating Independent Preionizing Pulses for Lasers

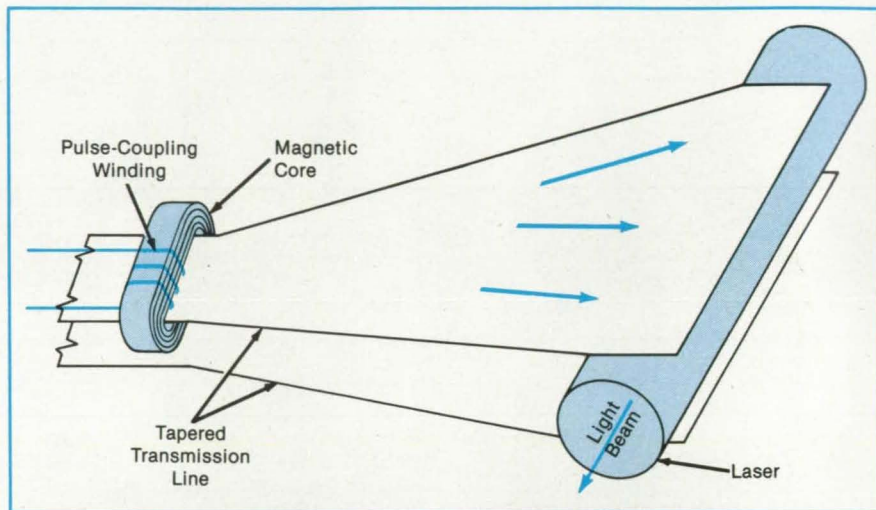
A saturable-core reactor also serves as a pulse transformer.

NASA's Jet Propulsion Laboratory, Pasadena, California

Another way to preionize the tapered-line-pulsed laser described in the preceding article offers somewhat higher efficiency and better controllability. The new approach provides greater independence between the shape and magnitude of the preionizing pulse and those of the main pulse. It also provides a more sharply rising preionizing pulse.

A simple pulse-coupling winding is attached to the core of the magnetic switch that energizes the laser (see figure). Under the control of a synchronizing circuit, a pulse is first applied to the pulse-coupling winding and the magnetic switch core. In its unsaturated state, the core acts as an efficient pulse transformer, sending the pulse as a preionizing peak to the laser. The synchronizing circuit then turns on a second, much larger pulse to the magnetic switch proper, which sends a larger firing pulse to the laser.

The pulse-coupling winding is simple, light in weight, low in bulk and power consumption, and inexpensive. It allows the preionizing pulse to be shaped independently for maximum efficiency and effectiveness and allows the main firing pulse to be given



A Simple Pulse-Coupling Winding on a saturable reactor core lets the core act as a pulse transformer, passing a preionizing pulse from the winding to the tapered transmission line, then to the laser. The laser is thus prepared for an independent firing pulse, which follows the preionizing pulse.

the best shape for its function.

This work was done by Thomas J. Pacala of Caltech for NASA's Jet Propulsion Laboratory. For further information, Circle 1 on the TSP Request Card.

Inquiries concerning rights for the commercial use of this invention should be addressed to the Patent Counsel, NASA Resident Office-JPL [see page 29]. Refer to NPO-16402.

Magnetically-Switched, Long-Pulse XeCl Laser

Output radiation is narrow in frequency and spatial extent.

NASA's Jet Propulsion Laboratory, Pasadena, California

Careful shaping of input pulses helps an XeCl excimer laser to produce a low-divergence, narrow-band light beam. A long (~ 100 ns) input pulse enables the radiation to pass a large number of times through the laser-cavity Fabry-Perot resonators, thereby improving the control of wavelength, bandwidth, polarization, and transverse modes. Another advantage of the increase in pulse length (from the previous value of 10 to 30 ns for an excimer laser) is that timing becomes less critical.

As shown schematically in the figure, the laser system includes a high-voltage power supply and a pulse-forming network. Before the main power pulse is applied, the laser is preionized by two rows of

30 resistively ballasted ultraviolet arcs, one row on each side. While the main pulse is being formed, it is withheld from the laser discharge tube by a saturable-inductor switch mounted on a tapered transmission line. The inductor saturates at the peak of the pulse, thereby allowing the pulse to pass along the transmission line to the discharge tube. The operation of the switch and transmission line is discussed more fully in the two preceding articles; "Pulse Coupling for Laser Excitation" (NPO-16403) and "Generating Independent Preionizing Pulses for Lasers" (NPO-16402).

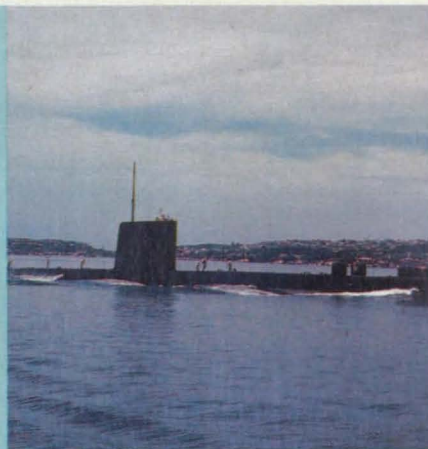
The 80-nF, 0.6- Ω pulse-forming network is charged to 16 kV in 150 ns from an 80-nF storage capacitor using a grounded-grid

thyatron. The voltage rise time of the network is 10 ns. The rise time is extended by the delay in saturation between the inner and outer laminations of the magnetic switch and by the residual switch inductance during saturation. The total voltage rise time at the laser is 20 ns.

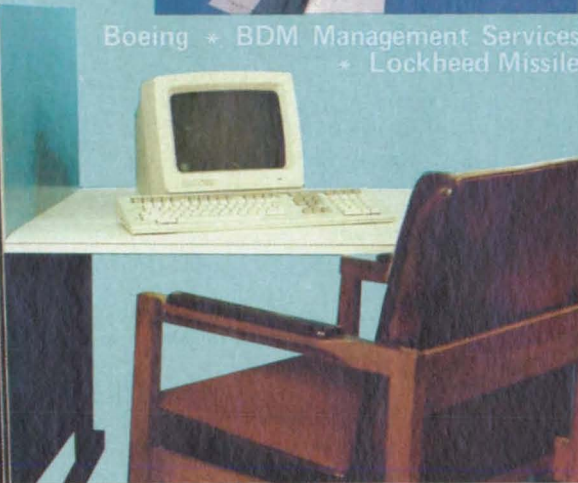
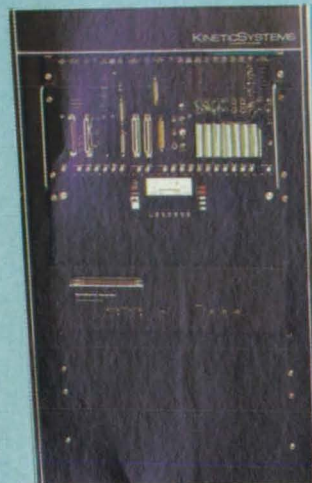
The laser discharge is 42 cm long, 0.7 cm wide, and 0.9 cm high. The gas mixture is typically 1 percent Xe, 0.1 percent HCl, 0.025 percent H_2 , and the balance Ne at 3 atm (3×10^5 N/m²) absolute pressure. The gas is circulated across the space between the electrodes at ~ 5 m/s, a speed sufficient for a pulse-repetition rate of 250 Hz.

The Fabry-Perot etalons are adjusted to select the oscillation frequency and to pro-

Bell Aerospace Textron * Naval Research Laboratory * Sperry * Draper Labs * TRW * McDonnell Douglas * Northrop Research * Ames Laboratory * Martin Marietta * Los Alamos National Laboratory * NASA * Hughes Aircraft * Naval Surface Weapons Center * Sandia Lab * United Technology * Bendix * Goodyear Aerospace * Oak Ridge National Laboratory * NOAA * Defense Nuclear Agency * E. G. & G. * General Electric * Livermore National Laboratory * Kirkland AFB *



Boeing * BDM Management Services * Lockheed Missile



Research and development • Flight simulation and training • Weapon guidance and control

When your projects call for real-time data acquisition and process control ... Call on KSC

For more than a decade, Kinetic-Systems Corporation has been supplying the aerospace and defense industries with real-time data acquisition and control systems . . . powerful, flexible, reliable systems based on the international CAMAC standard (IEEE-583) for Computer Automated Measurement And Control. *Weapons development, spacecraft testing, radar control, submarine technology, laser/particle beam research, flight simulation, jet propulsion, underground test project, R & D, quality control, and navigational in-*

struments testing are only a sampling of the areas where these CAMAC systems are proving their worth.

CAMAC offers you modular flexibility, limitless expansion, a high-speed data highway, and distributed intelligence capabilities. KSC offers you a choice of powerful LSI-11, PDP-11, or VAX-11 computer systems, easy-to-use software packages, and the widest range of process interface modules available to match your many real-time demands.

Your data acquisition and control system is easily designed and implemented using PC/DBS™, our **Process Control/Data Base System** software package. PC/DBS is the first comprehensive software tool for process automation with CAMAC . . . and you don't have to be a programmer to use it!

Ask about our aerospace and defense automation capabilities - from our total systems and supporting software to our customized configurations and training classes. See for yourself what KSC and CAMAC can do for you. Call us today!

Contact Us For More Information

KineticSystems Corporation

Standardized Data Acquisition and Control Systems

U.S.A.

11 Maryknoll Drive
Lockport, Illinois 60441
Phone: (815) 838 0005
TWX: 910 638 2831

West Coast Office:

(415) 797 2351 TWX: 910 997 0544
Northeast Regional Office:
(609) 921 2088 Telex: 833040
Southeast Regional Office:
(305) 425 9793 Telex: 441781

Europe (Service)

3 Chemin de Tavernay
1218 Geneva, Switzerland
Phone: (022) 98 44 45
Telex: 28 96 22

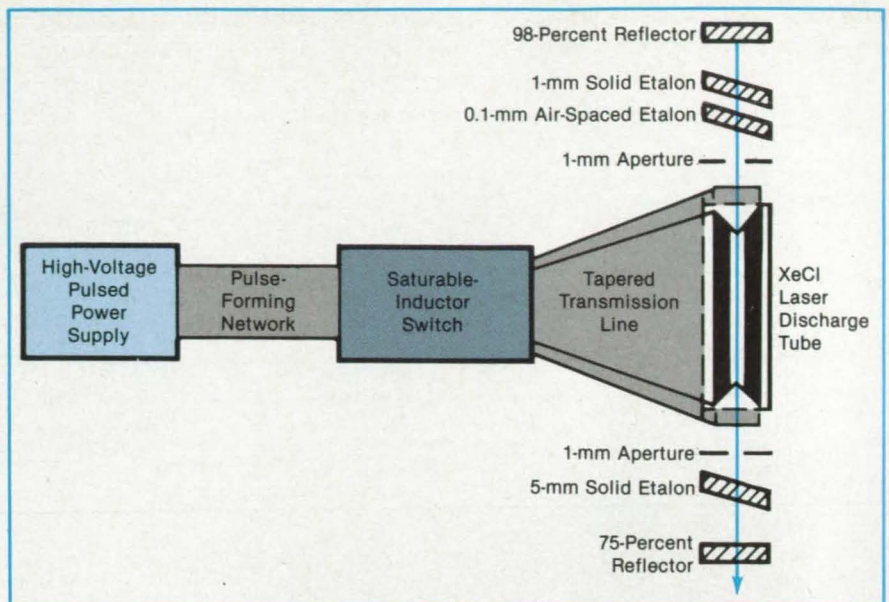
Europe (Marketing)

Gewerbestrasse 13
CH-4528 Zuchwil, Switzerland
Phone: (065) 25 29 25
Telex: 845/934648

vide a single, high-contrast interference-fringe pattern. The pulse duration and cavity length permit about 15 double passes (round trips) of the light beam through the laser cavity, resulting in a bandwidth of no more than $7 \times 10^{-4} \text{ \AA}$, as measured by the width and separation of the fringes. The output pulse duration at this line width is about 60 ns and the pulse energy between 5 and 10 μJ . The measured beam divergence is 0.2 mrad, which is at the diffraction limit.

This work was done by Thomas J. Pacala, Iain Stuart McDermid, and James B. Laudenslager of Caltech for NASA's Jet Propulsion Laboratory. For further information, Circle 41 on the TSP Request Card.

NPO-16410



The Long-Pulse Laser achieves a narrow-band output by multiple passes of the beam through precisely adjusted Fabry-Perot etalons. The pulse-forming network and saturable-inductor switch enable a fast (~ 20 ns) pulse rise to the peak voltage, followed by a long (~ 100 ns) residence at the peak.

Obtaining One-Degree Accuracy With Shaft Encoders

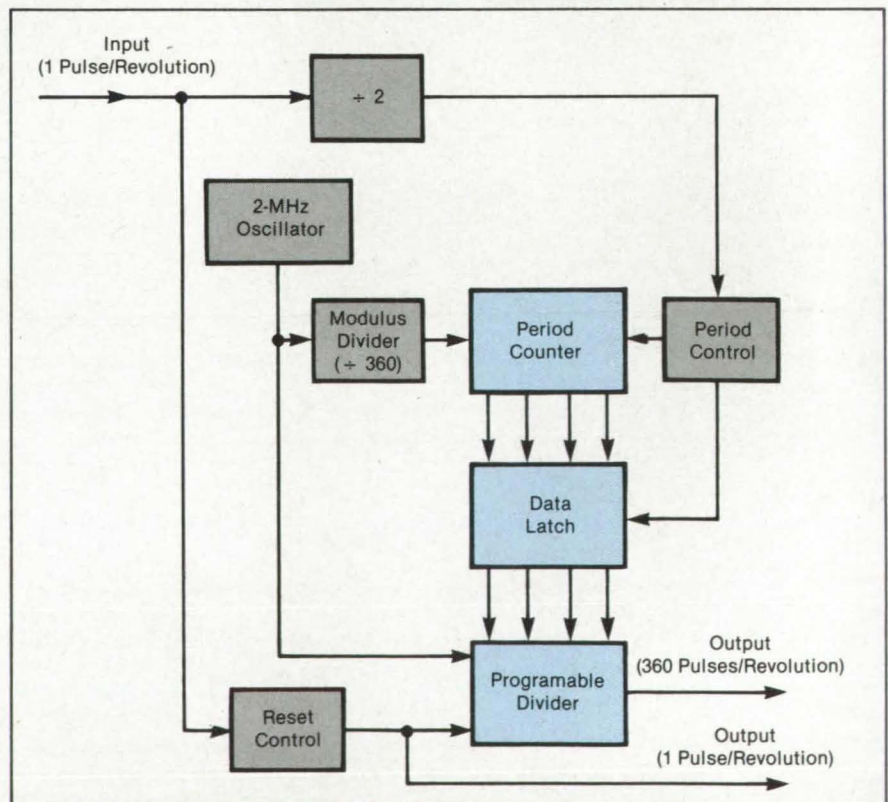
This circuit provides one pulse for each degree of rotation.

Langley Research Center, Hampton, Virginia

The circuit shown in the block diagram converts the output of a 1-pulse-per-revolution shaft encoder to a precise 360-pulses-per-revolution output. The circuit thus allows the shaft angular position to be measured with 1-degree accuracy. With simple modifications, the circuit can provide higher or lower resolution from single- or multiple-pulse-per-revolution sources.

Many existing shaft encoders have insufficient resolution for modern instrumentation and data-display systems. For example, some rotor-blade shaft encoders provide an angular resolution of only 5 degrees, whereas the associated laser-velocimeter data system requires 0.5-degree resolution. In electronic intelligence (ELINT) systems, the availability of only 1 pulse per revolution of the emitter antenna is common. The circuit described here is used to synchronize an aircraft beacon transponder-based plan-position indicator (PPI) display to a remote host interrogator search antenna.

The circuit is divided into five major sections: A stable reference-frequency source, a modulus divider, a period counter and latch, a programmable divider, and auxiliary control logic. The stable reference frequency source is a 2.0-MHz quartz-crystal



This Shaft-Encoder Circuit provides one output pulse for each degree of revolution. The circuit can be constructed using standard, commercially available components.



IN A NUTSHELL, BOEING CAN HELP WITH MILITARY/AEROSPACE ELECTRONICS.

Last year alone, Boeing Electronics Company supplied over a quarter billion dollars worth of high quality electronics. We can handle the toughest electronics assignments in the industry.

For instance, we've produced some of the most sophisticated microcircuits available. Including thick-film hybrids and thin-film circuits.

We can provide everything from concept develop-

ment to packaging and design. And Boeing delivers what it promises — on time.

If you have a special requirement for micro-circuits, power supplies, ceramic circuit boards, controllers or avionics, give us a call.

Contact Boeing Electronics Company, P.O. Box 3707, M/S 9A-10, Seattle, WA 98124.

Or call (206) 575-5755.

Boeing Electronics Company

Reliability By Design

Circle Reader Action No. 414

oscillator. The reference frequency is divided by the modulus divider. The divider reduces the reference frequency by the number of desired output pulses per input pulse.

The output from the modulus divider is fed to the period counter and latch. The period counter merely counts the number of pulses between two input trigger pulses. This number is latched, and the counter is reset. The latch is refreshed by alternating input pulses. The latched number is connected with a parallel bus to the program-

able divider, which divides the reference frequency by the number stored in the latch. The programmable divider is reset by each input trigger pulse to synchronize the output pulse train to the trigger.

Two systems have been constructed. The first is an antenna scan generator for a bistatic IFF ELINT display system, providing degree markers from a once-per-revolution trigger. The second is a 0.5-degree marker generator, coupled to a 5-degree rotorhead encoder, for a laser velocimeter system. This system also

includes a pulse counter to convert the programmable divider output pulses to a numerical value suitable for use by a computer. For low-frequency sources, this circuit has been demonstrated to be superior to a phase-locked-loop frequency multiplier.

This work was done by John M. Franke, James I. Clemmons, Jr., and Stephen B. Jones of Langley Research Center. For further information, Circle 58 on the TSP Request Card. LAR-13321

Microwave Power Combiner With Switching Diodes

Signal sources are switched in together or separately.

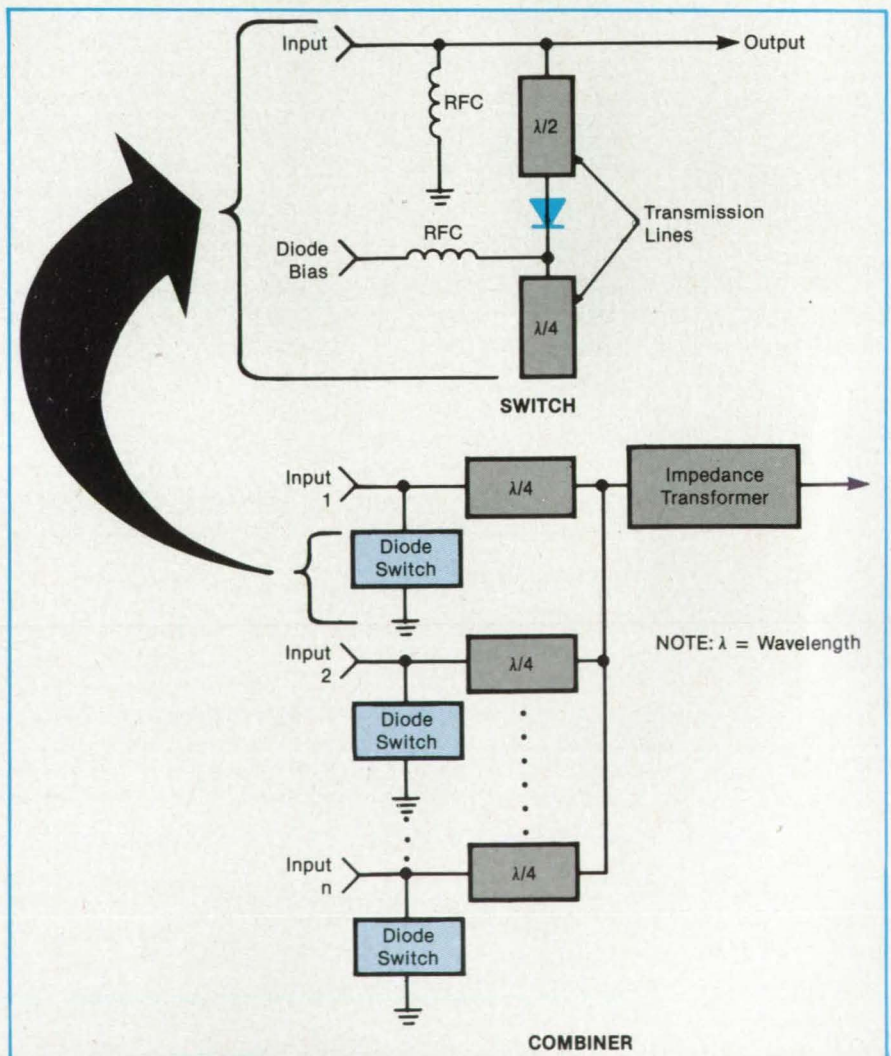
NASA's Jet Propulsion Laboratory, Pasadena, California

In a multiple-port microwave power combiner, each of the outputs of two or more power amplifiers of the same frequency and phase can be passed to a common output port separately or together. Each amplifier is connected to the combiner through a switch consisting of resonant structures, radio-frequency chokes, and a diode. The switches not only permit flexibility in the selection of amplifiers but also isolate the unused amplifiers from the network, all while operating at a relatively low power loss.

The operation of the switches and combiner is illustrated schematically in the figure, neglecting parasitic capacitances and inductances. In the switch, the open-circuited quarter-wavelength section of transmission line presents to the diode a radio-frequency (RF) short circuit to ground. This section also presents an open circuit for direct current, permitting the dc diode-switching bias to be injected.

The half-wave section reflects the diode impedance to the input/output line. When the diode is reverse biased, it presents a high RF impedance across the input/output line, thereby allowing the input signal to pass undisturbed along this line to the output. When the diode is forward biased, it presents a low RF impedance, which causes the input power to be reflected back to the amplifier. Thus, the switch is on when the diode is reverse biased and off when the diode is forward biased.

In the combiner, each switch is connected to the combining junction through a quarter-wave section. When a switch is off, the short circuit is transformed by the quarter-wave section to an open circuit at the combining-junction end. Thus, when a switch is off, it presents a high impedance



A Switching RF-Power Combiner with no moving parts is assembled from diodes, RF chokes (RFC's), and sections of transmission line. The combiner works at only one frequency because it depends on the impedance-transforming properties of quarter- and half-wave lengths of transmission line.

What we give you is just as important as what we take away.

Whether your requirement is a world-class 10 or a class 100,000 facility, the Engineering Division of Clean Room Products can effectively remove contaminants from your environment. That's important! But just as important as what we take away is what we give you.

We Give You Experience and Expertise.

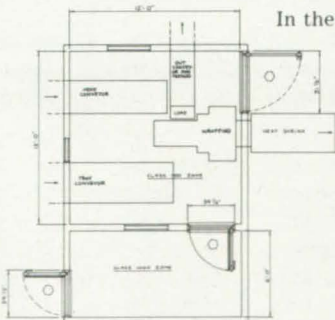
With over 1,000 clean room installations and thousands of work stations in industries like microelectronics, robotics, lasers, fiber optics, computer memories, and pharmaceuticals, CRP is uniquely qualified to research your requirements and provide the clean room solution that's right for you. From consultation through design and installation.



We Give You Flexibility.

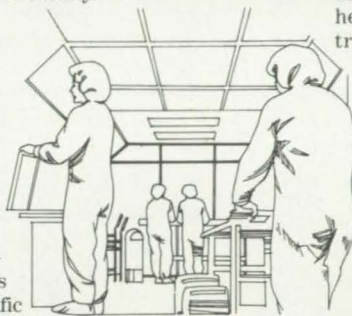
Industry process requirements, space restrictions, environmental conditions, and budgets vary greatly. CRP engineers have accommodated these needs with a cost-effective, phased system approach. It's flexible enough to handle any of your clean room needs, while meeting or exceeding government standards.

In Phase I, CRP engineers come to your site, work with the individuals involved with the production of your product, and carefully analyze your product and over-



all program. After achieving a working knowledge of your process and operation, we formulate a conceptual approach with design parameters that can be used for a new or upgraded facility.

Basic specifications and working drawings are developed in Phase II, and project objectives are clarified. The information developed at this point is specific enough to be used for contractor bidding or in-house construction.

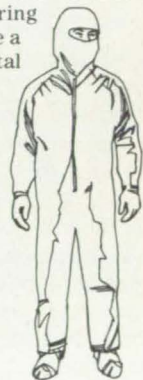


Phase III has a particular appeal to organizations that prefer to use their own personnel for actual construction. To assist your personnel and/or contractors, CRP engineers will provide on-site consultation/supervision during construction, facility startup, and final certification to performance specifications.

In the final phase, CRP engineers assume responsibility for designing and constructing a turnkey facility, complete with certification. Your only involvement is design approval and monitoring of the project as it moves through the stages of construction.

We Give You the Complete Clean Room Source.

The result of 25 years of R&D, our product line has set industry standards for quality and innovation. It's the most comprehensive selection of contamination control supplies available from any one source. Choose from over 100 products, including a full line of laminar flow units, clean room equipment, garments, and supplies. Many of them made in one of our own class 10/100 clean rooms. Combine that with extensive clean room engineering programs, and you have a single source with total compatibility.



We'll Give You a Head Start to High Productivity — Free!

To give you a better idea of what to look for when designing and constructing a clean room facility, we've prepared the CRP Clean Room Productivity Kit. To order your free copy, or for more information on CRP's complete line of products and services, call us at 516-968-8282, or mail the coupon below.

I want to know more about what Clean Room Products can give me. Send a free copy of your Clean Room Productivity Kit.

Name _____

Title _____

Company _____

Address _____

City _____ State _____ Zip _____

Clean Room Products, Inc., • Engineering Division
56 Penataquit Avenue, Bay Shore NY 11706

NTB 1185



Clean Room Products, Inc.

Productivity Through Engineered Environments

to the other switches and consequently does not load down any other amplifier that is feeding power to the combiner.

To match the impedances of the amplifiers and switches, the output-line impedance at the summing junction would have to be inversely proportional to the number of inputs that are switched on. Therefore, it is desirable to include some kind of impedance transformer at the output. Since the impedance changes with the state of the switches, an engineering compromise has to be made in the design of the trans-

former: For example, it may be necessary to select a transformation to an average or most frequently encountered output impedance.

Diodes for the switches must be selected to withstand the worst combination of operating faults. The peak-to-peak voltage that a reverse-biased diode may have to withstand could be several times the normal value obtained when all impedances are matched and all phase relationships are correct. For example, if the output is shorted, the voltages at all the diodes

are doubled. If an input is 180° out of phase, the voltage is multiplied several times at the affected diode. The diodes must also be able to withstand the forward-bias and worst-case-fault current and power.

This work was done by Bruce L. Conroy, Richard B. Postal, and James F. Boreham of Caltech for NASA's Jet Propulsion Laboratory. For further information, Circle 48 on the TSP Request Card. NPO-15775

Cassegrain-Antenna Gain Improvement

A feed with dual-shaped subreflectors economically increases antenna efficiency.

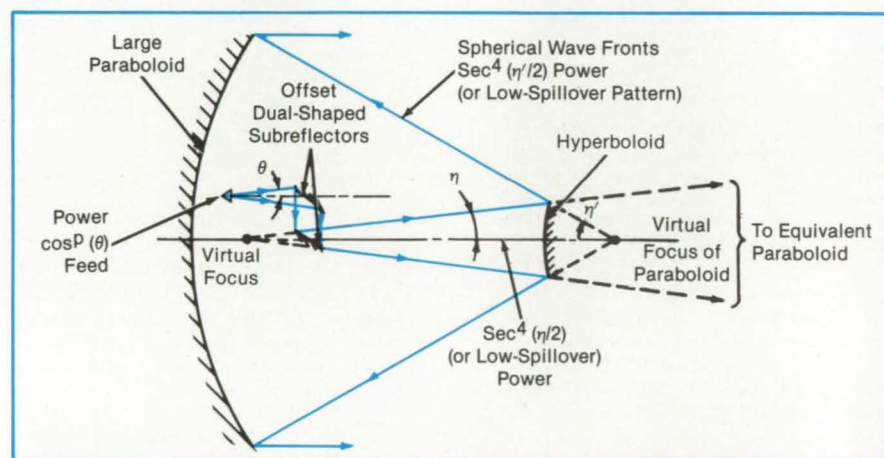
NASA's Jet Propulsion Laboratory, Pasadena, California

The efficiency of many existing large ground-based reflector antennas could be improved by 10 to 20 percent if their present feeds are replaced with new ones. The new feeds would each have two appropriately-shaped reflecting elements (see figure). Such an offset dual-shaped subreflector (DSS) feed would bring the gain of existing paraboloid or Cassegrain antennas up to that of reflector antennas of more recent design at a cost considerably lower than that for reshaping the existing reflecting surfaces.

Mathematical procedures have been developed for synthesizing nearly optimum shapes for the DSS elements of the new feeds. The synthesis is based on an extension of an approximate geometrical optics formulation developed previously for an offset dual-shaped high-gain antenna. In that antenna design, the power to be radiated was reflected first from a subreflector and then from a large reflector that produced a uniform phase and amplitude distribution. In the present DSS feeds, the first and second reflections are from offset subreflectors. The second reflection produces a spherical wave that feeds either the hyperboloidal element of a Cassegrain antenna or the main paraboloidal reflector.

The power distribution of the wave feeding the main reflector is designed to have a \sec^4 angular dependence and, if desired, an appropriate low spillover taper. This angular dependence cannot be produced by conic-section (spherical, paraboloidal, or hyperboloidal) reflecting surfaces unless a special relatively narrow-band feed is used (e.g., a Potter horn).

The synthesis problem is to find shapes for the subreflectors that satisfy the afore-



A modified antenna feed with dual-shaped subreflectors can yield a 10-to-20-percent improvement in the efficiency of existing large-aperture paraboloidal or Cassegrainian antennas.

mentioned phase and power-distribution constraints. By differentiation of the path-length equation, the phase constraint can be expressed as a differential. The power-distribution constraint is expressed as an integral that relates the feed-pattern and objective (\sec^4) pattern. Since there are to be two subreflector elements and only one such element is required to satisfy the phase constraint, some freedom remains in selecting the shape of the other element to obtain the required power distribution.

The key to finding approximate solutions that satisfy both constraints is an ad hoc assumption about the angular dependence of certain transformation functions appearing in the problem. The justification for the assumption is that when the feed pattern and the final scattered pattern have circular symmetric dependence, the assumption very often leads to practical

solutions.

Application of the assumption leads to a simultaneous pair of nontotal partial differentials that can be integrated along any path as a pair of simultaneous ordinary differential equations of first order. These yield a series of contours for the first subreflector. From these, a corresponding set of contours for the second subreflector is obtained by applying the phase constraint. The resulting DSS surfaces satisfy the phase constraint exactly and satisfy the power-distribution constraint to a close approximation.

This work was done by Victor Galindo and Alan G. Cha of Caltech and Raj Mittra of the University of Illinois for NASA's Jet Propulsion Laboratory. For further information, Circle 22 on the TSP Request Card. NPO-16327

Multiple-Winding Output Inductors for Power Converters

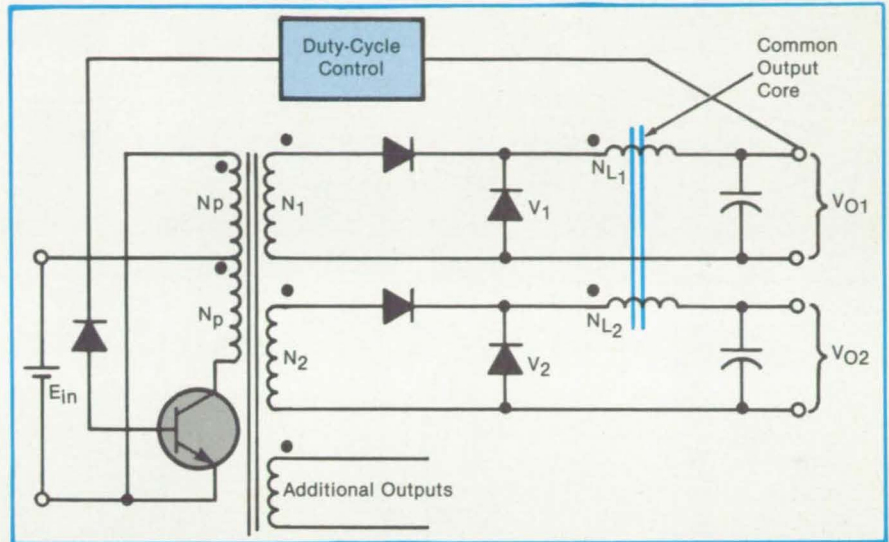
A numerical procedure determines the optimum core dimensions.

NASA's Jet Propulsion Laboratory, Pasadena, California

Power converters with multiple outputs having separate inductors for each output will have poor load regulation in a closed-loop system. This is because of the rectifier drops, copper losses, and transformer leakage inductance.

The closed-loop regulation of a power converter is improved from between 5 and 10 percent for individual inductors to between 1 and 2 percent if the inductors are wound on a common core. The total mass and volume is reduced about 35 percent for the same copper loss.

A design procedure has been developed for dc-to-dc power converters with multiple outputs having inductors wound on a common core (see figure). With a common core, the minimum load current consistent with good output regulation is lower, the output regulation is improved, and the total inductor size and weight is reduced. Details of the procedure may be obtained by requesting the Technical Support Package referenced at the end of this article. The inductor design procedure includes all that is necessary to select the proper magnetic core and size of the mag-



Many Output Windings (N_1 , N_2 , etc.) on a common core are less subject to voltage surges than they would be if they were wound on separate cores.

net wire for a given copper loss.

This work was done by Colonel W. T. McLyman of Caltech for NASA's Jet Pro-

pulsion Laboratory. For further information, Circle 9 on the TSP Request Card. NPO-16176

Improved Waveguide Laser Array

A new structure generates an intense, narrow beam.

NASA's Jet Propulsion Laboratory, Pasadena, California

An improved structure for an integrated array of $Al_xGa_{1-x}As$ diode lasers causes the array to oscillate predominantly in the fundamental supermode (with all units at the same phase), thereby producing an intense, narrow light beam. The new structure differs from the older ones in that the gain in the spaces between the laser channels is approximately equal to the gain in the channels.

In the new structure, the laser/waveguide channels are distinguished from the interchannel spaces in refractive index but not in gain. The refractive index of each channel is slightly higher than the index of the surrounding structure. This partially confines the light to the channels. In earlier versions, the spaces between the chan-

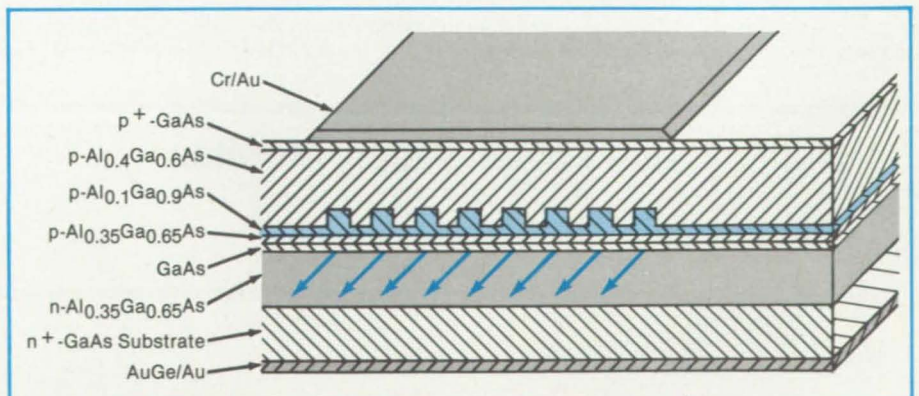


Figure 1. The Laser Array is formed of layers and channels of $Al_xGa_{1-x}As$ deposited epitaxially. In this structure, the layer, channel, and interchannel dopings are chosen so that the gain in the interchannel spaces is the same as the gain in the channels.

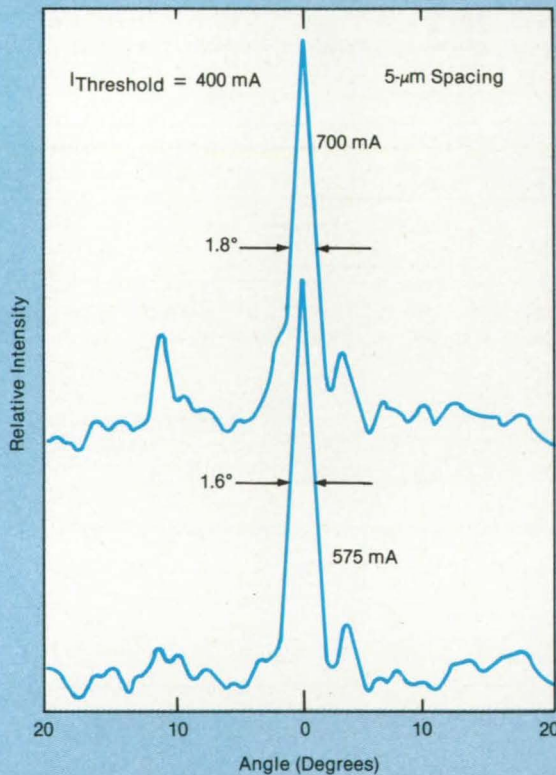
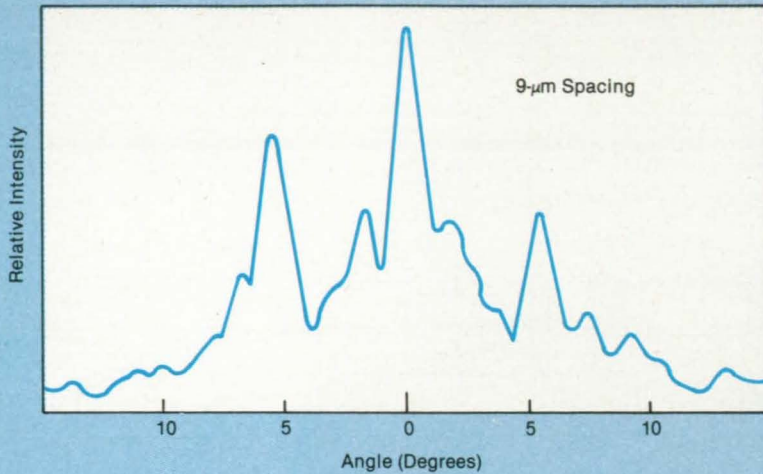


Figure 2. These **Far-Field Radiation Patterns** show the performances of laser arrays like the one in Figure 1. These measurements are performed in the plane of the laser junctions. The angles are measured with respect to the forward direction (the direction along the channels).

nels were absorptive. This favored oscillation in supermodes that were least absorbed in the interchannel spaces; that is, in the high-order supermodes. In the new structure, there is no longer a mechanism that favors the high-order supermodes, and the fundamental supermode can dominate.

Wafers with the improved laser arrays were prepared by liquid-phase epitaxial growth. First, the layers up to and including the p-Al_{0.1}Ga_{0.9}As layer containing the laser channels (see Figure 1) were grown on an n⁺-GaAs substrate. The spaces between the channels were then formed by etching with a 1:8:8 mixture of H₂SO₄, H₂O₂, and H₂O. The remaining laser ridges were then 0.5 μm high. Two lateral ridge (channel) spacings were used: Ridges 4.5 μm wide with a 9-μm period and ridges 2.5 μm wide with a 5-μm period.

The ridges were covered with a 4-μm-thick layer of Ge-doped p-Al_{0.4}Ga_{0.6}As. The ridges thus became buried laser/waveguide channels. The next layer was Ge-doped p⁺-GaAs, which was followed by a Cr/Au positive-side electrode. After lapping, a contact of AuGe/Au was deposited on the bottom. Laser arrays were cleaved from the wafer to a length of 250 μm.

Figure 2 shows the far-field radiation patterns in the laser-junction plane produced by lasers with the 9- and 5-μm spacings. The peaks at 0° and 5.5° in the 9-μm laser pattern correspond to those calculated when all lasers operate in phase. The lesser peaks surrounding the three main peaks correspond to a higher order mode. The width of the three main peaks is 1.3°, which is 1.6 times the diffraction-limited width.

The pattern for the 5-μm laser shows a single central peak. The width of 1.6° to 1.8° is only about 1.2 times the diffraction limit. This single narrow peak indicates that the radiation is well concentrated in the fundamental supermode.

This work was done by Seiji Mukai, C. P. Lindsey, J. Katz, E. Kapon, A. Yariv, and S. Margalit of Caltech for NASA's Jet Propulsion Laboratory. For further information, Circle 85 on the TSP Request Card. NPO-16500

A Quick Visual Power-Supply Monitor

A tricolor LED displays high, low, and intermediate output voltages.

Marshall Space Flight Center, Alabama

Power-supply voltages can be quickly monitored by a circuit equipped with a light-emitting-diode (LED) display. An oper-

ator looking at the display can quickly spot whether power output voltage is above, below, or within the acceptable limits.

The circuit as shown in the figure can monitor power-supply voltages between 5 and 15 volts. It has two potentiometers:

AFTER 35 YEARS AS HIS EMPLOYER, TELL HIM ABOUT DIRECT DEPOSIT AS A FRIEND.

Make sure the people who have given you so much through the years get everything they've got coming in the years ahead.

Direct Deposit lets your retiring employees send their Social Security straight to their checking or savings account. It's free, and it lets them enjoy the good life they deserve.

As an employer, send for a free Direct Deposit retirement planning kit today, and pass the information along...to a friend.

Write to—Direct Deposit (D1),
U.S. Treasury, Annex 1, PB-1100,
Washington, DC 20226.



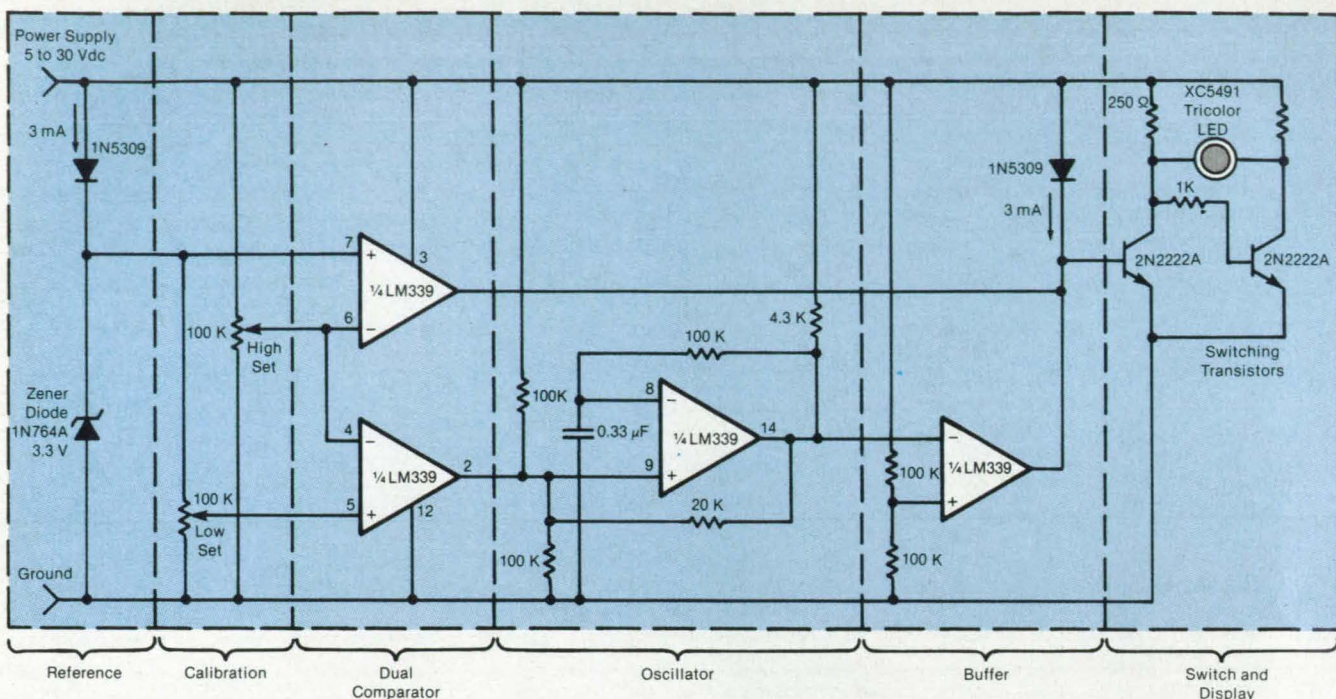
DIRECT DEPOSIT



A Public Service of This Publication & The Advertising Council

United States Treasury





This **Power-Supply Monitor** uses a tricolor LED display to indicate acceptable and unacceptable output voltages. A quick glance at the monitor shows the operator whether the voltage is above, below, or within the acceptable limits.

One to set the upper voltage limit, the other, the lower voltage limit. When the monitored voltage is above the set maximum, the LED display turns red. Yellow turns on for voltages below the set minimum, and green turns on for voltages between the high and the low settings.

The circuit does not need a separate

power supply. It is powered by the voltage it monitors.

Through simple modifications, the circuit can be adapted to monitor voltage differences between two power supplies. Should the monitored voltages differ by more than a set value, a visual or an audible alarm would warn the operator about

the difference. The circuit can also be modified for remote monitoring and the use of a separate power supply.

This work was done by Lloyd W. Taylor of The Johns Hopkins University, for Marshall Space Flight Center. No further documentation is available. MFS-26014

Controlling Transistor Temperature During Burn-In

A boiling refrigerant regulates temperature.

Marshall Space Flight Center, Alabama

A boiling refrigerant provides a simple temperature control for newly manufactured power transistors. Previously, transistor "burn in" — that is, operating the transistor continuously for an extended period to stabilize its characteristics — required a large heat sink to dissipate the heat generated at high power levels. Elaborate control electronics was also needed to maintain the transistor cases at the specified temperature.

The heat-transfer liquid is Fluorinert FC-77 (or equivalent). The liquid boils at 100° C, which is the specified temperature at which the transistor cases should be maintained during the burn-in with this technique. Refrigerants boiling at other temperatures might be used for burn-in at those temperatures, provided that they meet the requirements of safety and chemical compatibility with the compo-

nents under test.

The boiling fluid absorbs heat from the transistors without itself increasing in temperature, keeping the transistors within an acceptably narrow range between 98° and 101° C. In comparison with standard burn-in methods, more power can be dissipated in less area, and a large heat sink is not needed. Electronic controls are minimal, since the fluid itself regulates the transistor temperature.

The transistors are mounted on aluminum frames with cable harnesses for electrical power and grounding. The frames are lowered into an aluminum tank measuring 36 by 30 by 30 in. (91.4 by 76.2 by 76.2 cm). The tank is filled with the liquid to a level of 2 in. (5 cm) above the topmost row of transistors. A heavy aluminum lid containing coils of copper tubing is placed over the tank. Tap water flowing through the tubing keeps

the lid cool. Power to the transistors is turned on, and, as their temperature rises to about 100° C, the fluid starts boiling. The vapor condenses on the cool lid and returns to the tank.

Several safety controls are incorporated in the burn-in setup. A level sensor monitors the depth of liquid in the tank. A flow sensor measures the flow of water through the condensing coils. A conductivity probe monitors the liquid for the presence of water and other conductive contaminants. Thermocouples measure the case temperature of the transistors. If any of these instruments detects an abnormal condition, the burn-in system is automatically shut down.

This work was done by Bernard C. Scott of Martin Marietta Corp. for Marshall Space Flight Center. No further documentation is available. MFS-28076



I pledge allegiance to the flag of the United States of America. Unless, of course, my boss won't give me the time off because of meetings or inventory or my family has made plans for the weekend...

The National Guard and Reserve makes up a full one third of our nation's defense. They need one weekend a month and at least two weeks a year to train. When volunteers you know have to serve, don't give them a

hard time. We'd be a lot weaker without them. Protect their future while they protect yours. For more information, write Employer Support, Arlington, VA 22209. Or call 1-800-336-4590.



EMPLOYER SUPPORT OF THE GUARD & RESERVE

Keyboard With Voice Output

A voice synthesizer tells what key is about to be depressed.

Lyndon B. Johnson Space Center, Houston, Texas

A proposed keyboard would give an operator verbal identification of a key before it is actually pressed. The operator would lightly place a finger on the intended key, and a voice synthesizer would announce the key that has been selected. The operator could then follow through with the selection by pressing the key or could abandon the selection.

The verbal feedback is useful for blind operators or where dim light prevents a sighted operator from seeing the keyboard. It might also be used where the operator is busy observing other things — a remote manipulator for example — while keying data into a control system. In situa-

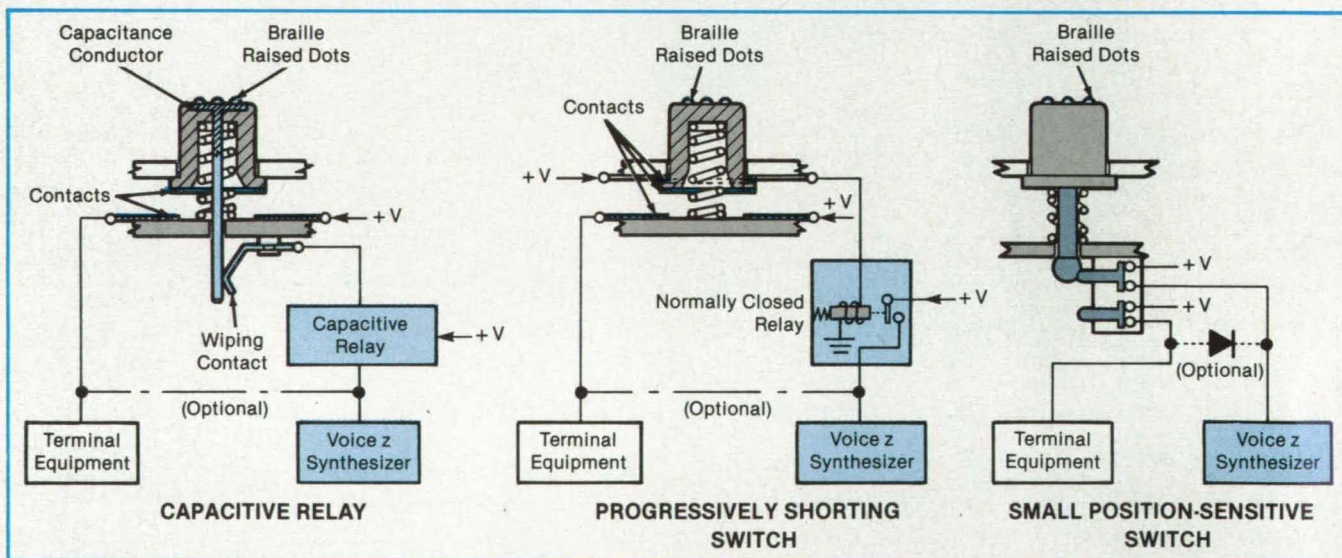
tions where correct data entry is critical, the feedback gives the operator added confidence. It can be used as a training aid for touch typing. It can also be used to train blind operators to use both standard and braille keyboards. The concept can be adapted to such equipment as typewriters, computers, calculators, telephones, cash registers, and on/off controls.

The voice synthesizer could be actuated by a light touch or by the proximity of a finger to a capacitive relay. Alternatively, the synthesizer could be actuated by a switch that is closed by a slight depression of the key (see figure): In this case, further depression would actuate the main switch

associated with this key. An audible beep or reactivation of the voice synthesizer could occur at this point to confirm that the key command has been received by the system. For further confirmation, the operator could depress another key to have the last character or group of characters reannounced.

This work was done by William C. Huber of **Johnson Space Center**. No further documentation is available.

Inquiries concerning rights for the commercial use of this invention should be addressed to the Patent Counsel, Johnson Space Center [see page 29]. Refer to MSC-20869.



A Variety of Electromechanical Devices can be used to actuate the voice synthesizer. In all of them, pushing the key to its limit will implement the command identified by the voice synthesizer.

Conductive Container for Semiconductor Devices

A container holds components securely while protecting them from electrostatic damage.

NASA's Jet Propulsion Laboratory, Pasadena, California

A container for semiconductor components not only protects them against mechanical damage but also ensures that they are not harmed by electrostatic dis-

charges. In addition, the container holds components in fixed positions so that they can be serialized and identified from their locations. The container is suitable for

holding components during both storing and shipping. Originally developed for microwave diodes, the container concept is readily adaptable to transistors and inte-

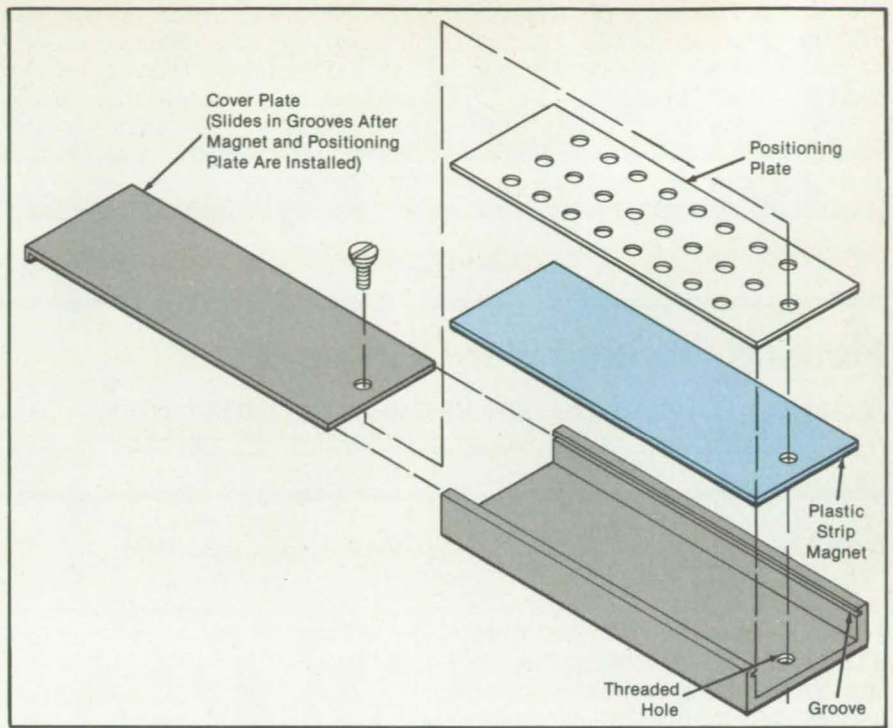
grated circuits.

When open, the container holds the components magnetically: Thus, the components must contain a magnetic alloy. One example is Kovar[®], an Fe/Co/Ni alloy commonly used in electronics to make glass-to-metal seals.

A plastic strip magnet is bonded to the container base with an adhesive. A positioning plate containing an array of holes (see figure) is placed over the strip magnet. The hole size and the plate thickness must be large enough to accommodate the components. A cover plate is slid into place along grooves in the sides of the container and fastened in the fully closed position with a screw.

The base, cover, and positioner plate are made of a conductive material such as metalized plastic. They thus exclude electric fields from the interior of the container and prevent electrostatic discharges into the components.

This work was done by John T. Rice of Caltech for NASA's Jet Propulsion Laboratory. For further information, Circle 66 on the TSP Request Card.
NPO-16110



A **Plastic Strip Magnet** is sandwiched between the container base and the positioning plate. A screw passes through the cover plate and engages a threaded hole in the base to complete the container assembly.

Low-Cost Humidity Sensor

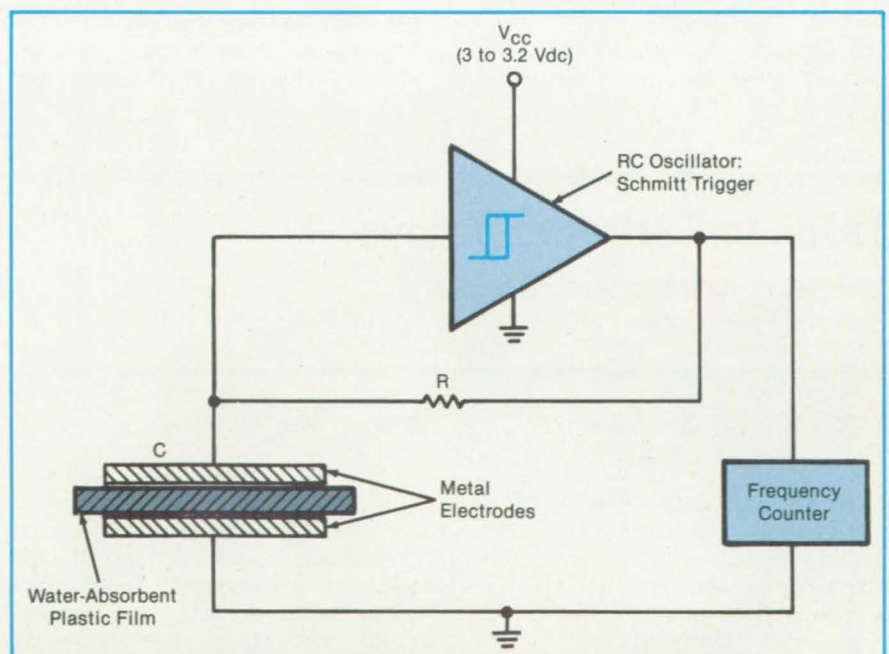
Moisture absorption changes frequency of an oscillator.

NASA's Jet Propulsion Laboratory, Pasadena, California

An electronic humidity sensor is simple, inexpensive, and produces an output that is readily used by indicator or control circuits. The sensor operates at a safe, low voltage and is relatively invulnerable to electrolysis effects.

The new sensor is a resistor/capacitor (RC) oscillator in which a water-absorbent plastic film is the insulator in the capacitive element. The capacitance of the film increases with the amount of water it absorbs from the air and thus reduces the oscillation frequency. A frequency counter produces a digital output that represents the change in frequency and hence the change in relative humidity. The sensor can be used to measure humidity in the atmosphere, in the soil, and in industrial gases, for example.

The RC oscillator is assembled from commercial components, except for the capacitor. A Schmitt-trigger-type integrated circuit is connected to the capacitor, which consists of a film of a commercially produced sulfonated fluorocarbon polymer, 2 inches (5.08 centimeters) square, sandwiched between perforated metal plates (see figure).



Moisture-Absorbing Plastic Film clamped between metal plates alters the capacitance in an RC circuit. Although sulfonated fluorocarbon is a good choice for the film because of its high water absorption and chemical resistance, such other materials as zirconia might also be used.

The oscillation frequency decreases almost linearly from about 100 to 16 kilohertz as the relative humidity increases from about 20 to about 76 percent.

The operating voltage is low enough that significant electrolysis of the absorbed water does not occur. The corrosion and polarization of electrodes that electrolysis

often causes are therefore not observed. The new sensor also offers better accuracy and resolution than do its predecessors, because frequency can be measured more readily than the picoampere or nanoampere currents produced as outputs in the older sensors.

This work was done by Eric G. Laue of

Caltech for NASA's Jet Propulsion Laboratory. For further information, Circle 68 on the TSP Request Card.

Inquiries concerning rights for the commercial use of this invention should be addressed to the Patent Counsel, NASA Resident Office-JPL [see page 29]. Refer to NPO-16544.

Floating-Emitter Solar-Cell Transistor

A conceptual transistor embedded in a photovoltaic diode promises to increase efficiency to more than 20 percent.

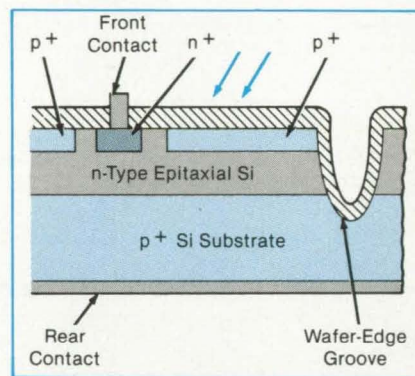
NASA's Jet Propulsion Laboratory, Pasadena, California

A proposed solar cell would incorporate a junction transistor for greater efficiency. Whereas the best conventional solar cells are about 15 percent efficient, the new device promises efficiencies greater than 20 percent.

The solar-cell transistor would have a front-surface contact, a rear contact, and a floating emitter. The figure shows one of the promising types of solar cells. A variety of other contact and junction configurations are possible, but in contrast with the one in the figure, they do not offer ease of fabrication in combination with high performance.

An n-type epitaxial layer of 50 μm thickness would be deposited on a 300- μm p^+ substrate. The relatively high thickness of the substrate makes the 3- to 6-in. (7.6- to 15.2-cm) silicon wafer less susceptible to breakage than ordinarily.

The processing steps are well known and within the capability of very-large-



The **Solar-Cell Transistor** has both front and back electrical contacts and an emitter/base/collector structure. The deep groove isolates the p^+/n junction from saw damage and electronic edge effects.

scale-integration technology. With an epitaxial layer thin enough so that the forward and reverse common-base current gains are near unity, and with all possible elec-

tron/hole recombination losses minimized, the open-circuit voltage will be high, the short-circuit current loss will be minimal, and efficiency will be greater than 20 percent. The rear collecting junction should also boost the open-circuit voltage and short-circuit current.

The solar-cell transistor would be relatively immune to variations in the common-emitter current gain between devices. Even for a 2-to-1 spread in this gain, the open-circuit voltage will vary only about 20 mV.

This work was done by Chih Tang Sah and Li Jen Cheng of Caltech for NASA's Jet Propulsion Laboratory. For further information, Circle 15 on the TSP Request Card.

Inquiries concerning rights for the commercial use of this invention should be addressed to the Patent Counsel, NASA Resident Office-JPL [see page 29]. Refer to NPO-16467.

Tester for Distress Beacons

Onboard monitor checks distress beacons en route.

Goddard Space Flight Center, Greenbelt, Maryland

Distress beacons on aircraft and boats can be checked for proper operation with the aid of the onboard monitor shown in the figure. The monitor:

- Determines whether a beacon is ready to transmit a distress signal,
- Checks the beacon by making it transmit a nondistress test signal on the distress frequency, and
- Resets the beacon for emergency use

after completion of the test.

The monitor is mounted in the aircraft cockpit or at the wheel of a boat. It is connected to the beacon electronics by a cable. The monitor is used with interface circuitry in the beacon, which acts as a buffer so that operation of the beacon is not adversely affected if the monitor is removed or if the connecting cable is accidentally short circuited.

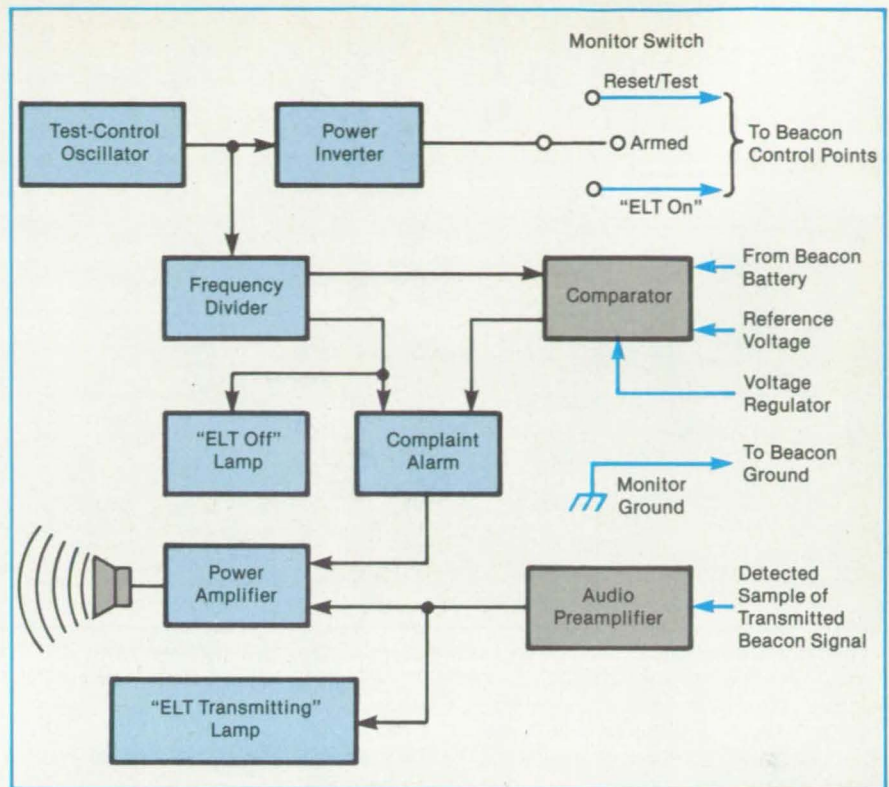
The monitor is used with emergency locating transmitters (ELT's) on aircraft and emergency position-indicating radio beacons (EPIRB's) on boats. Both the ELT's and the EPIRB's are essentially the same systems, transmitting an internationally recognized distress signal at 121.5 or 243 MHz, except the ELT's are activated by impact, and the EPIRB's by contact with water.

To test an ELT, a pilot sets the monitor

control switch to the reset/test position (see figure). The monitor then bypasses the impact-actuated switch and turns the beacon on. At the same time, the monitor disables the frequency modulator in the beacon audio-signal generator, which ordinarily repeatedly sweeps from about 1,600 to about 300 Hz two to four times per second (the distress signal required by law). Consequently, the transmitter is operating but emits a single tone not recognized as a distress signal: This prevents false alarms. If the beacon operates properly, the monitor emits the modulating tone and lights a lamp labeled "ELT transmitting."

When the pilot sets the monitor switch to the "armed" position, the beacon is ready to transmit a real distress signal. If the beacon battery power drops excessively or if the beacon starts transmitting, the monitor will illuminate indicator lamps and sound an alarm. The pilot also has the option of actuating the beacon distress signal manually by turning on the monitor switch.

Although ELT's transmit a standard distress signal and have similar circuits, there are some differences among units in switching the distress signal. Some are electrically latched, some mechanically. With mechanical latching, the switch stays closed once it is activated by impact. With electrical latching, the impact switch is closed only temporarily, but it turns on a silicon-controlled rectifier, which then remains latched in conduction. These differences entail slight differences in some parts of the monitor and interface circuits devoted to bypassing the impact switch. Since an EPIRB has no impact switch, it is



The **Aircraft Version of the Remote Monitor** supplies the pilot with visual and aural information about the condition of the distress beacon, which is usually placed near the tail.

not necessary to provide for bypassing it in the monitor.

This work was done by William R. Wade of Proteon, Inc., for **Goddard Space Flight Center**. For further information, Circle 70 on the TSP Request Card.

This invention is owned by NASA, and a

patent application has been filed. Inquiries concerning nonexclusive or exclusive license for its commercial development should be addressed to the Patent Counsel, Goddard Space Flight Center [see page 29]. Refer to GSC-12892.

Control Electronics for Solar/Flywheel Power Supply

Energy is automatically put into or taken out of flywheel motion.

Marshall Space Flight Center, Alabama

A control circuit automatically directs the flow of electrical energy to and from a motor with a flywheel that constitutes the storage element of a solar-power system. When the insolation is sufficient for charging, power is supplied by the solar-cell array to the load and to the motor. During periods of darkness, the motor is made to act as a generator, drawing kinetic energy from the flywheel and supplying it to the load.

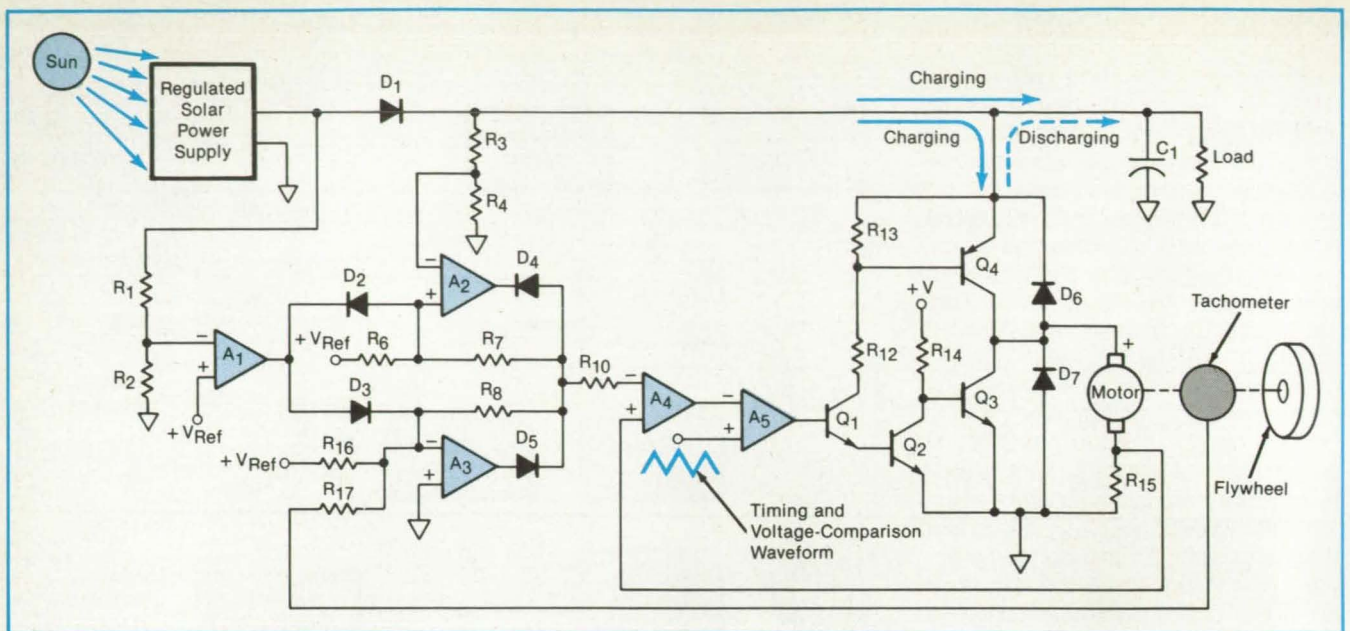
The control circuit (see figure) includes voltage comparators and amplifiers that measure the load voltage, source voltage, motor speed, and motor current. The motor-current feedback signal is derived

from the voltage across a series resistor, while the tachometer output voltage serves as the motor-speed feedback. The control signals developed by the amplifiers and comparators are applied to the switching transistors that commutate the motor current.

Pulses of voltage from the power-supply bus are applied to the motor at a typical repetition rate of 10 kHz. The repetition rate is that of an externally-generated sawtooth timing and voltage-comparison signal. The effective current and voltage applied to the motor, and therefore the average torque, are controlled by varying the pulse duration.

In the energy-storing (accelerating) mode, the pulses are sufficiently long to overcome the back emf of the motor and to force the accelerating motor current to a commanded value. When the motor speed reaches the maximum allowable, the pulse duration is reduced to a value just great enough to overcome frictional losses and maintain constant speed.

When the insolation is below the minimum for charging, the pulse duration is shortened. The back emf of the motor is allowed to force a reversal of the motor current, so that the motor supplies power to the bus. The average voltage applied to the load by the motor is adjusted by vary-



A **Feedback Control Circuit** adjusts the duration of voltage pulses applied to a motor in the energy-storing (accelerating) mode. It adjusts the duration of back-emf pulses applied to the load in the energy-withdrawing (decelerating) mode.

ing the duration of the back-emf pulses. The pulses are filtered out of the line voltage by the capacitor.

This work was done by Frank J. Nola of Marshall Space Flight Center. For fur-

ther information, Circle 26 on the TSP Request Card. MFS-25978

Reduced-Stress Mounting for Thermocouples

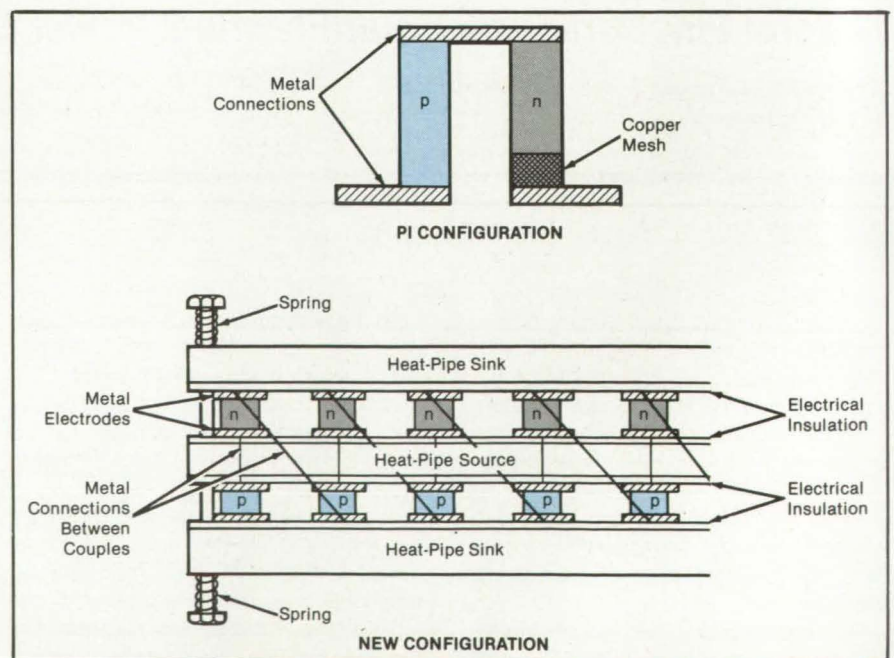
Mounting accommodates widely different coefficients of thermal expansion.

NASA's Jet Propulsion Laboratory, Pasadena, California

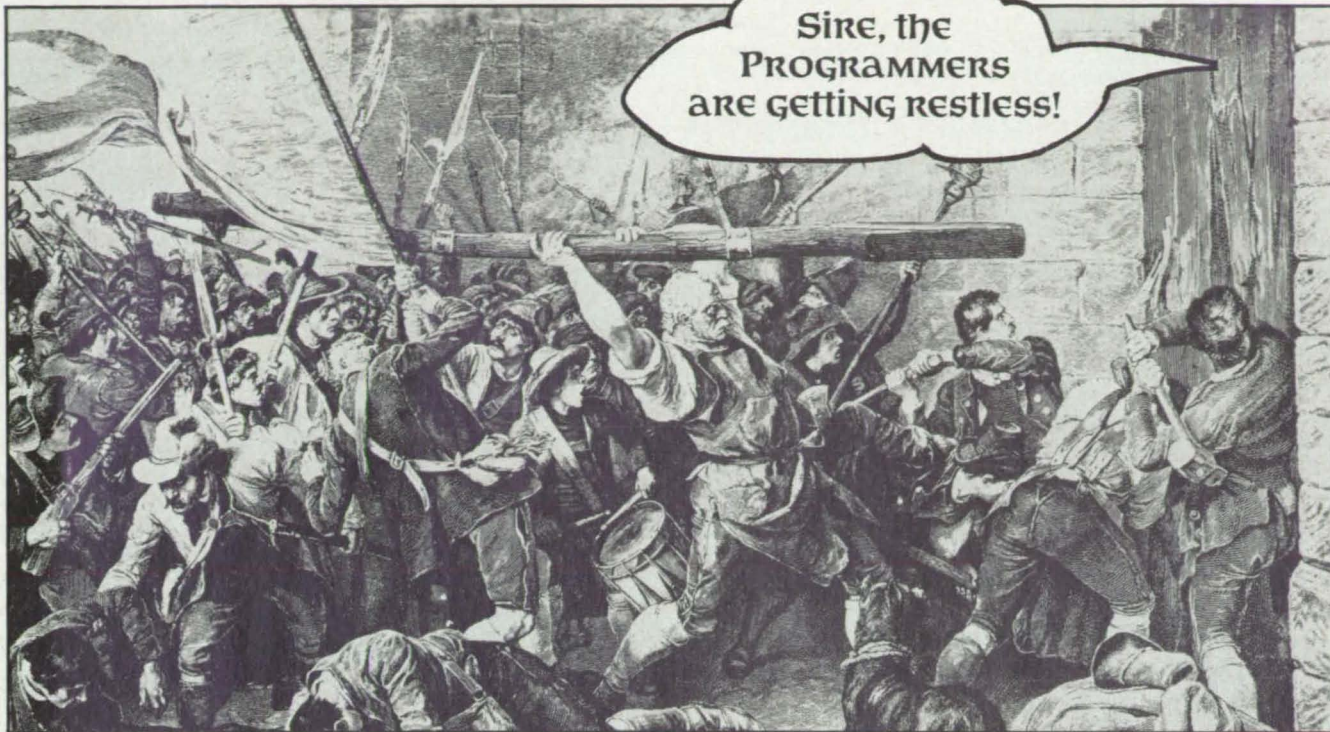
A way of connecting semiconductor materials in thermoelectric energy converters can reduce the stress caused by thermal expansion. The concept was originally developed for semiconductor thermocouples composed of lanthanum sulfide (the negative material) and boron carbide (the positive material). With increasing temperature, these semiconductors expand at different rates. When the different materials are joined, the stress due to the unequal expansion can result in eventual fatigue failure.

The conventional "pi" configuration for semiconductor thermocouples was adapted to lanthanum sulfide/boron carbide thermocouples by the addition of a copper wire mesh to one leg of the couple (see top of figure). The mesh can be compressed and expanded to accommodate thermal changes in dimensions of the legs.

In the new method (see bottom of figure), the legs of the thermocouple would be placed in separate n- and p-type arrays. The two arrays would contact a common heat pipe as a source but would have separate heat-pipe sinks. Wires would connect



Instead of Parallel n and p Legs in the pi configuration (above), legs of each type are arrayed together (below). The legs in each array change dimensions with temperature at a uniform rate.



On November 18, 1985, at SIGAda in Boston, ALSYS will open the doors to Ada . . .

With Ada compilers for 15 computer models

Apollo Domain DN300, DN320, DN330, DN400,
DN460, DN550, DN600, DN660.
SUN Workstations 2/50, 2/100, 2/120, 2/160, 2/170.
Hewlett-Packard 9000, Series 200, 300.

With an Ada cross-compiler

DEC VAX 11/730, 11/750, 11/780, 11/785, and MicroVAX I
Cross-Compiler to Altos ACS 68000.

With Ada training products

You Know Fortran—Ada is Simple
(12 Lesson Computer-Aided Instruction for those
who know Fortran.)

Lessons on Ada

(2-Volume, 27 lesson CAI course running on IBM-
PC and VAX.)

Ichbiah, Barnes and Firth on Ada

(27 video tape overview of Ada by language
designers.)

With Ada programming tools

AdaQuery

(Complete, searchable on-line Ada Language Refer-
ence Manual.)

AdaViewer

(Unique viewing tool for Ada programmers.)

With more compilers in development

IBM-370 Compiler under development at Alsys Ltd., U.K.

Hewlett-Packard 1000 Series A900 Compiler under de-
velopment at Alsys Ltd., U.K.

IBM-PC/AT and IBM-PC/XT Compilers under develop-
ment at Alsys, Inc., U.S.

Alsys, Inc. • 1432 Main Street • Waltham, MA 02154 • U.S.A. • Phone: (617) 890-0030 • Telex: 948536

Alsys, S.A. • 29, Avenue de Versailles • 78170 La Celle St. Cloud • France • Phone: (3)918.12.44 • Telex: 697569

Alsys, Ltd. • Partridge Hse. Newton Road • Henley-on-Thames • Oxon RG9 1EN, England • Phone: (0491) 579090 • Telex: 846508

© Ada is a registered trademark of the U.S. Government (AJPO).

metal electrodes on each n-type element to electrodes on the neighboring p-type elements. An electrically insulating layer would isolate the heat pipes from the legs while allowing heat transfer.

The net expansion (or contraction)

would be taken up by a spring mounting on the heat-pipe sinks. Temperature-induced stresses on the elements would thus be limited to those caused by the spring forces. The spring mounting would also support the sinks, eliminating much of the

support load on the fragile semiconductor legs.

This work was done by Charles Wood of Caltech for NASA's Jet Propulsion Laboratory. For further information, Circle 67 on the TSP Request Card. NPO-16513

Determining Internal Connections in Capacitors

A simple test shows which terminal is connected to the outer foil.

NASA's Jet Propulsion Laboratory, Pasadena, California

A simple electrical test shows which of two capacitor terminals is connected to the outer capacitor foil. The test makes it unnecessary to resort to X-ray inspection to distinguish the terminals.

For maximum reliability, the outside foil of a high-voltage capacitor should be connected to a particular point in a circuit — for example, to ground or to a low voltage. It is therefore necessary to determine which terminal is connected to the outer foil. The terminals are not always labeled on the component and, in some cases, are incorrectly labeled.

The test requires an oscilloscope and a square-wave signal generator with a source impedance of about 500 ohms. The signal-generator output is adjusted to about 10 V rms without an external load.

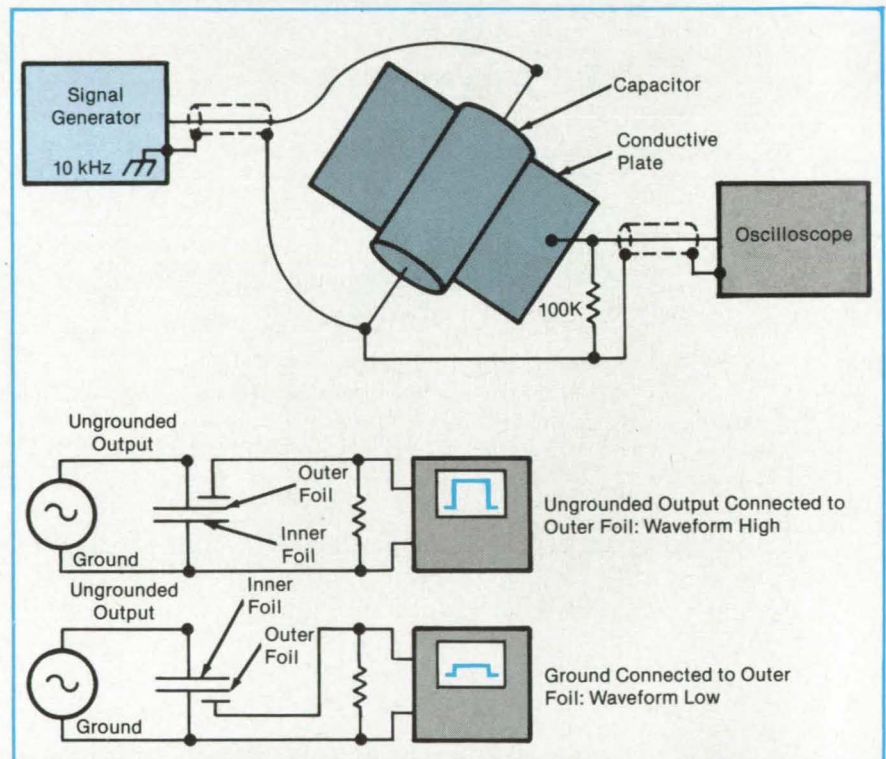
The oscilloscope probe is attached to a conductive plate that is placed under the capacitor (see figure). The oscilloscope ground is attached to one of the capacitor terminals and to the signal-generator ground. The ungrounded signal-generator output lead is connected to the other capacitor terminal.

The operator observes the display, reverses the capacitor terminals, and observes the display again. The display will show a higher voltage waveform when the ungrounded lead of the signal generator is attached to the outer capacitor foil.

The test can also be used to determine internal connections in multiple-element capacitors. In that case, the conductive plate has to be about as narrow as each

element. The strip is placed against the side of each element while the terminals are connected first one way, then the other. Again, a high reading on the oscilloscope identifies the outer-foil-connected terminal.

This work was done by Frank M. Ott and Michael F. Hanna of Caltech for NASA's Jet Propulsion Laboratory. For further information, Circle 79 on the TSP Request Card. NPO-16499



When the Outer Foil of a Capacitor is attached to the ungrounded signal-generator output lead, the oscilloscope displays a higher waveform amplitude. When the outer foil is joined to the grounded signal-generator output lead, the waveform amplitude is lower.

Accelerating Corrosion in Solar-Cell Tests

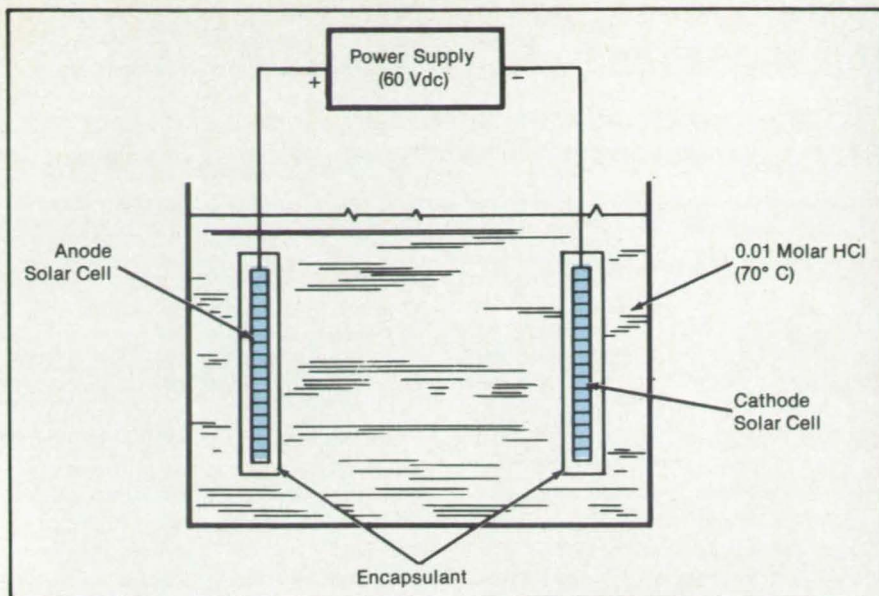
The degradation of metal contacts becomes evident in a few hours.

NASA's Jet Propulsion Laboratory, Pasadena, California

A simple electrochemical technique for accelerated testing of solar cells aids in

identifying corrosion mechanisms. Although developed specifically for cells with

Ti/Pd/Ag contacts, the technique can readily be adapted to other metal combinations.



In a **Simple Electrochemical Cell**, two silicon solar cells serve as an anode and cathode, respectively. The electrolytic medium and the voltage between them accelerate corrosion and migration interactions between the cell metal contacts and the plastic encapsulant.

A study employing the technique showed that the solar-cell encapsulant acts as an electrolyte that contributes to corrosion by allowing silver to migrate from the metal contact grid. The silver in the encapsulant reduces its transparency and thereby reduces cell efficiency. This finding was supported by measurements of the electrical performances of solar cells: Power output dropped because of corrosion products in the encapsulant around the metal contacts. According to the study, ethylene-vinyl acetate (EVA) copolymer is superior as an encapsulant to the commonly used polyvinyl butyral (PVB) because silver migration was detected in PVB but not in EVA.

A one-compartment electrochemical cell is used in the accelerated-corrosion-testing technique (see figure). Two encapsulated solar cells are immersed in 0.01 molar hydrochloric acid, a concentration that yields the requisite low pH of 2 for accelerated testing. A potential of 60 V is applied between the solar cells so that one becomes an anode, the other a cathode. This potential is typical of that between cells

and between cell strings and grounded metal frames in solar-cell modules. The electrolyte temperature is 70° C — well below the 100° C limit of encapsulation materials but high enough to accelerate corrosion.

In the study, the anode solar cells were removed from the electrolyte after 27 hours of immersion, and encapsulants were removed from the cells. Both the metal contact grids and the encapsulants were analyzed chemically. Scanning electron microscopy, energy-dispersive X-ray analysis, and electron spectroscopy were used.

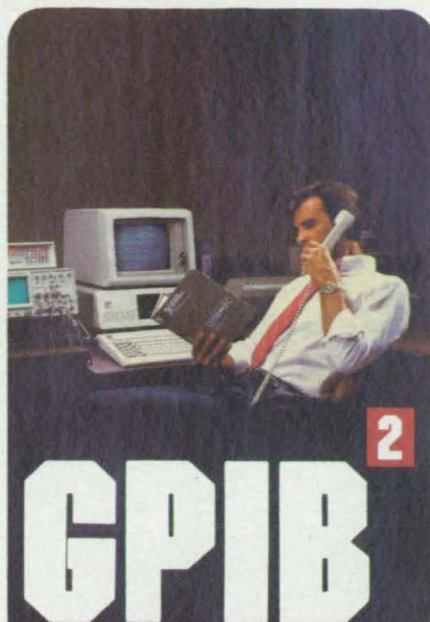
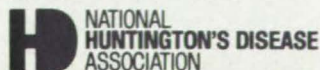
In PVB-encapsulated cells subjected to accelerated testing, only palladium and titanium were detected on the silicon wafer; no silver was present. The encapsulants, however, contained silver oxide, which was probably a product of silver from the metalization that was anodically oxidized in the electrochemical cell.

In the cathode solar cells, the encapsulants were largely delaminated after the test immersions. The delamination is attributed to the cathodic evolution of hydrogen gas on the metal surfaces.

This work was done by Hoda M. Shalaby of Caltech for NASA's Jet Propulsion Laboratory. For further information, Circle 21 on the TSP Request Card. NPO-16096

Imagine.

Imagine. With your help, our generation could be the one that beats Huntington's... forever. Please give generously to the National Huntington's Disease Association.



GPIB

IEEE-488 Interfaces and Bus Extenders For:

IBM PC, PCjr & COMPATIBLES

DEC UNIBUS, Q-BUS & RAINBOW 100

MULTIBUS, VMEbus STD & S-100

Full IEEE-488 functionality, with the most comprehensive language and operating system coverage in the industry. It takes experience to make IEEE-488 systems work with nearly 4000 devices available from more than 500 different manufacturers, and experience is what enables National Instruments to take the GPIB to the second power and beyond.



2 Your personal guarantee of unsurpassed customer support and satisfaction. CALL 1-800-531-GPIB for instant access to 100+ man-years of GPIB experience.

NATIONAL INSTRUMENTS
12109 Technology Blvd.
Austin, TX 78727
1-800-531-5066 512/250-9119
Telex: 756737 NAT INST AUS

IBM and PCjr are trademarks of International Business Machines. MULTIBUS is a trademark of Intel. DEC, UNIBUS, Q-BUS, and Rainbow 100 are trademarks of Digital Equipment Corporation.

Electronic Systems



Hardware, Techniques, and Processes

- 62 **Vibration-Free Raman Doppler Velocimeter**
- 63 **Modular, Fast, Two-Dimensional Cyclic Convolver**
- 64 **Rotating Capacitor Measures Steady Electric Fields**
- 65 **Generating Tunable Far-Infrared Laser Sidebands**
- 66 **Convolver for Pipelined-Image Processor**
- 67 **Single-Chip VLSI Reed-Solomon Encoder**
- 68 **Automatic Guidance for Remote Manipulator**
- 69 **Testing Electronic Devices for Single-Even Upset**
- 70 **Measuring Antenna Signal Delays**
- 74 **Multiplier Architecture for Coding Circuits**
- 76 **Improved Electronic Control for Electrostatic Precipitators**
- 77 **Picture-Element Comparator**
- 77 **Programable Pipelined-Image Processor**
- 78 **Function Generator for Image Processor**

Computer Programs

- 79 **Design of Linear Quadratic Regulators and Kalman Filters**

Vibration-Free Raman Doppler Velocimeter

Nonintrusive measurements of gas velocity, temperature, and pressure are possible in a highly vibrational environment.

Langley Research Center, Hampton, Virginia

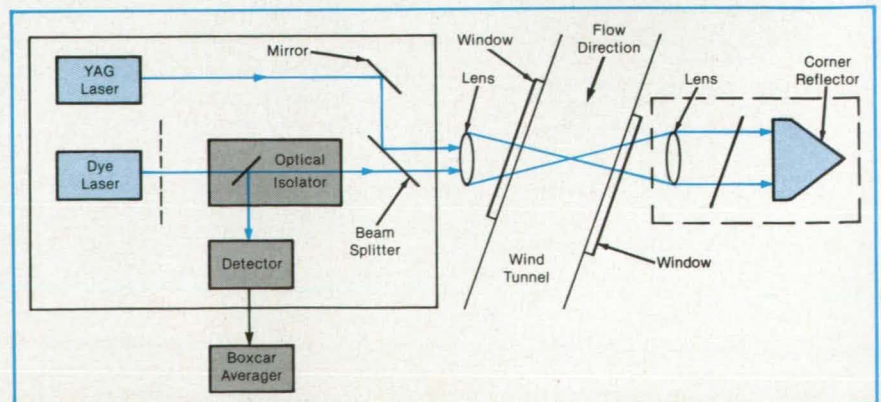
Laser Doppler velocimetry (LDV) has been used extensively for measuring flow velocities by tracking particles seeded into the flow. The seeding requirement, however, is often undesirable and sometimes impractical. A new method is under development to measure the flow velocity of the molecules directly by nonintrusive laser techniques. This method, combined with a vibration-free design, makes the flow-velocity measurements practical in severe vibrational environments.

The method is based on the Raman scattering of light from specific molecules in the flow, such as N_2 , O_2 , or H_2 . If the molecules are moving, the scattered light also exhibits a Doppler shift in frequency. The shift in the Raman spectra, therefore, can be related directly to the velocity of the molecules. Spontaneous Raman spectroscopy with a single laser could, in principle, be used, but weak signals and inadequate spectrometer resolution preclude such a measurement. The use of coherent (stimulated) Raman spectroscopy increases the signal by orders of magnitude and has a considerably higher resolution due to the narrow line widths associated with lasers.

In one version of coherent Raman spectroscopy, called stimulated Raman gain spectroscopy (SRGS), two lasers interact with the molecules, and the difference in frequency between these lasers is adjusted to be in resonance with a Raman shift exhibited by a specific molecule. Many geometrical arrangements can be envisioned for these two lasers. Two configurations, however, define the limits to their interactions with the molecules; namely, forward and backward scattering.

In forward scattering, the moving molecules "see" two laser beams, the frequencies of which are shifted in the same (spectral) direction and by about the same amount; hence, there is very little Doppler shift (and breadth) by which to measure velocity. In backward scattering, on the other hand, the molecules "see" one laser beam shifted in one spectral direction, while the other laser beam is shifted in the opposite direction. This results in a large Doppler shift (and breadth) that is considerably easier to measure. The ratio of Doppler shift to breadth is actually the same in both cases, but the larger shift exhibited in backward scattering (typically 15 times that for forward scattering) is easier to measure since it relaxes the stability and line width requirements placed on the lasers. This concept for measuring molecular velocities has been demonstrated in the laboratory, but the double-ended configuration employs tightly focused, counter-propagating laser beams and would be impossible to apply in severe vibrational environments such as in wind tunnels.

The solution to this problem is to mount both lasers on a single optical table and retroreflect one of the beams back onto itself. If this is done with a corner cube and lens (in effect, a retroreflector), as shown in the figure, the retroreflected beam is brought to the same focal point as the forward-directed beams. This situation occurs since a corner cube sends light back in the same direction from which it came. A lens is used to render a collimated (parallel) beam incident on the corner cube. This combination renders the desired focal point (within optical tolerances set by the



Raman Scattering and Retroreflection combine to yield a useful technique for wind-tunnel gas-flow mapping.

individual components) for the retro-reflected beam. The result is that this retro-reflected focal point is practically independent of lateral or rotational movements of the retrometer. In this manner, counter-propagating focused beams are easily attained with the simple requirement that the forward beams strike the retrometer. The retrometer can be moved (shaken) relative to the laser table, but this motion will not impact the overlapping of the two counter-propagating beams. Vibration-free overlap of the two counter-propagating beams is therefore attained.

The laser pump beam (directed toward the retrometer) simultaneously interacts with the probe beam in both the forward and backward directions. The detector will first sense a signal (gain/loss) from the backward scattering, followed by a signal from the forward scattering. The latter signal will be observed at a later time, given by the round-trip time for the probe beam to travel from the focal point to the retrometer

and back. Since the speed of light is about 1 foot (0.3 meters) per nanosecond and since the round trip is typically 10 feet (3 meters), this delay is about 10 nanoseconds, easily discriminated with a boxcar averager.

Thus, an additional advantage of the retrometer configuration is the nearly simultaneous observation of both forward and backward scattering. In this mode, the forward-scattered spectrum is essentially unshifted with respect to the backward-scattered spectrum and provides a nearly-zero-shift frequency reference. In other words, there is no requirement in this setup for an absolute frequency reference. It is also possible to measure the translational temperature of the gas by measuring the breadth (predominantly Doppler broadened) of the backward-scattered line.

Finally, the breadth of the forward-scattered line can be related to the pressure of the gas, since pressure broadening generally dominates over Doppler broadening in this case. Thus, the use of this system results in

a vibration-free velocimeter in which both forward and backward scattering can be observed simultaneously, yielding noninvasive point measurements of velocity, temperature, and pressure with a single optical system.

This work was done by Reginald J. Exton of Langley Research Center. Further information may be found in NASA TM-85808 [N84-25433/NSP], "Molecular Velocimetry Using Stimulated Raman Spectroscopy" [\$7]. A copy may be purchased [prepayment required] from the National Technical Information Service, Springfield, Virginia 22161.

This invention is owned by NASA, and a patent application has been filed. Inquiries concerning nonexclusive or exclusive license for its commercial development should be addressed to the Patent Counsel, Langley Research Center [see page 29]. Refer to LAR-13268.



Modular, Fast, Two-Dimensional Cyclic Convolver

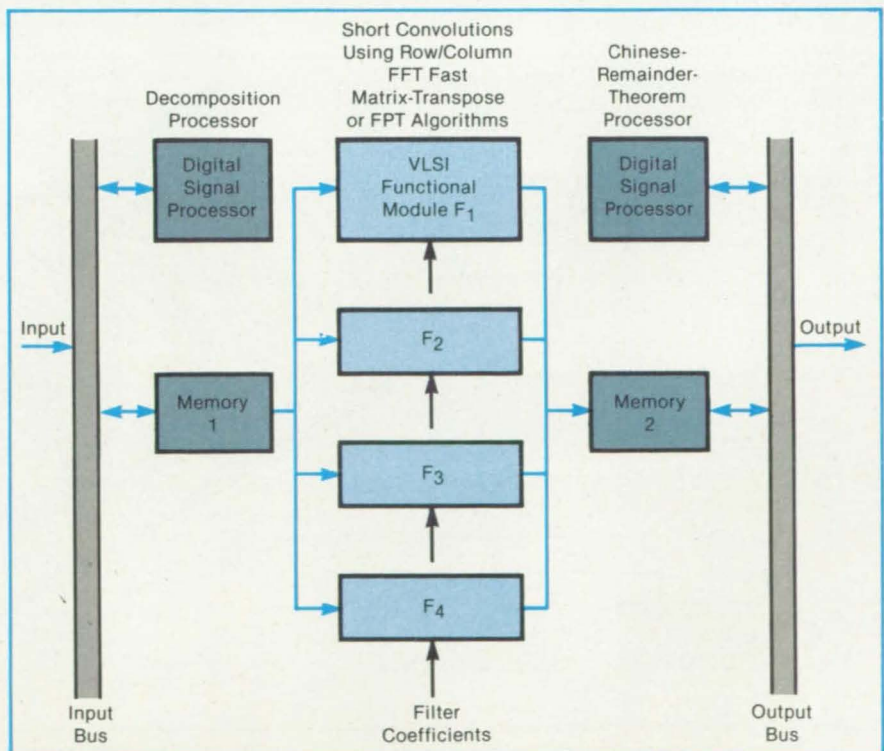
A synthetic-aperture-radar processor would include VLSI units to reduce cost, size, and power dissipation.

NASA's Jet Propulsion Laboratory, Pasadena, California

A proposed high-throughput, real-time synthetic-aperture-radar (SAR) processor would be built using a new, modular, two-dimensional cyclic convolver architecture based on polynomial factorization and designed for very-large-scale integrated (VLSI) circuitry. The new architecture would reduce the cost, size, and power dissipation of an SAR processor in comparison to the high-speed array-processor approach. The processor could also be used for other image- and data-processing applications involving two-dimensional Fourier transforms.

Present VLSI digital signal-processor chips are too slow and have too little on-chip memory to process the large SAR data arrays directly in real time. In the current state of the art, the fabrication of faster VLSI chips would lead to higher cost, lower yield, lower logic-component density, and higher power dissipation.

The new architecture circumvents these deficiencies by using an algorithm that transforms the calculation of the SAR two-dimensional cyclic convolution of a large data array into a form in which a group of identical two-dimensional cyclic convolver chips operates in parallel on a group of smaller data arrays. Three fast



A Fast, Modular, Two-Dimensional Cyclic Convolver would process large two-dimensional data arrays. The convolver includes VLSI signal processor chips that operate in parallel.

convolution algorithms that could be used in the chips are the row/column fast Fourier transform (FFT), the fast matrix transpose, and the fast polynomial transform (FPT).

The smaller data arrays are obtained from the original array by a decomposition process based on polynomial factorization. In this process, the two-dimensional convolution of the original array is first reexpressed as an N-point one-dimensional polynomial convolution and then decomposed into two N/2-point polynomial convolutions. This decomposition process is

repeated as many times as necessary to break the problem down into pieces small enough to be handled by the available chips.

The figure illustrates a case with two-level decomposition: The desired cyclic convolution of the original data array is obtained by using four VLSI convolvers in parallel on four smaller arrays, each containing one-fourth as many elements as the original array. The first digital signal processor (DSP), the decomposition processor, calculates the smaller arrays from the original array. The second DSP uses the Chi-

nese Remainder Theorem (CRT) to calculate the convolution of the original array from the convolutions of the four smaller arrays. The decomposition, convolution, and CRT circuits are pipelined so that they all operate simultaneously for high system throughput.

This work was done by Kuang Y. Liu of Caltech for NASA's Jet Propulsion Laboratory. For further information, Circle 31 on the TSP Request Card. NPO-16379

Rotating Capacitor Measures Steady Electric Fields

Rotating electrodes with self-contained electronics produce remote readings.

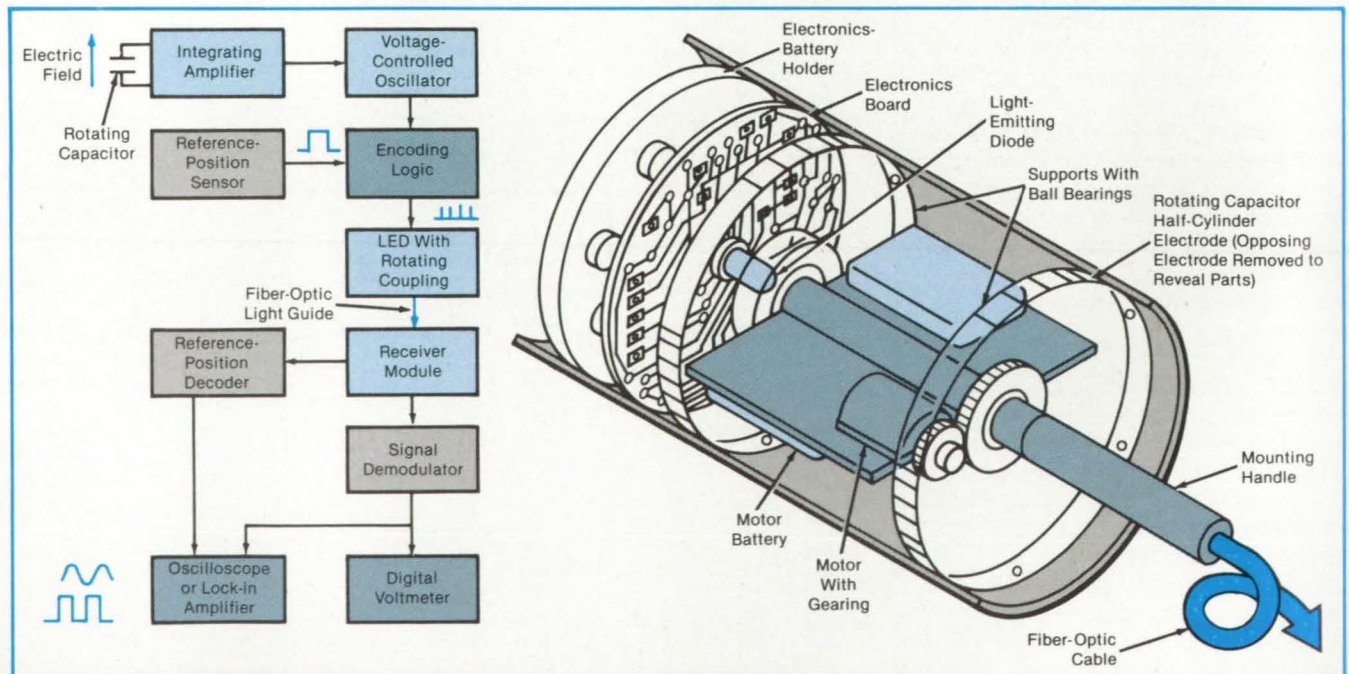
NASA's Jet Propulsion Laboratory, Pasadena, California

A portable sensor measures electric fields created by dc powerlines or other dc-high-voltage sources. It measures fields from 70 to 50,000 V/m with a linearity of 2 percent. The sensor can be used at any height above the ground. It measures both the magnitude and the direction of the field and provides signals representing these measurements to a remote readout device. The sensor functions with minimal disturbance of the field it is measuring.

The sensor employs a pair of opposed semicylindrical electrodes that rotate about their axis of symmetry (see figure). The electrodes constitute a capacitor: The electric field charges the capacitor and, as the electrodes rotate, the charges are exchanged between electrodes as alternating current at the rotational frequency. An operational amplifier measures the charge thus produced and generates a periodic signal of amplitude proportional to the field

magnitude. This signal modulates a voltage-controlled oscillator, which produces a train of pulses, the frequency of which varies from a central value of 10 kHz in proportion to the field magnitude.

So that the direction as well as the magnitude of the field can be determined, a phototransistor on the rotating electrodes passes before a stationary light-emitting diode (LED) once every revolution. The phototransistor, stimulated by the LED, pro-



Rotating Electrodes, consisting of half-cylindrical shells, cut through an electric field and gather charge as they do. Electronic circuitry gathers and processes the charge and generates synchronizing signals so that the magnitude and direction of the electric field are measured. The circuitry is mounted on a board that rotates with the electrodes.

vides reference pulses to the encoder. The phase relationship between the frequency of the field-magnitude pulses and the reference pulses is a measure of the angle of the field, and an encoder adds this information to the digital pulse train.

The signal-processing electronics rotate with the electrodes. An LED on the sensor converts the digital output of the encoder to light pulses for transmission by a fiber-optic light guide. A rotary optical coupler transfers the encoded light pulses to the light-guide cable. At the remote read-out device, the pulses are decoded and

displayed as field magnitude and direction.

A small dc motor drives the electrode shaft. A 9-V battery powers the motor. With a fresh battery, the sensor rotates at approximately 2,400 rpm. The rotational speed decreases as the battery is used, but the electric-field readout is independent of the speed within 1 percent down to about 600 rpm. Separate watch batteries supply power to the electronics. In its present form, this circuitry draws 8 mW.

The motor, batteries, electronics, and light-guide coupler are housed within the rotating electrodes, which form a cylinder

8 cm in diameter and 20 cm long. The size can be reduced to approximately 1 by 2 cm in a subsequent refined version. With a sensor this size, fields that are relatively uniform over only a few centimeters can be charted, and data can be gathered on electric fields after they have been perturbed by animals or humans.

This work was done by Alan R. Johnston, Harold Kirkham, and Bjorn Eng of Caltech for NASA's Jet Propulsion Laboratory. For further information, Circle 92 on the TSP Request Card. NPO-16550

Generating Tunable Far-Infrared Laser Sidebands

A new tunable source extends infrared spectroscopy into far infrared wavelengths.

NASA's Jet Propulsion Laboratory, Pasadena, California

A laser sideband source generates coherent radiation of continuously variable frequency at submillimeter and far-infrared wavelengths. Immediate applications are as a local oscillator for heterodyne systems and as a tunable source for spectroscopy.

The tunable far-infrared output is the sidebands produced by the mixing of signals from a fixed-frequency far-infrared laser and a tunable klystron. In the experimental apparatus (see figure), the laser beam is first passed through a polarizing Michelson interferometer. The polarizers are polyester-backed wire grids positioned so that the laser beam passes through each one without change other than a 10-percent attenuation.

An off-axis parabolic mirror with a focal length of 2.2 cm focuses the laser beam onto the mixer, which is a GaAs Schottky-barrier diode at the apex of an open corner-cube reflector. The laser power is quasi-optically collected and coupled to the mixer by a 1.7-mm-long phosphor bronze whisker antenna. The diode is soldered to a post that passes through the center of a waveguide in the corner cube.

Millimeter-wave radiation is generated by the klystron, then chopped by a ferrite modulator at the frequency best suited to the detector used to monitor the sidebands. The chopper output then passes into the waveguide and to the mixer.

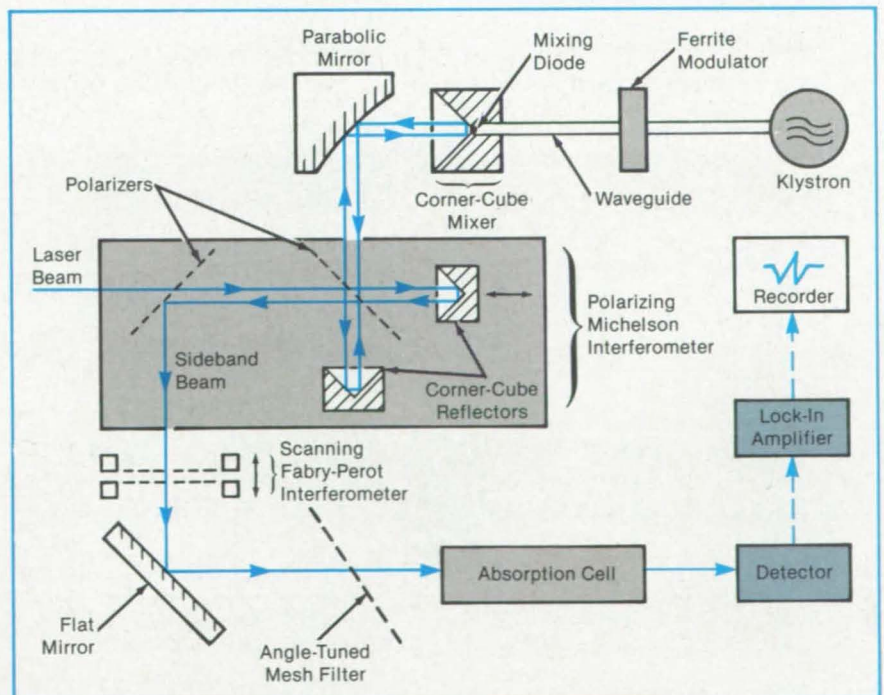
The laser and klystron signals are mixed nonlinearly in the diode, producing sidebands at the sum and difference frequencies. The unused laser power and the sideband power return to the interferometer along the path of the incident laser beam. The interferometer path difference is chosen so that the sideband polarization is

rotated by 90°, and the laser beam is not rotated.

In an ideal Michelson interferometer, all the sideband power and none of the laser power would be reflected out. Because of imperfections in the polarizers and their positioning, some laser power leaks through with the sidebands. A tunable Fabry-Perot interferometer filters most of the laser power out of the beam and selects the desired sideband. Further sup-

pression of the laser component is obtained with a mesh filter that acts as a sharp notch (narrow-band-rejection) filter. The notch frequency is tuned by adjustment of the angle of the filter with respect to the beam.

An absorption cell for spectroscopic studies is placed in the output path. The cell is filled with a material having a spectral absorption line within the frequency range of the mixer output. As the klystron is



Frequency-Tunable Far-Infrared Radiation is produced by the mixing of a fixed-frequency far-infrared laser beam with the output of a frequency-tunable klystron. By sweeping the klystron frequency in synchronism with a video display of the detector output, one obtains direct presentation of the absorption-cell spectrum.

scanned in frequency, the detector output is recorded to obtain an absorption spectrum of the material.

The system has been demonstrated at several frequency bands. Initially, the laser was operated at the 693-GHz line of formic acid while the klystron was tuned to 93 GHz and chopped at 1 kHz. Linear sweeps of the Fabry-Perot interferometer clearly indicated the generation of both sidebands with

an excellent signal-to-noise ratio. Sidebands were also generated at the numerous frequencies up to 3,200 GHz. Absorption-cell tests were also successful; for example, by use of the lower sideband of the formic acid line, the klystron was swept in frequency to scan the 599.92681-GHz absorption line of "heavy" water (HDO).

This work was done by Herbert M. Pickett and Jam Farhoomand of Caltech

for NASA's Jet Propulsion Laboratory. For further information, Circle 69 on the TSP Request Card.

Inquiries concerning rights for the commercial use of this invention should be addressed to the Patent Counsel, NASA Resident Office-JPL [see page 29]. Refer to NPO-16497.

Convolver for Pipelined-Image Processor

Data would be filtered rapidly with a few chips.

NASA's Jet Propulsion Laboratory, Pasadena, California

A convolver in the programable image-feature extractor processor described in the preceding articles would operate on square image portions of 3×3 picture elements. The convolver would produce a weighted sum of the nine picture elements and assign the sum as a new value to the element in the center. The specific choice of the convolution weights determines whether the convolver performs smoothing, spatial-frequency filtering, edge detection, or other forms of image processing.

The convolver (see figure) would be a custom-made very-large-scale integrated-circuit chip. Since three image lines must be available simultaneously for processing, two line buffers on external chips store the two previously scanned lines while the current line is being received and processed with them.

In low-level image-processing algo-

rithms, the convolution weights are usually small positive or negative integers, the extreme values of which differ by a factor of 20 or less. Consequently, 6 bits (including the sign) are used to represent the weights, since such a representation is adequate for all integers from -31 to $+31$. To prevent overflow in the output stream, scaling is done by shifting the input or output or both one or more bits; that is, dividing by a power of 2. In the internal chip data paths, 17 bits are used so that 12 significant bits will remain in the output even when an internal operation may require the subtraction of nearly equal quantities.

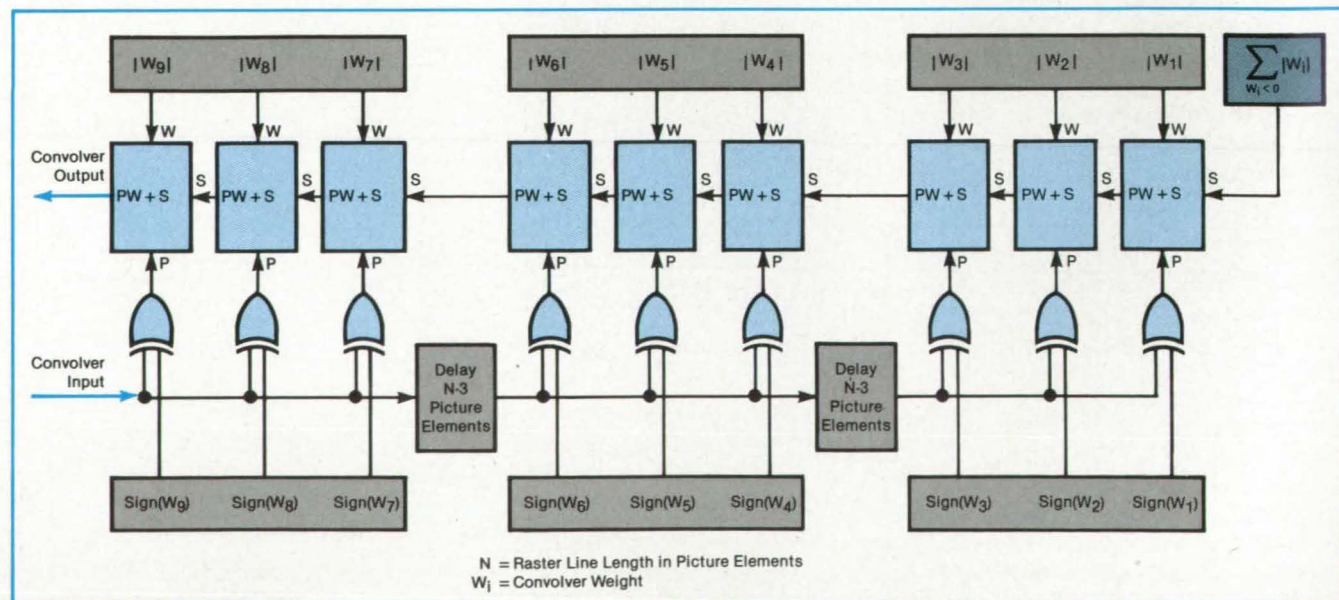
Signed arithmetic is done by using the ones complement of each picture-element value that is to be multiplied by a negative weight. This makes it possible to strip off the sign bit and use a uniform circuit architecture that operates with both positive

and negative weights. Because this scheme requires the ability to add an arbitrary number to the sum of the nine multiplications, the convolver can also be programmed to add numbers to the data stream that are unrelated to convolution weights.

The convolver will fit in a 64-pin package. The pins are apportioned among the input, output, line buffers, power, ground, clock, and programming computer. The convolver is designed to operate at a picture-element rate of 8 MHz.

This work was done by Brian Wilcox of Caltech for NASA's Jet Propulsion Laboratory. For further information, Circle 76 on the TSP Request Card.

Inquiries concerning rights for the commercial use of this invention should be addressed to the Patent Counsel, NASA Resident Office-JPL [see page 29]. Refer to NPO-16462.



A 3×3 Convolver would produce a weighted sum of the nine contiguous picture elements in a square. The data are processed through the convolver at the video scanning rate of the current raster line. The two previous lines are stored in the external buffers [(N-3)-element delays].

Single-Chip VLSI Reed-Solomon Encoder

The choice of algorithm permits compact design.

NASA's Jet Propulsion Laboratory, Pasadena, California

A Reed-Solomon (RS) encoder is based on the Berlekamp bit-serial multiplier algorithm. The RS code is standard, based on code words of 255 8-bit symbols, of which 223 symbols convey information and the remaining 32 are check symbols. This code enables the correction of up to 16 erroneous information symbols per word.

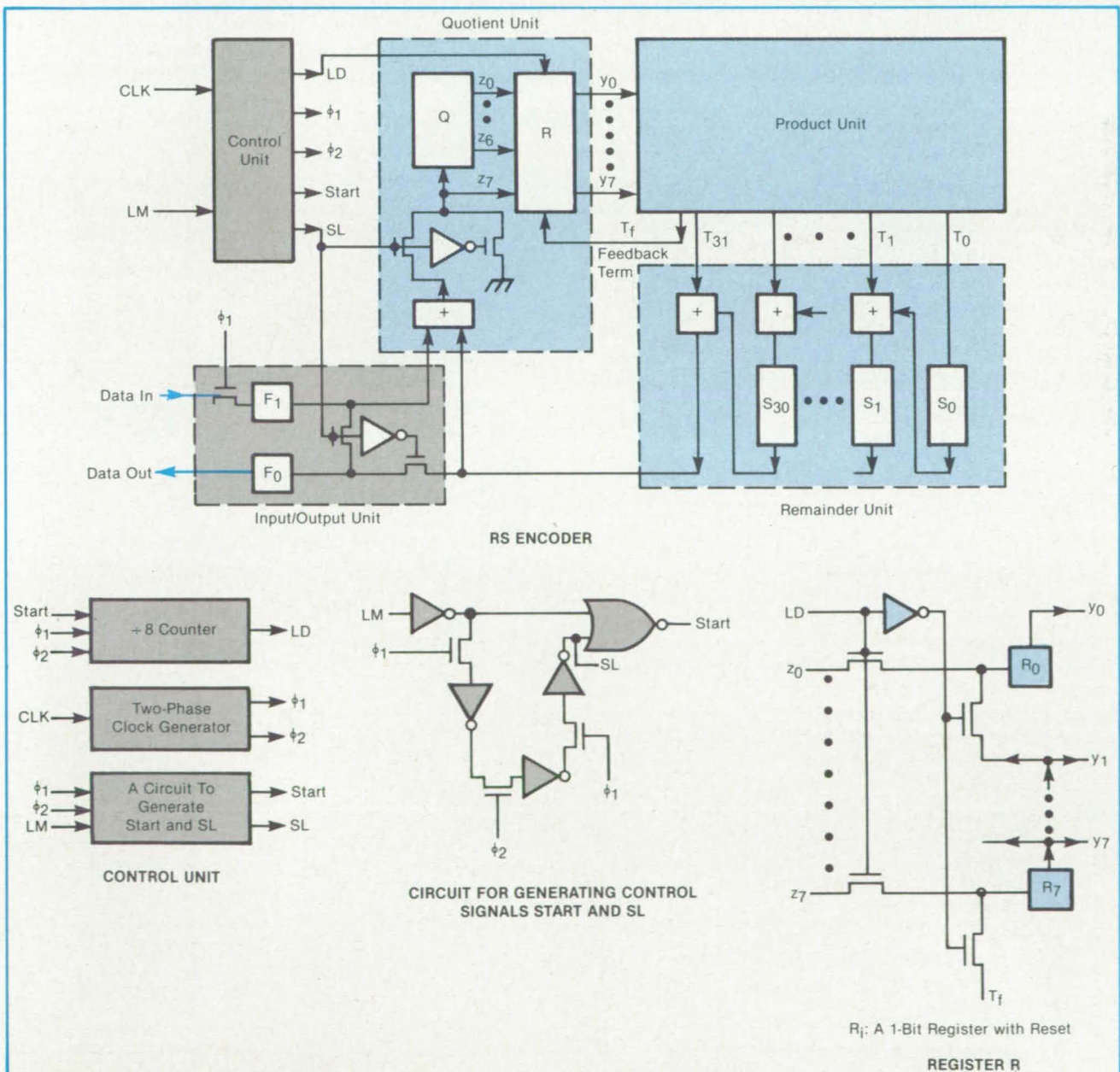
The Berlekamp algorithm is based on a code-generating polynomial with 32 roots that occur in reciprocal pairs. In contrast

with older RS encoders for long codes, those employing the Berlekamp algorithm do not require lookup tables to multiply two elements: Instead, they function only with shifting and exclusive-OR operations.

The encoder concept is illustrated in the figure. The information symbols are fed into the chip bit by bit. While the information symbols are being transmitted, the control signal LM (load mode) is set to logic "1." When there is no transmission or while

check symbols are being inserted, the LM is set at logic "0."

The input-data and LM signals are synchronized by the square-wave clock signal CLK, while the operations of the circuit and the output-data signal are synchronized by clock signals ϕ_1 and ϕ_2 . The signals CLK, ϕ_1 , and ϕ_2 are synchronized with each other but are not identical in phase and pulse width. The control signal START resets all registers and the divide-by-8 coun-



The **Encoder Concept** is based on a bit-serial algorithm that reduces the required circuit size. The symbols z_i , y_i , T_i , and S_i represent quantities calculated according to the algorithm.

ter before the encoding process begins for a code word.

The input/output unit includes flip-flops F_0 and F_1 . A pass transistor controlled by ϕ_1 is inserted before F_1 for synchronization. Control signal SL selects whether a bit of an information or check symbol is to be transmitted.

The product unit is a programmable logic array, chosen because it is easy to reconfigure for code-parameter changes. The remainder unit stores the coefficients of the remainder during the division process. The addition operation in this unit is a

modulo-2 addition or exclusive-OR operation.

Subunit Q is a 7-bit shift register with reset. Subunit R is an 8-bit shift register with reset and parallel load: The quantities z_i in Q are loaded in parallel into R under the control of signal LD every 8 clock cycles. These subunits store the currently operating coefficient and the next coefficient of the quotient polynomial. Immediately after all 223 information symbols are fed in, control signal SL changes to logic "0." Thenceforth, the contents of Q and R are zero, so that the values of the check symbols in the

remainder unit are retained.

The encoder will fit on a single very-large-scale negative-channel MOS integrated circuit chip. The circuit includes about 3,000 transistors.

This work was done by Trieu-Kie Truong of Caltech and L. J. Deutsch and I. S. Reed of the University of Southern California for NASA's Jet Propulsion Laboratory. For further information, Circle 8 on the TSP Request Card.
NPO-16122

Automatic Guidance for Remote Manipulator

A position sensor and mirror would guide the manipulator toward the object.

NASA's Jet Propulsion Laboratory, Pasadena, California

A mirror and combination light source and detector are part of a proposal for sensor-aided remote manipulation. The mirror would be mounted on an object to be grasped, while the light source and detector would be mounted on the manipulator arm (see figure). The sensor would measure the directions of the returning light beams. From these measurements, the position and orientation of the mirror would be determined.

The mirror would be a composite of a corner-cube reflector and plane reflectors. The sensor would consist of a lens and a detector in a package about 2 cm in diameter and 3 cm long. The detector, a silicon photovoltaic cell, would be divided into quadrants by etching through the junction layer. An output signal would be brought out by a lead from each quadrant. The lens would focus the incoming light onto a small spot on the detector.

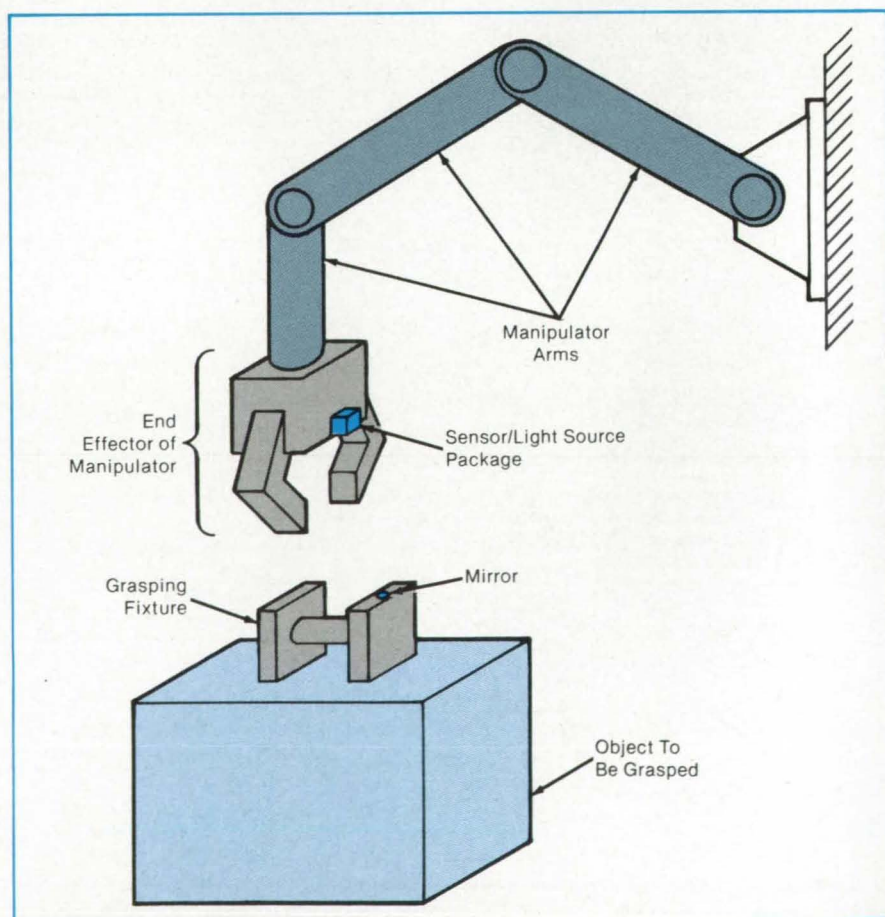
The light source would consist of three light-emitting diodes, each pulsed in turn so that the origin of the reflected light being sensed at a particular instant could be identified. The position of the light spot on the sensor and therefore the proportions of the signals from the four sensor quadrants would thus depend on which light-emitting diode is being pulsed and upon the orientation and position of the mirror.

With this pulsating and quadrant-sensing scheme, the light source/sensor would produce a total of six independent analog outputs. From the previously known geometric relationships among the light-emitting diodes, mirror facets, sensor components, and light beams, a microprocessor would turn these six outputs into the six

spatial coordinates that describe the relative position and orientation of the mirror.

In the remote-manipulator application

(see figure), the geometrical relationships between the object to be grasped and the manipulator must also be known in ad-



Grasping Becomes Automatic when the sensor begins to receive a signal from a reflector on the object to be manipulated. Light-emitting diodes on the manipulator produce light signals for the reflector, which is a composite of plane and corner reflectors.

vance and programmed into the microprocessor. Once having sensed the position and orientation of the object, the microprocessor would move the manipulator to the object. The grasping sequence would start with the operator moving the manipulator toward the object. When the sensor is close enough to receive valid signals from the mirror, it would take over control. The sensor output would drive the manipulator in such a way that the components of the

sensor output would approach a null. The effector fingers would then be closed automatically, and control would be returned to the operator.

The proposed scheme will be especially useful when the manipulator arm tends to flex or when the object is moving. The sensor and microprocessor can be designed to compensate for manipulator-arm oscillation.

This work was done by Alan R. Johnston

of Caltech for **NASA's Jet Propulsion Laboratory**. For further information, Circle 74 on the TSP Request Card.

This invention has been patented by NASA (U.S. Patent No. 3,888,362). Inquiries concerning nonexclusive or exclusive license for its commercial development should be addressed to the Patent Counsel, NASA Resident Office-JPL [see page 29]. Refer to NPO-13386.

Testing Electronic Devices for Single-Event Upset

Techniques for heavy-ion irradiation measurements are described.

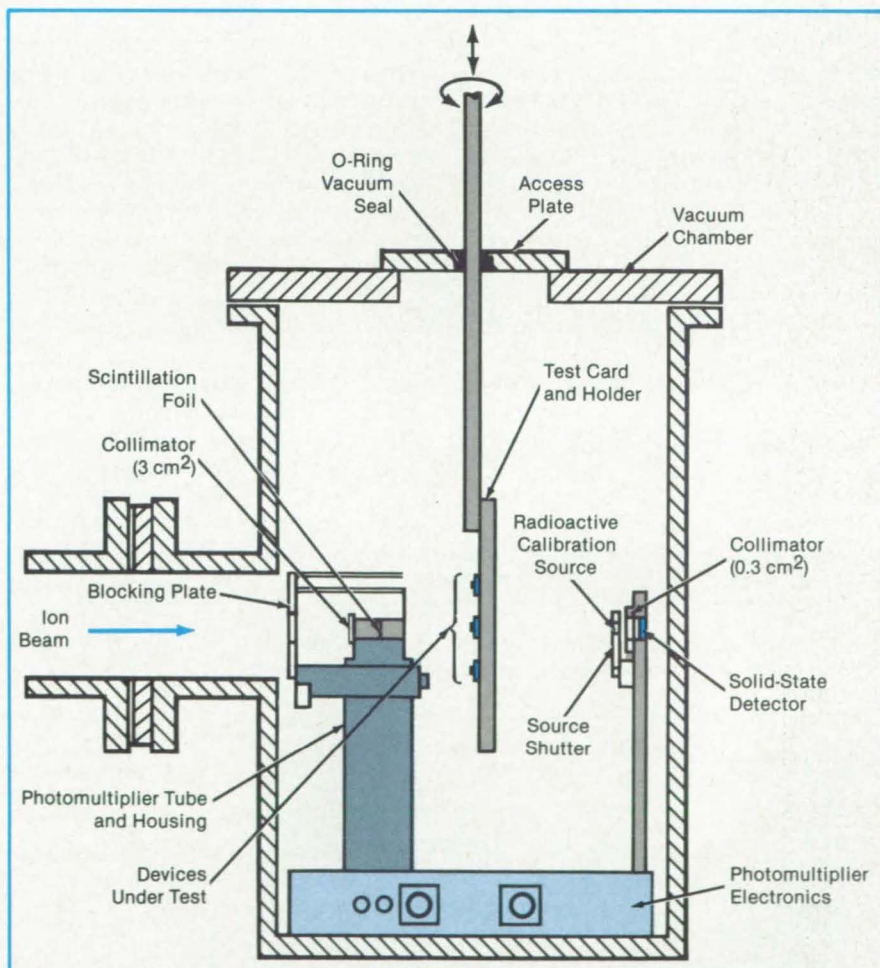
NASA's Jet Propulsion Laboratory, Pasadena, California

A report has been prepared that describes the equipment and summarizes both pretest and onsite procedures for the testing of digital electronic devices for susceptibility to single-event upset. The term "single-event upset" denotes a variety of temporary or permanent bit flips or latchup induced by single particles of ionizing radiation — such as appear in galactic cosmic rays or trapped radiation belts around some planets. In the tests, operating devices are irradiated with ion beams of known kinetic energy and flux density, while the devices are monitored for upsets. The techniques are applicable to logic and memory devices (random-access memories, microprocessors, and gate arrays, for example) that may be vulnerable to this type of radiation.

While natural radioactive sources are of some value, cyclotrons and Van de Graaff generators offer the advantages of selectability of ion species and adjustability of energy and particle flux. In addition to the devices under test (delidded to permit beam penetration), the equipment that must be brought to the ion-beam facility includes the following:

- Vacuum chamber;
- Beam-energy-measuring system;
- Beam-flux-measuring system;
- Beam-uniformity-measuring system;
- Circuit cards to mount the devices under test;
- Electromechanical positioner to move the circuit cards and devices; and
- An electronic testing system to exercise the device and record upsets.

The vacuum chamber is connected to the ion accelerator through the port that admits the ion beam (see figure) and is pumped down to a pressure of 10^{-5} torr. A well-designed chamber should have an ac-



A Vacuum Chamber houses the device under test while it is exposed to an ion beam. The vacuum chamber and associated equipment must be brought to the ion-beam facility for the test.

cess port for easy removal and insertion of the test card, valving to enable fast pump-down, and a vacuum feedthrough for the positioner so that the device can be rotated

and translated without breaking vacuum.

A remote angular-position control function is important because tilting a device with respect to a beam results in a longer

effective ion path through the sensitive volume of the device under test. Angular data can be used to determine whether the beam linear energy transfer (LET) is near the threshold LET of the device (large increase in the number of upsets with increasing angle) or whether the beam has a range that is limited in comparison with the device dimensions (large decrease in the number of upsets with increasing angle).

A scintillation foil and photomultiplier detect the passage of individual ions to meas-

ure the beam flux. A solid-state detector behind the device under test measures the beam energy. (A radioactive source can be slid into and out of place to calibrate this detector.) The beam uniformity is measured by a movable surface-barrier detector (not shown) mounted above the test card.

The complexity and cost of an ion-beam facility require an efficient combination of pretest and onsite preparation as well as a flexible approach to beam selection based

on experimental data. In addition, certain standards for recording the data are described in order to satisfy the needs of many different potential users.

This work was done by Donald K. Nichols, William E. Price, and Carl J. Malone of Caltech for NASA's Jet Propulsion Laboratory. For further information, Circle 50 on the TSP Request Card. NPO-16468

Measuring Antenna Signal Delays

Multipath errors are reduced yielding more precise delay measurements.

NASA's Jet Propulsion Laboratory, Pasadena, California

Signal delays in large dish antennas are measured by a method based on a commercial frequency-modulated instrument. Measurements are accurate within 3 ns on primary path lengths of 60 ns or more. A major benefit of the method is that the user can distinguish between the delay along the primary signal path and the delays along the multiple-reflection signal paths (multipaths), so that multipath errors can be minimized or made insignificant in the calibration of antenna delays. Large Cassegrain microwave antennas thus calibrated can measure the ranges of objects very accurately and can be synchronized more precisely with other antennas for very-long-baseline interferometry.

Previously, a horn transmitter on an antenna dish generated a signal, and the time

for the signal to reach the receiving horn at the antenna focal point was measured by a conventional phase-slope or amplitude-modulation technique. A major deficiency of this method was that the pattern of the transmitting horn often had poor directivity and large side lobes. The calibration signal therefore followed not only a direct path to the receiving horn, but also other paths because of unintentional illumination of the struts and sides of the receiving-horn housing.

In the improved technique, the instrument is a fault locator, a frequency-modulated radar system that can be operated at any center frequency in the microwave range from 1.7 to 12.4 GHz with sweep bandwidths ranging from 40 to 100 MHz. Ordinarily, the instrument is used to locate dis-

continuities in microwave transmission lines and measure the magnitudes of return losses as functions of the distances to the discontinuities. For the antenna measurements, the instrument was modified to operate in a one-way, transmission-only mode instead of its normal two-way, radar mode.

The principle of the operation is illustrated in Figure 1. The oscillator frequency is swept in a sawtooth pattern while the oscillator output is fed to a transmitting antenna and a receiving mixer. The mixer output is fed to a narrow-bandwidth IF amplifier, detected, and recorded. Since the frequency of the transmitted signal varies with time, the delay between the transmitted and received signals can be determined from the frequency differences between them.

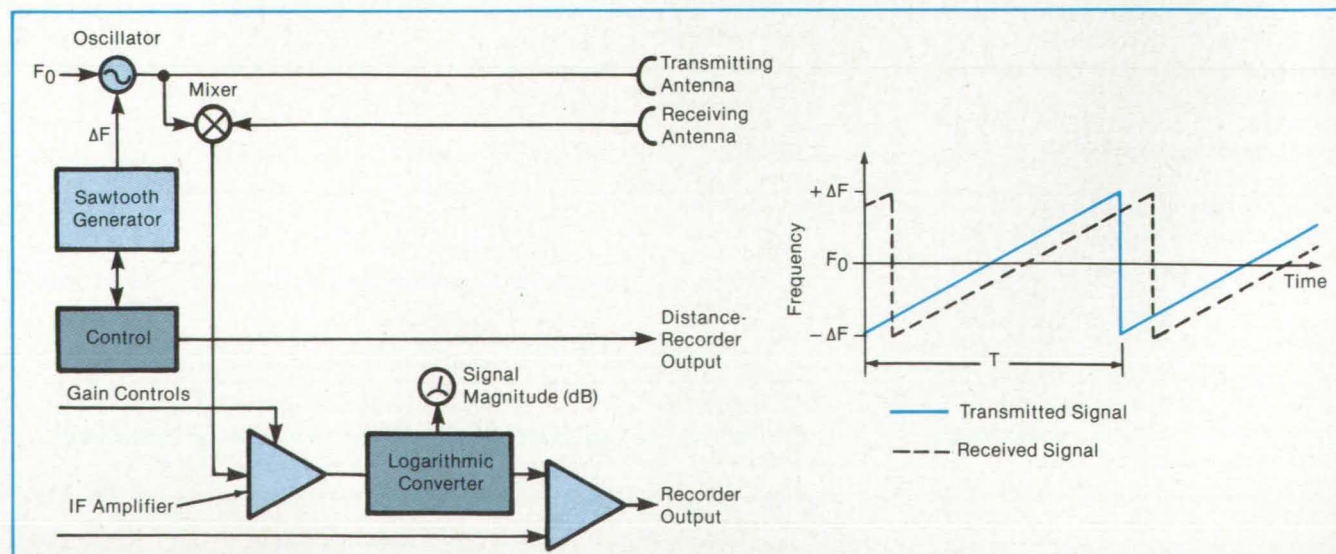


Figure 1. Antenna Delays Are Measured with a modified transmission-line-fault locator in terms of the differences in frequency between frequency-modulated transmitted and returned signals.



AFFORDABLE CESIUM CLOCK ACCURACY ANYWHERE, ANYTIME.

Collins NAVCORE I™ GPS receiver today offers laboratories Coordinated Universal Time (UTC) calibration accuracy within 100 nanoseconds. • The low-cost NAVCORE I™ GPS receiver is designed to be integrated into a variety of time-based systems—making precision equipment calibration much more affordable than an expensive cesium clock. NAVCORE I™ receiver eliminates the need for periodic off-site synchronization or waiting for an outside calibration service. • The Collins single-channel NAVCORE I™ receiver uses the currently available Navstar GPS coarse/acquisition (C/A) code to instantly deliver precise time and frequency at any site. Today GPS time signals are available from 16-20 hours daily worldwide. Contact your time-frequency equipment supplier for information on how the NAVCORE I™ GPS receiver can fit your specific time or frequency needs, or for a list of manufacturers offering NAVCORE I™ receivers contact Collins Industrial GPS Products, Rockwell International, Cedar Rapids, Iowa 52498, U.S.A. (319) 395-3234, Telex 464-421.

COLLINS GPS



**Rockwell
International**

...where science gets down to business

Aerospace / Electronics / Automotive
General Industries / A-B Industrial Automation

Circle Reader Action No. 354

Fiberite introduces the first Composite Materials



An Encyclopedia of Composite Materials As a designer of specialized products, you are only too aware of how difficult it is to find comparative data on various structural systems. This is especially true in the case of advanced composite materials information.

In response to this need, Fiberite has gathered all available data on our most widely used prepreg systems and arranged it in an easy-to-use tabular format. The resulting Fiberite Composite Materials

Selection Handbook has become the most unique reference tool available to engineers seeking comparative data on advanced composite prepreg systems.

Fiberite's put it all together

We've arranged data under three basic product categories – "250°F Systems", "350°F Systems" and "High Heat Systems". Each category contains basic information on a range of resin/fabric combinations. You can make side-by-side comparisons of the physical charac-

teristics of each system in any product category. Specific information on rheology, curing procedures and other properties for any system you select is available on request from Fiberite.



industry's Selection Handbook.



Sporting goods applications

Fiberite composite materials are tough, lightweight, non-corroding and dimensionally stable basic materials for high volume production.

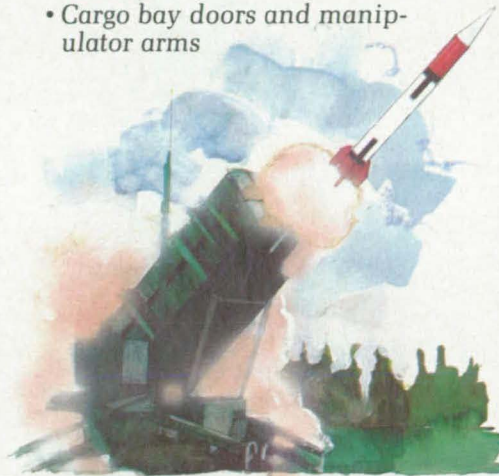
- Tennis, squash and racquetball rackets
- Golf club shafts
- Fishing rods
- Skis and ski poles
- Vaulting poles and javelins
- Boats, masts and booms



Aerospace applications are made to order for Fiberite composite materials. Light, yet strong, components offer low thermal

coefficients of expansion to cope with the temperature extremes encountered in orbit.

- Antennas and satellite platforms
- EMI shielding
- Telescopes
- Meteorite shrouds and primary structures
- Cargo bay doors and manipulator arms



Rockets and missiles Fiberite composite and ablative materials have dimensional stability, radar transparency and an ability to stand up to hostile environments.

- Radomes and nose cones
- Exit cones and nozzles
- Carbon/carbon leading edges
- Fins and rocket bodies
- Rocket and satellite motor cases
- Insulators, closures and igniters



Fiberite materials for helicopter applications

Glass, aramids and graphite provide high strength-to-weight ratios, excellent fatigue resistance and damage tolerance for such components as:

- Blades and rotor hubs
- Fuselage
- Main blade spar
- Ducting
- Interior panels and flooring
- Sponsons

Think of Fiberite before your design goes on the board

The earlier you involve our people in the design process, the sooner we'll be able to formulate a composite system that helps you meet the challenges of tomorrow's technology – CAD/CAM capabilities, automated fabrication, higher temperature service.

For more information, return this coupon or call 507/454-3611.

Yes, I would like a copy of your new Materials Selection Handbook.

I would also like more information on advanced composite materials for use in the following areas:

Name _____

Title _____

Firm _____

Address _____

City _____

State _____ Zip _____

Telephone _____ / _____

Application _____

Commercial Aircraft Missiles/Rockets

Military Aircraft Recreational

Helicopters ToolRite® Tooling

Satellites/Space Vehicles Materials Systems

Other _____

Mail to: Michael A. Edwards, Fiberite
501 West 3rd Street, Winona, MN 55987

FIBERITE[®]
AN ICI COMPANY

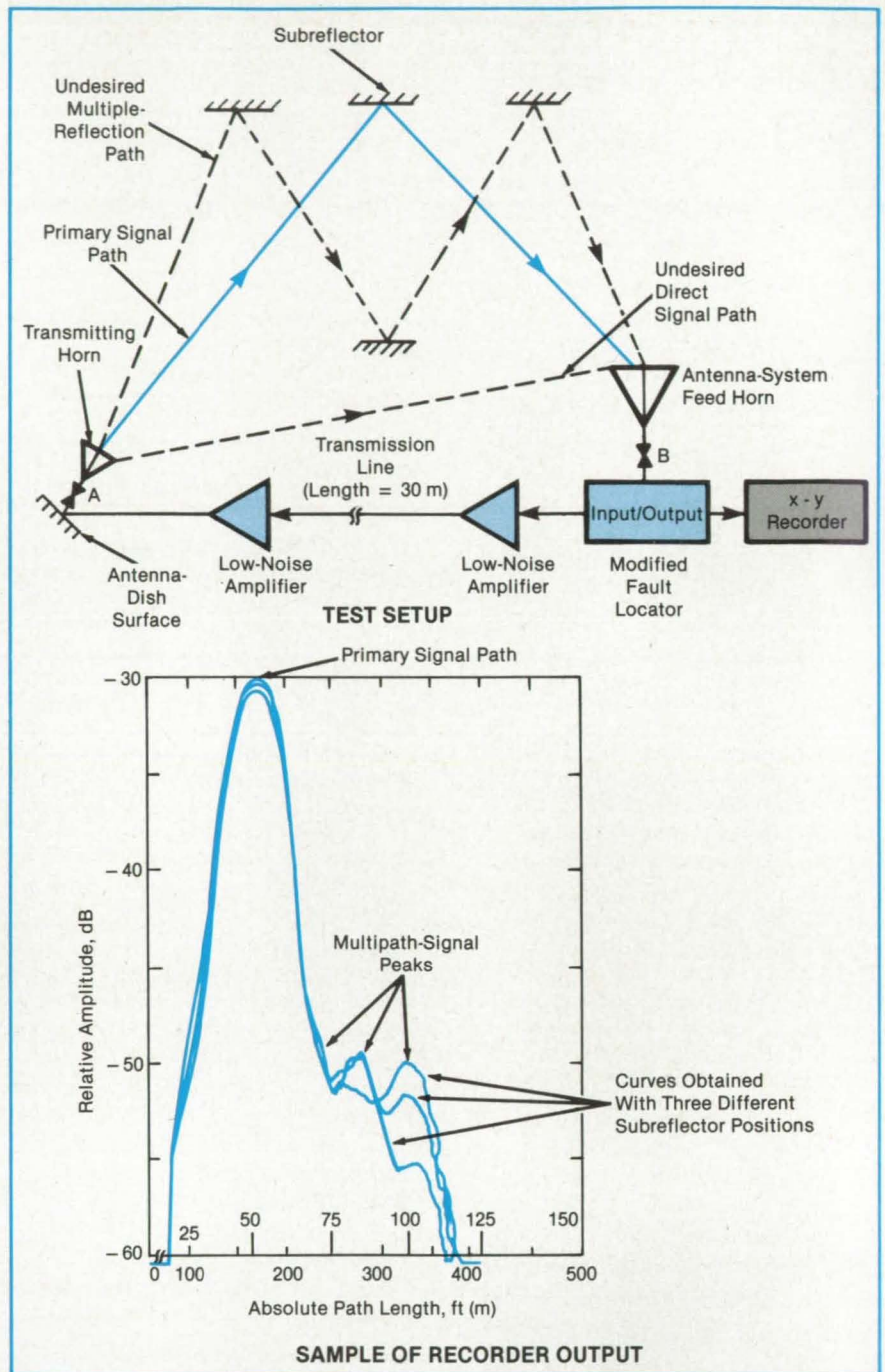
The delays can also be determined by varying the modulation rate ($2\Delta F/T$ in Figure 1) by the correct (known) amount such that the frequency difference remains constant.

The primary and multipath delays are determined by first recording the amplitude versus distance in the automatic plotting mode. Then the distance dial is adjusted manually to move the recorder pen to the positions of peak response on the recording and noting the corresponding distance readings on the instrument. The distance values are then converted to time delays. The largest amplitude occurs at the primary delay, while multipath reflections give smaller signal peaks at longer delays.

The modified fault locator is placed inside the antenna feed cone, close to the base of the antenna receiving horn. A 1.8-m cable connects the receiver output to the fault locator. Another cable connects the fault-locator output to the fault-locator transmitting horn at a place on the dish where a delay measurement is to be taken (see Figure 2). Amplifiers along this cable compensate for the airpath loss between the transmitting and receiving horns. In this configuration, the measured delay includes the internal delays of the fault locator. The fault-locator internal delay is measured separately with the cables disconnected from the transmitting and receiving horns and connected to each other through an attenuator. The internal delay thus measured is subtracted from the other measurements to obtain the antenna delays.

This work was done by Tommy Y. Otoshi and A. Ray Howland of Caltech for NASA's Jet Propulsion Laboratory. For further information, Circle 7 on the TSP Request Card.
NPO-15947

Figure 2. The **Modified Fault Locator** is placed on the antenna to measure the delay in the travel of the primary signal to the receiving horn through the reflector system of the antenna. It also measures the delays of undesired multipath signals that traverse the main signal path more than once or are reflected by structural parts. The recorder prints a plot of the signal response in which the multipath signals are readily distinguishable from the primary one. The plot shown here is for an antenna dish 64 m in diameter.



Multiplier Architecture for Coding Circuits

Finite-field arithmetic is performed in compact equipment.

NASA's Jet Propulsion Laboratory, Pasadena, California

Multipliers based on a new algorithm for Galois-field (GF) arithmetic are regular and expandable. Pipeline structures are used

for computing both multiplications and inverses. The designs are suitable for implementation in very-large-scale integrated

(VLSI) circuits.

To simplify the arithmetic operations and the circuitry, the algorithm exploits the

peculiar cyclic and modulo properties of arithmetic in the finite field $GF(2^m)$, where m is an integer. Three particularly useful properties are:

- For any two elements x and y in $GF(2^m)$, $(x + y)^2 = x^2 + y^2$;
- For any such element x , $x^{2^m} = x$; and
- If α is a root of any irreducible polynomial of degree m over $GF(2^m)$, then $\{\alpha, \alpha^2, \alpha^4, \dots, \alpha^{2^{(m-1)}}\}$ are in $GF(2^m)$ and constitute a complete set of the roots of the

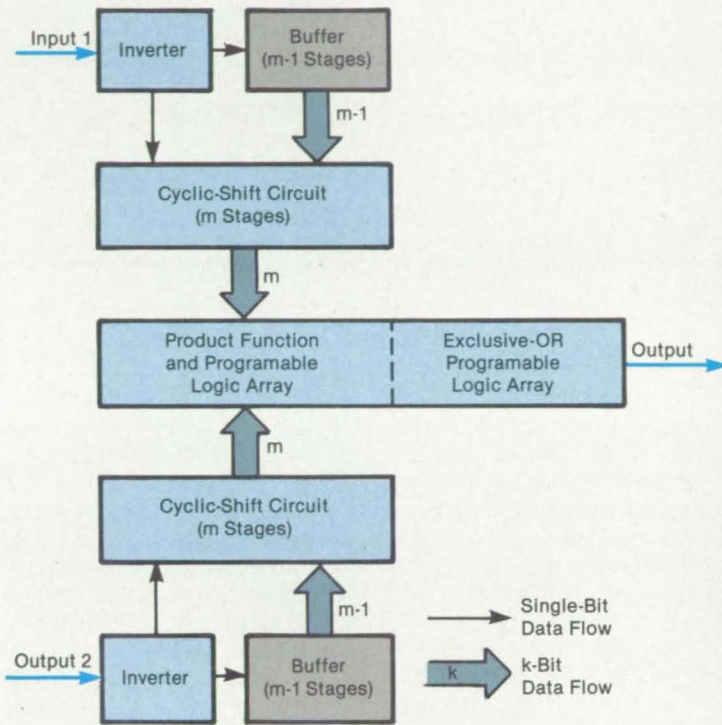
polynomial.

The field is represented by a normal basis, which is a set of elements $\{\alpha, \alpha^2, \alpha^4, \dots, \alpha^{2^{(m-1)}}\}$ with α chosen so that any element β can be expressed by

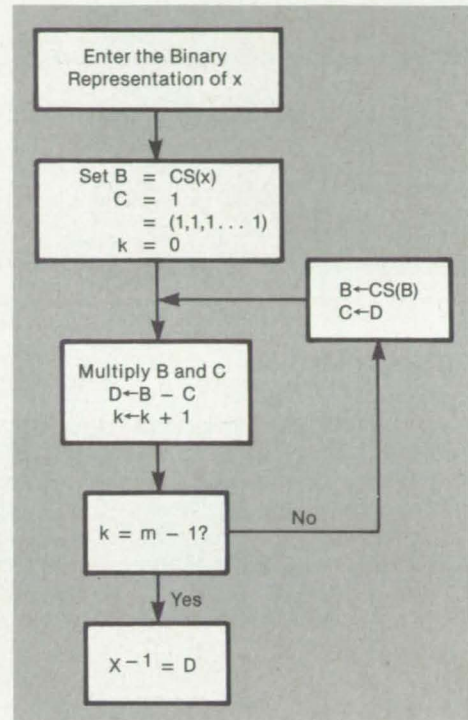
$$\beta = \sum_{k=0}^{m-1} b_k \alpha^{2^k}$$

where the b_k are binary digits, and modulo-2 addition is used. In this representation, the squaring of an element is accomplished by a simple cyclic shift of its binary digits. For any product digit, multiplication requires the same logic circuitry as for any other product digit. Adjacent product-digit circuits differ only in their inputs, which are cyclically shifted versions of each other.

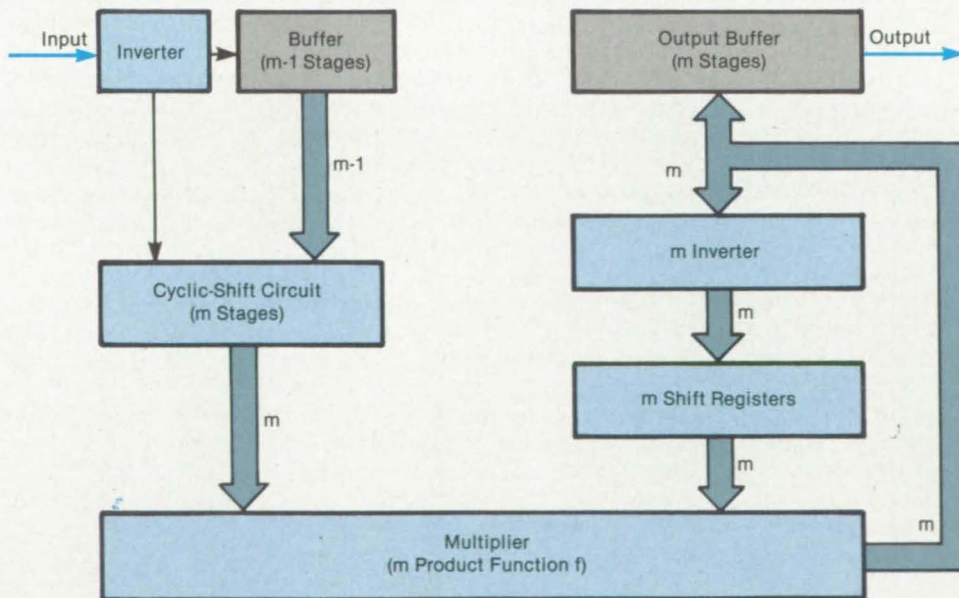
As a consequence of the property x^{2^m}



PIPELINE MULTIPLIER



INVERTING ALGORITHM



PIPELINE INVERTER

These Pipeline Multiplying and Inverting Systems can be implemented in VLSI. The multiplier (top left) exploits the special properties of normal-representation $GF(2^m)$ arithmetic. The inverting algorithm (top right) involves a series of multiplications. A pipeline inverter is shown at the bottom.

$= x$, the inverse element x^{-1} is easily found to be $x^{(2^m-2)} = x^2 \cdot x^{2^2} \cdot x^{2^3} \dots x^{2^{(m-1)}}$. Since squaring is done by a cyclic shift, the inverse of x is calculated by a sequence of cyclic shifts and multiplications using a recursive algorithm:

1. Obtain the cyclic shift (CS) of x ; that is, $x^2 = \text{CS}(x)$; let $B = \text{CS}(x)$, $C = 1$, and $k = 0$;
2. Obtain the product $D = B \cdot C$ and set $k(\text{new}) = k + 1$;

3. If $k = m - 1$, then stop because $D = x^{-1}$; if $k < m - 1$, let $B(\text{new}) = \text{CS}(B)$ and let $C(\text{new}) = D$; and
4. Return to step 2.

The figure illustrates the inverting algorithm and pipeline structures that calculate products and inverses. VLSI layouts have been done for multiplying and inverting circuits for $\text{GF}(2^4)$. This general type of inverter and multiplier architecture should be especially useful in performing the

finite-field arithmetic of Reed-Solomon error-correcting codes and of some cryptographic algorithms.

This work was done by Charles C. Wang, Trieu-Kie Truong, Howard M. Shao, and Leslie J. Deutsch of Caltech for NASA's Jet Propulsion Laboratory. For further information, Circle 97 on the TSP Request Card.

NPO-16363

Improved Electronic Control for Electrostatic Precipitators

The refuse-burner precipitator voltage is optimized.

Langley Research Center, Hampton, Virginia

A new microprocessor-based electronic control for electrostatic precipitators is in use at the Hampton/NASA/USAF Refuse-Fired Steam Generating Facility. The precipitators control pollution at this refuse-burning facility. The control solves the unique problems encountered with the precipitators in this application.

The electrostatic precipitators remove the particulate matter from the smoke created by the burning refuse. The smoke is exposed to an electrostatic field, and the particles become electrically charged and migrate to the electrically charged collecting surfaces.

To maximize particle collection, a precipitator should be operated at the highest practical field potential to increase both the particle charge and the electrostatic collection field. However, the maximum field potential at which the precipitator can operate is limited by sparking and arcing (electrical breakdown), which, if not controlled, can damage the precipitator and control system.

When the same type of fuel is burned continuously and the combustion is held relatively constant, the smoke is of a constant composition, and the magnitude of the electrostatic field for maximum particulate collection can be fairly constant. However, when refuse is burned or there are changes in the combustion, the composition of the smoke changes, requiring corresponding changes in the magnitude of the electrostatic field. Therefore, the point of maximum particulate collection cannot be held constant and an electronic control that can adjust rapidly to varying fuel and combustion is necessary to maintain precipitator efficiency.

The new microprocessor-based electronic control maintains the precipitator power at the maximum particulate-collection

level. The control automatically senses changes in the smoke composition due to variations in fuel or combustion and adjusts the precipitator voltage and current accordingly. Also, sensitive yet stable fault detection is provided.

A constant spark rate and setback are selected by the operator. Thereafter, the precipitator operation is fully automatic, requiring no further operator input.

Power is applied to the electrostatic precipitator in a series of ramps. At startup, the power level is increased at a fixed rate until the occurrence of the first spark or electrical breakdown in the gas stream. At this point, the control removes all power from the precipitator for a timed interval to allow the spark to extinguish.

Power is then reapplied over a timed interval at a rate called "fast ramp." The fast ramp quickly brings the power level back to a setback point that is proportionally lower than the spark level. The setback point and rate of rise of the fast ramp are calculated by the control from the varying spark level and the amount of setback desired (operator control).

Power is then increased at a rate called "slow ramp." The slow ramp searches for the new spark level. The rate of rise of the slow ramp is calculated by the control from the spark level and the number of sparks per minute desired (operator control). This sequence continues unless the spark level exceeds the current limit. Once the current limit is reached, the slow ramp stops climbing. Once another spark occurs, the ramp sequence is repeated. If the spark level is below the current limit, the number of sparks per minute will be the value selected independent of variations in fuel or combustion. This results in the maximum particulate collection possible for a given precipitator.

For precipitator/control protection, the primary ac current and voltage are sensed by the control, and the root mean square (rms) value of each is derived. This arrangement is used because each of these waveforms contains switching transients and spikes due to the switching action of the power silicon-controlled rectifiers and the dynamic impedance characteristics of the precipitator and its transformer/rectifier. The rms values of primary current and voltage are then compared; if an imbalance is found between them, a faulty condition is declared, and line power is removed from the precipitator.

Although the new microprocessor-based electronic control solves the problems encountered with electrostatic precipitators in refuse-burning applications, its features are applicable to any precipitator used with any fuel. True malfunctions are detected, yet the control does not needlessly shut down the operation. All calibration adjustments can be preset before installation, and no normal maintenance or field calibration is required. Major modifications of control parameters can be accomplished by reprogramming a plug-in electrically programmable read-only memory. The control can be applied in new facilities or in present precipitators as a retrofit package and can be tailored to any electrostatic-precipitator application.

This work was done by David F. Johnston of Langley Research Center. For further information, Circle 52 on the TSP Request Card.

Inquiries concerning rights for the commercial use of this invention should be addressed to the Patent Counsel, Langley Research Center [see page 29]. Refer to LAR-13273.

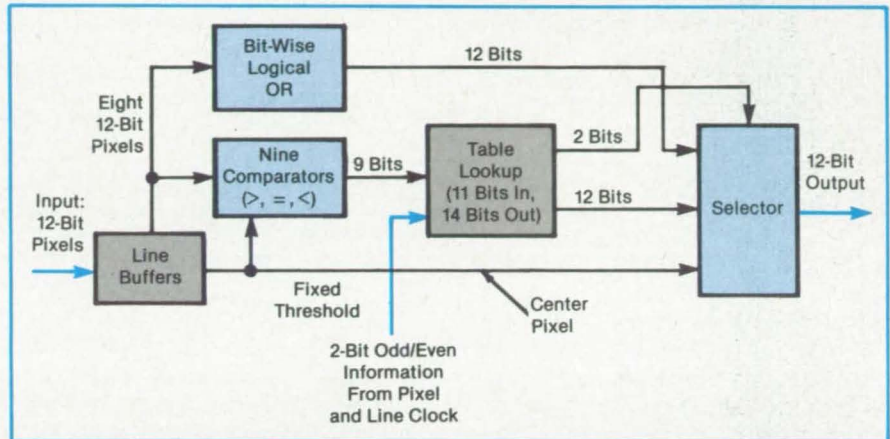
Picture-Element Comparator

A logic circuit identifies image features by comparing pixel data.

NASA's Jet Propulsion Laboratory, Pasadena, California

A proposed circuit, called a "neighborhood comparison operator," would compare data from neighboring picture elements (pixels) to find peaks, ridges, and valleys in the picture data. The circuit would also be able to expand or shrink pixel regions. The circuit concept was developed for the image-processing computer described in the preceding articles. The circuit handles a data stream of 12-bit pixels rather than the conventional 8 or 16 bits. The circuit would consist entirely of standard logic chips.

The circuit (see figure) stores two consecutive scan lines in line buffers. It performs a raster-to-window conversion with nine latches, thereby producing the nine pixel values of a 3-by-3-pixel window. The center pixel is compared with a programmable constant-threshold value, and its eight neighbors are compared with the center pixel or with the threshold. The outputs from the comparators form a representation of the greater-than, equal-to, or less-than relationships of the pixels in a 9-bit number. Two bits are appended to this value to indicate whether the center pixel number along its scan line is odd or even and whether the number of the scan line for that pixel is odd or even. The resulting 11-bit number is used to address a 2K-by-14-bit memory that has been programmed to produce two numbers in response to the input; an arbitrary 12-bit number from the memory table and a 2-bit number that, depending



The **Neighborhood Comparison Circuit** examines relationships between adjacent pixels. From data in a lookup table, it produces a 12-bit number representing the relationship and thereby can identify ridges, peaks, and valleys.

on the input number, directs the selector to choose as its 12-bit output the number from the table, the center pixel value, or a bit-wise logical OR derived from the eight neighbors of the center pixel.

When two's-complement representation is used and signed data are compared, the most significant bit (the sign bit) is first inverted. This procedure makes positive numbers (for which the sign bit is zero) compare as greater than negative numbers (for which the sign bit is 1).

Information about the address or evenness of the pixel position is included in the lookup table input so that subfields can be

implemented. The two odd-or-even bits allow four subfields to be defined, with different operations for each. This ensures that a line expressed as binary data is not lost if it is thinned to the width of a single pixel.

This work was done by Donald B. Gennery of Caltech for NASA's Jet Propulsion Laboratory. For further information, Circle 78 on the TSP Request Card.

Inquiries concerning rights for the commercial use of this invention should be addressed to the Patent Counsel, NASA Resident Office-JPL [see page 29]. Refer to NPO-16464.

Programmable Pipelined-Image Processor

Two-dimensional data would be processed via a pipelined approach.

NASA's Jet Propulsion Laboratory, Pasadena, California

A proposed computer would serve as a pipelined processor for imagery or other two-dimensional digital data. The processor would do feature extraction, smoothing, edge detection, texture measurement, and stereoscopic area correlation. It would also plan routes for obstacle avoidance by robots and would solve two-dimensional partial differential equations.

NASA Tech Briefs, Winter 1985

Parallel processing would be used to achieve the necessary speed for processing image data. In contrast with general-purpose computers, no time would be spent to repeatedly decode instructions during processing because the same operations would be performed repeatedly on the image data.

In the pipelined-image approach, the

system performs more than one arithmetic operation at a time on each picture element. Some operations are also performed simultaneously on corresponding elements in parallel data paths. The data would pass through the pipeline processor at the video-scanning rate (in most cases).

The processor consists of identical programmable computing modules (see figure,

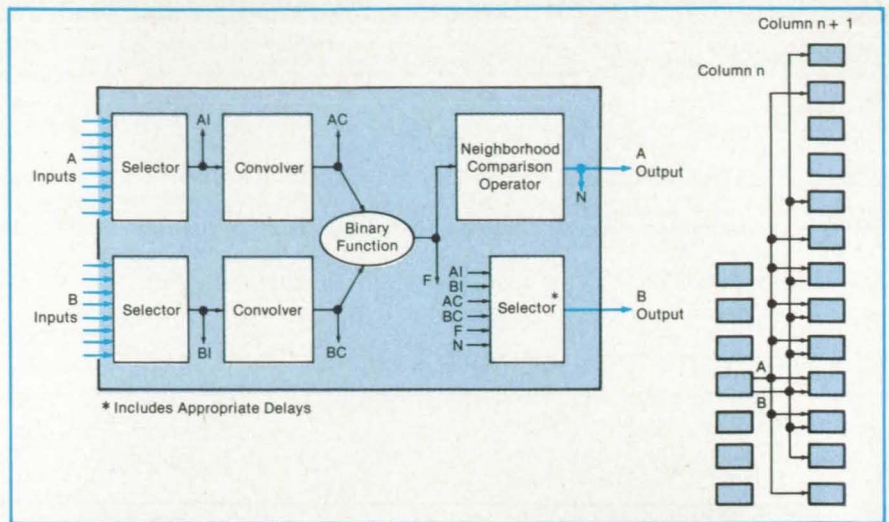
left) interconnected in a two-dimensional programmable arrangement. Each module, typically occupying one circuit card, contains binary arithmetic operators that use lookup tables. The module also includes convolvers and neighborhood comparison operators that perform such operations as finding local extrema, zero crossings, and directional extrema.

The processor receives image data as they emerge from external buffers or, more directly, from television cameras through analog-to-digital converters. The results of the computations are fed into the same or other image buffers. The delays caused by processing are taken into account by the circuit that reloads the buffers.

A flexible scheme is used to direct the flow of data to subsequent stages of the pipeline. For example, if a stage consists of a column of synchronized modules, the interconnection network enables the output of a module in a given row and column to be sent to any or all of a designated set of rows in the next column (see figure, right).

The concept has been worked out for an initial version of the processor, which is expected to process imagery of about 2,000 picture elements per line at 8×10^6 picture elements per second using 12-bit arithmetic. The processor would be programed by a commercial host computer through a direct-memory-access (DMA) interface.

Each binary function (which uses a quarter-megabyte lookup table) should be



The **Image Processor** would consist of modular units (left), each of which includes a set of computing elements of the types that are particularly useful in pipelined-image processing. A flexible interconnection scheme (right) would be used to route data to subsequent stages of the pipeline.

programmable in about 200 ms; all modules to be loaded with the same function would be programed in two 64K, 16-bit DMA transfers. The lookup table for each neighborhood comparison operator would be similarly programed in a 2K DMA transfer. The convolution weights, input selection, and other programing data would be inserted in an 80-word DMA burst for each module needing reprograming.

This work was done by Donald B. Gennery and Brian Wilcox of Caltech for NASA's Jet Propulsion Laboratory. For further information, Circle 77 on the TSP Request Card.

Inquiries concerning rights for the commercial use of this invention should be addressed to the Patent Counsel, NASA Resident Office-JPL [see page 29]. Refer to NPO-16463.

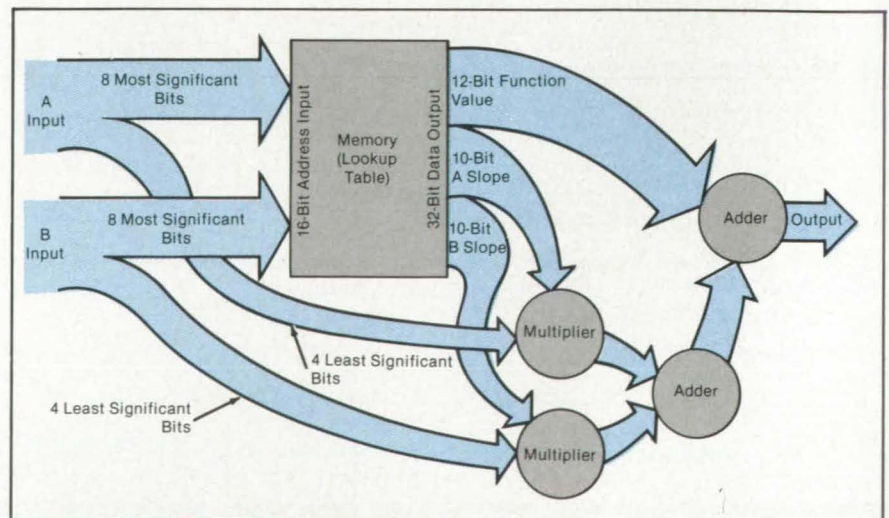
Function Generator for Image Processor

A custom-designed processing chip and commercial memory chips yield detailed data.

*NASA's Jet Propulsion Laboratory,
Pasadena, California*

A proposed binary-function generator would obtain data from lookup tables and linearly interpolate values from the data. The function generator would use commercial memory chips for the lookup tables and a custom-designed chip for interpolation. The concept was developed for the programable image-feature extractor described in the preceding article.

The eight most significant bits of two 12-bit input-function arguments, A and B, are used to address the 64K-by-32-bit lookup table (see figure). The four least significant bits in the input are directed to separate multipliers and used to interpolate between the lookup-table values. Twelve of the 32 table-output bits represent the value of the function at each of the 64K values stored in the table. The remaining 20 bits represent the interpolation slopes for arguments A and B.



The **Basic Elements of the Function Generator** are memory chips and an interpolator chip, which incorporates multipliers and adders. The memory includes CMOS static random-access devices. The 120 ns cycle time of these devices allows real-time processing of image data.

The interpolator multiplies each slope by the four least significant bits of the appropriate function argument and adds the two products. It discards the four least significant bits of the product sum and adds the remaining bits to the 12-bit function value looked up in the table to produce the final interpolated output.

A 32-bit-wide table was chosen because it accommodates the 12-bit word length of the system and still allows sufficient bits to describe the slopes over a wide range. The slopes can take positive or negative values from as low as 1/16 to as high as 32.

This work was done by Donald B. Gennery and Brian Wilcox of Caltech for NASA's Jet Propulsion Laboratory. For further information, Circle 75 on the TSP Request Card.

Inquiries concerning rights for the commercial use of this invention should be addressed to the Patent Counsel, NASA Resident Office-JPL [see page 29]. Refer to NPO-16461.

Computer Programs

These programs may be obtained at a very reasonable cost from COSMIC, a facility sponsored by NASA to make raw programs available to the public. For information on program price, size, and availability, circle the reference number on the TSP and COSMIC Request Card in this issue.

Design of Linear Quadratic Regulators and Kalman Filters

An interactive program includes over 60 predefined functions for system control, estimation, and response.

AESOP solves problems associated with the design of controls and state estimators for linear time-invariant systems. The systems considered are modeled in state-variable form by a set of linear differential and algebraic equations with constant coefficients. Two key problems solved by AESOP are the linear quadratic regulator (LQR) design problem and the steady-state Kalman filter design problem.

AESOP is interactive. The user can solve design problems and analyze the solutions in a single interactive session. Both numerical and graphical information are available to the user during the session.

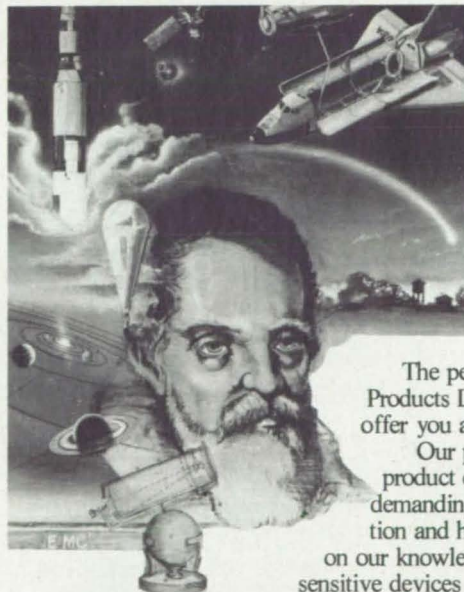
The AESOP program is structured around a list of predefined functions. Each function performs a single computation associated with control, estimation, or system response determination. AESOP contains over 60 functions and permits the easy inclusion of user-defined functions. The user obtains access to these functions either by inserting a list of desired functions in the order they are to be performed or by specifying a single function to be performed. The latter case is used when the choice of function and function order depends on the results of previous functions.

The available AESOP functions are divided into several general areas including (1) program control, (2) matrix input and revision, (3) matrix formation, (4) open-loop system analysis, (5) frequency response, (6) transient response, (7) transient function zeros, (8) LQR and Kalman filter design, (9) eigenvalues and eigenvectors, (10) covariances, and (11) user-defined functions. The most important functions are those that design linear quadratic regulators and Kalman filters. The user interacts with AESOP when using these functions by

inputting design weighting parameters and by viewing displays of designed system response. Support functions obtain system transient and frequency responses, transfer functions, and covariance matrices. AESOP can also provide the user with open-loop system information including stability, controllability, and observability.

The AESOP program is written in FORTRAN IV for interactive execution and has been implemented on an IBM 3033 computer using TSS 370. As currently configured, AESOP has a central-memory requirement of approximately 2M 8-bit bytes. Memory requirements can be reduced by redimensioning arrays in the AESOP program. Graphical output requires adaptation of the AESOP plot routines to whatever device is available. The AESOP program was developed in 1984.

This program was written by Bruce Lehtinen and Lucille Geysler of Lewis Research Center. For further information, Circle 37 on the TSP Request Card. LEW-14128



How will our experience benefit you?

The people of the ITT Electro-Optical Products Division, Fort Wayne operation, offer you a strong ally: **experience.**

Our people provide you with proven product development experience in such demanding applications as space exploration and high-tech research. You can rely on our knowledge for custom designed photosensitive devices to meet your particular needs.

From one device, to several thousand, you are provided with high-quality intensified solid-state-array cameras, image intensifiers, photomultipliers, image dissectors, photodiodes and accessories.

Ask for our catalog of Special Purpose Photosensitive devices. Put our proven experience to work for you.

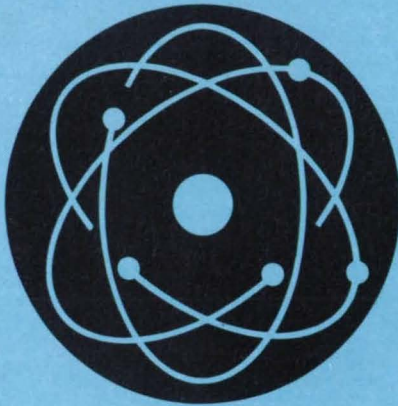
Contact ITT Electro-Optical Products Division • P.O. Box 3700 • Fort Wayne, IN 46801 • (219) 423-4341 • TWX: 810-332-1413 • Telex: 232-429.

Free full-color poster of above illustration if requested on your letterhead.

ELECTRO-OPTICAL PRODUCTS DIVISION

ITT

Physical Sciences



Hardware, Techniques, and Processes

- 80 Plotting Lightning-Stroke Data
- 82 Nebulization Reflux Concentrator
- 83 Tracking System for Infrared Spectrometer
- 84 Determining the Temperature Profile in a Cylindrical Sample
- 85 Intense Source of Polarized Hydrogen Atoms
- 85 Molecular Thermal-Electron Detectors
- 86 Detecting Trace Contaminants in the Atmosphere
- 88 Solid-State Detector for Trace Materials
- 90 Technique for Measuring Gas Conversion Factors
- 91 Compact Imaging Spectrometer
- 92 Liquid-Level Sensor for Containers in Motion
- 93 Hybrid Laser Would Combine Power with Efficiency
- 94 Wedged Fibers Suppress Feedback of Laser Beam
- 95 Determining Calibration Constants for Attitude Measurements

Books and Reports

- 96 Accuracy of Lidar Measurements of the Atmosphere
- 97 Adsorption of H₂, Ne, and N₂ on Activated Charcoal
- 97 Microwave Atmospheric-Pressure Sensor
- 97 Soil/Structure Interactions in Earthquakes
- 98 Equipment for Microgravity Research
- 98 Calculation Of Macrosegregation in an Ingot

Computer Programs

- 99 Kinematic Stirling Engine Performance
- 99 X-Ray Diffraction Analysis Program
- Deformable Subreflector Computed By Geometric Optics

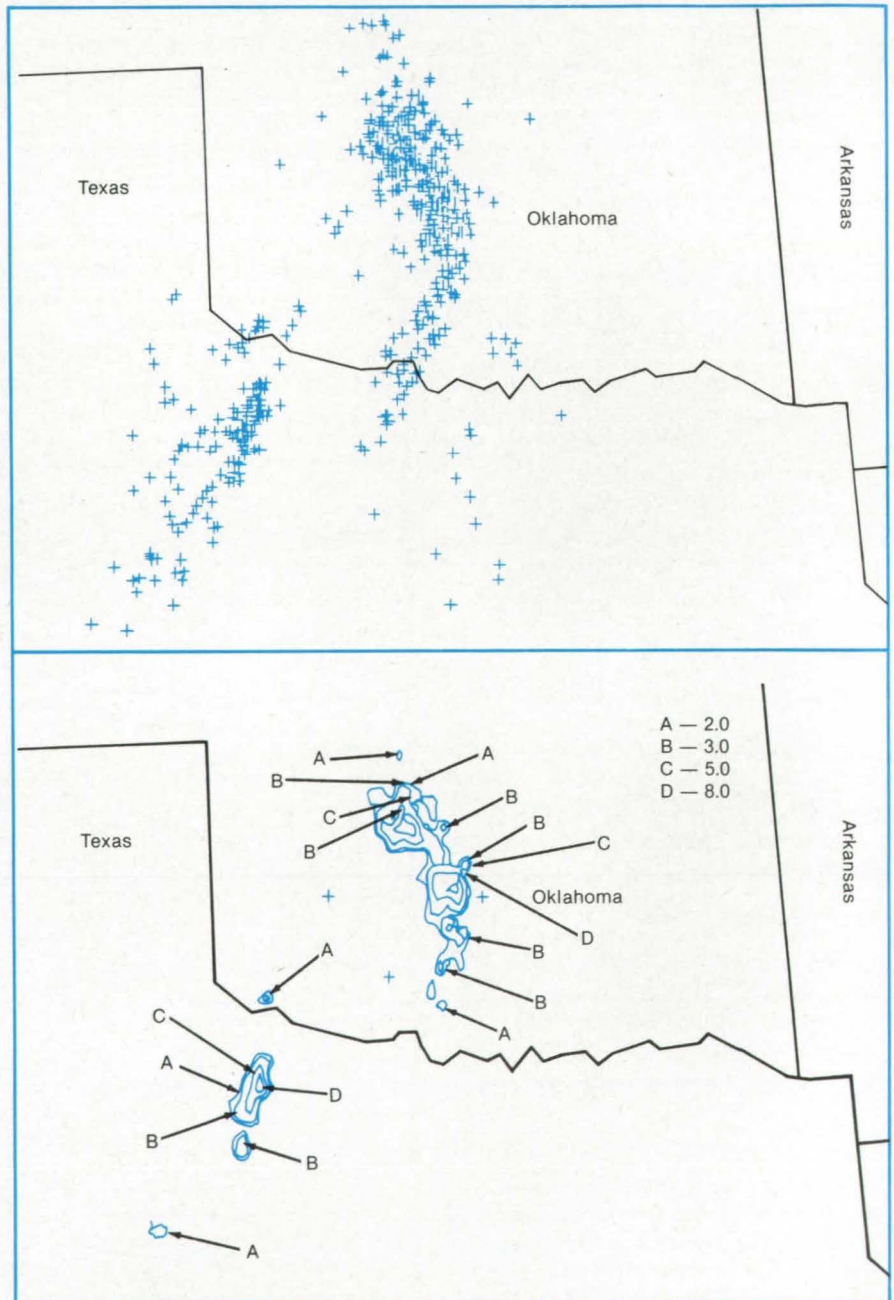
Plotting Lightning-Stroke Data

Density contours yield more meaningful information than point plots.

Marshall Space Flight Center, Alabama

Data on lightning-stroke locations become easier to correlate with cloud-cover maps with the aid of a new graphical treatment. In the past, lightning-stroke sites have been plotted individually on a conven-

tional geographic regional display (see top of figure). Such plots can be confusing when many strokes occur in a concentrated area, and it is difficult to relate them in a meaningful way to a plot of storm cen-



Plotted as individual points (top), data on lightning strokes are difficult to interpret because of overlap. Plotted as stroke-density contours (bottom), however, the data can be more readily comprehended. The plots show data from the 15-minute interval of 20:15 to 20:30 during the night of May 27, 1984.

The Science Of Optics: Phase Retrieval

Phase retrieval research at ERIM is opening up the possibility of diffraction-limited imaging despite the effects of atmospheric turbulence or other imaging system phase errors.

Phase Retrieval for Astronomy

Phase aberrations due to atmospheric turbulence severely limit the resolution of images obtained from large, earth-bound optical telescopes. One partial solution is the use of an interferometric sensor, such as Labeyrie's astronomical speckle interferometry, which measures the modulus (magnitude) of the Fourier transform of the object. Unfortunately, this technique loses the Fourier phase information, thus making it impossible to compute an image from the seemingly incomplete information.

To solve this problem, ERIM researchers developed phase retrieval algorithms which iteratively find a Fourier phase and consequently reconstruct an image that is consistent both with the measured Fourier modulus and the physical constraint that the image be

nonnegative. By this method much sharper pictures can be obtained than was previously possible.

Other Applications

Phase retrieval algorithms are also being used at ERIM to solve other problems, including sensing wavefronts for laser applications, producing diffraction-limited images from imperfect optical systems, and, with coherent light, possibly even producing images using no lenses at all.

Research in phase retrieval includes analytical study of the uniqueness of the solution, analyses of the sensitivity of image quality to noise, improvement of the convergence and robustness of reconstruction algorithms, and optical laboratory experiments for further proof of concept.

ERIM is a leader in advancing the state of the art in a number of areas in optics. Phase retrieval is one example. Others include 3-dimensional imaging sensors, optical computing, diffractive optics, and holography.

The Environmental Research

Institute of Michigan (ERIM) is a non-profit scientific research institute that performs contract research services for a variety of sponsors. Our sponsors include government organizations, industry, and universities.

Research at ERIM focuses upon remote sensing systems, devices, and techniques that span the electromagnetic spectrum. Within this broad research area, staff members employ their knowledge of modern electronics, optics, computer science, and infrared and microwave physics. All of the work is directed toward one end: to solve problems for sponsors, whether those problems are concerned with defense, outer space, or the factory floor.

Career Opportunities

ERIM's Infrared & Optics and Radar divisions have research and management positions available in Ann Arbor, MI, Washington, DC, and Los Angeles, CA. Positions are available at several levels in the following areas:

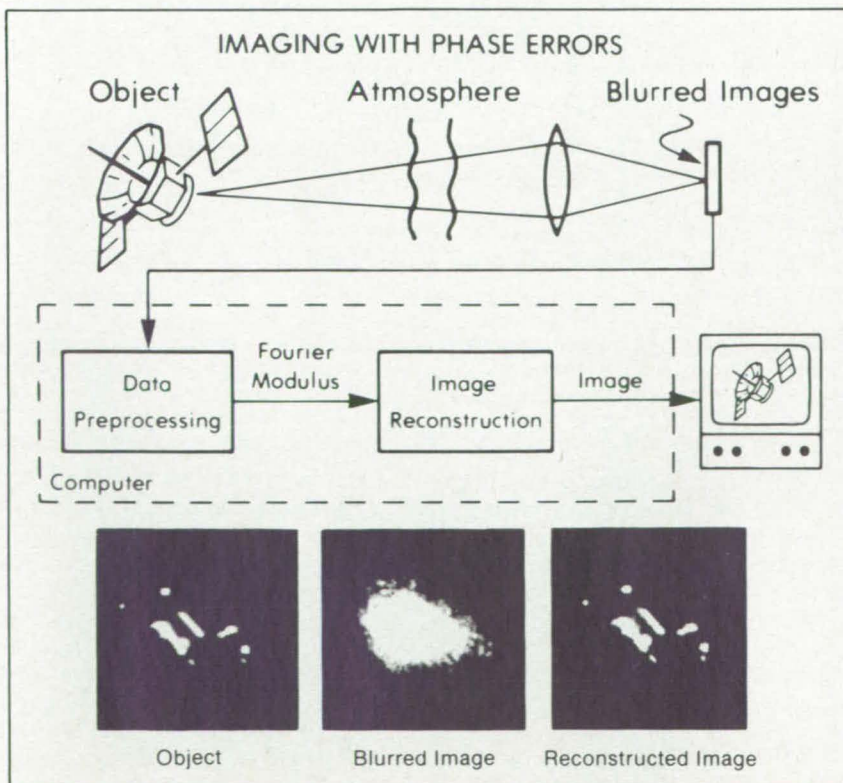
- E-O/IR System Design and Analysis
- Infrared Phenomenology
- Computer Vision
- Optical Computer Systems
- Phase Retrieval/Signal Reconstruction
- Radar System Engineering and Analysis
- Signal and Image Processing
- Microwave Scattering and Measurement Engineering
- Diffractive Optics

All positions require a BS, MS, or PhD in engineering, physics, mathematics, or statistics, along with appropriate work experience. Salary and benefits are highly competitive.

For details, telephone (313) 994-1200, ext. 260. Or send your resume to Personnel Administrator, Dept. IEO, ERIM, P.O. Box 8618, Ann Arbor, MI 48107.



U.S. Citizenship required
Equal opportunity employer



ters for the same region.

With the new treatment, the geographic region is divided by a grid into an array of cells. The number of lightning strokes in each cell is tabulated, and a value representing the density of lightning strokes is

assigned to each cell. With a contour-plotting routine, a computer draws contours of lightning-stroke density for the region (see bottom of figure). The shapes of the contours can then be compared directly with the shapes of the storm cells.

*This work was done by Frank B. Tatom and Robert A. Garst of Marshall Space Flight Center. No further documentation is available.
MFS-26019*

Nebulization Reflux Concentrator

Trace substances are removed from an atmosphere for analysis.

Langley Research Center, Hampton, Virginia

The nebulization reflux concentrator extracts and concentrates trace quantities of water-soluble gases for subsequent chemical analysis. As shown in the figure, the gas containing the soluble trace constituent(s) is blown through jet 1. Projecting into the outlet of this jet is the end of another tube, jet 2, which dips below the surface of a scrubbing liquid in a small reservoir. The velocity of the gas flowing past the end of jet 2 creates a partial vacuum that draws scrubbing liquid up the tube. When this liquid spills out into the gas stream, it is atomized or broken up into very small droplets. The fine spray formed by these droplets fills the chamber of the device, where intimate contact is made between the droplets and gaseous molecules.

For soluble gases, phase transfer occurs. The gaseous molecules of highly soluble constituents are collected in the droplets. The droplets of liquid impinge against a porous hydrophobic membrane, which is supported by a conical screen, where they coalesce into drops large enough to roll off the apex of the cone and return to the scrubbing-liquid reservoir. Although the hydrophobic membrane virtually blocks all transport of droplets, it offers little resistance to gas flow; hence, the device permits relatively large volumes of gas to be scrubbed efficiently with very small volumes of liquid. This means that analyzable quantities of contaminants can be concentrated in extracting solutions in much shorter times than with conventional techniques.

The hydrophobic membrane was made by shaping a commercially available polytetrafluoroethylene filter having a 1- μ m-diameter pore size around a wire screen cone, which is used for structural support. The shaped filter efficiently passes the vapor phase while almost completely repelling aqueous droplets. The droplets are subsequently dropped into the scrubbing-liquid reservoir to be recycled. The solution is then removed for chemical analysis. Water loss through the system can be

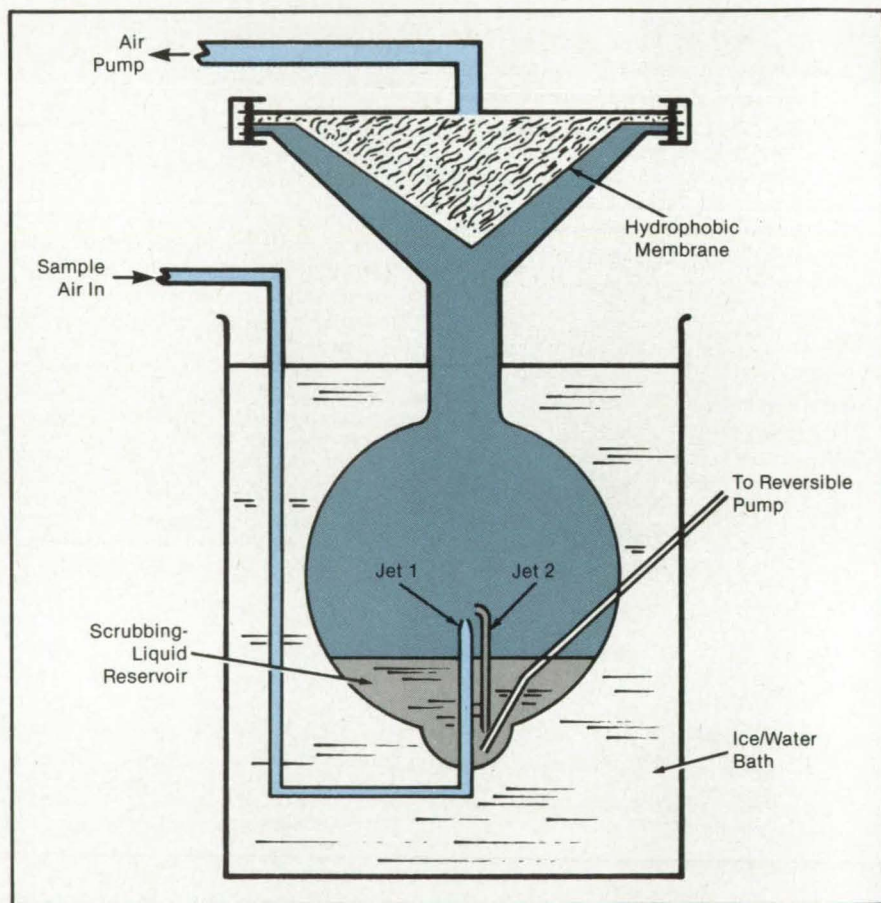
completely accounted for as vapor loss.

Test data comparing the efficiency of the concentrator with that of a conventional laboratory bubbler showed that the nebulization reflux concentration technique compared favorably to the bubbler for rapid extraction and preconcentration of gaseous hydrogen chloride and ammonia.

This work was done by Wesley R. Cofer III of Langley Research Center

and Vernon G. Collins of the College of William and Mary. For further information, Circle 39 on the TSP Request Card.

This invention is owned by NASA, and a patent application has been filed. Inquiries concerning nonexclusive or exclusive license for its commercial development should be addressed to the Patent Counsel, Langley Research Center [see page 29]. Refer to LAR-13254.



The Hydrophobic Membrane and Nebulizing Nozzles (Jets 1 and 2) form a scrubber for removing trace quantities of soluble gases or other contaminants from an atmosphere.

Tracking System for Infrared Spectrometer

Laser beams are returned from a moving reflector.

NASA's Jet Propulsion Laboratory, Pasadena, California

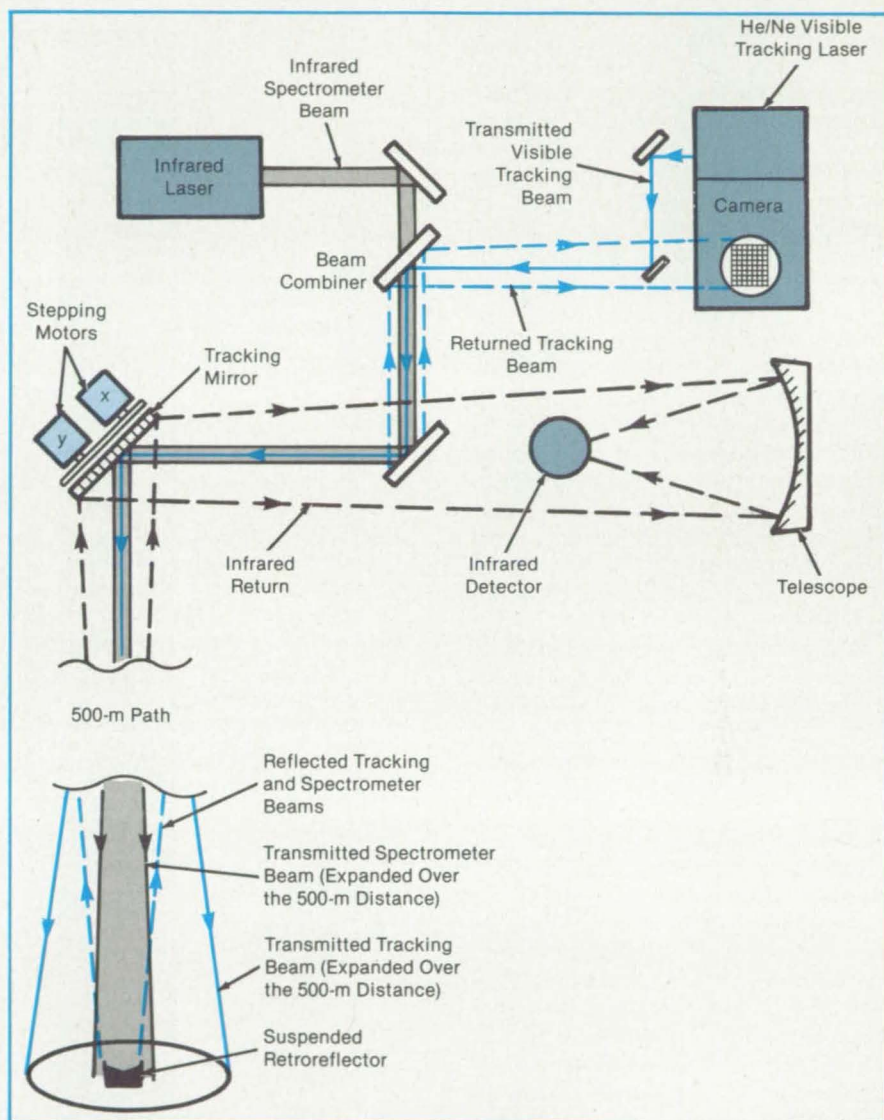
A visible laser tracking system for an infrared laser spectrometer keeps the probe infrared laser beam aimed at a moving reflector, thereby keeping the reflector image and the return laser beam within the spectrometer field of view. The system includes a tracking mirror that is tilted by stepping motors under microprocessor control to deflect the beams toward the continually changing reflector position.

The tracking system is part of a balloon-borne infrared laser spectrometer that measures the composition of the upper atmosphere at altitudes of about 25 to 40 km. To reduce the effects of outgassing from the balloon and gondola, the spectrometer measures infrared absorption over a path to and from a reflector hanging as much as 500 m below the gondola. Most of this 1,000-m path is far enough away that the effects of outgassing from objects adjacent to the instrument are negligible.

The suspended reflector swings like a pendulum below the instrument gondola. The tracking system, mounted in the gondola, uses a visible light beam from a helium/neon laser, distinct from the spectrometer beam from an infrared laser. The beam is directed to the reflector by mirrors and lenses (see figure) and broadens to a spot of 2 m diameter at the distance of 500 m. The reflector diameter is 14 cm. The axis of the spectrometer beam is maintained in a fixed orientation relative to that of the tracking beam. The tracking beam returned by the reflector to the gondola is projected on an array of light sensors in a television camera, and the camera output is fed to the microprocessor and controller.

In the first stage of tracking, the controller, under direction of the microprocessor, moves the tracking mirror so that the visible laser beam traces a spiral pattern at the reflector distance. As soon as the spiral scan picks up a glint from the reflected, visible tracking beam, the microprocessor moves the tracking mirror to position the glint at the center of a 32-by-32-picture-element central section of the 64,000-element camera array.

Every 0.05 s, the microprocessor updates the position of the glint with respect to the center of the array and computes a new scanning velocity that will move the tracking mirror in synchronism with any motion of the reflector. When tracking is fully maintained, the microprocessor turns



A Motor-Driven Tracking Mirror directs the visible tracking beam and the infrared spectrometer beam toward the reflector. Under microprocessor control, the tracking mirror keeps the beams aimed at the retroreflector.

to a fine-search algorithm, which moves the tracking mirror so that it samples different parts of the reflected tracking beam. At the same time, the microprocessor monitors the infrared beam reflected to the spectrometer receiving telescope. When the returned infrared power reaches a maximum, the system locks on the corresponding visible position for tracking. The fine-search algorithm allows for offset —

either intentional or accidental — between the axes of the tracking beam and the spectrometer beam.

This work was done by Robert A. Johnson, Christopher R. Webster, Robert T. Menzies, Guy B. Morrison, and James H. Riccio of Caltech for NASA's Jet Propulsion Laboratory. For further information, Circle 33 on the TSP Request Card. NPO-16440

Determining the Temperature Profile in a Cylindrical Sample

A power-series solution extrapolates from an axial temperature profile.

Marshall Space Flight Center, Alabama

The thermal profile in a homogeneous axisymmetric body can be determined throughout the body if the axial temperature profile is known at any radius. Previously, it was necessary to know the surface temperature profile to make such calculations.

The new theory was developed as an aid in research on the growth of mercury cadmium telluride for infrared detectors. In particular, it is applicable to Bridgman-Stockbarger growth, in which a round cylindrical ampoule of the molten ternary semiconductor is solidified directionally, from one end to the other.

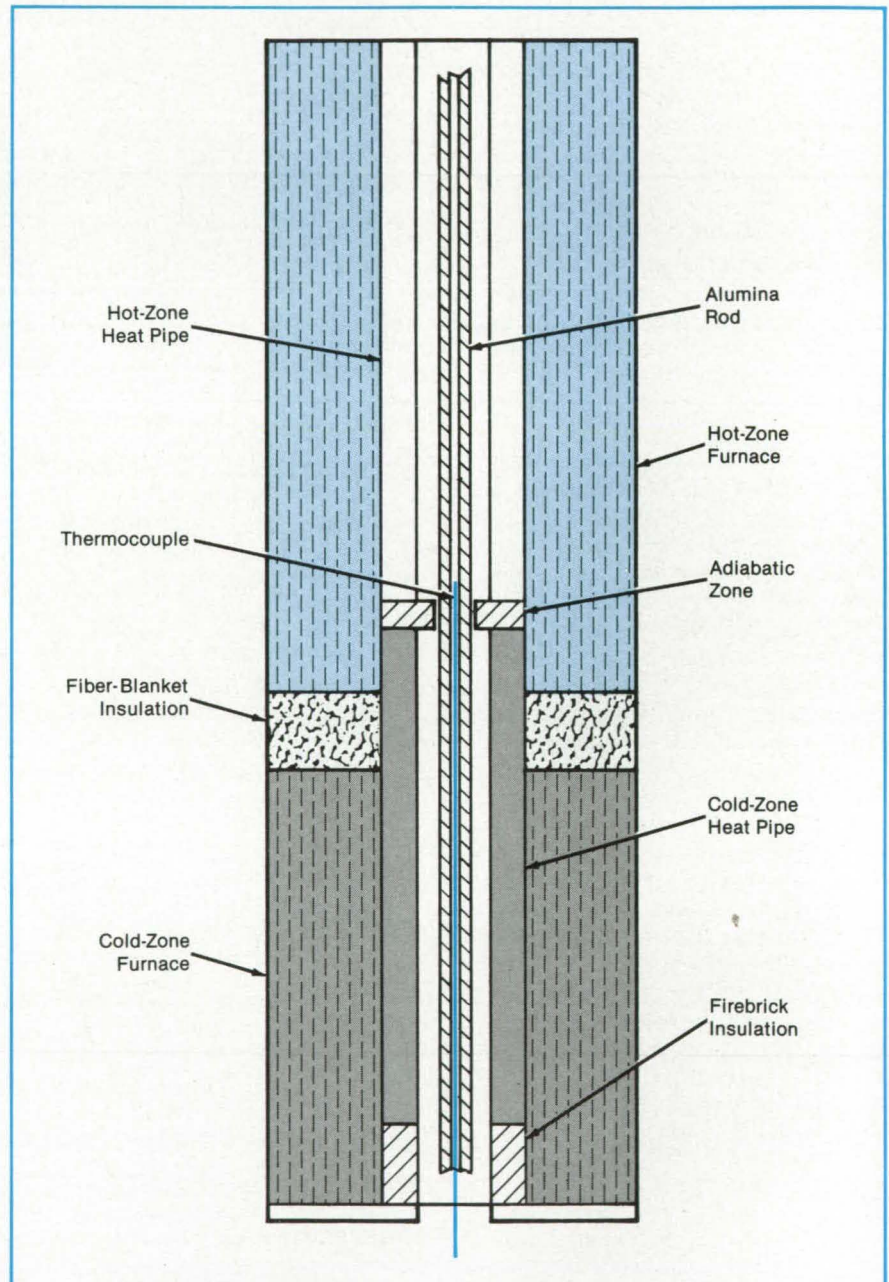
Simplifying assumptions are made for purposes of developing the mathematical solution: The cylinder is treated as being infinitely long, with constant thermal conductivity and specific heat, and without internal heat sources or sinks. In the steady state, the temperature field satisfies Laplace's equation.

The temperature is assumed to be expressible as a dual power series. Using the customary solution technique, the power-series coefficients are related to each other by recursion relations derived by inserting the power series into Laplace's equation.

If the temperature $T(b,z)$ is known as a function of axial position z along a line of constant radius $r = b$, this temperature profile can be used to determine some of the coefficients. The remaining coefficients are then determined from the recursion relations, thereby enabling the subsequent calculation of temperature $T(r,z)$ at any position in the rod. For example, the temperature $T(0,z)$ could be measured along the axis and the coefficients thereby obtained used to calculate $T(r,z)$.

To test the theory, temperature measurements were taken along an axial hole in an alumina rod. The rod was placed in a furnace (see figure) with hot and cold zones separated by an adiabatic zone. Although difficulties were encountered in fitting the theory to the experimental curves accurately, the calculated temperature profiles and isotherm locations agreed qualitatively with the behavior that basic physical principles would lead one to expect.

Only in determining radial temperature gradients did the theory present real difficulties. The isotherms were nearly flat



This **Furnace** was used to obtain the axial temperature profile of a rod of alumina. The alumina specimen was supported at the top and bottom of the hot and cold zones by jigs that allowed it to be aligned with the furnace axis. The top and bottom furnace openings and the gap between hot and cold zones were plugged with fiber insulation.

throughout the sample, and the resulting polynomial fits to the experimental data could not be resolved sufficiently to give consistent radial gradients at the surface.

This work was done by James Creed

Clayton of Semtec, Inc., for Marshall Space Flight Center. For further information, Circle 86 on the TSP Request Card. MFS-26013

Intense Source of Polarized Hydrogen Atoms

Atoms are produced magnetically according to total angular momentum.

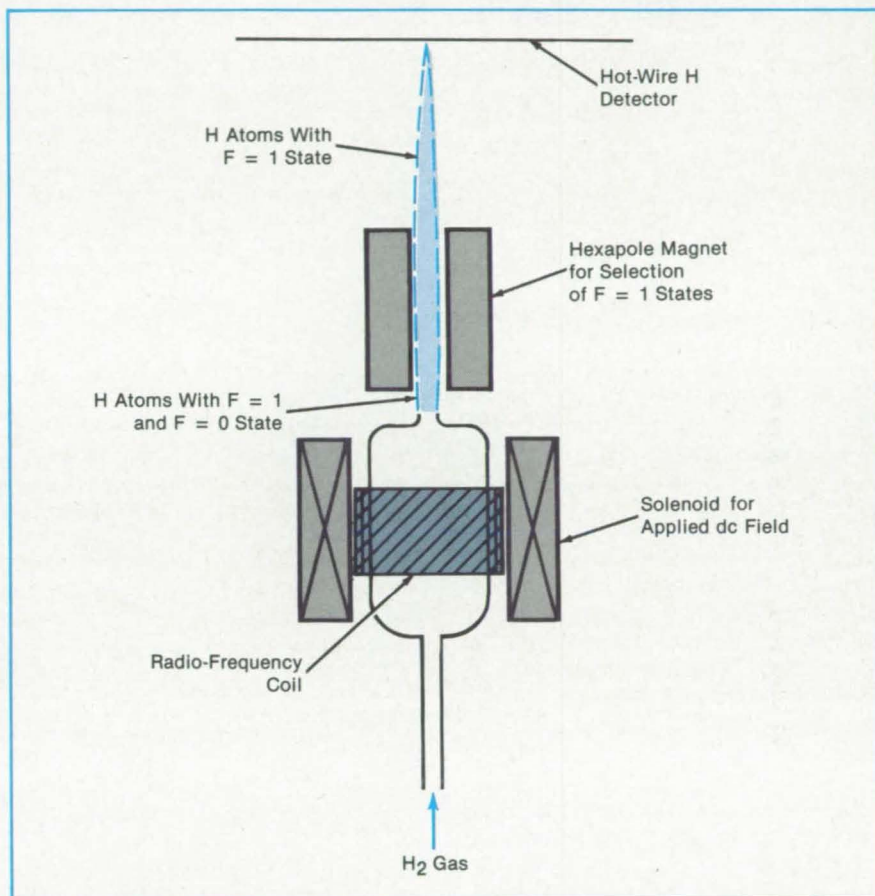
NASA's Jet Propulsion Laboratory, Pasadena, California

Atoms produced by the radio-frequency dissociation of hydrogen molecules are sorted according to their hyperfine states in an improved polarized hydrogen source. By use of a combination of dc magnetic fields, atoms of the upper hyperfine ground level $1S_{1/2}$, $F = 1$ are selected in numbers greater than those of the undesired $F = 0$ state.

The dissociator (see figure) operates under conditions typical of those in hydrogen masers, at a pressure of 250 mtorr (33 N/m^2) and a radio-frequency power of 7 W at 125 MHz. The magnetic field applied to the dissociator could range from 0 to 600 G, increasing the overall efficiency of the source by 10 to 200 percent. The degree of enhancement depends upon the field strength; for example, 230 G results in one of the higher peaks of polarized atom production.

The hexapole focusing magnet preferentially selects atoms in the desired state. The combination of the hexapole magnet and the dissociator with the applied magnetic field increases the number of desired atoms by a factor of 60 to 70, as compared to the combination of the hexapole magnet and a dissociator without the applied field. The source could be built with permanent magnets or electromagnets. Its principal utility is as a source of polarized hydrogen for masers or experimental studies.

This work was done by Lutfullah Maleki of Caltech for NASA's Jet Propulsion Laboratory. For further information, Circle 24 on the TSP Request Card. NPO-16434.



Solenoidal and Hexapolar Magnetic Fields turn an RF dissociator into an intense source of hydrogen atoms in the upper hyperfine ground level ($1S_{1/2}$, $F = 1$).

Molecular Thermal-Electron Detectors

Small energies are detected with high resolution and sensitivity.

NASA's Jet Propulsion Laboratory, Pasadena, California

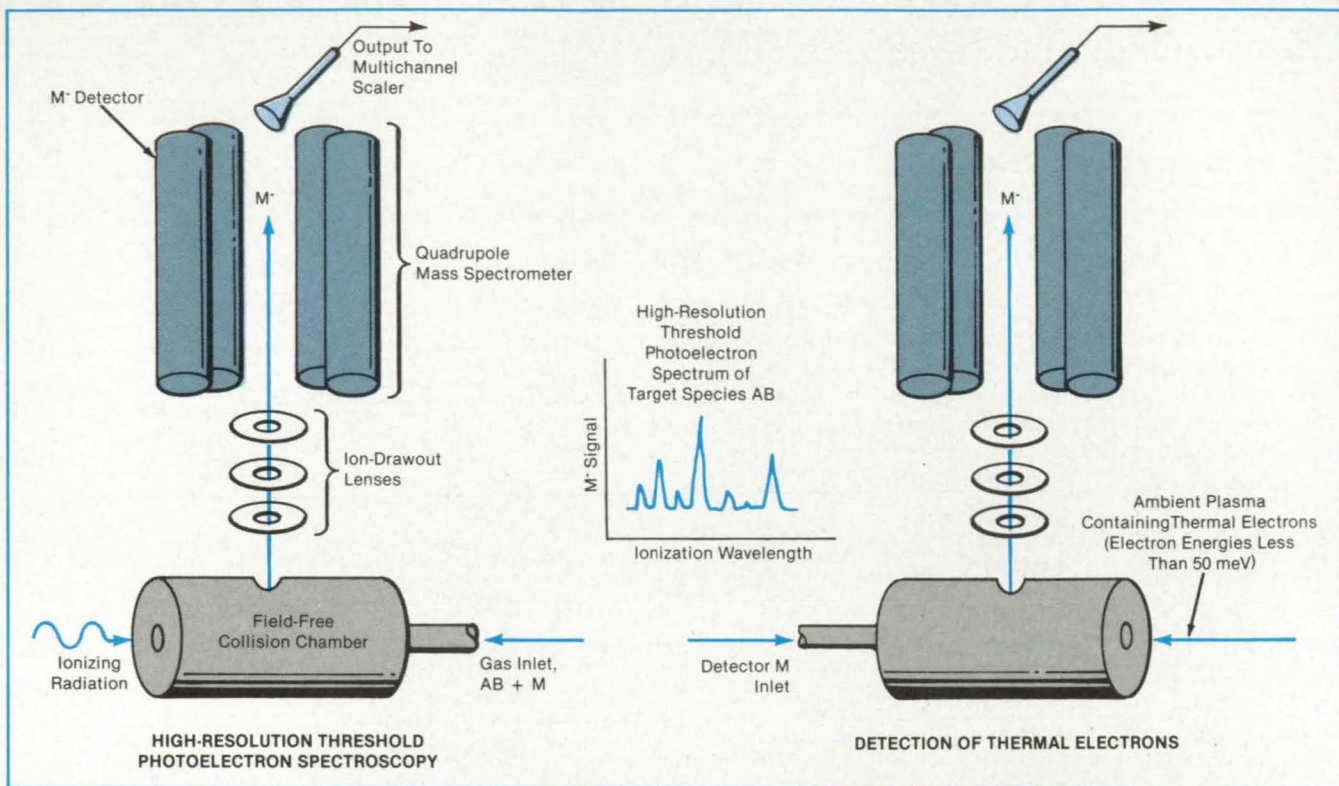
Low-energy electrons are detected with high resolution and sensitivity by their collisions with certain molecules. Molecules of CFCl_3 , CCl_4 , $2\text{-C}_4\text{F}_6$, and SF_6 have been used successfully to detect electrons having energies less than 10 meV. The mole-

cules $\text{C-C}_5\text{F}_8$ and $\text{C-C}_6\text{F}_{12}$ in particular have been found to have a nearly "delta function" response with respect to the attachment of zero-energy electrons.

An instrument based on molecular detection could perform high-resolution

threshold photoelectron spectroscopy. An instrument of this type could also be used to detect fluorocarbons and chlorocarbons in the upper atmosphere by their interaction with thermal electrons.

The technique is based on the formation



Detector Molecules (labeled "M") are used for both high-resolution threshold-photoelectron spectroscopy and thermal-electron detection. In the former case, low-energy electrons produced by ionizing radiation attach to the detector molecules. In the latter case, thermal electrons from a plasma attach to the detector molecules. The attachment products are negative M ions.

of negative ions by low-energy electrons and subsequent detection of the ions. The difficult process of extracting and focusing low-energy electrons is avoided. In the spectroscopy application, the compound to be analyzed is ionized by ultraviolet light (see left side of figure). At various ionization threshold energies, the compound produces thermal electrons that attach to the detector molecules, and the product negative ions are detected in a quadrupole mass spectrometer.

In the thermal-electron-detection application (see right side of figure), an ambient plasma is swept into a collision chamber.

The thermal electrons of the plasma attach to the detector molecules, and the mass-spectrometer signal produced by the attachment products is detected.

The collision chamber is designed to reduce stray electric fields to negligible levels and to prevent inelastic and superelastic collisions with the walls of the collision-chamber repeller element. A slotted, rhodium-plated copper repeller was found to be best; it results in an electron-attachment spectral-line width that is limited only by the spectrometer resolution in the threshold photoelectron spectroscopy application above, or by the ambient elec-

tron widths in the plasma detection scheme. The rhodium plating produces a surface that is effectively uniform in terms of contact potentials and patch fields. The slots reduce the number of inelastic and superelastic reflections of electrons back into the collision region.

This work was done by Ara Chutjian and Samuel Alajajian of Caltech for NASA's Jet Propulsion Laboratory. For further information, Circle 10 on the TSP Request Card.
NPO-16300

Detecting Trace Contaminants in the Atmosphere

A sensitive instrument uses two low-energy electron beams to detect certain molecules.

NASA's Jet Propulsion Laboratory, Pasadena, California

An experimental instrument identifies and measures trace contaminants in the atmosphere. When fully developed, the portable instrument is expected to be able to measure contaminant concentrations of

certain halogen containing molecules as low as one part per trillion.

The instrument employs electron beams to ionize the contaminant molecules by the dissociative attachment of

electrons (see figure). The negative ions are analyzed by a charged-particle detector and a mass spectrometer. The energies of the electron beams are adjusted to match the resonance dissociation ener-

TOTAL CAPABILITY



AVIONICS

RD-300 Solid-state, completely self-contained Weather Radar test set. RD-300 with oscilloscope can perform virtually all radar tests.

RD-301 Fully integrated, solid state simulator for testing airborne and narrow pulse marine radars. Responds to radar transmitter pulse widths of 50 ns to 30 μ s. Two independent range delay systems.

NAV-401L Self-contained ramp or bench test set for functional testing and calibration of MKR, VOR, LOC, G/S and COMM avionics.

NAV-402AP Similar in operation and appearance to NAV-401L plus additional features that permit testing of sophisticated autopilot systems.

ATC-600A Completely portable self-contained unit providing accurate Transponder/DME measurements on the ramp or bench.

NAV-750B Self-contained unit for semiautomatic functional testing and calibration of airborne VOR, LOC, G/S, MKR and COMM receivers.

NAV-750BR Automatic version of NAV-750B with step attenuator 0 dBm to -127 dBm.

COMM-760 NAV-750 accessory for semiautomatic testing of each of 720 or more channels of aircraft communications transceivers.

MLS-800 A menu driven ground station simulator for testing all parameters of airborne angle receivers on the ramp or bench. Optional IEEE-488.1978 interface.

ATC-1200Y3 Transponder/DME test set permits simulation of the ground station and airborne environment on the bench.

ATC-1400 Microprocessor-based test set to provide complete testing of modern Transponder/DME equipment with standard IEEE-488 Bus interface for automatic operation.



offers the most complete line of high performance avionics and communications test equipment available today.

Seeing is believing!

Call your distributor for complete technical information, brochure and demonstration — or contact IFR, Inc., 10200 West York Street, Wichita, Kansas 67215 U.S.A. Phone 316/522-4981 TWX 910-741-6952

Circle Reader Action No. 317

AVIONICS

T-1401 TACAN Bearing Simulator. Interfaces with ATC-1400 making a complete test station for ATC Transponder, DME and civil TACAN equipment.

TAC-1400A/A Microprocessor based unit for testing airborne TACAN equipment including Air-to-Air and Inverse TACAN. Meets military requirements for AN/ARM-135 TACAN test set.

WRX and WRC-7708 Weather Radar Test system, consisting of **RDC-7708, STD-7000, DF-7708**, terminal display and keypad, for a complete test station for Collins WXR-700C or WXR-700X weather radar. Also interfaces with Bendix. Meets ARINC-708 specifications.

COMMUNICATIONS

FM/AM-500A "Micro-Monitor" A complete, compact service monitor weighing only 16 lbs.

FM/AM-1100S Portable service monitor with built-in 70 dB Spectrum Analyzer. Continuous frequency coverage from 100 Hz to 1 GHz.

FM/AM-1200 A multi-function, microprocessor controlled, portable service monitor designed to test throughout the RF frequency range of 250 kHz to 1 GHz.

FM/AM-1500 A microprocessor-based, digitally synthesized service monitor utilizing keyboard entry system, LCD display for programmed frequency readout, processor controlled memory functions and CRT capable of alphanumeric or waveform displays. Optional cellular mobile test capabilities.

GENERAL PURPOSE

A-7550 A portable, digital Spectrum Analyzer utilizing two microprocessors, menu driven display modes and single function keyboard. Frequency ranges of 100 kHz to 1 GHz.

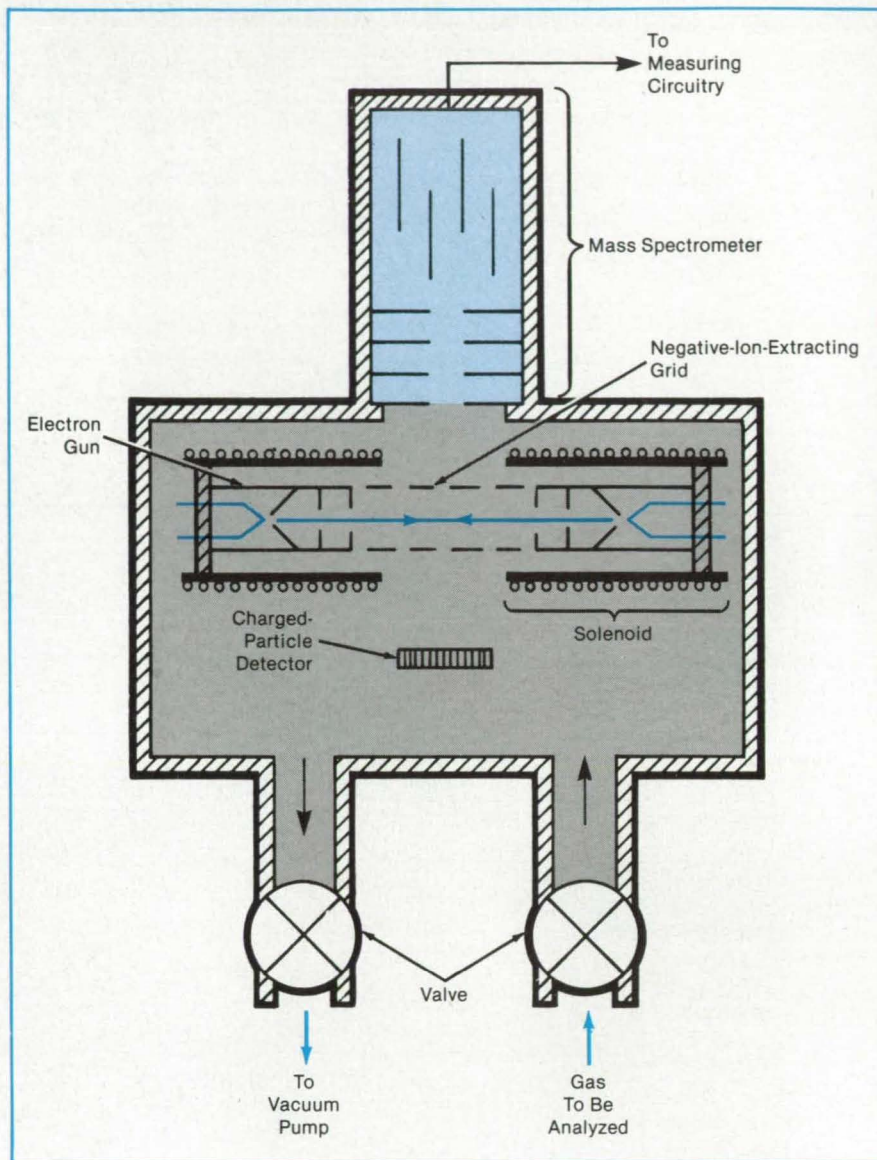
gies of the contaminant. The contaminant molecules are identified by the characteristic set of resonant energies and masses.

The ionization into negative ions is a low-energy process that produces few secondary electrons and photons from the instrument walls. Such secondary effects would contribute to inaccuracy in measurement. The low-energy beams ionize contaminants selectively, without significantly ionizing molecules of the surrounding air. As a result, the signal-to-noise ratio is high, and the instrument is highly sensitive.

Air or another gas to be analyzed flows into the path of opposed electron beams, the energies of which are varied between 0.5 and 20 electron volts. To collimate the electron beams, solenoids provide a magnetic field coaxial with the electron guns. The ions are extracted from the chamber and focused at the entrance aperture of a quadrupole mass spectrometer. Meanwhile, the gas is continuously pumped out of the chamber.

The use of two (or even more) electron beams greatly improves the size of the resonance peak for molecules in some rotationally and vibrationally excited states. One beam is used to excite the contaminant molecules while the energy of the other beam is varied to probe for the resonances. For carbon dioxide, for example, one beam at 1.2 electron volts raises the molecules to a vibrational state with a large excitation cross section. The energy of the other beam is then varied to obtain the rate of dissociation of the CO_2 into CO and O^- .

This work was done by Santosh K. Srivastava of Caltech for NASA's Jet Propulsion Laboratory. For further information, Circle 49 on the TSP Request Card. NPO-16225



Two Electron Beams impinge on flowing air, dissociating the contaminant molecules and producing ionized dissociation products in the stream. The ions are detected by a mass spectrometer.

Solid-State Detector for Trace Materials

Characteristic signals indicate the presence of certain chemicals.

NASA's Jet Propulsion Laboratory, Pasadena, California

A detector for trace chemicals senses as few as 10^{12} molecules of a given material on its surface. It contains no moving parts, is amenable to large-scale integration, and operates at room temperature. Potential applications are in industrial process control and in environmental analysis.

The detector is a thin-film, solid-state tunnel junction composed of layers of

aluminum, aluminum oxide, and gold on a glazed ceramic substrate. When a material is adsorbed on the gold, even in very small quantities, the tunneling characteristics are altered. The nature of the alteration depends on the material.

The aluminum layer, about 400 Å thick, is deposited by thermal evaporation through a mask. The intermediate oxide

layer then is grown to a thickness of about 20 Å on the aluminum layer by a dc glow discharge in an atmosphere of oxygen and water vapor. The gold is deposited on the oxide, also to a thickness of 400 Å, by thermal evaporation through a mask.

Detectors thus fabricated were tested by exposure variously to mercury, iodine, and bismuth. After the exposure, the sec-



**FOR
SALE**

SPACE

... on board NASA Tech Briefs' next launch

"NASA Tech Briefs WORKS for advertisers."

That's according to Bill Waskey, Director of Business Development for Fairchild Industries' Control Systems Division, and other executives now advertising in NASA Tech Briefs.

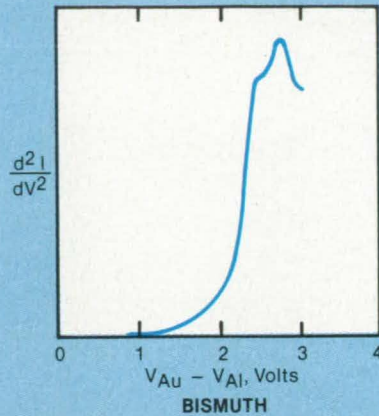
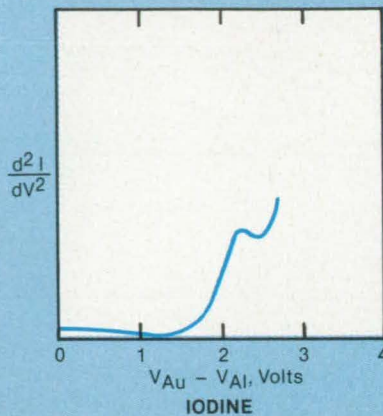
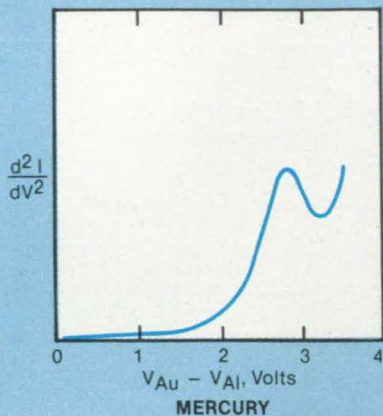
Companies like Rockwell, Amoco, Data General, and DuPont have already received more than 6200 top-quality responses to their ads in NASA Tech Briefs. If your company is on the leading edge of technology, shouldn't you be marketing in the #1 magazine on the leading edge of technology?

Confirm Your Space on Board.

To find out how you can be on board the next launch of NASA's official magazine, call Robin DuCharme, Dick Soule or Wayne Pierce in New York at (212) 490-3999; Irene Froehlich in Chicago at (312) 848-8120; or Bob Bruder in Los Angeles at (213) 477-5866.

NASA Tech Briefs

is published by
Associated Business Publications
41 East 42nd Street, Suite 921
New York, NY 10017



Characteristic Peaks appear in the tunneling spectra of thin-film tunnel junctions after exposure to mercury, iodine, and bismuth — all materials that readily diffuse into the outer gold films of the junctions. The spectra are plots of the second derivative of current with respect to voltage versus the voltage between metal layers.

ond derivative of current with respect to voltage was measured as a function of voltage between the gold and aluminum layers, the gold being at a higher potential than the aluminum. The exposure to mercury and iodine vapors was at room temperature for just a few minutes. Bismuth, on the other hand, was deposited 40 Å thick on the gold layer and heated at

120° C for 10 minutes.

In each case, the spectral features observed were characteristic of the adsorbed material (see figure). For repeated exposure to mercury, a device could be regenerated many times by heating: The heat drives off the adsorbed mercury and makes the device ready for use again. For iodine exposure, it is necessary only to

rinse the device in ethanol to regenerate it.

This work was done by John J. Lambe, Satish Khanna, Anilkumar P. Thakoor, and Henry G. Leduc of Caltech for NASA's Jet Propulsion Laboratory. For further information, Circle 89 on the TSP Request Card. NPO-16450

Technique for Measuring Gas Conversion Factors

The method is based on equalizing the partial pressures of oxygen in a test gas and in air.

Langley Research Center, Hampton, Virginia

A new technique for measuring calibration conversion factors for hydrocarbon mass flowmeters has been applied to a widely used type of commercial thermal mass flowmeter for hydrocarbon gases. The values of conversion factors for two common hydrocarbons measured using this technique are in good agreement with the empirical values cited by the manufacturer. Similar agreement can be expected for all other hydrocarbons. The technique is based on the Nernst theorem for matching the partial pressure of oxygen in the combustion product gases with that in normal air. It is simple, quick, and relatively safe, particularly for toxic/poisonous hydrocarbons.

Most current mass flowmeters for gaseous media depend on the thermal properties of the test gases. They are normally calibrated for air and then used for other gases by means of either a theoretical con-

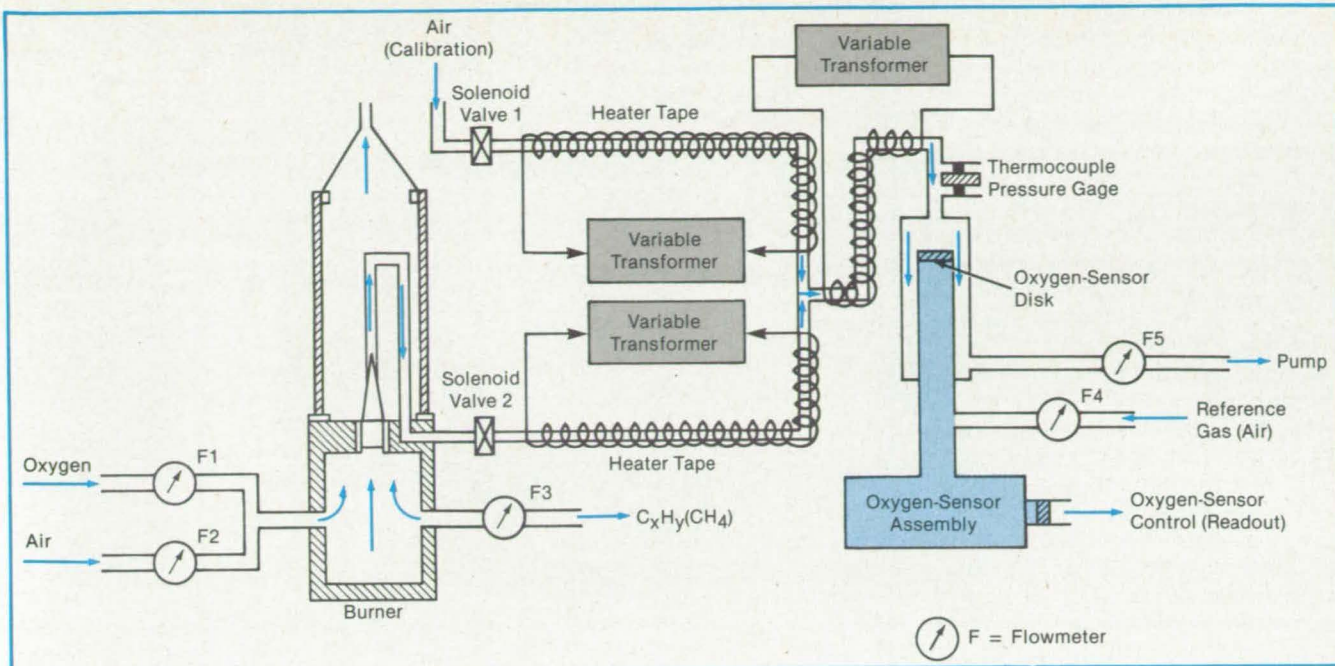
version factor or an empirical factor provided by the manufacturer. Since the theoretical conversion factors of many gases of interest, such as H₂, N₂, O₂, CO, CO₂, CCl₂F₂, and hydrocarbon (C_xH_y), do not agree with the experimental values, it is often necessary to determine their calibration conversion factors experimentally. This is particularly true for most of the hydrocarbons. Even though the process of calibrating mass flowmeters for hydrocarbons is not complicated, their conversion factors often are not available, particularly when the gases involved are rare or toxic. Any scheme that permits in situ measurements of conversion factors for all hydrocarbons would thus be of great interest to combustion chemists and others interested in synthetic fuel development.

The figure shows the experimental setup used for equalizing partial pressures of oxygen in the test gas and the calibration

air. Typically, the hydrocarbon under test would be burnt in oxygen-enriched air in a well-stirred combustor to ensure complete combustion. A fraction of the combustion products would be passed through the oxygen-partial-pressure monitor. For a particular dial setting of the hydrocarbon flowmeter, the oxygen flow rate would be adjusted to make the oxygen partial pressure in the combustion products the same as in the calibration air. This condition would be signaled by the production of the same cell output as is obtained when calibration air is used as the test gas. The hydrocarbon flowmeter conversion factor, F, would then be given by:

$$F = \frac{\text{Oxygen Flow Rate}}{\left(\frac{m}{n}\right)_{\text{Hydrocarbon}} \times \left(\frac{\text{Hydrocarbon}}{\text{Flow Rate on Dial}}\right)}$$

where m is the oxygen flow rate and n is the hydrocarbon flow rate.



The **Oxygen Partial Pressure** in hydrocarbon-combustion-product gases is monitored in this experimental arrangement.

Typical results obtained with methane and acetylene test gases are in good agreement with the empirical values listed by the flowmeter manufacturer. Also, it is apparent from the results obtained that the methane and acetylene conversion factors are independent of the oxygen flow rates as well as the carrier medium (air) flow rates.

This work was done by Jag J. Singh and Danny R. Sprinkle of **Langley Research Center**. Further information may be found in NASA TM-85676 [N83-33127/NSP], "A New Technique for Measuring Gas Conversion Factors for Hydrocarbon Mass Flowmeters" [7]. A copy may be purchased [prepayment required] from the National Technical Information Service,

Springfield, Virginia 22161.

This invention is owned by NASA, and a patent application has been filed. Inquiries concerning nonexclusive or exclusive license for its commercial development should be addressed to the Patent Counsel, Langley Research Center [see page 29]. Refer to LAR-13220.



Compact Imaging Spectrometer

The revised design improves spectral resolution in the visible and near infrared wavelengths.

NASA's Jet Propulsion Laboratory, Pasadena, California

An imaging spectrometer for use in crop and mineral resource-mapping experiments is a scaled-down version of the one described in "Reflecting Schmidt/Littrow Prism Imaging Spectrometer" (NPO-15801), page 481, *NASA Tech Briefs*, Vol. 8, No. 4 (Summer 1984). The new spectrometer also differs from the older one in that the 0.4-to-2.5- μm passband is now divided into two subbands at 1 μm .

Radiation from the scene strikes a reflecting Schmidt corrector plate located near the center of curvature of the primary spherical mirror (see figure). The reflected radiation illuminates the upper portion of the primary mirror and forms an image at its focal surface. A reflecting slit at the primary focal surface acts as a field stop and

serves as the entrance slit for the spectrometer section of the instrument.

The primary mirror collimates the radiation reflected by the slit and directs it toward a dichroic beam splitter, which separates the beam into the two wavelength bands. Separate dispersing prisms and corrector-plate/mirrors are used for each wavelength band.

Placing the correction-plate mirrors in the two beams at slightly different angles from the optical axes separates the two wavelength-dispersed images formed by the rays returning to the focal surface of the primary mirror. This image separation makes it possible to use a different charge-coupled-device detector array for each band without any gap in wavelength cover-

age. Handling the two bands separately improves dispersion linearity.

The revised performance specifications of the spectrometer include spectral resolutions of 10 nm in the visible/near infrared subband (to detect subtle changes in vegetation color) and 20 nm in the remaining infrared subband. The revised design includes two adjustable steering mirrors so that the field of view of the instrument can be aimed up to 45° forward or backward along one axis (along the groundtrack if the spectrometer is flown) and up to 20° to either side of this axis (across the groundtrack if the spectrometer is flown). The aim is adjustable in 1° increments in each direction.

To maintain accurate alignment, the

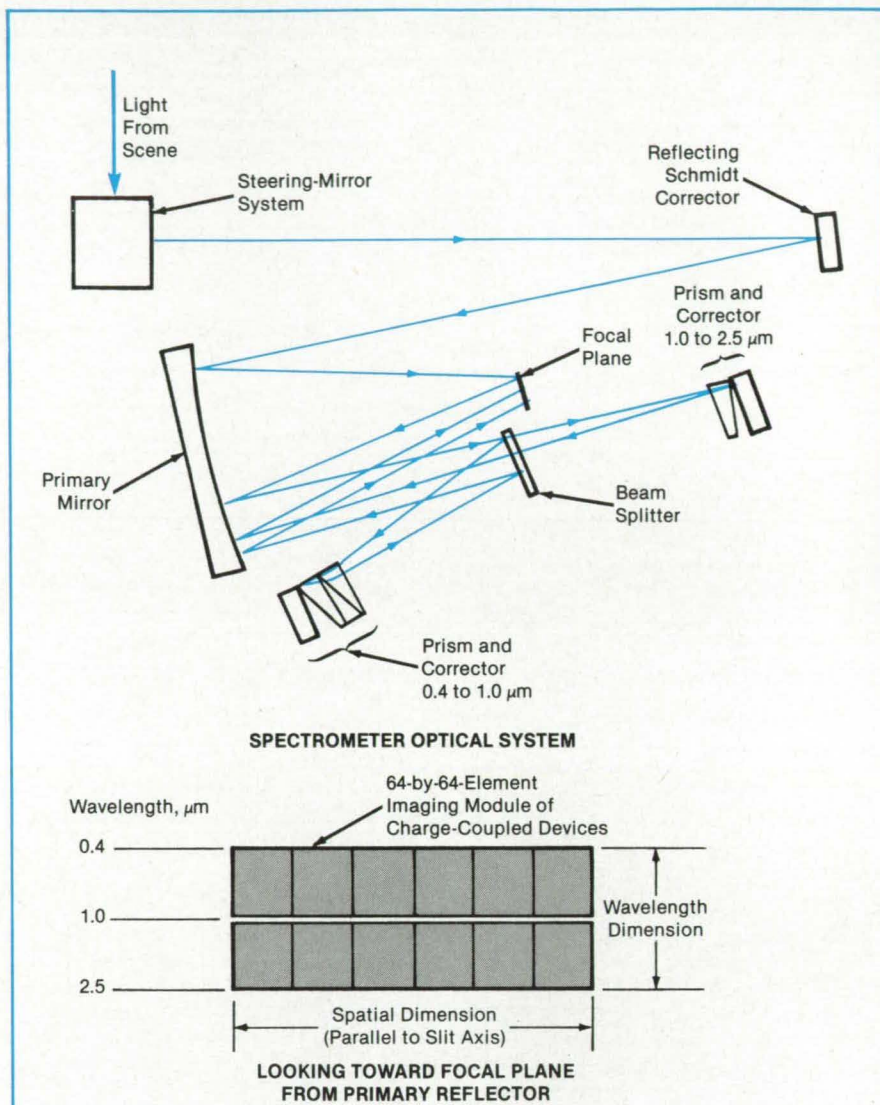
main optical system and the supporting structure for the two aiming mirrors are all mounted to the top plate of the instrument housing. The mirror that controls the aim along the groundtrack also doubles as a protective cover and, in the closed position, directs the instrument field of view to a spectral-line source for calibration.

The electronics and the detector cooler are located on the instrument baseplate; they are cooled by an external refrigerator to 120 K. This arrangement isolates the critical optical components from the heat-producing electronics and from the vibration of the cooler.

The optical parameters of the spectrometer include a primary-mirror focal length of 416 mm and an effective circular-aperture diameter of 11 cm (with a consequent focal ratio of $f/3.8$). The field of view is 2.8° . The signal-to-noise ratio of the instrument varies from about 100 to about 1,000 over most of the spectral region of interest.

The raw-data readout rate is 103×10^6 b/s. Four simple editing modes reduce the rate to or below 50×10^6 b/s. These include the selection of any subset of 128 spectral bands, the averaging of any contiguous set of up to four bands, the spatial averaging of any group of up to four contiguous picture elements, and the reduction of spatial coverage in increments of one picture element.

This work was done by John B. Wellman, Alexander F. H. Goetz, Mark Herring, and Gregg A. Vane of Caltech for NASA's Jet Propulsion Laboratory. For further information, Circle 73 on the TSP Request Card. NPO-16342



The **Compact Imaging Spectrometer** uses Schmidt/Littrow optics with a single spherical primary mirror. The steering mirrors and the two-spectral-band features are new.

Liquid-Level Sensor for Containers in Motion

The gamma-ray attenuation monitors the amount of fluid arbitrarily distributed within a container.

Langley Research Center, Hampton, Virginia

A nonintrusive technique monitors the fluid contents of sealed vessels, regardless of the fluid distribution inside the vessels. The technique is based on the differences in cesium-137 gamma-ray attenuation coefficients in air and the test liquids. Tests indicate that the technique provides accurate (better than ± 10 percent) information about the residual fluid content in sealed vessels.

The new method was originally developed

for use on spacecraft, where the absence of gravity causes a fluid to become distributed throughout the interior of its container. Since conventional liquid level sensors are useless in such situations, a new approach was required. The one developed could be used to measure the fluid content in closed containers on high-maneuvering aircraft where accelerations cause the fluid to become distributed throughout the container.

The figure shows a schematic diagram of the concept. The container is modeled as a rectangular volume, with a planar, uniform gamma-ray source on one face and a planar detector on the opposite face.

The computer program used with the new technique models the stochastic process in which a gamma ray traverses a medium subject to multiple Compton scattering. The vessel modeled is a closed container of exterior dimensions l by $2d$ by $2d$

NASA Tech Briefs, Winter 1985

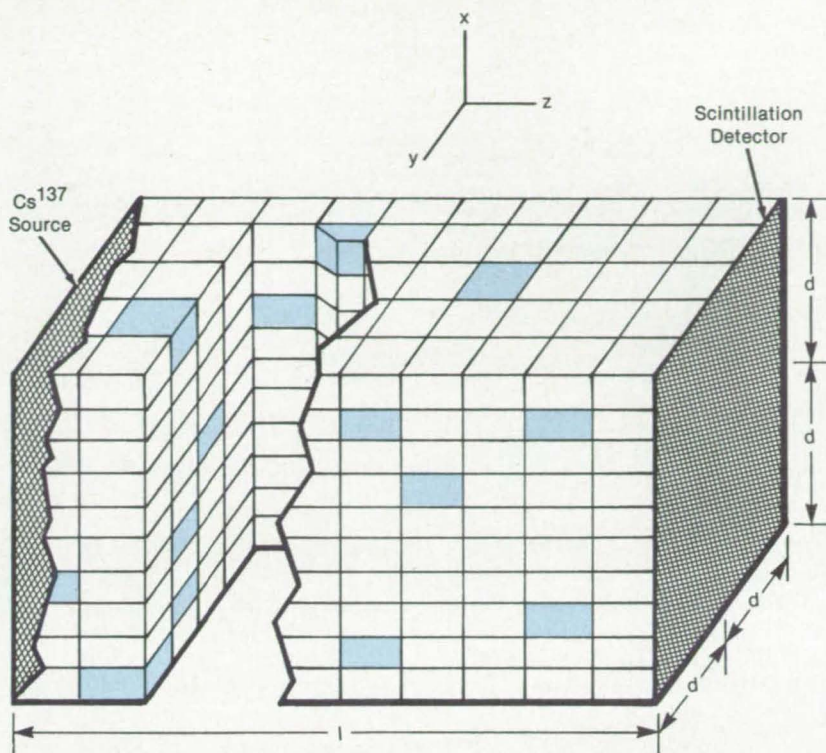
holding variable amounts of a fluid located randomly within it. The interior of the container is subdivided into smaller volumes such that the cross section in any plane parallel to the x-z plane is an $n \times n$ uniform grid. The parameters l , d , and n are defined by the user as program input.

The program identifies each cell with an integer index between one and the total number of cells. If a cell is designated to contain fluid, the electron density (and thus the scattering properties) for that cell is assigned a value corresponding to the fluid. All cells are initially assigned an electron density value corresponding to air.

The program generates formatted output on two files. One file contains a record of the program input followed by a graphic display of the fluid distribution and the transmission probability for each distribution. Each distribution from "no fluid" to "100 percent fluid" is illustrated for each set, with the transmission for each distribution printed below the corresponding display. Following this display, a summary for all sets is generated containing the average transmission and its standard deviation for each distribution.

The second file provides a brief summary for each distribution including the number of counts, the number not counted, and the number of particles dropped for x, y, or z coordinates outside the region or for energy below the cutoff value. In addition to the formatted output, the program generates a graphic output presenting the transmission versus fluid content.

This work was done by Jag J. Singh of



Fluid Is Arbitrarily Distributed in cells throughout the interior of a closed container. Each cell contributes to the attenuation of gamma rays on their way from the source to the detector. The detector readings, therefore, give a measurement of the total fluid content of the container.

Langley Research Center and Gerald H. Mall of Computer Sciences Corp. Further information may be found in NASA TM-85754 [N84-17560/NSP], "A Nonintrusive Nuclear Monitor for Measuring Liquid Con-

tents in Sealed Vessels" [\$8.50]. A copy may be purchased [prepayment required] from the National Technical Information Service, Springfield, Virginia 22161. LAR-13327

Hybrid Laser Would Combine Power With Efficiency

A Nd:YAG laser would be pumped by semiconductor lasers at its ends.

NASA's Jet Propulsion Laboratory, Pasadena, California

According to a recent NASA proposal, an efficient laser system could be constructed by using two semiconductor lasers to pump a neodymium yttrium aluminum garnet (Nd:YAG) device. The hybrid concept was originally developed for optical communication over interplanetary distances. In space or on Earth, it would allow digital transmission at data rates of several megabits per second with a reasonably sized optical aperture of 20 cm.

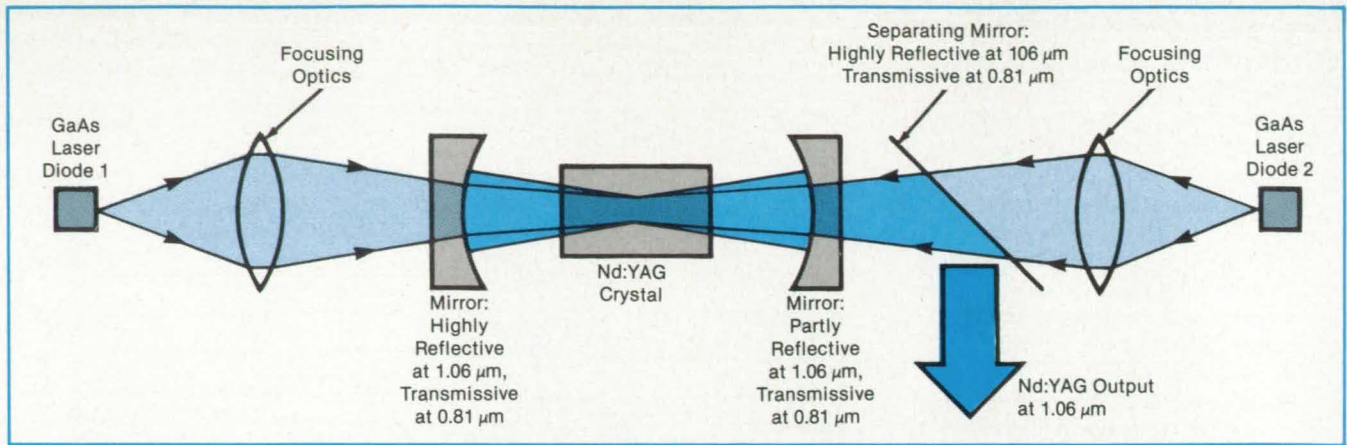
By itself, a GaAs laser produces only a few tens of milliwatts of power with relatively low coherence and spectral purity. A Nd:YAG laser, on the other hand, is difficult

to pump efficiently (an efficiency of only about 0.1 percent is typical). A combination of the devices, however, would allow efficient pumping and would yield 1 W or more of optical power at an overall efficiency of about 10 percent.

The light from two or more GaAs lasers would be focused to small spots on the ends of a Nd:YAG rod (see figure). The GaAs beams, at a wavelength of $0.81 \mu\text{m}$, stimulate the Nd:YAG laser to emit light at $1.06 \mu\text{m}$. With a suitable choice of focusing optics, the GaAs spots can be varied from 50 to $100 \mu\text{m}$ in diameter to coincide with the diameter of the resonant volume of the

YAG rod. Moreover, the GaAs beams would penetrate deeply into the rod: The Nd:YAG crystal is highly absorbent to light at the GaAs wavelength. The end-pumping configuration thus allows the Nd:YAG laser to make maximum use of the energy from the GaAs lasers.

This is in contrast to a conventional side-pumping configuration in which GaAs lasers are arrayed along the length of the Nd:YAG rod. Much of the light from the GaAs passes through the rod without being absorbed in the resonant volume. As a result, a maximum efficiency of only about 0.5 percent is possible with side pumping.



The beams from **Two GaAs Lasers** are efficiently coupled for pumping a Nd:YAG crystal. The combination of lasers exploits the best features of each.

Extremely small optical elements can be used to collect and deliver the pump light, and the size and weight of the system would therefore be small. The separation between mirrors in the laser resonator would be 5 cm, and the mirrors would have a radius of curvature of 5 cm.

The distortion from temperature-induced changes in the index of refraction of the Nd:YAG crystal is expected to be minimal, even though the pumping intensity will be about 10 kW/cm². Such effects as thermal "lensing," in which radial thermal gradients give the rod a lenslike distortion, and

thermal birefringence, in which thermal stress tends to depolarize the light beam, should be negligible.

This work was done by Donald L. Sipes, Jr., of Caltech for NASA's Jet Propulsion Laboratory. For further information, Circle 72 on the TSP Request Card. NPO-16173

Wedged Fibers Suppress Feedback of Laser Beam

An improved optical fiber has a beveled output end and a wedged input end to reduce optical feedback losses.

Langley Research Center, Hampton, Virginia

When an injected laser is coupled into an optical fiber, emission instabilities arise because of optical feedback losses from the fiber into the laser. Coupling efficiencies as high as 80 percent, however, have been obtained by shaping the end of a multimode fiber into an obtuse-angled wedge. Because the slanted sides eliminate the back reflection, such a wedged fiber can achieve high coupling efficiency. The relation (see Figure 1) between the fiber acceptance half angle and the wedge angle in a typical wedge-ended fiber is given by:

$$\theta = \sin^{-1} \{ n_2 \sin[\phi + \cos^{-1}(n_2/n_1)] \} - \phi$$

In order to investigate the ability of the wedged fiber to suppress optical feedback, a laser was mounted on a temperature-stabilized block and operated at a constant current with an output of about 3 mW. After the spectrum was recorded, a wedged fiber was interposed between the laser and the spectrometer, and the spectrum was again recorded. The two spectra were in close agreement. The advantage of the wedge, however, can be lost if there is in-

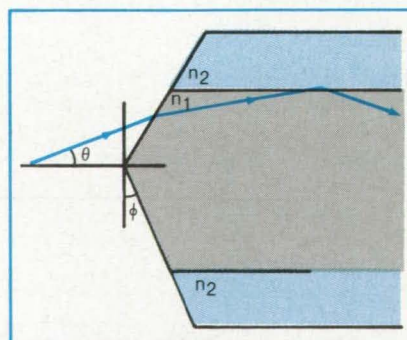


Figure 1. The **Input End of the Multimode Fiber Is Wedge Shaped** to obtain high coupling efficiency with reduced optical feedback.

ternal reflection from the output end of the fiber. These reflections can be eliminated with a beveled output end (see Figure 2). The bevel angle ω must satisfy the inequality:

$$90^\circ - \sin^{-1}(1/n_1) < \omega < 90^\circ - \cos^{-1}(n_2/n_1)$$

It is desirable to use the smallest possible ω to increase the attenuation of internally reflected light, but internal reflection

should be avoided too close to the critical angle where reflectivity rises steeply above 4 percent. Most of the fiber terminations in this work had angles in the 50° to 55° range, the bevel angle for total internal reflection being approximately 47°. The output beam with such terminations is inclined toward the bevel, and the angle δ between the beam direction and the fiber axis is given by:

$$\delta = \sin^{-1}(n_1 \sin \epsilon) - \epsilon$$

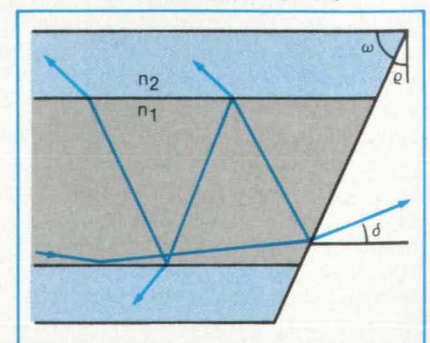


Figure 2. The **Output End of the Fiber Is Beveled** to reduce optical feedback.

High coupling efficiency and feedback suppression can thus be combined by shaping the input end of a multimode fiber into a wedge and by beveling the output end at a suitable angle. With such fibers,

the laser is not perturbed, and the spectrum measured at the fiber output is a faithful reproduction of the spectrum measured when the laser radiates into free space. This work was done by Ivan Ladany of

RCA Corp. for Langley Research Center. No further documentation is available. LAR-13074

Determining Calibration Constants for Attitude Measurements

An algorithm based on the method of least squares is programmed for a desk-top computer.

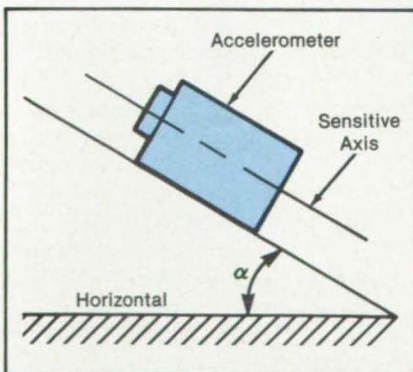
Langley Research Center,
Hampton, Virginia

An algorithm based on the method of least squares determines the calibration constants of seismic instruments for precise attitude measurements. The algorithm was successfully used on a desk-top computer to reduce the calibration data from a precision linear accelerometer.

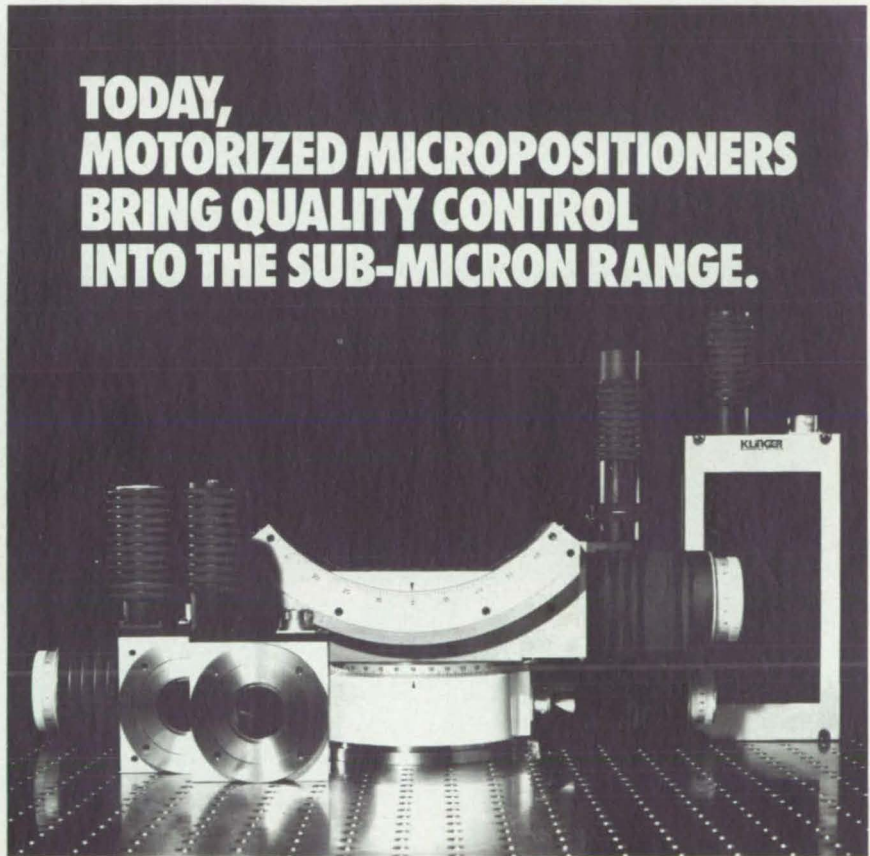
Seismic instruments such as inclinometers or low-range accelerometers can be used to make attitude measurements, as shown in the figure. If the inclination angle α is taken as the input, the output of the instrument is directly proportional to $\sin \alpha$. Ideally, the input and output are related as:

$$e = Sg(\sin \alpha)$$

where e = output signal (volts),
 S = sensitivity (volts/gram),
 g = local gravitational constant,
and α = input angle (degrees).



An Accelerometer can be used to make attitude measurements. The algorithm described in the text can be used to determine calibration constants for this measurement.



**TODAY,
MOTORIZED MICROPOSITIONERS
BRING QUALITY CONTROL
INTO THE SUB-MICRON RANGE.**

IT DOESN'T SEEM A BIT BEYOND
KLINGER SCIENTIFIC

Our linear stages have up to $0.1 \mu\text{m}$ linear accuracy, some with essentially zero backlash that'll carry 100 kg.

Our rotation stages and goniometric cradles measure to 0.001° .

These make possible systems with travel ranges up to 1,250 mm and speeds from 0-200 mm/second for wafer and mask alignment, tracking systems, remote sensing and imaging, laser alignment, fiber optics test and measurement, robotics, disc cer-

tification, calibration and testing mass information storage, with a host of R & D applications.

Klinger is world leader in micropositioning. With a philosophy that says the best is always a bargain in the long run. Write or phone us for our free catalog. Klinger Scientific Corporation, 110-20 Jamaica Avenue, Richmond Hill, NY 11418. (718) 846-3700.

In practice, however, this equation is modified to include two sources of error: The mechanical misalignment ϕ and the electrical bias b . Thus, the input/output relationship becomes:

$$e = b + Sg\sin(\alpha + \phi)$$

where b = bias signal (volts) and ϕ = vertical component of the misalignment angle (degrees).

In theory, the three unknowns, b , S , and ϕ , can be established from a "three-point" calibration process, but, in general, many more data points are taken in order to perform a statistical analysis on the experi-

mental data. The algorithm is a procedure that determines the calibration constants b , S , and ϕ using the method of least squares.

The algorithm was programed and run successfully on a commercially available desk-top computer. It simplifies determinations of accelerometer calibration constants, and it can be used in the field to verify accelerometer stability.

This work was done by Ping Tchong and Tom D. Finley of Langley Research Center. For further information, Circle 12 on the TSP Request Card.
LAR-13214

Books and Reports

These reports, studies, and handbooks are available from NASA as Technical Support Packages (TSP's) when a Request Card number is cited; otherwise they are available from the National Technical Information Service.

Accuracy of Lidar Measurements of the Atmosphere

Sources of error in calibration of systems and interpretation of data are examined.

A report reviews sources of systematic error in laser radar (lidar) measurements of particles in the atmosphere. The report applies particularly to stationary pulsed carbon dioxide lidars of the type used to measure backscatter from aerosols in the troposphere. It provides information for calibrating such systems accurately and consistently and interpreting their data correctly. Much of the discussion is also useful in calibrating mobile and airborne lidars, lidars operating at wavelengths other than those of carbon dioxide lasers, and continuous-wave lidars.

The report examines the physics of atmospheric backscatter measurements. It considers data-acquisition errors, data-processing errors, the influence of the telescope overlap function (defined as the fraction of the transmitted pulse energy that is within the receiver field of view), calibration with a hard target, and mathematical models of atmospheric attenuation.

The largest potential source of error is the telescope overlap function. If the function is neglected or inaccurately modeled, measurements can be significantly in error. Although errors from other sources may be smaller, they nevertheless must be considered.

This work was done by Michael J. Kavaya and Robert T. Menzies of Caltech for NASA's Jet Propulsion Laboratory. Further information may be found in NASA CR-173738 [N84-28067/NSP], "Aerosol Backscatter Lidar Calibration and Data Interpretation" [\$10]. A copy may be purchased [prepayment required] from the National Technical Information Service, Springfield, Virginia 22161. NPO-16493



"IMPRISONED"

by design limitations of your current

GHz BRAGG CELL?



BREAK
OUT...

...with
 brimrose

ACOUSTO-OPTIC MODULATORS at their finest!

APPLICATIONS:

- GHz OPTICAL MODULATORS
- LASER CAVITY DAMPERS
- BROADBAND LASER DEFLECTORS
- LASER BEAM STEERING
- RADIO ASTRONOMY
- VARIABLE RANGE SIMULATORS
- OPTICAL COMPUTING
- RF SPECTROMETER
- FIBER OPTIC COMMUNICATIONS
- LASER DISK MODULATORS
- EW SYSTEMS
- FREQUENCY IDENTIFICATION

- 30 DAY DELIVERY ON SELECTED ITEMS

FEATURES:

- 90% RF WATT EFFICIENCY AT 1 GHz
- CELLS FROM 25 MHz to 3 GHz
- BANDWIDTHS TO 1 GHz
- FULL RANGE OF AO MATERIALS
- 2-D LASER DEFLECTORS
- 6" DEFLECTION ANGLES
- LARGE SCALE PRODUCTION CAPABILITIES
- 96% YIELDS
- ENGINEERING DESIGN
- PERFORM GOVERNMENT CONTRACTUAL WORK
- CUSTOM FABRICATION

AND MORE!

compare our devices with the best of them: HARRIS, ITEK, CRYSTAL-TECH, and TELEDYNE.

brimrose bragg cells: Worth "bragging" about.

for information
call or write:

brimrose corporation of america
7720 belair road
baltimore, maryland 21236
(301) 668-5800
telex 910-997-6817 brimrosecorp

Adsorption of H₂, Ne, and N₂ on Activated Charcoal

Adsorption isotherms and heats of adsorption were determined at pressures from 1 to 80 atmospheres.

A 9-page report presents measured adsorption isotherms of hydrogen, neon, and nitrogen on activated charcoal for temperatures from 77 to 400 K and pressures from 1 to 80 atmospheres (0.1 to 8.1 MPa). Heats of adsorption calculated from the isotherms are also presented.

The new results extend to higher pressures than previous data. Data in this region were needed for use in designing a workable gas-adsorption compressor.

The isotherms were determined by noting the equilibrium pressure and temperature inside a constant volume. A stainless-steel adsorption cell of 14.35 cm³ volume held 7.38 g of charcoal, which was packed into an open foam copper matrix (2 percent by volume) to enhance heat transfer to and from the charcoal. The cell temperature was measured with a silicon diode thermometer and controlled with a 40-W heater and a gas heat switch to a 77-K heat sink.

The adsorption cell was connected to a chamber of calibrated volume, which in turn was connected to both a vacuum system and a gas supply. To control experimental conditions, there was a valve in each of the lines connecting these components.

The report gives expressions, based on the ideal-gas law, which show the relationship between different definitions of the volume of gas adsorbed and which are used in describing low-pressure isotherms. Of these, V_E , which includes only the part of the fluid under the direct influence of the adsorption force, is recommended as the most useful because it is independent of the intergranular structure and the packing pattern of the charcoal cell. Another defined volume, V_T , differs from V_E by including the fluid inside the microscopic voids in the charcoal.

Two different analytic expressions that fit adsorption data are given: One for hydrogen and one for neon and nitrogen. The data on the heats of adsorption are presented tabularly. These data agree with previous results, where available.

This work was done by Chung K. Chan, Emanuel Tward, and Kourosh I. Boudaie of Caltech for NASA's Jet Propulsion Laboratory. To obtain a copy of the report, "Adsorption Isotherms and Heats of Adsorption of Hydrogen, Neon, and Nitrogen on Activated Charcoal," Circle 95 on the TSP Request Card.
NPO-16329

Microwave Atmospheric-Pressure Sensor

The difference in signal absorption between two frequencies is a measure of the atmospheric pressure.

A report describes tests of a microwave pressure sounder (MPS) for use in satellite measurements of atmospheric pressure. When fully developed, the MPS may furnish valuable data for predicting weather at low cost. Such an instrument is not only feasible but also accurate, according to tests of a simplified version on an airplane.

The MPS is a multifrequency radar operating between 25 and 80 GHz. It determines the signal absorption over a vertical path through the atmosphere by measuring the strength of echoes from the ocean surface. The MPS would operate even with cloud cover, and it is suitable for use on current meteorological satellites. After further development, it should be able to measure not only surface pressure but also liquid and vaporous water content and surface wind speed as well.

Two channels in the broad oxygen-absorption band at 60 GHz would be used to measure the total oxygen in the air column. The surface pressure would then be calculated from the total-oxygen measurement by taking into account the effects of the vertical temperature profile and other atmospheric variables. These variables would be determined from measurements in four channels outside the 60-GHz oxygen-absorption band.

The simplified MPS tested in the aircraft used only two channels and operated with much shorter pulses than will be necessary from a satellite in space. The channels were in the lower wing of the oxygen-absorption band at 50.402 and 50.218 GHz. The two frequencies were close enough that the average surface reflectivities were equal. The difference in absorption between the two was thus predominantly a measure of the abundance of oxygen in the air column and of the pressure difference between the surface and the aircraft.

The initial flight tests, conducted over the Pacific Ocean near northern California, were used to check the operating characteristics of the instrument. The second series of tests, over the Beaufort Sea, demonstrated measurements over sea ice. The third series was carried out in a tropical environment over the Atlantic Ocean near Puerto Rico. On each flight, measurements were made at altitudes between 10,000 and 40,000 ft (3 and 12 km).

Differential absorption measurements were made with a precision of 0.01 dB. The variation of differential absorption with altitude corresponded with theory within an equiva-

lent pressure accuracy of ± 3.4 mbar (± 340 Pa).

This work was done by Dennis A. Flower, Gordon E. Peckham, and W. John Bradford of Caltech for NASA's Jet Propulsion Laboratory. To obtain a copy of the report, "Experimental Validation of a Millimeterwave Radar Technique To Remotely Sense Atmospheric Pressure at the Earth's Surface," Circle 51 on the TSP Request Card.
NPO-16496

Soil/Structure Interactions in Earthquakes

A computer simulation of these interactions promises to improve Earthquake resistant structures.

In an effort to improve the design of Earthquake-resistant structures, a mathematical study was undertaken to simulate the interactions among the soil, foundation, and superstructure during various kinds of vibrational excitation. The system was modeled as three lumped masses connected vertically by springs, with the lowest mass connected to a horizontal vibrator (representing the ground) through springs and a dashpot. The behavior of the springs was described by elastic or elastoplastic force/deformation relationships. These relationships were used to approximate nonlinear system behavior as well as soil/foundation-interface behavior.

The study includes a general background discussion and review of the literature concerning the use of finite-element and lumped-parameter/impedance models. A review of seismicity in the Eastern United States is included. Theoretical considerations for the computer modeling of soil/structure systems are presented, along with a discussion of the capabilities (types of problems, input, and output) required of a program to perform such modeling.

Two superstructure models, three soil-behavior models, and two soil stiffnesses were examined in various combinations. The simulation was carried out with a FORTRAN computer program called "DYNA," which was developed for such lumped-parameter/impedance models.

The analysis was performed in the time domain rather than the frequency domain so that behavior parameters could be modified more easily during a program run and so that the immediate output could be interpreted more readily. Moreover, a time-domain analysis can simulate nonlinear effects directly, rather than base them on average values of deformation, and can account for a sequence of events as they actually occur.

Some preliminary conclusions were drawn from the responses of the models to harmonic ground accelerations. For the systems examined and a given soil-behavior model, an increase in soil stiffness decreases foundation displacements and increases superstructure responses. For a given soil stiffness, the response of the superstructure tends to be greatest when the soil behavior is elastic and least when the soil behavior is plastic; that is, when the foundation wallows. Overall increases of damping in the structure and soil/structure system decrease the peak deformation of the first story and the displacement of the top mass while increasing the rotational response of the foundation.

The DYNA computer program is expected to be used in future studies. Modifications that would increase the accuracy and utility of the program include certain elaborations of some of the simple model elements, increasing the number of response parameters in the output, and adding the ability to accept recorded seismic events as inputs. Studies might include simulations of taller, more flexible structures, transient (as distinguished from harmonic) ground movements, and the correlation of computer simulations with experimental data from real structures.

This work was done by George W. Ramey, Raymond K. Moore, Chai H. Yoo, Thomas D. Bush, Jr., and James M. Stallings of the Auburn University for Marshall Space Flight Center. For further information, Circle 44 on the TSP Request Card. MFS-27078

Equipment for Microgravity Research

Equipment ranging from containers to spacecraft is cataloged.

An illustrated catalog describes equipment and facilities available for experiments under low-gravity conditions. The catalog may encourage scientific and commercial organizations to investigate the benefits of conducting research and manufacturing activities in a microgravity environment.

In a section on experimental apparatus, the catalog covers 14 equipment items:

- General-purpose furnace;
- Automated directional solidification furnace;
- Advanced automated directional solidification furnace;
- Static column electrophoretic system;
- Isoelectric focusing experiment;
- Single-axis acoustic levitator;
- Three-axis acoustic levitator;
- Acoustic containerless experiment

system;

- Electromagnetic levitator furnace;
- Fluid experiment system (crystal growth, convection, phase transitions, surface physics, and bubble behavior);
- Fluids experiment apparatus (modular experiments in general liquid chemistry, crystal growth, fluid mechanics, thermodynamics, cell culturing, and other areas);
- Vapor crystal-growth system;
- Monodisperse-latex reactor system; and
- Solute-diffusion apparatus.

For each item, the catalog describes the capabilities and mode of operation. It lists key operating characteristics (such as temperature ranges, voltages, and powers) and physical characteristics (such as dimensions and masses). It gives the parameters of the specimens that the apparatus can accommodate. It describes instrumentation on the apparatus and the types of data that can be acquired from it. Drawings and photographs of the apparatus accompany the description.

In a section on research facilities, the catalog covers drop tubes, drop towers, microgravity research aircraft, ground-based levitators, a float-zone experiment system, and Space Shuttle facilities. Included in the Space Shuttle facilities are the Orbiter middeck, the Orbiter payload bay, modular storage lockers, experimental-apparatus containers, the materials science laboratory, the materials experiment assembly, and standardized aluminum cans for small, self-contained experiments. For each item, the catalog provides text and illustrations.

This work was done by James A. Fountain of Marshall Space Flight Center. To obtain a copy of the catalog, "Microgravity Science and Applications," Circle 84 on the TSP Request Card. MFS-27094

Calculation of Macrosegregation in an Ingot

An interactive computer program uses a new numerical technique to model solidification.

A report describes both a two-dimensional theoretical model of macrosegregation (the separating into regions of discrete composition) in the solidification of a binary alloy in a chilled rectangular mold and an interactive computer program embodying that model. The model evolved from previous ones that were limited to calculating the effects of interdendritic fluid flow on the final macrosegregation for a given input

temperature field under the assumption of no fluid flow in the bulk melt.

The theory incorporates the effects of thermally induced convection in the bulk melt and of heat flow throughout the ingot in the macrosegregation calculation in the solid/liquid region. The theoretical model enables one to calculate the rate of development of the solid and the temperature distribution in the ingot; the only thermal input data required are the heat-transfer coefficient at the chilled side of the mold and the temperature of the chill.

Due to subtleties in the nonlinear form of the macrosegregation equations, it was necessary to resort to a new numerical technique to solve the problem. This technique, called the "discrete-flux method," applies to a broad class of moving-boundary problems.

In the discrete-flux method, the physical conservation relations are preserved both analytically and in discrete form. Finite-difference equations simulate the heat flow through a discrete computational mesh. The resulting discrete form of the moving boundary conditions is explicit.

The heat- and mass-flow equations are first transformed to body-fitted curvilinear coordinates, retaining both the enthalpy and the temperature as dependent variables. Conserving finite-difference approximations are then made for each of the interior and boundary coordinates. The movements of the interfaces are then obtained, subject to the conditions that maintain the correct heat-flux relations at the interfaces.

An interactive computer program to perform these calculations is designed for use by nonprogramers. The user selects the process parameters and the alloy composition and controls the selection of both graphical and tabular output as modeling progresses. The report includes an operating guide, flow charts, and a list of subroutine names and functions, but not the source code.

As implemented, the model neglects convection in the bulk liquid (the region where no solidification has taken place). The report suggests an approach for including a coupling of the convective field in the bulk liquid to the convective field in the solid/liquid zone.

This work was done by David R. Poirier and Anna L. Maples of General Electric Co. for Marshall Space Flight Center. Further information may be found in NASA CR-171030 [N84-23752/NSP], "Analysis and Calculation of Macrosegregation in a Casting Ingot: Exhibits 'C' and 'E' " [\$11.50]. A paper copy may be purchased [prepayment required] from the National Technical Information Service, Springfield, Virginia 22161. The report is also available on microfiche at no charge. To obtain a microfiche copy, Circle 83 on the TSP Request Card. MFS-27068

Computer Programs

These programs may be obtained at a very reasonable cost from COSMIC, a facility sponsored by NASA to make raw programs available to the public. For information on program price, size, and availability, circle the reference number on the TSP and COSMIC Request Card in this issue.

Kinematic Stirling Engine Performance

Calculated power and efficiency characterize performance.

A computer program was developed for analyzing the thermodynamic characteristics of a kinematic Stirling engine. (A kinematic engine has pistons connected by mechanical linkages to a crankshaft.) The program computes time-varying piston positions, pressures, and gas temperatures in each of the gas-control volumes into which the engine working space is divided. The engine performance is characterized by calculations of power and efficiency (both indicated and brake). The inputs to the code are the engine geometrical parameter, engine-operating conditions, and indexes that specify various options available. This computer model represents a compromise between other publicly available models that are either less mathematically rigorous and faster or more mathematically rigorous and slower than the model described here.

The model predicts engine performance for a given set of engine-operating conditions (i.e., mean pressure, boundary temperatures, and engine speed). Fixed heater-tube and coolant-inlet temperatures are assumed; gas physical properties vary with temperature. For the test-case engine, one of the four identical engine working spaces is modeled, and the resultant power is multiplied by 4 to account for the four working spaces. The working-space model includes two pistons, the piston-swept volumes — the expansion and compression spaces, three heat exchangers — the heater, regenerator and cooler, and four adiabatic connecting ducts. The pistons are positioned as func-

tions of time according to the specified frequency. The working space is divided into appropriately sized control volumes for analysis. Flow resistances and heat-transfer coefficients are calculated for each control volume at each time step over the engine cycle. Within each gas volume, the continuity and energy equations are integrated with respect to time; a simplified momentum equation (pressure drop is a function of a friction factor and flow rate) and an equation of state are also used in the calculations.

The basic computer model equations are applied to each of the control volumes. The temperatures, masses, heat-transfer coefficients, and flow rates for each of the control volumes and interfaces (except the appendix gap volumes and interfaces) are represented by dimensioned variable names in the computer model.

The required engine-operating conditions that must be entered into the model are: Heater-tube outside-wall temperatures (the combustor is not modeled), expansion- and compression-space inside-wall temperatures, cooling-water-inlet temperature, cooling-water flow rate, engine speed, and mean pressure. The cooler-tube inside-wall temperature is solved by iteration but is constant during any one cycle. Cylinder and regenerator-housing temperatures for conduction calculations can either be inputs or can be calculated from heater and cooler input temperatures.

Losses due to imperfect heat transfer and appendix-gap pumping losses are an integral part of the cycle calculations. The appendix-gap pumping calculations assume isothermal appendix gaps. A cold appendix gap is included for the sake of generality; however, its volume is very small for the sample case, and its effect is negligible. Heat-conduction and piston-shuttle losses are calculated and are accounted for in the efficiency calculations.

The pressure-drop calculations are based on a simplified momentum equation that neglects gas inertia. Pressure-drop calculations are also decoupled from the basic thermodynamic calculations for the working space to neglect pressure-wave dynamics.

Two passes through the thermodynamic calculations are made to more accurately model the effect of the decoupled pressure-drop calculations on engine performance. The calculated power loss due to pressure drop is about the same whether one or two passes are made. However, in the second-pass calculations, the effect of pressure drop on heat transfer to and from the engine and on mass trans-

fer with the engine is more accurately modeled; the net effect on predicted performance is to increase the basic power (power before pressure-drop loss) and efficiency of the engine.

The program is written in FORTRAN IV for use on an IBM 370 computer.

This program was written by Roy C. Tew, Jr., of Lewis Research Center. For further information, Circle 55 on the TSP Request Card.
LEW-14092

X-Ray Diffraction Analysis Program

The program analyzes derivatives and separates overlapping peaks.

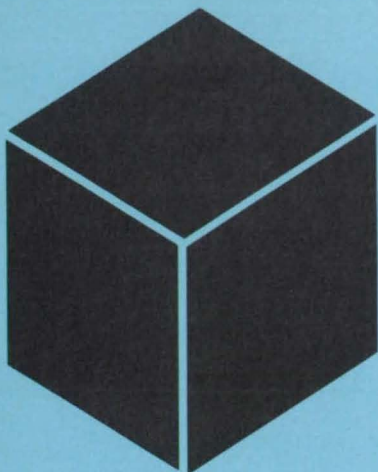
SOPAD separates overlapping peaks and analyzes the derivatives of X-ray diffraction data. In the qualitative and quantitative analysis of X-ray diffraction data, overlapping profiles introduce difficulties that prevent an accurate determination of peak positions and the areas under the diffraction peaks. This problem is prevalent in complex multielement alloys and in certain metal/matrix composites because of the large number of phases present. SOPAD helps the analyst to get the most information out of the available diffraction data.

SOPAD uses a Marquardt-type nonlinear regression routine to refine initial estimates of the individual peak positions, intensities, shapes, and half-widths. Data-smoothing routines and second-derivative routines are included to aid in making estimates of the number of peaks and their positions. The Pearson-VII distribution, which requires only four parameters per peak, is used to describe and refine the individual peaks. Also included is the capability to treat doublets without increasing the total number of parameters.

SOPAD is written in FORTRAN 77 for batch execution and has been implemented on a CDC CYBER 175-series computer with a central-memory requirement of approximately 68K (octal) of 60-bit words. SOPAD was developed in 1983.

This program was written by K. E. Wiedemann and J. Unnam of Vigyan Research Associates, Inc., and S. V. N. Naidu and C. R. Houska of the Virginia Polytechnic Institute & State University for Langley Research Center. For further information, Circle 14 on the TSP Request Card.
LAR-13276





Hardware, Techniques, and Processes

- 100 Measuring Resistivities of Small Fibers
- 102 Solvent-Resistant, Thermally Stable Poly(Carbonate-Imides)
- 104 Chromium Ions Improve Moisture Resistance of Epoxy Resins
- 105 Fast-Response Oxygen-Monitoring and Control System
- 106 Measuring Thermoelectric Properties Automatically
- 107 Insulation Blankets for High-Temperature Use
- 108 Colorless, Transparent, Aromatic Polyimide Films
- 109 Phenoxy Resins Containing Pendent Ethynyl Groups
- 110 Micronized-Coal Burner Facility
- 111 Cobalt Ions Improve the Strength of Epoxy Resins
- 112 Alkane-Based Urethane Potting Compounds
- 113 High-Strength, Low-Shrinkage Ceramic Tiles
- 114 Research Furnace for Crystal Preparation
- 115 Lightweight Protective Garments
- 116 Ultrasonic Mixing of Epoxy Curing Agents
- 117 Ultra-High-Molecular-Weight Silphenylene/Siloxane Polymers
- 118 Cast Iron with High Carbon Content
- 118 Beta Silicon Nitride Whiskers

Books and Reports

- 119 Mechanical Design Handbook for Elastomers
- 120 Solidifying Cast Iron in Low Gravity
- 121 Constitutive Equations of Aging in Polymers

Measuring Resistivities of Small Fibers

Resistivities of graphite and SiC/Si₃N₄ fibers are measured easily and accurately.

Marshall Space Flight Center, Alabama

A technique for measuring the electrical resistivities of fibers of graphite, silicon carbide/silicon nitride mixture, and other materials used in composites is simple, accurate, and reproducible. It is suitable for monofilament fibers with diameters of about 10 to 50 μm . It can also be adapted to tow fiber strands.

A fiber, the diameter of which has been measured, is placed on a clean glass plate. A bead of silver-filled epoxy resin is applied to one end of the fiber, attaching it to the plate. After the fiber settles down to the surface from the disturbance of applying the resin, a bead of the resin is applied to the other end of the fiber. As the second bead is applied, the fiber is gently pulled taut so that it stretches between the beads in a straight line. It is not necessary to wait for the epoxy to cure. The mixed, uncured resin is viscous and holds the fiber securely.

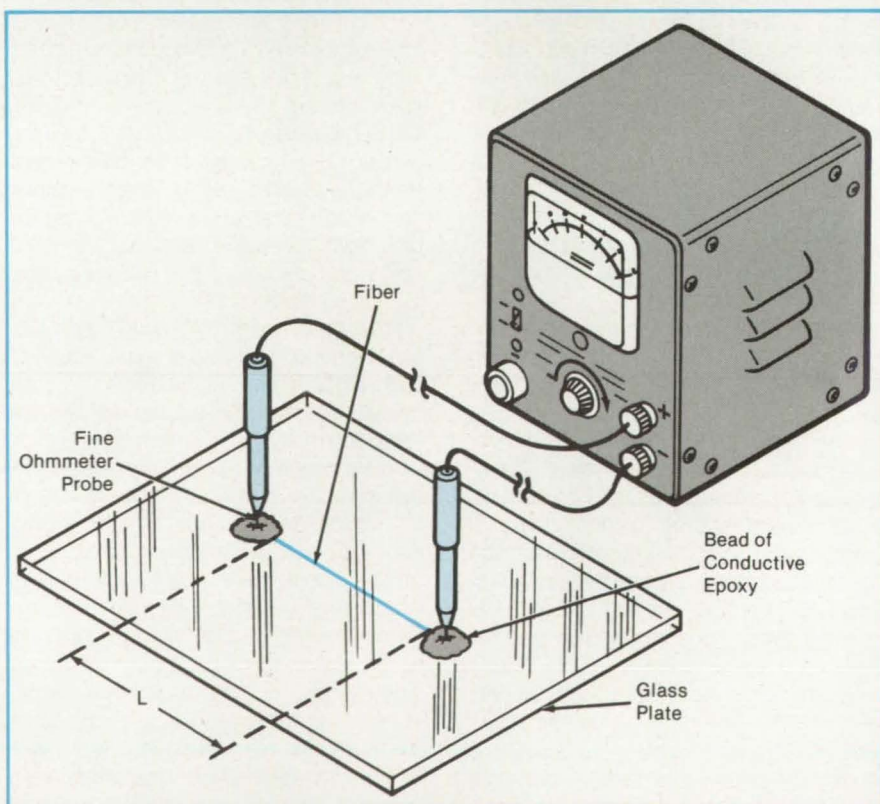
Ohmmeter probes are placed on opposite ends of the fiber, and the resistance between the probes is measured (see figure).

One advantage of not waiting for the epoxy beads to cure is that the probe points can be pressed into them to establish good electrical contact with the fiber. The contact resistance is negligible.

The distance along the fiber between the resin/fiber junctions is then measured with the aid of a divider, ruler, or other convenient instrument. The resistivity ρ is calculated from the measured resistance R , the length L , and the cross-sectional area A of the fiber, according to $\rho = RA/L$.

This work was done by Julia Daniels, Johnny M. Clemons, Frank E. Ledbetter, and Benjamin G. Penn of Marshall Space Flight Center and David J. Crouse of the Tennessee Technological University. No further documentation is available.

Inquiries concerning rights for the commercial use of this invention should be addressed to the Patent Counsel, Marshall Space Flight Center [see page 29]. Refer to MFS-28077.



A **Small-Diameter Fiber** is held at its ends by two beads of metal-filled epoxy resin. The electrical resistance of the fiber is measured by the ohmmeter probes inserted in the beads before they harden. The softness and high conductivity of the uncured beads assure good electrical contact between the probes and the fiber.

SCHOTT ... Precision Optical Glass Made in America and More!!!



Schott Glass Technologies is geared to work with the largest production quantities or the smallest prototype development right here in the USA. Our 300,000 square feet of manufacturing facilities, backed by our scientific knowledge and technical skills, are ready to work for you at every stage of your program.

Our in-house research and development is among the most modern of its kind

anywhere. And we have the marketing and sales know-how to assure you that products made from Schott materials or components get to your customers on time and to specification.

And, above all, Schott Glass Technologies has the widest range of precision optical glass and components available in the Western Hemisphere today.

OPTICAL DIVISION

- OVER 250 TYPES OF OPTICAL GLASSES
- FIBER OPTICS RODS
- HIGH HOMOGENEITY GLASS BLANKS FOR MASSIVE OPTICS
- ZERODUR® — LOW EXPANSION MATERIAL
- PHOSPHATE AND SILICATE LASER GLASSES
- CERENKOV COUNTERS

COMPONENTS DIVISION

- CRT FACEPLATES
- SCIENTIFIC FILTER GLASS
- INTERFERENCE FILTERS
- CRT CONTRAST ENHANCEMENT FILTERS
- FIBER OPTICS SPECIALTIES
- B-270/CLEAR SHEET GLASS
- X-RAY LEAD GLASS
- RADIATION SHIELDING GLASS AND WINDOWS

OPHTHALMIC DIVISION

- CROWN GLASS — CLEAR AND TINTS
- 1.60 LIGHTWEIGHT CROWN GLASS
- HIGH-LITE® — HIGH INDEX LOW DENSITY GLASS
- SUN MAGIC® PHOTOCROMICS — FOR SUNWEAR
- PHOTOCROMICS — FOR PRESCRIPTION
- INDUSTRIAL SAFETY GLASS
- UV FILTERING CROWN
- SPECIALTY GLASS

TECHNICAL SERVICES

- CONTRACT RESEARCH AND DEVELOPMENT
- CUSTOM MELTING
- ANALYTICAL/PHYSICAL/OPTICAL MEASUREMENTS

— and the list goes on . . .

Our commitment . . .

**Research & Development, Manufacturing, Sales, Service — Total Capability
. . . your advantage.**

 **SCHOTT™**
GLASS TECHNOLOGIES INC.

400 York Ave., Duryea, Pennsylvania 18642
(717) 457-7485 TWX 510-671-4535
Telefax (717) 457-6960

Circle Reader Action No. 383

Solvent-Resistant, Thermally Stable Poly(Carbonate-Imides)

A polyimide backbone with carbonate moieties yields high temperature stability and high solvent resistance.

Langley Research Center, Hampton, Virginia

New polymers and copolymers based on a polyimide backbone with carbonate moieties exhibit high temperature capability. Because of the carbonate unit, many of these materials also exhibit high order or crystallinity. All of the new imide-containing polymers are insensitive to acetone.

Commercial polymers based on the inclusion of carbonate units are thermoplastic (300° C processing temperature) and have high impact resistance in an amorphous state. However, they lose their toughness as they crystallize. The commercial polycarbonates have a heat-distortion temperature in the range of 130° to 140° C and withstand continuous use at temperatures up to 120° C. These systems exhibit crazing and loss of properties when exposed to many organic solvents. Acetone is particularly deleterious to polycarbonates. Thus, there is a need for a solvent- and thermal-resistant aromatic resin that can be cured between 180° and 300° C.

The new poly(carbonate-imide) exhibits significantly increased temperature resistance and shows less sensitivity to solvents

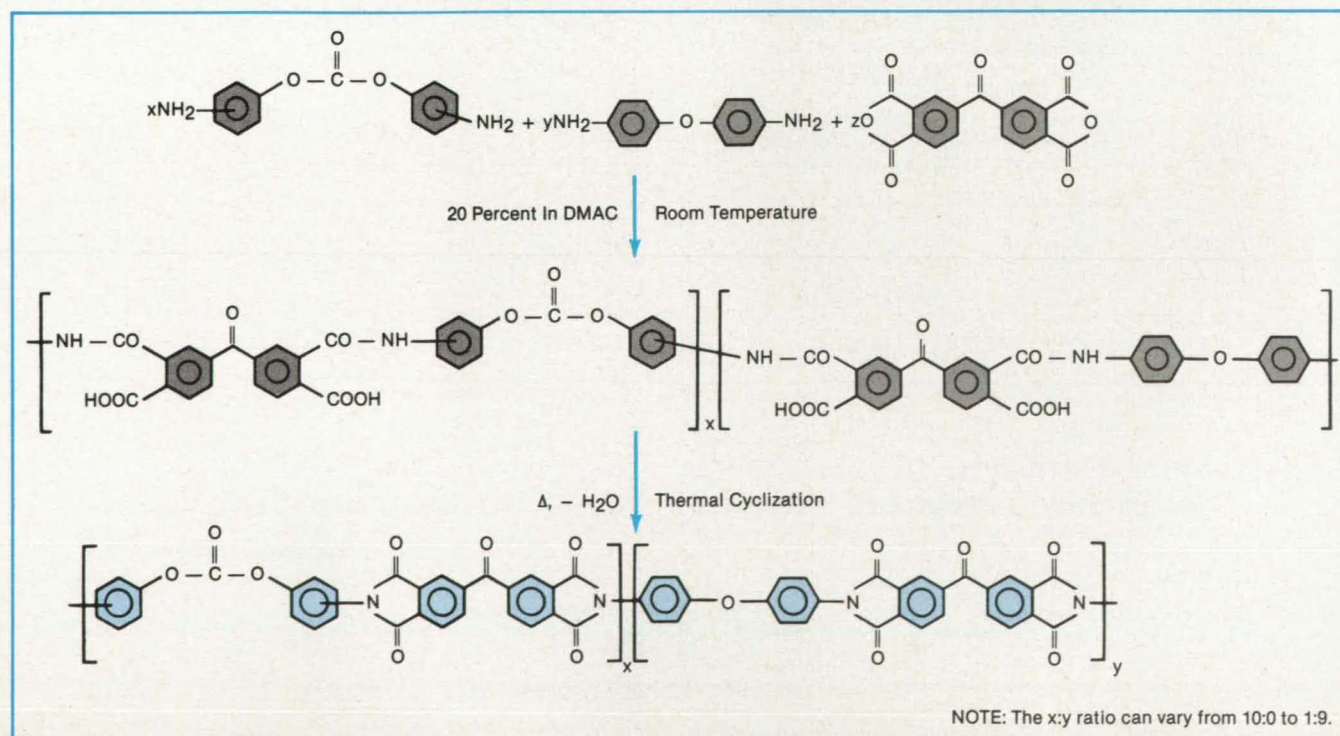
than commercial polycarbonates. By incorporating a carbonate unit into a polyimide backbone at varying yields and of varying structures, a series of ordered or crystalline thermoplastic polymers is produced that is solvent-resistant and has heat-distortion temperatures in excess of 140° C.

The poly(carbonate-imides) are prepared according to the reaction scheme shown in the figure. They were characterized for heat-distortion temperature using a differential scanning calorimeter (DSC), so the temperature of the transition of the polymer from the glassy state to the rubbery state (T_g) could be measured. All of the poly(carbonate-imides) prepared have higher temperature capabilities than the commercial systems. In fact, the lowest T_g is 190° C compared to 130° to 140° C for the commercial systems. The highest T_g of 278° C is twice that for the commercial systems. The inherent viscosities for the poly(carbonate-imides) ranged from 0.59 to 0.65 dl/g, indicating that all had very similar molecular weights.

The DSC studies show that systems where x is greater than 2 have crystalline transitions or highly ordered glass-to-rubber transitions that are common with the polycarbonates but not common with the base polyimide where $y = 10$. The crystalline melts occur in the temperature range of 325° to 450° C. Also, for several of the copolymers, X-ray diffraction studies show that in systems where x is greater than 4, the systems exhibit crystalline structure.

This work was done by Terry L. St. Clair and Noel T. Wakelyn of Langley Research Center, Shubha Maudgal of the National Research Council, and John R. Pratt of the Mississippi University for Women. For further information, Circle 71 on the TSP Request Card.

Inquiries concerning rights for the commercial use of this invention should be addressed to the Patent Counsel, Langley Research Center [see page 29]. Refer to LAR-13292.



This Reaction Scheme is used in preparing the new poly(carbonate-imides). The general structure of the new materials is seen at the bottom of the figure.



Ad
Council

Photo: Peter B. Kaplan

If you still believe in me, save me.

For nearly a hundred years, the Statue of Liberty has been America's most powerful symbol of freedom and hope. Today the corrosive action of almost a century of weather and salt air has eaten away at the iron framework; etched holes in the copper exterior.

On Ellis Island, where the ancestors of nearly half of all Americans first stepped onto American soil, the Immigration Center is now a hollow ruin.

Inspiring plans have been developed to restore the Statue and to create on Ellis Island a permanent museum celebrating the ethnic diversity of this country of immigrants. But unless restoration is begun now, these two landmarks in our nation's heritage could be closed at the very time America is celebrating their hundredth anniversaries. The 230 million dollars needed to carry out the work is needed now.

All of the money must come from private donations; the federal government is not raising the funds. This is consistent with the Statue's origins. The French people paid for its creation themselves. And America's businesses spearheaded the public contributions that were needed for its construction and for the pedestal.

The torch of liberty is everyone's to cherish. Could we hold up our heads as Americans if we allowed the time to come when she can no longer hold up hers?

Opportunities for Your Company.



You are invited to learn more about the advantages of corporate sponsorship during the nationwide promotions surrounding the restoration project. Write on your letterhead to: The Statue of Liberty-Ellis Island Foundation, Inc., 101 Park Ave, N.Y., N.Y. 10178.



Save these monuments. Send your personal tax deductible donation to: P.O. Box 1986, New York, N.Y. 10018. **The Statue of Liberty-Ellis Island Foundation, Inc.**

Chromium Ions Improve Moisture Resistance of Epoxy Resins

Cr (III) ions bind free hydroxyl groups on the epoxy chain.

Langley Research Center, Hampton, Virginia

A broad spectrum of thermosetting epoxy resins is used on commercial and military aircraft, primarily as composite matrices and adhesives. Epoxy resins, however, tend to absorb moisture, causing objectionable plasticization of the material and depression of the polymer glass-transition temperature. Although chromium-complex coupling agents have reduced moisture absorption at the interface between resin and reinforcement, moisture absorption at the resin surface and into the bulk of the polymer remains a problem. The relatively high water uptake capacity of epoxy resins is due to the presence of hydroxyl groups in the epoxy chains that attract polar water molecules.

In a new technique, a chromium-ion-containing epoxy with improved resistance to moisture can be produced where the chromium ions are believed to prevent the absorption of water molecules by coordinating themselves to the hydroxyl groups

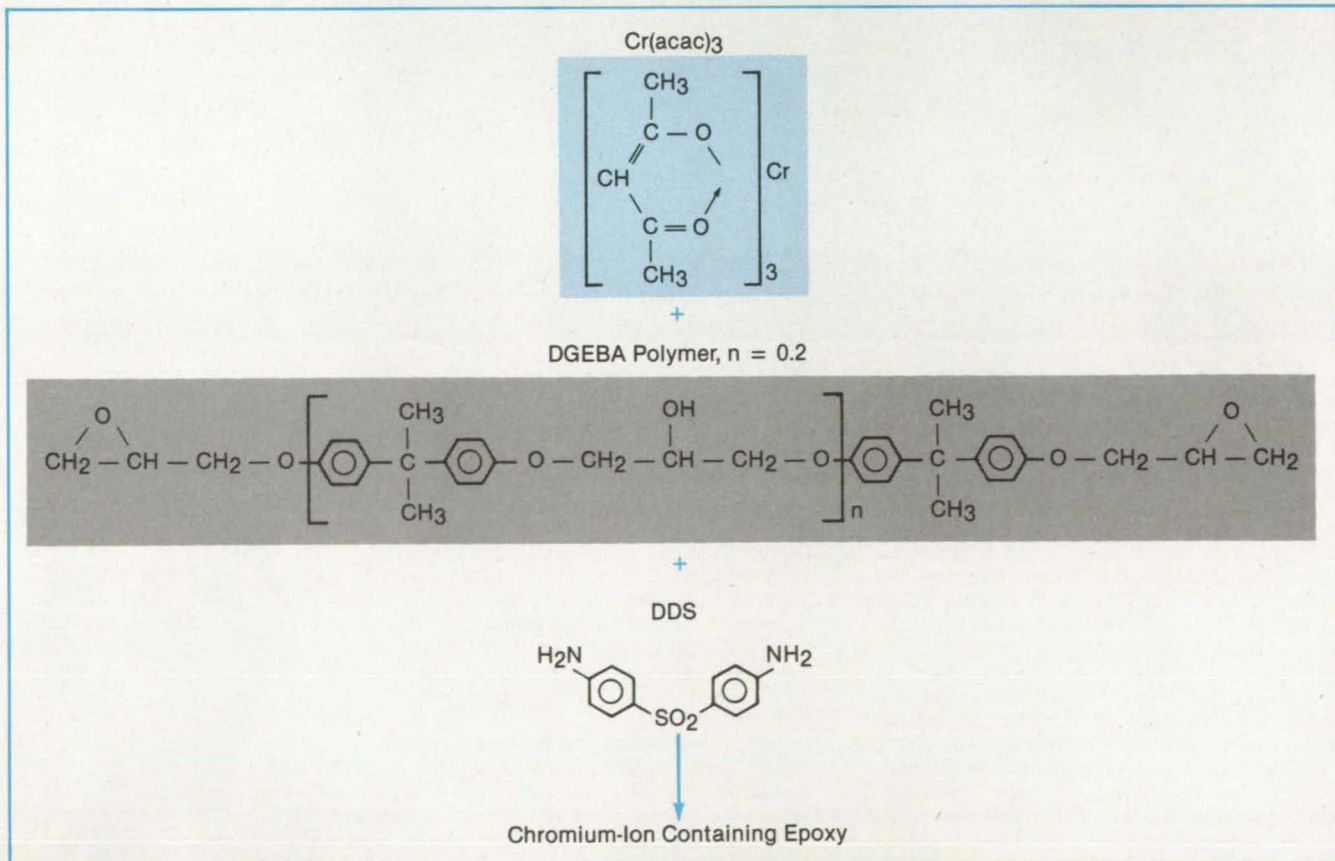
on the epoxy chain. One of three processes developed in this new technique for producing an epoxy with improved moisture resistance involves:

1. Addition of chromium ions to a preheated epoxide;
2. Addition of a diamine curing agent;
3. Thermosetting of the chromium-ion-containing epoxy resin by curing at 140° C; and
4. Further heating at 204° C to postcure the polymer.

The chromium ions are added in the form of tris(acetylacetonato)chromium (III) complex [abbreviated "Cr(acac)₃"] at a concentration of 1 to 13 percent by weight of the complex (0.1 to 1.1 percent metal) to an epoxide based upon the diglycidyl ether of bisphenol A (DGEBA) that has been preheated at 130° to 135° C. While maintaining this temperature, an aromatic diamine [4,4'-diaminodiphenyl sulfone (DDS)] curing agent is stirred into the epoxy mixture.

A reaction scheme is shown in the figure. Two additional processes have been developed to produce similar results using a tetraglycidylmethylenedianiline epoxide.

The ultimate success of improved moisture resistance for epoxy resins according to this technique is dependent upon the presence of the Cr(acac)₃. Of all the possible ligands that can coordinate to the chromium atom in a Cr (III) complex, hydroxyl is the most stable. By binding free hydroxyl groups on the epoxy, the chromium prevents water molecules from attacking the polymer. Any Cr (III)-containing salts, complexes, or organometallic complexes that have a Cr (III) atom available for hydroxyl coordination could be useful in this technique. Success of this technique is also dependent upon the solubility of the chromium complex in the epoxy resin. The solubility allows the Cr (III) ions to chemically interact with the polymer chain rather than to act merely as an inert filler.



Chromium Ions Are Added to an Epoxide to form a moisture-resistant epoxy resin. The aromatic diamine DDS is stirred into the preheated mixture to cure it.

It is anticipated that this improved epoxy formulation will be useful as a composite matrix resin, adhesive, or casting resin for applications on commercial and advanced aircraft. This improvement has been made without a sacrifice in the mechanical properties of the polymer.

This work was done by Anne K. St. Clair, Terry L. St. Clair, Diane M. Stoakley, Jag J. Singh, and Danny R. Sprinkle of **Langley Research Center**. For further information, Circle 59 on the TSP Request Card.

This invention has been patented by NASA (U.S. Patent No. 4,510,277). Inquir-

ies concerning nonexclusive or exclusive license for its commercial development should be addressed to the Patent Counsel, Langley Research Center [see page 29]. Refer to LAR-13226.

Fast-Response Oxygen-Monitoring and Control System

New ZrO_2 sensors are intended for hypersonic-vehicle testing.

Langley Research Center, Hampton, Virginia

A system for monitoring and controlling the oxygen concentration in CH_4/O_2 /air combustion product gases in the Langley 8-Foot High-Temperature Tunnel has been tested in the laboratory. The oxygen sensor is a Y_2O_3 -stabilized ZrO_2 ceramic disk maintained at $843^\circ C$. The overall system response time has been reduced to about 0.2 second, which is equal to or less than 1 percent of the tunnel run time. When the test gas oxygen concentration differs from the normal air concentration by 25 percent or more, an alarm sounds, and an emergency tunnel shutdown signal operates.

The most frequently used electrochemical oxygen detectors are the solid-state ceramic oxide devices such as ZrO_2 and TiO_2 sensors. Of these two types, ZrO_2 sensors are faster and more dependable in transient combustion environments. The ZrO_2 device is based on the Nernst equation, which relates the oxygen partial pressures on its opposite sides with the voltage potential difference developed across them. The recommended operating temperature range for ZrO_2 sensors is 600° to $850^\circ C$. The high temperature is necessary in order to produce the vacancies that effect the oxygen ion diffusion through the sensor disk.

The sensor is made of a high-temperature Y_2O_3 -stabilized ZrO_2 ceramic electrolyte disk coated with porous platinum electrodes on both sides (see figure). The platinum electrodes are sufficiently porous to permit ready diffusion of gases through them.

Oxygen, or an oxygen-containing gas such as air, is supplied to one side of the disk, and the test gas is supplied to the other side (see figure). Oxygen molecules arriving at the heated electrode are dissociated and converted to doubly charged oxygen ions, with the platinum electrode providing the necessary electrons. The O^{2-} ions combine with the vacancies and diffuse through the heated ceramic disk to the other side, where they convert to neu-

tral O_2 molecules with the platinum electrode taking up the extra electrons.

When the concentration of oxygen is different on the two sides of the disk, more oxygen ions migrate from the high-oxygen-concentration side to the low-oxygen-concentration side. This ion flow provides an electronic imbalance that results in a voltage difference between the two platinum electrodes. The voltage difference is a function of the disk temperature and the oxygen partial pressures on the two sides of the disk.

Because, in practice, the pressure is not usually exactly equal on the two sides of the sensor and the sensor matrix has impurities and imperfections, a practical relationship between the sensor output and the oxygen partial pressures on the two sides is given by the following equation:

$$E = A \ln \left(\frac{P_1}{P_2} \right) + C(P)$$

where A = a mathematical constant, T = the ZrO_2 disk temperature, and $C(P)$ = the

Super durable Kapton®

performs reliably year after year

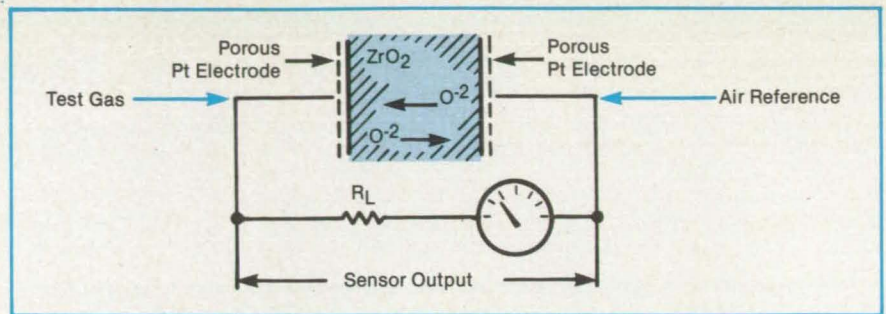
Components made with KAPTON polyimide film provide enduring performance in hostile environments and harsh chemicals. They handle temperatures from $-269^\circ C$ to $240^\circ C$. They survive millions of flexes. Dielectric strength and tensile strength are excellent.

If your components need to perform reliably year after year, consider durable KAPTON, made only by Du Pont. For facts and a free sample, write Du Pont Co., KAPTON Rm. X40804, Wilmington, DE 19898.



cell constant, which is determined by calibration with known gas mixtures at known pressures. Because of the extreme sensitivity of the Nernst voltage to the ZrO_2 disk temperature, it is necessary to use a feedback loop, based on a thermocouple signal, to maintain the sensor temperature at a constant, high level of $843^\circ C$. A NiCr/NiAl thermocouple is used to monitor the temperature of the ZrO_2 sensor. An error signal, generated by comparing the thermocouple signal with a predetermined set point, is then used to maintain the sensor at $843^\circ C$.

Initially, the ZrO_2 oxygen sensor was calibrated using various mixtures of N_2 and O_2 at room temperature. The system was then modified to include hydrocarbon combustion products in the test gas stream. Finally, the system was modified so that a controlled amount of oxygen gas was introduced in the air prior to methane combustion, as would be the case in the combustor of the wind tunnel. The O_2 -to- CH_4 flow rate ratio was adjusted to produce the same oxygen sensor output as obtained with the room air. Samples of the room air and the exhaust gas were analyzed using a gas chromatograph. The oxygen concentration in the exhaust gas was



The ZrO_2 Disk Oxygen Sensor is used to relate oxygen partial pressures on its opposite sides with the voltage across them.

equal to that in the room air, confirming the accuracy and reliability of operation of the oxygen-monitoring system.

In actual wind-tunnel operation, the exhaust (test) gas signal will be compared with the air signal, and the error signal will be used to control the oxygen spray rate in the combustor air. This will keep the exhaust gas oxygen partial pressure at the level of that in the air.

This work was done by Jag J. Singh, William T. Davis, and Richard L. Puster of Langley Research Center. Further information may be found in NASA TP-2218 [N84-11460/NSP], "Proposed Fast-

Response Oxygen Monitoring and Control System for the Langley 8-Foot High-Temperature Tunnel" [\$8.50]. A copy may be purchased [prepayment required] from the National Technical Information Service, Springfield, Virginia 22161.

This invention is owned by NASA, and a patent application has been filed. Inquiries concerning nonexclusive or exclusive license for its commercial development should be addressed to the Patent Counsel, Langley Research Center [see page 29]. Refer to LAR-13257.

Measuring Thermoelectric Properties Automatically

A microcomputer increases measurement accuracy, improves operator productivity, and reduces test time.

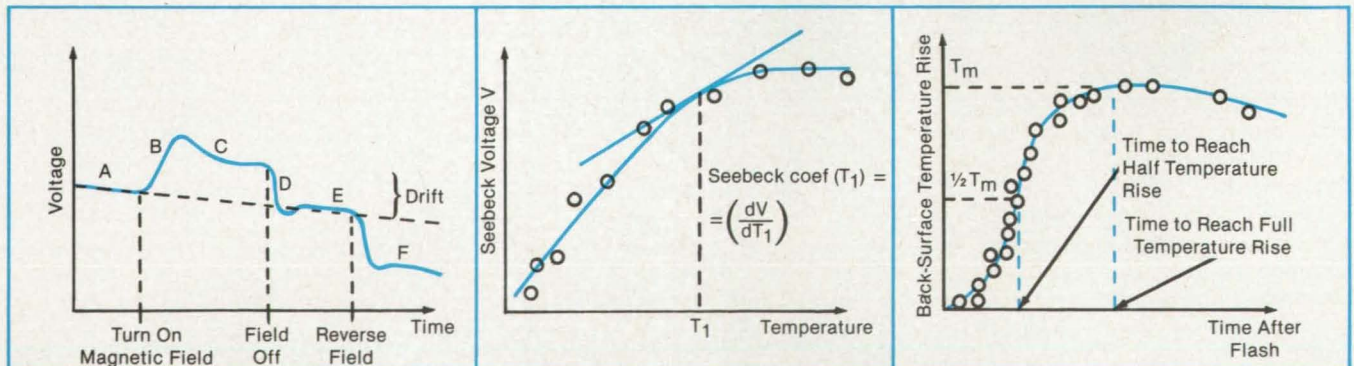
NASA's Jet Propulsion Laboratory, Pasadena, California

A microcomputer-controlled system speeds up measurements of Hall voltage, Seebeck coefficient, and thermal diffusivity in semiconductor compounds for thermoelectric-generator applications. With the microcomputer system, a large data

base of these parameters can be gathered over a wide temperature range.

For Hall-effect measurements, the microcomputer reduces the measurement time at each temperature from about 2 days to about 1 hour. The microcomputer also

automatically eliminates readings from unstable regions of the voltage-versus-time characteristic of material (see figure). The Hall-voltage measurement is obtained by averaging measurements in the stable regions for forward and reverse magnetic



Three Basic Thermoelectric Properties are measured rapidly and with minimal human interaction. Hall-voltage readings are accepted only during the stable intervals A, C, E, and F. The Seebeck coefficient is determined from the differentiation of the least squares polynomial fit of the voltage-versus-temperature curve. For thermal diffusivity, the back-surface temperature versus time is recorded, and times to reach the peak temperature rise and half the peak temperature rise are calculated.

fields. The averaging procedure is repeated for eight different combinations of electric probes and directions of current.

The computer also records the high and low values for each measurement point. It periodically displays results to the operator and asks whether they are acceptable. The operator can repeat any portion of the test if the data are suspect. The measurements are repeated for many temperatures over the expected operating range of the material. Clearly, gathering Hall-voltage data would be both tedious and error prone by manual methods.

For measurements of the large-thermal-gradient Seebeck coefficient, the micro-computer takes control once the test specimen is inserted in a test fixture; no human intervention is necessary. The temperature of the cold side of the sample is held con-

stant, while the temperature of the hot side is increased by the computer. At preset temperature increments — every 10° C, for example — the computer stores the cold- and hot-side temperatures and the Seebeck voltage. Once the variation of the Seebeck voltage with temperature has been determined, the computer finds the Seebeck coefficient from the slopes of the voltage-versus-temperature curve.

Thermal diffusivity is determined by the flash method, in which a sensor measures the temperature of the back surface of a sample resulting from a flash of heat on the front surface. The accuracy of the thermal-diffusivity measurement depends on the accuracy with which peak temperature and halftime (the time it takes for the rear surface to reach one-half the peak temperature rise) can be measured, and this is

where computerized data acquisition comes into play.

The digitized points that make up the curve of back-surface temperature versus time are transferred from a digital oscilloscope to the computer. The computer then finds a curve that fits the points and differentiates the curve. The point where the slope of the equation is zero corresponds to the peak temperature. With the peak temperature determined, the computer then finds the halftime value by interpolating between the origin and the peak temperature.

This work was done by Artur Chmielewski and Charles Wood of Caltech for NASA's Jet Propulsion Laboratory. For further information, Circle 99 on the TSP Request Card. NPO-16507

Insulation Blankets for High-Temperature Use

Lightweight, flexible material resists intense heat.

Ames Research Center, Moffett Field, California

An insulating blanket resists temperatures up to 1,500° F (815° C). It is useful where high-temperature resistance, flexibility, and ease of installation are important — for example, as insulation for odd-shaped furnaces and high-temperature ducts, as curtains for furnace openings and for fire control, and as conveyor belts in hot processes.

The blanket is a quilted composite consisting of two face sheets: the outer one of silica, the inner one of silica or other glass cloth with a center filling of pure silica glass felt sewn together with silica glass threads (see figure). The felt fibers have diameters ranging from 1 to 3 μm . The fibers are amorphous silica rather than crystalline; thermal expansion is therefore low, and crystalline inversions causing sudden changes in volume do not occur. A major advantage of the blanket insulation is its low mass density — about 8 lb/ft³ (128 kg/m³). It is lighter than the ceramic tile insulation used on the Space Shuttle, for example.

The new insulating blanket is manufactured in various thicknesses from 1/8 to 2 inches (3.2 to 50.8 mm) in a standard 33-by-33-inch (83.8- by 83.8-cm) size. Small pieces can be cut from stock for application to sharp corners or areas of complex curvature. It is quilted in squares approximately 1 inch (2.54 cm) on a side. The outside layer of the blanket can be coated with a moisture-resistant material. The inside layer can be bonded directly to the metal or

Boeing 747s now use Kapton®

#1 in wire insulation for aerospace

The 707, 727, 737, 757, 767 and now the 747. Boeing relies on KAPTON polyimide film to meet their high-temperature wire insulation requirements. The reasons: KAPTON saves weight and space. It won't melt, drip or propagate flame. And even in a current overload condition, it emits practically no smoke.

Learn why Boeing and other leading aerospace manufacturers rely on KAPTON, made only by DuPont.

For a new booklet on why nearly all high-performance aircraft use KAPTON, write DuPont Company, KAPTON, Room X40804, Wilmington, DE 19898.

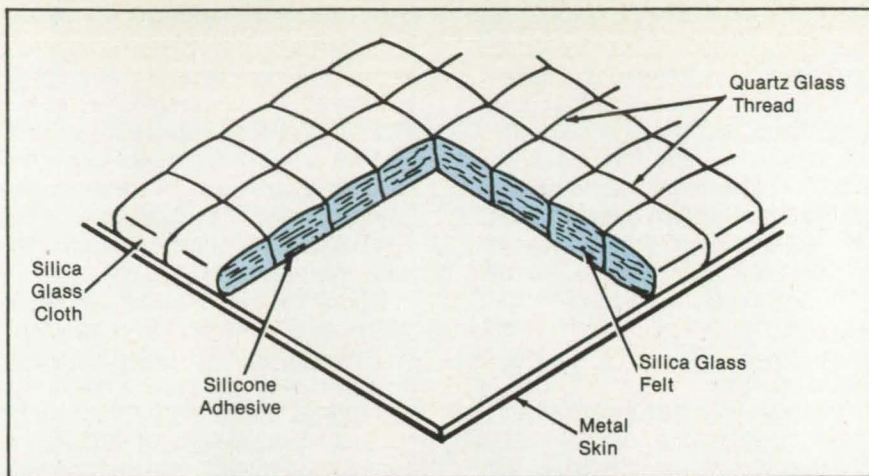


Circle Reader Action No. 400

other skin of the object to be insulated by a room-temperature-vulcanizing adhesive (RTV-560 or equivalent). This adhesive, applied at a thickness of 0.010 inch (0.25 mm), keeps weight low and minimizes thermal-expansion stress during temperature changes.

This work was done by Howard Goldstein, Daniel Leiser, Paul M. Sawko, Howard K. Larson, Carlos Estrella, and Marnell Smith of Ames Research Center and Frank J. Pitoniak of the U.S. Air Force. No further documentation is available.

Inquiries concerning rights for the commercial use of this invention should be addressed to the Patent Counsel, Ames Research Center [see page 29]. Refer to ARC-11453.



Flexible, Reusable Insulation for surfaces is composed of quilted silica felt covered on the top by silica and on the bottom by silica or other glass cloth. The insulation can withstand temperatures of 1,500° F (816° C).

Colorless, Transparent, Aromatic Polyimide Films

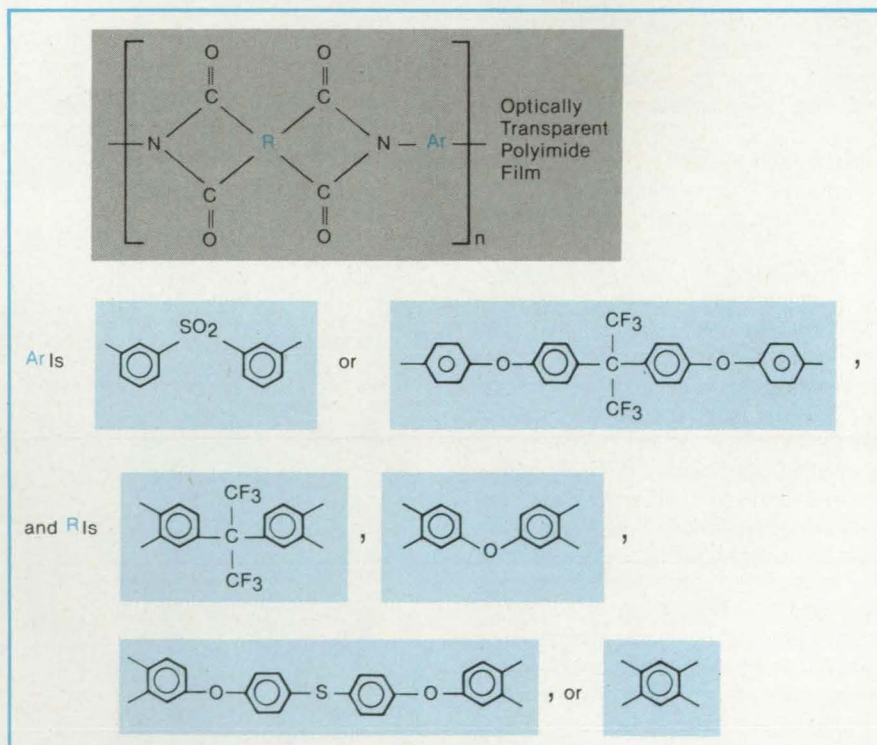
Essentially colorless, 90-to-100-percent transparent films are obtained in a two-part process.

Langley Research Center, Hampton, Virginia

A new process yields aromatic condensation polyimide films that are essentially colorless. These films are between 90- and 100-percent transparent at the visible wavelength of 500 nm, compared to 60 to 70 percent for commercial polyimide film of equal thickness.

Linear aromatic condensation polyimide film is used in many aerospace and commercial applications. These polyimides are known for their bright yellow color. Further, the intensely colored aromatic polyimides, upon aging in a space environment, become even less transparent, as low as 30 percent. The need exists, therefore, for high-temperature, flexible polymeric film and coating materials that have high optical transparency in the 300-to-600-nm range of the electromagnetic spectrum for applications on antennas, solar cells, and thermal-control coating systems.

The new process involves two conditions: (1) Purification of both aromatic diamine and aromatic dianhydride monomers and the solvent used as a medium, and (2) separation or removal of chromaphoric centers and reduction of both inter- and intra-chain electronic interactions that cause absorption in the ultraviolet/visible range by introducing bulky groups and "separator" groups into the polymer molecular structure. Both conditions must be used concurrently to produce polyimide films with maximum optical transparency.



Optically Transparent Polyimide Films are made from a variety of aromatic condensation polyimides. The films range from very pale in color to colorless.

For the first condition, at least one recrystallization or sublimation of the aromatic diamine and dianhydride monomers was necessary to prevent impure starting materials from discoloring the final polyimide film.

It was also necessary to use distilled solvent as a reaction medium.

The second condition involves use in the monomers of bulky groups such as $-CF_3$ or SO_2 groups and "separator" groups

such as —O— linkages that can reduce electron affinity and overall conjugation in the polymer chain. Incorporation of electron-withdrawing groups in the diamine portion of the polymer structure reduces the formation of inter- and intra-chain charge-transfer complexes that cause large absorptions in the UV-visible range. Incorporation of large, bulky groups into either the diamine or dianhydride monomers reduces the amount of chain-to-chain electronic interactions and thereby discourages charge-transfer-complex formation.

In this process, a highly purified aromatic diamine is dissolved in a distilled amide-type solvent such as dimethylacetamide. A highly purified dianhydride is then added to the diamine solution at room temperature to form a polyamic acid. This resin is then spread onto a glass plate to

form a film using a doctor blade with a specified blade gap. The polyamic acid film is then thermally converted to the polyimide by heating to 300° C.

Optical transparency of the films was determined not only by physical appearance but by transmission UV-visible spectroscopy. Spectra of 0.2 mil (0.005 mm) thick films showed strong absorptions with cutoffs located between 300 and 400 nm (UV region) compared to a cutoff between 450 and 500 nm (visible region) for a commercial polyimide film of equal thickness. As a result of this process, high optical transparency was obtained for a variety of aromatic condensation polyimides (see figure).

Films were prepared that range from very pale in color to colorless, compared to the bright yellow color of conventional commercial aromatic polyimide film. This

increased transparency was achieved at no sacrifice in thermal stability, flexibility, toughness, or mechanical properties. These features make the films extremely attractive as films or coating materials for aerospace applications or for any other applications where high optical transparency or thermal stability is required.

This work was done by Anne K. St. Clair, Terry L. St. Clair, Keziban S. Ezzell, and Robert M. Ely of Langley Research Center. For further information, Circle 28 on the TSP Request Card.

This invention is owned by NASA, and a patent application has been filed. Inquiries concerning nonexclusive license for its commercial development should be addressed to the Patent Counsel, Langley Research Center [see page 29]. Refer to LAR-13351.

Phenoxy Resins Containing Pendent Ethynyl Groups

Cured resins show greatly improved resistance to heat and solvents.

Langley Research Center, Hampton, Virginia

Linear phenoxy resins are widely used in a variety of applications, such as adhesives, coatings, moldings, and blow-molded bottles. However, these resins are extremely sensitive to certain solvents and have relatively low tolerance to heat. By reacting phenoxy resins with various amounts of an ethynyl-containing acid chloride, one obtains phenoxy resins containing different amounts of pendent ethynyl groups. When exposed to elevated temperatures, a thermally induced reaction of the ethynyl groups results in branching and cross-linking. (A catalyst could be used to lower the cure temperature, but it is unnecessary.) As a result of the curing reaction, the use temperature and solvent resistance of the cured modified phenoxy resins are greatly increased over previous phenoxy and modified phenoxy resins.

Ethynyl-containing phenoxy resins were prepared from the reaction of phenoxy resins with ethynyl-substituted aryl acid chlorides such as 4-ethynylbenzoyl chloride, as shown in the figure. The ethynyl content can be readily controlled simply by controlling the amount of 4-ethynylbenzoyl chloride used or by coreaction of the pendent hydroxy groups on the phenoxy resins with mixtures of the ethynyl-substituted aryl acid chloride and other acid chlorides such as benzoyl chloride. In controlling the ethynyl content, the cross-link density of the cured resin can be controlled accordingly. If desired, residual hydroxy groups

Heat resistant Kapton®

#1 in wire insulation for aerospace.

DuPont KAPTON polyimide film.

A high-performance wire and cable insulation rated for 200°C continuously and up to 400°C for short periods. Won't melt, drip or propagate flame. Practically no smoke in a fire.

Send for more information and a list of wire manufacturers. Write DuPont Co., Room X40804, Wilmington, DE 19898.

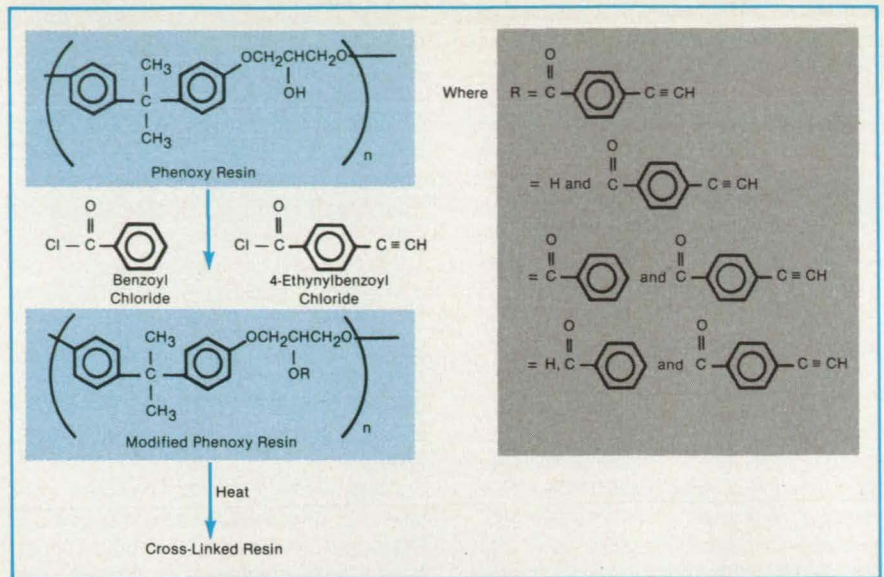


Circle Reader Action No. 399

can be left in the phenoxy resin without adverse effects. This general concept can be extended to virtually any polymer containing such groups as OH, NH₂, NHR, and SH, which are capable of reacting with an acid chloride.

The ethynyl-containing phenoxy resins have excellent shelf life in solution or in bulk. The cured ethynyl-containing phenoxy resins offer lower moisture absorption, higher use temperatures, and better thermal stability over state-of-the-art cross-linked phenoxy resins. Depending upon the cross-link density, the cured ethynyl-modified phenoxy resins are solvent resistant but still thermoformable and relatively tough. These modified resins show potential for use as adhesives, composite matrices, solvent-resistant coatings, membranes, insulators, and films.

This work was done by Paul M. Hergenrother of Langley Research Center. Further information may be found in NASA TM-85747 [N84-16338/NSP], "Phenoxy Resins Containing Pendent Ethynyl Groups" [7]. A copy may be purchased [prepayment required] from the National



Ethynyl-Containing Phenoxy Resins are prepared by the reaction shown. Control of the ethynyl content in turn controls the cross-link density.

Technical Information Service, Springfield, VA 22161.

Inquiries concerning rights for the commercial use of this invention should be ad-

ressed to the Patent Counsel, Langley Research Center [see page 29]. Refer to LAR-13222.

Micronized-Coal Burner Facility

It is used in testing materials for turbines fueled by a coal/oil mix.

Lewis Research Center, Cleveland, Ohio

The micronized-coal (coal-in-oil mix) burner facility was developed to fulfill a need to generate erosion/corrosion data on a series of superalloy specimens. The specimens were to be subjected to cyclic heating and cooling in a high-velocity, hot gas stream using coal-in-oil fuel.

Due to the energy crisis caused by the reduction in availability of crude oil, there was a serious need for alternative energy schemes to reduce the dependence of the United States on foreign oil. One scheme that had been attempted in the past involves the use of a mixture of coal particles in fuel oil (COM) with the coal in the mixture being as high as 50 weight percent. The use of COM has the advantage of reducing the amount of oil used while still allowing the COM to be handled and burned as a liquid.

In the past, most attempts to use COM have been with regard to its use in utility boilers and blast furnaces. However, because of the rapidly expanding use of gas turbines for applications such as electrical generation, it would be extremely advantageous to operate such turbines on COM. Attempts to operate gas turbines on pow-

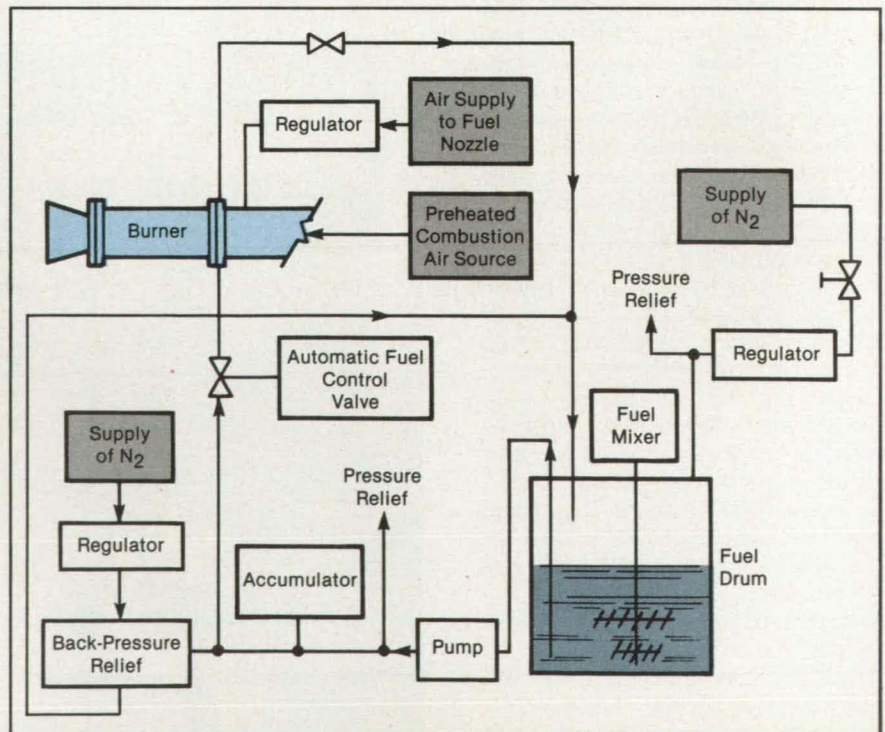


Figure 1. The **Micronized-Coal Burner Facility** was designed to generate erosion/corrosion data on superalloys used in gas turbines.

dered coal alone have been unsuccessful. Not only were there problems of handling and preparing the coal, but the ash from the burned coal particles caused unacceptable erosion of the turbine blades.

In order to successfully operate a gas turbine using COM, there are two primary conditions that must be met. First, there must be adequate atomization of the COM and second, minimization of coking of the burner. Meeting these conditions will be achieved only by clean burning and flame stability.

The object of the facility is to provide for coal-in-oil mixture in a combustor or burner system (see Figure 1) in which ash resulting from burning the mixture is of submicron particle size. The burner system comprises a burner section, a flame exit nozzle, a fuel-nozzle section, and an air tube by which preheated air is directed into the burner section. A regulated airflow at a controlled pressure is delivered to a fuel nozzle where it is mixed with fuel. A liquid pump is provided to direct a mixture of coal particles and oil from a drum to the nozzle at a desired rate and pressure. The fuel mixer in the drum is provided to keep the coal particles uniformly distributed in the coal-in-oil mixture.

The burner section (see Figure 2) has an inner wall that is separated from an outer wall. This arrangement reduces heat transfer from the combustion zone to provide more complete burning of the fuel. The spray nozzle includes an axially centered passageway through which regulated pressurized air in oil is directed. COM is directed through radial passageways corresponding to axial passageways that communicate with the central passageway. As the COM flows through the radial passageways into the central passageway, the regulated air pressure causes atomization of the COM.

The spray nozzle is supported in a nozzle

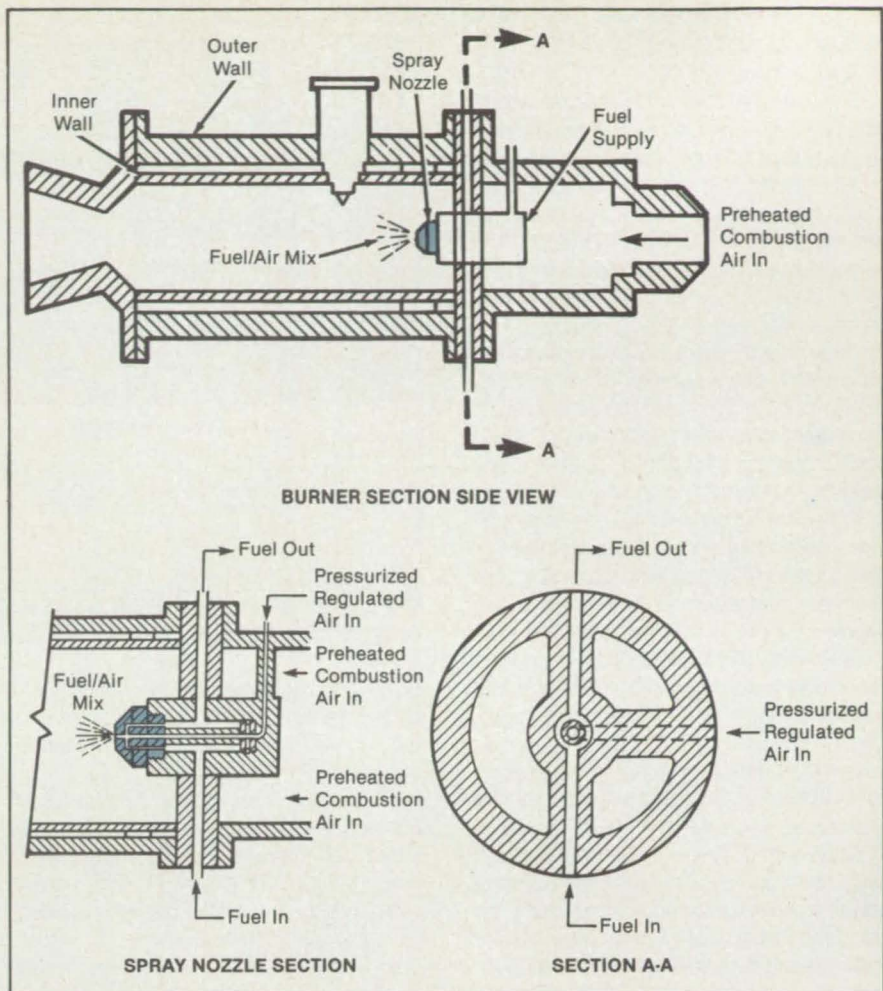


Figure 2. The **Burner**, which includes a spray nozzle with a fuel supply, has an inner wall and an outer wall to reduce heat transfer.

zle body, which includes passageways for air, for entrance of the fuel mixture, and for exit of excessive fuel mixture. Preheated combustion air passes around the nozzle body and into the burner chamber.

This work was done by F. D. Calfo and M. W. Lupton of **Lewis Research Center**. For further information, Circle 60 on the

TSP Request Card.

This invention has been patented by NASA (U.S. Patent No. 4,425,854). Inquiries concerning nonexclusive or exclusive license for its commercial development should be addressed to the Patent Counsel, Lewis Research Center [see page 29]. Refer to LEW-14131.

Cobalt Ions Improve the Strength of Epoxy Resins

The addition of cobalt ions increases the flexural strength of TGMDA resins by 10 to 95 percent.

Langley Research Center, Hampton, Virginia

Epoxy resins are extremely versatile materials, offering ease of processing, chemical resistance, high adhesive strength, low density, and high electrical insulation. One drawback of highly cross-linked epoxy resins is their brittleness and accompanying low mechanical strengths. A technique

has been developed for improving the mechanical strength of epoxy resins by adding cobalt ions in the form of tris(acetylacetonato)cobalt (III) complex [abbreviated "Co(acac)₃"].

One of three new processes for producing a cobalt ion-containing epoxy with im-

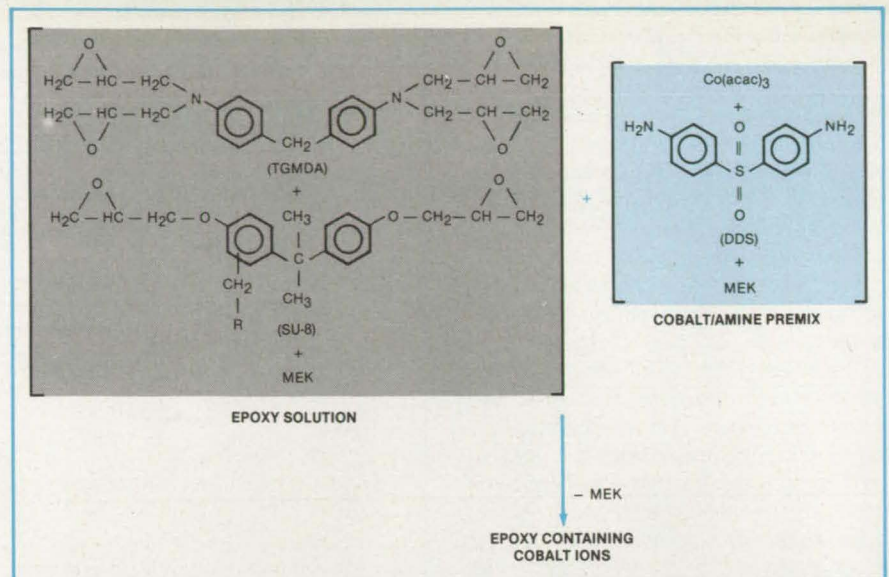
proved mechanical properties involves:

1. Combining epoxides and solvent;
2. Combining cobalt ions, diamine curing agent, and solvent to form a pre-mix;
3. Adding the pre-mix to the epoxide solution;
4. Degassing the cobalt ion-containing

- resin at 115° to 125° C;
 5. Curing at 150° C; and
 6. Postcuring at 177° C.

The epoxy solution in this process comprises a tetraglycidylmethylenedianiline (TGMDA) epoxide (61.5 percent by weight), an epoxidized phenolic novolac commercially known as SU-8 (5.0 percent by weight), and a low-boiling-temperature solvent such as methyl ethyl ketone (MEK) (33.5 percent by weight). A premix is prepared separately containing Co(acac)₃ (1.3 to 11.6 percent by weight), an aromatic diamine curing agent such as 4,4'-diaminodiphenyl sulfone (DDS) (20.1 to 22.4 percent by weight), and a low-boiling-temperature solvent such as MEK (6.8 to 7.6 percent by weight). The cobalt/amine premix is added to the epoxy solution so that the final mixture contains 43.5 to 46.2 percent premix and 53.8 to 56.5 percent epoxy solution. The reaction scheme is shown in the figure.

Solid cast disks prepared from cobalt ion-containing epoxy resins were tested for flexural strength and stiffness. Incorporation of cobalt ions into the epoxies increased the flexural strength of the resins by 10 to 95 percent. Suitable resins for this technique include any liquid or solid TGMDA resins. The improved mechanical properties achieved with TGMDA-based cobalt ion-containing epoxies were not attained using a more linear difunctional epoxy resin. It is anticipated that this im-



The Epoxy Solution and Cobalt/Amine Premix are combined, degassed, cured, and post-cured to form a cobalt ion-containing epoxy.

proved epoxy formulation will prove useful as a composite matrix resin, adhesive, or casting resin for applications on commercial and advanced aircraft.

This work was done by Diane M. Stoakley and Anne K. St. Clair of Langley Research Center. Further information may be found in NASA TM-85715 [N84-13309/NSP], "Cobalt Ion-Containing Epoxies" [\$7]. A copy may be purchased [prepayment required] from the National Techni-

cal Information Service, Springfield, Virginia 22161.

This invention has been patented by NASA (U.S. Patent No. 4,473,674). Inquiries concerning nonexclusive or exclusive license for its commercial development should be addressed to the Patent Counsel, Langley Research Center [see page 29]. Refer to LAR-13230.

Alkane-Based Urethane Potting Compounds

Lowered viscosity makes these prepolymers usable as potting materials.

Marshall Space Flight Center, Alabama

New low viscosity urethanes are easily mixed, molded, and outgassed. The alkane-based urethanes resist hydrolysis and oxidation and have excellent dielectric properties.

A low-viscosity alkane-based urethane prepolymer is prepared by a one-step reaction of either isophorone diisocyanate or methyl-bis(4-cyclohexyl isocyanate) with a hydrogenated, hydroxy-terminated polybutadiene (HTPBD). The curing agent is a diol or amine that acts as a chain extender or cross-linker, which allows the prepolymer to reach its final molecular weight and converts it to a thermoset material via cross-links. The curing agents used in experiments were trimethylene glycol, di-p-aminobenzoate and 1,4-butanediol.

For tests of the new material, speci-

Property	NASA Specification	Experimental Alkane-Based Urethanes
Hardness, Shore A	60-90	57-96
Tensile Strength, psi	1,500 Minimum	400-3,000
Tear Strength, psi	175 Minimum	52-434
Elongation, percent	200 Minimum	74-525
Viscosity, Initial at 25° C, P	450 Maximum	20-500
Application, Life At 25° C, h	1 Minimum	2-10
Coefficient of Thermal Expansion, -55° to +100° C	175 × 10 ⁻⁶ Maximum	162-324 × 10 ⁻⁶

A Comparison of Mechanical Properties of new alkane-based urethanes with NASA standards for potting compounds shows a wide range of values.

mens were prepared by heating the curing agent with HTPBD, stirring isocyanate or diisocyanate into the mixture, degassing, and pouring the mixture into molds for

sheet material. The compound was cured in air at 70° C for 12 hours and at 120° C for 18 hours. A variety of HTPBD and isocyanate or diisocyanate combinations

were formulated.

The molecular weights of the new alkane-based urethanes tested varied from 300 to 4,000, depending on the choice of HTPBD. Those materials with molecular weights up to 2,500 exhibited viscosities low enough and working life long enough for those materials to be used as potting compounds.

The thermal stability of the experimental alkane-based urethanes was as high as, or higher than, that of those previously avail-

able. The dielectric properties and hydrolytic stabilities were excellent. The mechanical properties varied widely, depending on the formulation (see table). Many formulations met most NASA mechanical requirements. However, no single formulation met all the requirements. In general, the mechanical properties were not as good as those of ether- and ester-based urethanes.

This work was done by Donald E. Morris of Marshall Space Flight Center. Further

information may be found in NASA TM-82544 [N83-34047/NSP], "Development of Low Viscosity Alkane-Based Urethane for Connector Potting Applications" [\$8.50]. A paper copy may be purchased [prepayment required] from the National Technical Information Service, Springfield, Virginia 22161. The report is also available on microfiche at no charge. To obtain a microfiche copy, Circle 62 on the TSP Request Card.

MFS-27047

High-Strength, Low-Shrinkage Ceramic Tiles

Flexural strength and other properties are improved by additives.

Lyndon B. Johnson Space Center, Houston, Texas

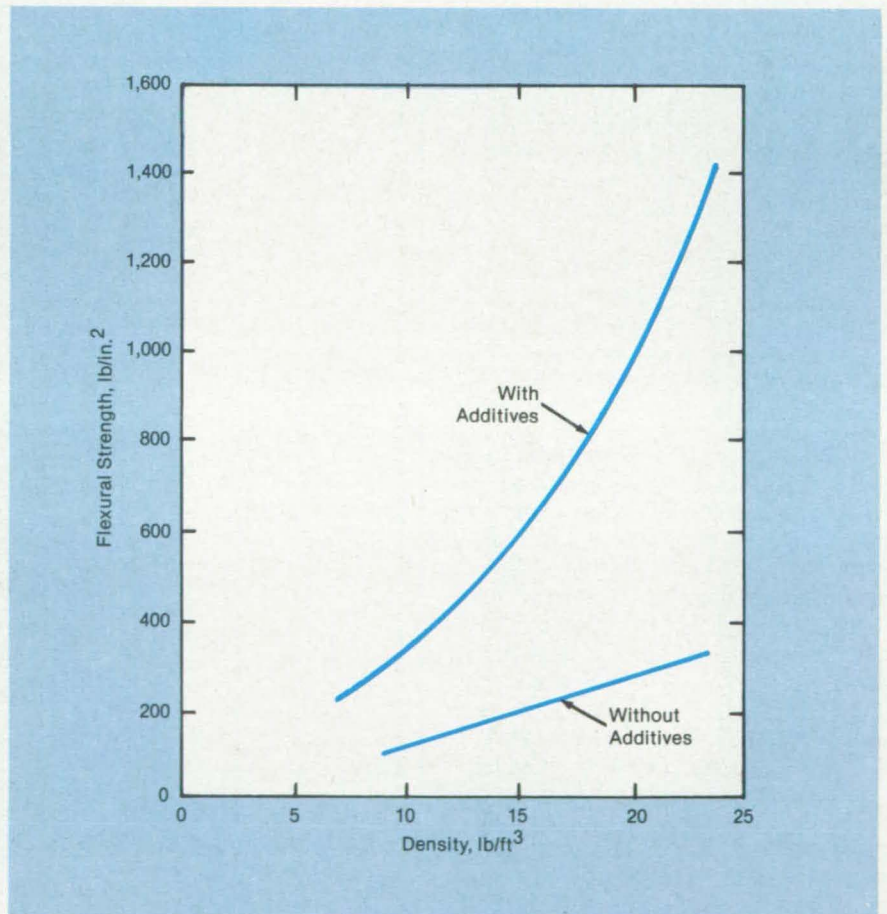
The addition of refractory fibers and whiskers to insulating tiles composed primarily of fibrous silica, such as those used on the skin of the Space Shuttle orbiter, greatly improves their properties. For example, modifying the formulation with 15 percent alumina fibers and 2.85 percent boron nitride multiplies the flexural strength by a factor of 2 or 3 while maintaining the same low density as that of the all-silica tiles (see figure). Added benefits are an increase in the modulus of elasticity and less deformation and shrinkage at temperatures above 2,300° F (1,260° C).

Although originally developed to provide the Space Shuttle with tiles of greater strength and dimensional stability, the new composition is also suitable for lightweight, thermally-stable mirror blanks and as furnace and kiln insulation. The improved tiles are made with current tile-fabrication processes.

The tile ingredients are blended with de-ionized water to form a thick slurry and cast to shape. After drying, the tiles are heated. Boron nitride is especially useful because it resists oxidation up to about 1,830° F (1,000° C), then slowly dissociates to boron trioxide and nitrogen gas during subsequent heating to higher temperatures.

The boron addition promotes eutectic sintering and provides a strong borosilicate bond at fiber junctions. At the tile-firing temperature of 2,350° F (1,290° C), the slowly-released boron trioxide has time to react as it diffuses throughout the tile to all the silica fibers, producing uniformly bonded intersections. The boron trioxide content also inhibits crystallization of the silica during exposure to high temperatures. Crystallization — which would make tiles brittle — does not exceed 5 percent when boron-

NASA Tech Briefs, Winter 1985



For a Given Density, tiles containing silicon carbide and boron additives are stronger in flexure than are tiles made from silica alone. In addition, the tiles with additives are nearly immune to heat distortion, whereas pure-silica tiles shrink and become severely distorted.

containing tiles are heated to 2,300° F (1,260° C) for 15 hours.

This work was done by William H. Wheeler and John F. Creedon of Lockheed

Missiles & Space Co., Inc., for Johnson Space Center. For further information, Circle 64 on the TSP Request Card. MSC-20654

Research Furnace for Crystal Preparation

Temperature profiles are accurately controlled by three independent heaters.

Langley Research Center, Hampton, Virginia

A three-zone furnace originally developed for materials research in zero gravity has been tested and characterized for the preparation of lead-tin-telluride (LTT) crystals. Tests show that the temperature in the furnace can be controlled to obtain a constant rate of movement of a high-temperature isotherm down the length of the furnace. The tests also show that a temperature gradient on the order of $20^{\circ}\text{C}/\text{cm}$ can be obtained in the furnace while a 900°C isotherm is moved. A functional dependency of growth rate on perturbations during the growth has been derived and shows the importance of avoiding nonsteady growth rates and changing temperature gradients.

LTT is a compound semiconductor that can be considered a binary mixture of lead-telluride molecules and tin-telluride molecules. The pseudobinary phase diagram shows that the two materials are fully miscible. A mixture of 20 percent tin telluride and 80 percent lead telluride was chosen for NASA's zero-gravity experiment. This combination, which solidifies in a temperature range around 900°C , dictates the temperature at which the furnace should be characterized.

A schematic of a furnace is shown in Figure 1. There are three heaters in the furnace and a water-cooled heat extractor that makes contact with the end of the cartridge. Control software brings the separate heaters to any desired temperature. Careful selection of temperature profiles allows a particular isotherm to be moved down the length of the furnace at a fixed rate. Directional solidification can be achieved by either moving the furnace and the sample relative to each other or by ramping a temperature gradient through the furnace at a constant rate. Since the furnace is designed to be stationary with no moving parts, its temperature profiles must be characterized, and a procedure must be developed for controlling the temperatures in the three zones so that a solidification front passes down the specimen at a constant growth rate with a sufficiently high temperature gradient to avoid constitutional supercooling.

Since the fabrication of an LTT sample is quite time consuming and the sample can be solidified only once without risk of ampoule breakage (which can result in

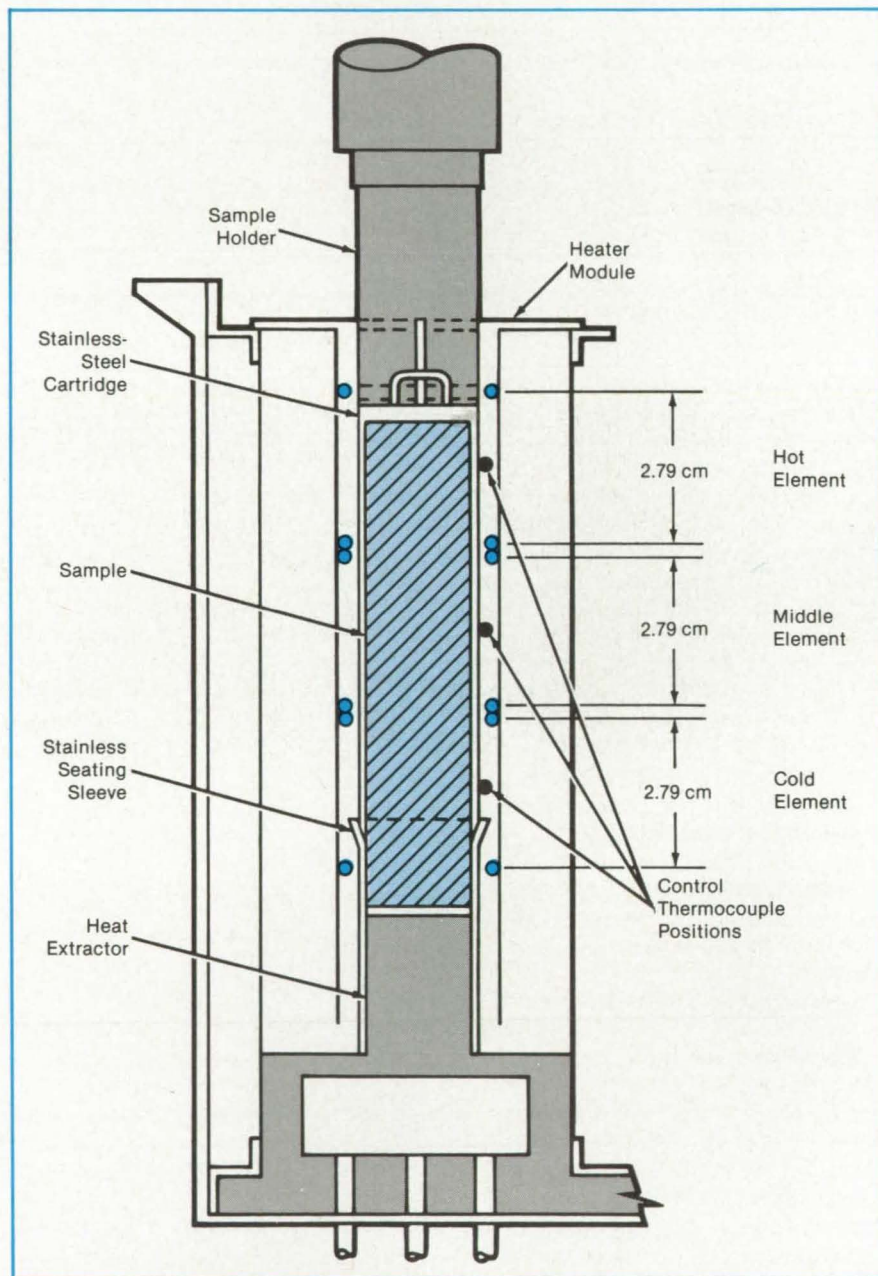


Figure 1. A Schematic of the Furnace Module in the general purpose research furnace shows relative positions of the heater elements, the heat extractor, the positioning sleeve, and the sample.

corrosion of the interior of the furnace), it was decided to make most of the characterization tests with relatively inert materials that have thermal characteristics similar to those of LTT. The first series of tests was carried out on a boron nitride sample

with six thermocouples measuring axial temperatures along the solid rod. The next sample tested was fused silica with six thermocouples at various positions.

A timetable was deduced from position/temperature data to program the software

to control the set points for the various furnace zones such that a constant rate of movement would be obtained for the 900° C isotherm. Figure 2 shows a portion of the curve for the position as a function of time. As can be seen, the rate in this part of the furnace is very nearly constant as was the case over the entire range covered by the thermocouples. Preliminary tests on a PbTe-SnTe sample showed that the furnace is capable of producing the required temperature gradients in LTT.

This work was done by Roger K. Crouch, Archibald L. Fripp, Jr., William J. Debnam, Jr., and Ivan O. Clark of Langley Research Center, J. M. Zwiener of Marshall Space Flight Center, and F. M. Carlson of Clarkson University. Further information may be found in NASA TM-85718 [N84-13211/NSP], "Characterization of the General Purpose Research Furnace for Low-G Directional Solidification Experiments" [\$7]. A copy may be purchased [prepayment required] from the National Technical Information Service, Springfield, Virginia 22161. LAR-13302

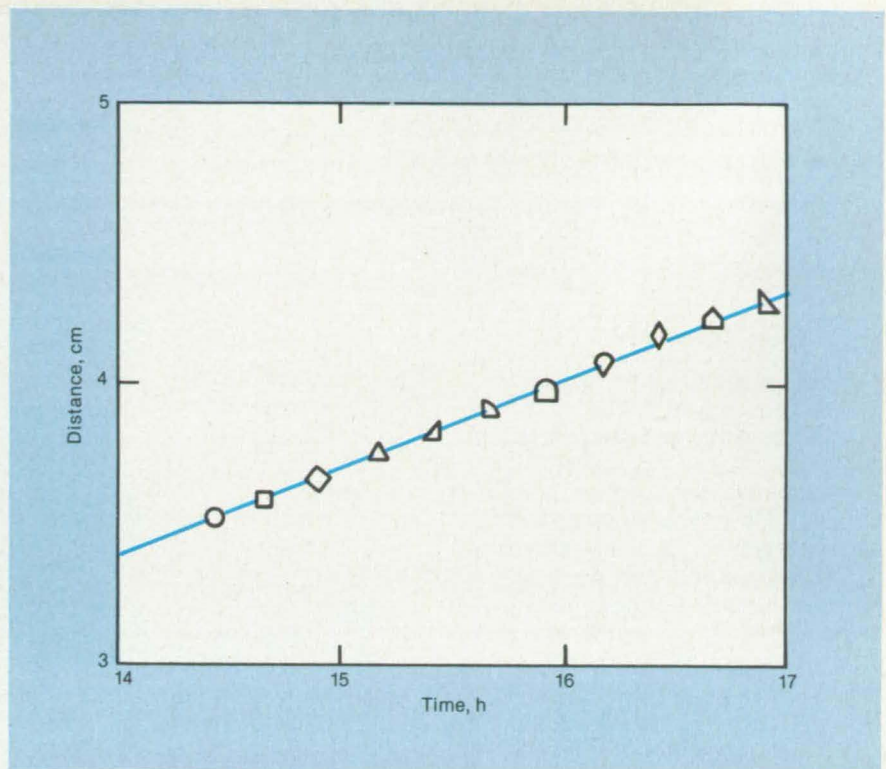


Figure 2. The **Interface Position as a Function of Time** shows the constant rate of change of the 900° C temperature for this region of the furnace.

Lightweight Protective Garments

Polyacrylate-rubber-coated fabric would selectively transmit water vapor and carbon dioxide.

NASA's Jet Propulsion Laboratory, Pasadena, California

A proposed garment material would protect the wearer from poisonous chemicals, bacteria, and radioactive particulates. At the same time, the garment would allow heat, moisture, and carbon dioxide to pass from the inside to the outside so that the wearer remains comfortable.

The garment would be made of cotton fabric on which a thin layer of polyacrylate rubber has been deposited by calendaring or spraying. It would be lighter and cooler than existing protective garments made of two layers of canvas separated by a core of activated charcoal and a chlorinated compound. Moreover, it would not release grains of core material. Such grains can embed themselves in the wearer's skin, causing irritation.

Polyacrylate rubber was selected for the garment material because it transmits water vapor and carbon dioxide at high rates. The rates could be adjusted to the values required for human comfort by varying the rubber formulation. At the same time, polyacrylate rubber would

transmit large-molecule chemical agents at low rates — many orders of magnitude lower than the rates for moisture and carbon dioxide. In addition, such agents could be destroyed within the polyacrylate rubber layer by reactive additives.

Because the polyacrylate rubber is non-porous, it would not pass bacteria and viruses. For the same reason, the layer would exclude radioactive dust. If radioactive materials become lodged on the surface of the garment or trapped in it by chemical reaction, the garment could be discarded.

An example of a reactive additive is calcined magnesium oxide, which could be mixed with the polyacrylate in proportions as great as 44 percent by weight. The magnesium oxide would react with moisture from the wearer to form magnesium hydroxide. This alkaline material would then react with the phosphate moiety of the small amount of phosphate-based warfare agent that would penetrate into the rubber layer. The agent would then be neutralized

by the formation of insoluble magnesium phosphates.

Acid hydrolysis additives could also be included in the rubber, either alone or in combination with alkaline hydrolysis additives. Similarly, oxidants, precipitants, complexing reagents, and others could be added to destroy harmful chemicals. Of course, such reagents and their products must be bound in the rubber so that they would not escape to become skin irritants, lung irritants, or carcinogens.

It would probably not be necessary to vulcanize the rubber. If vulcanizing is done, however, the curing agent should be selected carefully. Polyamines should be avoided, for example, because they are skin irritants. Fortunately, nonallergenic vulcanizing compounds are available.

This work was done by Eugene R. du Fresne of Caltech for NASA's Jet Propulsion Laboratory. For further information, Circle 91 on the TSP Request Card. NPO-16510

Ultrasonic Mixing of Epoxy Curing Agents

Uniform mixing is obtained at relatively low temperatures, without adding solvent.

Langley Research Center, Hampton, Virginia

Aircraft of the future will require high-performance polymer matrices to fully achieve the weight savings possible with composite materials. Some potentially useful polymer/curing agent combinations cannot be mixed properly because of the high melting temperatures of the curing agents. As an example, when curing agent A is heated to its melt temperature of 242° C and mixed into epoxy resin, the result is uncontrollable, very rapid curing. If solvent is used to lower the melt temperature, residual solvent evolution during subsequent processing causes voids and degradation of properties in the final part. Another curing agent is a fluffy, low-density crystalline material that is difficult to blend into the epoxy.

A new ultrasonic mixing technique alleviates these problems. The technique has been used to mix several curing agents/epoxy combinations. The major component of the commercially available base epoxy resin used is tetraglycidylmethyl-enedianiline (TGMDA).

The ultrasonic unit used is the commercial ultrasonic generator with transducer and horn shown in Figure 1. Maximum power output for the unit is 300 W. A polyimide release film is taped to the end of the horn to form a cup for the resin and curing agent during excitation. The curing agents are hand mixed into the epoxy resin at 30° C before ultrasonic blending.

The mixing ratios of the samples are 26.3 parts per hundred, by weight, for the two conventional systems and 22.5 parts per hundred for the two experimental systems. Prior to ultrasonic treatment, the samples are opaque, lumpy, viscous liquids, each colored a darker shade than the natural color of the curing agent.

The samples are placed in the cup with the top of the ultrasonic horn forming the bottom of the cup. They are ultrasonically treated until they became amber colored and transparent. The peak temperature reached while mixing the high-melting curing agent A with TGMDA is around 150° C after mixing for 10 min. The other three curing agents take between 1 and 4 min to dissolve, reaching peak temperatures of 90° to 100° C for very short times.

After ultrasonic mixing, the resin samples are cured in an air-circulating oven. Because ultrasonic agitation drives



Figure 1. In the **Ultrasonic Mixing System** the cup holds the resin and curing agent during acoustic excitation.

out entrapped air, degassing is not necessary before cure.

All curing agents were successfully blended into the epoxy resin using this ultrasonic technique (see Figure 2). Gel permeation chromatograms of the ultrasonically mixed and of melt-mixed samples indicated no premature polymerization or

significant differences in the compositions of either mixing technique.

Ultrasonic mixing of resins is a useful technique to dissolve curing agents into liquid resins to obtain uniform mixing while avoiding uncontrolled advancement of the resin. This technique also precludes the need for solvents that give processing

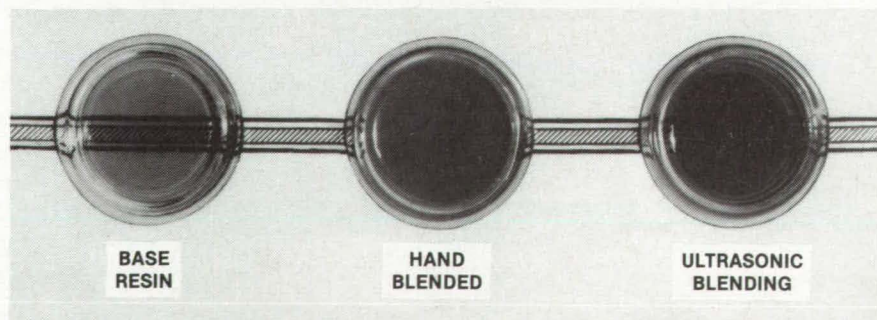


Figure 2. The **Transparent Ultrasonic Blend** demonstrates effective mixing of the curing agent into the resin using the ultrasonic technique.

problems during final cure.

This work was done by William T. Hodges of the U.S. Army Structures Laboratory and Terry L. St. Clair of Langley Re-

search Center. Further information may be found in NASA TM-85643 [N83-27018/NSP], "Ultrasonic Mixing of Epoxy Curing Agents" [\$7]. A copy may be purchased

[prepayment required] from the National Technical Information Service, Springfield, Virginia 22161. LAR-13307

Ultra-High-Molecular-Weight Silphenylene/Siloxane Polymers

A new process produces highly stable synthetic rubbers.

Marshall Space Flight Center, Alabama

Elastomers having molecular weights above 1 million have been made by two-stage polymerization. Such elastomers retain their mechanical properties even after long exposure to high-temperature oxidizing environments. A laboratory process was scaled up to yield 50-gram quantities of the elastomer without loss of molecular weight.

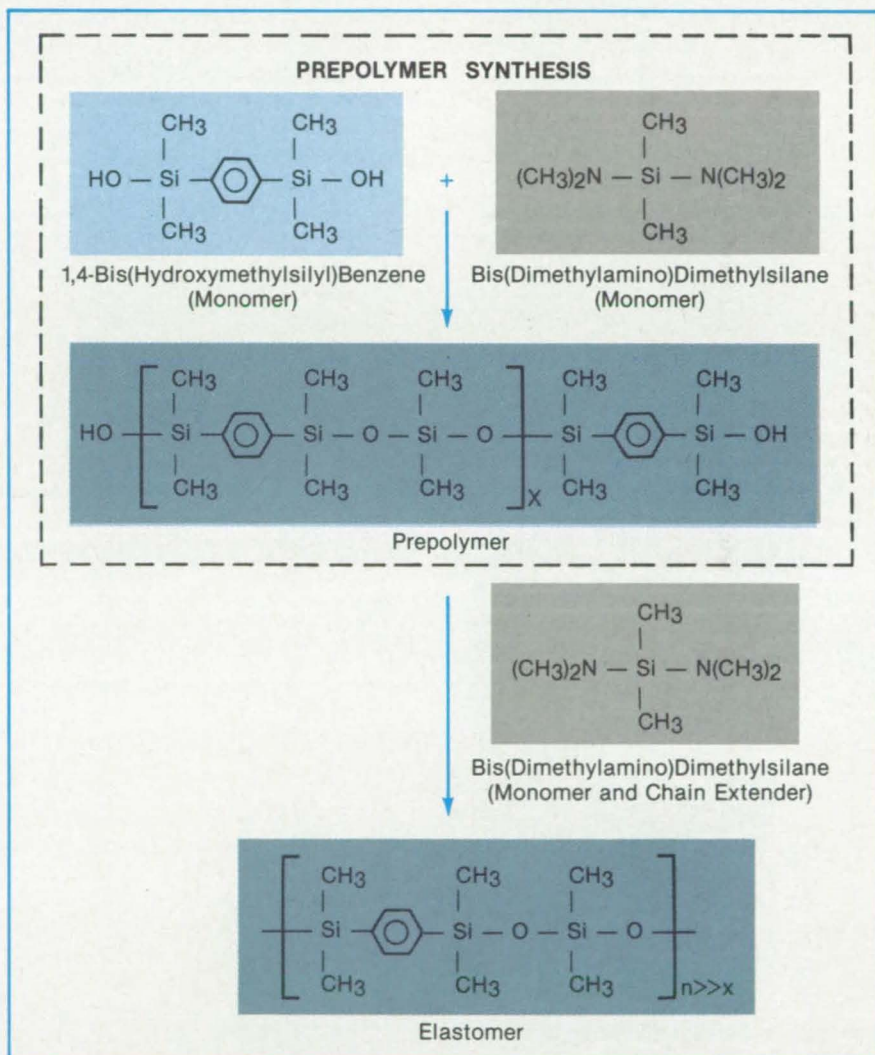
The two-stage process proved to be far more successful than synthesis from reactive monomers. The process involves the synthesis of a silanol-terminated prepolymer and subsequent extension of the prepolymer chain with additional aminosilane monomer.

In an experiment, a prepolymer was synthesized (see figure) by the reaction of 1,4-bis(hydroxymethylsilyl)benzene with bis(dimethylamino)dimethylsilane in toluene in a nitrogen atmosphere at 109° to 112° C. After cooling, the prepolymer was precipitated in methanol, purified, and dried. The polymer was synthesized by reacting the prepolymer with more bis(dimethylamino)dimethylsilane in the same manner as before.

Molecular weights near and above 10⁶ were obtained consistently. The greater effectiveness of the two-stage technique in comparison with the reactive-monomer process is probably a result of the greater control of stoichiometry afforded by the former. The multistage method allows the chain-extending monomer to be added in precise amounts between the stages.

This work was done by W. J. Patterson, N. H. Hundley, and L. M. Ludwick of Marshall Space Flight Center. Further information may be found in NASA Technical Paper 2295 [N84-19564/NSP], "Ultra-High Molecular Weight Silphenylene-Siloxane Polymers" [\$7]. A paper copy may be purchased [prepayment required] from the National Technical Information Service, Springfield, Virginia 22161. The report is also available on microfiche at no charge. To obtain a microfiche copy, Circle 80 on the TSP Request Card. MFS-27065

NASA Tech Briefs, Winter 1985



The Steps in the Two-Stage Polymerization Process are the synthesis of the prepolymer and the synthesis of the elastomer with the additions of the chain-extending monomer to the prepolymer.

Cast Iron With High Carbon Content

Solidification in low gravity would ensure uniform distribution of graphite.

Marshall Space Flight Center, Alabama

A method has been proposed for solidifying high-carbon cast iron without carbon particles segregating at the upper surface. Solidification would be carried out in low gravity, for example on an airplane flying a free-fall parabolic trajectory.

On Earth, buoyant forces on the relatively light carbon particles cause them to float to the top of the molten iron. However, at low gravity, the carbon particles would be distributed homogeneously throughout the iron.

The proposed method is based on experiments on solidification in an airplane flying parabolic arcs. Graphite flotation in samples of a few millimeters in size was reduced to between one-hundredth and one-

thousandth its "normal" values.

Hypereutectic (high-carbon) cast iron directionally solidified in low gravity has large, unaggregated carbon nodules distributed evenly throughout the casting. In contrast, cast iron of the same overall composition solidified in the same manner but, at Earth gravity, has large, aggregated modules concentrated at the top of the casting.

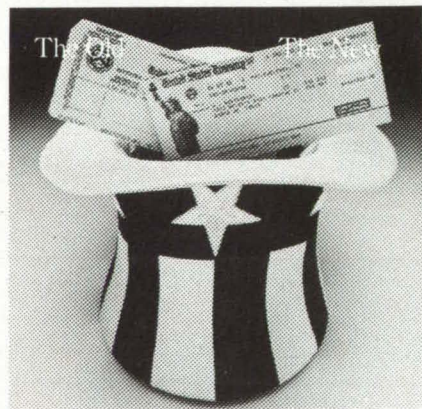
Similarly, hypereutectic flake cast iron directionally solidified in low gravity has large flakes of carbon scattered uniformly throughout the casting and often aligned with the direction of solidification. The same cast iron solidified at Earth gravity has no large flakes in the bottom portion of

the casting and large aggregated flakes in the upper portion.

Many different microstructures could be obtained by the proposed technique, and the percentage by weight of carbon that could be retained in the melt would be much higher than it is at present. For example, by increasing the weight fraction of carbon to more than 10 percent, the volume fraction of carbon would be increased to over 50 percent, resulting in an iron/carbon composite of greatly reduced density.

This work was done by Peter A. Curreri of Marshall Space Flight Center and John C. Hendrix and Doru M. Stefanescu of the University of Alabama. No further documentation is available. MFS-28014

U.S. Government Checks Have A Brand New Look.



In the coming months, all punched-card government checks will be replaced by the new U.S. Government check.

The design features the Statue of Liberty over a multicolored background ranging from light blue to pale peach. A pattern of the letters "USA" is printed in pale blue on the reverse side.

Be looking for the new checks. And please keep in mind that the old punched-card checks are still good!

Department of the Treasury
Financial Management Service

A public service of this publication.

Beta Silicon Nitride Whiskers

A process forms whiskers of strong, stable, heat-resistant material.

NASA's Jet Propulsion Laboratory, Pasadena, California

A process for growing fibrous beta silicon nitride may help to meet the potentially great demand for silicon nitride ceramics. These ceramics have high tensile strength and resistance to thermal shock, which make them an attractive choice for high-temperature engine parts.

The process is a modification of an existing process for growing whiskers of cubic silicon carbide and alpha silicon nitride. Silicon monoxide, generated by the reaction of carbon and silica at 1,450° C, is reacted with a stream of ammonia mixed with hydrogen, carbon monoxide, and/or nitrogen. The JPL version of the process uses higher temperatures and flow rates in conjunction with a simple tubular configuration of the reaction chamber.

The silicon nitride forms as a layer of white corklike material, up to 6 mm thick, covered with a satin-textured parallel

growth of whiskers. The whiskers are single crystals of beta silicon nitride, about 1 μm in diameter and up to 5 cm long. The corklike material appears to be a lightly packed mesh of submicron beta silicon nitride whiskers.

The whiskers are expected to find application as reinforcement in composite silicon nitride ceramic parts. The corklike material may be useful in its present form for thermal barrier tiles. Work must still be done, however, to identify what catalyst, if any, is operating in the process and to relate process parameters to the form and composition of the products.

This work was done by R. James Holliday of the John Brown University and Paul J. Shlichta of Caltech for NASA's Jet Propulsion Laboratory. For further information, Circle 3 on the TSP Request Card. NPO-16409

Books and Reports

These reports, studies, and handbooks are available from NASA as Technical Support Packages (TSP's) when a Request Card number is cited; otherwise they are available from the National Technical Information Service.

Mechanical Design Handbook for Elastomers

Step-by-step procedures are presented for designing elastomer dampers.

A *Mechanical Design Handbook for Elastomers* has been written that reviews the state of the art in elastomer-damper technology with particular emphasis on the applications of high-speed rotor dampers. It is a self-contained reference but does include some theoretical discussion to help the reader understand how and why dampers are used for rotating machines.

This handbook presents a step-by-step procedure for the design of elastomer dampers and detailed examples of actual

elastomer damper applications. Dampers of this type have been shown to be effective for controlling rotor vibrations; however, a historic lack of design data and designer experience with elastomer dampers has inhibited the expansion of their application. The term "elastomer" refers to a large variety of synthesized polymers as well as to natural rubber. The purpose of this handbook is to provide such data in a compact and convenient form and to encourage the use of elastomer dampers and elastomeric damping treatments.

A portion of the design data contained in this handbook is relevant to many mechanical design problems and applications of elastomers. For example, the elastomer dynamic-property data may be utilized in the design of structural supports for shock and vibration isolation and insulation. Some basic information regarding the effect of structural damping is included in this work. Specific information concerning the design of such structural members is beyond the scope of this handbook, but an extensive bibliography is provided at the conclusion of each chapter to aid the design engineer in finding a solution to the problem.

The specific steps required for the design of elastomer dampers are reviewed in detail and include the procedures and justifications for the selection of a particular elastomer material and a particular elas-

tomers configuration as well as the details involved in the design of the damper hardware. In order to provide as complete a reference as possible, a full range of such physical properties as density and thermal conductivity are also provided for a large variety of elastomer compositions. Such considerations as compatibility with fluid, ozone, and adhesives are also presented along with specific compatibility data for several elastomer materials.

For the designer who finds it necessary to determine the dynamic properties for a particular elastomeric material, or for an elastomeric material for which the dynamic properties are not available, a thorough discussion of the most common dynamic-property test methods is presented. This handbook includes a detailed description of the procedure for performing the base-excitation resonant-mass test, which is the most versatile and the least sensitive to instrumentation error. Detailed examples of existing elastomer dampers are discussed, along with the steps encountered in the design process, to provide the reader with a complete picture of the design procedure.

This work was done by M. Darlow and E. Zorzi of Mechanical Technology, Inc., for Lewis Research Center. Further information may be found in NASA CR-3423 [N81-26461/NSP], "Mechanical Design Handbook for Elastomers" [\$28]. A copy may be

**THE GOOD NEWS IS
WHAT WE PUT IN THIS BOX.
BUT THE GREAT NEWS IS
WHAT YOU GET OUT.**



INTRODUCING SONIX
DIGITAL AIR PRESSURE STANDARD

Sonix is here! It's the new pressure transducer that's small, accurate, rugged and stable. And best of all, it outputs data in corrected engineering units.

Because Sonix is a smart transducer, its applications go far beyond calibration of other transducers. And since the internal micro-computer compensates for systematic and temperature-dependent errors, you get reliable, repeatable results.

To find out more great news, call or write PSI...the leaders in digital pressure measurement technology.

- $\pm 0.01\%$ F.S. accuracy/stability
- Corrected digital output
- Applications include metrology, flight test and lab calibration

PSI PRESSURE SYSTEMS

15 Research Drive, Hampton, VA 23666
(804) 865-1243

Circle Reader Action No. 378

purchased [prepayment required] from the National Technical Information Service, Springfield, Virginia 22161. LEW-14160

Constitutive Equations of Aging in Polymers

Stress-relaxation and creep chemomechanical behavior are analyzed.

A theoretical paper presents solutions of equations that describe polymeric aging. The solutions apply under such loading conditions as constant strain (stress relaxation), constant strain rate, and stress relaxation with a sudden change of cross-link density. These theoretical models form a framework for predicting the chemomechanical aging behavior of elastomers and polymers.

The previous constitutive equation describing the relaxation behavior of time-dependent, chemically unstable materials was developed by employing the irreversible thermodynamics of internal variables and Eyring's absolute-reaction-rate theory. Related equations (also developed previously) include a set of evolution equations that can account for the effect of the

chemical-cross-link density on the relaxation rate and a rate equation that describes mechanically coupled chain-scission processes.

The report begins with a review of the previously derived equations in the context of deformation kinetics. These equations, which represent the coupled chemomechanical behavior of a polymer, are quite general and apply irrespective of the constitutive properties of a material. They are, however, complicated and highly nonlinear, and hence not tractable analytically in the general case.

In applying the equations to particular cases, simplification is achieved by selecting such particular conditions as constant temperature or by making specific, simplifying assumptions about the nature of the process being modeled. For example, in the first of three cases considered, relaxation is assumed to occur without chain scission. The resulting equation states that the shift factor due to the cross-link density is an exponential rather than a power function of chemical cross-linking density. The temperature dependence is included implicitly.

In the second case, chain scission is assumed to occur without physical relaxation and at constant temperature. The equation derived under these assumptions is shown to be in agreement with certain high-temperature scission-process data where

no physical relaxation occurs.

In the third case, both physical relaxation and chemical aging are assumed to occur simultaneously. With constant temperature assumed, three different loading histories are investigated: Stress relaxation, constant strain rate, and stress relaxation with a sudden change of cross-link density.

In the final section of the report on creep behavior, the introduction of the Gibbs free energy leads to constitutive equations expressed as functions of stress and temperature. Using a three-element model that is mathematically equivalent to the model of two springs in parallel, with one of them in series with a dashpot, the equations thus derived show, for the first time, the relations between mechanical models and internal variables in the creep expressions. The final set of equations presented describes the coupled chemomechanical behavior of a nonaging network polymer undergoing simple creep at constant temperature and stress. These equations explicitly express the effect of chain scission on the creep rate.

This work was done by Steven T. J. Peng of Caltech for NASA's Jet Propulsion Laboratory. To obtain a copy of the report, "Constitutive Equations of Aging Polymeric Materials," Circle 90 on the TSP Request Card. NPO-16480

MEASURE RPM INSTANTLY Pioneer Model DT36M Digital TACHOMETER

Continuous Digital Readout
60 to 50,000 RPM
Visible Light Beam makes aiming easy
No Wires or Mechanical Connections Required
Memory stores last reading

with memory

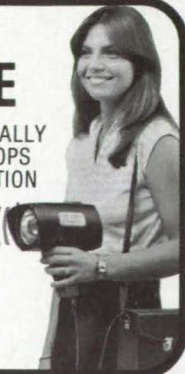
A highly accurate photoelectric digital display tachometer incorporating Pioneer's own patented* circuitry. Accuracy: ± 1 RPM over entire range • Large 5 Digit LCD Display • Crystal Controlled Time Base for stability • Battery operated using 2-1.5 V "AA" batteries 1-9V alkaline battery • No calibration required



Pioneer Model DS-12V Battery Powered PORTA-STROBE

Ideally suited for a wide range of industrial, institutional and educational applications. Sturdy and compact, it can be operated for visual and digital measurement of rotary, reciprocating or linear motions. Adjustment also allows viewing the action in slow motion to study interacting parts. Can also be used as a remote electronic digital tachometer for direct measurement of RPM (speed) without special reflective tape or markings. RPM results are updated and recorded approx. every half second on a 5-digit LED display. Can also be operated on 120V 60Hz AC line. Speed range 0 to 12,000 RPM with accuracy to 1 RPM.

VISUALLY
STOPS
MOTION



THE **PIONEER**
ELECTRIC & RESEARCH CORPORATION
743 Circle Avenue • Forest Park, Illinois 60130 • Phone 312/771-8242

There is a Solution.

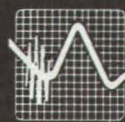
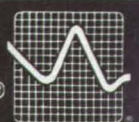
- memory loss
- board failure
- read-write errors
- "hung" equipment
- costly downtime

The above headaches, caused by spikes, surges, transients, common and normal mode noise, effect all micro-processor based equipment.

A word of caution:

The industry today is being inundated with filters and surge suppressors of all types, shapes and prices. Do not be misled by grossly exaggerated performance claims. Tycor® has been the leader in the AC Power Line Filter Industry for 10 years and its products continue to meet and exceed the rigid performance tests imposed by the industry.

The New Improved High Efficient...

 **TYCOR** 

Solidifying Cast Iron in Low Gravity

Directional solidification can produce higher carbon content alloys and directional thermal conductivity.

A report describes a study of the solidification of cast iron in low and normal gravity. Because flotation, sedimentation, and convection are suppressed, alloys that solidify at nearly zero gravity have unusual and potentially useful characteristics.

The study was conducted in an airplane that repeatedly flew along parabolic trajectories. During these maneuvers, the gravitation perceived in the airplane was about 0.001 to 0.1 of its normal value for 20 to 30 seconds. A directional-solidification furnace was used to slowly advance the solid/liquid interfaces along rod-shaped cast iron samples of 4-mm diameter. For each sample, controlled solidification was continued through several dives. The known solidification rate of the sample was then correlated with accelerometer data to determine the gravity level during solidification at any point in the sample.

In low-phosphorus, flake-graphite samples, bands of coarse graphite appeared in

the regions solidified under low gravity. The coarsening is explained by the absence of flotation, which allows long flakes of graphite to be incorporated into the solidification front.

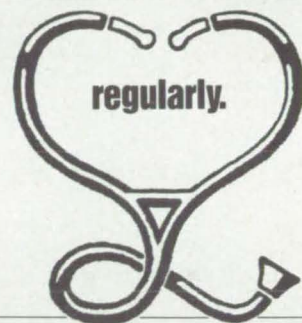
High-phosphorus, flake-graphite iron samples had larger eutectic cells in the low-gravity zones. These cells were followed by bands of coarse graphite. Thus, it seems that convection favors increased nucleation.

The spheroidal-graphite samples were similar to the flake-graphite samples in that they had bands of larger graphite nodules corresponding to regions of low gravity. This is a consequence of graphite flotation in normal gravity and incorporation of the graphite in the solidification front in low gravity.

Thus, it appears that iron/carbon alloys made at low gravity can have greater carbon content (as high as 5 to 10 percent) than those made at Earth gravity because the carbon particles do not float to the top of the melt. With directional solidification, low-gravity iron/carbon alloys might also be made with highly directional properties. For example, thermal conductivity can be made very high along the solidification axis and very low across this axis.

This work was done by J. C. Hendrix, P. A. Curreli, and D. M. Stefanescu of Marshall Space Flight Center. To obtain a copy of the report, "Directional Solidification of Flake and Spheroidal Graphite Cast Iron in Low and Normal Gravity Environment," Circle 43 on the TSP Request Card. MFS-27069

**Have a heart-to-heart
with your doctor. . .**



American Heart Association
WE'RE FIGHTING FOR YOUR LIFE

Employers

Willing workers available now at as little as 1/2 your usual cost.

Under the new Job Training Partnership Act, businesses that hire and train the jobless will receive up to 50% of on-the-job training costs. And you may qualify for tax credits of up to 50% of the first year salary.

No business too large or too small.

This is your chance to get the help you've needed, but thought you couldn't afford.

Call your local private industry council or write **National Alliance of Business**, P.O. Box 7207, Washington, D.C. 20044

A Public Service of
This Publication



Tycor AC Power Line Filters . . .

the **POWERful** Solution. ✓

Tycor filters eliminate the need for dedicated lines, costly re-boots, decrease downtime, service calls, board replacement, and the need for large spare parts inventory. They have proven to be cost effective in less than 3 days on problem sites and 90 days on typical sites.

(actual field evaluations by national companies show an 81% decrease in service calls)

TYCOR ELECTRONIC PRODUCTS LTD.

Head Office:
6107 - 6th Street S.E.
Calgary, Alberta, Canada
T2H 1L9

**FOR A DISTRIBUTOR
NEAREST YOU CALL
TOLL FREE:
1-800-661-9263**



TYCOR®





122 Mass Spectrometer for Airborne Micro-Organisms

Books and Reports

124 Preadapting to Weightlessness

Mass Spectrometer for Airborne Micro-Organisms

Bacteria flow continuously to an analytical instrument.

NASA's Jet Propulsion Laboratory, Pasadena, California

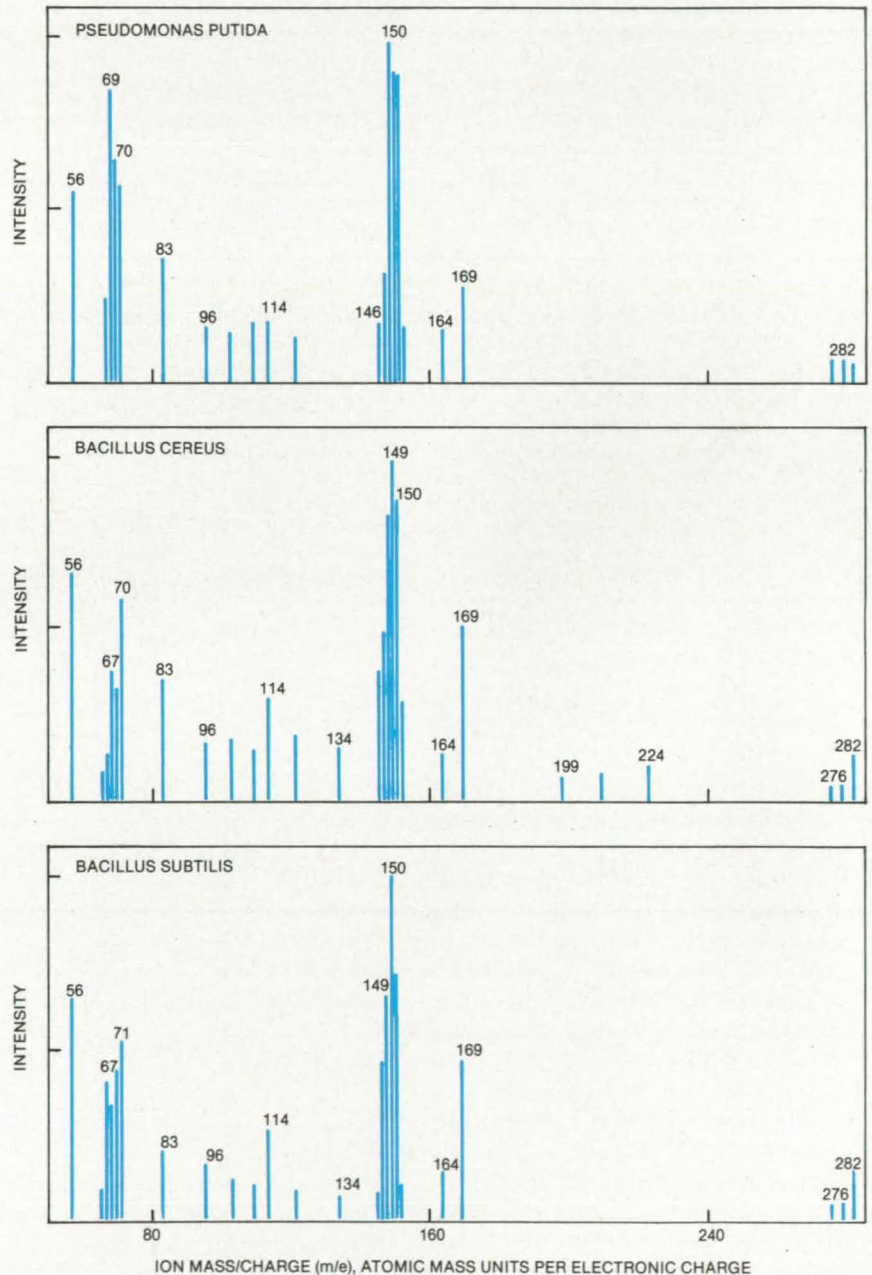


Figure 2. **Mass Spectra** for three different microbe species illustrate their discernible differences. Because they are made from essentially the same molecular building blocks, the micro-organisms share similar spectral features — for example, intense peaks at about 150 mass units. However, the relative intensities of the various peaks differ among the species. Some distinguishing mass peaks can also be seen.

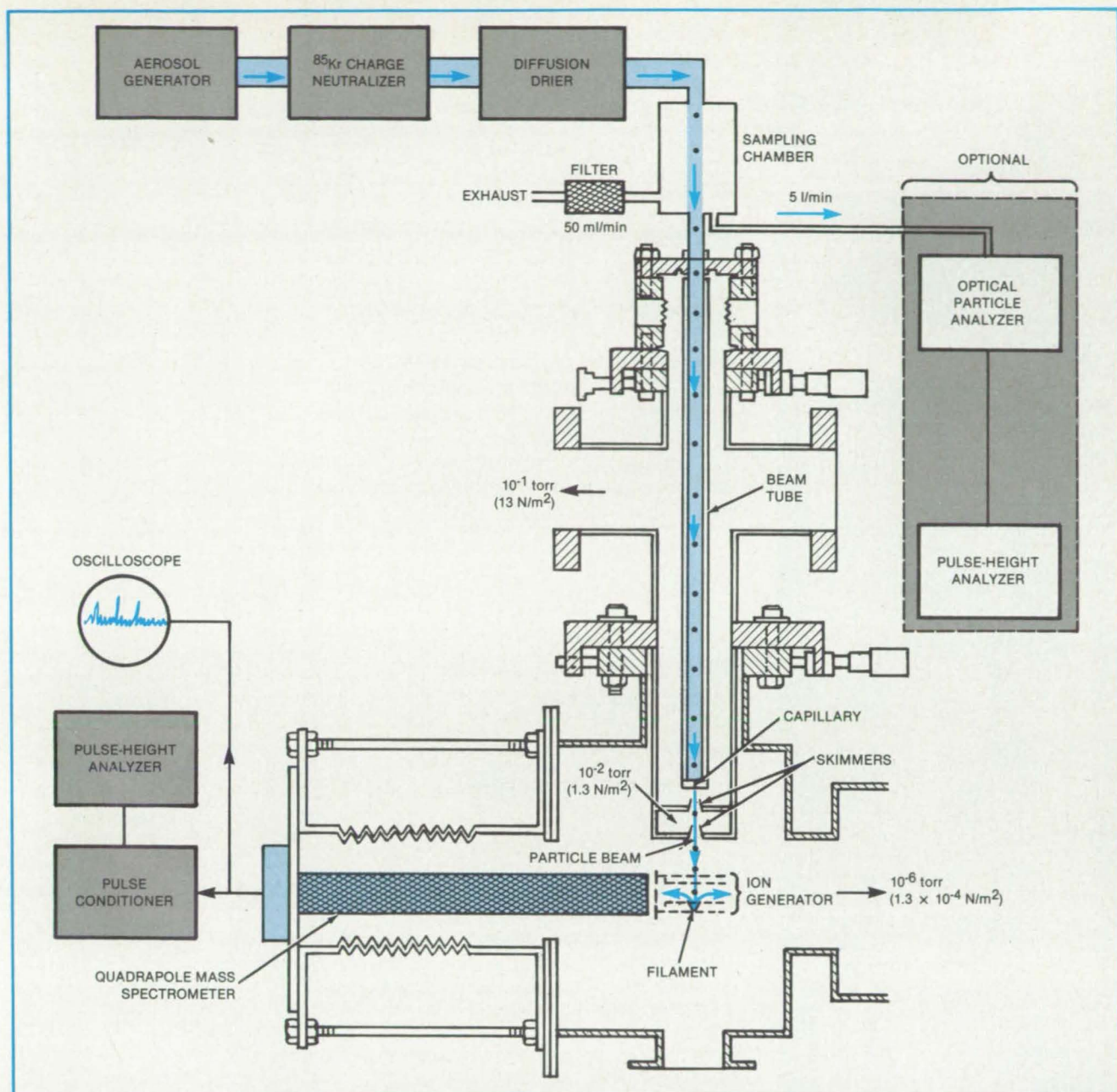


Figure 1. The **Sampling System** includes an injection apparatus that introduces bacteria particles in the form of a beam into the source of the mass spectrometer. The particles are volatilized on a hot filament, then ionized, then analyzed in the mass spectrometer.

Bacteria and other micro-organisms may be identified continuously with the aid of a new technique for producing samples for a mass spectrometer. The technique generates an aerosol of the organisms and feeds it to the spectrometer. A given species of organism produces a characteristic set of peaks in the mass spectrum and might thereby be identified. The technique may be useful for monitoring bacterial makeup in environmental studies and in places where cleanliness is essential, such as hospital operating rooms, breweries, and pharmaceutical plants.

In the laboratory version of the system, any one of three species of bacteria is allowed to deposit and grow for 40 hours in a culture medium composed of tryptone,

yeast extract, glucose, and sodium chloride. The culture is harvested by repeated washing with distilled water, then suspended in distilled water and refrigerated. In preparation for analysis, the sample medium is converted from water to ethanol by washing in a series of water/ethanol solutions of increasing ethanol concentration, ending with 100 percent ethanol.

An aerosol containing the biological particles is generated by nebulizing the liquid suspension. A stream of nitrogen gas carries the aerosol through a charge neutralizer, then through a drier. The aerosol, after expansion into vacuum through the capillary nozzle, produces a beam of bacteria particles. The heavier aerosol particles continue on a straight path into the mass spec-

trometer (see Figure 1), whereas the light carrier-gas molecules are pumped off upstream of the nozzles.

The particles impinge on a hot rhenium filament at 740° C in the ion source of a quadrupole mass spectrometer. The particles vaporize on the filament and are ionized by electron bombardment at an energy of 40 electron volts. The ions are accelerated into the mass spectrometer, where the spectral measurements are made. The particle-injection-and-ion-generation scheme is highly efficient: Up to 70 percent of the material in the aerosol reaches the spectrometer.

A burst of ions lasting for about 100 microseconds is produced by each micro-organism. Bacterial species can be distin-



**...DEVELOPED FOR
N.A.S.A.
...USED BY
ASTRONAUTS ON
SPACE FLIGHTS**



Chrome Space Pen with flight button point retraction. Refills readily available.

\$10.00

Probably the world's most dependable pen. The patented pressurized cartridge developed for NASA permit these pens to write at any angle (even upside down) in severe temperatures -50° to +400°F, over glossy or greasy surfaces, under water and up to 3 times longer than ordinary pens.



Chrome pocket/purse pen with distinctive Space Shuttle emblem. Unique compact design.

\$12.50



Fisher Space Pens are available wherever better pens are sold. Corporate logos and emblems are available. You may order or request further information by contacting:

PAUL C. FISHER
743 Circle Avenue
Forest Park, IL 60130
(312) 366-5030

guished via slight differences in their mass spectra (see Figure 2). The average intensity of mass peaks is determined from the pulse-height distribution of about 1,000 ion bursts. Although the laboratory version of the system requires a bacterial culture to generate a number of particles large enough to sample, work is in progress to develop a more sensitive system that can operate directly

from ambient air. It should eventually be possible to obtain a complete mass spectrum from a single particle.

This work was done by Mahedeva P. Sinha and Sheldon K. Friedlander of UCLA for NASA's Jet Propulsion Laboratory. For further information, Circle 102 on the TSP Request Card. NPO-16359

Books and Reports

These reports, studies, and handbooks are available from NASA as Technical Support Packages (TSP's) when a Request Card number is cited; otherwise they are available from the National Technical Information Service.

Preadapting to Weightlessness

This training concept could prevent motion sickness.

A report discusses the physiological and physical concepts of a proposed training system that would precondition astronauts to a weightless environment. The system could prevent motion sickness, which is often experienced during the early part of an orbital flight. It may also help to prevent seasickness and other forms of terrestrial motion sickness.

In one form of the proposed system, a training subject sits on a three-dimensional platform that can pitch, roll, and yaw slightly. Belts and braces prevent the subject from moving the head or torso. A box measuring 8 feet (2.4 meters) on a side surrounds the subject. Projectors outside the box cast images of visual scenes on its walls.

The system would change the scene in response to attempted head and body movements by the subject. The change would simulate the motion that would be observed by the subject if he or she were weightless. In space, the entire visual scene moves in reaction to a head movement, and changes in the perceived scene are different from those that would be observed if the body was not weightless. For example, when the subject uses the controls to command forward movement, the scene on the front wall enlarges, the scenes on the side walls pan rearward, and the table pitches the subject back slightly.

In addition to this simulation of translational movement, rotation is simulated by rotating the box instead of the subject. The subject's head is prevented from moving, but transducers in the head restraint sense the forces of incipient movement and generate the signals that rotate the box.

The training would affect the subject's perception of inner-ear signals, visual signals, and kinesthetic motion perception. The changed perception would resemble that of astronauts who have spent many days in space and have adapted to weightlessness.

The effect of the force of gravity on the inner ear is minimized during training by maintaining the gravity vector close to the vertical axis of the subject's body regardless of the orientation of the box. The effect of gravity is further reduced by computer control of the visual scene motion and the slight pitch, roll, and yaw of the table. Gravity "washout" algorithms, some of which have already been developed for aircraft simulators, can be used for this purpose.

Subjects would probably become motionsick when they first use the simulator. With repeated exposures, however, the brain would learn how to deal with the unfamiliar stimuli, and the symptoms would diminish.

This work was done by Millard F. Reschke of Johnson Space Center, and Donald E. Parker and A. P. Arrott of Miami University.

Title to the invention described in this report has been waived under the provisions of the National Aeronautics and Space Act (42 U.S.C. 2457(f)) to the Miami University, Oxford, Ohio 45056.

MSC-20847

Capture the Glory!

Now you can own this collector's print, commemorating Columbia's exploits, at an exceptional introductory price.

Noted aviation artist Ken Kotik has captured *Columbia* in all its glory to commemorate the completion of four test flights and the first operational mission, STS-5. This fine print—truly a collector's item—depicts the orbiter in full color, side view, with every feature crisply detailed.

Arranged beneath the ship, also in full color, are the five distinctive mission patches. But what makes Ken Kotik's work most unique is his method of creating a 'historical panorama' via individual vignettes surrounding the side view of *Columbia*.

Educational as well as eye-appealing, these scenes, which are expertly rendered in a wash technique, include such subjects as the orbiter under construction at Rockwell, on the launch pad, at touch-down and during transit on its 747 carrier. Concise copy, hand-written by the artist, accompanies each vignette. (*Important:* The greatly reduced print reproduced here is intended only to show style—at the full 32" by 24" size, all copy is clearly readable.)

About the artist.

Ken Kotik, a 37-year old Colorado native, has been a professional commercial artist for the past 14 years. In his own words, he "eats, drinks and sleeps flying." It shows in the obvious care and attention he brings to each print or mural. When not at his drawing board creating artworks for such prestigious institutions as the Air Force Academy, Ken can be found at the controls of his Schweitzer sailplane, in which he competes nationally. A self-taught artist, he specializes in airbrush-applied acrylic techniques. *Space Shuttle Columbia: The Pathfinder* is his first work on the space program, and the original art has been accepted by the Smithsonian Air and Space Museum for its permanent collection.

About the artwork.

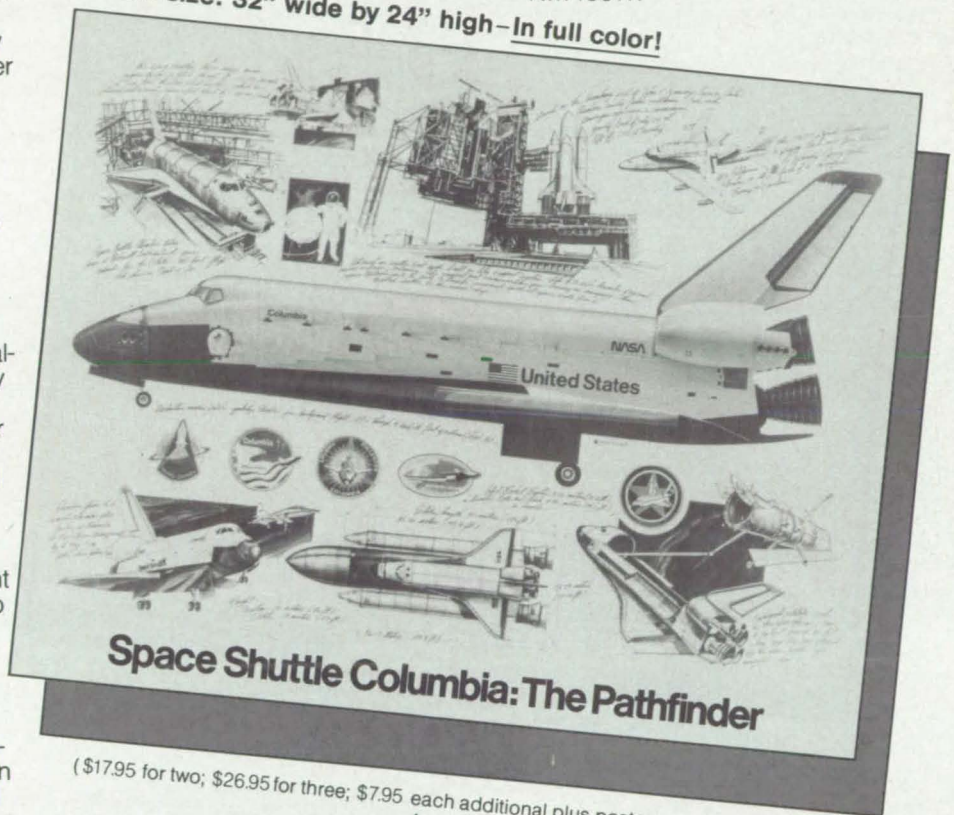
Space Shuttle Columbia: The Pathfinder was printed in five colors, after individual press proving, on exhibit-quality 80 lb text 'Hopper Feltweave' textured paper. The feltweave texture yields properties most desirable for framing and display.

About ordering.

Each *Columbia* print comes packed in a sturdy mailing tube and will be shipped upon receipt of your order at the introductory price of \$9.95. Please allow two to three weeks for delivery. There is a one-time *first class* postage and handling charge of \$2.50 for each order. (If you order

three prints, for example, you still include only \$2.50 for postage and handling to cover the entire order.) To ensure that you receive your prints without delay, fill out and mail the coupon today, *including check or money order only* and local tax where applicable. If coupon has been clipped, mail your order to: NASA Tech Briefs, Columbia Print Offer, 41 E. 42nd St., New York, N.Y. 10017.

Actual size: 32" wide by 24" high—In full color!



(\$17.95 for two; \$26.95 for three; \$7.95 each additional plus postage and handling.)

ONLY \$9.95 EACH

MONEY BACK GUARANTEE

If not completely satisfied, return undamaged print, in wrapper, within 10 days for a full refund of print purchase price.

Mail to: NASA Tech Briefs
Columbia Print Offer
41 East 42nd St.
New York, N.Y. 10017



Note: One print \$9.95; two \$17.95; three \$26.95; each additional \$7.95, plus \$2.50 postage and handling per order.

Please rush _____ Columbia prints.
I have enclosed \$ _____ plus \$2.50
for *first class* postage and handling.
Total enclosed: \$ _____.

Name _____

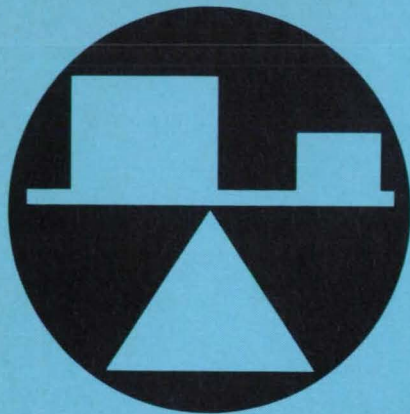
Address _____

City _____ State _____ Zip _____

New York State residents add 7% sales tax.
New York City residents add 8.75% sales tax.

Please add my name to your mailing list
for future print offerings.

SS-1



Hardware, Techniques, and Processes

- 126 Latch for Telescoping Structures
- 127 Water-Thickness Gage
- 128 Rotary Speed Sensor for Antilocking Brakes
- 129 Calculating Bearing Forces from Strain-Gage Signals
- 130 Photo-Optical Blade-Vibration-Data Acquisition System
- 131 Locking Pull Pin
- 131 Distributing Radiant Heat in Insulation Tests
- 132 Smoothed Two-Dimensional Edges for Laminar Flow
- 133 Fuel Gage for Sloshing Tanks
- 134 Calibrating Pressure Transducers at Cryogenic Temperatures
- 135 Braille Reading Systems
- 136 Hydraulic Cylinder with an Integral Position Indicator
- 137 Shaft Axial-Displacement Sensor
- 137 Accelerated Stress-Corrosion Testing
- 138 Miniature Microphone Adaptor
- 139 Electronic/Hydraulic Level Gage
- 140 Advanced Vapor-Supply Manifold
- 141 Titanium Heat-Pipe Wicks
- 141 Microphone Boom for Aircraft-Engine Monitoring
- 142 Thermal-Diode Sandwich Panel
- 143 Reduction of Vane Noise in Wind-Tunnel Nozzles
- 144 Squeeze-Film Damper Controls High Vibrations
- 145 Noise-Path Measurements in Aircraft Structures
- Books and Reports**
- 145 Stiffness Study of Wound-Filament Pressure Vessels
- Computer Programs**
- 146 Predicting the Performance of an Axial-Flow Compressor
- 147 Axial-Flow Compressor Performance with Water Ingestion
- 147 Flow Through Gas-Turbine Ducts
- 147 Automated Design Synthesis
- 148 Radiation View-Finder Program with Interactive Graphics
- 148 Four-Cylinder Stirling Engine Control Simulation
- 149 Solution of Radiation and Convection Heat-Transfer Problems
- 149 Orbit Transfer Programs
- 150 Bearing Thermal Performance Prediction
- 150 Three-Dimensional, Subsonic, Turbulent Juncture Region Flow
- 150 Zero-Lift Wave Drag of Complex Aircraft Configurations

Latch for Telescoping Structures

A four-bar linkage is activated by the relative movement of longeron sections.

Langley Research Center, Hampton, Virginia

A latch for a three-member telescoping column was originally developed for the deployment of an antenna 122 meters in diameter. Illustrated in Figure 1, the antenna is being designed as a candidate Space Shuttle cargo.

The deployable column along the axis of the antenna is an open lattice structure with three longerons as the principal load-bearing members. The column is divided into telescoping sections that deploy, one section at a time. The latch automatically locks the sections into position during deployment and unlocks them when the antenna is restowed. The latch is a four-bar linkage using the over-center principle for locking, with Belleville spring washers to absorb deflections.

The main column is composed of 23 tel-

escoping sections. Each section has three longerons spaced 120° apart with a latch located at the end of the longerons. There are 63 identical latches in the column. The latch fits within the 0.75-in. (19.05-mm) diameter longeron. A servomotor applies a tensile force to cables that are threaded through each set of longerons. The same servomotor may be used for retrieval by pulling on a single cable that is threaded through the center of the column and is attached to the top column section.

Deployment of column sections initiates the rotation of an actuator arm (see Figure 2) that is extended into the housing at the base of each longeron. As longerons B and C move relative to longeron A, the latch restraining arm and actuator arm rotate. The actuator arm rotates into an over-center

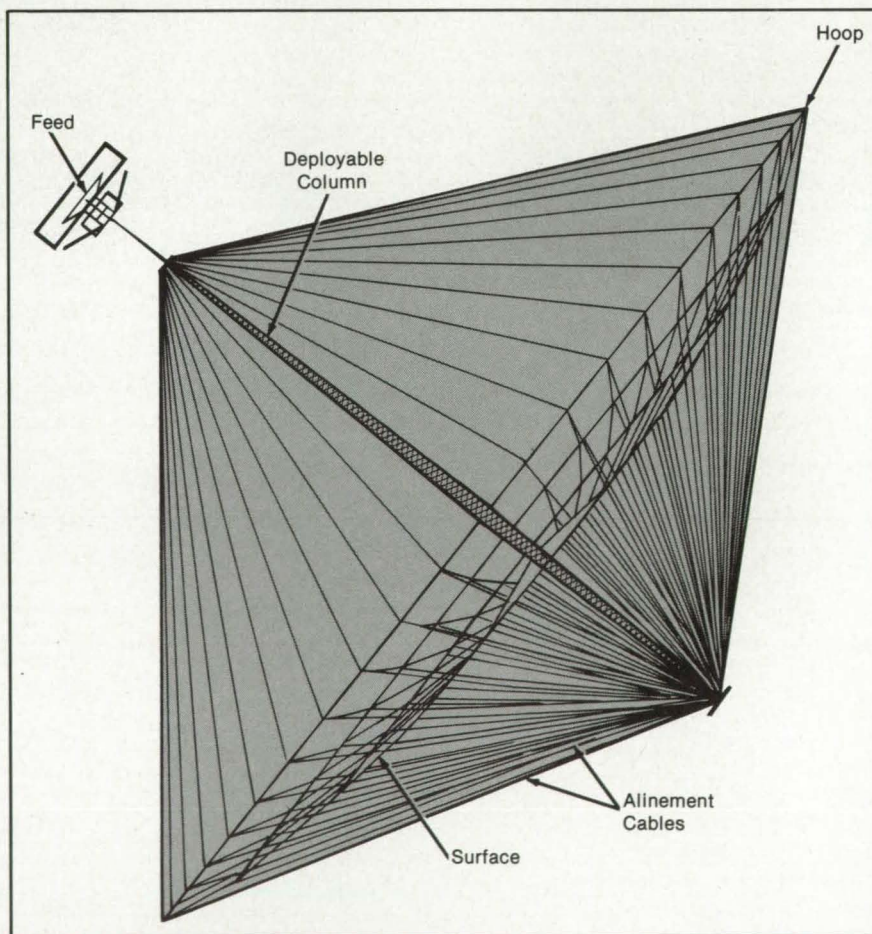


Figure 1. The Large Hoop/Column Antenna must be deployed and restowed while in orbit. It is divided into telescoping sections that are deployed after the antenna is placed in orbit. The antenna may be as large as 400 ft (122 m) in diameter, with the electronic feed system suspended on a 279-ft (85-m) column.

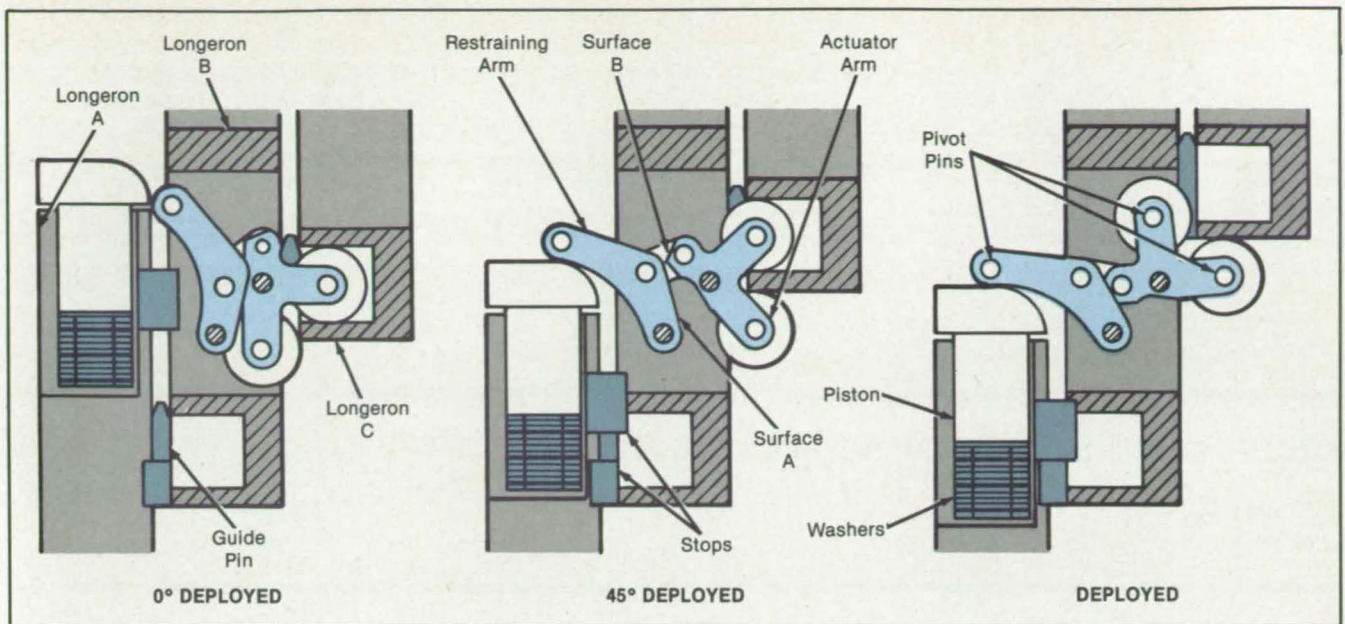


Figure 2. The **Restraining Arm** and **Actuator Arm** control movement in the deployment sequence. Deployment of the column sections initiates latching.

position, locking the linkage. After latching over center, further rotation is stopped when surface A of the restraining arm mates with surface B of the actuator arm. The stops of longerons A and B merge into position engaging two guide pins, which force alignment and restrain shearing motion.

The Belleville spring washers and piston housed at the top of each longeron are an integral part of the latching mechanism. As the restraining arm swings toward the

locked position, it drives the piston against the washers causing them to compress. (In general, over-center mechanisms rely on the four-bar linkage to deflect when moving to an over-center position. This was unacceptable for the latch because the small size caused excessive stress in the pins and linkage.) The Belleville spring washers absorb most of the deflections and limit the maximum force necessary to latch. The resulting preload of spring and actuator arms is set to provide a rigid column for the ex-

pected external loads.

This work was done by Elvin L. Ahl, Jr., of Langley Research Center. For further information, Circle 93 on the TSP Request Card.

This invention is owned by NASA, and a patent application has been filed. Inquiries concerning nonexclusive or exclusive license for its commercial development should be addressed to the Patent Counsel, Langley Research Center [see page 29]. Refer to LAR-13169.

Water-Thickness Gage

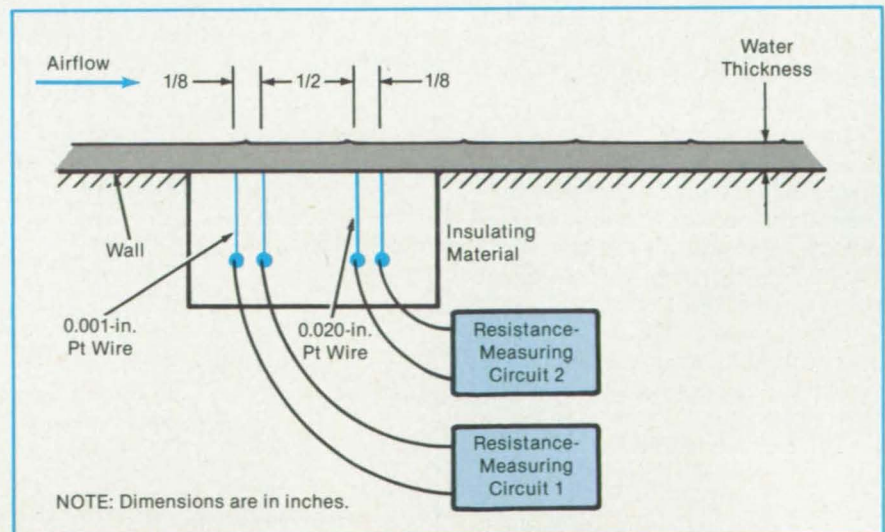
Dual-sensor measurement is independent of water conductivity.

Langley Research Center, Hampton, Virginia

A gage for determining the depth of water buildup on the outside of aircraft is relatively simple to operate and yields a result independent of the conductivity of the water. The gage can be used to evaluate the effects of water on lift and to detect water weight excesses.

The gage is shown schematically in the figure. It features two pairs of conducting platinum wires, with 0.001-in. and 0.020-in. (0.025-mm and 0.508-mm) diameters, respectively, immersed in an insulating material. Two ac circuits measure the resistance between each pair.

If a single pair of wires is used in an ac resistance-measuring circuit (ac to prevent electrolysis or polarization), the output is a function of both water thickness and water conductivity for a given electrode geometry. The use of two pairs of wires eliminates the effects of the variable con-



The **Dual-Sensor Gage** eliminates the effects of water conductivity, providing a direct correlation between resistivity and water thickness.

ductivity of the water and yields resistance changes that are directly related to the water thickness.

Successful tests of the dual-gage sensor have shown that a gage wire pair with a sufficiently small circular cross section yields a resistance change that is nearly independent of water thickness. This determines the resistivity. If the gage has wires with diameters several times the water thickness, the relationship between resistivity and thickness is linear. The combination of the two outputs then gives the water

thickness. If water thicknesses smaller than the small wire sensor are encountered, results are in error. Thus, the small wire should be smaller than the thinnest sheet of water measured.

This work was done by Leonard M. Weinstein of Langley Research Center. No further documentation is available on the dual-thickness gage. Preliminary results of a test to evaluate a single sensor for measuring water-film thickness are presented in NASA TM-85796 [N84-27677/NSP], "Preliminary Indications of Water

Film Distribution and Thickness on an Airfoil in a Water Spray" [\$7]. A copy may be purchased [prepayment required] from the National Technical Information Service, Springfield, Virginia 22161.

This invention is owned by NASA, and a patent application has been filed. Inquiries concerning nonexclusive or exclusive license for its commercial development should be addressed to the Patent Counsel, Langley Research Center [see page 29]. Refer to LAR-13342.

Rotary Speed Sensor for Antilocking Brakes

It uses inlet pressure, rather than outlet pressure, for the control signal.

NASA's Jet Propulsion Laboratory, Pasadena, California

A sensor based on fluidic principles produces a negative pressure approximately proportional to rotational speed. The sensor is being developed as part of an antilocking brake system for motorcycles. It uses the inlet pressure rather than the outlet pressure as the braking-control signal, eliminating the pressure pulsations caused by the pump vanes and thus ensuring a low-noise signal.

The sensor is a centrifugal air pump that is turned by one of the motorcycle wheels. Air enters the pump through orifice plates, and the suction is taken off through a port in the pump inlet plenum (see figure).

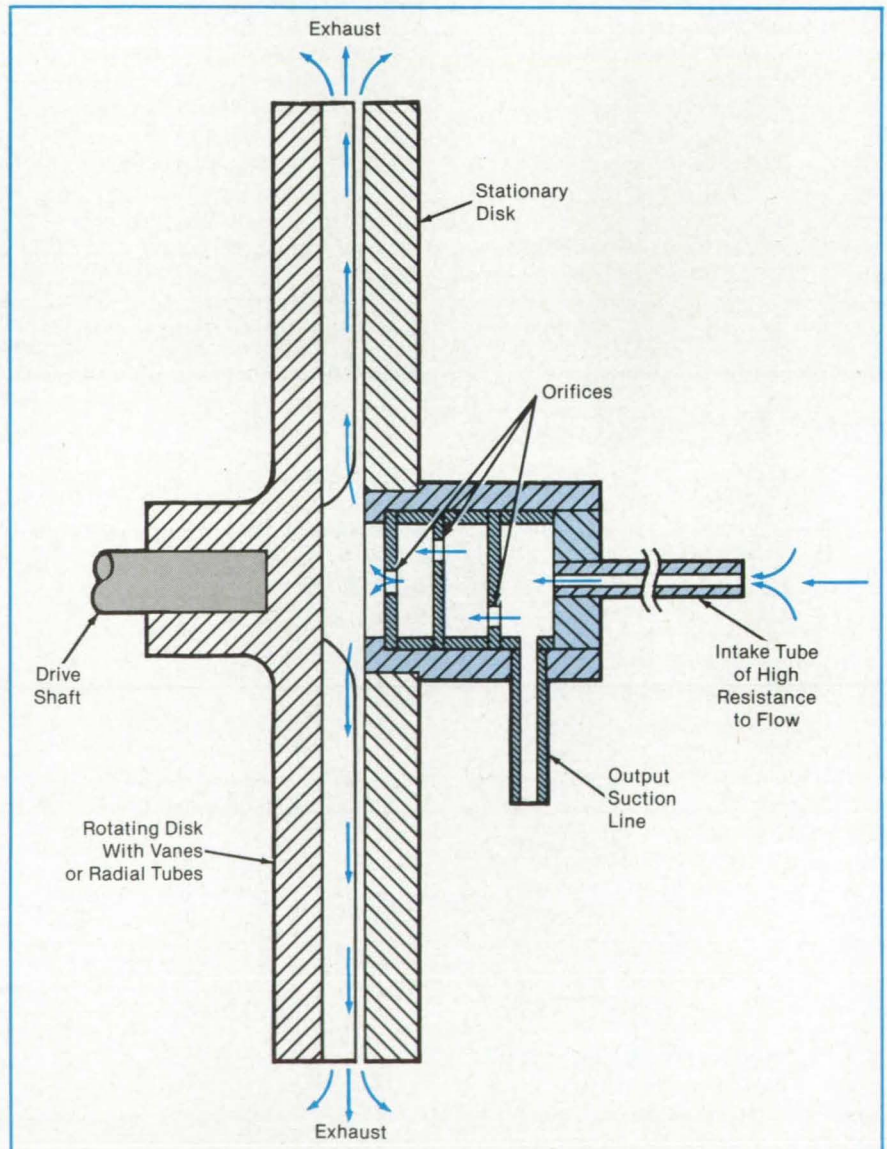
The suction (negative pressure) at a simple inlet would be proportional to the square of the pump angular speed. However, the combination of orifice plates and intake resistance results in a negative-pressure output that varies approximately linearly with angular speed.

Before the vacuum signal enters the main fluidic amplifier of the control system, it passes through a fluidic differentiator. This component produces a signal that is approximately proportional to the rotary acceleration of the pump.

In a prototype recently tested, the vacuum signal lagged changes in rotary speed by about 64 milliseconds. However, by optimizing the volume of the inlet plenum and the resistances of the orifices, it should be possible to reduce the response time one quarter of its present value.

This work was done by C. Martin Berdahl of Caltech for NASA's Jet Propulsion Laboratory. For further information, Circle 5 on the TSP Request Card.

Inquiries concerning rights for the commercial use of this invention should be addressed to the Patent Counsel, NASA Resident Office-JPL [see page 29]. Refer to NPO-16479.



The **Centrifugal Air Pump** creates a suction at a port in its inlet plenum. The suction increases approximately linearly with pump speed.

Calculating Bearing Forces From Strain-Gage Signals

Orthogonal force components are obtained with minimal processing.

Marshall Space Flight Center, Alabama

A technique for obtaining force components on a cylindrical bearing holder uses pairs of opposing strain gages. Signals proportional to the outputs of pairs of opposing gages are subtracted from each other. The subtraction nearly eliminates crosstalk between orthogonal force components. Since the output is two signals proportional to the orthogonal force components, the instantaneous load vector can be displayed simultaneously on an oscilloscope. The outputs can also be processed for simultaneous or subsequent analog or digital analysis. The technique should be quite useful in testing rotating machinery.

As shown in Figure 1, four gages are placed at 90° intervals on the circumference of the bearing holder. The output of each gage includes two strong components, the first of which is due to lateral motion (along the local radius) and the second, to elliptical distortion. The equations in the figure are equivalent to

$$\frac{1}{2} \left(\frac{S_1}{K_1} - \frac{S_3}{K_3} \right) =$$

$$F \cos \theta + \frac{1}{2} F \left(\frac{L_1}{K_1} - \frac{L_3}{K_3} \right) \cos 2\theta$$

and

$$\frac{1}{2} \left(\frac{S_2}{K_2} - \frac{S_4}{K_4} \right) =$$

$$F \sin \theta + \frac{1}{2} F \left(\frac{L_4}{K_4} - \frac{L_2}{K_2} \right) \cos 2\theta$$

Since in practice $L_1/K_1 \approx L_3/K_3$ and $L_4/K_4 \approx L_2/K_2$, the elliptical-distortion terms proportional to $\cos 2\theta$ are small and can be neglected. The remaining terms, $F \cos \theta$ and $F \sin \theta$, are just the orthogonal force components F_x and F_y , respectively. The multiplication and subtraction to obtain these components are easily done electronically.

The gage coefficients K_i and L_i must be known in advance to set the amplifier gains for the multiplications. To obtain the coefficients for each gage, a calibration curve is generated by applying a load at various angular positions relative to the gage (see Figure 2). The coefficients are calculated by adding and subtracting the values at the 0° and 180° points of the curve.

This signal-processing technique is equally applicable to rotating as well as to stationary loads. For a machine rotating at angular speed ω , the angle at time t is given

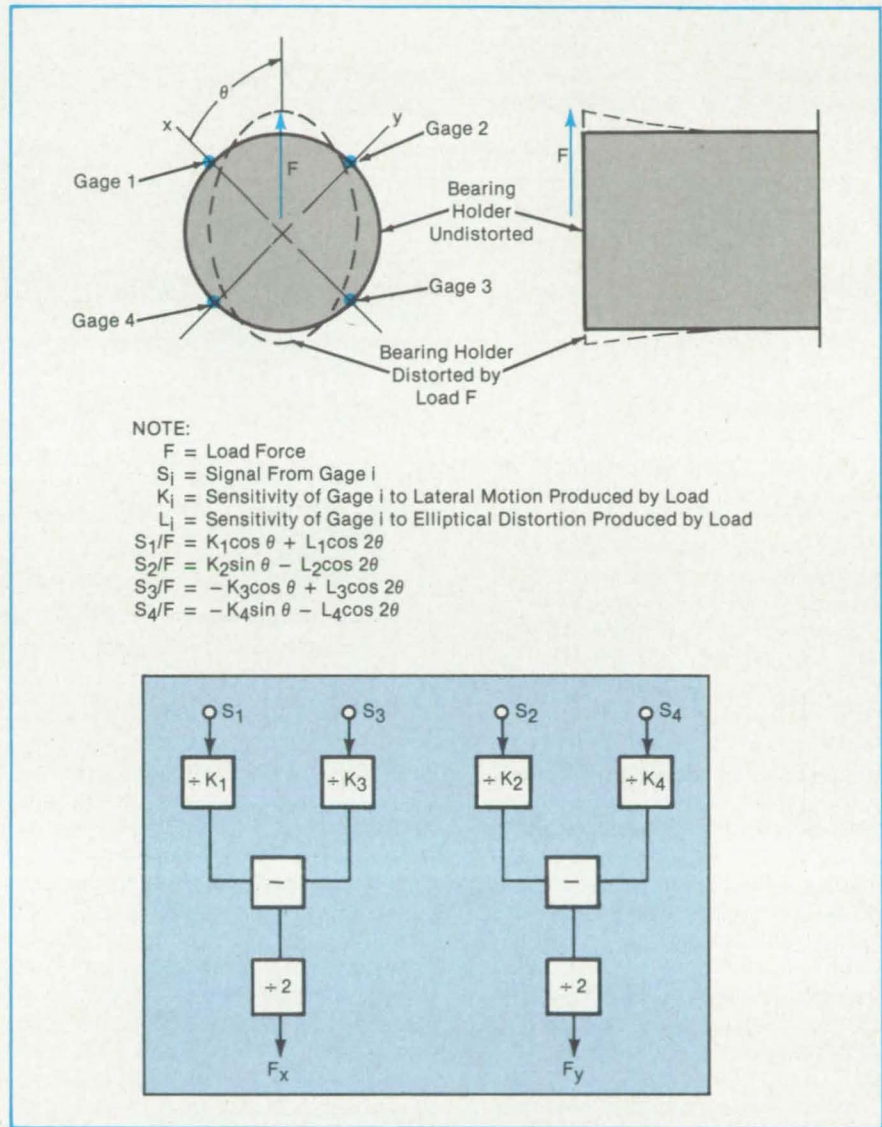


Figure 1. Strain Gages at 90° Intervals produce signals proportional to the lateral motion and elliptical distortion of the cantilevered bearing holder. Gage signals are divided and subtracted by the circuitry shown in the block diagram to obtain perpendicular components F_x and F_y of loading force F .

by $\theta = \omega t$. The force components of the signals have angular frequency ω , while the small elliptical-distortion components have angular frequency 2ω . It should therefore be possible to reduce the error components by low- or band-pass-filtering the subtractor outputs.

This work was done by J. R. Fenwick of Rockwell International Corp. for Marshall Space Flight Center. For further information, Circle 11 on the TSP Request Card. MFS-29000

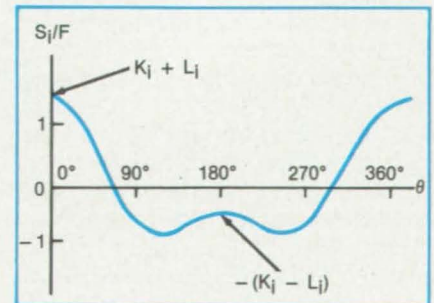


Figure 2. A Typical Calibration Curve shows the ratio of gage output signal to loading force at various loading angles, θ . Here, $K_i = 1$ and $L_i = \frac{1}{2}$.

Photo-Optical Blade-Vibration-Data Acquisition System

Many optical probes monitor the blades on a spinning stage.

Lewis Research Center, Cleveland, Ohio

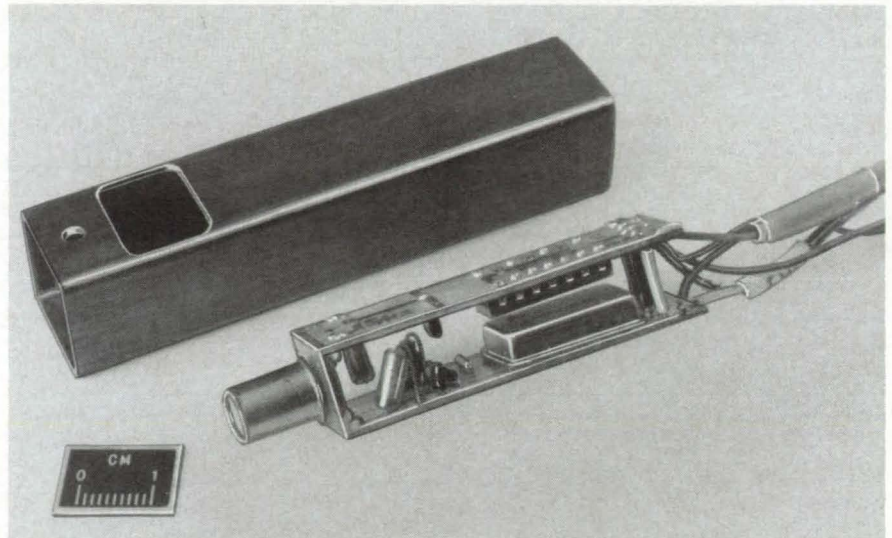
Techniques have been developed for measuring blade vibrations using optical sensors fixed in a casing around a bladed turbine-engine stage. Basically, the time of passage of an undeformed blade is computed very accurately. The actual time of passage of each blade as it passes each optical probe is measured. Time differences are then directly related to the amount of blade-tip deflection. Samples of blade-tip deflection from all of the probes are then assembled to represent vibration histories of each of the blades.

The measurement system coordinates and assembles the inputs of many optical probes (see figure) in order to monitor all of the blades on a spinning stage. Several points on every blade are monitored in order to develop a quantitative measure of the overall bladed-stage response.

Experimental determinations of blade-vibration phenomena in gas-turbine engines are extremely important to the advanced development of these engines. Many aspects of these vibrations were difficult to adequately predict or measure in any quantitative fashion. These include certain aspects of response to forced vibrations, blade-flutter phenomena, and complex engine/structural interactions that occur during transient excitations. Advanced turbine-engine development requires a broader accounting for blade-vibration phenomena to meet future design goals for increased performance, decreased weight, fuel economy, and minimized user cost.

Traditionally, blade-vibration phenomena on rotating members have been studied using strain gages. Signals generated on the blades are passed through either multi-channel sliprings or telemetry devices. Significant problems with these approaches include the degradation or loss of strain-gage signals due to the hostile operating environment. Furthermore, the number of measurement points is limited by the capacity of available slipring devices.

It is very difficult to quantitatively determine actual vibration patterns on rotating bladed stages with the limited number of measurement points available with strain-gage techniques. In part, this is due to the complexity of these vibration patterns and the need to monitor many points in order to fully characterize these motions. With this new system, the difficulties normally asso-



An Optical Probe is fixed in a casing to monitor the deflection of turbine-blade tips.

ciated with strain-gage life and durability can be reduced. The costs associated with the mounting of the strain gages and the installation and maintenance of sliprings can be avoided.

The complex bladed-disk responses become increasingly more complicated as the stage is spun at operating speeds. The effects of aerodynamic and centrifugal loading and nonharmonic excitation result in very complex deformation patterns. Experimental methods were required for the measurement of many points on these rotating systems in order to develop a better assessment of the dynamical state of the entire assembly. Holographic imaging methods with optical derotating prisms provide an excellent source of qualitative modal information for rotating stages that are visible. Strain-gaging methods are limited when considering a many-bladed structure because of the number of strain gages required and the limited number of channels available on slipring devices or telemetry systems.

The instrumentation concept for measuring blade-tip displacements employs optical probes and an array of microcomputers. The concept represents a hitherto unknown instrumentation capability for the acquisition and direct digitization of deflection data concurrently from all of the blade tips of an engine rotor undergoing flutter or forced vibrations. System measurements

are made using optical transducers that are fixed to the case. Measurements made in this way are the equivalent of those obtained by placing three surface-normal-displacement transducers at different positions on each blade of a bladed stage.

The system directly digitizes a time deflection history containing a minimum of 2,048 points for each of the three measurement locations on each blade. For a 64-blade rotor operating at 18,000 rpm, 393,216 data points are taken in a minimum sampling period of 70 ms. Alternate modes of operation can expand the sampling period or acquire additional data from only selected subsets of the blading. Provisions within the design automatically correct the data points for variations in rotor speed, nominal blade-to-blade and instrumentation probe misalignments, and either blade data points that are missed or extraneous blade data generated by foreign objects passing the optical probes.

This work was done by Louis J. Kiraly of Lewis Research Center and John L. Frarey of Mechanical Technology, Inc. Further information may be found in NASA TM-81382 [N80-14113/NSP], "Digital System for Dynamic Turbine Engine Blade Displacement Measurements" [\$7]. A copy may be purchased [prepayment required] from the National Technical Information Service, Springfield, Virginia 22161. LEW-12887

Locking Pull Pin

Redundancy secures this pin against shock and vibration.

NASA's Jet Propulsion Laboratory, Pasadena, California

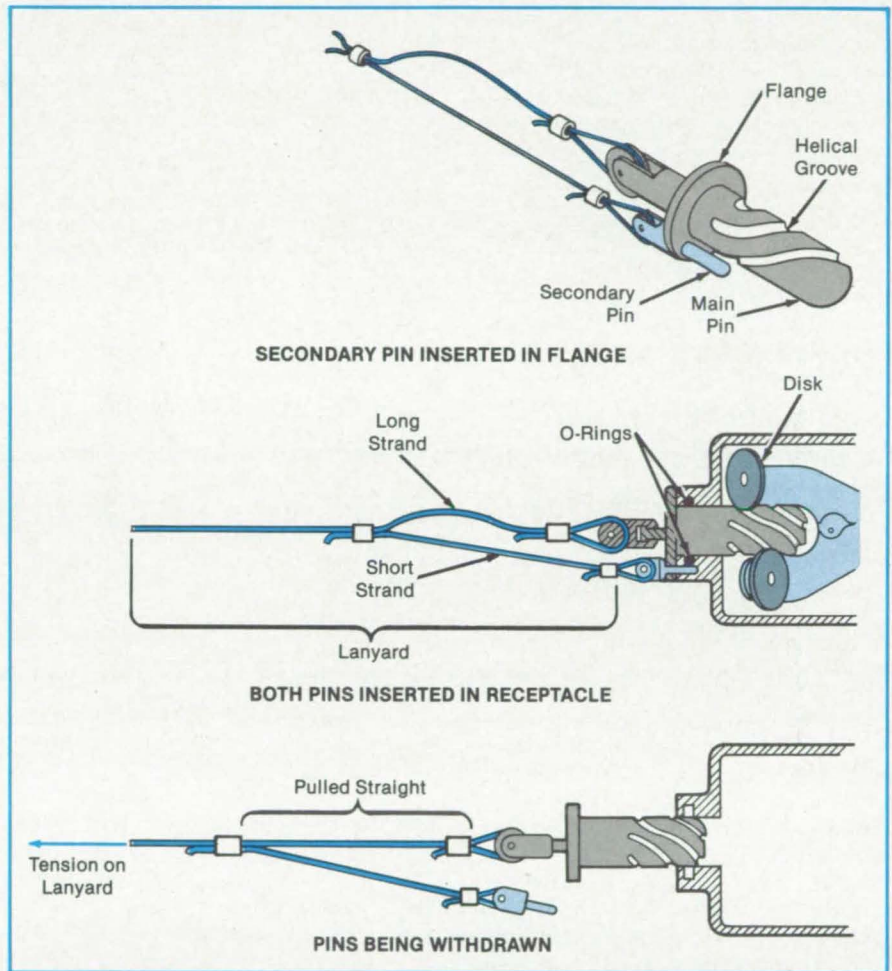
A proposed self-locking pull pin cannot be accidentally released by shock or vibration but can be intentionally released by a pull on a lanyard. Any rotational movement of the main pin traps a secondary pin, which then prevents further rotation and disengagement of the main pin.

The secondary pin is inserted in a flange on the main pin (see figure). The main and secondary pins are inserted in a receptacle in which a pair of rotating disks engage helical grooves on the main pin. An O-ring helps to prevent the pins from rotating by exerting friction. A pull on the main pin can only force it out if the pin could spiral out by rotating between the disks. However, the secondary pin, secure in its own hole in the receptacle, prevents the main pin from rotating. Moreover, the rotational force of the main pin would also act on the secondary pin, pressing it against its wall and locking it even more securely in its hole.

A lanyard with end strands of different lengths can be used to extract the pull pin. A pull on the lanyard would first apply tension to the shorter strand, which is attached to the secondary pin. The tension would pull the secondary pin out of its hole. The tension would then shift to the longer strand attached to the main pin. Without the secondary pin to restrain it, the main pin would rotate and withdraw from the receptacle.

This work was done by Thomas O. Killgrove of Caltech for NASA's Jet Propulsion Laboratory. For further information, Circle 88 on the TSP Request Card.

Inquiries concerning rights for the commercial use of this invention should be addressed to the Patent Counsel, NASA Pasadena Office-JPL [see page 29]. Refer to NPO-16233.



The **Vibration-Resistant Pull Pin** is shown with the secondary pin inserted in the flange of the main pin at the top, fully inserted in its receptacle at the middle, and being withdrawn by the lanyard at the bottom. As long as the secondary pin is in the receptacle, the main pin cannot be extracted.

Distributing Radiant Heat in Insulation Tests

A silicon carbide blanket spreads heat more uniformly over the insulation specimens.

Lyndon B. Johnson Space Center, Houston, Texas

A thermally radiating blanket of stepped thickness distributes heat over an insulation sample during thermal vacuum test. NASA Tech Briefs, Winter 1985

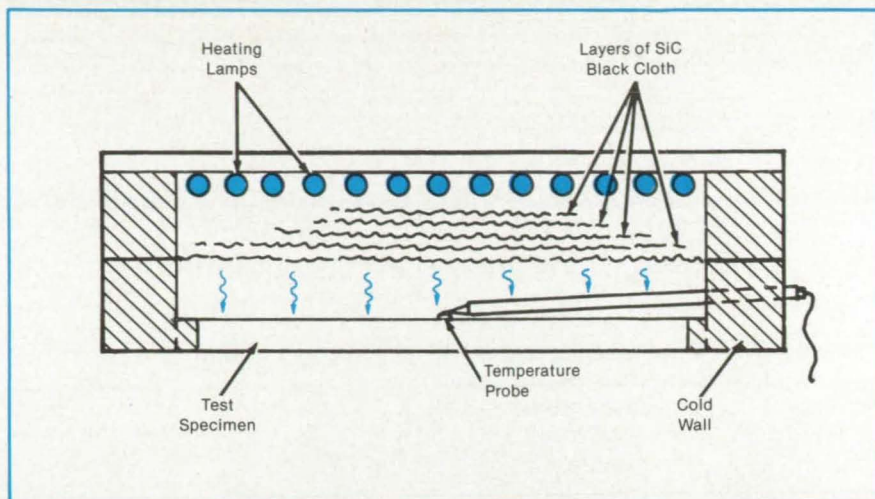
ing. Developed for testing surface-insulation tiles used on the Space Shuttle, the blanket technique reduces the temper-

ature variation over the insulation surface to $\pm 25^\circ\text{F}$ ($\pm 14^\circ\text{C}$). Previously, it varied by as much as $\pm 100^\circ\text{F}$ ($\pm 56^\circ\text{C}$).

The blanket is placed in a test chamber between quartz heating lamps and the insulation specimen (see figure) to serve as a secondary, heat-distributing radiator. The blanket is built up from layers of silicon carbide cloth. The loose weave of a single layer passes 30 to 35 percent of the incident thermal radiation.

The layers are stacked in order of diminishing area, with the greatest thickness at the center. This thickness profile delays the heating of the middle but allows heat to be radiated quickly to the periphery of the specimen, which is ordinarily hard to heat because of the cold chamber wall and unevenness of the lamp reflectors.

The blanket allows one to use the entire chamber area. It smooths out the temperature gradients that would otherwise be caused by uneven reflector or sample surfaces, or by the differing emissivities. Since edge effects are reduced, the area of the insulation specimen can be as large as the lamp array. A temperature probe is positioned at the center of the specimen. When the probe calls for more heat, more heat is



Woven of Silicon Carbide Fibers, a blanket spreads heat from quartz lamps evenly over the insulation sample. Because of fewer blanket layers toward the periphery of the sample, more heat initially penetrates there for a more uniform heat distribution.

initially applied at the periphery to keep it at about the same temperature as that of the center.

This work was done by Heinz J. Freitag,

Amador R. Reyes, and Mark C. Ammerman of Rockwell International Corp. for Johnson Space Center. No further documentation is available. MSC-20878

Smoothed Two-Dimensional Edges for Laminar Flow

A passive method is proposed for installing leading-edge devices on natural-laminar-flow wings.

Langley Research Center, Hampton, Virginia

A new concept allows a passive method for installing flaps, slats, ice-protection equipment, and other leading-edge devices on natural-laminar-flow (NLF) wings without causing a loss of laminar flow. Two-dimensional roughness elements in laminar boundary layers are strategically shaped to increase the critical (allowable) height of the roughness. This would facilitate the installation of the leading-edge devices by practical manufacturing methods.

Modern airframe construction methods involving bonded or milled aluminum skins or composite skins are sufficiently free from roughness or waviness for successful use of NLF for drag reduction. However, currently accepted NLF wing-design practices exclude the installation of leading-edge devices to preserve the smoothness of the leading edge so that laminar flow can be maintained. On modern production airplane wings, an orthogonal step (forward or aft facing) or a gap typically results at the joint between the main skin panels and the leading edge. These steps or gaps typically are sufficiently large to cause the transition of the laminar boundary layer to a turbulent boundary layer at the protuber-

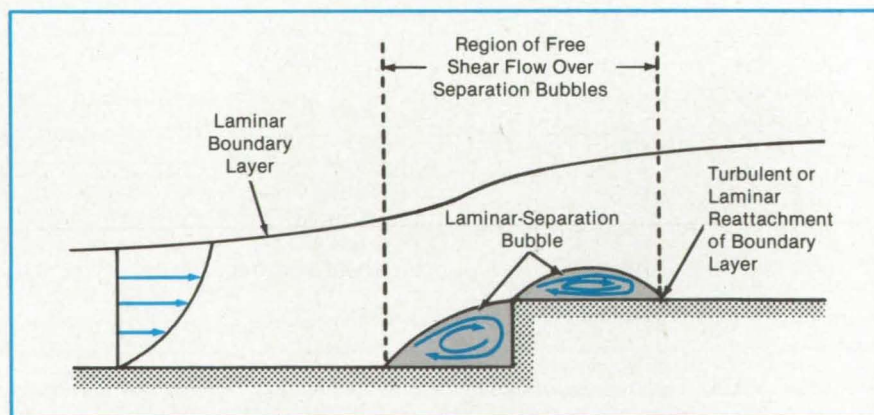


Figure 1. Laminar Separation Bubbles caused by a conventional two-dimensional roughness element step force the boundary layer off the surface, which can result in transition to a turbulent boundary layer.

ance, greatly increasing the wing drag.

The principal manufacturing challenge is to produce wings with skin joints that meet the allowable step- or gap-size requirements for laminar flow. These joints must be designed with margins that allow for dimensional stability of the structure over the life of the aircraft. This new concept permits much larger, specially shaped

forward-facing steps and gaps in laminar flow and thus significantly alleviates the disparity between modern airframe production tolerances and the maximum size for steps and gaps in laminar boundary layers that are allowable without causing transition.

A step with orthogonal, sharp edges can cause transition by generating laminar

separation bubbles as shown in Figure 1. These bubbles force the boundary layer off the surface, forming a free shear layer in which inflectional instabilities can cause rapid transition to a turbulent boundary layer. Similarly, gaps in the surface can cause transition across the laminar separation region within the gap. By proper shaping of the forward-facing step or gap, it is possible to modify the geometry of the resulting laminar separation regions.

As shown in Figure 2, it may be possible to modify or entirely eliminate the secondary separation region, greatly reducing the inflectional instability disturbances in the boundary layer and thus allowing a larger step height (h) without causing transition. Flight test results support this relationship between step shape and critical step height in laminar boundary layers. For a simple, rounded, forward-facing step, critical step height increases by more than

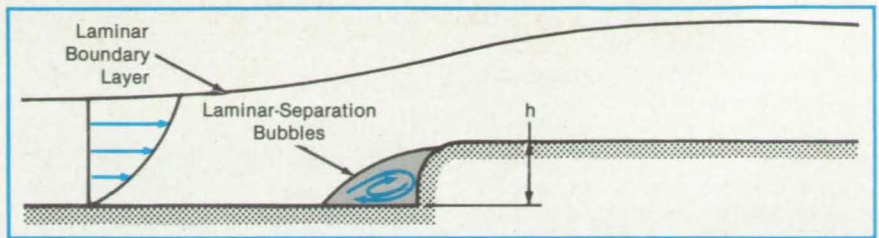


Figure 2. A Shaped, Two-Dimensional Roughness Element can control or eliminate laminar separation regions.

50 percent relative to an orthogonal sharp-edged step.

This work was done by Bruce J. Holmes and Chen-Huei Liu of Langley Research Center; Glenn L. Martin, Christopher S. Domack, and Clifford J. Obara of Kentron International, Inc.; Ahmed Hassan of the Arizona State University; and Max D. Gunzburger and Roy A. Nicolaidis of Carnegie-Mellon University. For further in-

formation, Circle 40 on the TSP Request Card.

This invention is owned by NASA, and a patent application has been filed. Inquiries concerning nonexclusive or exclusive license for its commercial development should be addressed to the Patent Counsel, Langley Research Center [see page 29]. Refer to LAR-13255.

Fuel Gage for Sloshing Tanks

Dynamic measurements of the tank pressure are converted to a readout of the volume of remaining fuel.

Langley Research Center, Hampton, Virginia

A new gage accurately measures the fuel remaining in a moving, or sloshing, tank. It measures the tank air (or other gas) pressure and the time required for the pressure to change from one preselected level to another. This time measurement is directly proportional to the volume of air. A data processor computes the relative volumes of air and fuel in the tank.

Conventional gages measure the level of the surface of the fuel at one or more locations in the tank. However, variations in fuel level due to sloshing and to changes in attitude and acceleration of the vehicle, especially in the shallow fuel tanks in airplane wings, lead to hazardous errors in the indication of the quantity of fuel remaining.

The new gage controls the flow of air (or other gas) into and out of the space above the fuel in the tank and measures the pressure in the tank. The gage has the capability to reverse the direction of flow at selected pressure levels. A timer and data processing device measures the time interval required for the pressure in the tank to change between two preselected levels. The volume of fuel remaining in the tank is computed by the data processor from the value of this time interval.

Figure 1 shows a laboratory model of a gage. Details of the timer/data processor are shown in Figure 2.

The fuel tank is supplied with air from a NASA Tech Briefs, Winter 1985

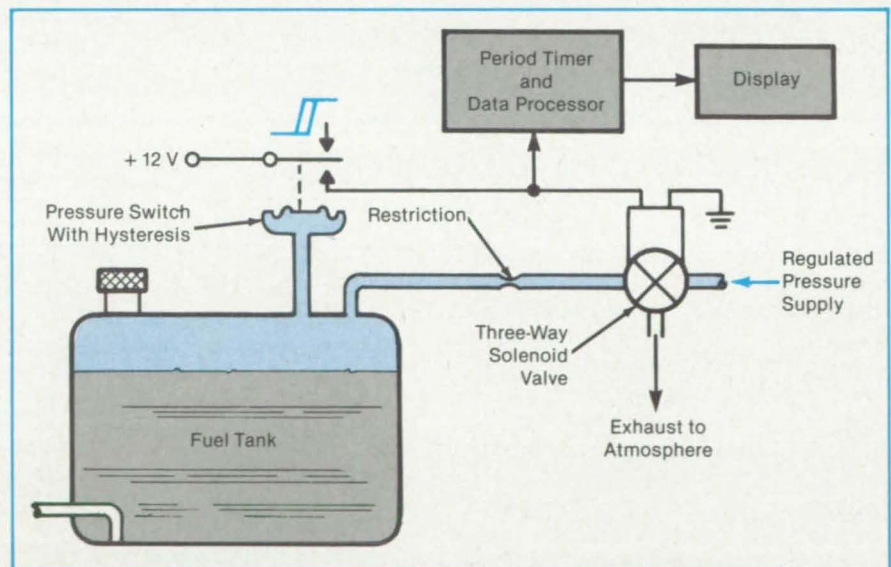


Figure 1. The Volume of Air in the Space Above the Fuel is directly proportional to the time required to change the pressure in the tank between two preselected pressure levels, regardless of the attitude or agitation of the fuel tank.

2-psi ($13.7 \times 10^3 \text{ N/m}^2$) supply. The direction of airflow is controlled by a solenoid valve that, when energized, allows air to flow from the pressure supply to the tank through a restriction. When not energized, the solenoid vents the tank to the atmosphere through the same restriction.

The pressure switch consists of a dia-

phragm, exposed on its lower side to the tank pressure, in contact with a micro-switch. This assembly has mechanical hysteresis, so that the switch snaps over to one contact when the pressure in the tank reaches approximately 0.4 psi ($2.8 \times 10^3 \text{ N/m}^2$) and drops back to the other contact when the pressure is reduced to about 0.2 psi



($1.4 \times 10^3 \text{ N/m}^2$). It is connected to the solenoid valve in such a way that the pressure in the tank is cycled up and down continuously between these two levels.

The timer/data processor is also connected to the contacts of the pressure switch and converts the time required for the tank pressure to rise from 0.2 psi to 0.4 psi into a proportional measure of the volume of air in the tank. This value is subtracted from the known total tank volume to obtain the value of the fuel volume, which is then displayed on the digital indicator.

For example, when used with a 30-gal (114-l) tank, the counter is loaded with the number "30.0" during the time when the tank is vented to the atmosphere. The oscillator is disabled during this time of the cycle. As soon as the pressure switch indicates the low limit of 0.2 psi, the solenoid valve is actuated to increase the tank pressure, and the oscillator is turned on so that the counter starts counting down from 30.0. When the upper pressure limit of 0.4 psi is reached, the solenoid valve cuts off the air pressure supply and vents the tank to the atmosphere. At the same time, the oscillator is again disabled, and the number remaining in the counter is transferred to the internal latch in the digital display assembly where it remains and is displayed until the next cycle is completed. The coun-

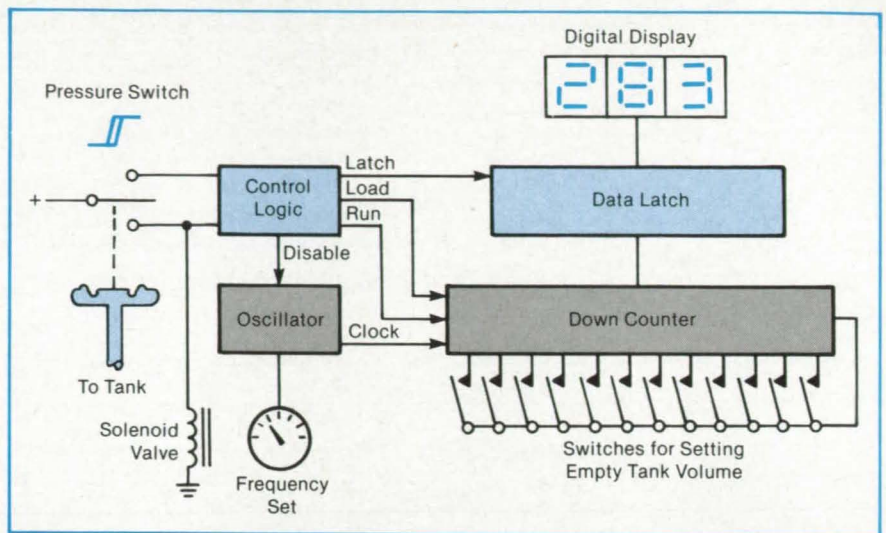


Figure 2. The **Data Processor Computes the Air Volume** and subtracts it from the total fuel tank volume to obtain the volume of fuel.

ter is again loaded with the total volume number, 30.0, and the cycle is repeated.

In this way, the gage produces a count proportional to the volume of air in the tank and simultaneously subtracts it from the total volume of the tank to produce a count proportional to the volume of liquid fuel remaining in the tank. It does this at each charge/discharge cycle and holds the result on a digital display until the next cycle

is complete.

This work was done by H. Douglas Garner and William E. Howell of Langley Research Center. No further documentation is available.

Inquiries concerning rights for the commercial use of this invention should be addressed to the Patent Counsel, Langley Research Center [see page 29]. Refer to LAR-13147.

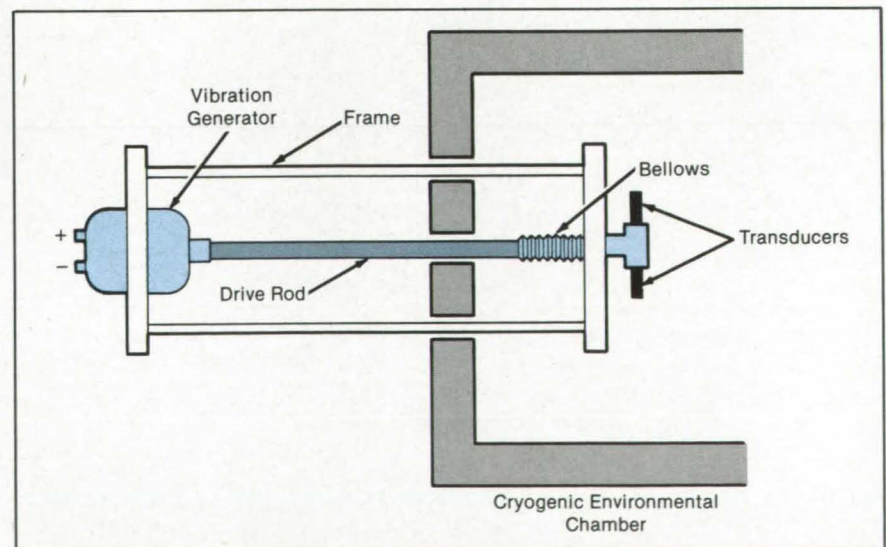
Calibrating Pressure Transducers at Cryogenic Temperatures

A reciprocating bellows generates a sinusoidal pressure wave with a calculable peak-to-peak value.

Langley Research Center, Hampton, Virginia

The development at Langley Research Center of the National Transonic Facility, a cryogenic wind tunnel for high-Reynolds-number aerodynamic research, has introduced several new measurement requirements, one of these being dynamic pressure measurement at cryogenic temperature. Pressure transducers are currently calibrated statically, using a step-function method at both ambient and cryogenic temperatures, and dynamically, using quick-opening-valve/shock-tube techniques at ambient temperatures. Accordingly, a technique and system have been developed for the dynamic calibration of pressure transducers at cryogenic temperatures.

The dynamic calibration system is based on the reciprocation of a sealed metal bellows that produces a sinusoidal pressure with a calculable peak-to-peak value. Given the linear bellows displacement L , the volume V of the transducer-bellows assembly, the bellows cross-



To **Calibrate Transducers** immersed in a cryogenic environment, a sealed reciprocating bellows generates a sinusoidal dynamic pressure. The transducer manifold assembly and bellows are immersed in the cryogenic environment to minimize gradients in the controllable cryogenic temperature.

sectional area A , and the initial internal static pressure P , the peak-to-peak dynamic pressure P_{p-p} can be calculated. Two expressions are used to calculate the value PV according to the ideal-gas law. One accounts for the compression of the bellows and the other for the expansion during its sinusoidal reciprocation:

$$(PV)_c = (P + \Delta P_1)(V - \Delta V_1)$$

$$(PV)_e = (P - \Delta P_2)(V + \Delta V_2)$$

Solving for the changes in pressure due to compression and expansion and then substituting $AL/2$ for the changes in volume due to compression and expansion, the expression for peak-to-peak sinusoidal dynamic pressure becomes:

$$P_{p-p} = 4 PVAL/(4V^2 - A^2L^2)$$

As shown in the figure, the primary element of the calibration system is a reciprocating bellows that develops the time-varying pressure waveform applied to the

transducers. Calibration is performed by comparing the response of the transducers to the time-varying pressure calculated from the measured linear motion of the bellows. The bellows is reciprocated using a small vibration generator mounted outside the cryogenic chamber and linked to the bellows by a steel drive rod. Dynamic pressure is controlled by adjusting the static helium pressure in the bellows and by controlling the amplitude of the vibration. The vibration generator, helium pressure-control valves, and instrumentation are located outside the environmental chamber.

The linear displacement of the bellows is measured using a proximity probe mounted on the drive rod. The transducer outputs are measured and recorded using a digital storage oscilloscope. The temperature inside the chamber is measured using a copper/constantan thermocouple, and the static helium pressure inside the bellows is measured using a digital pres-

sure gage connected to the bellows through a tube.

The system has a dynamic pressure measurement uncertainty of approximately 11 percent and is capable of producing a peak-to-peak dynamic pressure amplitude of 1.4 kPa over a frequency range of 40 to 100 Hz and a temperature range of 100 to 300 K. It provides an unprecedented capability of both static and dynamic calibration of pressure transducers from ambient to cryogenic temperatures.

This work was done by Barry V. Gibbens of Langley Research Center. Further information may be found in NASA TM-85695 [N84-11458/NSP], "A Technique for Dynamically Calibrating Pressure Transducers at Cryogenic Temperatures" [\$7]. A copy may be purchased [prepayment required] from the National Technical Information Service, Springfield, Virginia 22161. LAR-13242

Braille Reading Systems

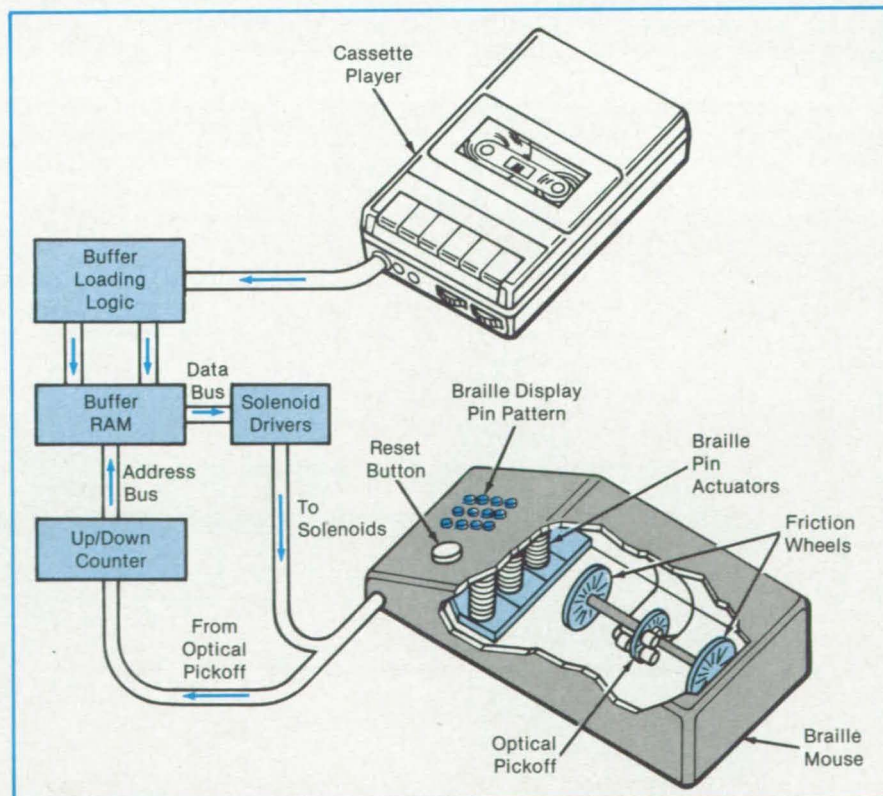
Similar to dot-matrix printers, these two electromechanical concepts would be relatively inexpensive to manufacture.

Langley Research Center, Hampton, Virginia

Two proposed electromechanical systems for making braille characters could be produced relatively inexpensively. Similar in operating principle to dot-matrix printers, the two methods use electronically actuated pins to reproduce characters from information stored on magnetic tape.

In the first method, one or more pins would be scanned over a blank page and energized at intervals to emboss the text on paper, one or more dots at a time. The pins could be driven by solenoids, piezoelectric transducers, or pneumatic actuators. Inexpensive paper could be used for a one-time reading, or more durable material could be used for a permanent record. Low-definition graphics would also be possible. If speed were not important, this printer would be simple and inexpensive to produce.

The text for the printer would be read from a tape in a form that would directly produce the braille characters and would be fed into a RAM buffer one or more pages at a time. The paper would be roller fed using a constant speed motor, and the solenoid-operated embossing pins would be scanned across the page by a lead screw or cable drive operated by the same motor. Optical pickoffs on the two drives would address the buffer to produce the



The Braille "Mouse" could be used to step through the addresses of the RAM using an optical pickoff disk.

embossed dots in the proper sequence to build up the desired characters. The machine could be arranged so that a person could read the text as it emerged from the embosser.

In the second approach, a hand-held device containing one or more character-generator cells would be used by the reader to scan the lines of text manually. This device, which is illustrated in the figure, would be similar to the "mouse" used as a computer input device. It would be swept manually over a flat surface and would scan through the character addresses of the RAM containing the text by means of a wheel running on the flat surface and driving an optical pickoff disk, which consecutively steps through the ad-

resses of the RAM. As the RAM addresses are stepped through, the character contained in each address is presented to the reader's fingers by the character generator in much the same way as if he or she had run the fingers over an embossed series of characters. Several consecutive characters could be presented at one time, using several character-generator cells on the mouse, to speed up the reading process.

A conventional mouse operates in two dimensions using two orthogonally oriented pickoff wheels. It would be easy for the blind reader, using a two-dimensional scan, to run off a "line of print." It may be preferable, however, not to define line length at all, but to simply store the characters in memory in a single line. The mouse

would then be constructed with a single pickoff wheel, oriented for horizontal motion, which would step through the RAM continuously from beginning to end. When the reader reached a convenient point in the text, he or she would simply lift the mouse and return it to the left-hand side of the work area and thus start a new "line." The mouse could also be "backed up" to catch any missed characters.

This work was done by H. Douglas Garner of Langley Research Center. No further documentation is available.

Inquiries concerning rights for the commercial use of this invention should be addressed to the Patent Counsel, Langley Research Center [see page 29]. Refer to LAR-13306.

Hydraulic Cylinder With an Integral Position Indicator

An LVDT is contained within the hydraulic cylinder.

Langley Research Center, Hampton, Virginia

A linear variable differential transformer (LVDT) incorporated within the cylinder of a hydraulic actuator gives a precise readout of the position of the piston relative to the cylinder. The LVDT is contained completely within the actuator. The actuator was originally developed for use in the wind-tunnel model-helicopter suspension system at Langley Research Center. This system requires precise positioning and position readout for computer control of model motions. Minimal space is available for motion cylinders, and precise, continuous position readout (with no steps or pulses) is required. This device provides continuous and accurate position indication of a hy-

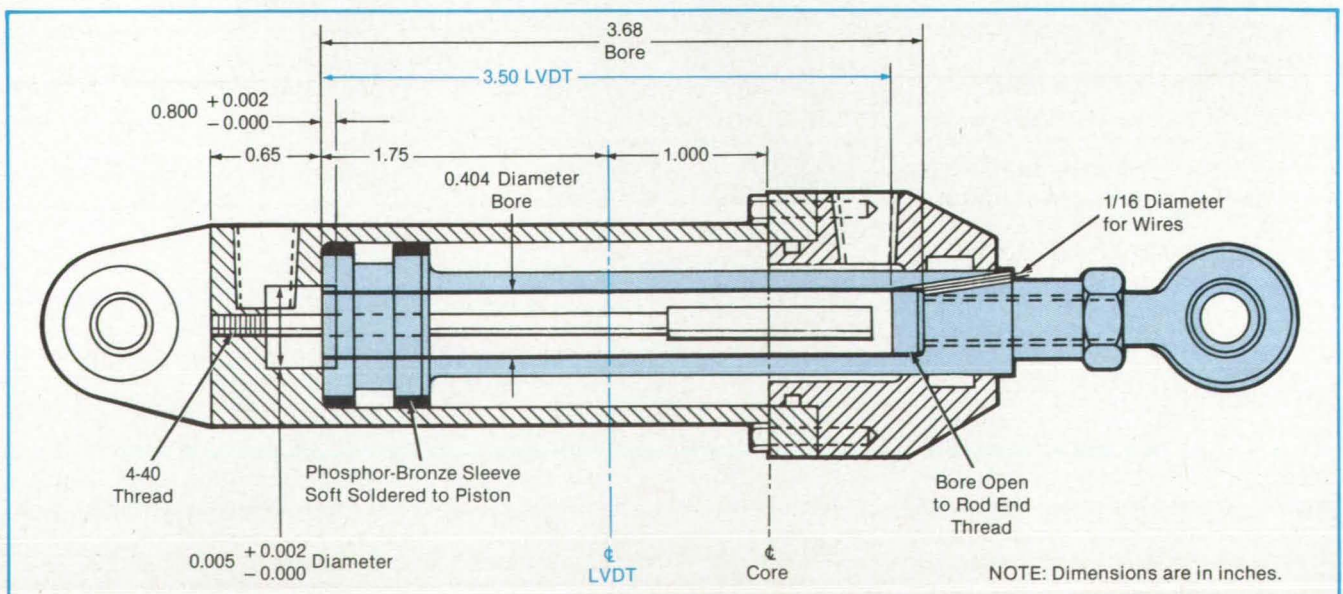
draulic cylinder by means of an integral, coaxially mounted LVDT.

The LVDT (see figure) produces an electrical output proportional to the displacement of its movable iron core relative to its surrounding coils. The core support rod is screwed into the base of the barrel, and the coil portion is welded into the piston rod with the wires exiting beyond the rod seal area.

When the piston of the actuator is extended and retracted, the coils of the LVDT move back and forth over the fixed core, varying the electrical output of the LVDT for a remote readout of the exact distance that the actuator rod is extended.

The LVDT is compact and does not require dynamic seals against hydraulic pressure or any electronics mounted on the actuator. This actuator, as a result, is no larger than it would be without position indication. The LVDT is completely enclosed and protected from abuse, and the continuous position indication provided is the most accurate and repeatable currently available.

This work was done by Garland O. Goodwin of Kentron International, Inc., for Langley Research Center. No further documentation is available.
LAR-13095



This Actuator With a Completely Enclosed LVDT gives a precise readout of the position of the piston relative to the cylinder.

Shaft Axial-Displacement Sensor

A magnetic rotation sensor is modified to detect axial travel.

Marshall Space Flight Center, Alabama

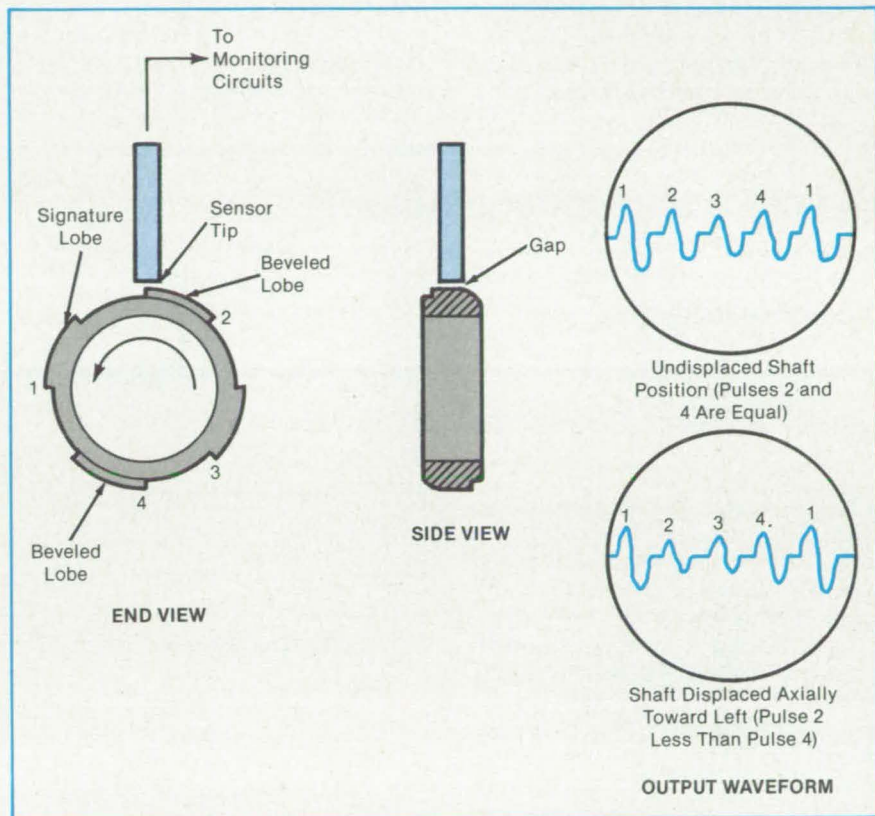
The shaft-speed sensor on a turbopump is readily adapted to indicate shaft axial displacement as well as rotational speed. The adaptation makes it unnecessary to install a separate displacement sensor, which would require an additional access port on the pump. The combined speed/displacement sensor would be used for performance analysis and for pump control.

The modified sensor exploits an effect that is ordinarily considered a less desirable feature of magnetic speed sensors — the decrease in output voltage with increasing sensor gap. The adaptation consists of beveling certain lobes on the shaft-speed encoder nut. For example, lobes 2 and 4 on a four-lobe nut can be beveled, the bevel on lobe 2 being on a side opposite the bevel on lobe 4 (see figure). Axial displacement of the shaft then alters the gap between those lobes and the sensor tip, with a consequent alteration in the output waveform.

In the example of the figure, axial shaft motion to the right makes lobe 2 pass closer to the tip, while lobe 4 passes farther from it. The pulse output at lobe 2 then increases while that of lobe 4 decreases. Conversely, a shaft motion to the left is indicated by an increase in sensor pulse output at lobe 4 and a decreased output at lobe 2.

This work was done by Arthur J. Hill of Rockwell International Corp. for Marshall Space Flight Center. For further information, Circle 46 on the TSP Request Card.

Inquiries concerning rights for the com-



As the **Speed-Encoder Nut Rotates**, its lobes induce a voltage in the speed/displacement sensor tip. Longitudinal movement of the shaft alters the gap between beveled lobes and the pickup and thus alters the waveform produced by those lobes.

mercial use of this invention should be addressed to the Patent Counsel, Marshall

Space Flight Center [see page 29]. Refer to MFS-29048.

Accelerated Stress-Corrosion Testing

A unified approach detects crack initiation and early-stage crack-growth rates.

Langley Research Center, Hampton, Virginia

New test procedures for accelerated stress-corrosion testing of high-strength aluminum alloys are faster and provide more quantitative information than traditional pass/fail tests. Experiments have demonstrated that extremely small amounts of cracklike damage can be readily detected in small specimen cross sec-

tions 0.125 in. (3.18 mm) in diameter. Also, there is an optimum exposure time for accurate results.

The new method uses data from tests on specimen sets that are exposed to a corrosive environment at several levels of applied static tensile stress for selected exposure times and then subsequently ten-

sile tested to failure. The breaking loads are converted to an "apparent" tensile strength for further analysis. Comparing these data with similar data from control specimens, both unexposed and exposed unstressed to the corrosive environment, makes it possible to separate the stress-corrosion cracking response from general

or localized corrosion.

The breaking-strength data with the alloy strength and toughness values are used in a new elastic/plastic fracture-mechanics model to calculate an "effective flaw size." This estimation of the flaw depth and growth rate is used to rate the stress-corrosion-cracking performance of corrosion-resistant alloys. The results are not biased by the material strength and fracture toughness or the test specimen size.

The breaking-strength data are further analyzed by an extreme-value statistical method to get survival probabilities and statistically defined stress-corrosion cracking threshold stresses for the sample

material. These stress-corrosion performance ratings tend to be significantly more discriminating than those obtained from traditional pass/fail analysis of smooth specimen data.

These new test procedures were used to investigate three tempers of 7075 aluminum alloy plate. The predicted combinations of breaking strength and flaw depth agree very well with actual measurements made on tensile specimens 0.125 and 0.225 in. (3.18 and 5.72 mm) in diameter containing "small" flaws introduced by either fatigue or stress-corrosion cracking.

This method is potentially applicable to other degrading phenomena (such as fatigue, corrosion fatigue, fretting, wear, and

creep) that promote the development and growth of cracklike flaws within a material.

This work was done by the Aluminum Company of America for Langley Research Center. Further information may be found in NASA CR-172387 [N85-11218/NSP and N85-11219/NSP], "A Study of Environmental Characterization of Conventional and Advanced Aluminum Alloys for Selection and Design" [Phase 1: Literature Review, \$13; Phase 2: The Breaking Load Test Method, \$25]. Copies may be purchased [prepayment required] from the National Technical Information Service, Springfield, Virginia 22161. LAR-13337

Miniature Microphone Adapter

This probe is insensitive to aeroacoustic disturbances in a high-velocity flow.

Langley Research Center, Hampton, Virginia

Narrow tubes are frequently used to conduct acoustic energy to microphones for noise measurements in small ducts and intricate machinery. Characteristically, these devices lose sensitivity with increased frequency because of the length and diameter of the tube, the acoustic impedance of the microphone cartridge, and the volume between the microphone diaphragm and the tube-terminating volume. Small condenser microphones also have been used for aeroacoustic measurements, but these suffer significant aeroacoustic disturbances because the adapters and preamplifier must be very close to the microphone.

A critical requirement for such a microphone probe tube is that it be small and aerodynamically shaped to minimize aeroacoustic disturbances that distort the measurements. On the other hand, the need for accurate, stable amplitude and phase calibration and uniform sensitivity over the frequency range of interest requires that the sensing element be located very near the probe-sensing ports.

These design requirements are achieved by a new microphone adapter that permits the installation of a commercially available condenser microphone 1/8 inch (3 mm) in diameter at the location of the sensing ports, with a remotely located preamplifier. The microphone has a high-impedance source and a low-level electrical output signal; therefore, the adapter was designed with a minimum capacitance to avoid degradation of microphone sensitivity. The adapter is shown in Figure 1.

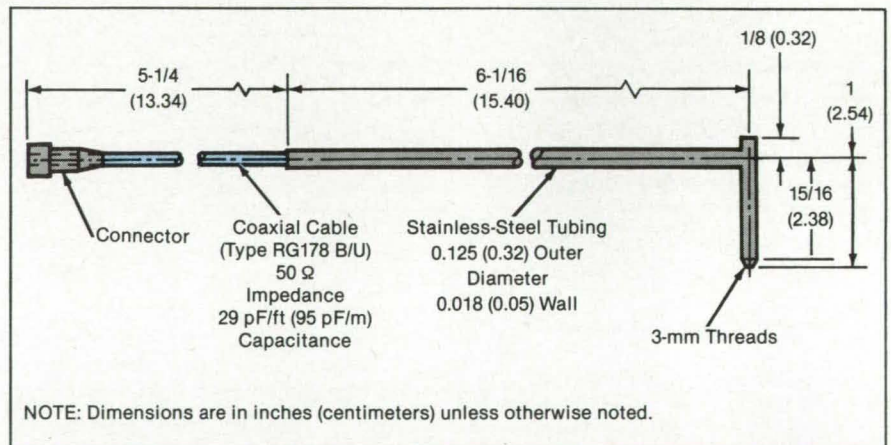


Figure 1. This **Microphone Adapter** permits the installation of a small condenser microphone at a sensing port.

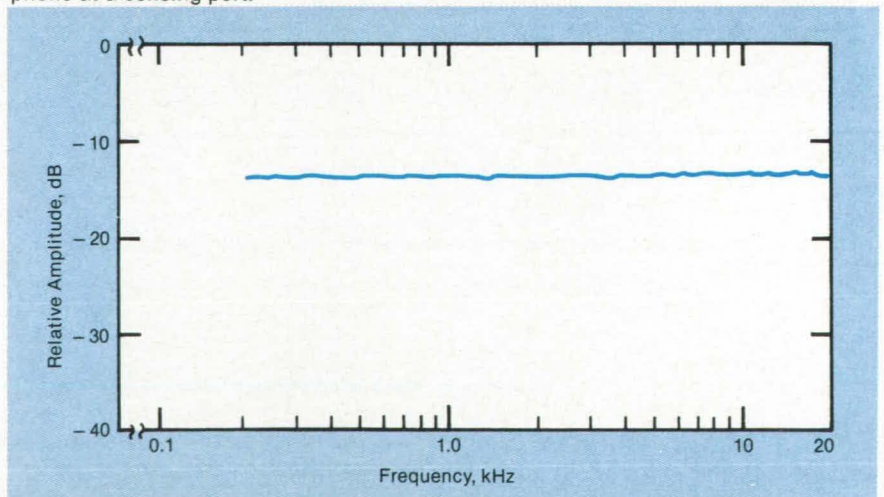


Figure 2. The **Sensitivity Degradation** of the adapter and microphone is compared with the same microphone with a commercially available adapter.

Figure 2 illustrates the sensitivity degradation, 14 dB, of the adapter and microphone compared with the same microphone with a commercially available adapter. The cable length of this configuration can be shortened to improve the sensitivity by about 4 dB, i.e., with a sensitivity degradation of 10 dB.

Although this probe was designed pri-

marily for duct aeroacoustic measurements, it can be used for aeroacoustic measurements in jet flow and for multiple acoustic measurements in a small space where correlation of the measurements is desirable. With state-of-the-art technology, it is feasible to develop a small preamplifier to complement the probe design.

This work was done by James C.

Manning and John W. Simpson of Langley Research Center. To obtain a set of four construction drawings, Circle 57 on the TSP Request Card.

Inquiries concerning rights for the commercial use of this invention should be addressed to the Patent Counsel, Langley Research Center [see page 29]. Refer to LAR-13210.

Electronic/Hydraulic Level Gage

Machine parts or structures are leveled faster than with optical surveying instruments.

Marshall Space Flight Center, Alabama

A system for checking the levelness of machines and structures requires less time and labor than do conventional optical systems. The system measures differences in elevation to within 0.002 in. (0.05 mm).

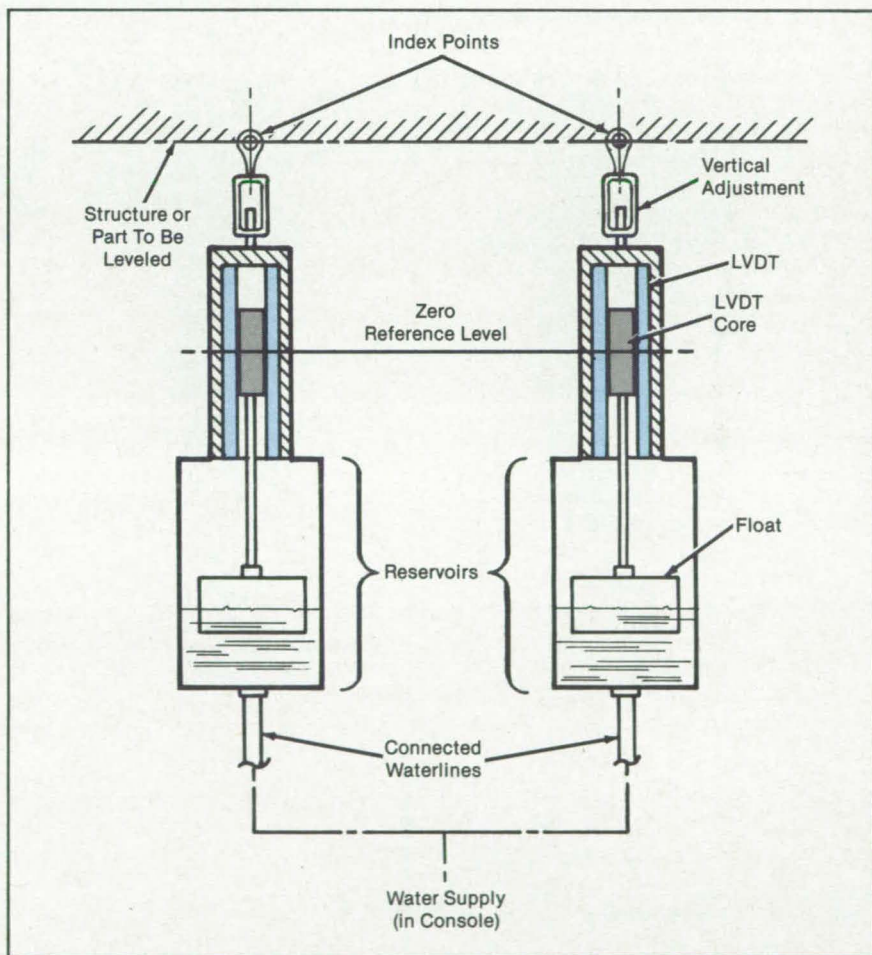
In conventional leveling, a pair of telescopes are alined in the same plane by sighting them on a vertical scale. Operators at both telescopes then sight on the designated index marks on the part to be leveled. They direct another operator at a hoist or other lifting device to raise or lower one end of the part until the index marks are in the plane of the scopes. At this point, the part is known to be level.

With the new system, floats in water reservoirs are suspended at index points on opposite ends of the part to be leveled (see figure). The floats are attached to core rods in the windings of linear variable-differential transformers (LVDT's). The output voltage of each LVDT is proportional to the difference in height between the middle of the core rod and the middle of the winding. Since the reservoirs are connected to the same water supply, the water in them is at the same level. Thus, if the part is out of level — that is, if one end is higher than the other — the voltages of the LVDT's will be different. On the other hand, if the part is level, the voltages will be identical.

The electrical outputs and the water supply are connected to a console. Electronic circuitry in the console converts the LVDT outputs into a level difference and displays the value to the operator on a digital indicator. The console also illuminates lamps that tell the operator in which direction to move the part to restore levelness.

A small pump on the console fills the reservoirs. An automatic shutoff control, actuated by the LVDT outputs, prevents overflow.

The float shape and material proved to be critical for obtaining repeatable measurements. The best results were produced



Floats at Opposite Ends of a Structure determine the positions of cores in linear variable-differential transformers. The outputs of the LVDT's are carried by cables to a control console, where they are displayed to an operator as a difference in core levels and therefore of the ends of the structure.

by a polypropylene cylinder 2¾ in. (69.9 mm) in diameter and 1¾ in. (44.4 mm) high. A clearance of 0.25 in. (6.4 mm) between the floats and the reservoir walls is sufficient to eliminate the effects of friction and suction on the measurements.

This work was done by B. Hanninen and D. Hartley of Martin Marietta Corp. for Marshall Space Flight Center. For further information, Circle 87 on the TSP Request Card. MFS-28066

Advanced Vapor-Supply Manifold

A new four-port valve helps eliminate dead gas volume and contamination.

Langley Research Center, Hampton, Virginia

An advanced vapor-supply manifold solves the problem of manifold purging. The design virtually eliminates dead gas volumes in the manifold system. The system incorporates a special valve into the manifold in such a way that the leaks and contamination problems of previous systems, which use tees and three-port valves, are minimized or eliminated in both the main manifold line and in the supply line.

Figure 1 shows the new valve. The primary difference between this design and that of the three-port valve consists of the addition of the fourth port, marked "A" on the figure. This port virtually eliminates the dead airspace present on the supply side of the three-port valve in the closed position. Thus, a continuous flow of vapor from the supply line through line "A" thoroughly purges contaminants that may initially remain in the valve when it is closed.

In addition, a continuous flow is permitted through the main manifold line whether the valve is in the open or closed position. When the valve is closed, there is no intermixing between the two lines, and virtually no dead airspace exists in the manifold main line or in the supply/purge line. When the valve is open, the two gas flows can intermix. Therefore, this valve constitutes a cross fitting when it is open and two separate lines when it is closed.

Figure 2 shows a system incorporating a gaseous source and the four-port valve as the manifold valve. With the manifold valve closed and the purge valve open, the mass-flow controller is adjusted to the desired flow. The purge valve is then closed and the manifold valve opened to introduce the vapor to the manifold. When the vapor is no longer desired in the manifold, the manifold valve is closed and the purge valve opened to flush out any contaminating vapors that entered the supply line from the manifold.

The manifold is currently being used at Langley Research Center to upgrade a NASA-owned chemical vapor-deposition system. It should be of considerable use in gas manifold systems where even small amounts of gaseous impurities constitute a problem or where more than one gaseous material is used in a single system.

This work was done by Ivan O. Clark, William J. Debnam, Jr., Archibald L. Fripp,

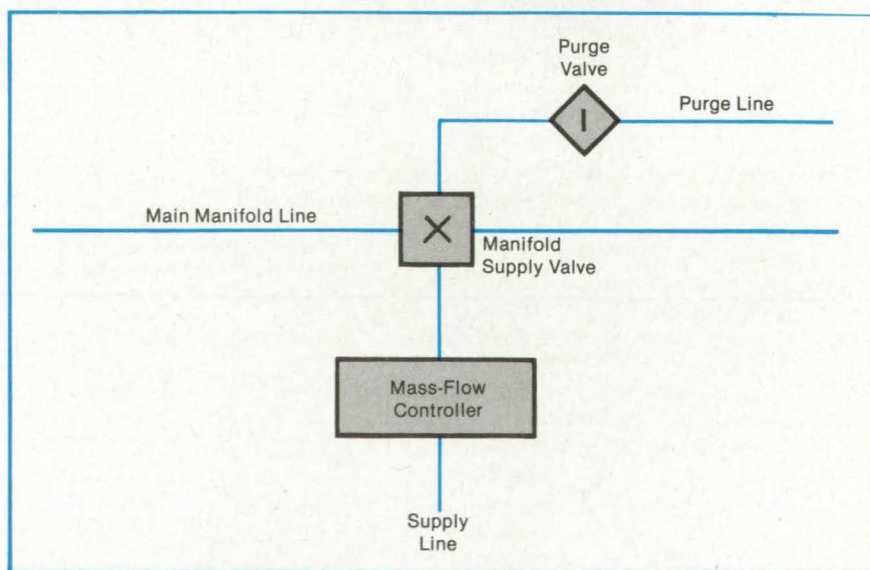
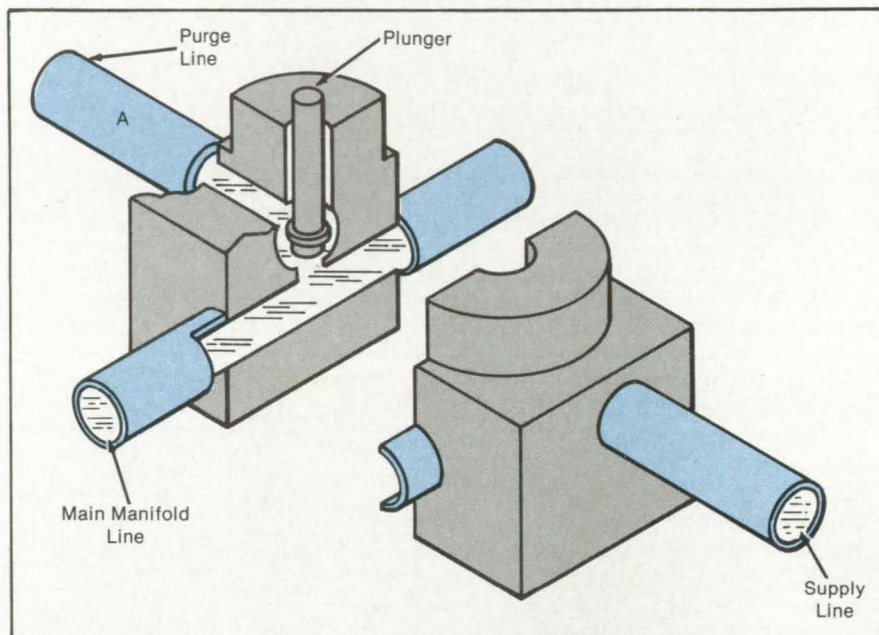


Figure 2. The **Four-Port Manifold Valve and Purge Valve** are used to flush out contaminating vapors.

Jr., and Roger K. Crouch of **Langley Research Center**. No further documentation is available.

This invention is owned by NASA, and a patent application has been filed. Inquiries concerning nonexclusive or exclusive license for its commercial development

should be addressed to the Patent Counsel, Langley Research Center [see page 29]. Refer to LAR-13259.

Titanium Heat-Pipe Wicks

Titanium offers advantages over aluminum.

Marshall Space Flight Center, Alabama

Sintered titanium offers several advantages over sintered aluminum as a material for heat-pipe wicks. Titanium is both strong and light. Its thermal conductivity is only one-seventh that of aluminum, and it can therefore be used when a high thermal resistance is needed to prevent boiling of the working fluid.

In a study, sintered titanium powder wicks were prepared under a variety of conditions. The wicks were tested to identify those conditions that yield the best

wicking characteristics. The key sintering conditions were titanium particle size, alloy constituents, time, pressure, and temperature. The best wicks were subjected to further measurements of such properties as thermal conductivity, density, pore size, and permeability.

An all-titanium heat pipe was made with the best type of wick. Such characteristics as heat flux, evaporator temperature drop, and life expectancy were measured. Data were gathered for a variety of working

fluids: Acetone, ammonia, water, and chlorofluoromethanes.

This work was done by Robert Shaubach, G. Yale Eastman, and Donald M. Ernst of Thermacore, Inc., for Marshall Space Flight Center. No further documentation is available.

Inquiries concerning rights for the commercial use of this invention should be addressed to the Patent Counsel, Marshall Space Flight Center [see page 29]. Refer to MFS-26016.

Microphone Boom for Aircraft-Engine Monitoring

Accuracy of engine-noise measurements is improved by reducing boundary-layer effects.

Ames Research Center, Moffett Field, California

A microphone for measuring aircraft engine noise is mounted on a lengthwise boom that is supported away from the fuselage and engine (see Figure 1). This configuration minimizes the boundary-layer effects and pressure doubling that would be present if the microphone were mounted in the aircraft fuselage.

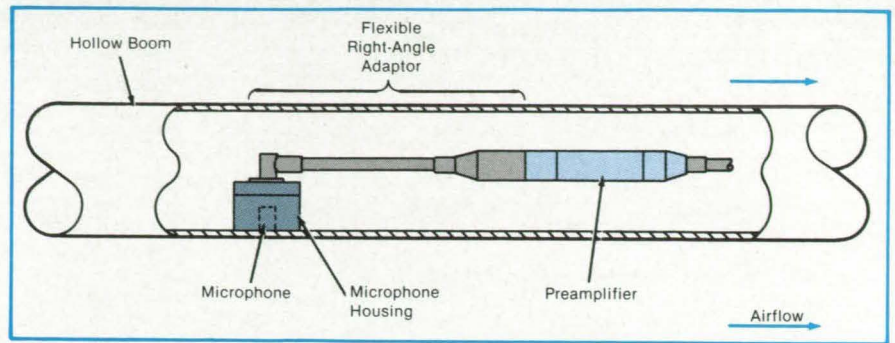
The microphone is mounted inside the boom with the diaphragm flush with the outside edge and facing the noise source parallel to the airflow (see Figure 2). Accelerometers in the boom tip sense vertical and lateral boom vibrations. These measurements are used to correct vibrational errors in the acoustic measurements.

This work was done by R. Cohn, M. Economu, and W. Albrecht of Ames Research Center. No further documentation is available.
ARC-11495



Figure 1. **Measurement Errors** introduced by such boundary-layer flow effects as pressure doubling are avoided by positioning an acoustic sensor at a distance from the aircraft fuselage. This boom-mounting principle can also be adapted to wind-tunnel measurements.

Figure 2. The **Microphone and Preamplifier** are mounted inside the boom, with the diaphragm of the microphone flush with the boom surface.



Thermal-Diode Sandwich Panel

This panel transfers heat in only one direction.

Langley Research Center, Hampton, Virginia

A proposed thermal diode sandwich panel transfers heat in one direction, but when the heat load is reversed, it switches off and acts as a thermal insulator. It has been proposed to control temperature in spacecraft and in supersonic missiles to protect internal electronics. In combination with conventional heat pipes, it can be used in solar panels and other heat-sensitive systems.

The diode sandwich panel (see figure) consists of face sheets lined with wicking material on a honeycomb core that is constructed from wicking material. The lower wick has smaller capillaries than the upper wick to ensure that the capillary force is greater in the direction of the lower wick. The honeycomb wick has pores of the same or larger size than those of the lower wick but has pores smaller than those of the upper wick. The entire sandwich panel is welded shut by sidewalls, hermetically sealing the panel.

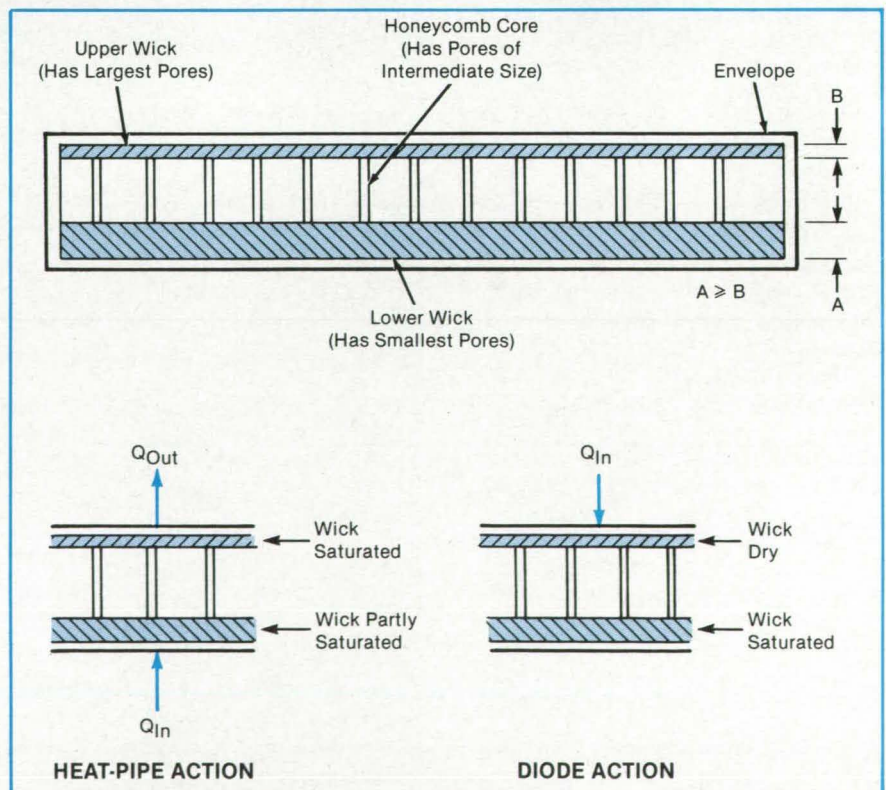
A processing tube is provided for filling the panel with working fluid and for processing. During processing, the panel is filled with working fluid of sufficient quantity to saturate the lower wick only, the upper wick remaining dry. Then, all noncondensable gases are pumped out, leaving the working fluid and its vapor inside the panel. During the processing of heat pipes, noncondensable gases flow to the cold end (condenser) and are pumped out. In a honeycomb sandwich panel, it is very difficult to confine noncondensable gases near the exhaust port to permit their removal. The processing tube, which is lined internally with a wick, is welded onto the sandwich panel. During processing, this tube is cooled, and the entire vapor chamber becomes an evaporator; the processing tube then becomes a condenser and a

trap for noncondensable gases. The trapped noncondensable gas can then be evacuated to complete heat-pipe processing.

When heat is applied to the lower face of the panel, fluid evaporates and condenses at the top. Then the condensate returns to the lower wick by capillary action, producing normal heat-pipe operation. When heat is applied at the top, fluid evaporates and is trapped in the lower wick. Since the capillary forces are greater at the lower wick, fluid remains at the bottom. The upper wick

dries out, and heat-pipe action (heat transfer) stops. Thus the heat-pipe sandwich panel becomes a thermal insulator. The terms "top," "bottom," "upper," and "lower" are used here to simplify the explanation of the panel's performance. This device will operate in zero gravity or any orientation in a 1-g field.

This work was done by Algerd Basiulis of Hughes Aircraft Co. for Langley Research Center. No further documentation is available.
LAR-13121



The **Thermal-Diode Sandwich Panel** acts as a heat-transfer device or as an insulator, depending on the relative heat loads.

Reduction of Vane Noise in Wind-Tunnel Nozzles

Foam-layered vanes reduce low-frequency pulsations and high-frequency noise.

Langley Research Center, Hampton, Virginia

A major aerodynamic problem in the Langley Research Center 4-by-7-Meter (Wind) Tunnel is a very-low-frequency pulsation (1 to 4 Hz) when the tunnel is operated in the open-throat mode. This pulsation not only creates unrealistic flow in the tunnel, but it also induces unsafe resonances in some model/sting systems.

An interim solution to this problem was the installation of staggered triangular vanes around the perimeter of the jet exit nozzle. However, these vanes increased the background noise levels above 5 kHz by 10 to 20 dB.

The vane-induced noise was reduced by adhering a thin layer of porous material such as foam to the downwind surface of the vanes, particularly near the sharp trailing edges, to prevent the occurrence of edge tones (see Figure 1). Other modifications made to aerodynamically streamline the vane structure were rounding the leading edges and smoothly fairing the trailing edges. A boundary layer trip was applied to the leading edge to prevent laminar tone shedding from the trailing edge.

Measurements of background noise in the open test section were made with the modified vane structure and compared to background noise measured with the untreated vanes and the "clear tunnel." Figure 2 shows the measured background noise levels for an inflow location at a tunnel speed of 120 kn (62 m/s). The effect of the treatment is to reduce noise levels by 10 to 20 dB in the higher frequency range. Online observations of the velocity fluctuations with the treated vanes installed confirmed that the pulsation was favorably reduced.

This work was done by Ruth M. Martin and Thomas F. Brooks of Langley Research Center, and Danny R. Hoad of the U.S. Army Structures Laboratory. For further information, Circle 94 on the TSP Request Card. LAR-13333

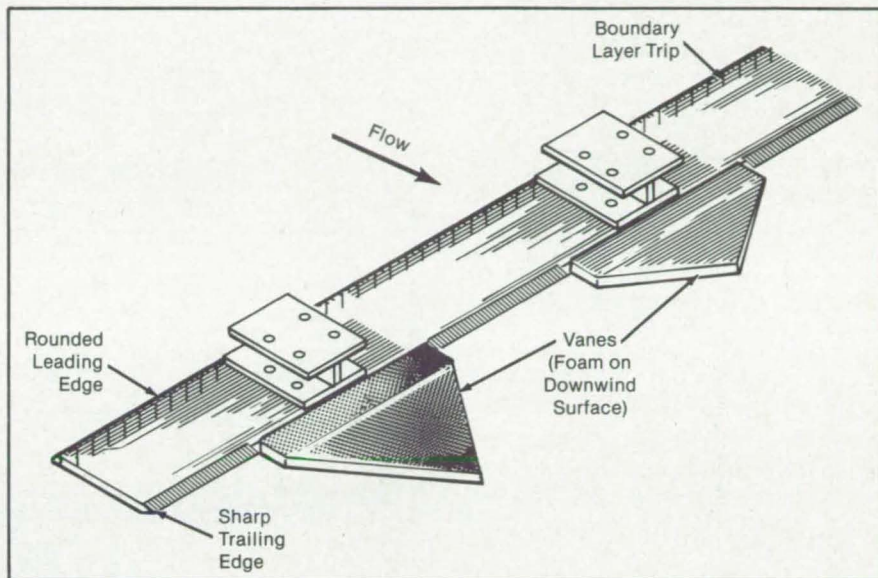


Figure 1. The **Thin Layer of Foam** is attached to the downwind surface of the vanes to prevent edge tones.

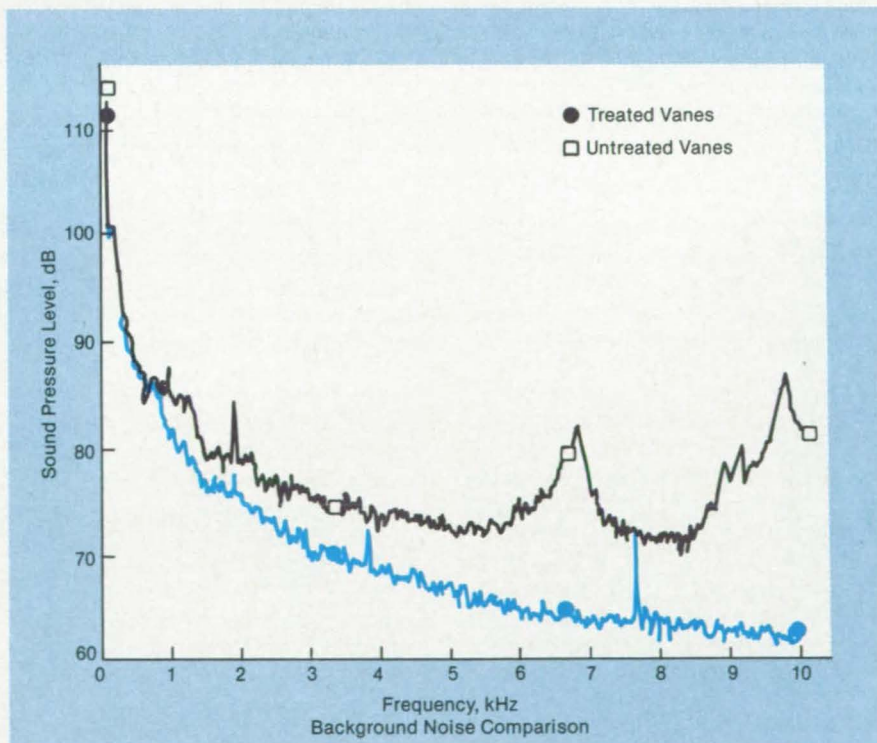


Figure 2. **Foam-Layered Vanes** reduce wind-tunnel background noise at higher frequencies.

Squeeze-Film Damper Controls High Vibrations

Two oil films control bearing load when operating above critical speed with a high imbalance.

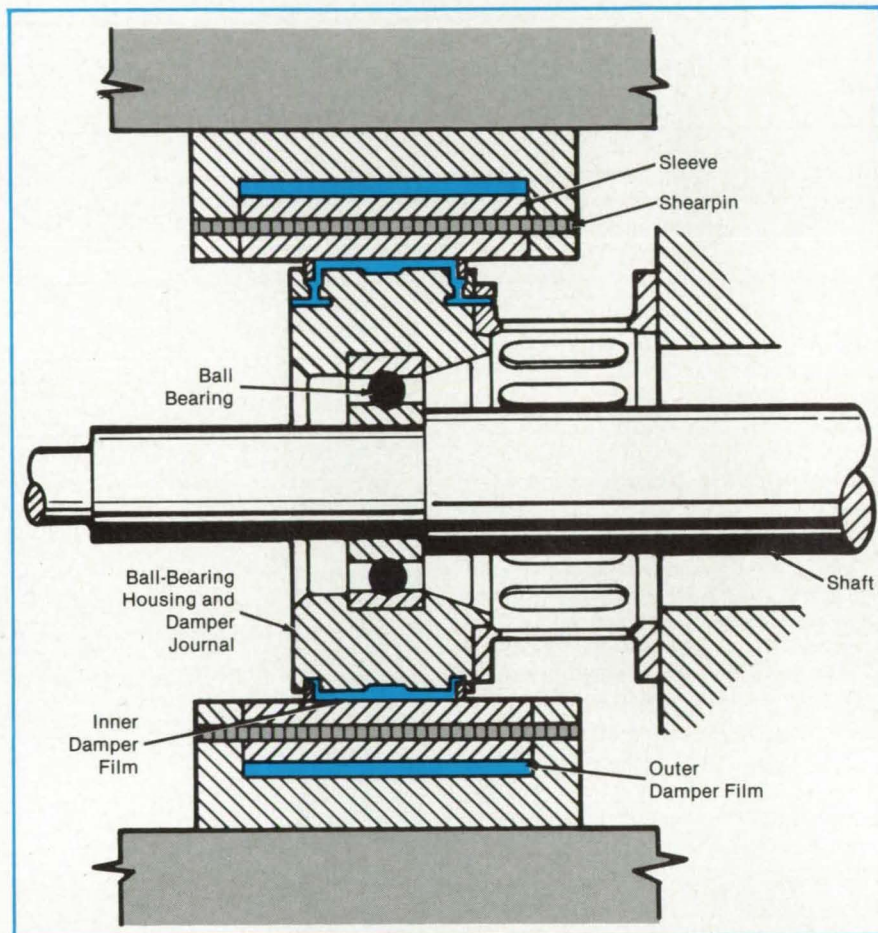
Lewis Research Center, Cleveland, Ohio

A dual-clearance (two oil films) squeeze-film damper has been developed for controlling vibrations in aircraft turbine engines and other rotating machinery. A conventional squeeze-film damper would be overloaded and no longer effective in controlling vibration amplitudes and bearing forces if the shaft imbalance would rise appreciably above the design value of the damper. The new damper under normal conditions uses only one low-clearance film. Under high imbalance, both films are active, controlling shaft vibration in a near-optimum manner and allowing continued operation until a safe shutdown can be made.

As shown in the figure, both squeeze-film dampers operate in series. During normal operation, the sleeve separating the two damper films is fixed in place by two or more shearpins. Only the inner film is active; behavior is then identical to that of the single-film damper. The clearance is only as high as is required for the rotor imbalance likely to occur in normal operation; thus, the rotor radial location can be closely controlled.

In the event of rotor-blade loss or some other occurrence that increases the imbalance, the damper load rises until the strength of the shearpins is exceeded. The pins shear, allowing the sleeve to move, and activate the outer damper film. The two films then operate in series; that is, the bearing load is transmitted first through the inner film, then through the sleeve and outer film to the machine structure. The outer film will generally have a larger clearance than the inner film to accommodate the larger amplitude of motion necessarily accompanying the higher imbalance. The inner and outer dampers will continue to operate together until the imbalance is corrected and new shearpins are installed.

Oil-supply passages are not shown in the figure; however, oil is typically supplied through a feed hole in the outer side of the outer film. The inner damper receives its oil from the outer damper via a feed hole in



The **Inner and Outer Damper Films** operate in series. During normal operation, only the inner film is active. However, during high imbalance, the shearpins break and bring the outer damper film into play.

the sleeve. The outer damper shown is of closed-end design. It was found that a shorter length for the damper would suffice compared to an open-end damper.

The dual-clearance damper was designed to (1) maintain close control of rotor radial location during normal operation; i.e., when the rotor is well balanced; (2) maintain control of vibration amplitude and bearing load during operation above the critical speed with high imbalance; and (3)

allow safe deceleration through the critical speed with high imbalance.

This work was done by David P. Fleming of **Lewis Research Center**. For further information, Circle 61 on the TSP Request Card.

Inquiries concerning rights for the commercial use of this invention should be addressed to the Patent Counsel, Lewis Research Center [see page 29]. Refer to LEW-13506.

Noise-Path Measurements in Aircraft Structures

Portable equipment separates airborne and structure-borne noise in aircraft.

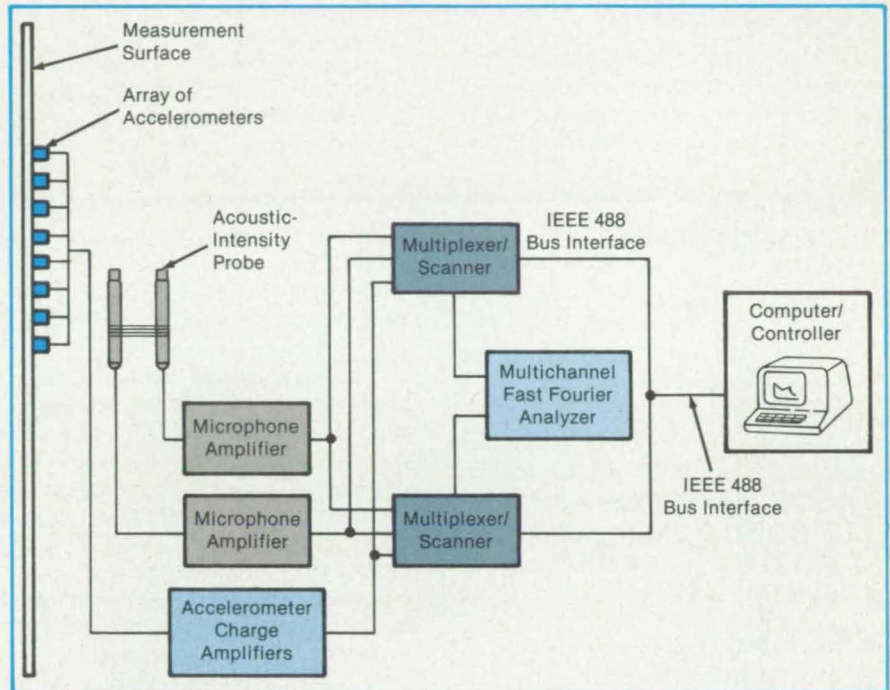
Langley Research Center, Hampton, Virginia

The system illustrated in the figure determines the amount of radiated sound power that can be separately attributed to airborne and structure-borne paths in aircraft. It can also be used to evaluate vibrating plates and thin shells.

The sound transducers include an array of lightweight, miniature piezoelectric accelerometers and a two-microphone probe. A multichannel Fast Fourier Transform (FFT) analyzer/computer is used for analog-to-digital conversion and to analyze the spectrum of each of the input signals. An averager is used to sum and average the spectra produced by the array of accelerometers and the FFT computer. An acoustic-radiation-efficiency computer calculates and stores the radiation efficiency for both purely acoustic excitation of the structure and purely vibrational excitation of the structure. The noise-path-identification computer is used to calculate and display the acoustic sound power caused by the acoustic excitation and the vibrational excitation for a particular combination of simultaneous acoustic and vibrational inputs.

The plate or thin-shell structure is subjected simultaneously to the acoustic and vibrational sources of noise. The acoustic and vibrational inputs may be the result of a single source or of several incoherent or coherent sources. The radiated acoustic power and the space-averaged surface velocity of the plate or thin-shell structure are then measured using the acoustic-intensity probe, accelerometers, and computers.

The radiated acoustic power and the space-averaged surface-velocity data are used in conjunction with acoustic-radiation-efficiency information obtained during calibration to compute the results. The noise-path-identification computer predicts the amounts of the radiated



Noise-Path Identification in Aircraft is performed in flight by this system.

acoustic power attributed to acoustic sources of input or airborne paths and vibrational sources of input or structure-borne paths.

The device operates exclusively in the low frequency regime and is accurate in the frequency regime below the coincidence frequency of the plate or thin-shell structure under investigation. The equipment is compact and portable and can be applied to single or multiple highly coherent sources of excitation. Since the device works on the principles of conservation of energy and superposition of two simple linear solutions, it is applicable to all types of acoustic and vibrational inputs.

This work was done by Michael C. McGary and William H. Mays of Langley Research Center. Further information may be found in NASA TP-2079 [N83-11838/NSP], "A New Measurement Method for Separating Airborne and Structure-borne Noise Radiated by Aircraft-Type Panels" [\$8.50]. A copy may be purchased [prepayment required] from the National Technical Information Service, Springfield, Virginia 22161.

Inquiries concerning rights for the commercial use of this invention should be addressed to the Patent Counsel, Langley Research Center [see page 29]. Refer to LAR-13017.

Books and Reports

These reports, studies, and handbooks are available from NASA as Technical Support Packages (TSP's) when a Request Card number is cited; otherwise they are available from the National Technical Information Service.

Stiffness Study of Wound-Filament Pressure Vessels

Theory and experiments are presented for strong, lightweight composite structures.

A report presents a theoretical and experimental study of the stiffness of lightweight, jointed pressure vessels made of wound graphite fibers and epoxy. These vessels are intended to replace heavier steel cases on the Space Shuttle solid rocket booster engine. The vessel has to be accommodated by existing casting, transportation, and erection facilities, but

no comparable jointed wound-filament pressure vessel has been manufactured to provide the necessary confidence in fabrication procedures and criteria. Equally important, the new case has to comply with the existing structural load limits, but no comparable stiffness and dispersion data were available before the study.

The specimens were fabricated from layers of graphite fibers, wet with epoxy, which were on an aluminum mandrel. The segment ends were thickened with interspersed layers of axially oriented fibers to reduce pinhole bearing stresses and local deformations. The segments were cured at 390° F (199° C).

The report presents the results of vibrational tests of one-quarter-scale models of wound-filament pressure vessels. Each was a segmented case 350 in. (8.89 m)

long with an inside diameter of 36.25 in. (0.92 m). Metal and composite joints simulated those of the full-scale vessel, and the helical filament-wrapping angle was 29°, as in the full-scale vessel. Data are tabulated for specimen thickness, fiber volume fraction, load, and strain. Similar data are presented for preliminary tests on a full-scale component; namely, the aft segment of the motor case.

The report also discusses a mathematical model for the behavior of the graphite/epoxy laminate in the wound structure. The model is intended to predict the responses to loads for all operational conditions, including those during static firing, tilting while on the firing pad, lift-off, ascent, reentry, and splashdown. The report compares the model predictions with the test data and suggests ways of adjusting the model

to bring predictions into agreement with measured values.

This work was done by V. Verderaime of Marshall Space Flight Center. Further information may be found in NASA Technical Paper 2377 [N84-33521/NSP], "Development of In Situ Stiffness Properties for Shuttle Booster Filament Wound Case" [\$10]. A paper copy may be purchased [prepayment required] from the National Technical Information Service, Springfield, Virginia 22161. The report is also available on microfiche at no charge. To obtain a microfiche copy, Circle 100 on the TSP Request Card.

Inquiries concerning rights for the commercial use of the technology described in this report should be addressed to the Patent Counsel, Marshall Space Flight Center [see page 29]. Refer to MFS-27086.

Computer Programs

These programs may be obtained at a very reasonable cost from COSMIC, a facility sponsored by NASA to make raw programs available to the public. For information on program price, size, and availability, circle the reference number on the TSP and COSMIC Request Card in this issue.

Predicting the Performance of an Axial-Flow Compressor

This computer code can be used in the development of multistage axial-flow compressors.

A stage-stacking computer code (STGSTK) has been developed for predicting the off-design performance of multistage axial-flow compressors. The code uses a meanline stage-stacking method. Stage and cumulative compressor performance is calculated from representative meanline velocity diagrams located at rotor inlet and outlet meanline radii.

Numerous options are available within the code: (1) Nondimensional stage characteristics may be input directly or calculated from stage design performance input; (2) stage characteristics may be modified or off-design speed and blade reset; and (3) rotor design deviation angle may be modified for off-design flow, speed, and blade-setting angle.

The axial-flow compressor is widely used in aircraft engines. In addition to its inherent

advantage of high mass flow per frontal area, it can give very good aerodynamic performance. However, good aerodynamic performance over an acceptable range of operating conditions is not easily attained.

Both experimental and analytical programs can be used in the development process for multistage axial-flow compressors. Since compressor experimental development in test facilities is expensive and time consuming, any insight into the onset and location of troublesome flow regimes that can reduce the amount of testing is very valuable. One natural information source is experimental data from similar compressor stages. But such data in sufficient detail are rarely available. New compressors are usually extrapolations from the data of their predecessors.

Analytical methods that contain good flow modeling are an alternative way of gaining the insight needed for compressor development. There are several levels of sophistication for analytical programs; but in general, only the level of sophistication required to evaluate the relevant flow phenomenon is desired in order to minimize complexity and to give high computational efficiency. Compared with other more sophisticated two- and three-dimensional models for compressor flow, the stage-stacking method is very simple. The simplicity of a one-dimensional compressible flow model enables the stage-stacking method to have excellent convergence properties and short computer run time. The simplicity of the model results in manageable computer codes that ease the incorporation of correlations directly linked to experimental test data to directly model real flow phenomena.

The stage-stacking computer code was developed and used at the Lewis Research Center during the past several years. It has been routinely used to generate performance maps for compressors evaluated experimentally. The performance predictions

of the code have agreed with the measured performance. The code either accepts nondimensional stage characteristics as input or calculates these characteristics from aerodynamic input available from compressor design codes.

Many of the code options use correlations that are normally obtained from experimental data. These empirical correlations permit modeling of the trends in stage and overall performance by a simple one-dimensional, stage-stacking technique. However, the correlations may only be accurately applied to predict the performance of compressors similar to those used in deriving the empirical correlations. The code is developed so that users may modify the correlations to suit their needs.

For off-design compressor performance prediction, the main features of the stage-stacking method are simplicity, fast convergence, and the ability to directly incorporate correlations from experimental data to model real flow conditions. The method used has the following properties:

1. It is a one-dimensional, compressible-flow model with fast convergence;
2. Overall stage performance is represented by meanline velocity diagrams at the rotor inlet and outlet;
3. It includes options to calculate the stage characteristics and to adjust them for blade reset and real flow effects;
4. Experimental test data can be applied directly to correlations that model real flow conditions; and
5. Accurate off-design predictions can be made for a limited range of compressors. The computer program is written in FORTRAN IV for use on an IBM 370 computer. For a related computer code see the following article.

This program was written by Ronald J. Steinke of Lewis Research Center. For further information, Circle 103 on the TSP Request Card. LEW-14025

Axial-Flow Compressor Performance With Water Ingestion

Code predicts how water ingestion affects the performance of a jet-engine compressor.

A stage-stacking computer code (WISGSK) has been developed for the prediction of off-design axial-flow compressor performance with water ingestion. The code uses a meanline stage-stacking method; stage and cumulative compressor performance is calculated utilizing representative triangles located at rotor inlet and outlet mean radii.

The aerothermomechanical interactions arising during air/water droplet mixture flow are taken into account in terms of four processes: (1) Changes in blade performance parameters (deviation and efficiency), (2) centrifugal action due to flow rotation, (3) heat and mass transfer processes between the gaseous and liquid phases, and (4) droplet instability and breakup. The last three are introduced at the exit of each blade row. The aerodynamic performance of a stage is based on estimated rules for deviation and efficiency with air/water mixture flow.

Water ingestion into jet engines may arise due to various circumstantial reasons: High humidity in the air resulting in condensation of water at the inlet, tire-generated spray entering the airstream during takeoff and landing on rough runways with puddles of water, and flight through rainstorms. It has been found that such water ingestion can lead to a loss of performance, engine mismatch, loss of surge margin, and, in some cases, undesirable mechanical and aeroelastic effects. Both steady-state and transient performances are affected as well as the operational margins in the control system. With ingestion of large amounts of water, water may flow through the engine at low power settings, and a flameout may occur at higher power settings.

The code provides options for the calculation of performance with mixtures of gases such as air and water vapor and air/water droplet mixtures with different water contents. The code is useful for obtaining preliminary estimates of overall performance of compressors with water ingestion given the design point details corresponding to airflow and the nature of corrections for air/water mixture flow.

Calculations may be performed along any stream tube selected in the compressor with specified (1) mass flow and mixture composition at entry, (2) area change, and (3) work input at appropriate rotor locations. The program is written in FORTRAN IV for

use on an IBM 370 computer. For a related computer code see the preceding article.

This program was written by T. Tsuchiya and S.B. Murthy of Purdue University for Lewis Research Center. For further information, Circle 104 on the TSP Request Card. LEW-14026

Flow Through Gas-Turbine Ducts

It describes ducts with struts, vanes, and 90° bends.

An existing computer program, the Axisymmetric Diffuser Duct code (ADD code), which calculates compressible turbulent swirling flow through axisymmetric ducts, has been modified to permit calculation of flows through small gas-turbine ducts with struts, guide vanes, and large degrees of turning. The code improvements include a new coordinate generator, an endwall loss model, and a generalized geometry capability to describe struts and guide vanes in ducts that turn more than 90 degrees. An improved output format has been developed to provide the solution on any arbitrary plane in the duct.

The ADD code has produced accurate and reliable calculations of flows in gas-turbine engine components. It has been successfully applied to predicting the performance of the subsonic portion of mixed compression inlets and to predicting the pressure recovery of high-mach-number diffusers. Additional applications have been to straight-wall annular diffusers, effects of inlet distortion on diffuser performance, and mixing of two coaxial streams, and further calculations were made for swirling flow in a precombustion diffuser and for an inlet with inlet guide vanes.

Finally, the ADD code has been applied to the solution of flows in small axial-flow turbines and has been modified to treat flows with a small separation bubble, flows with large compressible axisymmetric streamline curvatures, and nonequilibrium turbulent flows that require a two-equation (k, ϵ) turbulence model.

The ADD code can be applied to the solution of flows in annular ducts that have significant radial flow components as found in small gas-turbine engines. An algorithm is used to calculate the coordinate mesh with no restrictions as to flow turning in the axisymmetric plane. It employs a second-order integration formula that exactly integrates the singularities (poles) that occur at each corner of the n -sided polygon used to represent the duct with a Schwartz-Christoffel transformation. This method is used to generate a coordinate mesh that is constructed from the streamlines and potential lines of the plane potential-flow solution.

In the present approach, strut and guide-vane effects appear in the governing turbulent-flow equations as gap-averaged a priori body forces. These body forces are obtained using blade-element theory, which treats the mainstream flow through the cascade as if it were two-dimensional and inviscid. The airfoil section cascade performance is obtained using empirical data.

The present version of the ADD code contains these empirical relations for National Advisory Committee for Aeronautics (NACA) 65 series airfoils and NACA four-digit series airfoils. This procedure using the ADD code produces good predictions of the flow field through a compressor inlet guide vane. In particular, the exit flow angles, the mean streamwise velocities, and the mean crossflow velocities in the endwall boundary layer were shown to be modeled quite well. The loss mechanism, however, accounted only for blade profile loss and endwall friction loss. A simple endwall loss model to account for three-dimensional effects in the blade passage based on the Papailiou correlation has been incorporated into the code.

The calculated flow properties can be presented along the coordinate potential lines or arbitrary output lines. This option is specified by the user and allows the ADD code output to be readily compared to data taken in nonorthogonal coordinates. Computed results compared favorably with experimental results. The program is written in FORTRAN IV for use on an IBM 370/3033 computer.

This program was written by O. L. Anderson, G. B. Hankins, Jr., and D. E. Edwards of United Technologies Corp. for Lewis Research Center. For further information, Circle 36 on the TSP Request Card. LEW-14095

Automated Design Synthesis

It can be used for constrained and unconstrained function minimization.

The Automated Design Synthesis (ADS) program is a general-purpose numerical optimization program containing a wide variety of algorithms. It is assumed that the user prepares an analysis problem capable of computing the objective function and constraints. The program should be able to accept as part of its input the design variable quantities. The optimization process is carried out by ADS coupled with the user's program.

ADS can be used for both constrained and unconstrained function minimization. The solution of the general problem is sep-

arated into three basic levels: Strategy, Optimizer, and One-Dimensional Search. By choosing the Strategy, Optimizer, and One-Dimensional Search, the user is given flexibility in creating an optimization program that works well for a given class of design problems. ADS has already found significant applications in the area of structural synthesis (minimum-weight design).

Strategy options that may be invoked in ADS include:

1. Sequential unconstrained minimization using the exterior-penalty-function method;
2. Sequential unconstrained minimization using the linear, quadratic, or cubic extended interior-penalty-function method;
3. Augmented-Lagrange-multiplier method;
4. Sequential linear programming;
5. Method of centers (method of inscribed hyperspheres); and
6. Sequential quadratic programming.

Optimizer options available include:

1. Fletcher-Reeves algorithm for unconstrained minimization,
2. Davidon-Fletcher-Powell (DFP) or Broydon-Fletcher-Goldfarb-Shanno (BFGS) variable metric method for unconstrained minimization, and
3. Regular or modified Method of Feasible Directions (MFD) for constrained minimization.

One-Dimensional Search options include:

1. Find the minimum of a constrained or unconstrained function using just a Golden Section method or a Golden Section method followed by a polynomial interpolation, and
2. Find the minimum of a constrained or unconstrained function using polynomial interpolation/extrapolation with or without first finding bounds on the solution.

ADS is invoked by a user-supplied driver program. ADS does not call user-supplied subroutines. Instead, it returns control to the calling program when function or gradient information is needed. This provides considerable flexibility in program organization and restart capabilities.

ADS can be used in four principal modes:

1. Default control parameters and finite-difference gradients,
2. Override default parameters and finite-difference gradients,
3. Default parameters and user-supplied gradients, and
4. Override default parameters and user-supplied gradients.

The first mode is the simplest "black-box" approach. The second mode allows the user to "fine tune" the program for efficiency. The third and fourth modes permit analytic gradients to be supplied, when known, for considerable efficiency improvements.

ADS is written in FORTRAN 77 for inter-

active or batch execution and has been implemented on a CDC CYBER 170-series computer with a central-memory requirement of approximately 150K (octal) of 60-bit words. The ADS program was developed in 1984.

This program was written by Garret N. Vanderplaats of the Naval Postgraduate School for Langley Research Center. For further information, Circle 54 on the TSP Request Card.
LAR-13341

Radiation View-Factor Program With Interactive Graphics

Six programs help analyze radiation flux.

VIEW is six computer programs for determining view factors, graphically displaying surfaces, and evaluating the solar irradiation of an assemblage of surfaces. These programs offer the thermal engineer a powerful system for view-factor determination.

For spacecraft, space structures, solar receivers, industrial furnaces, and other design situations, radiation is the dominant heat-transfer mechanism. Accurate determination of the radiant flux is necessary for engineering analyses. The central program of this system (VIEWC) computes the longwave radiant-energy exchange factors between the surfaces that make up an enclosure. Other VIEW programs support the user working with VIEWC.

VIEWC computes the view factors between surfaces. These views may be obstructed either by other surfaces or by the surfaces for which the view factors are being computed. The view factors are generally computed by the contour-integration technique originally developed by Mittal and Stevenson. When there is the possibility that the radiation between any two surfaces is obstructed, their view factor is usually calculated by a double-area-integral technique because of the difficulties in defining the contour.

Structures are defined to VIEWC in terms of a collection of flat surfaces, each of which has three or four edges (i.e., a triangle or a quadrilateral). There are several ways to enter the data for VIEWC. One way is compatible with the usual finite-element surface definitions, allowing the use of finite-element mesh generation programs to create input for VIEWC. The VIEWCI program eliminates excess common nodes in free-form data input, thus reducing the amount of storage required.

VIEWI is an interactive graphics program for generating the surface information needed for VIEWC. The surfaces may

be generated singly or in groups, and the user may manipulate them to create the desired structure. VIEWI may also be used to generate finite-element, two-dimensional meshes.

VIEWCM combines the output from two VIEWI sessions to make a composite body. VIEWG provides interactive graphical display of the surfaces generated by VIEWI, with full hidden-line removal and storage of the picture for high-speed processing (e.g., rapid rotation or perspective viewing of the structure).

VIEWWS computes the solar radiation falling on a structure and the solar radiation that is reflected from the Earth (albedo). Input is the same as VIEWC, with additional data on the position of the structure with respect to the Sun and Earth. VIEWWS runs in either batch or interactive mode and computes the solar load as a function of orbital position. Output from VIEWWS includes: Solar view factor, Earth's longwave view factor, reflected solar view factor, and total solar load.

The VIEW programs are written in FORTRAN 77 for batch and interactive execution. They have been implemented on a CDC 6000-series computer with the largest program having a central-memory requirement of approximately 220K (octal) of 60-bit words. The graphics routines are based on the Tektronix PLOT10 system and assume the use of Tektronix 4010 terminals or emulators. Version 5.5 of VIEW was released in 1984.

This program was written by Ashley F. Emery of the University of Washington for Langley Research Center. For further information, Circle 53 on the TSP Request Card.

LAR-13299

Four-Cylinder Stirling Engine Control Simulation

This model includes engine mechanical-drive dynamics and vehicle-load effects.

A four-cylinder, Stirling-engine, transient-engine-simulation computer program has been developed. The program is intended for control analysis. The associated engine model has been simplified to shorten computer calculation time. The model includes engine mechanical-drive dynamics and vehicle-load effects. The computer program also includes subroutines that allow (1) acceleration of the engine by addition of hydrogen to the system and (2) braking of the engine by short circuiting of the working spaces. Subroutines to calculate degraded engine performance (e.g., due to piston-ring and piston-rod leakage) are provided. The program is modular to allow easy modification of individual routines.

Proposed control schemes for four-cylinder Stirling engines require that the working spaces not remain isolated. One such scheme is engine braking by short circuiting. In this case, all four working spaces are connected to high- and low-pressure manifolds. Flow enters or leaves a working space depending on the pressure differential and the orientation of the check valves between the pressure manifolds and the working spaces. A complete four-cylinder model was needed to analyze this control problem.

In the model, four cylinders are interconnected by four working spaces. Each working space contains three volumes — one for the expansion space and the heater, one for the regenerator, and one for the cooler and the compression space. Each volume is assumed to be at constant temperature. Variations in volume temperature can be scheduled as a function of engine speed.

Differential forces on the pistons are translated into torque through the vehicle drive geometry and summed to form total torque. Torque due to engine friction is subtracted to form brake torque. This is available to drive the auxiliaries and the vehicle load. The vehicle inertia and the gear ratio are used to compute the effective load. The summation of torques is integrated to give engine speed and again to give crank angle. The crank angle is used to generate piston position. The model can be run in this manner, or piston position can be inserted as a function of time with torque and cycle performance calculated at constant speed.

The simulation is modular to allow for each modification of the model. An input routine is provided in which the user specifies the transient to be run by setting switches and supplying the proper geometric and engine data. The output is also selected by the user by setting a switch in the input routine. A printout at the desired printout increment can be selected.

The simulation has been run to generate both steady-state and transient results. Power and torque predictions from the simulation compare well with experimental data over a wide range of engine speeds and pressures. The simulation is capable of predicting steady-state performance with piston-ring leakage and short circuiting between the working spaces.

This program is written in FORTRAN IV for use on an IBM 370 computer.

This program was written by Carl J. Daniele and Carl F. Lorenzo of Lewis Research Center. For further information, Circle 56 on the TSP Request Card. LEW-14106

Solution of Radiation and Convection Heat-Transfer Problems

Fin-type conduction problems are solved with radiative or convective boundary conditions.

A computer program P 5399 B has been developed to accommodate a variety of fin-type heat conduction applications involving radiative or convective boundary conditions with additionally imposed local heat flux. The program can also accommodate a significant variety of one-dimensional heat-transfer problems that do not correspond specifically to fin-type applications.

The objective was development of a rapid, efficient, and convenient computer program for solution of radiation fin problems in thermal analysis. Such problems are classified mathematically as double boundary-value problems. They are posed by an ordinary differential equation not amenable to direct closed-form solution. Prior techniques involved laborious effort employing parametric curves or, alternately, detailed numerical modeling for a general-purpose heat transfer computer program. Prior techniques were extremely inefficient, and the parametric approach could not accommodate lengthwise variations in thermophysical properties, environments, or geometry.

The heat-transfer application is represented by a second-order ordinary differential equation and is posed as a two-point boundary value problem. An implicit finite-difference method is used to approximate the differential equation, and the Newton-Raphson method is employed with a tridiagonal linear equation technique to solve the system of implicit difference equations.

The program computes fin-node temperature, while boundary-node temperatures are constrained. The vertical linkages may represent either radiation or convection and could easily be contrived to represent conduction. Moreover, fin nodes may have additional heat flux and need not have vertical linkages. Thus, the program can easily accommodate all but a few specialized one-dimensional heat-transfer analyses as well as many two-dimensional analyses. However, it contains no special provision for computation of boundary-condition heat rates.

Temperature-dependent input data are accommodated by a simple namelist format. Graphical output data are displayed interactively or in batch mode.

The program is written in FORTRAN IV for the CYBER 172 computer. It can achieve an order-of-magnitude reduction

SOLAR DYNAMIC POWER SYSTEM

Small Scale Rankine Cycle Power Generation System is being developed by Centrifugal Piston Expander Inc. to produce electrical power from any heat source, including solar energy, through the use of its Rotary Piston Expander/Engine Prototype (Pat. Pending) which operates with low pressure requirements (as little as 30 psig working gas pressure) without a crankshaft in a rankine cycle system to produce power with instantaneous torque from low to high heat source. Variable displacement capability is available.

Written inquiries invited:

**Centrifugal Piston
Expander Inc.
515 Busby
San Antonio, Texas 78209
(512) 824-3093**

Circle Reader Action No. 417

in CYBER 172 run time when employed as a substitute for current general-purpose heat-transfer programs.

This program was written by R. F. O'Neill of General Dynamics Corp. for Lewis Research Center. For further information, Circle 34 on the TSP Request Card. LEW-13978

Orbit Transfer Programs

Fast, approximate solutions and exact solutions are obtained.

A collection of computer programs have been developed that solve the problem of transfer between noncoplanar circular orbits for spacecraft with chemical propulsion systems. The programs are set up to find Hohmann-type solutions, with burns near the perigee and apogee of the transfer orbit. They are not set up to find bielliptical or other non-Hohmann maneuver types. They will solve transfers with fairly long burn arcs but will not solve continuous-burn, spiral transfers. They will solve "divided-burn" transfers: Transfers in which the perigee (or apogee) burns are divided into repeated smaller perigee (or apogee) burns in order to reduce the average burn arc length and improve transfer fuel efficiency.

The programs model the propulsion system as either constant thrust or constant acceleration. A spherical Earth gravity model is used.

The solutions obtained are optimal with respect to fuel use; that is, the final mass of the spacecraft is maximized with respect to the controls. The controls assumed here are the direction of thrust and the thrust on/off times. The spacecraft continuously varies its orientation during the burns so as to track the optimal thrust direction.

Two basic programs are given. The first, referred to as the "exact solution," gives complete, exact time histories of transfers. The exact spacecraft position, velocity, and optimal thrust direction are given throughout the maneuver as are the optimal thrust switch points, transfer time, and fuel cost.

The exact solution programs are fairly large, iterative programs. Two versions are given: One for noncoplanar (3-D) transfers and a faster version for transfers between coplanar orbits (2-D transfers).

The second, or "approximate solution," program gives approximate information on the transfer time and fuel cost but provides no detail of the trajectory. The approximations are accurate for transfers when burn arcs are relatively small.

The advantages of the approximate solution are that it is a much simpler and faster program and that it has no difficulty converging on a solution. The approximate solution is used to estimate initial conditions for the exact solution. It can be used in divided-burn transfers to find best numbers of burns with respect to time. It is useful by itself in relatively efficient, short burn-arc transfers. The programs are written in FORTRAN IV for use on a DEC computer.

This program was written by J. V. Breakwell of the Stanford University for Lewis Research Center. For further information, Circle 35 on the TSP Request Card. LEW-14089

Bearing Thermal Performance Prediction

Better estimates are obtained when the lubricant density is considered.

A parameter that describes the density of the lubricant/air mixture within a bearing was required as input for computer codes used for thermal analysis and temperature distributions in ball and roller bearings. The parameter is called the lubricant percent volume or cavity factor (XCAV). It is used primarily in the calculation of ball or roller drag and, therefore, significantly affects calculated bearing-heat generation and temperature distribution.

An equation for lubricant percent volume in the bearing cavity XCAV was derived based upon experimental data from three sizes of angular-contact ball bearings run over a range of speeds and lubricant flow rates. Previously, it had been established that values of XCAV in the range from 2 to 5 percent should be used, but little basis existed for selection of the actual value to be used. For more critical high-speed aerospace ball and roller bearing applications where jet lubrication or under-*race* lubrication is used, a more precise estimate of XCAV is required for reasonable thermal-performance predictions.

Bearing-heat generation and temperature distribution were calculated using the computer program SHABERTH, an existing program for analysis of shaft and bearing thermal performance [described in "Thermal Performance of Shaft Bearing Systems" (LEW-12761) on page 269 of *NASA Tech Briefs*, Vol. 3, No. 2]. By comparing predicted and experimental heat generation and temperature, the following equation for XCAV was derived:

$$XCAV = 8.62 \times 10^5 W^{0.37} N^{-1} D_m^{-1.7}$$

either jet or under-*race* lubrication. Using values of XCAV determined with this equation, the thermal performance of thrust-loaded, angular-contact ball bearings can be accurately predicted with the computer program SHABERTH. The new equation accounts for the sensitivity of XCAV to shaft speed, lubricant flow rate, and bearing size, and provides a significant improvement over previous estimation methods. where W is the lubricant flow rate through the bearing cavity, in gal/min; N is the shaft speed, in rpm; and D is the bearing pitch diameter, in in.

The equation was found to be valid for angular-contact ball bearings having bore diameters ranging from 35 to 167 mm, with

This program was written by Richard J. Parker of Lewis Research Center. Further information may be found in NASA TP-2275 [N84-18654/NSP], "Comparison of Predicted and Experimental Thermal Performance of Angular Contact Ball Bearings" [\$7]. A copy may be purchased [prepayment required] from the National Technical Information Service, Springfield, Virginia 22161.

LEW-14163

Three-Dimensional, Subsonic, Turbulent Juncture Region Flow

Finite-element methodology is used in predicting the flow near wing/body, wing/winglet, and pylon/wing junctures.

CMC3DPNS predicts three-dimensional, subsonic, turbulent aerodynamic juncture region flow. This versatile program for comprehensive flow-field analysis applies finite-element methodology to nonlinear field problems.

A prime requirement in computational flow mechanics is flow prediction in juncture regions formed by the intersection of aerodynamic surfaces, such as wing/body, wing/winglet, and pylon/wing. In most instances, the associated flow is three-dimensional, subsonic with variable density, and turbulent. An order-of-magnitude analysis of the subsonic, three-dimensional, steady time-averaged Navier-Stokes equations for semibounded aerodynamic juncture geometries yields the parabolic Navier-Stokes equations. CMC3DPNS solves these equations to predict the juncture-region flow.

In CMC3DPNS, the numerical solution of the pressure Poisson equation, resulting from the parabolic Navier-Stokes equations, is cast into complementary and particular parts, yielding an iterative interaction algorithm with an exterior three-dimensional potential flow solution. A parabolic transverse momentum equation set is constructed, with robust enforcement of first-order continuity effects accomplished by a penalty differential constraint concept within a finite-element solution algorithm. A Reynolds stress constitutive equation, with low-turbulence Reynolds-number wall functions, is employed for closure using parabolic forms of the two-equation, turbulent kinetic energy dissipation.

CMC3DPNS is written in FORTRAN 77 for batch execution and has been implemented on a CDC CYBER 205 computer with a memory requirement of approximately 250K (octal) of 64-bit words. The CMC3DPNS code is not vectorized and should be readily adaptable to the CDC CYBER 70/170-series computers with the FORTRAN V compiler. CMC3DPNS was developed in 1982.

This program was written by A. J. Baker, P. D. Manhardt, and J. A. Orzechowski of Computational Mechanics Consultants, Inc. for Langley Research Center. For further information, Circle 20 on the TSP Request Card. LAR-13263

Zero-Lift Wave Drag of Complex Aircraft Configurations

Total drag and the wave-drag coefficient are calculated.

WAVDRAG calculates the supersonic zero-lift wave drag of complex aircraft configurations. The numerical model of an air-

craft is used throughout the design process from concept to manufacturing. WAVDRAG incorporates extended geometric input capabilities to permit use of a more accurate mathematical model. With WAVDRAG, the engineer defines aircraft components as fusiform or nonfusiform in terms of traditional parallel contours or nonintersecting contours in any direction. In addition, laterally asymmetric configurations can be simulated.

The calculations in WAVDRAG are based on Whitcomb's area-rule computation of equivalent bodies, with modifications for supersonic speed. Instead of using a single equivalent body, WAVDRAG calculates a series of equivalent bodies, one for each roll angle. The total aircraft configuration wave drag is the integrated average of the equivalent-body wave drags through the full roll range of 360 degrees.

WAVDRAG currently accepts up to 30 user-defined components containing a maximum of 50 contours as geometric input. Each contour contains a maximum of 50 points. The mach number, angle of attack, and coordinates of angle-of-attack rotation are also input. The program warns of any fusiform-body line segments having a slope larger than the mach angle.

WAVDRAG calculates total drag and the wave-drag coefficient of the specified aircraft configuration. The equivalent-body areas for each component at the specified roll angles are also available.

WAVDRAG is written in FORTRAN 77 for batch execution and has been implemented on a CDC CYBER 170-series computer with a central-memory requirement of approximately 110K (octal) of 60-bit words. The program was developed in 1983.

This program was written by Charlotte B. Craidon of Langley Research Center. For further information, Circle 13 on the TSP Request Card.
LAR-13223

Keep your working parts in order.



American Heart Association
WERE FIGHTING FOR YOUR LIFE

ENHANCE YOUR PRODUCT RELIABILITY!

Manufacturers nationwide rely on the high quality and timely delivery of Aurora Bearing Company products. Select from a complete family of general purpose, economy, extra strength and heavy-duty rod ends to 2" bore size. Quality 1-piece race, swaged construction, precision ground balls for maximum trouble-free performance. Aurora Bearing, THE MOTION TRANSFER SPECIALISTS, will customize units to your special materials and linkage requirements.

Aurora Bearing is an OEM supplier of rod ends and special linkages to the following industries:

- HEAVY TRUCKING & TRANSPORTATION
- PRINTING EQUIPMENT
- AUTOMATION & PACKAGING MACHINERY
- AIRCRAFT—AEROSPACE
- OFF-HIGHWAY CONSTRUCTION EQUIPMENT
- FARM MACHINERY AND EQUIPMENT
- RACING CARS OF ALL TYPES
- AND MANY MORE...

Let Aurora Bearing apply its manufacturing, application, and design expertise to your needs. Call or write today for technical assistance, price and delivery on your rod end and special linkage applications.



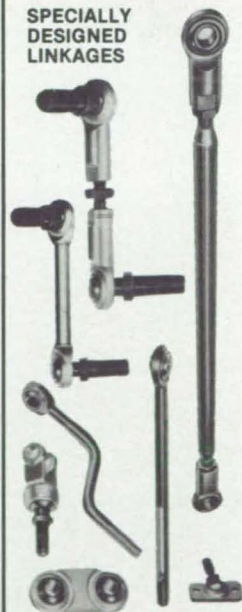
WRITE FOR CURRENT CATALOG

**TELEX: 280079 AUR BRGS
THE MOTION-TRANSFER SPECIALISTS**

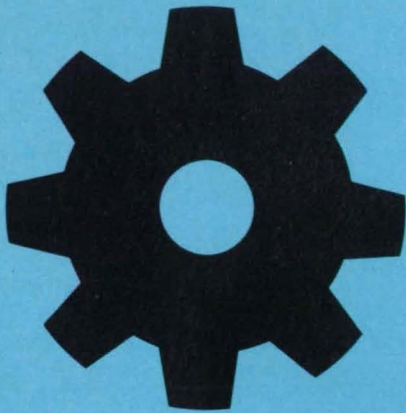
STANDARD ROD ENDS



SPECIALY DESIGNED LINKAGES



AURORA BEARING COMPANY
970 South Lake Street
Aurora, IL 60506 • Phone (312) 859-2030



Hardware, Techniques, and Processes

- 152 Pumped, Two-Phase Heat-Transfer Loop
- 153 Hydrogen Refrigerator Would Cool Below 10 K
- 154 Agglomeration-Free Distributor for Fluidized Beds
- 154 Adjustable-Angle Drill Block
- 155 Rotary Joint for Heat Transfer
- 156 Carbon/Carbon Pistons for Internal Combustion Engines
- 157 Calculating Flow-Angle Deviation in Rotary Pumps
- 157 Rough/Smooth Rotary Seal
- 158 Peristaltic Pump with a Stable Output

Books and Reports

- 159 Systems Engineering of Electric and Hybrid Vehicles
- 160 Vibrational Effects of Turbopump Housing Flexibility

Computer Programs

- 161 Dynamic Effects of Internal Spur-Gear Drives

Pumped, Two-Phase Heat-Transfer Loop

A liquid-and-vapor circulator can either heat or cool.

Lyndon B. Johnson Space Center, Houston, Texas

A proposed two-phase heat-transfer system would deliver coolant to equipment as a liquid and remove it as a vapor. Alternatively, the system could heat equipment by delivering vapor and removing condensed liquid. The two-phase scheme, which was originally proposed for use on the Space Shuttle, is effective for heat transfer over long distances.

When the system operates in the cooling mode, liquid is pumped to plates that absorb the surrounding heat (see figure). The plates contain capillary grooves through which the liquid flows, cooling the plates and the equipment mounted on them. As the liquid absorbs heat from the plates, it evaporates into a vapor line and passes to a condenser. There, the liquid transfers its heat to a radiator and condenses. The condensed liquid is recirculated by the pump.

Liquid flow is controlled by a valve on each plate. The valves may be conventional expansion valves like those in refrigerators. A valve would sense the plate temperature with a sensing bulb. As the bulb temperature increases, its contents would create increasing pressure on a diaphragm in the valve, and the diaphragm would open the valve to admit more liquid to the plate. Alternatively, the liquid flow may be controlled by a valve equipped with an ultrasonic transducer that senses the liquid in the plate.

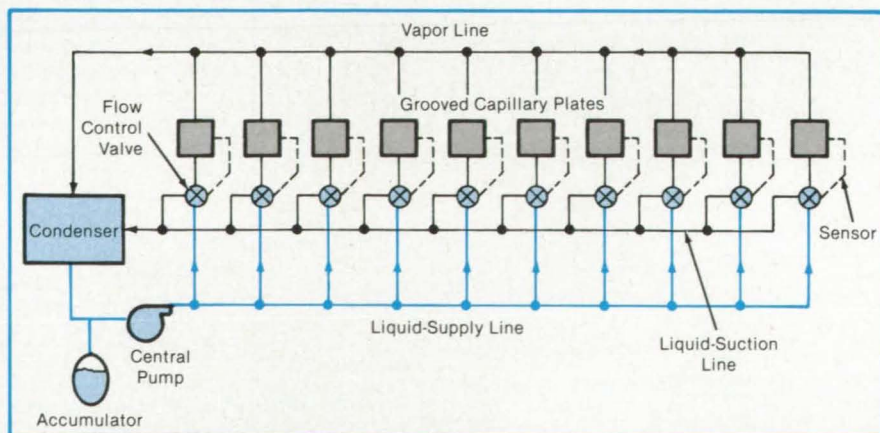
If the system is used to heat the plates, vapor would flow into the plates, where it would release heat of condensation. A control valve would admit the condensed liquid to a liquid-suction line, which would return it to the pump inlet for recirculation.

The two-phase system offers these advantages over a single-phase system.

- The loop would operate at a nearly constant temperature — with a differential of about 5° C instead of the 40° C of single-phase systems. Moreover, all heat-transfer locations would operate at the same temperatures, and equipment could thus be placed on any plate.
- Less pumping would be needed because the extra heat capacity afforded by evaporation and condensation would reduce the required flow rate. Radiator weight would be reduced for the same reason.
- Equipment to be heated could draw waste heat more conveniently from other equipment instead of using electrical heating.
- Parallel branches could readily be added to the loop.

This work was done by Fred Edelstein of Grumman Aerospace Corp. for Johnson Space Center. No further documentation is available.

Inquiries concerning rights for the commercial use of this invention should be addressed to the Patent Counsel, Johnson Space Center [see page 29]. Refer to MSC-20841.



Heat-Transfer Plates can either remove heat from or supply heat to equipment. If the temperature of a plate is high, its valve opens the liquid-supply line to the plate, and cooling results. If the plate temperature is low, the valve opens the liquid-suction line to the plate, and heating ensues.

Hydrogen Refrigerator Would Cool Below 10 K

Concept for cryogenic cooling would use energy from low-grade heat.

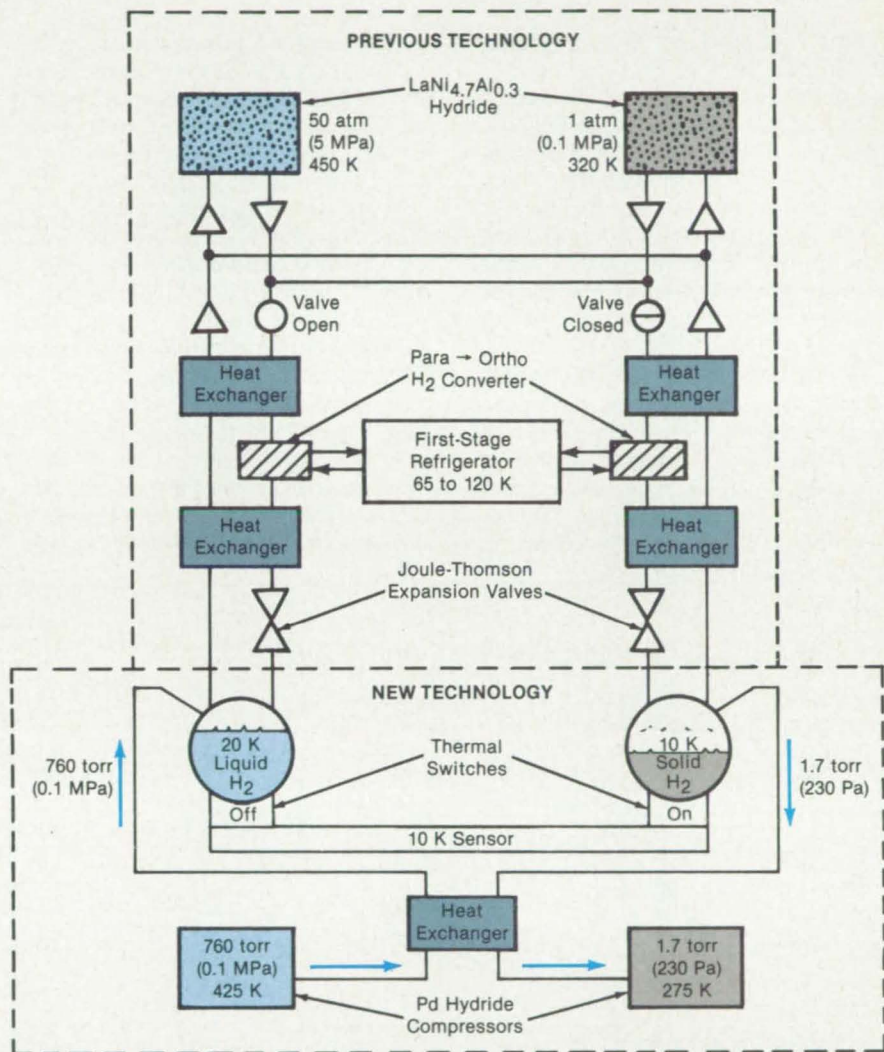
NASA's Jet Propulsion Laboratory, Pasadena, California

A proposed closed-cycle hydrogen refrigerator would use low-level heat energy to cool objects to a temperature of 10 K. The refrigerator would need only a fraction of the energy of previous equipment with similar low-temperature capability. The unit would be compact and light in weight. With valves as the only moving parts, it should be reliable for many years.

The new hydrogen refrigerator concept was developed for cooling sensitive infrared detectors for airborne and aerospace cameras. It overcomes an earlier limitation of hydrogen cryogenic cooling systems in that it can cool below the freezing temperature of hydrogen (13.8 K). It offers advantages over helium-based systems for extremely low temperatures. For example, it can operate on waste or solar heat instead of electrical energy. It is simpler mechanically and less subject to wear. It conserves and recycles its working fluid rather than expending it and thus can function for many years rather than just a few months. Aside from aerospace applications, the hydrogen refrigeration concept might be adapted to cooling superconducting magnets on magnetically levitated railcars, nuclear-particle accelerators, and a variety of other cryogenic equipment.

The refrigerator employs two stages. The first stage, using previously developed technology based on the absorption and release of hydrogen by lanthanum pentanickel, produces liquid hydrogen at a temperature of about 20 K. The liquid hydrogen fills one of two containers in the second stage (see figure). When the container is full, the liquid-hydrogen supply is cut off, and the hydrogen vapor in the container is absorbed in a vessel containing a low-pressure hydride material, such as palladium, which has a high affinity for hydrogen, at a temperature of 275 K. As a result of the absorption, the pressure in the liquid-hydrogen container drops to 1.7 torr (230 N/m²). As the pressure falls, the hydrogen cools and solidifies, stabilizing at about 10 K. The solid hydrogen sublimates at the low container pressure, removing heat from an infrared sensor (or other object) as it does so.

The sublimated gas enters a heat exchanger, where it pre-cools gas that is being returned to an alternate liquid-hydrogen



The Hydride Refrigeration System with few moving parts comprises a 20-K first stage and a below-10-K second stage.

vessel from an alternate palladium absorber that has been heated to 425 K to release the hydrogen. When the solid hydrogen has sublimated completely, the system switches to the alternate liquid-hydrogen vessel, and the alternate palladium absorber is cooled to 275 K to absorb hydrogen. The cycle then repeats. Thermal switches connect first one hydrogen vessel, then the other, to the heat load, depending on which container is sublimating its solid hydrogen content.

The cycle time is fairly lengthy. About

120 g of solid hydrogen, cooling at a rate of 100 mW at 10 K, may require about a week to sublime completely.

This work was done by Jack A. Jones of Caltech for NASA's Jet Propulsion Laboratory. For further information, Circle 4 on the TSP Request Card.

Inquiries concerning rights for the commercial use of this invention should be addressed to the Patent Counsel, NASA Resident Office-JPL [see page 29]. Refer to NPO-16393.

Agglomeration-Free Distributor for Fluidized Beds

Spiral-flow distributor prevents bed particles from gathering on it.

NASA's Jet Propulsion Laboratory, Pasadena, California

A new gas distributor for fluidized beds prevents hot particles from reacting on it and forming a hard crust. In the reduction of iron ore in a fluidized bed, for example, the ore particles do not sinter on the distributor and perhaps clog it or otherwise interfere with gas flow. The new distributor is also relatively cool. Thus, in the fluidized-bed production of silicon, inflowing silane does not decompose until it is within the bed of hot silicon particles and can deposit on them.

Called a "spiral distributor," the new unit consists of overlapping plates, each plate being shaped like a sector of a circle (see figure). The plates are welded together at the center. Gaps between the plates admit flowing gas. The gas swirls into the bed, creating a turbulent zone with a low density

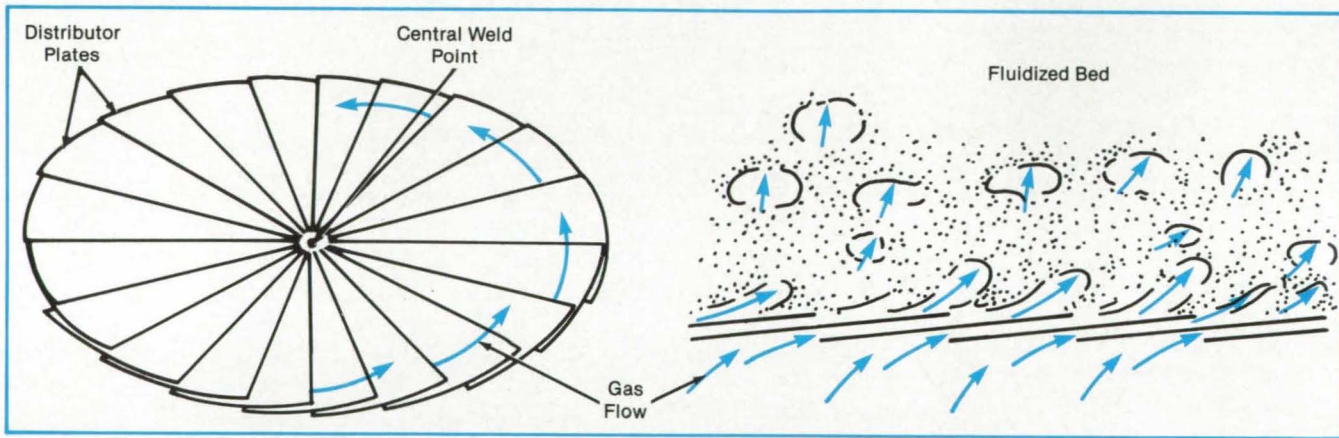
of solid particles immediately above the distributor plate. Above the turbulent zone, the particles form a conventional fluidized bed. The turbulent flow above the spiral distributor keeps the particles moving so that they do not rest on it and adhere.

A working model of the spiral distributor was compared with a conventional distributor made of porous, sintered stainless steel. In the spiral distributor, the number of plates was varied between 24 and 32, and the interplate gap was varied from 0.214 to 0.813 millimeter. For both types of distributor, three types of particles were used to fill the fluidized bed: Sand, silicon, and zirconia.

For the spiral distributor, the pressure drop was always lower than for the conventional distributor, enabling the blower to consume less power. At high gas speeds,

the spiral distributor gives a better quality of fluidization; pressure fluctuations across the bed are low, gas bubbles are small, and contact of the gas with solids is greater. Indeed, for such high-density bed-particle materials as zirconia, the fluidization quality is better for all gas speeds. At low gas speeds, for all types of particles, the transfer of heat from the bed to the spiral distributor is less than to a porous distributor operating at the same gas-feed conditions and bed temperature.

This work was done by Fan OuYang of the Institute of Chemical Metallurgy, Academia Sinica, and Octave Levenspiel of the Oregon State University for NASA's Jet Propulsion Laboratory. For further information, Circle 42 on the TSP Request Card. NPO-16466



The Plates of the Spiral Distributor are arranged to direct the incoming gas into a spiral flow. The turbulence in the flow reduces the frequency of contact between fluidized-bed particles and the distributor. There appears to be no tendency for particles to collect at the central weld point.

Adjustable-Angle Drill Block

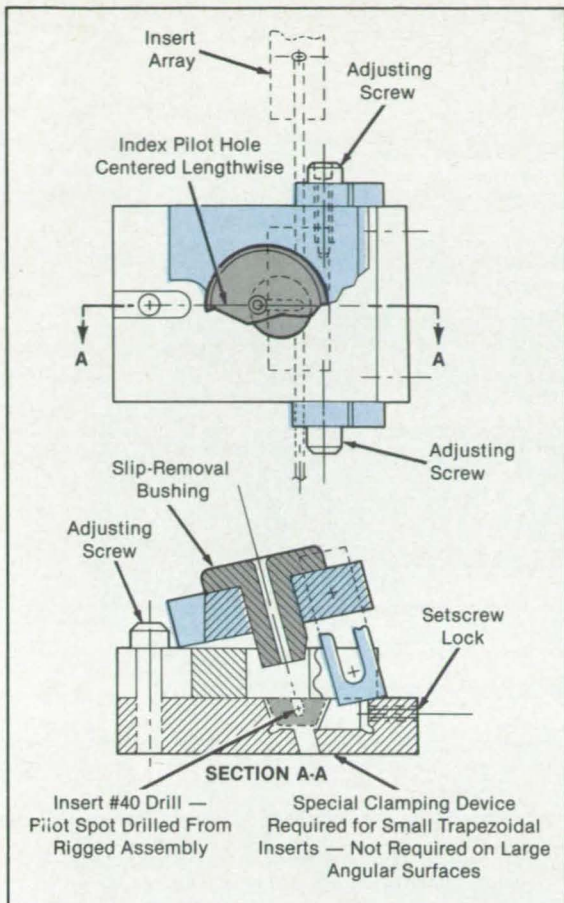
Holes are drilled at a precise angle to the surface of a structure.

Langley Research Center, Hampton, Virginia

The adjustable block illustrated in the figure helps to drill precise holes at an angle to the surface of a structure. It has

been used in fabricating wind-tunnel models, where holes drilled at an angle in one part have to be "transferred" and drilled at

the same angle in a mating part. Improperly aligned parts could fail during wind-tunnel tests, causing expensive damage to the



1. With the assembly in the rigged position, drill a pilot hole (using a #40 drill with a #10 sleeve) in the inserts through jig-bored installation holes in the support structure.
2. Remove the insert arrays. Do not rotate the inserts arrayed on threaded stock. The center distances of threaded holes must be maintained for accurate reinstallation in assemblies.
3. Fit the arrayed insert into the adjustable angle drill block.
4. Center the pilot hole lengthwise. Tighten the setscrew lock.
5. Loosen the adjusting screws.
6. Insert a dowel through the #40 slip-removal bushing and into the pilot hole. Adjust the angle and location of the angle block.
7. Lock the adjusting screws with the dowel in place. Check the alignment. The dowel should slip fit through the pilot hole and bushing.
8. Using a #40 drill, drill through the insert.
9. Using a #25 (0.1495-in.) drill (tap size drill for 10-24 thread) and a # 25 slip-removable bushing, drill through the insert.
10. With a #10 (0.1935-in.) slip-removable bushing and a 10-24 starting tap, tap through the insert.
11. Chamfer and deburr the tapped hole.
12. Repeat the operations for all inserts.

The **Adjustable Angular Drill Block** accurately transfers hole patterns from mating surfaces that are not normal to each other. The drilling procedure is shown at the right.

tunnel and to the model being tested. The hole angle is transferred precisely by using the adjustable-angle drill block. A procedure for drilling holes using the block is given in the figure. The block is applica-

ble to the transfer of nonperpendicular holes in mating contoured assemblies in the aircraft industry. It also is useful in general manufacturing to transfer mating installation holes to irregular and angular

surfaces. *This work was done by Frank H. Gallimore of McDonnell Douglas Corp. for Langley Research Center. No further documentation is available. LAR-13101*

Rotary Joint for Heat Transfer



A mixture of liquid sodium and potassium fills the interface between the rotating and stationary sections.

Marshall Space Flight Center, Alabama

A proposed rotary joint would exchange heat between two heat pipes — one rotating and one stationary. The joint would accommodate varying heat loads with little temperature drop across the interface. Originally proposed to exchange heat between rotating spacecraft sections, the joint would be leakproof and easy to assemble. It would also provide structural support to the heat pipes.

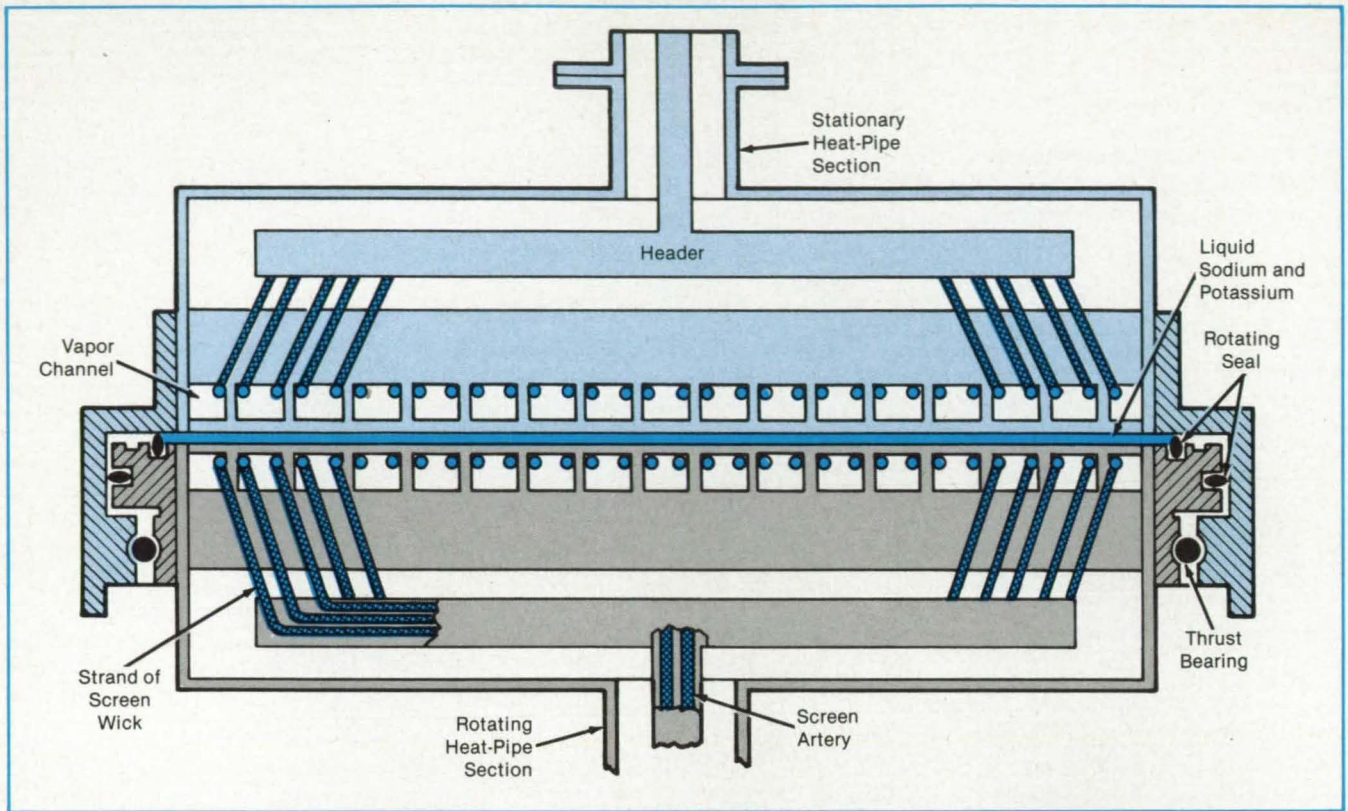
According to the concept, a heat pipe enters the center of the disklike stationary section of the joint (see figure). There, the wicks in the central artery of the heat pipe

separate into multiple strands that lead to concentric channels on the rotary-interface side of the stationary disk. The rotating heat pipe is connected to the rotary section of the joint in the same way. A thrust bearing links the stationary disk to the rotary disk. A mixture of liquid sodium and potassium lies between the two disks and is contained by a rotary seal. Thus, heat from the concentric grooves in one disk flows through the walls of the disk, through the liquid alloy, and into the opposite disk.

The pipes, disks, and wicks would be

made of aluminum, selected for its high thermal conductivity, light weight, and compatibility with the heat-pipe and disk-gap fluids. The pipes, arteries, channels in the disks, and wicks would be lined with sintered powdered aluminum. The wick systems of the stationary and rotating disks are identical, with tunnel arteries fit into the channel corners.

Acetone would be the working fluid in the heat pipes proposed for the original NASA application. It transfers heat effectively in the 0°-to-40° C range of operating temperature. It also has a low vapor pres-



A Thin Layer of Liquid Sodium/Potassium Alloy carries heat from one member of the rotary joint to the other. The liquid conducts heat efficiently while permitting relative motion between the members. Polypropylene rings contain the liquid without interfering with rotation.

sure and thus allows thin-walled parts and, consequently, low temperature drops. Liquid sodium/potassium alloy was selected as the disk-gap medium because it is compatible with aluminum, has high thermal conductivity, and does not evaporate readily at the anticipated operating atmospheric pressure.

Polypropylene is the material of choice for the rotary seal. It is compatible with the liquid alloy and produces little outgassing.

More tests are needed, however, to determine whether a polypropylene seal has adequate life. A lightweight ball-type bearing was designed for the joint; the bearing will probably not require lubrication or, at most, will need molybdenum disulfide dry lubricant.

The disk-on-disk structure offers efficient heat transfer. When operating at 56 percent of capacity, it is expected to transfer 10 kW of heat with an overall temperature

drop of only 5° C.

This work was done by R. Shauback of Thermacore, Inc., for Marshall Space Flight Center. No further documentation is available.

Inquiries concerning rights for the commercial use of this invention should be addressed to the Patent Counsel, Marshall Space Flight Center [see page 29]. Refer to MFS-26015.

Carbon/Carbon Pistons for Internal Combustion Engines

Carbon/carbon material reduces piston weight and eliminates piston rings.

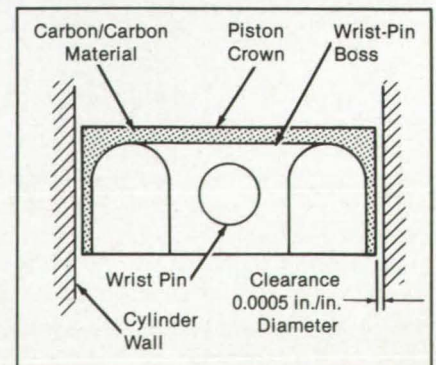
Langley Research Center, Hampton, Virginia

The carbon/carbon piston performs the same function as aluminum pistons in reciprocating internal combustion engines while reducing weight and increasing the mechanical and thermal efficiencies of the engine. The carbon/carbon piston concept (see figure) features a low piston-to-cylinder wall clearance — so low, in fact, that piston rings and skirts are unnecessary. These advantages are made possible by the negligible coefficient of thermal expansion of carbon/carbon [0.3×10^{-6} in./in./° F (0.54×10^{-6} cm/cm/° C)]. Aluminum, in comparison, has a coefficient of thermal ex-

pansion over 40 times that of carbon/carbon.

The carbon/carbon material maintains its strength at elevated temperatures, allowing the piston to operate at higher temperatures and pressures than a comparable metal piston. The high emittance and low thermal conductivity of the carbon/carbon piston will improve the thermal efficiency of the engine because less heat energy is lost to the piston and cooling system. The elimination of rings reduces friction, thus improving mechanical efficiency.

Besides being lighter than an aluminum piston for the same application, the carbon/



A Carbon/Carbon Piston Eliminates Piston Rings and allows a minimal piston skirt length.

carbon piston will produce cascading effects that will reduce the weight of other reciprocating components such as the crankshaft, connecting rods, flywheel, and balances, thus improving specific engine performance. The engine can run at higher speeds than an aluminum piston engine, again improving specific engine performance.

An alternate carbon/carbon piston con-

cept includes the use of a carbon/carbon cylinder wall provided by a carbon/carbon sleeve in a cylinder block of a more conventional material. This modification further increases the specific power and thermal efficiency by lowering heat losses to the coolant.

This work was done by Allan H. Taylor of Langley Research Center. No further

documentation is available.

This invention is owned by NASA, and a patent application has been filed. Inquiries concerning nonexclusive or exclusive license for its commercial development should be addressed to the Patent Counsel, Langley Research Center [see page 29]. Refer to LAR-13150.

Calculating Flow-Angle Deviation in Rotary Pumps

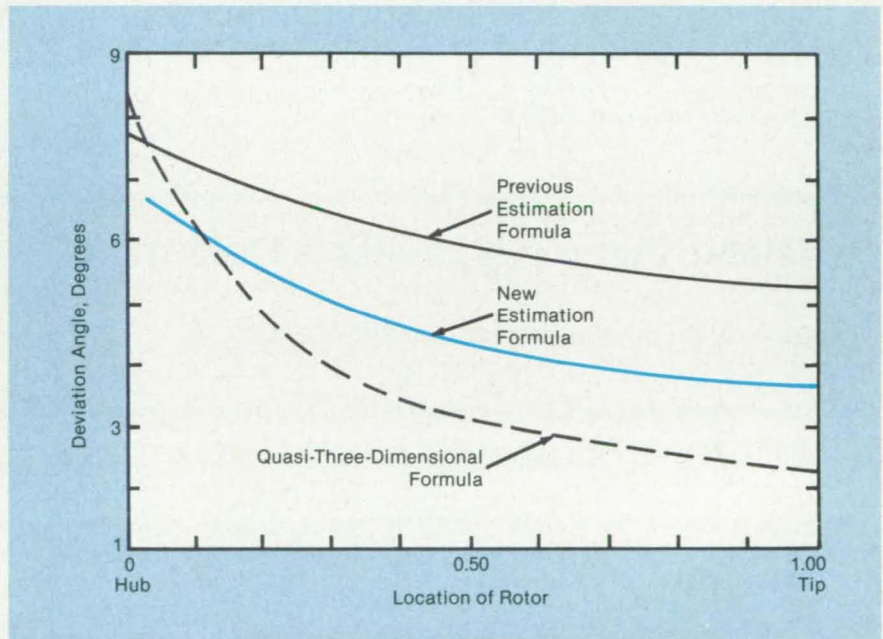
The difference between rotor-blade angle and flow angle is computed.

Marshall Space Flight Center, Alabama

A new mathematical formula calculates the difference between the angle of an impeller blade and the angle of flow. The formula can be used for inducers of mixed-flow pumps. With the formula, calculations can be made more quickly and accurately than with previously available formulas (see figure).

The formula is adapted from a NASA formula for the impeller slip factor. The slip-factor formula is applied locally to an inducer or to a mixed-flow-rotor exit station to derive an equation for the local slip factor. The slip-factor equation is then used to develop an equation for the local rotor-discharge deviation angle. The deviation angle is expressed in closed form as a function of the local discharge blade angle, the rotor axial-length-to-radius ratio, the local flow coefficient, and the local slip coefficient.

This work was done by S. Y. Meng and R. B. Furst of Rockwell International Corp. for Marshall Space Flight Center. For further information, Circle 101 on the TSP Request Card. MFS-29062



The **Deviation Angle Estimated by the New Formula** is closer to that predicted by a quasi-three-dimensional solution than the angle calculated from a previously used estimation formula.

Rough/Smooth Rotary Seal

Contrasting mating surfaces increase strength and decrease leakage.

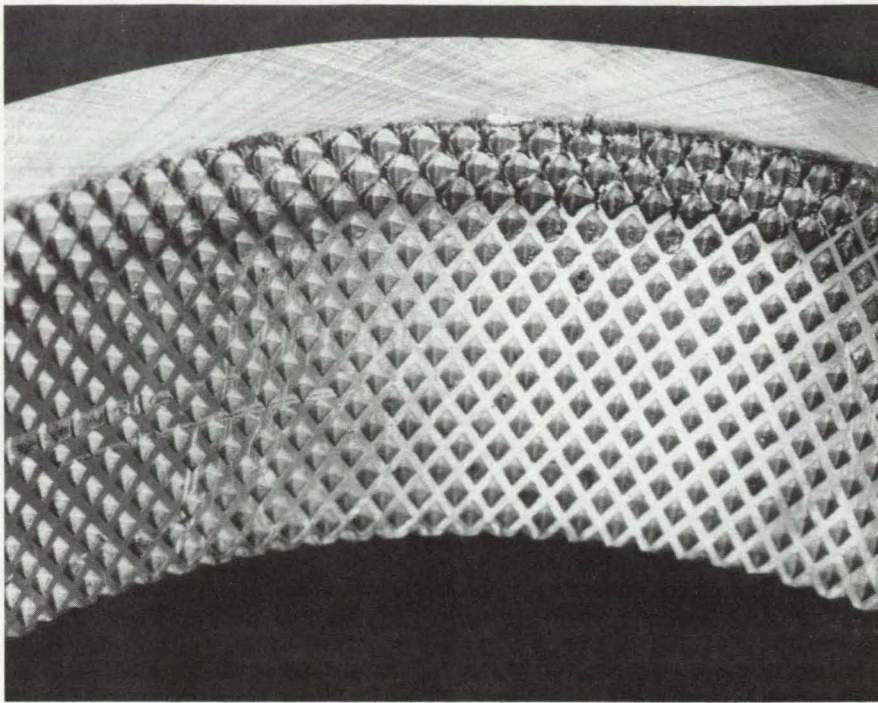
Marshall Space Flight Center, Alabama

A rotary seal for a turbopump combines the low leakage of a labyrinth seal with the high load capacity of a smooth-surface annular seal. The new seal acts as a strong journal bearing that provides high stiffness —

about the same as that of the ball bearings for the turbopump shaft. The seal thus shares the load with the ball bearings and prolongs their lives. At the same time, the seal allows minimal leakage of fluid from

the pump. By combining leakage control and bearing functions, the seal makes multiple seals unnecessary and thus allows compact design.

The seal employs a stator section with a



rough surface (see figure) and a mating rotor section with a smooth surface. The stator is roughened to a finish of about $800\ \mu\text{in.}$ ($20\ \mu\text{m}$), and the rotor is smoothed to a finish of $8\ \mu\text{in.}$ ($0.2\ \mu\text{m}$). The rough/smooth seal design reduces the axial velocity of the fluid and thereby reduces leakage. It also reduces the tangential velocity of the fluid, thereby increasing the dynamic stability.

The rough/smooth seal has been used in a high-pressure liquid-oxygen pump. Its high load capacity has been confirmed in rocket-engine tests, and its ability to control leakage has been demonstrated in a water test.

This work was done by W. C. Chen and E. D. Jackson of Rockwell International Corp. for Marshall Space Flight Center. No further documentation is available. MFS-19947

A **Stator Seal Insert** is produced with a deliberately roughened surface to improve load-bearing capacity and reduce leakage.

Peristaltic Pump With a Stable Output

Pumping channels prevent permanent changes in flow rate due to loss of elasticity.

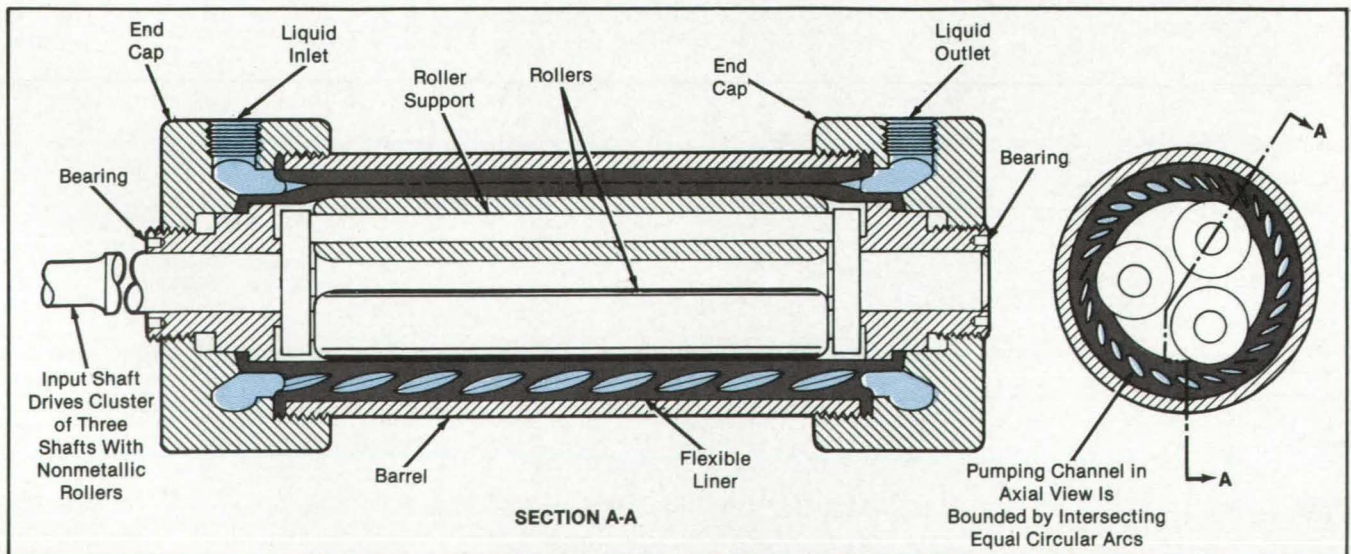
Lyndon B. Johnson Space Center, Houston, Texas

A proposed design for a peristaltic pump would decrease the flow-rate change that results from the loss of elasticity. In a conventional peristaltic pump, plastic tubing is squeezed repeatedly to move

liquid through it. After a brief operation, the volume of liquid displaced by squeezing changes because the tubing acquires a permanent "set" as a result of the large deflections imposed on its wall. In critical lab-

oratory or hospital applications, the tubing must be repositioned in the pump periodically so that a fresh section is available.

Instead of the tubing, the new pump uses a special flexible liner as the pumping



Rollers Squeeze Channels in a liner molded from a durable elastomer such as silicon rubber. For the three rollers depicted here, the helix angle of the channels is larger than 120° .

channel. The liner is molded as a single piece of flexible plastic with helical internal channels (see figure).

Three rollers move around the inner wall of the liner, compressing the channels and forcing liquid before the constrictions. As the rollers move on, the channels open elastically, drawing in liquid from the inlet port and making it available when the rollers return. The dimensions and shapes of the channels in the liner are chosen to minimize fatigue stresses caused by the repeated squeezing. Therefore, the liner should not acquire a noticeable set.

Every channel must be closed by a roller to prevent backflow. This means that the angle between rollers must always be less than the helix angle of the channels. If only one roller were used, for example, the helix angle would have to be greater than 360°.

In an alternative version of the pump, the rollers would be on the outside wall of the liner. In this configuration, the rollers would be belt- or gear-driven, rather than directly driven by a motor, so that an inlet connection could be made for the liquid.

This work was done by Joseph A. Chandler of Johnson Space Center. No further documentation is available.

Inquiries concerning rights for the commercial use of this invention should be addressed to the Patent Counsel, Johnson Space Center [see page 29]. Refer to MSC-20907.

Books and Reports

These reports, studies, and handbooks are available from NASA as Technical Support Packages (TSP's) when a Request Card number is cited; otherwise they are available from the National Technical Information Service.

Systems Engineering of Electric and Hybrid Vehicles

Hybrid vehicles are sought by optimizing electric- and combustion-engine combinations.

A technical paper notes that systems engineering principles can be applied to the development of electric and hybrid vehicles such that system performance requirements support the overall program goal of reduced petroleum consumption. The paper discusses the iterative design approach dictated by systems analyses. In addition to the obvious performance parameters of range, acceleration rate, and energy consumption, systems engineering

SPACE THE NEW FRONTIER

The Equity Research Department of
Shearson Lehman/American Express Inc.

and

The Center for Space Policy, Inc.
advisors to the U.S. Government and Industry
are pleased to announce

SPACE

the first monthly analysis of commercial
investment opportunities in space.

The financial expertise of SHEARSON LEHMAN/AMERICAN EXPRESS and the special knowledge of THE CENTER FOR SPACE POLICY have teamed to offer a totally new investment service to help investors evaluate these and other opportunities in this New Frontier.

For information contact: James P. Samuels, Shearson Lehman/American Express, 2 World Trade Center, New York, NY 10048. (212) 321-5722 or Brad M. Meslin/David Lippy. CENTER FOR SPACE POLICY, INC. 1972 Massachusetts Avenue, Cambridge, MA 02140, (617) 576-2266/2828

Circle Reader Action No. 384

also considers such major factors as cost, safety, reliability, comfort, the necessary supporting infrastructure, and availability of materials.

Petroleum consumption can be reduced by the use of electrical energy from utilities to charge batteries in electric and hybrid vehicles. Electrical generation by utilities is not entirely free from petroleum dependence. However, only about 10 to 15 percent of the current U.S. utility baseload is produced by burning oil. During offpeak periods, enough excess generating capacity is available to charge a large number of electric and hybrid vehicles.

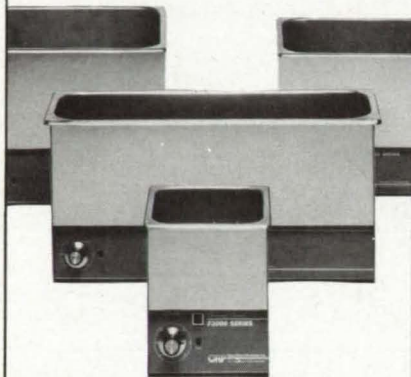
In discussing systems analysis of the

developmental ETV-1 electric car, the paper observes that the vehicle is highly efficient and well designed, but the practical driving range is severely limited by battery capacity. Because of this, there is concern that all-electric vehicles may never be purchased in sufficient numbers to satisfy petroleum-saving goals.

The hybrid approach retains much of the petroleum independence of all-electric vehicles while providing the greater range of gasoline and diesel-powered vehicles. Such vehicles contain a battery-powered electric motor and a conventional gasoline or diesel engine. Hybrid vehicles have been designed according to three basic



A sound cleaning investment.



When it comes to ultrasonic cleaners, more and more industries are making the sound decision...new F3000 series Ultrasonic Cleaners from Clean Room Products.

F3000 cleaners are available in nine sizes, covering a range of capacities from 1/2 to 7 1/2 gallons. Innovative circuit design offers the most efficient cleaning available, while protecting sensitive parts from damage. Automatic self-tuning compensates for changes in liquid level, temperature, and parts loading. And plug-in circuit modules mean easy maintenance. In addition, CRP chemists have compounded five new solutions to meet every ultrasonic cleaning requirement.

For over 20 years, CRP has specialized in providing complete clean room environments, equipment, and supplies. Our six divisions are professionally managed and staffed to serve your every clean room need.

To find out more about F3000 series Ultrasonic Cleaners or other clean room products and services, write or call today.

CRP

Clean Room Products, Inc.

Productivity Through
Engineered Environments

56 Penataquit Avenue
Bay Shore, NY 11706
516-968-8282

operating strategies:

- In the internal-combustion-engine-peaking strategy, the electric subsystem tries to supply all propulsion energy, with internal-combustion assistance available for acceleration when required;
 - In the electric-motor-peaking strategy, the internal-combustion engine fuel system supplies most of the propulsion energy, with possible assistance from the electric subsystem during acceleration or on command by the driver; and
 - In a blended strategy, both the internal-combustion and electric subsystems supply power continuously according to a sharing scheme suited to the capabilities of each power subsystem and administered by the vehicle control system.
- Computer simulations of conceptual hybrid-vehicle designs show that variations of the internal-combustion-engine-peaking strategy offer the best petroleum savings.

Based on computer simulations of expected driving cycles, it appears that hybrid vehicles offer the greatest potential petroleum savings when used primarily for low-speed stop-and-go driving. If the driving is under electric power with perhaps an occasional boost from the internal combustion engine for high acceleration, a substantial amount of petroleum will be saved, without sacrificing individual mobility of the internal-combustion engine.

This work was done by Donald W. Kurtz and Richard R. Levin of Caltech for NASA's Jet Propulsion Laboratory. To obtain a copy of the report, "EHV Systems Technology — Principles and Current Status," Circle 65 on the TSP Request Card. NPO-15871

Vibrational Effects of Turbopump Housing Flexibility

A flexible housing may be more stable than a rigid one.

Methods of computer simulation of turbopump vibrations are described in a report. For aircraft and aerospace service, high-speed, high-performance turbomachinery should be as light in weight as possible. Of course, a certain amount of mass is needed in the turbomachine housing for stiffness. The report addresses the question of how much extra weight is necessary.

Rotor stability was analyzed on six advanced turbopumps designed to operate at speeds ranging from 28,057 to 110,000 r/min and pressures up to 8,000 lb/in.² (55 MPa). Interestingly, the analyses have shown that under certain conditions, a flexible housing may be more stable than a rigid one. Specifically, if the support stiffness ratio is at least 3:1 and preferably 5:1, a turbopump will tolerate higher rotational speeds than if

it were completely rigid. A housing-to-rotor weight ratio of at least 6:1 is also recommended, partly to ensure the reliability of computational results and partly because this ratio is representative of existing turbopumps.

The report also describes an analytical program developed for a personal computer from several large programs for a mainframe computer. The new program allows complex rotor and housing configurations to be analyzed in a much shorter time and in an interactive mode. The program, called RSTAB, is written in FORTRAN and has the accuracy and summation capability of its larger predecessors.

Root-locus analysis was found to provide an interesting and useful output; the roots in the speed range of a pump are plotted in the complex plane as loci of speed. The plot indicates the change in resonant frequency and closed-loop damping as speed is increased. Troublesome resonant modes in the system can be readily tracked; the effect of system changes on the roots can be seen easily.

This work was done by J. R. Fenwick and R. B. Tarn of Rockwell International Corp. for Marshall Space Flight Center. Further information may be found in NASA CR-171147 [N84-33811/NSP], "Research Study for Effects of Case Flexibility on Bearing Loads and Rotor Stability" [\$22]. A paper copy may be purchased [prepayment required] from the National Technical Information Service, Springfield, Virginia 22161. The report is also available on microfiche at no charge. To obtain a microfiche copy, Circle 45 on the TSP Request Card.

MFS-27083

Are you reading someone else's copy of NASA Tech Briefs?

Qualified engineers and other new product development personnel can receive their own personal copies of NASA Tech Briefs by checking the subscription box and filling in one of the bound-in cards.

Computer Programs

These programs may be obtained at a very reasonable cost from COSMIC, a facility sponsored by NASA to make raw programs available to the public. For information on program price, size, and availability, circle the reference number on the TSP and COSMIC Request Card in this issue.

Dynamic Effects of Internal Spur-Gear Drives

Three programs perform static, dynamic, and stress analyses.

A set of computer programs has been developed for studying the dynamic effects of internal spur-gear drives. Spur gears have been used for many years and are important in transmitting power from

one rotating shaft to another. The use of an external gear inside of an internal gear provides a compact arrangement, but its dynamics have not been studied as much as those of the more common arrangement of two external gears side by side. This new analysis procedure can be used for gear combinations leading up to and exceeding the "very high contact ratio" (VHCR) of three. Parametric studies with these new computer programs have already revealed an impressive list of advantages of internal spur-gear drives over external spur-gear drives.

The analysis package consists of three computer programs that perform static, dynamic, and stress analyses, respectively. Output from the three programs includes the static and dynamic loads, variations in transmission ratio, sliding velocities, maximum contact pressures, and tooth-bending stress acting on the gear teeth. These new programs provide an analysis procedure applicable to involute profiles and minor deviations from this profile as a result of modifications, imperfections, and circumferential deflections.

Because of the potential noninvolute profile and the effect of radial deflection on tooth position, an interactive procedure is used to calculate the statically indeterminate problem of multitooth contacts, circumferential deflection, and contact ratio. The static analysis can also be adapted for determining the gear mesh stiffness of a planet and ring gear assembly. The maximum tooth-bending stress of the external and internal gear is determined by "Cornell's method." These programs provide for the very detailed and advanced modeling of internal spur-gear drives.

These programs are written in FORTRAN IV for batch execution and have been implemented on an IBM 370-series computer with the largest having a central-memory requirement of approximately 220K of 8-bit bytes. These programs were developed in 1983.

These programs were written by A. Printz, R. Kasuba, J. L. Frater, and R. August of the Cleveland State University for Lewis Research Center. For further information, Circle 38 on the TSP Request Card. LEW-14167



Clearing Winter Storm, Yosemite National Park, California 1944. Photography by Ansel Adams. Courtesy of the Ansel Adams Publishing Rights Trust. All rights reserved.

SOME OF THE GREATEST THINGS IN AMERICA NEVER CHANGE. SOME DO.

U.S. Savings Bonds now pay higher variable interest rates—like money



Paying Better Than Ever.

market accounts. Plus, you get a guaranteed return. You can buy Bonds at almost any financial institution. Or easier

yet, through your Payroll Savings Plan. For the current interest rate and more information, call toll-free 1-800-US-Bonds.

U.S. SAVINGS BONDS
Paying Better Than Ever

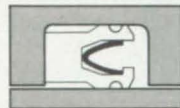
Variable rates apply to Bonds purchased on and after 11/1/82 and held at least 5 years. Bonds purchased before 11/1/82 earn variable rates when held beyond 10/31/87. Bonds held less than 5 years earn lower interest.

A public service of this publication.

New! Metal Spring/PTFE Seals With Unique Dual-Lip Design For Double Leak Protection



Greene, Tweed MSE™ Series F are the only metal spring/PTFE seals with two lips to offer double leak protection and trap lubricant for longer life. These low-friction, self-lubricating seals for rod, piston and face sealing applications—



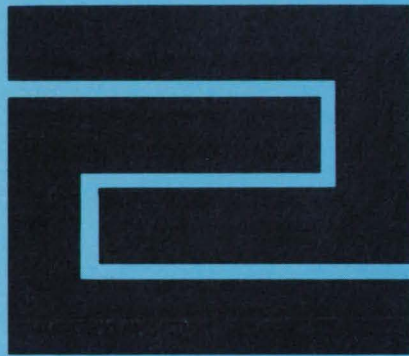
- Provide excellent static and dynamic sealing at pressures to 10,000 psi.
- Operate at temperatures from cryogenic to 500F+.
- Fit MIL-G-5514F glands.
- Are compatible with aggressive aerospace fluids, and are non-contaminating.

MSE seals are available in a variety of PTFE's and spring energizers; they are ideal for applications in fuel systems, emergency blow down systems, electronic cooling systems, etc.

Call or write for details.

GREENE, TWEED & CO

North Wales, PA 19454 • USA • (215)256-9521



Hardware, Techniques, and Processes

- 162 Dent-Removing Tool
- 162 Zone Refining by Laser
- 164 Apparatus for Sizing and Rewinding on Graphite Fibers
- 165 Inexpensive Masks for Film Deposition

Dent-Removing Tool

A sliding hammer removes minor dents in metal structures.

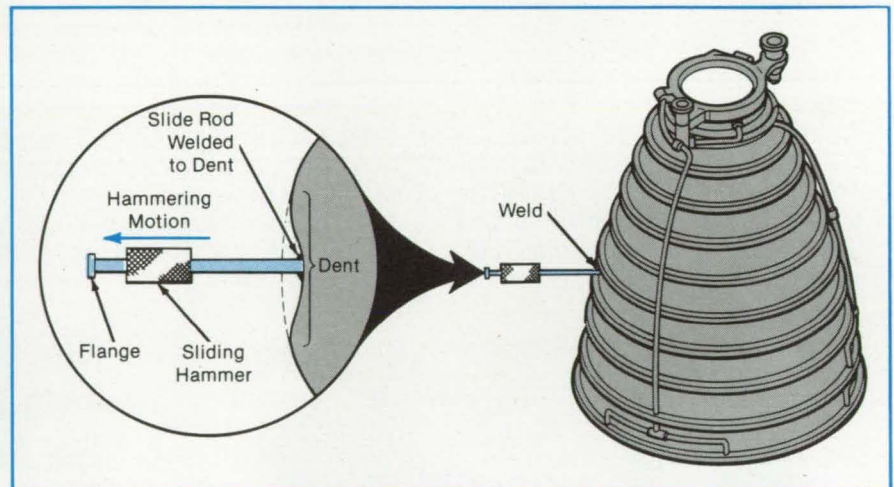
Marshall Space Flight Center, Alabama

Small dents in metal parts and structures can be evened out quickly with the aid of a simple tool. Originally used to remove dents on the Space Shuttle main-engine nozzle, the tool is a variation of the sliding-hammer dent puller used in automotive bodywork.

The user first tack welds the tip of the slide rod to the dent (see figure). Next, the user slides the hammer away from the dent so that the hammer strikes a flange at

the end of the rod. The impact of the hammer pulls out the dent. The hammering is repeated until the dented metal is even with the surrounding surface. The slide rod is unwelded, and the surface finish is restored.

This work was done by Teresa Leipham and Jewel E. McCarroll of Rockwell International Corp. for Marshall Space Flight Center. No further documentation is available.
MFS-29044



The **Impact of the Sliding Hammer** on the rod flange pulls out a dent. The tool was developed for removing small defects in the Space Shuttle main-engine nozzle, pictured here.

Zone Refining by Laser

Silicon wafers were melted by this microcomputer-controlled system.

Marshall Space Flight Center, Alabama

A system has been developed for studying the use of a laser beam for zone-refining semiconductors and metals. The specimen would be scanned with a focused CO₂ laser beam in such a way that a thin zone of molten material would move along the specimen and sweep impurities with it.

As shown in the figure, the laser beam is directed by mirrors to a galvanometer-driven scanning mirror, which in turn directs the beam to a stage driven by a stepping motor. The beam scans rapidly back and forth across the specimen as the specimen is translated slowly by the main

translation stage in a direction perpendicular to the scanning motion. The center of the beam thus traces a zigzag path on the specimen. Because of the relative speed of the scanning motion, the heated zone appears as a line that translates along the specimen.

The melt zone can be up to 1 centimeter wide and can be moved a maximum distance of 10 centimeters. The laser spot diameter at sharpest focus is 0.5 millimeter. The focusing lens is mounted on a small stage, also driven by a stepping motor, so that the laser spot size can be adjusted. The laser power can be varied from 10 to

NASA Tech Briefs, Winter 1985

American Business Leaders Who Do Not Join The War On Government Waste And Fight The Deficit — Are Shooting Themselves And Our Country In The Foot!



Here's Why

Despite "promising" economic forecasts and the public's patient "wait and see" attitude, the deficit is at record levels. So is wasteful and inefficient spending in government.

Many executives are openly decrying the deficit as the one thing that can derail the economy in 1985 and beyond. Among the consequences:

- A collision between the private sector and the U.S. Treasury for access to the credit markets.
- Reduced worth of personal and corporate portfolios.
- Increased taxes that will slash growth and inspire layoffs.
- The transfer of a bigger deficit and unwieldy debt to the next generation.

Business leaders need to get the attention of those politicians and bureaucrats who are dragging their feet in cutting waste and inefficiency in government.

Fortunately, the hard work is already done

The ground work has been laid by the Grace Commission Report, which details 2,478 ways to reduce federal waste, inefficiency and over-spending. Once adopted these proposals would save \$424.4 billion over three years, and effectively get America out of hock.

The report provides solid evidence that government waste and inefficiency can be reduced. It provides practical ways to cut waste without weakening our national defense and eliminating necessary subsidy programs.

What you can do as a business leader

We need your help to distribute the Citizens Against Waste Petition to be served on the 99th Congress, to let the lawmakers know there's some real pressure building among their constituents to cut the deficit and stop waste.

Sponsor a petition center that includes a 24" x 37" Poster for display and the 500-petition display (a 10,000-name potential).

The cost is only \$40.00 delivered prepaid.

The display takes up less than one square foot of space and is an investment that is sound business practice for all concerned.

The deficit is the one economic culprit that can single handedly derail the economy, slash growth, inspire layoffs and reduce the worth of personal and business finances — not only for 1985, but for years to come.

It is essential that more and more Americans pool their efforts and their money to establish a vocal and powerful group to pressure those politicians and bureaucrats who insist on wasting tax dollars and using government funds for their own pet projects,

Not to mention, the urgent need for all public officials to become more accountable, answerable, and responsive to the American taxpayer.

Pressure works!

Politicians do and will respond if the numbers of petitions are big enough.

In fact, they'll buckle under.

It's been proven in the past that pressure works. From the Child Labor Law, the Women's Right To Vote, Workmen's Compensation, the Civil Rights Act, and the recent and very successful efforts to curb drunk driving by SADD and MADD, we have seen that Congress WILL respond time and again. But only when they're convinced that the people are serious.

Citizens Against Waste — Who We Are

Citizens Against Waste is a nonprofit foundation of bipartisan and concerned citizens from all walks of life, who've come together to "educate" the Federal bureaucratic spenders and waste makers in Congress about the absolute necessity to curb overspending, waste and inefficiency to eliminate the deficit.

Citizens Against Waste

1511 K Street NW,
Washington, D.C. 20005

ATTN: J. P. Bolduc, President

Dear Mr. Bolduc:

Here is my order for _____
petition centers @ \$40.00 each.

Check enclosed for \$ _____

Name _____

Title _____

Company _____

Address _____

City _____

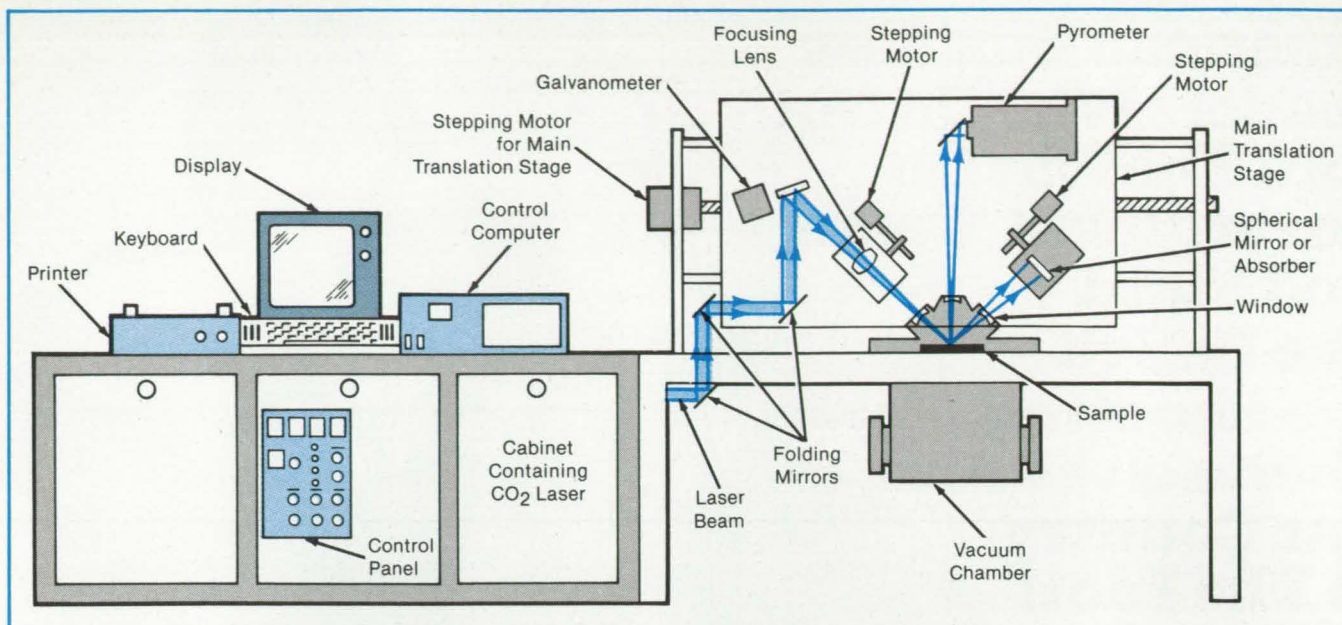
State _____ Zip _____

Enclose a PR kit on how we can spread the word that the petition centers are available in our business.



A Petition to Our Government
As the true owners of the U.S. government, we protest the appalling waste of our money by those we entrust to spend it. We demand action, not discussion, to stop the excessive and unnecessary squandering of government funds for foolish projects, wasteful programs and inefficient operations and ineffective measures taken against those in Congress and the federal bureaucracy who irresponsibly authorize and misspend our tax dollars.

For more information,
call **1-800-USA-DEBT.**



The **Zone-Melting System** comprises a microcomputer, a laser, electromechanical and optical components for beam control, a vacuum chamber that holds the specimen, and a sensor for determining the specimen temperature.

85 watts. In experiments, silicon wafers were melted at 50 watts; however, a nickel alloy specimen could not be melted even at the maximum power.

The apparatus holds the specimen in a vacuum chamber. Two windows on opposite sides of the chamber allow the laser beam to enter and exit at 45° angles with the vertical. The beam reflected from the specimen and leaving the vacuum chamber can be either absorbed or reflected back to the specimen to increase the energy directed to the specimen. A third window, at the top of the chamber, allows a py-

rometer to view the specimen.

A microcomputer controls the system. The system includes a real-time clock; analog-to-digital converters for monitoring the laser power meter; and driving circuits for the stepping motors, scanning mirrors, and laser-beam shutter. Peripheral equipment includes a keyboard, a cathode-ray-tube display, a printer, and a dual floppy-disk drive.

This work was done by Donald B. Griner of **Marshall Space Flight Center**. Further information may be found in NASA TM-86459 [N84-32805/NSP], "Laser Furnace

Technology for Zone Refining" [\$8.50]. A paper copy may be purchased [prepayment required] from the National Technical Information Service, Springfield, Virginia 22161. The report is also available on microfiche at no charge. To obtain a microfiche copy, Circle 47 on the TSP Request Card.

Inquiries concerning rights for the commercial use of this invention should be addressed to the Patent Counsel, Marshall Space Flight Center [see page 29]. Refer to MFS-27084.

Apparatus for Sizing and Rewinding Graphite Fibers

Research-scale apparatus sizes commercially available wound fibers, improving wetting during resin impregnation.

Langley Research Center, Hampton, Virginia

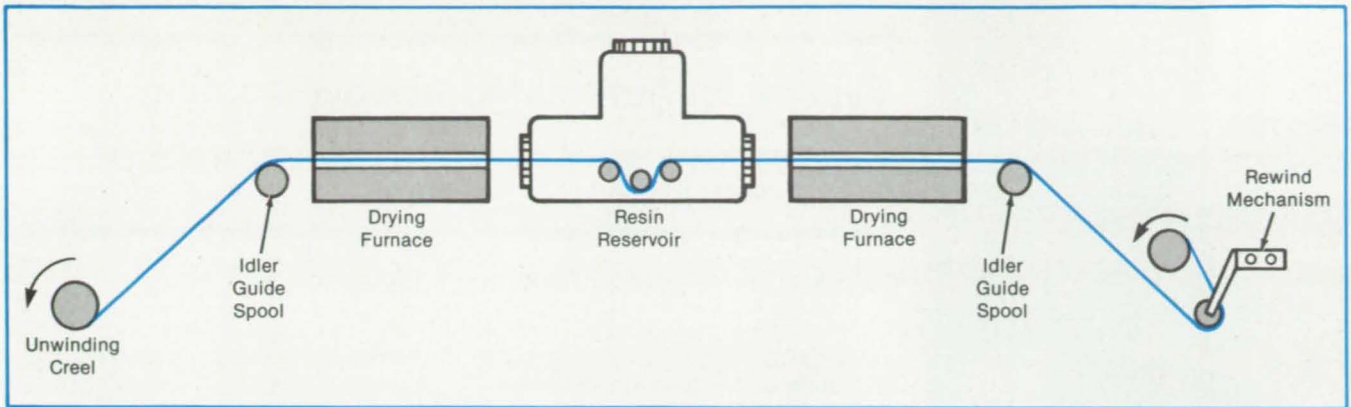
A new technique applies a sizing solution to unsized graphite tow, thereby improving fiber wetting during resin impregnation, drum winding, and laminate molding. The equipment is ideally suited for research and development of new sizing solutions. It was designed especially for applying thermoplastic sizing solutions to graphite tow consisting of 3,000 to 12,000 filaments per tow, but it will accommodate other solutions, other filament counts, and materials other than graphite.

The new apparatus is diagrammed in the figure. A spool of unsized graphite tow, commercially available and wound on standard cardboard cores, is attached to

an unwinding creel. An idling spool guides the tow and provides tension. The tow is pulled through a tube furnace lined with Pyrex (or equivalent) glass tube to drive off atmospheric moisture. From there, it proceeds through the resin reservoir, which is made by welding three polyethylene bottles together, installing orifices at both ends, and adding spreader bars to spread the tow as it travels through the solution. A typical sizing solution is 0.5 percent by weight polysulfone in methylene chloride solvent. The tow is pulled through a second drying furnace to drive off the methylene chloride solvent, pulled through a second idler spool, and finally rewound on a spool

for further processing.

This technique was developed because there is no commercial equipment available on a small (research) scale to mechanically unwind, size, dry, and rewind fiber tows. Poor wetting of fibers during resin impregnation results in resin-poor areas, or dry spots, after laminating and molding. These areas subsequently result in voids within the composite, causing delamination and early failure. Sizing compounds (very low concentrations of the intended impregnating resin system or constituents of such resin, usually less than 1 percent by weight) are applied to the fibers to provide environmental protection, to enhance



The **Resin Reservoir Is a Closed System** containing the highly volatile methylene chloride vapors. There is also a ventilation system directly over the resin reservoir.

wetting during resin impregnation causing the resin to encapsulate individual filaments, and to prepare the fiber surfaces chemically to receive additional resin in order to improve bonding strength at the fiber/resin interface.

The method is used in research and de-

velopment at Langley Research Center to solve wetting problems incurred in processing graphite-reinforced thermoplastic composites. This concept can be used to apply sizing compounds on fiber tows or yarn-type reinforcement materials used in composite technology. Sizing solutions can

consist of compounds compatible with thermosets as well as thermoplastics.

This work was done by Maywood L. Wilson and Clarence E. Stanfield of Langley Research Center. No further documentation is available.
LAR-13323

Inexpensive Masks for Film Deposition

Overlapping openings in superimposed masks would define narrow lines.

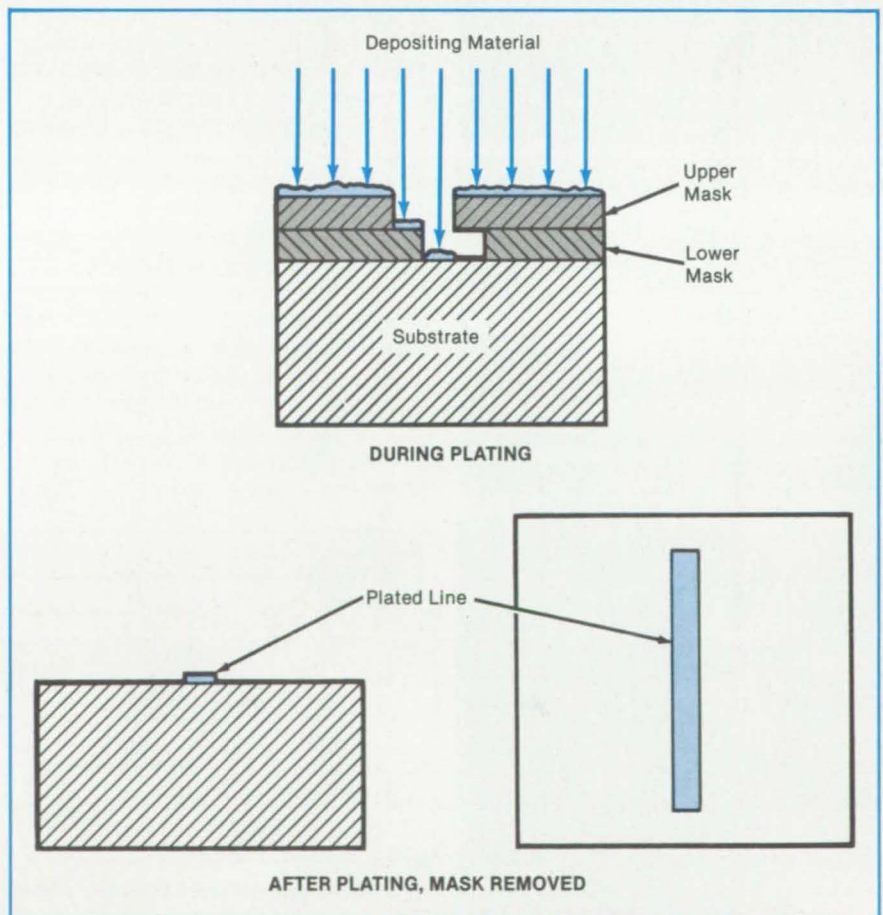
*NASA's Jet Propulsion Laboratory,
Pasadena, California*

Sputtered or sprayed lines less than 2 millimeters wide could be made by superimposing masks with partially overlapping openings. Slits would first be cut in the masks by stamping or other economical process. Then the masks would be superimposed so that the slits define new openings that are narrower than the original slits (see figure).

This two-mask process may be cheaper than making a narrow slit in a single mask by chemical etching or electrical-discharge machining. By repeatedly shifting one mask with respect to the other, the same pair of masks might be used to make lines of various widths.

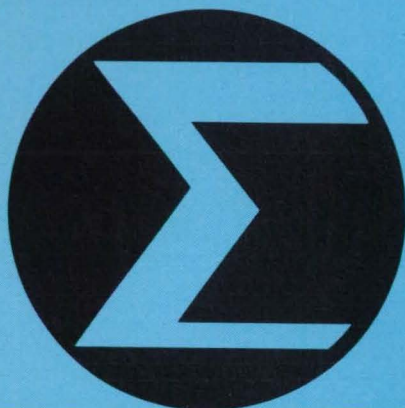
The masks would ordinarily be cut from shimstock typically 0.001 to 0.040 inch (0.025 to 1.0 millimeter) thick. The edge of the line defined by the upper mask will be sharper if the lower mask is kept as thin as possible. The upper mask can be made thicker to lend structural support to the lower one.

This work was done by William R. Conley of Illinois Tool Works, Inc., for NASA's Jet Propulsion Laboratory. For further information, Circle 98 on the TSP Request Card
NPO-16416



A Composite Mask for Depositing a Narrow Line is made by positioning two masks with wider openings so that the two openings overlap partially. The component masks can be made by stamping the openings in shimstock.

Mathematics and Information Sciences



Hardware, Techniques, and Processes

- 166 System for Automated Troubleshooting
- 167 Geometric Representations for Discrete Fourier Transforms
- 168 Maximum-Likelihood Parameter-Estimation Algorithm

Books and Reports

- 168 Optimum Cyclic Redundancy Codes for Noisy Channels
- 175 Numerical Aerodynamic Simulation Facility
- 175 Comparison of Decision Models

Computer Programs

- 176 Numerical Methods for Classical Sampled-System Analysis
- 176 Software Comparison
- 177 Image-Processing Educator
- 177 Manipulation of Numbers with Many Digits
- 177 Printer Graphics Package

System for Automated Troubleshooting

Algorithms follow human patterns in diagnosing faults in electromechanical systems.

NASA's Jet Propulsion Laboratory, Pasadena, California

New algorithms for diagnosing problems in electromechanical systems based on artificial intelligence techniques can be used to locate faults with minimal human intervention. After being given information on the system architecture, electrical connections, types of parts, and failure modes, the algorithms apply "reasoning" processes patterned after those of humans.

The system troubleshoots common problems. If experience with the system shows that certain problems have been overlooked, it is easy to add the necessary rules and factual knowledge to the program.

The diagnostician alternates between explanation and either confirmation or denial (see figure). The explanation phase seeks to find the cause of a detected or hypothesized malfunction. The software works backward from either the malfunction presented to it or the confirmed cause of the malfunction (itself a malfunction), thus building a chain of causes. The confirmation or denial phase seeks evidence for or against the hypothesized cause.

In the explanation process, a symptom or cause is matched against a rule in the data base that contains the symptom or cause as its result. Usually, more than one rule matches, and the preconditions of all such rules then become candidate explanations. Some rules can be eliminated because they specify facts that cannot be matched against given facts of the data base — such as system architecture or connections. Of the remaining candidates, each in turn undergoes a confirmatory process until only one confirmed cause remains. If no cause is confirmed, the chain

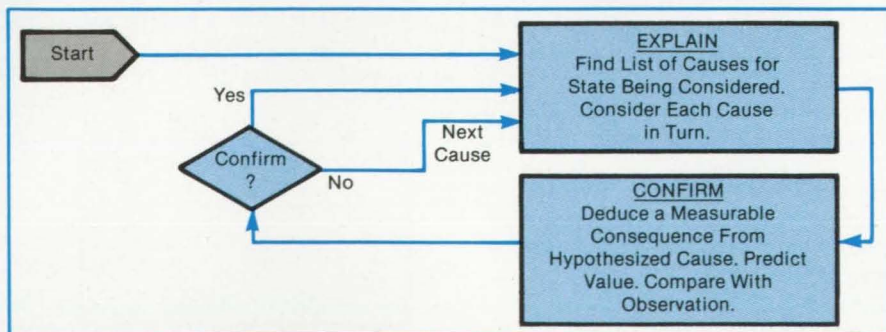
of explanation unwinds to a previously confirmed level, and the software tries alternative hypothetical causes. The process quits only after it has exhausted all alternatives.

When the process confirms a cause judged to be sufficiently explanatory, determined by the person designing the diagnosis, it may find an "advice" message associated with the terminating rule that suggests a cure for the problem and displays the message to the user. A user who wants a more detailed explanation may request the process to continue and have the explanation extended to a deeper level of system detail.

To confirm a diagnostic condition, the system searches its knowledge base for a rule having preconditions that match those of the candidate. The rule predicts what selected values of system performance will be measured if the candidate explanation is true. Each such prediction is compared with actual measurements until either all predictions are matched or any is denied.

When a system consists of relatively independent subsystems, the software is programmed to operate in a "focus" mode. Such independent subsystems have unique symptoms that characterize faulty operation. The diagnostician checks each subsystem in turn until a set of symptoms for faulty operation is confirmed, or there are no subsystems left to check.

When a system consists of subsystems that influence each other by passing signals, the software uses a "trace" mode. Several kinds of knowledge have to be supplied to the program by the user for this mode. Signal paths have to be defined as



Troubleshooting Software Operates Like a Human technician troubleshooting a system. First, it attempts to locate a fault to within a particular subsystem. Having narrowed down the problem to a particular subsystem, it then tries to characterize the problem within that subsystem. During this process, it is guided by comparisons between predicted measurements and actual data.

do input and output ports and the kinds of signals to be expected at each test point in the signal path.

The diagnostician can generate tests as well. Starting with measured inputs to a system that are hypothesized to be at fault, it will propagate those subjects along the

connection paths specified in the data base (equivalent to a circuit diagram) and simulate correct operation and outputs. These can be compared with actually measured outputs to detect errors. By complex reasoning processes, parts of the circuit that may have caused the observed errors

may be singled out by the diagnostician.

This work was done by Leonard Friedman of Caltech for NASA's Jet Propulsion Laboratory. For further information, Circle 23 on the TSP Request Card. NPO-16339

Geometric Representations for Discrete Fourier Transforms

Periodicity and Hermiticity lead to economy in storage of transform values.

Marshall Space Flight Center, Alabama

Simple geometric representations show the symmetry and periodicity of discrete Fourier transforms (DFT's). The representations help in visualizing the requirements for storing and manipulating transform values in computations. The representations are useful in any number of dimensions, but particularly in the one-, two-, and three-dimensional cases, which are often encountered in practice.

The three-dimensional DFT (also called the "fast" Fourier transform) $X(k_1, k_2, k_3)$ for a function $x(n_1, n_2, n_3)$ has periodicity N_i in each axis: For example,

$$X(k_1, k_2, k_3) = X(k_1 \pm N_1, k_2, k_3)$$

where k_i and N_i are integers, and N_i = the number of points in the Fourier sum along the i th axis. This relationship enables one to generate the transform values for negative arguments from those for positive arguments by means of $X(-k) = X(N - k)$. One very useful relation of this type is

$$X\left(\frac{N}{2} + m\right) = X\left(-\frac{N}{2} + m\right)$$

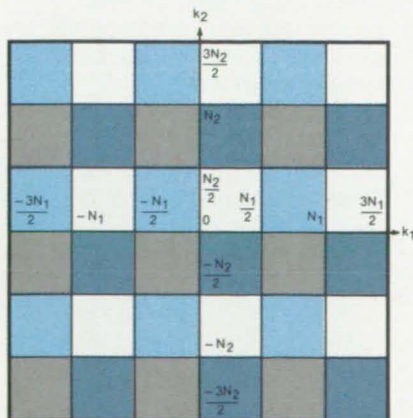


Figure 1. The **Two-Dimensional DFT** repeats all over the transform plane with periodicity in each axis equal to the number, N , of sampling points along that axis. Here, corresponding points in boxes of identical color have identical transform values.

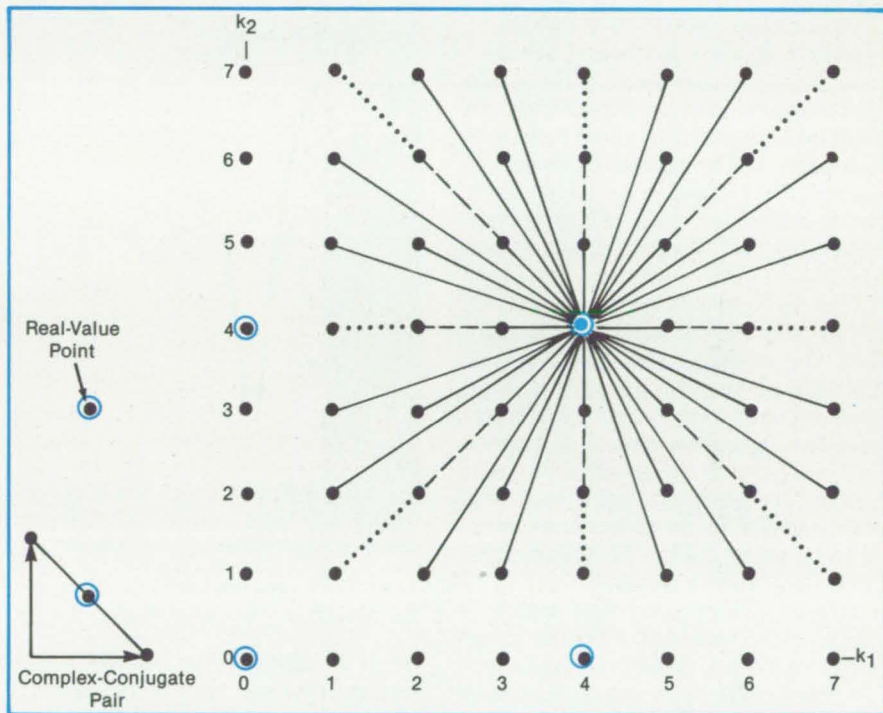


Figure 2. **Within a Quadrant**, two-dimensional 8-by-8 DFT values that are complex conjugates of each other lie at points opposite each other at equal distances from the point 4,4 on lines through the point 4,4.

Thus, it is possible to generate any transform value as long as any N contiguous value is known along each axis. These symmetry and periodicity properties are illustrated geometrically in Figure 1 for a two-dimensional DFT.

The DFT also has the Hermitian property

$$X(k_1, k_2, k_3) = X^*(-k_1, -k_2, -k_3)$$

Combining this with the periodicity relations results in sets of equations for generating transform values that are complex conjugates of each other. For a two-dimensional DFT, one such set is:

$$X\left(\frac{N_1}{2} + m_1, k_2\right) = X^*\left(\frac{N_1}{2} - m_1, -k_2\right)$$

and

$$X\left(\frac{N_1}{2} + m_1, \frac{N_2}{2} + m_2\right) = X^*\left(\frac{N_1}{2} - m_1, \frac{N_2}{2} - m_2\right)$$

The geometric significance of these equations is that the transform must have real values at the corners of the rectangles defined by progressing in increments of $N/2$ points along each axis from the origin, and that the transform values of points equidistant from the real-value points on the opposite ends of lines through the real-value points are complex conjugates of each other. These properties are illustrated for the first quadrant of a two-dimensional DFT in Figure 2.

Using the combination of properties illustrated in the figures, the DFT of any argument is easily generated from the values in the four quadrants surrounding the origin. All other values follow from periodicity: The identical value is reached by moving two blocks along either axis or diagonally

from any point.

This work was done by C. Warren Cambell of **Marshall Space Flight Center**. Further information may be found in NASA Technical Paper 2332 [N84-24114/NSP], "Geometric Interpretations of the Discrete Fourier Transform (DFT)" [\$7]. A

paper copy may be purchased [prepayment required] from the National Technical Information Service, Springfield, Virginia 22161. The report is also available on microfiche at no charge. To obtain a microfiche copy, Circle 6 on the TSP Request Card. MFS-27072

Maximum-Likelihood Parameter-Estimation Algorithm

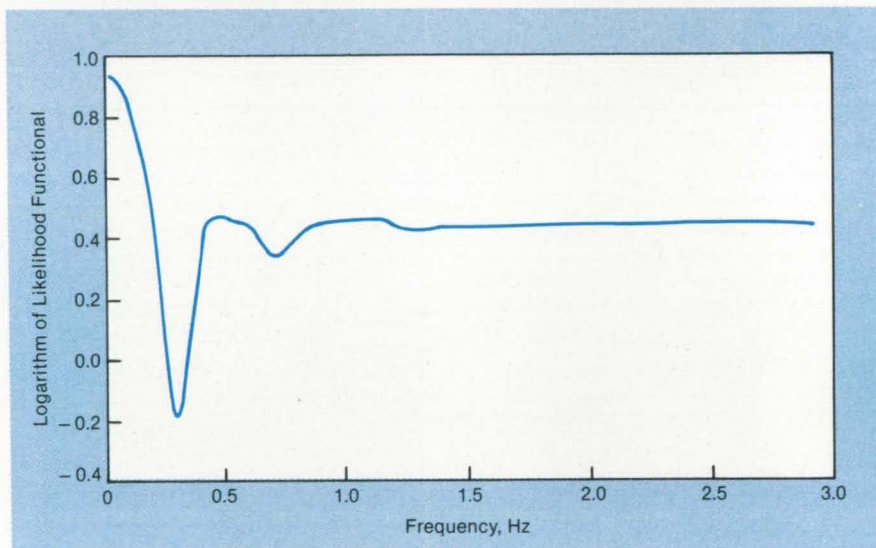
Treating errors as uncorrelated white noise is realistic and computationally efficient.

NASA's Jet Propulsion Laboratory, Pasadena, California

An efficient version of a maximum-likelihood algorithm has been devised for calculating normal-mode frequencies and damping parameters of a vibrating system from experimental data where both process noise and measurement noise are present. The method should be applicable in the vibration analysis of such complicated structures as vehicles, aircraft, and spacecraft.

The new algorithm is a simplification of an existing maximum-likelihood formulation using a Kalman filter that allows for both process and measurement noise. The new algorithm incorporates the assumption that measurement-noise covariance can be treated as a given rather than as a parameter to be determined. This assumption simplifies the computation and guarantees that the Kalman filter gains correspond to a physical system.

The most likely parameters are identified by the minimization of a performance index called the "likelihood functional." The Newton-Raphson method is used to minimize the likelihood functional. Estimates of the values of the parameters, which are required to start the process, are used to design a Kalman filter for state estimation. A related filter that indicates the sensitivity of the state estimate to the parameters to be determined is obtained from derivatives of the Kalman filter. The state estimates and the derivatives are used to calculate the gradient of the likeli-



Local Minima in a Likelihood Functional for a flexible beam occur at the frequencies of the first three vibrational modes.

hood functional. In the Newton-Raphson update, new estimates of the parameter values are calculated. Using the new parameter values in each iteration as input for the next, the entire process is repeated until convergence is achieved.

When the likelihood functional is plotted as a function of frequency or damping ratio, the result is a smoothly varying curve with a round-bottomed local minimum at each modal frequency or damping ratio (see figure). In such a situation, rapid con-

vergence is obtained when the parameter estimates used to start the first iteration are reasonably close to the correct values. Nevertheless, one must select the initial parameters with care, since incorrect values sometimes cause the likelihood functional to diverge.

This work was done by Daniel B. Eldred, Massih Hamidi, and Guillermo Rodriguez of Caltech for **NASA's Jet Propulsion Laboratory**. For further information, Circle 30 on the TSP Request Card. NPO-16320

Books and Reports

These reports, studies, and handbooks are available from NASA as Technical Support Packages (TSP's) when a Request Card number is cited; otherwise they are available from the National Technical Information Service.

Optimum Cyclic Redundancy Codes for Noisy Channels

Recommended 24- and 32-bit CRC codes are given.

The capabilities and limitations of cyclic redundancy codes (CRC's) for detecting transmission errors in data sent over relatively noisy channels (e.g., voice-grade telephone lines or very-high-density storage media) are discussed in a 16-page report. Because of the prevalent use of bytes that are multiples of 8 bits in data transmis-

Multiple Pages Missing from Available
Version

sion, the report is primarily concerned with cases in which both the block length and the number of redundant bits (check bits for use in error detection) included in each block are multiples of 8 bits.

The authors derive theorems that are then used to calculate safe upper and lower bounds on block lengths for 16-, 24-, and 32-bit CRC's with largest minimum Hamming distances of 4, 6, and 8. (Codes of distances 4, 6, and 8 can be used to detect any error of no more than 3, 5, and 7 bits, respectively, in a block or to correct any error up to 1, 2, and 3 bits, respectively.)

The cases of distance-6, 24-redundant-bit and distance-8, 32-redundant-bit CRC's are analyzed thoroughly; specific polynomials recommended for use in calculating the check bits for each of these types of codes are also given. The recommended polynomials are of low weight (low number of terms). The lowest-weight 24- and 32-bit polynomials found had 6 and 10 terms, respectively. It was also found that there are no 16- or 24-bit CRC's minimum of distances ≥ 8 .

The 16-bit CRC polynomial

$$p(x) = X^{16} + X^{12} + X^5 + 1$$

specified in the X.25 packet-communication-link standard is shown by the authors to be optimum for the 16-bit, distance-8 case. However, being of Hamming distance 4, this code will fail to detect some errors of 4 or more bits per block and is useful only in links with low input-bit-error probabilities.

This work was done by Edward C. Posner and Phillip Merkey of Caltech for NASA's Jet Propulsion Laboratory. To obtain a copy of the report, "Optimum Cyclic Redundancy Codes for Noisier Channels," Circle 32 on the TSP Request Card. NPO-16406

Numerical Aerodynamic Simulation Facility

Its history, status, and future plans are presented in a 22-page report.

The NASA numerical aerodynamic simulation (NAS) facility described in a 22-page report will provide an advanced computational aerodynamics service by the mid- to late-1980's for use by government laboratories, industry, and academia. The facility will be continually upgraded as computer technology advances.

The facility, which is expected to begin operating by late 1985, will support both local and remote users. The User Interface Group, comprising representatives of the

aerospace industry, universities, and government agencies, serves as a forum for the discussion of such user-oriented issues as the selection of user languages, management policy, equipment required for remote access, and data protection.

The sustained computational speed of the facility is expected to be 250×10^6 floating-point operations per second; its memory at least 64×10^6 64-bit words. By 1987, the speed and memory should each be increased by a factor of 4 and the network will be expanded to support at least 100 users simultaneously on a time-sharing basis. The operating system and network will be capable of using equipment from a number of manufacturers.

The facility will house the NAS Processing System network, which includes the following eight subsystems:

- High-speed processor,
- Support processing,
- Work stations,
- Graphics,
- Mass storage,
- Long-haul communications,
- High-speed data network, and
- Local-area network.

The report lists nine candidate problems for inclusion in initial tests of the system. These represent a balance of fundamental fluid physics research and applied computational aerodynamics and aerothermodynamics. A computational chemistry problem; namely, the simulation of crack initiation and propagation, is also a candidate.

It is expected that 90 percent of the available high-speed processor time will be devoted to fluid dynamics and aerodynamics and 10 percent to chemistry, atmospheric modeling, aircraft structural analysis, and astrophysics. By user affiliation, usage is expected to be about 55 percent NASA, 20 percent Department of Defense, 15 percent industry, and 5 percent universities. The report does not state the allocation of the remaining 5 percent.

In reviewing the history and future of computational aerodynamics, the report lists computational requirements for treating a series of increasingly complex problems involving the equations of fluid dynamics. The most demanding problem is the full Navier-Stokes treatment of time-varying supersonic/subsonic flow with laminar/turbulent transitions and turbulence dissipation, requiring 10^{12} to 10^{15} grid points.

This work was done by V. L. Peterson, W. F. Ballhaus, Jr., and F. R. Bailey of Ames Research Center. To obtain a copy of the report, "Numerical Aerodynamic Simulation (NAS)," Circle 96 on the TSP Request Card.

Inquiries concerning rights for the commercial use of the technology described in this report should be addressed to the Patent Counsel, Ames Research Center [see page 29]. Refer to ARC-11497.

Comparison of Decision Models

The results predicted by linear and multiplicative decision models are compared.

Two methods of multiattribute decision analysis are compared in a report. One method employs a linear utility model. The other utilizes a multiplicative utility model. The report is based on interviews with experts in automotive technology to obtain their preferences regarding 10 new types of vehicles.

Thirty-nine people were asked to express their preferences for these attributes: Initial cost, life-cycle cost, maintainability, safety, relative fuel economy, and refueling time. All the vehicles are intended to operate with nonpetroleum fuel and to have a 250-mile (400-kilometer) range. The propulsion systems included a methanol spark-ignition engine, a solid-polymer-electrolyte fuel cell, three different types of batteries in an all-electric configuration, and five different types of batteries in a hybrid configuration with a methanol-fueled engine.

The interviewees were drawn from the following groups or functions associated with advanced vehicles:

- Fleet purchasing or management,
- Research in an automobile manufacturing firm,
- Corporate decisionmakers in automobile manufacturing,
- Consumer, professional, and market-analysis organizations,
- Fuel suppliers,
- Organizations conducting advanced-vehicle research for utility companies,
- Utility companies, and
- Government and university researchers.

Rankings were calculated for the 39 interviewees and for the 8 groups they represent. For the individuals, several variations of the multiattribute decision models were used, including versions in which the less important attributes were disregarded. For the groups, three different group-decision rules were used. In addition, direct rankings were obtained from 31 of the participants who responded to questionnaires.

In general, the rankings were consistent among individuals, different group-decision rules, and different multiattribute utility models. The rankings from the linear model were virtually identical to the rankings from the multiplicative model. Although some interview and computation time could have been saved by using only one model, the fact that both agree lends additional credibility to the results.

The direct rankings required the least effort and, for the most part, agreed with the rankings from the linear and multiplicative



models. The direct rankings, however, give no insight into risk preferences or the relative importance of various attributes. Such insights are often at least as valuable as the rankings themselves.

This work was done by Abe Feinberg, Ralph F. Miles, Jr., and Jeffrey H. Smith of Caltech and Ernest M. Scheuer of the California State University for NASA's Jet Propulsion Laboratory. To obtain a copy

of the report, "A Comparison of Multiattribute Decision Models," Circle 25 on the TSP Request Card. NPO-16446

Computer Programs

These programs may be obtained at a very reasonable cost from COSMIC, a facility sponsored by NASA to make raw programs available to the public. For information on program price, size, and availability, circle the reference number on the TSP and COSMIC Request Card in this issue.

Numerical Methods for Classical Sampled-System Analysis

Algorithm selection is simplified for the control-system analyst.

SAMSAN provides the control-system analyst with self-consistent computer algorithms that support large-order control-system design and evaluation studies. It emphasizes sampled-system analysis.

Control-system analysts have access to a vast array of published algorithms to solve an equally large spectrum of computational problems related to controls. The analyst usually spends considerable time and effort in bringing these published algorithms to an integrated operational status and often finds them less general than desired. SAMSAN reduces the burden on the analyst by providing a set of algorithms that have been well tested and documented and that can be readily integrated for solving control-system problems. Algorithm selection for SAMSAN has been biased toward numerical accuracy for large-order systems with computational speed and portability being considered important but not paramount.

In addition to containing relevant sub-routines from EISPAK for eigenanalysis and from LINPAK for the solution of linear systems and related problems, SAMSAN contains the following capabilities:

1. Reduction of a real nonsymmetric matrix to block diagonal form via a real similarity-transformation matrix that is well conditioned with respect to inversion;
2. Solution of the generalized eigenvalue problem with balancing and grading;

3. Computation of all zeros of the determinant of a matrix of polynomials;
4. Matrix exponentiation and the evaluation of integrals involving the matrix exponential with an option to first block diagonalize;
5. Root locus and frequency response for single-variable transfer functions in the S, Z, and W domains;
6. Several methods of computing zeros for linear systems;
7. Reduction of a set of linear ordinary differential equations or finite-difference equations to a set of almost decoupled generalized coordinate equations;
8. Integration of a system of ordinary differential equations using a fixed- or variable-step standard Runge-Kutta algorithm or by using the general-purpose package of numerical integration algorithms DEPACK;
9. Computation of characteristic gains and phases, principal gains and phases, robustness, and sensitivity measures for a return-ratio (transfer-function) matrix at a particular point in the complex plane;
10. The ability to read a NASTRAN-generated OUTPUT2 data file and produce a data file compatible with the SAMSAN routines; and
11. The ability to generate documentation "on demand."

All matrix operations in the SAMSAN algorithms assume nonsymmetric matrices with real double-precision elements. There is no fixed size limit on any matrix in any SAMSAN algorithm; however, it is generally agreed by experienced users, and in the numerical error analysis literature, that computation with nonsymmetric matrices of order greater than about 200 should be avoided or treated with extreme care. SAMSAN attempts to support the needs of application-oriented analysis by providing:

1. A methodology with unlimited growth potential,
2. A methodology to insure that associated documentation is current and available "on demand,"
3. A foundation of basic computational algorithms that most control-analysis procedures are based upon,
4. A set of checkout and evaluation programs that demonstrate the use of the algorithms on a series of problems that are structured to expose the limits of each algorithm's applicability, and
5. Capabilities that support both a priori and a posteriori error analysis for the

computational algorithms provided.

The SAMSAN algorithms are coded in FORTRAN IV for batch or interactive execution and have been implemented on a DEC VAX series computer. An effort was made to ensure that the FORTRAN source code was portable and, thus, SAMSAN may be adaptable to other machines. The SAMSAN package was developed in 1982 and last updated in 1984.

This program was written by Harold P. Frisch and Frank H. Bauer of Goddard Space Flight Center. For further information, Circle 82 on the TSP Request Card. GSC-12827

Software Comparison

The program compares similarly structured files, line by line.

The Software Comparison Package (SCP) compares similar files. Normally, these are 90-character files produced by the CDC UPDATE utility from program libraries that contain a FORTRAN source code plus an identifier. The SCP can also be used to compare load maps, cross-reference outputs, and UPDATE corrections sets. In short, it can help wherever line-by-line comparison of similarly structured files is required.

An important feature of the SCP is the automatic generation of update directives (in standard CDC UPDATE format) that can be later applied to a program library to change one set of routines into the other. Often, only part of this set may be useful, but experience has shown it to be a time-saver. In cases where major modifications are anticipated and a complicated history of overlapping corrections have been applied to a routine, it is often easiest to use the SCP to generate a single correction deck that summarizes all changes.

The SCP program is written in FORTRAN IV for batch execution and has been implemented on a CDC CYBER 70-series computer. Dimensioned for comparing routines up to 2,500 lines long, the program has a central-memory requirement of approximately 200K (octal) of 60-bit words. The SCP program was developed in 1984.

This program was written by David C. Blanchard of McDonnell Douglas Corp. for Johnson Space Center. For further information, Circle 16 on the TSP Request Card. MSC-20777

Image-Processing Educator

This program explores the digital processing of remotely sensed images by microcomputers.

The Apple Image-Processing Educator (AIPE) explores the ability of microcomputers to provide personalized computer-assisted instruction (CAI) in the digital image processing of remotely sensed images. AIPE is a "proof-of-concept" system, not a polished production system. User-friendly prompts provide access to explanations of common features of digital image processing and of sample programs that implement these features.

Currently available features include:

- Density Slicing — Assigns color codes to ranges of gray scale values,
- Statistics — Generates image statistics for whole images or training areas,
- Filter — Demonstrates the effects of bandwidth bypass filters,
- Transverse — Displays a histogram of pixel values for a selected channel or line in an image, and
- Contable — Calculates and displays a "confusion matrix" for two color-coded images.

A sample image is included with the AIPE system so that instruction is self-contained.

The AIPE system is written in Applesoft BASIC and Integer BASIC for interactive execution on the Apple II or Apple II+ computers with the Disk II Subsystem, DOS 3.3, a color monitor, and 48K of 8-bit bytes. The AIPE system was developed in 1979-1980.

This program was written by Fred J. Gunther of Computer Sciences Corp. for Goddard Space Flight Center. For further information, Circle 27 on the TSP request Card.
GSC-12933

Manipulation of Numbers With Many Digits

Underflow and overflow are prevented in programs generating extreme numbers.

PRECISION is designed for the manipulation of numbers with an accurate retention of up to thousands of digits per number. It combines the double-precision capabilities of a floating-point-variable format with the basically unlimited string length of a literal-variable format to provide multiple-

NASA Tech Briefs, Winter 1985

precision results. The input and output are in literal format and are restricted only by machine limitations, time considerations, or a user-defined limit to the number of decimal places required. The use of PRECISION will prevent underflow and overflow in programs that generate extreme numbers such as probability theory, statistics, and scientific applications.

Basic PRECISION functions include addition, subtraction, multiplication, division, and integer powers. Extremely large or small numbers can be handled by use of a PRECISION function that converts them to standard scientific notation. PRECISION functions also exist for multiplication, division, and integer powers of numbers in scientific notation. A program is converted to PRECISION arithmetic by replacing +, -, *, and ÷ with the appropriate PRECISION operator.

PRECISION was written in APL for use with interactive or batch programs and has been implemented on a Honeywell Sigma-series computer with a central memory requirement of approximately 16K bytes. It was written in 1984.

This program was written by Leonard W. Howell and Marshall Patrick of Marshall Space Flight Center. For further information, Circle 63 on the TSP Request Card.
MFS-28048

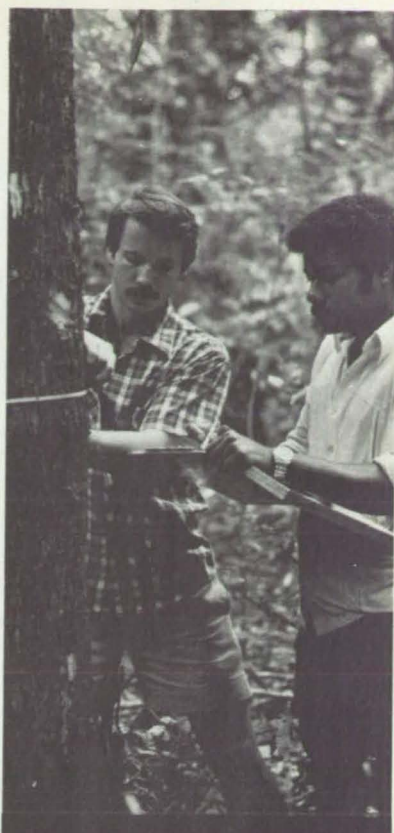
Printer Graphics Package

New symbols can be easily created from available symbols.

The Printer Graphics Package (PGP) is a tool for making two-dimensional symbolic plots on a line printer. PGP was created to support development of a Heads-Up Display (HUD) simulation, and many of its standard symbols were defined with the HUD in mind. Available symbols include the circle, triangle, quadrangle, window, line, numbers, and text. Additional symbols can be easily added or built up from available symbols. The user gains access to the PGP from a driver program. Output is a collection of line-printer plots 13 inches (33 cm) square. The available plotting area is 132 by 106 print positions.

The PGP routines are written in FORTRAN IV for batch execution and have been implemented on a CDC CYBER 70-series computer with a central memory requirement of approximately 52K (octal) of 60-bit words. The PGP routines were developed in 1984.

These routines were written by David C. Blanchard of McDonnell Douglas Corp. for Johnson Space Center. For further information, Circle 17 on the TSP Request Card.
MSC-20778



You have to
go a long way
to save a
tree in your
own backyard.

As a Peace Corps volunteer, you could help stop the deforestation that is affecting the world's environment.

The Peace Corps trains volunteers with forestry degrees or experience. Call toll-free 800-424-8580. And put your experience to work where it can do a world of good.

U.S. Peace Corps.
The toughest job
you'll ever love.

A Public Service of This Publication



Subject Index



A

ACOUSTIC MEASUREMENT
Miniature-microphone adapter page 138 LAR-13210

ADAPTERS
Miniature-microphone adapter page 138 LAR-13210

ADSORPTION
Adsorption of H₂, Ne, and N₂ on activated page 97 NPO-16329

AERODYNAMIC DRAG
Zero-lift wave drag of complex aircraft configurations page 150 LAR-13223

AERODYNAMICS
Numerical aerodynamic simulation facility page 175 ARC-11497

AGING (MATERIALS)
Constitutive equations of aging in polymers page 121 NPO-16480

AIR QUALITY
Detecting trace contaminants in the atmosphere page 86 NPO-16225

AIRCRAFT CONFIGURATIONS
Zero-lift wave drag of complex aircraft configurations page 150 LAR-13223

AIRCRAFT ENGINES
Microphone boom for aircraft-engine monitoring page 141 ARC-11495

AIRCRAFT HAZARDS
Water-thickness gage page 127 LAR-13342

AIRCRAFT INSTRUMENTS
Shaft axial-displacement sensor page 137 MFS-29048
Water-thickness gage page 127 LAR-13342

AIRCRAFT LIGHTS
Tester for distress beacons page 56 GSC-12892

AIRCRAFT NOISE
Noise-path measurements in aircraft structures page 145 LAR-13017

AIRCRAFT STRUCTURES
Noise-path measurements in aircraft structures page 145 LAR-13017

AIRFOIL THICKNESS
Water-thickness gage page 127 LAR-13342

ALGORITHMS
Maximum-likelihood, parameter-estimation algorithm page 168 NPO-16320

ALGORITHMS
System for automated troubleshooting page 166 NPO-16339

ALGORITHMS
Determining calibration constants for attitude measurements page 95 LAR-13214

AMIDES
Solvent-resistant, thermally stable poly(carbonate-imides) page 102 LAR-13292

ANALYZERS
Solid-state detector for trace materials page 88 NPO-16450

ANALYZERS
Detecting trace contaminants in the atmosphere page 86 NPO-16225

ANGULAR RESOLUTION
Obtaining one-degree

accuracy with shaft encoders page 44 LAR-13321

ANTENNA FEEDS
Cassegrain-antenna gain improvement page 48 NPO-16327

ANTENNAS
Cassegrain-antenna gain improvement page 48 NPO-16327
Measuring antenna signal delays page 70 NPO-15947

ARCHITECTURE (COMPUTERS)
Multiplier architecture for coding circuits page 74 NPO-16363

ATMOSPHERE SCATTERING
Accuracy of lidar measurements of the atmosphere page 96 NPO-16493

ATMOSPHERIC COMPOSITION
Nebulization reflux concentrator page 82 LAR-13254

ATMOSPHERIC IMPURITIES
Detecting trace contaminants in the atmosphere page 86 NPO-16225

ATMOSPHERIC PRESSURE
Microwave atmospheric-pressure sensor page 97 NPO-16496

ATOMIZERS
Mass spectrometer for airborne micro-organisms page 122 NPO-16359

ATOMS
Intense source of polarized-hydrogen atoms page 85 NPO-16434

AXIAL FLOW PUMPS
Peristaltic pump with a stable output page 158 MSC-20907

B

BATCH PROCESSING
Manipulation of numbers with many digits page 177 MFS-28048

BEACONS
Tester for distress beacons page 56 GSC-12892

BEARINGS
Bearing thermal performance prediction page 150 LEW-14163
Calculating bearing forces from strain-gage signals page 129 MFS-29000

BEDS (PROCESS ENGINEERING)
Agglomeration-free distributor for fluidized beds page 154 NPO-16466

BOOMS (EQUIPMENT)
Microphone boom for aircraft-engine monitoring page 141 ARC-11495

BORON FIBERS
Measuring resistivities of small fibers page 100 MFS-28077

BRaille
Braille reading systems page 135 LAR-13306

BRAKES (FOR ARRESTING MOTION)
Rotary speed sensor for antilocking brakes page 128 NPO-16479

BURNERS
Micronized-coal burner facility page 110 LEW-14131

C

CALIBRATING
Calibrating pressure transducers at cryogenic temperatures page 134 LAR-13242
Determining calibration constants for attitude measurements page 95 LAR-13214

CAPACITORS
Determining internal connections in capacitors page 60 NPO-16499

CARBON DIOXIDE LASERS
Zone refining by laser page 162 MFS-27084

CARBON FIBERS
Apparatus for sizing and rewinding graphite fibers page 164 LAR-13323
Measuring resistivities of small fibers page 100 MFS-28077

CASES (CONTAINERS)
Conductive container for semiconductor devices page 54 NPO-16110

CASSEGRAIN ANTENNAS
Cassegrain-antenna gain improvement page 48 NPO-16327

CAST ALLOYS
Solidifying cast iron in low gravity page 120 MFS-27069

CASTING
Cast iron with high carbon content page 118 MFS-28014

CATALOGS (PUBLICATIONS)
Equipment for microgravity research page 98 MFS-27094

CERAMICS
Beta silicon nitride whiskers page 118 NPO-16409
High-strength, low-shrinkage ceramic tiles page 113 MSC-20654

CHANNEL NOISE
Optimum cyclic redundancy codes for noisy channels page 168 NPO-16406

CHARCOAL
Adsorption of H₂, Ne, and N₂ on activated page 97 NPO-16329

CHIPS (ELECTRONICS)
Single-chip VLSI Reed-Solomon encoder page 67 NPO-16122

CIRCUIT PROTECTION
Conductive container for semiconductor devices page 54 NPO-16110

COAL
Micronized-coal burner facility page 110 LEW-14131

COAL UTILIZATION
Micronized-coal burner facility page 110 LEW-14131

COBALT
Cobalt ions improve the strength of epoxy resins page 111 LAR-13230

CODERS
Obtaining one-degree accuracy with shaft encoders page 44 LAR-13321
Single-chip VLSI Reed-Solomon encoder page 67 NPO-16122

COMPARATORS
Picture-element comparator page 77 NPO-16464

COMPRESSORS
Axial-flow compressor performance with water ingestion page 147 LEW-14026

Predicting the performance of an axial-flow compressor page 146 LEW-14025

COMPUTER GRAPHICS
Printer graphics package page 177 MSC-20778
Radiation view-factor program with interactive graphics page 148 LAR-13299

D

DECISION THEORY
Comparison of decision models page 175 NPO-16446

DECISIONS
Comparison of decision models page 175 NPO-16446

DEPOSITION
Inexpensive masks for film deposition page 165 NPO-16416

DESIGN ANALYSIS
Automated design synthesis page 147 LAR-13341
Dynamic effects of internal spur-gear drives page 161 LEW-14167

DETECTION
Molecular thermal-electron detectors page 85 NPO-16300

DIGITAL FILTERS
Convolver for pipelined-image processor page 66 NPO-16462

DIGITAL SIMULATION
Calculation of macrosegregation in an ingot page 98 MFS-27068
Design of linear quadratic regulators and Kalman filters page 79 LEW-14128
Dynamic effects of internal spur-gear drives page 161 LEW-14167
Flow through gas-turbine ducts page 147 LEW-14095
Four-cylinder Stirling engine control simulation page 148 LEW-14106
Solution of radiation and convection heat-transfer problems page 149 LAR-13978

DIGITAL SYSTEMS
Testing electronic devices for single-event upset page 69 NPO-16468

DIGITAL TECHNIQUES
Modular, fast, two-dimensional cyclic convolver page 63 NPO-16379

DISPLAY DEVICES
A quick visual power-supply monitor page 50 MFS-26014

DRILLING
Adjustable-angle drill block page 154 LAR-13101

DRILLS
Adjustable-angle drill block page 154 LAR-13101

DUCTED FLOW
Flow through gas-turbine ducts page 147 LEW-14095

COMPUTER PROGRAMS
Automated design synthesis page 147 LAR-13341
Bearing thermal performance prediction page 150 LEW-14163
Design of linear quadratic regulators and Kalman filters page 79 LEW-14128

Image-processing educator page 177 GSC-12933

Manipulation of numbers with many digits page 177 MFS-28048

Orbit transfer programs page 149 LEW-14089

Printer graphics package page 177 MSC-20778

Radiation view-factor program with interactive graphics page 148 LAR-13299

Software comparison page 176 MSC-20777

Three-dimensional, subsonic, turbulent juncture region flow page 150 LAR-13263

X-ray diffraction analysis program page 99 LAR-13276

Zero-lift wave drag of complex aircraft configurations page 150 LAR-13223

COMPUTERIZED SIMULATION
Numerical aerodynamic simulation facility page 175 ARC-11497
Soil/structure interactions in Earthquakes page 97 MFS-27078
Vibrational effects of turbopump housing flexibility page 160 MFS-27083

CONCENTRATORS
Nebulization reflux concentrator page 82 LAR-13254

CONSTITUTIVE EQUATIONS
Constitutive equations of aging in polymers page 121 NPO-16480

CONTROL
Numerical methods for classical sampled-system analysis page 176 GSC-12827

CONTROL SIMULATION
Numerical methods for classical sampled-system analysis page 176 GSC-12827

CONVECTION HEAT TRANSFER
Solution of radiation and convection heat-transfer problems page 149 LAR-13978

CORROSION
Accelerated stress-corrosion testing page 137 LAR-13337

CORROSION TESTS
Accelerated stress-corrosion testing page 137 LAR-13337
Accelerating corrosion in solar-cell tests page 60 NPO-16096

CRACK INITIATION
Accelerated stress-corrosion testing page 137 LAR-13337

CROP IDENTIFICATION
Compact imaging spectrometer page 91 NPO-16342

CRUCIBLES
Research furnace for crystal preparation page 114 LAR-13302

CRYOGENIC COOLING
Hydrogen refrigerator would cool below 10 K page 153 NPO-16393

CRYOGENIC WIND TUNNELS
Calibrating pressure transducers at cryogenic temperatures page 134 LAR-13242

CRYSTAL GROWTH
Research furnace for crystal preparation page 114 LAR-13302

CYLINDERS

Hydraulic cylinder with an integral position indicator
page 136 LAR-13095

E**EARTH ATMOSPHERE**

Accuracy of lidar measurements of the atmosphere
page 96 NPO-16493

EARTHQUAKES

Soil/structure interactions in Earthquakes
page 97 MFS-27078

ELASTOMERS

Mechanical design handbook for elastomers
page 119 LEW-14160

Ultra-high-molecular-weight silphenylene/siloxane polymers
page 117 MFS-27065

ELECTRIC CONTACTS

Accelerating corrosion in solar-cell tests
page 60 NPO-16096

Determining internal connections in capacitors
page 60 NPO-16499

ELECTRIC FIELD STRENGTH

Rotating capacitor measures steady electric fields
page 64 NPO-16550

ELECTRIC FIELDS

Rotating capacitor measures steady electric fields
page 64 NPO-16550

ELECTRIC HYBRID VEHICLES

Systems engineering of electric and hybrid vehicles
page 159 NPO-15871

ELECTRIC MEASUREMENT

Measuring thermoelectric properties automatically
page 106 NPO-16507

ELECTRIC POWER SUPPLIES

A quick visual power-supply monitor
page 50 MFS-26014

ELECTRIC PULSES

Generating independent preionizing pulses for lasers
page 42 NPO-16402

ELECTRIC TERMINALS

Determining internal connections in capacitors
page 60 NPO-16499

ELECTRICAL FAULTS

System for automated troubleshooting
page 166 NPO-16339

ELECTRICAL RESISTIVITY

Measuring resistivities of small fibers
page 100 MFS-28077

ELECTROMECHANICAL DEVICES

Braille reading systems
page 135 LAR-13306

GEARS

System for automated troubleshooting
page 166 NPO-16339

ELECTRONIC EQUIPMENT TESTS

Testing electronic devices for single-event upset
page 69 NPO-16468

ELECTRONS

Molecular thermal-electron detectors
page 85 NPO-16300

ELECTROSTATIC PRECIPITATORS

Improved electronic control for electrostatic precipitators
page 76 LAR-13273

ENGINE CONTROL

Four-cylinder Stirling engine control simulation
page 148 LEW-14106

ENGINES

Kinematic Stirling engine performance
page 99 LEW-14092

EPOXY COMPOUNDS

Ultrasonic mixing of epoxy curing agents
page 116 LAR-13307

EPOXY RESINS

Chromium ions improve moisture resistance of epoxy resins
page 104 LAR-13226

Cobalt ions improve the strength of epoxy resins
page 111 LAR-13230

ERROR ANALYSIS

System for automated troubleshooting
page 166 NPO-16339

ERROR DETECTION CODES

Optimum cyclic redundancy codes for noisy channels
page 168 NPO-16406

EXCIMER LASERS

Magnetically-switched, long-pulse XeCl laser
page 42 NPO-16410

Pulse coupling for laser excitation
page 40 NPO-16403

F**FABRICATION**

Colorless, transparent, aromatic polyimide films
page 108 LAR-13351

Controlling transistor temperature during burn-in
page 159 NPO-15871

FUEL TANKS

Fuel gage for sloshing tanks
page 133 LAR-13147

FUNCTION GENERATOR

Function generator for image processor
page 78 NPO-16461

FURNACES

Research furnace for crystal preparation
page 114 LAR-13302

G**GARMENTS**

Lightweight protective garments
page 115 NPO-16510

GAS ANALYSIS

Technique for measuring gas conversion factors
page 90 LAR-13220

GAS LASERS

Magnetically-switched, long-pulse XeCl laser
page 42 NPO-16410

GAS TURBINE ENGINES

Squeeze-film damper controls high vibrations
page 144 LEW-13506

GAS TURBINES

Flow through gas-turbine ducts
page 147 LEW-14095

GEARS

Dynamic effects of internal spur-gear drives
page 161 LEW-14167

GEOMETRY

Geometric representations for discrete Fourier transforms
page 167 MFS-27072

GRAPHITE

Apparatus for sizing and rewinding graphite fibers
page 164 LAR-13323

GUIDANCE SENSORS

Automatic guidance for remote manipulator
page 68 NPO-13386

H**HAMMERS**

Dent-removing tool
page 162 MFS-29044

HANDBOOKS

Mechanical design handbook for elastomers
page 119 LEW-14160

HEAT EXCHANGERS

Pumped, two-phase heat-transfer loop
page 152 MSC-20841

HEAT PIPES

Rotary joint for heat transfer
page 155 MFS-26015

Titanium heat-pipe wicks
page 141 MFS-26016

HEAT TRANSFER

Pumped, two-phase heat-transfer loop
page 152 MSC-20841

Rotary joint for heat transfer
page 155 MFS-26015

Solution of radiation and convection heat-transfer problems
page 149 LAR-13978

HEATING EQUIPMENT

Pumped, two-phase heat-transfer loop
page 152 MSC-20841

HOT ELECTRONS

Molecular thermal-electron detectors
page 85 NPO-16300

HUMIDITY

Low-cost humidity sensor
page 55 NPO-16544

HUMIDITY MEASUREMENT

Low-cost humidity sensor
page 55 NPO-16544

HYDRAULIC EQUIPMENT

Hydraulic cylinder with an integral position indicator
page 136 LAR-13095

HYDROCARBON COMBUSTION

Technique for measuring gas conversion factors
page 90 LAR-13220

HYDROGEN

Hydrogen refrigerator would cool below 10 K
page 153 NPO-16393

HYDROGEN ATOMS

Intense source of polarized-hydrogen atoms
page 85 NPO-16434

HYPERSONIC WIND TUNNELS

Fast-response oxygen-monitoring and control system
page 105 LAR-13257

I**IMAGE PROCESSING**

Convolver for pipelined-image processor
page 66 NPO-16462

Function generator for image processor
page 78 NPO-16461

Image-processing educator
page 177 GSC-12933

Picture-element comparator
page 77 NPO-16464

Programmable pipelined-image processor
page 77 NPO-16463

IMAGING TECHNIQUES

Compact imaging spectrometer
page 91 NPO-16342

Convolver for pipelined-image processor
page 66 NPO-16462

IMIDES

Solvent-resistant, thermally stable poly(carbonate-imides)
page 102 LAR-13292

INDUCTORS

Multiple-winding output inductors for power converters
page 49 NPO-16176

INFRARED LASERS

Generating tunable far-infrared laser sidebands
page 65 NPO-16497

INFRARED SPECTROMETERS

Compact imaging spectrometer
page 91 NPO-16342

Tracking system for infrared spectrometer
page 83 NPO-16440

INFRARED TRACKING

Tracking system for infrared spectrometer
page 83 NPO-16440

INGOTS

Calculation of macrosegregation in an ingot
page 98 MFS-27068

INSULATION

Insulation blankets for high-temperature use
page 107 ARC-11453

INTERNAL COMBUSTION ENGINES

Carbon/carbon pistons for internal combustion engines
page 156 LAR-13150

IONIZING RADIATION

Testing electronic devices for single-event upset
page 69 NPO-16468

IRON

Cast iron with high carbon content
page 118 MFS-28014

J**JACKETS**

Insulation blankets for high-temperature use
page 107 ARC-11453

K**KALMAN FILTERS**

Design of linear quadratic regulators and Kalman filters
page 79 LEW-14128

L**LAMINAR FLOW**

Smoothed two-dimensional edges for laminar flow
page 132 LAR-13255

LASER

Pulse coupling for laser excitation
page 40 NPO-16403

LASER DOPPLER VELOCIMETERS

Vibration-free Raman Doppler velocimeter
page 62 LAR-13268

LASER PUMPING

Hybrid laser would combine power with efficiency
page 93 NPO-16173

LASERS

Generating independent preionizing pulses for lasers
page 42 NPO-16402

Generating tunable far-infrared laser sidebands
page 65 NPO-16497

Hybrid laser would combine power with efficiency
page 93 NPO-16173

Improved waveguide

laser array
page 49 NPO-16500

Magnetically-switched, long-pulse XeCl laser
page 42 NPO-16410

Wedge fibers suppress feedback of laser beam
page 94 LAR-13074

Zone refining by laser
page 162 MFS-27084

LATCHES

Latch for telescoping structures
page 126 LAR-13169

Locking pull pin
page 131 NPO-16233

LEADING EDGE FLAPS

Smoothed two-dimensional edges for laminar flow
page 132 LAR-13255

LEVEL (HORIZONTAL)

Electronic/hydraulic level gage
page 139 MFS-28066

LIGHTNING

Plotting lightning-stroke data
page 80 MFS-26019

LINKAGES

Latch for telescoping structures
page 126 LAR-13169

LIQUID LEVELS

Liquid-level sensor for containers in motion
page 92 LAR-13327

LOADS (FORCES)

Calculating bearing forces from strain-gage signals
page 129 MFS-29000

LOGIC CIRCUITS

Multiplier architecture for coding circuits
page 74 NPO-16363

Picture-element comparator
page 77 NPO-16464

LOW GRAVITY MANUFACTURING

Cast iron with high carbon content
page 118 MFS-28014

LOW GRAVITY

Solidifying cast iron in low gravity
page 120 MFS-27069

M**MACHINE TOOLS**

Adjustable-angle drill block
page 154 LAR-13101

MAINTENANCE

Dent-removing tool
page 162 MFS-29044

MANIFOLDS

Advanced vapor-supply manifold
page 140 LAR-13259

MANIPULATORS

Automatic guidance for remote manipulator
page 68 NPO-13386

MASS SPECTROMETERS

Mass spectrometer for airborne micro-organisms
page 122 NPO-16359

MEASURING INSTRUMENTS

Electronic/hydraulic level gage
page 139 MFS-28066

Rotating capacitor measures steady electric fields
page 64 NPO-16550

MECHANICAL DRIVES

Dynamic effects of internal spur-gear drives
page 161 LEW-14167

MICROCOMPUTERS

Image-processing educator
page 177 GSC-12933

Measuring thermoelectric properties automatically
page 106 NPO-16507

MICROMODULES

Conductive container for semiconductor devices
page 54 NPO-16110

MICROORGANISMS

Mass spectrometer for airborne micro-organisms
page 122 NPO-16359

MICROPHONES

Microphone boom for aircraft-engine monitoring
page 141 ARC-11495

Miniature-microphone adapter
page 138 LAR-13210

MICROWAVE SENSORS

Microwave atmospheric-pressure sensor
page 97 NPO-16496

MICROWAVE SWITCHING

Microwave power combiner with switching diodes
page 46 NPO-15775

MINIATURE ELECTRONIC EQUIPMENT

Solid-state detector for trace materials
page 88 NPO-16450

MIXING

Ultrasonic mixing of epoxy curing agents
page 116 LAR-13307

MOISTURE METERS

Low-cost humidity sensor
page 55 NPO-16544

MOISTURE RESISTANCE

Chromium ions improve moisture resistance of epoxy resins
page 104 LAR-13226

MONITORS

A quick visual power-supply monitor
page 50 MFS-26014

Tester for distress beacons
page 56 GSC-12892

MOTOR VEHICLES

Rotary speed sensor for antilocking brakes
page 128 NPO-16479

MOUNTING

Reduced-stress mounting for thermocouples
page 58 NPO-16513

N**NAVIGATION AIDS**

Tester for distress beacons
page 56 GSC-12892

NEODYMIUM LASERS

Hybrid laser would combine power with efficiency
page 93 NPO-16173

NOISE MEASUREMENT

Noise-path measurements in aircraft structures
page 145 LAR-13017

NOISE REDUCTION

Reduction of vane noise in wind-tunnel nozzles
page 143 LAR-13333

NUMERICAL ANALYSIS

Ada[®] + PC

**General
Systems**

IT ADDS UP!

That's right, when you think of working with Ada on a PC you know the solution has to add up to be General Systems.

Why burden yourself with expensive systems when ours will cost less, compile faster, and be portable?

The heartbeat of our system is an Ada compiler (up to 3,200 lines per minute) and a circuit board that plugs directly into the expansion slot of your IBM PC, XT, AT or compatible machine.

Thinking of converting your system to Ada or simply trying to find a way of not tying up your Main Frame? Why not contact us to find out more about our Ada systems and our Ada instructors and programming pool.

*Ada is a registered trademark of the U.S. Government Ada Joint Program Office (AJPO)

IBM is a registered trademark of the International Business Machines Corporation.

**Complete
ADA Systems from \$2695.00***

*Includes Compiler

Call or write:
General Systems Corporation
P.O. Box 250
Ansonia, Connecticut 06401
(203) 776-8990

OPTIMIZATION
Automated design synthesis
page 147 LAR-13341

ORBITS
Orbit transfer programs
page 149 LEW-14089

OSCILLATION DAMPERS
Squeeze-film damper controls high vibrations
page 144 LEW-13506

OXYGEN
Fast-response oxygen-monitoring and control system
page 105 LAR-13257

OXYGEN ANALYZERS
Fast-response oxygen-monitoring and control system
page 105 LAR-13257

P

PARAMETRIZATION
Maximum-likelihood, parameter-estimation algorithm
page 168 NPO-16320

PERFORMANCE PREDICTION
Bearing thermal performance prediction
page 150 LEW-14163

Kinematic Stirling engine performance
page 99 LEW-14092

PHENOLIC EPOXY RESINS
Phenoxy resins containing pendent ethynyl groups
page 109 LAR-13222

PHENOLIC RESINS
Phenoxy resins containing pendent ethynyl groups
page 109 LAR-13222

PHOTOVOLTAIC CELLS
Floating-emitter solar-potting compounds
page 112 MFS-27047

cell transistor
page 56 NPO-16467

PINS
Locking pull pin
page 131 NPO-16233

PIPELINING (COMPUTERS)
Programmable pipelined-image processor
page 77 NPO-16463

PIPES (TUBES)
Titanium heat-pipe wicks
page 141 MFS-26016

PISTONS
Carbon/carbon pistons for internal combustion engines
page 156 LAR-13150

PLOTTERS
Plotting lightning-stroke data
page 80 MFS-26019

POLYCARBONATES
Solvent-resistant, thermally stable poly(carbonate-imides)
page 102 LAR-13292

POLYIMIDES
Colorless, transparent, aromatic polyimide films
page 108 LAR-13351

POLYMER PHYSICS
Constitutive equations of aging in polymers
page 121 NPO-16480

POLYMERIC FILMS
Colorless, transparent, aromatic polyimide films
page 108 LAR-13351

POLYMERIZATION
Ultra-high-molecular-weight silphenylene/siloxane polymers
page 117 MFS-27065

POSITION INDICATORS
Hydraulic cylinder with an integral position indicator
page 136 LAR-13095

POTTING COMPOUNDS
Alkane-based urethane

page 56 NPO-16467

POWER CONVERTERS
Multiple-winding output inductors for power converters
page 49 NPO-16176

POWER SUPPLY CIRCUITS
Control electronics for solar/flywheel power supply
page 57 MFS-25978

Microwave power combiner with switching diodes
page 46 NPO-15775

PRECIPITATORS
Improved electronic control for electrostatic precipitators
page 76 LAR-13273

PRESSURE SENSORS
Calibrating pressure transducers at cryogenic temperatures
page 134 LAR-13242

Microwave atmospheric-pressure sensor
page 97 NPO-16496

PRESSURE VESSELS
Stiffness study of wound-filament pressure vessels
page 145 MFS-27086

PRINTERS (DATA PROCESSING)
Printer graphics package
page 177 MSC-20778

PROTECTIVE CLOTHING
Lightweight protective garments
page 115 NPO-16510

PULSE GENERATORS
Generating independent preionizing pulses for lasers
page 42 NPO-16402

Pulse coupling for laser excitation
page 40 NPO-16403

PUMPS
Calculating flow-angle deviation in rotary pumps
page 157 MFS-29062

Peristaltic pump with a stable output
page 158 MSC-20907

Rough/smooth rotary seal
page 157 MFS-19947

PURGING
Advanced vapor-supply manifold
page 140 LAR-13259

R

RADIATION DAMAGE
Testing electronic devices for single-event upset
page 69 NPO-16468

RADIATIVE HEAT TRANSFER
Solution of radiation and convection heat-transfer problems
page 149 LAR-13978

RATINGS
Comparison of decision models
page 175 NPO-16446

REFRIGERATORS
Hydrogen refrigerator would cool below 10 K
page 153 NPO-16393

REMOTE MANIPULATOR SYSTEM
Automatic guidance for remote manipulator
page 68 NPO-13386

RESEARCH FACILITIES
Numerical aerodynamic simulation facility
page 175 ARC-11497

ROTATING SHAFTS
Obtaining one-degree accuracy with shaft encoders
page 44 LAR-13321

Shaft axial-displacement sensor
page 137 MFS-29048

S

SANDWICH STRUCTURES
Thermal-diode sandwich panel
page 142 LAR-13121

SEALS(STOPPERS)
Rough/smooth rotary seal
page 157 MFS-19947

SEISMOGRAPHS
Determining calibration constants for attitude measurements
page 95 LAR-13214

SEMICONDUCTOR DEVICES
Conductive container for semiconductor devices
page 54 NPO-16110

SIGNAL MEASUREMENT
Measuring antenna signal delays
page 70 NPO-15947

SIGNAL PROCESSING
Modular, fast, two-dimensional cyclic convolver
page 63 NPO-16379

SIGNAL TRANSMISSION
Optimum cyclic redundancy codes for noisy channels
page 168 NPO-16406

SILICON NITRIDES
Beta silicon nitride whiskers
page 118 NPO-16409

SIZING (SURFACE TREATMENT)
Apparatus for sizing and rewinding graphite fibers
page 164 LAR-13323

SOLAR CELLS
Accelerating corrosion in solar-cell tests
page 60 NPO-16096

Floating-emitter solar-cell transistor

SOLAR GENERATORS
Control electronics for solar/flywheel power supply
page 57 MFS-25978

SOLIDIFICATION
Calculation of macrosegregation in an ingot
page 98 MFS-27068

Solidifying cast iron in low gravity
page 120 MFS-27069

SOLOMON COMPUTERS
Single-chip VLSI Reed-Solomon encoder
page 67 NPO-16122

SPACE TOOLS
Equipment for microgravity research
page 98 MFS-27094

SPECTROMETERS
Compact imaging spectrometer
page 91 NPO-16342

SPEED INDICATORS
Shaft axial-displacement sensor
page 137 MFS-29048

STIFFNESS
Stiffness study of wound-filament pressure vessels
page 145 MFS-27086

STIRLING CYCLE
Four-cylinder Stirling engine control simulation
page 148 LEW-14106

Kinematic Stirling engine performance
page 99 LEW-14092

STRAIN GAGES
Calculating bearing forces from strain-gage signals
page 129 MFS-29000

SUBSONIC FLOW
Three-dimensional, subsonic, turbulent juncture region flow
page 150 LAR-13263

SURVEYS
Electronic/hydraulic level gage page 139 MFS-28066

SWITCHING CIRCUITS
Microwave power combiner with switching diodes page 46 NPO-15775

SYNTHETIC APERTURE RADAR
Modular, fast, two-dimensional cyclic convolver page 63 NPO-16379

SYNTHETIC RUBBERS
Ultra-high-molecular-weight silphenylene/siloxane polymers page 117 MFS-27065

SYNTHESIZERS
Keyboard with voice output page 54 MSC-20869

SYSTEMS ENGINEERING
Systems engineering of electric and hybrid vehicles page 159 NPO-15871

T

TANKS (CONTAINERS)
Liquid-level sensor for containers in motion page 92 LAR-13327

TEMPERATURE MEASUREMENT
Determining the temperature profile in a cylindrical sample page 84 MFS-26013

TEMPERATURE PROFILES
Determining the temperature profile in a cylindrical sample page 84 MFS-26013

TESTS
Distributing radiant heat

in insulation tests page 131 MSC-20878

THERMAL INSULATION
Distributing radiant heat in insulation tests page 131 MSC-20878

High-strength, low-shrinkage ceramic tiles page 113 MSC-20654

Insulation blankets for high-temperature use page 107 ARC-11453

Thermal-diode sandwich panel page 142 LAR-13121

THERMAL PROTECTION
Thermal-diode sandwich panel page 142 LAR-13121

THERMAL RADIATION
Radiation view-factor program with interactive graphics page 148 LAR-13299

THERMAL VACUUM TESTS
Distributing radiant heat in insulation tests page 131 MSC-20878

THERMOCOUPLES
Reduced-stress mounting for thermocouples page 58 NPO-16513

THERMOELECTRICITY
Measuring thermoelectric properties automatically page 106 NPO-16507

THIN FILMS
Inexpensive masks for film deposition page 165 NPO-16416

TILES
High-strength, low-shrinkage ceramic tiles page 113 MSC-20654

TOOLS
Dent-removing tool page 162 MFS-29044

TRACE ELEMENTS
Solid-state detector for

trace materials page 88 NPO-16450

TRACKING (POSITION)
Tracking system for infrared spectrometer page 83 NPO-16440

TRANSFER ORBITS
Orbit transfer programs page 149 LEW-14089

TRANSISTORS
Controlling transistor temperature during burn-in page 52 MFS-28076

TRANSISTORS
Floating-emitter solar-cell transistor page 56 NPO-16467

TUNABLE LASERS
Generating tunable far-infrared laser sidebands page 65 NPO-16497

TURBINE ENGINES
Photo-optical blade-vibration-data acquisition system page 130 LEW-12887

TURBINE PUMPS
Rough/smooth rotary seal page 157 MFS-19947

Vibrational effects of turbopump housing flexibility page 160 MFS-27083

TURBOCOMPRESSORS
Axial-flow compressor performance with water ingestion page 147 LEW-14026

Predicting the performance of an axial-flow compressor page 146 LEW-14025

TURBOMACHINE BLADES
Photo-optical blade-vibration-data acquisition system page 130 LEW-12887

TURBOSHAFTS
Shaft axial-displacement

sensor page 137 MFS-29048

TURBULENT FLOW
Three-dimensional, subsonic, turbulent junction region flow page 150 LAR-13263

TYPEWRITERS
Keyboard with voice output page 54 MSC-20869

U

ULTRASONIC AGITATION
Ultrasonic mixing of epoxy curing agents page 116 LAR-13307

URETHANES
Alkane-based urethane potting compounds page 112 MFS-27047

V

VALVES
Advanced vapor-supply manifold page 140 LAR-13259

VELOCITY MEASUREMENT
Vibration-free Raman Doppler velocimeter page 62 LAR-13268

VIBRATION DAMPING
Squeeze-film damper controls high vibrations page 144 LEW-13506

VIBRATION EFFECTS
Vibrational effects of turbopump housing flexibility page 160 MFS-27083

VIBRATION MEASUREMENT
Photo-optical blade-vibration-data acquisition system page 130 LEW-12887

VIBRATION SPECTRA
Maximum-likelihood, parameter-estimation algorithm page 168 NPO-16320

VIDEO DATA
Programmable pipelined-image processor page 77 NPO-16463

VOICE
Keyboard with voice output page 54 MSC-20869

VOLTAGE CONVERTERS (DC TO DC)
Multiple-winding output inductors for powerconverters page 49 NPO-16176

W

WATER DEPTH
Water-thickness gage page 127 LAR-13342

WATER INJECTION
Axial-flow compressor performance with water ingestion page 147 LEW-14026

WATERPROOFING
Chromium ions improve moisture resistance of epoxy resins page 104 LAR-13226

WAVEGUIDE LASERS
Improved waveguide laser array page 49 NPO-16500

WEIGHTLESSNESS
Preadapting to weightlessness page 124 MSC-20847

WEIGHTLESSNESS SIMULATION
Preadapting to weightlessness page 124 MSC-20847

WIND TUNNEL NOZZLES
Reduction of vane noise in wind-tunnel nozzles

page 143 LAR-13333

WIND TUNNELS
Reduction of vane noise in wind-tunnel nozzles page 143 LAR-13333

WING TANKS
Fuel gage for sloshing tanks page 133 LAR-13147

WINGS
Smoothed two-dimensional edges for laminar flow page 132 LAR-13255

X

X-RAY DIFFRACTION
X-ray diffraction analysis program page 99 LAR-13276

Z

ZIRCONIUM OXIDES
Fast-response oxygen-monitoring and control system page 105 LAR-13257

ZONE MELTING
Zone refining by laser page 162 MFS-27084

Are You a Subscriber?

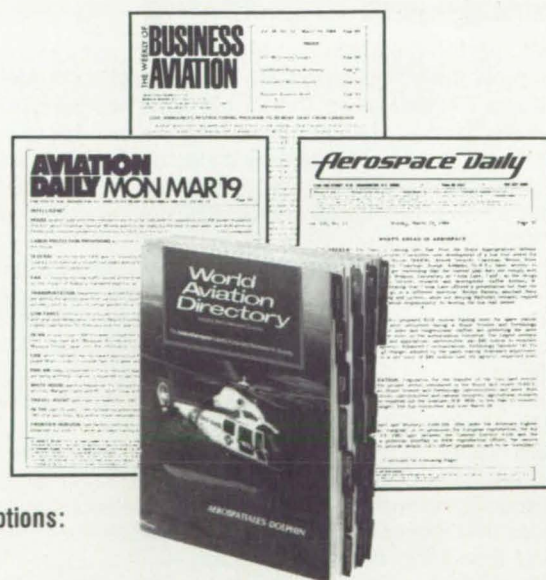
The most relied-upon
"intelligence/communications"
network serving the
aviation/aerospace industry
worldwide.

Write on company letterhead or call for FREE trial subscriptions:

- 3 weeks of Aerospace Daily
- 30 day inspection of World Aviation Directory
- 3 weeks of Aviation Daily
- 4 weeks of Business Aviation
- Plus 1 month test of Aerospace Online*

*Aerospace Daily is now on-line as part of a comprehensive network of electronic databases called **Aerospace Online**. Call 202-822-4691 for a one month test at only a nominal cost.

1156 15th St., NW • Washington, DC 20005 • 202-822-4600



A FRAMEWORK FOR ACTION: Improving Quality and Productivity in Government and Industry

The following recommendations were drafted at the 1984 NASA-sponsored "Symposium on Quality and Productivity: Strategies to Improve Operations in Government and Industry." They represent the collective wisdom of the more than 650 top executives from major American corporations, government agencies and universities who attended the symposium, which focused on the challenge of improving quality and productivity through effective managerial practices.

The major findings of the symposium are organized into nine themes, three of which were presented on pages 186—191 of the Fall 1985 issue of NASA TECH BRIEFS. In this issue, we continue our presentation with themes four through six. (The remaining three themes will be presented in a future issue.) Each theme encompasses a set of recommended actions and management practices that have been shown to contribute to high quality and productivity—organizational imperatives in this era of the increasingly competitive global marketplace.

THEME 4: Make Innovation Rewarding: Encouraging Innovation and Risk-Taking

Maintaining the creativity and the risk-taking attitude that make an organization successful is a major task of maturing organizations. It is well known that innovation is key to organizational survival in a fast changing economy. The true risk for any organization is to believe risk-taking is unnecessary for long-term survival. Management needs to recognize the proper place for innovation and risk-taking and create an environment that supports and rewards it.

"... One essential step in renewing an organization is to set up a system for the care and feeding of innovators... a sponsor... proper awards... and the need to know what will happen to them if they fail..." (Lewis Lehr, 3M Company)

Organizations typically go through a life cycle. When they are young, they are characterized by flexibility and innovation, and are usually staffed by a group of people with a strong drive for success. As they expand and mature, organizations tend to become specialized and segmented. Informal dialogue tends to be replaced by a preoccupation with formal policy and control. Instead of designing for success, Lehr points out, mature organizations tend to be more concerned with avoiding errors. "Playing it safe" becomes paramount. George Seegers of Citibank, N.A., describes the fate of Central Leather, once the nation's 24th largest company:

"Central Leather failed to adopt new shoemaking techniques and equipment, and some time ago took its rightful place in the graveyard of companies that decided to 'play it safe!'"

Survival in today's economy depends on an organizational philosophy that nurtures risk-taking and innovation.

"... companies that take risks generally prosper. The *true* risk for any company is to believe that risk-taking is unnecessary for long-term growth and survival." (Seegers)

Recommendation 4.1 Provide a Climate for Creativity

Lehr identifies three considerations in the care and feeding of innovators. First, they need a sponsor who can help obtain resources and shield the project if it falters. Second, innovators should be appropriately rewarded according to individual values. IBM's Corporate Fellows Program provides one example. Fellows are free to roam the company to select problems that interest them. The third consideration is the cost of failure. Innovators must be assured that failed projects will not cost them their jobs.

Harold Edmondson of Hewlett-Packard describes a supportive climate for innovation as one that allows people to be creative, challenges the person by providing progressively more demanding creative experiences, provides direction for creative energy, provides measures for assessing success, and provides tangible rewards, e.g., status, resource support and peer awards.

"Zealous volunteer champions. Innovators. Quite simply, they are *the key* to renewal in an organization. And we don't even need to look for them. They'll find us if we let them." (Lehr)

Recommendation 4.2 Recognize the Place for Risk-Taking

Innovation is not equally applicable or desirable in all parts of an organization. Furthermore, innovation is frequently accompanied by risk and additional costs. Management must therefore decide when these risks and costs are warranted by the potential gains. As Seegers points out:

"The first lesson to be learned is that you must have a detailed, well-thought-out template... for reaching your objective. The second is that you have to know when to follow the plan, and when to ignore parts of it... What every large

organization—and especially the government—needs is periodic reviews of all activities, just to make sure that an obvious, somewhat risky, but better way of doing things is not being overlooked.”

The timing of innovation is also important. Should the focus be at the early stage of a project, a later stage, or should one strive for innovation throughout the process? The answer can be derived only from a well-thought-out business strategy which explicitly addresses the areas in which innovation in product or process is appropriate. John Franke of the U.S. Department of Agriculture had an interesting point of view on the benefits of some risk-taking.

“Stirring the pot upsets and causes some disruption. But we feel the disruption is worth it. It provides the energy for new approaches and new methods.”

THEME 5: Build Dedication, Pride and Team Effort: Promoting Participative Management

Successful organizations have a very high level of performance “over and above” that expected from their employees. Management needs to encourage and provide positive support for employee participation to maintain organization vigor. Middle management anxieties need to be addressed in this process, and mechanisms such as employee suggestion programs and quality circles should be used to sustain high levels of employee participation, so that employees feel committed and involved in the organization’s success.

“The spirit of entrepreneurship may start at the top, but it is the middle levels where the attention to detail and commitment to quality make or break an entrepreneurial dream.” (George Seegers, Citibank, N.A.)

Organizations that face strong competitive and budgetary challenges are forced to make full use of all resources. Although most organizations give lip-service to the slogan that people are their most important resource, management actions often tell a different story. Many employees are inhibited from making contributions to quality and productivity because they are not encouraged by management to participate in planning for improvements, problem solving, and other work-related decisions. Nevertheless, employees on the shop floor, in the office areas, and at various levels of management are extremely knowledgeable about their work and are aware of task-related problems.

Employees who are allowed to participate in decision-making have a commitment to make those decisions work. Participation gives an employee the opportunity to learn and master the environment as well as the chance to be recognized for making a contribution.

“Forty-one thousand suggestions, 17 thousand adopted. \$52 million saved. People just naturally become more productive when they are given something to live for, work for, and hope for.” (Malcolm Stamper, The Boeing Company)

Recommendation 5.1 Make a Long-Term Commitment to Participative Management

“The basic philosophy behind our way of doing things is to recognize that the employee on the job is often the best fitted to give advice about how to do that job. . . . Just being involved in carrying out the tasks of a company without ever having a voice in the development of policies or procedures is not sufficient participation.” (John Felton, McCormick & Co.)

The journey toward a participative organization begins with a clear commitment to the philosophy of involving people as a “way of doing business.” This commitment must start at the top, representing a long-term dedication which is conveyed in words and in accord with the organizational structure and systems.

The Dana Corporation management explains its company phil-

osophy, “The Dana Style,” in a handout given to all employees:

“The people of Dana, who are doing the job, know best how it should be done and they share the responsibility to decide what their job is, and to judge how well it is done.”

(Carl Hirsch, Dana Corporation)

In a unionized environment, the commitment to participation will necessarily involve the joint actions of management and labor and may be institutionalized through the collective bargaining process. In order to succeed, however, according to Jack Sheinkman of the Amalgamated Clothing and Textile Workers Union, union and management must view each other as equal partners in a long-term effort. He further notes that contractual agreements must include an explicit provision that the productivity improvement program will not lead to layoffs and will neither undermine nor supplant collective bargaining, but rather extend the process.

Recommendation 5.2 Build Supportive Management Structures and Policies

There is a wide range of employee involvement techniques: e.g., suggestion systems, quality circles, multiple management, labor management committees and employee stock ownership plans. The particular form chosen to elicit employee participation does not appear to be as important as the fact that some structured process exists and that the process enjoys a broad base of support among those affected. Participative processes are implemented in accordance with the unique characteristics of each organization; there are no formulas or ready-made programs to guarantee success.

Mechanisms that encourage the flow of communication to upper management tend to increase commitment to the job and promote high levels of motivation.

“More than anything else, quality or excellence stem from the people of an organization: their motivation, their drive and, most importantly, the way they relate to one another.”

(John Jackson, IBM)

Once the commitment has been made to move toward a more participative organization, a supportive management structure must be put into place. According to Charles Joiner, Mead Corporation, this may mean reducing the levels of management, broadening the span of control and reducing staff:

“It is important to entrust a person with the job and then trust him/her to do it without unneeded bureaucratic red tape or management hierarchy.”

In the early stages, participation alone may be enough to sustain a participative management style. In the long run, though, to sustain high levels of participation, organizations must make it clear to employees how the fruits of their participation are distributed.

“Our stock purchase plan gets people to identify with Dana by making them owners of the company. Last year Dana people put out \$17 million of their own money (along with \$5 million in Dana’s matching contributions) to buy 846,000 shares of stock.” (Hirsch)

Other means of rewarding employees include bonuses, management recognition and enhancing status. Unfortunately, when organizations attempt to provide a more participative organizational climate, performance appraisal systems, promotion and compensation systems and other controls may, unless modified, work in opposition to these goals. Management must periodically review these systems to ensure that they support participative management if this philosophy is to become institutionalized.

Recommendation 5.3 Address the Concerns of Middle Managers

Over the long run, no participative management process can be sustained without the involvement and support of middle managers. What is this “middle management problem”? Throughout this report, we have discussed the need to involve top management in launching any quality/productivity effort. As David Hamilton from Intel put it:

"Senior management must set realistic goals for productivity improvement throughout . . . and be willing to hold middle management accountable for performance against these goals."

Gaining enthusiastic support among rank-and-file employees generally presents few problems. Unfortunately, the benefits to be derived from a productivity effort are not so readily apparent to middle management, for they tend to perceive themselves as being held accountable for a process over which they exercise little control. Moreover, middle managers may grumble that their role in the decision-making process has been usurped, at least until they become sufficiently involved in carving out a new relationship with employees.

One barrier to this support is lack of skill in operating in this "new" mode. McCormick and Company has solved this problem through a well-established program called multiple management. This involves giving middle managers a greater voice in running the business through the establishment of "junior" boards of directors.

"The result at McCormick was small teams of employees meeting regularly on a voluntary basis to identify, to analyze, and to solve work-related problems—real company problems involving packaging, product development, productivity, cost reduction, distribution, sales, quality and inventory control." (Felton)

When introducing participative management processes, considerable effort should be devoted to identifying and confronting the fears and concerns of middle managers. For example, is it realistic to expect middle management support if top management does not allow middle managers to participate in decisions that affect them?

THEME 6: Uncork Individual Talent: Controlling Bureaucracy

As successful organizations mature, they tend to become preoccupied with controls and checks that are narrowly focused, parochial and inflexible. This process results in overregulation of activity, discourages initiative and slows down responsiveness to changing conditions. Management needs to thwart this tendency through decentralization and by providing freedom and protection for its innovators.

"Pushing responsibility to the farthest point of the organization is the best way to make entrepreneurship a reality." (Carl Hirsch, Dana Corporation)

Organizational barriers that inhibit entrepreneurship need to be broken. The true purpose of an organization is to support the individuals within it so they can be responsive to the organization's goals and be innovative and effective. Experience has shown that as successful organizations mature, there is a tendency for bureaucratic symptoms to begin to erode the organization's effectiveness. Typically, it becomes preoccupied with controls and checks that are narrowly focused, parochial and inflexible. This maturation process, if unabated, leads to organizational decline as it loses the ability to adapt to the needs of the customers and meet the challenges of technology and the growth of competition.

"In any organization, the inertia is on the side of those who play it safe . . . Bureaucracy begins when people are less concerned with being right than with not being found wrong." (George Seegers, Citibank, N.A.)

Government laws, rules and regulations also have impeded the ability of organizations to remain flexible and adapt to change.

Recommendation 6.1 Increase Employee Initiative Through Decentralization

F. Blake Wallace describes how GM is dealing with the bureaucracy issue:

"Decentralization is what our new GM organization is all

about. We've got to move faster in designing new products and bringing them to market. We've got to cut out bureaucracy, eliminate redundancy, and make more efficient use of our people. And probably most important of all, we've got to uncork individual talent . . . by giving our people the opportunity to take risks, assume responsibility . . . and earn rewards." (Wallace, quoting General Motors Chairman Roger Smith)

It is possible for management to thwart the bureaucratic symptoms of maturing organizations through decentralization and by providing greater freedom for the innovators. Managers must examine the given tasks and structure of an organization in such a way that the people who are supposed to make it work have the best chance to do so. The danger can be in placing people in various slots simply because it supports some form of an organization, whether it is effective or not. Often in bureaucracies, performance at lower organizational levels is hampered by the need to check with multiple layers of management before a decision can be made. This stifles individual motivation, initiative and creativity. Arlene Triplett of the U.S. Office of Management and Budget describes a government field manager's frustration:

"One of the problems with productivity in the government is that the poor guys out there in the field trying to deliver services to the taxpayers have to go through five and six layers of management before they can get simple decisions like, 'Can I replace my secretary? Can I buy a file cabinet?'"

Recommendation 6.2 Resist the Tendency to Overregulate, and Provide Incentives for Productivity Improvement

"For all the tools we have tried and texts we have studied, the real secret to improved productivity in our society is that simple but all-elusive commodity, plain old-fashioned *trust*—confidence in people and faith in their integrity." (Malcolm Stamper, The Boeing Company)

An example of overregulation in the Federal procurement process was discussed by John Mittino, who described the Department of Defense's efforts during the last three and a half years to improve productivity with its contractors. This effort began with 32 initiatives to shorten and simplify the acquisition process. At the present time, priority is being given to six management areas which Mittino says provide the greatest challenge and the greatest potential payback. These areas include: program stability, multi-year procurement, economic production rates, realistic budgeting, support and readiness, and competition.

Another example of continuing DoD efforts to enhance contractor quality and productivity is through the use of contract incentives in its Industrial Modernization Incentives Program. NASA also is using the contractual process to encourage improved contractor performance.

"Incentive contracts have always been our primary tool to motivate business in the R&D environment. We are now placing increasing reliance on this controversial tool to focus on developing even more innovative and cost-effective ways of doing business." (Gerald Griffin, Johnson Space Center)

Griffin further stated that 15-year contracts were planned to give contractors the opportunity to introduce long-range improvements. Later on, a fixed-price contract is envisioned to inject greater productivity and cost consciousness incentives. These new contracts will allow NASA to delegate extensive management responsibilities to the contractor as NASA reduces its day-to-day involvement in operations support.

In his review of initiatives undertaken by the President's Commission on Industrial Competitiveness, Executive Director Egils Milbergs outlined some components of a recently passed bill which will "modify the antitrust laws to permit precompetitive R&D ventures." A central goal is to reduce paperwork and costs for industry and government. □

Look for more on quality and productivity in the next issue of NASATech Briefs.



Sperry Opportunities

Sperry and the future in Space: You have the choice.

Sperry's Space Systems Division has openings for aerospace professionals who want to help us meet the challenges of tomorrow's space business. Join us in working with advanced programs for NASA, DoD and space commercialization.

Advanced Systems Development

Lead the development of front-end concepts and innovative designs. Positions are available in both spacecraft and payload system technology in the areas of **Mission Analysis, Communications, Guidance & Control, Optics and Signal Processing.**

Program Development

Apply your technical background and business development skills to NASA and defense programs.

Your responsibilities will include customer contact, applications engineering and technical marketing and planning.

Make the right Choice

If you have prior space experience or related qualifications and are ready to help us develop future space business, send your resume and salary history, in confidence, to Clarence Williams, Sperry (NASA-E636), M/S DV5C, P.O. Box 21111, Phoenix, AZ. 85036.



Equal Employment Opportunity/Affirmative Action Employer
U.S. citizenship is required.

Letters

The "Letters" column is designed to encourage a wide exchange of ideas among *NASA Tech Briefs* readers. To contribute a request for information or to respond to such a request, use the feedback cards in this issue, or write or call: Manager/Technology Transfer Division, P.O. Box 8757, Baltimore/Washington International Airport, MD 21240; (301) 859-5300. While we can print only a small number of letters, we will endeavor to select those that are varied and of wide interest.

TANSTAAFL'S LAST STAND

Thank you for reprinting TANSTAAFL in the Summer 1985 issue of *NASA Tech Briefs*. Many of my associates have enjoyed receiving copies and passing them around.

The thing that's ironic is that not one in a thousand of us who read TANSTAAFL will admit that we may be part of the problem, performers in the government circus, at best, and possibly workfare recipients, at worst.

Circuses and space programs are wonderful things. Both improve the quality of life. But how much of either is enough can only be decided by the free market, and any industry that exists largely on government subsidization is sure to provide more of its commodity than we need, most likely where we need it least.

When government provides free circuses, we should all ask, "Instead of what?" TANSTAAFL.

Andrew E. Barniskis
Principal Consultant
Applied Dynamics and Ballistics Co.
Levittown, PA

TECH BRIEFS AT WORK

Just read my first copy of NTB—Summer 1985, Vol. 9, No. 2. How refreshing! One of the most stimulating publications I've seen in years.

Having migrated from technical engineering into managerial work over the years, I had concluded that technology had passed me by. Your magazine restores my confidence; even I am able to understand most of it. Your editors do communicate well.

I was particularly delighted by the article "Low Friction Joint For Robot Fingers," page 140. When I was a youngster building model airplanes, 35 years ago, this same concept worked well for control surface hinges. Our design motivation then, however, was not low friction. We couldn't afford model shop hinges.

Thanks for an excellent publication.

R.E. Hine
Clinton, TN

I depend on Tech Briefs to keep me updated on solar power research and to catalyze creative thought in solar as well as other technical areas. I have used Tech Briefs as a source of information for advising builders and contractors of residential homes for years. I generally find your publication most helpful.

James F. Long
VP Research & Dev.
Seaborn, Inc.
Freeport, FL

The availability of the report "Predicting Leakage in Labyrinth Seals" (NTB, Summer '85, p. 149) is of particular interest, because we regularly supply lip seals and flow re-

strictor bushings along with our mechanical seals. Because of our test lab work load, we don't have time to test a lot of "small hardware," so the information on calculating labyrinth flow should help us in predicting bushing behavior. We can also compare it with our own equations, which are developed in-house. The lip seal report may provide us with an alternate auxiliary sealing method.

Rich Piccirilli
Borg-Warner
Temecula, CA

I like your new format and current style. *NASA Tech Briefs* has helped solve or suggested solutions to many problems too numerous to mention here.

Alvord Rubino
Senior Design Engineer
Budd Lake, NJ

I have been selecting material for stress measurements at cryogenic temperatures in biological materials. *NASA Technical Support Packages* have supplied necessary data on stainless steel dimensional changes at low temperatures.

Jerry D. Leaf
Research Associate
UCLA Medical Center
Los Angeles, CA

From each issue of *NASA Tech Briefs*, certain tech briefs are selected because they are likely to have either direct or indirect impact on our processes or products. These tech briefs are then circulated among key people who are involved with the specific technology.

Normand L. Peterson
Technical Specialist
Hercules Inc.
Magna, UT

Your articles on engine efficiencies have aided in the development of modifications, designed and built by us for use on large and small gasoline and diesel engines.

Anthony Petrone
Petrone's Automotive Supplies
Erie, PA

Recently I was designing a low-power battery back-up supply for a communications terminal. An auto-reset circuit breaker at 24VDC to react at 5 Amp was required, which was not available on the open market. I was introduced to *NASA Tech Briefs* and found the DC solid state circuit breaker and requested the information package (MFS-25172). The circuit derived from this information worked perfectly in the prototype and the design package was accepted. Thanks again.

Dale A. Richardson
Tracor Applied Sciences
Virginia Beach, VA

WANTED: LAMBERTIAN REFLECTOR

We are looking for a white Lambertian reflector for use in niyag lasers with a binder that does not degrade in the presence of UV light.

D. Hatchfield
Coherent General, Inc.
Sturbridge, MA

For help in finding the Lambertian reflector, we suggest you contact the *NASA Industrial Applications Center* nearest you. These Centers offer computerized access to a comprehensive collection of scientific

and technical documents produced by *NASA*, by other government agencies, and by corporate and academic research organizations around the world. Each Center also has a professional staff that can help you evaluate your information needs and assist you with solutions to specific technical problems. For the location of the *Industrial Applications Center* nearest you, see page 29, this issue.

ONE MORE TIME

We have completed the *NASA Tech Briefs* subscription request form, at your request, nine times in the last year and a half.

Why is this necessary? Please respond!

T. Pappan
Technology Transfer
Corunna, MI

The recent commercialization of *NASA Tech Briefs* makes it necessary for subscribers to complete a qualification form once a year in order to continue to receive our free publication.

Our records indicate that you were deleted from our mailing list in early 1984 due to a late return of a recircularization form. Since then you have returned two incomplete subscription requests. Though you are on our mailing list, it is necessary for you to complete the subscription form in its entirety once a year in order to continue your free subscription.

We hope to have your understanding for this requirement and apologize for any inconvenience caused by such a request. We are forwarding all *NASA Tech Briefs* you conceivably might have missed in the last 18 months.

Editor's Note: *NASA Tech Briefs* will make every effort to inform subscribers well in advance that they need to complete a new qualification form, and to insure that they continue to receive *NASA Tech Briefs* without interruption. In return, we ask that you complete the form after the first request to do so.

CORRECTIONS

First the good news: I like the new *NASA Tech Briefs*. They're a big improvement over the old ones.

Now the "questionable" news: a five-jewel propulsed laser? Is that anything like a five-jewel watch?

Are you sure you don't mean five-joule, the SI (Système International) unit of energy?

Insincerely yours,
W.R. Bozman
Albuquerque, NM

Editor's Reply: Indeed we do. Our apologies for this oversight and our thanks for pointing it out.

In the Summer 1985 issue of *NASA Tech Briefs*, management of the Venus Radar Mapper (VRM) Project, which was featured on the front cover, was incorrectly attributed to the Ames Research Center. The VRM Project is managed by the Jet Propulsion Laboratory, Pasadena, California. Ames Research Center is responsible for management of the Pioneer Missions, including the Pioneer Venus Orbiter. We regret the error.

ARTIFICIAL WETLANDS

Please send me any information you may have regarding the creation of artificial wetlands with natural waste.

John Freis
Oneida, WI

The following documents, available from the American Institute of Aeronautics and Astronautics (see address below), contain the information you requested:

A80-49996, *The Production Of Substitute Natural Gas And Recyclables From Municipal Solid Waste*

A80-49974, *The Potential In Denmark For Substituting Natural Resources By Waste Incineration Products.*

You may also wish to purchase the following publications from the National Technical Information Service (see address below):

N85-19548, *Removal Of Heavy Metals By Artificial Wetlands*

N82-77262, *Validation Of Predictive Models For Geologic Disposal Of Radioactive Waste Via Natural Analogs*

N84-18794, *Salton Sea Geothermal Field, California, As A Near-Field Natural Analog Of A Radioactive Waste Repository In Salt*

N77-26032, *Improved Waste-Treatment Systems Design Based On The Natural Thermal Environment*

N76-24771, *Natural Methods Of Purifying Waste Water And Utilizing Them In Agriculture, Bibliography, Parts 1 and 2*

Please write to AIAA and NTIS directly to inquire about costs and mailing arrangements.

KUDOS & CHRONOGRAPHS

My main interest is in electronics and communications. Your magazine has opened a new door for my company with your unique circuits and articles. Keep up the good work!

How about some info on chronographs?

Steve W. Teegarden
Ft. Collins, CO

You may wish to purchase the following publications from the American Institute of Aeronautics and Astronautics (AIAA), Technical Information Service (see address below): A76-30479, *Pico-Femtosecond Electrooptic Chronograph*; A69-26598, *The Use of the YuS-38M Chronograph For Testing High-Speed, Curtain-Type Shutters*; A68-32677, *Device For Making Chronograph Imprints.*

You may also wish to purchase the following documents from the National Technical Information Service (NTIS) (see address below): N70-74327, *Assembly Of An Electric Chronograph With Automated Output On Punched Cards For Use In The Observatory With A Transit Instrument*; N70-74099, *The Solenoid-Electrostatic Aberdeen Chronograph.* Please write to AIAA and NTIS directly to inquire about costs and mailing arrangements.

To inquire about the availability and cost of documents published by the American Institute of Aeronautics and Astronautics, write: AIAA, Technical Information Services, 555 West 57th Street, New York, NY 10019. To purchase publications from the National Technical Information Service, write: NTIS, 5285 Port Royal Road, Springfield, VA 22161.

U.S. Postal Service Statement of Ownership, Management and Circulation (Required by 39 U.S.C. 3685) 1A. Title of Publication: NASA Tech Briefs B. Publication No. USPS 014531x 2. Date of Filing: 10-8-85 3. Frequency of Issue: Quarterly A. No. of Issues Published Annually: 4 B. Annual Subscription Price: \$50.00 4. Complete Mailing Address of Known Office of Publication (Street, City, County, State and Zip Code (Not Printers): Associated Business Publications, Inc., 41 East 42nd Street, New York, New York 10017-5391 (New York County) 5. Complete Mailing Address of the Headquarters or General Business Office of the Publishers (Not Printers): Associated Business Publications, Inc. 41 East 42nd Street, New York, N.Y. 10017-5391 6. Full Names and Complete Addresses of Publisher, Editor, and Managing Editor: Publisher (Name and Complete Mailing Address): Bill Schnirring, Associated Business Publications, Inc., 41 East 42nd Street, New York, New York 10017-5391; Editor (Name and Complete Mailing Address): Bill Schnirring, Associated Business Publications, Inc., 41 East 42nd Street, New York, New York 10017-5391; Managing Editor (Name and Complete Mailing Address): Rita Nothaft, Associated Business Publications, 41 East 42nd Street, New York, NY 10017-5391 7. Owner: (If owned by a corporation, its name and address must be stated and also immediately thereunder the names and addresses of stockholders owning or holding 1 percent or more of total amount of stock. If not owned by a corporation, the names and addresses of the individual owners must be given. If owned by a partnership or other unincorporated firm, its name and address, as well as that of each individual must be given. If the publication is published by a non-profit organization, its name and address must be stated.): (Full Name and Complete Mailing Address): Associated Business Publications, Inc., Bill Schnirring, Melissa Schnirring, Luke Schnirring, Frank Nothaft, Jr., Frank Nothaft, III, Rita Ursula Nothaft, Patricia Neri, Wayne Pierce, all at Associated Business Publications, Inc., 41 East 42nd Street, New York, New York 10017-5391 8. Known Bondholders, Mortgagees, and Other Security Holders Owning or Holding 1 Percent or More of Total Amount of Bonds, Mortgages or Other Securities (If there are none, so state): None, Complete Mailing Address: None 9. For Completion by Nonprofit Organizations Authorized to Mail at Special Rates (Section 411.3, DMM only) The purpose, function, and nonprofit status of this organization and the exempt status for Federal income tax purposes (Check one) Have Not Changed During Preceding 12 Months Have Changed During Preceding 12 Months (If changed, publisher must submit explanation of change with this statement.) 10. Extent and Nature of Circulation Average No. Copies Each Issue During Preceding 12 Months; Actual No. Copies of Single Issue Published Nearest to Filing Date: A. Total No. Copies Printed (Net Press Run): 94,125; 94,999 B. Paid Circulation 1. Sales Through Dealers and Carriers, Street Vendors and Counter Sales: —; 2. Mail Subscriptions: 79,271; 79,104 C. Total Paid Circulation (Sum of 10B1 and 10B2): 79,271; 79,104 D. Free Distribution by Mail, Carrier or Other Means Samples, Complimentary, and Other Free Copies: 7,459; 6,700 E. Total Distribution (Sum of C and D): 86,730; 85,804 F. Copies Not Distributed 1. Office Use, Left Over, Unaccounted, Spoiled After Printing: 7,395; 9,195 2. Returns From News Agents: —; G. Total (Sum of E, F1 and 2)—Should equal net press run shown in A): 94,125; 94,999 11. I certify that the statements made by me above are correct and complete. Signature and Title of Editor, Publisher, Business Manager, or Owner: Frank Nothaft, Business Manager. 12. For Completion by Publishers Mailing at the Regular Rates (Section 132.121, Postal Service Manual) 39 U.S.C. 3626 provides in pertinent part: "No person who would have been entitled to mail matter under former section 4359 of this title shall mail such matter at the rates provided under this subsection unless he files annually with the Postal Service a written request for permission to mail matter at such rates." In accordance with the provisions of this statute, I hereby request permission to mail the publication named in item 1 at the phased postage rates presently authorized by 39 U.S.C. 3626. Signature: Frank Nothaft, Business Manager.

Classifieds

Classified advertising rates and specifications are as follows: Set in 6 point light type face, with up to five words at beginning of copy in bold caps. Count box numbers as six words.

50 words or less \$ 125
100 words \$ 175

Check or money order must accompany order to: Classified Advertising Manager, NASA Tech Briefs, Suite 921, 41 East 42nd Street, New York, NY 10017-5391.

NASA CERTIFICATION—HAND SOLDERING TRAINING. Engineers, technicians, assemblers and inspectors can now get the training needed to verify their ability to perform/inspect high-reliability hand soldering. Upon completion, students will be NASA certified. For information call 301/426-3794 or write to Technology Transfer Company, P.O. Box 32457, Pikesville, MD 21208.

Advertiser's Index

A-E Systems Management, Inc.	(RAC 327*)	6
A.L. Design, Inc.	(RAC 342)	38
Alsys, Inc.	(RAC 341)	59
Aurora Bearings	(RAC 413)	151
Boeing Electronic	(RAC 414)	45
Brimrose	(RAC 415)	96
Brisk Heat Corp.	(RAC 416)	21
Celerity Computing	(RAC 352)	25
Centrifugal Piston	(RAC 417)	149
Clean Room Prods.	(RAC 322)	47
Clean Room Prods.	(RAC 321)	160
Collins Industrial GPS Products, Rockwell International	(RAC 354)	71
Du Pont-KAPTON	(RAC 399,400,401)	105, 107, 109
Eastman Kodak	(RAC 339)	35
Erim	(RAC 319)	81
Fairchild Control Systems Co.	(RAC 357)	15
Fiberite	(RAC 307)	72-73
Fisher Pen Company	(RAC 358)	124
GAF Corporation	(RAC 359)	12
General GE Electric	(RAC 361)	Cov.II-1
General Systems Corp.	(RAC 306)	180
Greene, Tweed & Co.	(RAC 328)	161
Harris Aerospace	(RAC 410)	22-23
Honeywell Inc. Space and Strategic Avionics Division	(RAC 364)	190, Cov.III
IBM Federal Systems Division	(RAC 365)	30-31
IBM Information Systems	(RAC 390)	10-11
IFR Inc.	(RAC 317)	87
ITT Electro-Optical Products	(RAC 403)	79
Kinetic Systems	(RAC 316)	43
Klinger Scientific Corp.	(RAC 368)	95
Lockheed California Company	(RAC 408)	4-5
Martin Marietta	(RAC 372)	Cov.IV
McDonnell Douglas Corp.	(RAC 412)	7
Metal Bellows Corp.	(RAC 348)	61
National Instrument	(RAC 377)	120
Pioneer Electric	(RAC 378)	119
Post Offers	(RAC 380)	37
Pressure Systems, Incorporated	(RAC 383)	101
Rockwell International Corp./ Rocketdyne Division	(RAC 384)	159
Schott Glass Technologies Inc.	(RAC 393)	41
Shearson Lehman/American Express	(RAC 308)	120
Sperry Corp.—Recruitment	(RAC 309)	121
Texas Instruments DSG	(RAC 409)	16-17
Tycor Electric Products Ltd.	(RAC 394)	2
Tycor Electric Products Ltd.	(RAC 419)	8
United States International Trading Co., Inc.	(RAC 419)	8
Vitro Corporation	(RAC 396)	9
Western Graffec	(RAC 310)	13
World Aviation Directory		181
Wyle Laboratories Scientific Services & Systems Group		9
Xerox		13

*RAC stands for Reader Action Card. For further information on these advertisers, please circle the RAC number on the Reader Action Card elsewhere in this issue. This index has been compiled as a service to our readers and advertisers. Every precaution is taken to ensure its accuracy, but the publisher assumes no liability for errors or omissions.

ABOUT THE NASA TECHNOLOGY UTILIZATION PROGRAM

Thumb Index



NASA TU Services



New Product Ideas



Electronic Components and Circuits



Electronic Systems



Physical Sciences



Materials



Life Sciences



Mechanics



Machinery



Fabrication Technology



Mathematics and Information Sciences



Subject Index

This document was prepared under the sponsorship of the National Aeronautics and Space Administration. NASA Tech Briefs is published quarterly and is free to engineers in U.S. industry and to other domestic technology transfer agents. It is both a current-awareness medium and a problem-solving tool. Potential products . . . industrial processes . . . basic and applied research . . . shop and lab techniques . . . computer software . . . new sources of technical data . . . concepts . . . can be found here. The short section on New Product Ideas highlights a few of the potential new products contained in this issue. The remainder of the volume is organized by technical category to help you quickly review new developments in your areas of interest. Finally, a subject index makes each issue a convenient reference file.

Further information on innovations—Although some new technology announcements are complete in themselves, most are backed up by Technical Support Packages (TSP's). TSP's are available without charge and may be ordered by simply completing a TSP Request Card, found at the back of this volume. Further information on some innovations is available for a nominal fee from other sources, as indicated. In addition, Technology Utilization Officers at NASA Field Centers will often be able to lend necessary guidance and assistance.

Patent Licenses—Patents have been issued to NASA on some of the inventions described, and patent applications have been submitted on others. Each announcement indicates patent status and availability of patent licenses if applicable.

Other Technology Utilization Services—To assist engineers, industrial researchers, business executives, Government officials, and other potential users in applying space technology to their problems, NASA sponsors Industrial Applications Centers. Their services are described on pages 28-32. In addition, an extensive library of computer programs is available through COSMIC, the Technology Utilization Program's outlet for NASA-developed software.

Applications Program—NASA conducts applications engineering projects to help solve public-sector problems in such areas as safety, health, transportation, and environmental protection. Two applications teams, staffed by professionals from a variety of disciplines, assist in this effort by working with Federal agencies and health organizations to identify critical problems amenable to solution by the application of existing NASA technology.

Reader Feedback—We hope you find the information in *NASA Tech Briefs* useful. A reader-feedback card has been included because we want your comments and suggestions on how we can further help you apply NASA innovations and technology to your needs. Please use it; or if you need more space, write to the Manager, Technology Transfer Division, P.O. Box 8757, Baltimore/Washington International Airport, Maryland 21240.

Advertising Reader Service—Reader Action Card (RAC): For further information on the advertisers, please circle the RAC number on the separate Reader Action Card in this issue.

Change of Address—If you wish to have *NASA Tech Briefs* forwarded to your new address, use the Subscription Card enclosed at the back of this volume of *NASA Tech Briefs*. Be sure to check the appropriate box indicating change of address, and also fill in your identification number (T number) in the space indicated. You may also call the Manager, Technology Utilization Office, at (301) 859-5300, ext. 242 or 243.

This document was prepared under the sponsorship of the National Aeronautics and Space Administration. Neither Associated Business Publications, Inc., nor anyone acting on behalf of Associated Business Publications, Inc., nor the United States Government nor any person acting on behalf of the United States Government assumes any liability resulting from the use of the information contained in this document, or warrants that such use will be free from privately owned rights. The U. S. Government does not endorse any commercial product, process, or activity identified in this publication.

Mission **A**ccomplished



Both the award-winning Mall At 163rd Street in Miami, Fla. (left) and the East Towne Mall in Knoxville, Tenn. are completely enclosed by permanent Fiberglas fabric roofs. The material was originally used in the space program during the Apollo era.

Fabric structures are nothing new—that is, temporary fabric structures. Tents have been around for quite awhile, and although tepees and covered wagons have come and gone, a permanent fabric structure material has recently taken its place on the American landscape.

What to wear to the moon is the question that spurred the development of a lightweight, flexible and durable fabric made of woven Fiberglas® coated with Teflon®. During the Apollo program, NASA sought to improve upon the fabrics it had used in fashioning space suits for the Mercury and Gemini astronauts, and began its search for a durable and noncombustible material that was also thin, lightweight and flexible.

At the time, Owens-Corning was developing a glass fiber yarn that could be woven into a fabric. The fabric was then coated with Teflon for added strength, durability and hydrophobicity—the ability to repel moisture. The material met NASA specifications and was used in space suits throughout the Apollo era.

The technology developed for the space program soon found additional

applications. The health care market required flame-resistant draperies and the Fiberglas fabric was adapted for that use. A more recent application is in the construction field, where a heavier version of the Fiberglas fabric is used as a permanent covering—or roof—for an airport terminal in Saudi Arabia, animal enclosures at zoos in Boston and North Carolina, stadiums in Michigan and Canada, and shopping malls in Miami, Fla., Knoxville, Tenn., Houston, Texas, San Mateo, Cal., and Albany, N.Y.

The construction adaptation of the Fiberglas fabric is marketed under the trade name Sheer-Fill® by O.C. Bird Air of Buffalo, New York, a joint venture fabric structures company owned by Owens-Corning and Chemical Fabrics. (Structo-Fab, a trade name registered by Owens-Corning prior to the joint venture agreement, is currently being phased out.)

Sheer-Fill is gaining popularity with building engineers and owners for a number of reasons. The fabric's translucency value, which ranges from 4 to 18 percent, reduces lighting needs and its reflectivity lowers cooling costs, so Sheer-Fill is considered energy effi-

Through the technology transfer process, many of the systems, methods and products pioneered by NASA are re-applied in the private sector, obviating duplicate research and making a broad range of new products and services available to the public.

cient. The Teflon coating reduces maintenance costs by increasing the fabric's resistance to moisture, temperature extremes and deterioration. Pound for pound, Sheer-Fill is stronger than steel and weighs less than five ounces per square foot. These factors combine to lower initial costs and speed construction.

Architects are favorably impressed with Sheer-Fill as well. It combines the aesthetic appeal of light, airy and unobstructed spans with a degree of space utilization that invites innovative design concepts—domes, atriums and sharply sloping roofs reminiscent of circus tents.

Typically, fabric structures are built in one of two ways. Either they're tension structures that are supported by a network of cables and pylons, or air-supported structures that consist of an outer membrane and an inner liner. The area between these two layers is inflated to maintain the pressure differential necessary for roof rigidity.

The air-supported structure concept is also being applied in creating domes to protect and shield radar and microwave antennas. The radome® provides an electromagnetic window for the microwave landing control antennas used by air traffic controllers, and the FAA is currently using radomes in developing its experimental wind shear detection radar system. Again, the material in use is Teflon-coated fiberglas fabric, all of which goes to show just how far innovative technology can travel—from the earth to the moon and back. □



NEYWELL AEROSPACE AND DEFENSE

HONEYWELL AERO

NEYWELL AEROSPACE AND DEFENSE

HONEYWELL AE

WELL AEROSPACE AND DEFENSE

HONEYW

LL AEROSPACE AND DEFENSE

EY

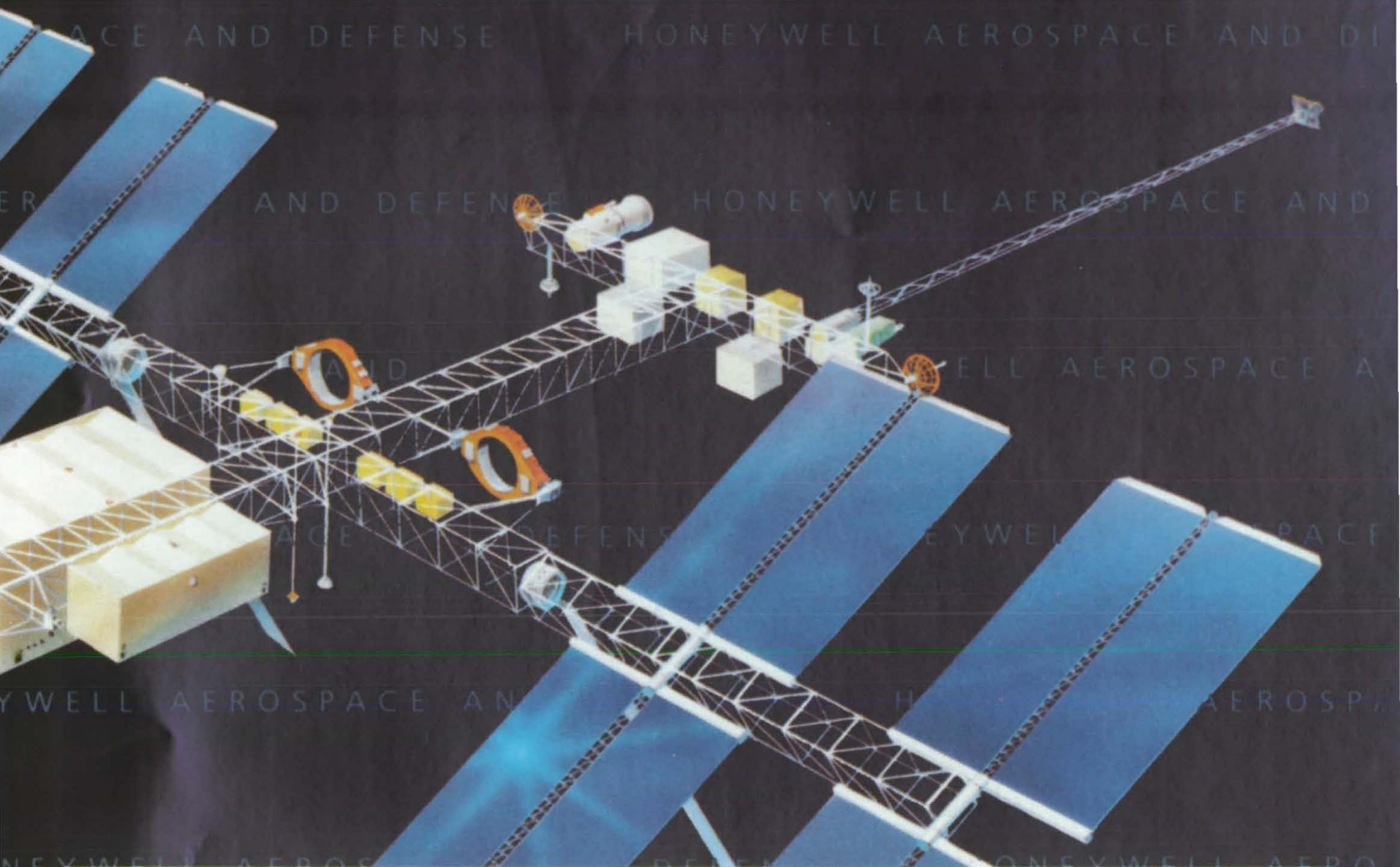
AEROSPACE AND DEFENSE

HON

CE AND DEFEN

E AND DE

E AND



Zero defects at zero gravity.

When you're working on America's first space station, the ultimate goal is zero defects at zero gravity.

Which is why NASA depends on Honeywell Reliability to make outer space ideas a reality.

Honeywell has played a major role in every one of NASA's manned space missions, from the X15 through Gemini and Apollo, to SkyLab and the Space Shuttle. And now we're working with other leaders in the aerospace industry to engineer critical control systems for life support, power distribution and guidance and navigation for NASA's first space station, scheduled for deployment in the mid-1990s.

Honeywell combines advanced technology with reliable performance to insure America's space program will succeed well into the 21st century — and beyond.



Honeywell Reliability

Together, we can find the answers.

Honeywell

Circle Reader Action No. 364

©1985 Honeywell Inc.

A BUILDING SITE LIKE NO PLACE ON EARTH.

Some structures needed in space are just too big to launch in one piece. Too large and too fragile even to stand alone on Earth, intricate sections can be brought up on successive shuttle flights, plucked from the orbiter by station robot arms, assembled into massive structures by the space station crew, and released to their own orbits. The miracle of microgravity will make light

work of such space construction.

One example is the 20-meter diameter Large Deployable Reflector infrared telescope NASA is planning for the mid-1990s. Consisting of some 100 pieces—large mirrors and supporting structures—when assembled and deployed, the device will permit a variety of deep space investigations.

Without the manned space

station, structures of this size would not be possible.

We think that's a very good reason to build a building site like no place on Earth.

With Eastman Kodak and NASA, McDonnell Douglas is planning the precision techniques needed for construction in space. We are teamed with Honeywell, IBM, Lockheed and RCA for major definition and design work on the station.



MCDONNELL DOUGLAS